Investigations into the underlying cellular mechanism of the alcohol-electro-oculogram

Paul Alexander Constable

PhD Thesis

Submitted to City University, London, UK

Department of Optometry and Visual Sciences, Henry Wellcome laboratories for Visual Science, City University, London, UK

The Wolfson Centre for Age-Related Diseases, King's College London, London, UK

May 2007

Table of Contents

I Figure List

II Table List

Acknowledgements

I would like to thank the following individuals for their support and encouragement throughout the preparation of this thesis:

Prof Geoffrey Arden
Prof John Lawrenson
Dr Diana Dolman
Prof Joan Abbott
Dr Ali Hussain
Dr Joanne Cunningham

For
Helle, Miles, Mum and Mam.

Funding for this work was provided by

The British Retinitis Pigmentosa Society, UK
The College of Optometrists, UK
The South Devon and Cornwall Institute for the Blind, UK

III Abstract

The aim of this study was to determine the underlying cellular mechanism by which ethanol alters the standing potential of the human eye (the ethanol electro-oculogram). Ussing chamber experiments using animal explants of retinal pigmement epithelium and retina, as well as cultured retinal pigment epithelial cells grown on filter inserts, were conducted to determine whether the retinal pigment epithelium was the target for ethanol. The human retinal pigment epithelial cell line, ARPE-19 was used to investigate changes in intracellular calcium concentration in response to ethanol. Human studies involving patients with cystic fibrosis were performed to determine the likely ionic channel involved in the ethanol-electro-oculogram.

Results indicated that ethanol was capable of elevating intracellular calcium concentration but that the source was from the extracellular pools. The likely ionic channel responsible for the light evoked electro-oculogram is the L-type calcium channel and this channel could be the route through which ethanol mediates the calcium-signal based on this finding. The amplitude of the ethanol evoked electro-oculogram was not dependent upon one functional chloride channel affected in cystic fibrosis and regulated by cyclic adenosine monophosphate dependent protein kinase A. This finding supports the role of a calcium-gated basolateral chloride channel being responsible for the ethanol-electro-oculogram. The fast oscillations in the cystic fibrosis subjects also showed higher or normal responses which are supportive of a recent finding in an animal model of this condition.

The findings of this study indicate that the ethanol-electro-oculogram is dependent upon calcium signalling. The earlier clinical studies have also shown that the ethanol-electro-oculogram is affected more than the light electro-oculogram in early retinal degenerations. Therefore, the results presented would suggest that calcium signalling is impaired in early retinal degenerations.

IV Abbreviations

Abbreviation	Definition
$[Ca^{2+}]_{in}$	Intracellular Calcium Concentration
AA	Arachidonic Acid
AC	Adenylate Cyclase
ADP	Adenosine Di-Phosphate
AM	Acetoxymethyl
ANOVA	Analysis of Variance
ARMD	Age-Related Macular Degeneration
ATP	Adenosine Tri-Phosphate
***a*-value**	Ratio of R_{Apical} to R_{Basal} Resistance
bFGF	Basic-Fibroblast Growth Factor
BM	Bruch's Membrane
BPE	Bovine Pituitary Extract
BSA	Bovine Serum Albumin
CaCC	Calcium-Activated Chloride Channel
cAMP	Cyclic Adenosine Mono-Phosphate
CIC	Chloride Channel
CF	Cystic Fibrosis
CFHBSS	Calcium-Free Hank's Balanced Salt Solution
CFTR	Cystic Fibrosis Transmembrane Conductance Regulator
CRALBP	Cellular Retinaldehyde Binding Protein
cGTP	Cyclic Guanosine Tri-Phosphate
CNS	Central Nervous System
DAG	Diacyglycerol
DIDS	4,4'-Diisothiocyanostilbene-2,2-disulphonate
ddH_2O	Double Distilled Water
DMEM	Dulbecco's Modified Eagle's Medium
DMSO	Di-Methylsulphoxide
DR:LT	Dark Rise : Light-trough Ratio
ECACC	European Collection of Animal Cell Culture
EDTA	Ethylenediaminetetraacetic Acid
EGF	Epidermal Growth Factor
EGTA	Ethylene-bis(oxyethylenenitrilo)tetraacetic acid
ENaC	Epithelial Sodium Channel
EOG	Electro-Oculogram
ER	Endoplasmic Reticulum
ERCA	Endoplasmic Reticulum Ca^{2+}-ATPase Pump
ERG	Electroretinogram
F and F_o	Fluorescent Emission and Fluorescent Emission at Baseline
F12	Ham's F12 Medium
FCS	Foetal Calf Serum Heat Inactivated
FITC	Fluorescein-Isothiocyanate
FO	Fast Oscillation
FSH	Follicular Stimulating Hormone
$GABA_A$	gamma-aminobutryic acid type A
GDP	Guanosine Di-Phosphate

GJ	Gap Junction
GTP	Guanosine Tri-Phosphate
HBBS	Hank's Balanced Salt Solution
HEK 293	Human Embryonic Kidney Cells -293
HEPES	N-(2-Hydroxyethyl)piperazine-N'-(2-ethanesulfonic acid)
HGF	Hepatocyte Growth Factor
HVA	High Voltage Activated
IGF	Insulin Growth Factor
IP_3	Inositol 1,4,5-Triphosphate
IP_3-R	Inositol 1,4,5-Triphosphate-Receptor
ISCEV	International Society for Clinical Electrophysiology of Vision
K_{ir}	Inward Rectifying Potassium Channel
LRR	Light-Rise Receptor
LVA	Low Voltage Activated
M199	Specialised Medium 199
MDCK	Madin-Darby Canine Kidney
MDR	Multi Drug Resistance
MEM	Modified Eagle's Medium
NA	Numerical Aperture
NBD	Nucleotide Binding Domain
NCX	Sodium Calcium Exchanger
ORCC	Outward Rectifying Chloride Channel
PBS	Phosphate Buffered Saline
PDGF	Platelet Derived Growth Factor
PEDF	Pigment Epithelial Derived Growth Factor
pH_{in} or pH_{out}	Intracellular or extracellular pH
P-gp	P-Glycoprotein
PIP_2	Phosphatidylinositol -4,5-Bisphosphate
PMCA	Plasma Membrane Ca^{2+}-ATPase pump
PKC (A)	Protein Kinase-C or –(A)
PLC-β	Phospholipase-C_β
PTK	Protein Tyrosine Kinase
R_{Apical} or R_{Basal}	Apical or Basal Membrane Resistance
RCS	Royal College of Surgeons
R-value	Ratio of Fluorescent Change = $(F-F_o)/F_o$
Rh	Rhodopsin
RP	Retinitis Pigmentosa
RPE	Retinal Pigment Epithelium
RT-PCR	Reverse Transcriptase-Polymerase Chain Reaction
SD	Standard Deviation
SEM	Standard Error of the Mean
SM	Specialised Medium
T3	3,3',5-Triiodo-L-Thyronine Sodium Salt
TEP	Trans Epithelial Potential
TER	Trans Epithelial Resistance
V_{Apical} or V_{Basal}	Voltage at Apical or Basal Membrane
VEGF	Vascular Endothelial Growth Factor
V_M	Membrane Voltage
VMD	Vitelliform Macular Dystrophy
ZA	Zonula Adherens
ZO	Zonula Occludens

1 Introduction

The RPE was described as a pigmented membrane 'composed of small oblong bodies, analogous to globules' (Mondini, 1790). As the specifications of microscopes improved individual hexagonal cells containing melanin granules could be observed (Jones, 1833). For a long time the RPE was thought to be the analogue of a camera's black light absorbing inner surface, but it is now recognised that the RPE performs a vast array of functions necessary to photoreceptor survival. For review see Strauss, (2005). The structure of the RPE reflects the range of its different functions. The apical surface of the RPE is composed of microvilli that interdigitate with the outer segments of the photoreceptors. The RPE forms tight inter-cellular junctions that create a barrier between the outer retina and the underlying choriocapillaris (Marmor, 1998). The basement membrane of the RPE is continuous with Bruch's membrane. The melanin within the melanosomes of the RPE absorbs light to reduce scatter (LaVail and Gorrin, 1987; Sardar *et al.*, 2001). One of the important roles of the RPE is the phagocytosis of shed photoreceptor outer segments (Young and Bok, 1969). The process of phagocytosis with the daily shedding of rod and cone outer segmnents and their ingestion and degradation by the RPE is accomplished by several steps. The shed photoreceptors bind to integrin αv5β receptors on the apical membrane of the RPE (Finnermann *et al.*, 1997; Lin and Clegg, 1998) which then leads to activation of Mer tyrosine kinase signalling pathway for internalisation of the outer segments (Wu *et al.*, 2005).

The RPE also participates in the transport of essential amino acids, fatty acids and is responsible for the isomerisation of all-*trans*-retinal into 11-*cis*-retinal for use by the photoreceptors in phototransduction (Miller and Steinberg, 1979; Bridges *et al.*, 1984, 2001a, 2002). The RPE also provides protection from reactive oxygen species by the production of glutathione, mitochondrial superoxide dismutases and absorption of free radicals by melanin (Atalla *et al.*, 1988; Kasahara *et al.*, 2005; Seagle *et al.*, 2005; Wang *et al.*, 2006). The RPE also contains at the apical and basal membranes numerous ionic channels, pumps and co-transporters that regulate pH, fluid transport and the ionic composition of the sub-retinal space (Hughes *et al.*, 1984; Miller and Farber, 1984; Miller and Edelman, 1990; Gallemore *et al.*, 1993; Gallemore and Steinberg, 1993). The ionic currents that flow across the apical and basal membranes through the ion channels, pumps and co-transporters generate an electrical potential at each membrane. This potential is termed the trans epithelial potential (TEP) and underlies the ocular standing potential of the eye (Steinberg *et al.*, 1983).

This study is primarily concerned with the slow voltage and current changes across the RPE in response to light and ethanol. There is currently no sensitive and specific clinical electrophysiological test to assess the physiology of the RPE. The light-EOG relies upon a signal transduction from the rods to the RPE and therefore it is not specific for RPE function (Griff and Steinberg, 1982). Clinical tests involving fluorescein angiography and red free fundus photography provide information about the integrity of the RPE barrier but they do not provide a means of assessing the physiology of the RPE.

The clinical relevance of the light-EOG has been questioned for some time and more recently it has been suggested that the light- and alcohol-EOGs are too variable to be of any clinical value (Marmor, 1991; Marmor and Wu, 2005). However, the light-EOG continues to be a useful and reliable measure of the interaction between the photoreceptors and the RPE. The light-EOG is a sensitive test for Best's disease (Weleber, 1989) as well as being important for the early detection and monitoring of drug toxicity as in the case of the anti-epileptics, vigabatrin (Lawden *et al.*, 1999; Harding *et al.*, 2002) and lamotrigine (Arndt *et al.*, 2005). The EOG is a sensitive measure of visual function for patients prescribed desferrioxamine (Iron chelator) following repeated blood transfusion (Hidajat *et al.*, 2004) and is a useful screening tool during clinical trials to ascertain whether a novel drug is toxic (Theischen *et al.*, 1993). The light-EOG is said to be abnormal in seasonal-affected disorder (Lam *et al.*, 1991) and is crucial in the diagnosis of acute zonal outer retinopathy (Francis *et al.*, 2005). It is of course abnormal in cases of retinal degenerations, but in such disorders, the electro-retinogram (ERG) is the preferred diagnostic test.

The first complete description of the human light-dark sequence was due to Kris, (1958). However, the clinical utility was established by Arden who showed that the light-EOG was reduced when there was gross retinal degeneration, anoxia or drug toxicity to the outer-retina and RPE (Arden, 1962; Arden and Barrada, 1962; Arden *et al.*, 1962; Arden and Kelsey, 1962; Arden and Kolb, 1966). The light-EOG records the change in the ocular standing potential over time. In the initial dark phase, there is a fall in the standing potential to a minimum as the eye dark-adapts over a period of 15 to 20 minutes. When the retina is illuminated, the standing potential rises with a peak voltage occurring approximately 8 to 12 minutes after light onset. The ratio of this peak voltage to the dark-adapted trough minimum voltage is known as the Arden ratio. The peak voltage in the light is dependent upon a normal interaction between the RPE and photoreceptors. For review see, Arden and Constable, (2006).

Ethanol also produces a voltage change across the dark-adapted eye in man (Skoog *et al.*, 1975; Arden and Wolf, 2000b) and sheep (Knave *et al.*, 1974) that mimics the slow light-evoked voltage change. The clinical utility of the alcohol-EOG has been assessed in patients with age-related macula degeneration (ARMD) and retinitis pigmentosa (RP) (Arden and Wolf, 2000a, 2003; Arden *et al.*, 2000). In all of the conditions, the alcohol-EOG was smaller than the light-EOG. Therefore, the alcohol-EOG may provide greater sensitivity and may be a more specific test of RPE function than the light-EOG. Consequently, the underlying mechanism by which ethanol interacts with the RPE may provide valuable insights into the aetiology of these retinal degenerations.

1.1 Embryology

The development of the RPE, retina Bruch's membrane and the choriocapillaris is a co-ordinated and integrated process (Hollyfield and Witkovsky, 1974; Rizzolo and Li, 1993; Rizzolo *et al.*, 1994; Rahner *et al.*, 2004; Mitsuda *et al.*, 2005). In man, the optic cup develops from the neuroectroderm during the fourth week of gestation and comprises two layers of cells. The outermost layer of columnar epithelial cells develops into the RPE and the inner layer develops into the neural retina. This decision is regulated by a variety of signals that are not exclusive to the developing eye-cup (Buse *et al.*, 1993). Pigmentation of the RPE is detectable at five to six weeks gestation (Hollenberg and Spira, 1972). At seven weeks the lateral folds and apical microvilli are present and the tight junctional proteins are present (Mund *et al.*, 1972). By the eighth week, the RPE has developed gap- and zonula adherens-junctions (Fisher and Linberg, 1975). Developments of the inner segments of the photoreceptors are apparent at 10 - 15 weeks gestation and the outersegments are present at 20 weeks in man (Rizzolo, 2006).

1.2 Structure

The apical membrane of the RPE faces the photoreceptors with which it maintains a close association through apical microvilli. The basal plasma membrane of the RPE has small infoldings that increase the surface area for efficient exchange of metabolites, water and nutrients into and from the underlying choroidal circulation. The RPE contains adenosine tri-phosphate (ATP) generating mitochondria, melanin-containing melanosomes, lysosomes and phagosomes for the digestion of shed photoreceptor disks (Marmor, 1998).

1.2.1 Cytoskeleton

The RPE's structure is maintained by a cytoskeleton with a circumferential actin band at the cell apex. The cytoskeleton provides a framework to which the junctional proteins are attached and also provides a flexible and strong scaffold so that the RPE can change shape and maintain its structural integrity (Owaribe *et al.*, 1981, 1986, 1988). The apical processes also possess actin filaments and in chick, these exert tension on the retina to aid the close association of these two structures (Philp and Nachmias, 1985). The cytoskeleton is composed of three basic elements: microfilaments, intermediate filaments and microtubules. The microfilaments form a network within the cortex of the cell and are composed of actin filaments that are cross linked with α-actinin (Burnside and Bost-Usinger, 1998). In chick RPE the microtubules extend into the apical microvilli. However, in man these microtubules are absent and actin filaments are present instead (Turksen *et al.*, 1989). A network of microtubules use the hydrolysis of guanosine tri-phosphate (GTP) to perform reorganisation of intracellular organelles (Klyne and Ali, 1981), cell motility (Campochiaro and Glaser, 1986) and contribute to phagocytosis (Irschick *et al.*, 2006). The microtubules give structural integrity to the RPE and are composed of dimmers of β-tubulin and γ-tubulin (Rizzolo and Joshi, 1993; Bollimuntha *et al.*, 2005). Intermediate filaments have a diameter between that of the microfilaments and the microtubules and are comprised of an acidic

and basic cytokeratins which provide structural support for the RPE. Cytokeratins 8 and 18 are found in human RPE (McKechnie *et al.*, 1988; Owaribe *et al.*, 1988; Fuchs *et al.*, 1991). The expression of cytokeratins 18 and 19 is associated with RPE migration (Robey *et al.*, 1992) and the difference in expression profiles of cytokeratins can be used to differentiate between phenotypically distinct RPE cells in culture (McKay and Burke, 1994; Casaroli-Marano *et al.*, 1999).

1.3 Junctional Proteins

The barrier properties of the RPE are created in part by the intercellular junctional proteins that create a seal with low permeability between the RPE cells. This paracellular pathway between the cells provides one route for ions and water to pass between the retina and underlying choroid. There is also a transcellular route for the passage of ions, water and metabolites through the ionic channels of the RPE's plasma membranes (Joseph and Miller, 1991; Anderson, 2001). The intercellular junctions are assembled from several proteins that link the RPE cells together and determine the barrier properties of the cell monolayer. One protein, zonula occludens (ZO)-1 (Stevenson *et al.*, 1986) is a scaffolding protein that links cytoplasmic proteins (occludins) to the actin cytoskeleton on the inner face of the plasma membrane with extracellular proteins (claudins) that interlink with complimentary claudins on the plasma membrane of the adjoining cell (Schafer *et al.*, 1992; Konari *et al.*, 1995; Yanagihara *et al.*, 2001). In chick RPE, it is the expression levels of claudins and not ZO-1 that determines the electrical resistance of the barrier (Ban and Rizzolo, 2000b; Peng *et al.*, 2003; Rahner *et al.*, 2004). There are approximately 24 families of vertebrate claudin proteins whose expression changes with the development of the tight junction and disease (Kojima *et al.*, 2002; Lu *et al.*, 2004). Claudins are selectively permeable to ions; however all permit the passage of K^+ (Colegio *et al.*, 2002, 2003). For review see Van Itallie and Anderson, (2006). The zonula adherens junctions act as focal points of contact around the RPE, and develop just prior to tight junction formation. The proteins forming the adherens junctions are composed of Ca^{2+}-dependent cadherin proteins associated with the actin circumferential band (Miyaguchi, 2000). In the RPE, E-cadherin forms the adherens junction and this protein is attached to the cytoplasmic microfilament by vinculin and catenins (Marrs *et al.*, 1995).

Gap junctions are formed in the lateral plasma membranes to permit intercellular signalling and the sharing of small molecules such as ATP (Himpens *et al.*, 1999; Pearson *et al.*, 2004, 2005). The gap junction is formed by six connexin proteins (Goodenough, 1974) with alterations in their configuration regulating intercellular communication (Unwin and Ennis, 1984).

The RPE's basement membrane is formed from vitronectin, collagen types I, III, and IV, fibronectin and laminin with the RPE secreting these proteins *in vitro* (Turksen *et al.*, 1984, 1985, 1989; Campochiaro *et al.*, 1986; Ho and Del Priore, 1997; Tsukahara *et al.*, 2002; Tezel *et al.*, 2004). Laminin is the main component associated with attachment of the RPE to Bruch's membrane (Crawford and Vielkind, 1985). A transmembrane linking protein, integrin, links the

basement membrane to the intracellular cytoskeletal proteins talin and vinculin thereby anchoring the RPE to Bruch's membrane (Philp and Nachmias, 1987; Philp *et al.*, 1990). The RPE's basement membrane is continuous with Bruch's membrane that is divided into an inner collagenous layer, elastin layer, outer collagenous layer and the basement membrane of the choriocapillaris (Hollenberg and Burt, 1969). With age, the nature of Bruch's membrane changes and the accumulation of basal laminar deposits and collagenous debris reduce the permeability of the underlying membrane (van der Schaft *et al.*, 1993; Starita *et al.*, 1997). Figure 1.1 overleaf shows a schematic representation of a mammalian RPE cell with a representation of some of the cytoskeletal proteins and complexes present.

Figure 1.1 The RPE – Basic Structure

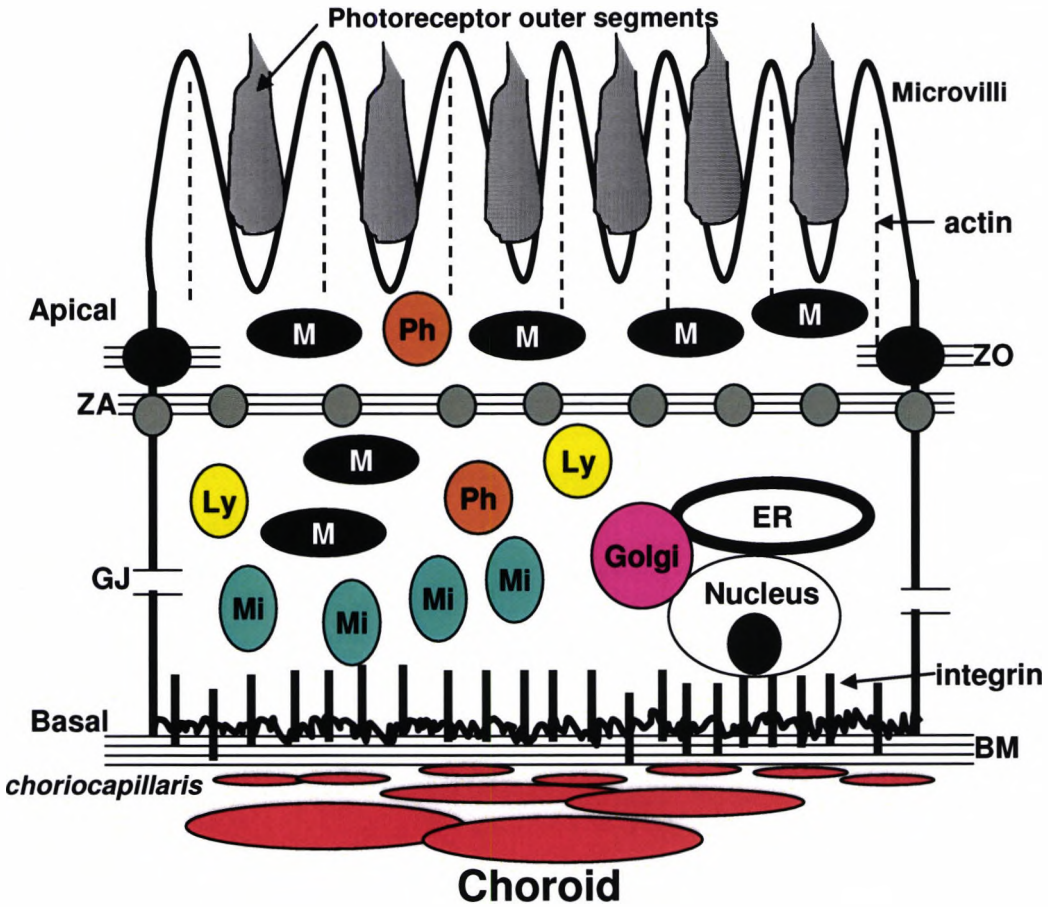

Schematic showing an RPE chick cell with the apical microvilli interdigitating with the photoreceptor outer segments. The inner section of the RPE contains melanosomes (M) that absorb stray light. Phagocytosis of shed photoreceptor outer segments is performed by Phagosomes (Ph) which then fuse with Lysosomes (Ly) to further digest the photoreceptor outer segments. The RPE has mitochondria (Mi), an endoplasmic reticulum (ER) which acts as an intracellular reservoir of Ca^{2+} and protein synthesis along with the Golgi apparatus. The RPE is polarised by virtue of the tight junctional proteins and cytoskeleton. At the apical margins, a circumferential belt composed mainly of actin filaments surrounds the RPE. This band is associated with zonula adherens proteins (ZA) and form tight adhesive complexes between E-cadherins that are linked to the plasma membrane of adjoining RPE cells. The zonula occludens (ZO) junctions are associated with claudins and occludins that regulate the permeability of the paracellular pathway. The apical microvilli contain actin bundles that both give structure and contribute to the phagocytosis of rod outer segments. Gap junctions (GJ) between cells allow intercellular communication and are formed by connexins. The basement membrane of the RPE is continuous with Bruch's Membrane (BM). The transmembrane protein integrin (black bars) forms attachments to the laminin, collagen and fibronectin components of BM and connects with the RPE's cytoskeleton. BM is continuous with the choriocapillaris of the vascular choroid.

1.4 Signal Transduction

A cell must be able to adapt to changes in the immediate environment. A number of receptors and signalling proteins and second messengers are present in all cells that enable this adaptability. It is assumed that the light-rise of the EOG is dependent upon a signal being released from the rods that binds to an RPE apical membrane receptor and this initiates the release of a second messenger within the RPE that then alters the basolateral membrane chloride conductance (Gallemore *et al.*, 1988). The pathways for signal transduction and amplification within a cell are numerous but two key intracellular second messengers are cyclic adenosine monophosphate (cAMP) and Ca^{2+}. Both of these second messengers have been implicated in altering the basal membrane conductance of chloride channels and could potentially contribute to the alcohol-EOG.

1.4.1 G-Proteins

One likely pathway that either ethanol or the light-rise substance could alter membrane conductance is by the activation of a G-protein coupled receptor. G-proteins are involved in the signal transduction of extracellular ligands that vary in nature from ions, peptides, proteins, lipids, nucleotides odours or light as seen in the phoptoisomerisation of rhodopsin (Rh). For reviews see, Waters *et al.*, (2004) and Nash and Osborne, (1996). Heterotrimeric G-proteins are composed of three subunits (α, β and γ) and span the cell membrane. The protein complex is coupled to an extracellular receptor that when bound to its ligand enables modulation of intrcellular signalling cascades that may either be inhibitory or excitatory. The nature of the α-subunit defines the G-protein family and so the G_s family all contain the α_s subunit.

One receptor associated with the G_s protein is the β-adrenergic receptor. In the inactive state the α_s subunit binds guanosine di-phosphate (GDP). Following ligand binding to the β-adrenergic receptor the G_s protein undergoes a conformational change enabling the release of GDP which is rapidly replaced by guanosine tri-phosphate (GTP) owing to the higher cytosolic concentration. The G_α subunit then dissociates from $G_{\beta\gamma}$ and uses the hydrolysis of GTP to catalyse the formation of cAMP by the membrane-bound protein, adenylate cyclase (AC) (Rodbell *et al.*, 1971). The generation of cAMP is able to catalyse the activation of the protein kinase-A enzyme (PKA) that in its active state can phosphorylate specific amino acids on proteins to modulate their function. It is also possible for the $G_{\beta\gamma}$ and G_α subunits to act as synergists or antagonists on the same or different target proteins to regulate intracellular signalling (Gilman, 1987). Once GTP is hydrolysed into GDP, the G-protein reassembles.

The generation of PKA by the RPE is important as one of the basolateral chloride channels is regulated by PKA (Anderson *et al.*, 1991c). This channel, the cystic fibrosis transmembrane conductance regulator (CFTR) may play an important role in the electrophysiological responses of the RPE (Blaug *et al.*, 2003; Reigada and Mitchell, 2005).

The generation of a Ca^{2+} response by G-proteins involves a different mechanism belonging to the G_q family. In one example, an agonist binds to the receptor associated with G_q. This step leads to the activation of the enzyme, phospholipase-C_β (PLC-β) which rapidly cleaves the membrane-bound phospholipid, phosphatidylinositol-4,5-bisphosphate (PIP_2) (Smrcka *et al.*, 1991) into two key signalling molecules. One is Inositol 1,4,5-triphosphate (IP_3) and the other is diacyglycerol (DAG) which act as second messengers to raise intracellular Ca^{2+} concentration ($[Ca^{2+}]_{in}$) by two separate pathways.

1: IP_3: Ca^{2+} released from the intracellular stores of the endoplasmic reticulum (ER) is dependent upon the IP_3-receptor (IP_3-R) that forms an intracellular Ca^{2+} channel (Spat *et al.*, 1986). IP_3 can move in the cytosol to the ER where it binds to the receptor and releases Ca^{2+}. However, there is a negative feedback loop and increasing levels of cytosolic-free Ca^{2+} inhibit the IP_3-R to ensure cytosolic Ca^{2+} levels do not remain elevated. For review see Berridge *et al.*, (2003).

Re-uptake of Ca^{2+} into the ER is also regulated by the ER-calcium-ATPase pump (ERCA). This pump is inhibited by thapsigargin (Lytton *et al.*, 1991) and/or cyclopiazonic acid (Seidler *et al.*, 1989). The use of these drugs is commonly used to demonstrate that Ca^{2+} is derived from ER stores by inhibiting re-uptake of Ca^{2+}. Physiologically, ERCA is inhibited by phospholamban in its unphosphorylated state (Tada and Kadoma, 1989). Phosphorylation of phospholamban by various kinases acted upon by second messengers exerts fine control over cytosolic free calcium by increasing re-uptake of Ca^{2+} (Tada and Inui, 1983). One further regulator of cytosolic free Ca^{2+} is calmodulin that acts as a Ca^{2+} receptor and once bound can modulate cellular functions through protein phosphorylation such as cellular migration, cell attachment and differentiation (Kishi *et al.*, 2000; Smith-Thomas *et al.*, 2000).

2: DAG: Two separate signalling pathways are influenced by the generation of DAG. Firstly as a modulator of Ca^{2+}-signalling it activates the membrane bound inactive protein-kinase C (PKC) that also requires elevation of intracellular Ca^{2+} to translocate across the plasma membrane for activation by DAG. Once active, PKC then phosphorylates proteins to modulate their function (Mitchell, 1982a, b). The second interaction of DAG is to release the polyunsaturated fatty acid arachidonic acid (AA) from the plasma membrane. AA is then further metabolised into potent autocrine and paracrine signalling molecules that are associated with inflammation and pain regulation. For review see Sigal, (1991).

The elevation of $[Ca^{2+}]_{in}$ by an external agonist is important because Ca^{2+} is capable of increasing the basolateral membrane chloride currents of two ionic channels. Bestrophin and a Calcium Activated Chloride Channel (CaCC) that have both been proposed to participate in the light-rise of the EOG (Marmorstein *et al.*, 2006; Rosenthal *et al.*, 2006).

1.4.2 Protein Tyrosine Kinases

Protein tyrosine kinases (PTKs) are membrane-bound proteins which act as enzymes by directly phosphorylating tyrosine residues in intracellular target proteins after extracellular activation by growth factors such as epidermal growth factor (EGF), insulin derived growth factor (IGF) or platelet-derived growth factor (PDGF) (Glenney Jr, 1992; Schlessinger and Ullrich, 1992). Integration of PTKs and G-protein signalling pathways provides an alternative means by which G-protein activation and signalling pathways can interact with PTKs to modulate cell physiology. For review see, Waters *et al.*, (2004). Of importance to the RPE is the regulation of PTKs and the L-type Ca^{2+} channel. This ion channel's gating is determined not only by membrane voltage, but also phosphorylation by PTK and PKC. The PTK associated with this regulation in the RPE belongs to the non-receptor tyrosine kinase family that lack an extracellular binding domain but retain the intracellular tyrosine kinase catalytic domain (Strauss *et al.*, 1997). Growth factor regulation of PTKs provides a means of regulating $[Ca^{2+}]_{in}$ by altering the conductance of L-type Ca^{2+} channels (Rosenthal *et al.*, 2005). The L-type Ca^{2+} channel is now seen as the principal channel responsible for the generation of the Ca^{2+}-signal associated with the light-rise of the EOG (Marmorstein *et al.*, 2006).

1.5 Membrane Voltage

The changes in membrane voltage (V_M) are determined by the net currents that flow across the cell membranes. The resting V_M results from the difference in ionic concentrations across the plasma membrane and the relative permeability of the membrane to the ions present in the cytosol and the extracellular spaces. Alterations in the permeability or conductance of the membrane to the ions by the gating of ionic channels leads to a change in V_M as ionic currents pass across the membrane.

Since ions are electrically charged, their movement through ionic channels causes a change in the charge across the lipid bilayer. For example, as positively charged potassium ions move out of a cell, the interior becomes negatively charged with respect to the exterior and so V_M hyperpolarises. This change in voltage eventually opposes the movement of the ions and an equilibrium is established approximating to the Nernst equilibrium potential (Nernst, 1888). See equation 1.i.

$$\mathbf{E_X = [(R \times T) / (z \times F)] \times \ln ([X]_{out} / [X]_{in})} \text{— } \mathbf{1.i}$$

Where:

E_X = Equilibrium potential (Volts) of ion X.

$[X]_{out}$ = Concentration of ion X outside cell (mM).

$[X]_{in}$ = Concentration of ion X inside the cell (mM).

R = The Gas Constant (8.314 $J.K^{-1}.mol^{-1}$).

T = Absolute temperature (K).

F = Faraday's constant (96,500 $C.mol^{-1}$).

z = Valence of ion or charge e.g. Cl^- = -1; Ca^{2+} = +2.

The RPE develops an electrical potential that is dependent upon ions being held away from their equilibrium or Nernst potential. The ionic channels, pumps and cotransporters move ions against the electrochemical gradients so that an electrical potential is established. The opening of ionic channels enables certain ions to move towards their equilibrium potential creating ionic currents and a change in V_M. It is these changes in ionic currents that generate the alterations in the ocular standing potential recorded with the EOG. The foundation of the ocular standing potential is the trans-epithelial potential (TEP) of the RPE that is established between the basal and apical membrane voltages.

1.6 Trans Epithelial Potential and Resistance

Because there is a different population of ionic channels in the apical and basal membrane of the RPE, a TEP is established across the RPE. There is also a trans-epithelial resistance (TER) that is established in part by the tight-junctions. The resistance that forms the paracellular pathway through which ions may pass is denoted R_s. The conductance of the apical and basal membranes to ions also creates a resistance (R_{Apical}) and (R_{Basal}) respectively. The TEP is defined in the RPE as the difference between the basal membrane voltage (V_{Basal}) and the apical membrane voltage (V_{Apical}). See equation 1.ii on following page.

Steinberg modelled the RPE on an electrical circuit in which the apical membrane was electrically coupled to the basal membrane (figure 1.2 overleaf). In this equivalent circuit, V_{Apical} is represented by a battery (E_A) in series with a resistance (R_A) and a current pump that represents the apical NaKATPase pump. The battery represents the net ionic currents across the apical membrane. Similarly the basal membrane is represented by a resistance (R_B) in series with a battery (E_B). The apical and basal membranes are electrically coupled through the paracellular resistance that may be assumed to be constant. Because of this electrical coupling a change in the membrane voltage at either the apical or basal membrane is shunted to the other membrane so that there is a delayed and smaller change in the V_M at the opposite membrane (Miller and Steinberg, 1977; Gallemore and Steinberg, 1993).

Figure 1.2 Electrical Circuit Model of the RPE

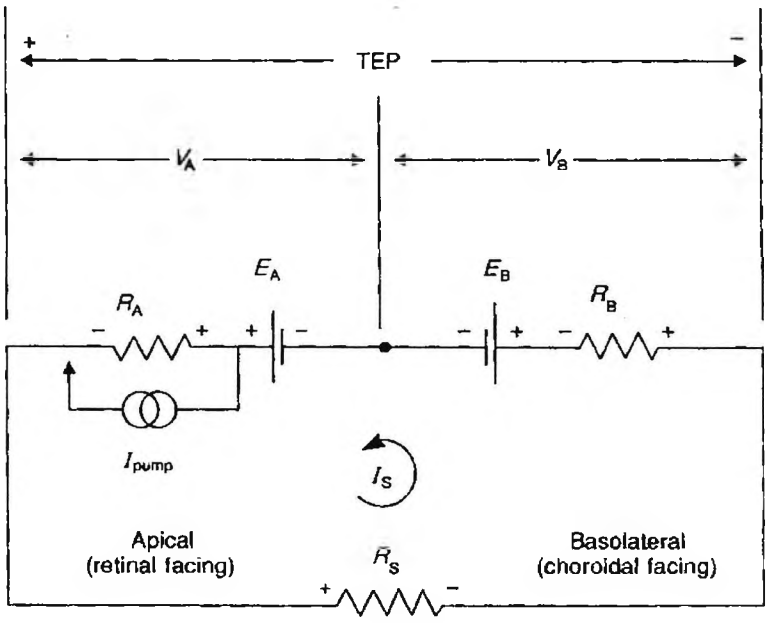

The equivalent electrical circuit of the RPE as modelled by Miller and Steinberg, (1977). The apical and basal membrane voltages are represented by a resistance and battery in series. The apical membrane has another current source, the NaKATPase pump that is depicted by the pump. The apical and basal membranes are electrically coupled by the tight junctions that have a finite and near constant resistance. This electrical coupling means that a change in the membrane potential at one membrane results in a change at the opposite membrane of equal sign but smaller magnitude.

The RPE's apical membrane is hyperpolarised with respect to the basal membrane owing to the differences in the batteries (ion channels) in the apical and basal membranes. The TEP is defined as the difference between the basal and apical membrane voltages so that the TEP is positive for the RPE (equation 1.ii). This positive TEP also creates a current loop from the basal to apical membrane (I_s) that flows through the paracellular resistance (R_s). The TER can be derived from the equivalent electrical circuit and is expressed in equation 1.iii (Miller and Steinberg, 1977). For review see Gallemore *et al.*, (1997).

$$\mathbf{TEP = V_{Basal} - V_{Apical}} \qquad \mathbf{— 1.ii}$$

$$\mathbf{TER = [R_s \times (R_{Apical} + R_{Basal})] / (R_{Apical} + R_{Basal} + R_S)} \qquad \mathbf{— 1.iii}$$

1.7 Voltage Gated Channels

The RPE contains numerous ionic channels, pumps and co-transporters that all contribute to the 'battery' at the apical and basal membranes. The opening of an ion channel may be dependent upon a number of different factors such as, an external ligand, phosphorylation, cell volume or the membrane voltage. Voltage gated ion channels were observed in the giant squid axon by Hodgkin and Huxley, where it was shown that the conductance of the ion channels varied as a function of V_M (Hodgkin and Huxley, 1952 a-c). The investigators were able to hold or clamp V_M at a holding potential and record the current. Using this technique a plot of how current varied with voltage was drawn with the slope of the curve representing the conductance.

Hodgkin and Huxley introduced the term 'rectification' to describe ionic channels whose I-V relationship was non-linear as was found with the voltage gated Na^+ and K^+ channels of the axon. The conductance or open probability of the channel depended upon V_M in these excitable membranes.

Some of the RPE's ionic channels also display rectification, in that their conductance varies as a function of V_M. Channels are termed *inward* or *outward* rectifiers depending upon how their conductance changes in relation to hyperpolarisation or depolarisation of V_M. An inward rectifier increases conductance in response to hyperpolarisation of V_M and an outward rectifier increases conductance in response to a depolarisation of V_M.

Ion channels may not display rectification but still be dependent upon V_M for opening. One example is the L-type Ca^{2+} channel[1] where the inward Ca^{2+}-current increases as the membrane depolarises. For this voltage dependent ionic channel, the I-V curve is bell-shaped with a reduction of current as the membrane depolarises further. (See figure 1.3 overleaf).

[1] L-type Ca^{2+} channel is a voltage dependent Ca^{2+} channel with a 'Long' deactivation time giving sustained Ca^{2+} currents into the cell.

Figure 1.3 Voltage-dependent L-type Ca^{2+} Currents in the RPE

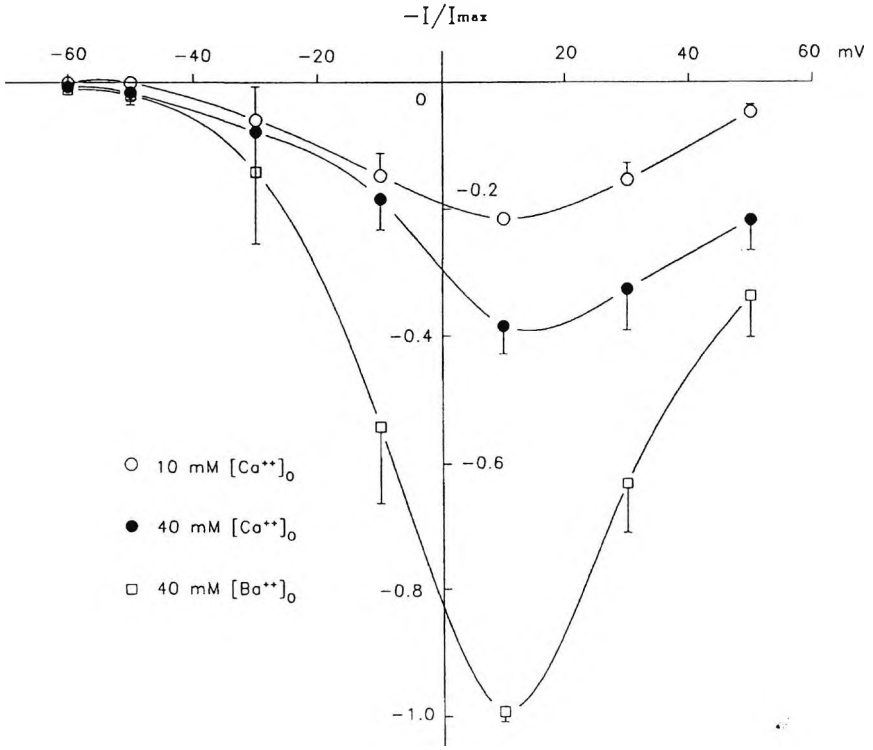

The I-V curve of the voltage dependent L-type Ca^{2+} currents recorded from the rat RPE. The inward current increases as the membrane voltage depolarises with a maximum at ~ +10 mV and then falls as the membrane voltage is further depolarised. In this case Ba^{2+} ions were used as well as Ca^{2+} ions because the L-type Ca^{2+} channel has a greater permeability to Ba^{2+} than Ca^{2+} so the inward current was greater and easier to record. In contrast Co^{2+} ions are less permeable through the L-type Ca^{2+} channel pore and so exhibit a reduced current. From Ueda and Steinberg (1993).

1.7.1 The Ocular Standing Potential

The German neurophysiologist, Du Bois–Reymond demonstrated that amongst different potentials of the frog there was a potential across the eye with the cornea positive with respect to the posterior globe (Du Bois Reymond, 1849). The EOG is an approximate measure of the TEP of the RPE that is the main contributor to the ocular standing potential (Gallemore *et al.*, 1998). The ocular standing potential is recorded with electrodes placed at the inner and outer canthus of each eye or at the outer canthi of both eyes with an earth electrode positioned at a suitable location between the active electrodes (eyebrow or forehead). The current and voltage generated by the RPE is normal to the surface of the globe. Therefore, the resultant potential lies normal to the optic axis and as the eyes execute horizontal saccades; the magnitude of the standing potential is recorded. The size of the potential falls in the dark and rises in the light. Figure 1.4 shows the ocular standing potential and how the amplitude alters between dark and

light. The ratio of the peak voltage in the light phase to the minimum voltage in the dark phase represents the Arden ratio and is reduced when either the RPE and/or rods are diseased.

Figure 1.4 The Electro-Oculogram

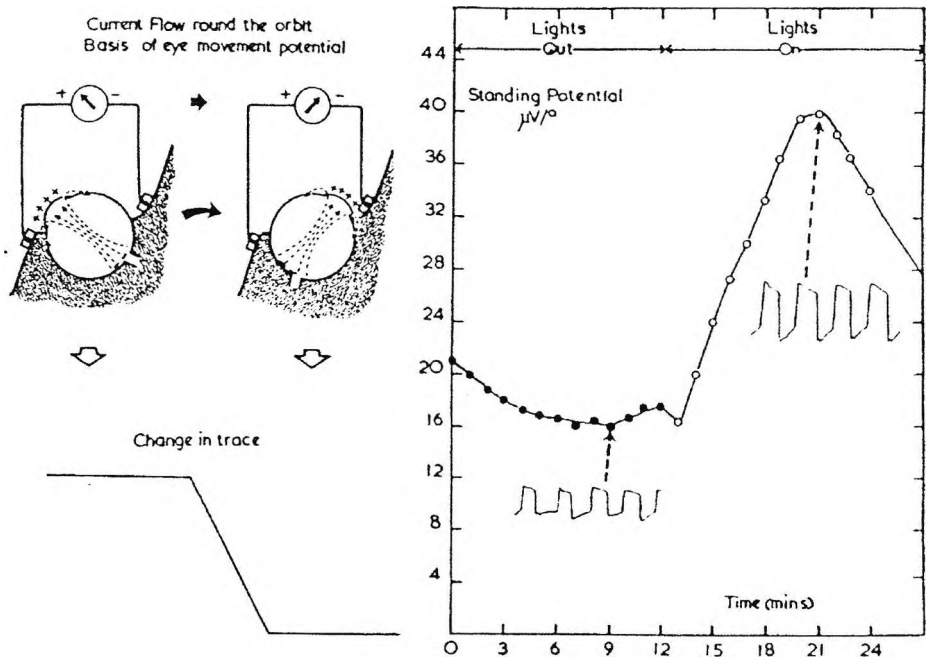

The ocular standing potential is recorded between two differential electrodes. As the eye moves left and right the potential changes. In the dark, the amplitude falls creating the dark-trough of the EOG and in light the amplitude rises generating the light-rise of the EOG. In the figure the square waves are the voltages recorded from the electrodes as the eyes perform horizontal saccades. In the dark this potential falls so that the amplitude of the square wave also decreases. In light the ocular standing potential increases which is seen in the increase in the amplitude of the square waves at the light-rise peak. The ratio of the peak to trough voltage represents the Arden ratio and is typically > 1.87. The standing potential is measured in this instance using μV/deg which is the actual potential divided by 30° (the visual angle through which each saccade was performed). From Arden, (1962).

The mechanism of the EOG depends upon changes in the membrane voltage of the RPE and this is determined by the ionic channels and signalling pathways within the RPE. However, a change in the RPE's membrane voltages also contributes to two other clinical tests that utilise light. One is the c-wave that occurs ~ 10 seconds after light onset and is, in part, generated by the apical membrane of the RPE hyperpolarising which produces a positive change in the TEP (Steinberg *et al.*, 1970). The second light induced effect on the standing potential of the eye can be seen by alternating between light and dark cycles at one-minute intervals. In the dark phase the standing potential increases and in the light phase the standing potential falls creating a fast oscillation (FO) that has a period of 60 - 75 seconds. The FOs are believed to be due to a decrease in Cl^- transport by CFTR (Blaug *et al.*, 2003).

1.8 Ionic Channels Associated with the EOG

The principal ionic channels of the RPE that are known to be or are implicated in the changes in membrane voltage associated with the c-wave, the FOs and the light-EOG are summarised in table 1.1 overleaf. At the apical membrane, there is the inward rectifying K^+ channel, the Na-K-2Cl cotransporter, NaKATPase pump and CFTR. At the basal membrane, CFTR is present as well as bestrophin, CaCC and the L-type Ca^{2+} channel. ClC chloride channels have also been identified in a foetal human RPE cell line but their localisation is unknown.

Table 1.1 Ionic Channels and Transporters in Mammalian RPE

Channel	Gating/Regulation	Localisation	I-V curve	EOG	Reference(s)
K_{ir}	Hyperpolarisation	Apical/Basal	Inward Rectifier	c-wave	Hughes and Takahira, (1996)
CFTR	ATP and PKA	Apical/Basal	Linear	FO ? and EOG ?	Wills *et al.*, (2000); Blaug *et al.*, (2003); Reigada and Mitchell, (2005)
CaCC	Calcium	Basal	Linear	EOG	Ueda and Steinberg, (1994); Loewen *et al.*, (2003)
Bestrophin hBest 1-4	Calcium Cell swelling	Basal	Linear Inward and Outward Rectifiers	EOG ?	Marmorstein *et al.*, (2000); Fischmeister and Hartzell, (2005)
L-type Ca^{2+}	Bestrophin Depolarisation PTK, PKC	Basal	Voltage dependent	EOG	Mergler *et al.*, (1998); Strauss *et al.*, (2000); Rosenthal *et al.*, (2006)
ClC	PKA Cell swelling	Apical/Basal?	Mild outward rectification?	?	Wills *et al.*, (2000)
Na-K-2Cl	Cell Volume	Apical	—	FO	la Cour *et al.*, (1997)
NaKATPase	ATP	Apical	—	—	Miller *et al.*, (1978)

Summary of principal channels involved in alterations of membrane voltage in the electrophysiological responses associated with mammalian RPE.

1.8.1 Chloride Channels of the RPE

Chloride channels have been shown to be responsible for the change in the TEP of the RPE associated with the light-rise of the EOG (Gallemore and Steinberg, 1993). However, the nature of these channels and their involvement in the depolarisation of the basal membrane that leads to the light-rise has yet to be fully elucidated. This is in part due to the non-selective nature of chloride channel blockers but also the many other regulatory kinases that modulate gating. For reviews see Nilius and Droogmans, (2003) and Eggermont, (2004). In the RPE there are three main chloride channels expressed that could be implicated in the alcohol-EOG.

1.8.1.1 Cystic Fibrosis Transmembrane Conductance Regulator (CFTR)

Cystic fibrosis (CF) is an autosomal recessive disorder caused by mutations in the gene encoding for CFTR (Rich *et al.*, 1990). The gene responsible for CFTR encodes for a chloride channel that belongs to the ATP-Binding Cassette family (Riordan *et al.*, 1989; Rommens *et al.*, 1989; Dean and Allikmets, 2001). The intracellular portion of CFTR consists of two nucleotide binding domains (NBD1 and NBD2) separated by a large polar regulatory domain with sites for phosphorylation by PKA and PKC (Riordan *et al.*, 1989). CFTR protein is expressed in cultured adult human RPE cells (Weng *et al.*, 2002) as well as in the transfected human RPE foetal cell line (Wills *et al.*, 2000). It has been localised to the basal and apical membranes in primary human foetal RPE explants where it appears to localise to a greater extent at the basal membrane (Blaug *et al.*, 2003).

The predominant mutation in Caucasian CF is a deletion of phenylalanine at position 508 in NBD1 and is termed the Δ508 mutation (Cutting *et al.*, 1990; Lemna *et al.*, 1990). This mutation results in CFTR being unable to reach the plasma membrane (Puchelle *et al.*, 1992) and is degraded in the ER (Yang *et al.*, 1993). Gating of CFTR depends upon the priming of the channel with PKA at the intracellular regulatory domain and binding of ATP at NBD1 and the hydrolysis of ATP at NBD2 (Li *et al.*, 1988; Vergani *et al.*, 2005). For reviews see Riordan, (2005) and Linsdell, (2006). CFTR currents are non–rectifying when Cl^- concentrations are symmetrical across the membrane (Anderson *et al.*, 1991a, b; Kartner *et al.*, 1991).

1.8.1.2 Role of CFTR in the RPE

CFTR is thought to play a role in fluid regulation by the RPE because it can transport Cl^- (Blaug *et al.*, 2003). However, if CFTR was significantly involved in fluid regulation then it would be expected that CF individuals would be prone to retinal oedema which is not observed (Loewen *et al.*, 2003). However, CFTR could produce current and voltage changes across the RPE and transport molecules through the membrane which could affect other ionic channels as well as potentially playing a role in the regulation of intracellular pH (pH_{in}). CFTR has a major role in regulating pH of the gut (Kopelman *et al.*, 1988) and the lung where CFTR apparently controls a direct HCO_3^- conductance (Coakley *et al.*, 2003), which accounts for the acidic nature of the

airway mucosa in CF sufferers. Whether CFTR plays a role in regulating pH_{in} in mammalian RPE is unknown. CFTR is implicated in altering the conductance of at least three other ionic channels. One is the inhibition of the epithelial sodium channel (ENaC) (Ismailov *et al.*, 1996) and inward rectifying K^+ channels (K_{ir}), (Loussouarn *et al.*, 1996). However, CFTR also is implicated in activating outward rectifying chloride channels (ORCC) (Schwiebert *et al.*, 1995; Peterson *et al.*, 1997; Braunstein *et al.*, 2004). For review see, Kunzelmann, (2001).

However, the transport of ATP by CFTR is of more interest to the RPE. Experiments using bovine RPE and a human RPE cell line also suggest that CFTR increases ATP in the sub-retinal space following activation (Reigada and Mitchell, 2005). It has been proposed that the transport of ATP could contribute to the light-rise of the EOG by stimulating Ca^{2+}-signalling (Peterson *et al.*, 1997; Reigada *et al.*, 2005; Reigada and Mitchell, 2005).

1.8.2 Calcium-Activated Chloride Channel (CaCC)

The CaCC is a chloride channel that is regulated by an increase in intracellular $[Ca^{2+}]$. CaCCs were first identified in *Xenopus* oocytes where a rise in $[Ca^{2+}]_{in}$ following fertilisation led to a depolarisation of the oocytes that prevented further entry of sperm (Miledi, 1982; Barish, 1983). CaCCs are believed to be responsible for fluid regulation in the RPE via ATP or adrenergic coupled regulation (Peterson *et al.*, 1997, 1998; Rymer *et al.*, 2001). A partially inhibitable CaCC current by 4,4'-diisothiocyanostilbene-2,2'-disulphonic acid (DIDS) was first identified in neo-natal rat RPE (Ueda and Steinberg, 1994). However, these currents were short-lived and only responded to non-physiological ranges of $[Ca^{2+}]_{in}$. In canine RPE CaCCs are expressed in the basal membrane and contribute to fluid secretion to a greater extent than cAMP activated chloride channels (Loewen *et al.*, 2003). CaCC channels have also been demonstrated in human foetal (Quinn *et al.*, 2001) and bovine RPE with stimulation with epinephrine (Rymer *et al.*, 2001) or ATP (Peterson *et al.*, (1997).

1.8.3 Bestrophin

Best's vitelliform macular dystrophy (VMD) (Best, 1905) is an inherited autosomal dominant disease with a variable age of onset from childhood to adulthood (Renner *et al.*, 2005). It is characterised by a central 'egg-yolk' vitelliform lesion at the macula that eventually develops into a disciform scar impairing vision. The gene responsible for Best's (*VMD2*) has been identified (Forsman *et al.*, 1992; Petrukhin *et al.*, 1998; Marchant *et al.*, 2001). It codes for the bestrophin protein, which is specifically expressed at the basal membrane of human, porcine and macaque RPE (Marmorstein *et al.*, 2000). There are four human homologues of human bestrophin (hBest 1-4) with differing I-V relationships (Tsunenari *et al.*, 2003).

Several mutations of *VMD2* result in Best's disease that are phenotypically similar with a decreased light-rise and macular lesions (Marchant *et al.*, 2001). However, there is a report of

normal light-rises in individuals with Best's disease and mutations in *VMD2* which indicates that bestrophin may not be essential for the development of the light-rise (Pollack *et al.*, 2005).

Bestrophin was predicted to form an ionic channel based upon its amino acid sequence (Gomez *et al.*, 2001). The first evidence that bestrophin was a chloride ion channel gated by Ca^{2+} was demonstrated when hBest1 and hBest2 were transfected into human embryonic kidney cells (HEK 293). Whole cell recordings identified a Cl^- conductance that was increased by $[Ca^{2+}]_{in}$ (Sun *et al.*, 2002). Furthermore, the expression of *Xenopus* bestrophin (xBest-2a) that shares homology to hBest-2 into HEK 293 cells also showed Ca^{2+}-activated chloride currents. When mutant *Xenopus* bestrophins were expressed there was a loss of or reduction of the Ca^{2+}-activated chloride current depending upon the mutant (Qu *et al.*, 2003). Furthermore, when mouse bestrophin (mBest2) was expressed into three different mammalian cell lines a Ca^{2+}-activated chloride channel was present whose permeability and anion selectivity were altered by mutations (Qu *et al.*, 2004; Qu and Hartzell, 2004). In a patch clamp study Ca^{2+} was shown to increase the chloride current in hBest4 but the activation and deactivation of these currents were very slow and therefore other signalling mechanisms were proposed to be involved in modulating the opening and closing of the channel (Tsunenari *et al.*, 2006). These studies all strongly suggested that bestrophin was the Ca^{2+}-gated chloride channel responsible for the light-rise. However, this model has become more complicated with recent findings in animal models of Best's.

Marmorstein *et al.*, (2004) transfected rat RPE with wild-type isoform of human bestrophin (hBest-1) or two mutant variations (W93C and R218C). Recordings were made of the ERG and EOG components. The authors found that in rats over expressing wild-type bestrophin the amplitude of the light-rise was reduced which would not be expected if bestrophin was the chloride channel responsible for this response. However, the time to peak was faster in the wild-type transfected group. The authors concluded that bestrophin may not generate the light-rise but serves as an intermediary in this response and may modulate the timing of the response. Of the two mutant bestrophins, the W93C reduced the light-rise amplitude more than the R218C. However, in the W93C mutant the light-rise response was the fastest of any of the transfected rats but the R218C mutant did not alter the timing of the response (Marmorstein *et al.*, 2004).

The question of whether bestrophin is or is not a CaCC has been raised by the observation that bestrophin increases the rate of entry of Ca^{2+} through L-type Ca^{2+} channels into the RPE (Rosenthal *et al.*, 2006). Bestrophin now appears not to be a chloride channel but a regulator of Ca^{2+} influx. The initial signal from the photoreceptors to the RPE that initiates the light-rise is still unknown but it has been suggested that ATP may be light-rise substance (Peterson *et al.*, 1997; Reigada and Mitchell, 2005; Marmorstein *et al.*, 2006). When $[Ca^{2+}]_{in}$ was increased in mouse RPE with ATP the change in $[Ca^{2+}]_{in}$ was five fold higher in *Vmd2* null mice compared to controls which is the only direct experimental evidence for ATP being the light-rise substance (Marmorstein *et al.*, 2006). Bestrophin is now seen as a regulator of Ca^{2+} entry as well as re-

uptake of Ca^{2+} by the ER. Bestrophin does not seem to contribute to the increased basolateral Cl^- conductance that generates the light-rise.

Bestrophin may also play a role in volume regulation. Whole cell recordings from transfected cells expressing human or mouse bestrophins (hBest1 or mBest2) showed a large decrease in current when the extracellular solution was hyperosmolar. A slight increase in current was found when the extracellular solution was hypo-osmotic (Fischmeister and Hartzell, 2005).

1.8.4 ClC Chloride Channels

These channels are distributed throughout the body in epithelia, skeletal muscle and neurons. ClC (chloride channels) were first identified in the electric organ of the *Torpedo* ray (White and Miller, 1979). Nine types of ClC channels have been identified in mammals and ClC-2 activates slowly at hyperpolarising membrane voltages and has a linear I-V curve (Thiemann *et al.*, 1992). The diversity of ClC-2 distribution implies that it has a key role to play in epithelial and non-epithelial cells. The electrophysiology of the different types of ClC channel is not identical. ClC-2 has slight inward rectification in the range from -180 mV to +50 mV that is slowly activated both by hyperpolarisation, extracellular acidification, PKA and AA (Cuppoletti *et al.*, 1993; Jordt and Jentsch, 1997; Tewari *et al.*, 2000). ClC channels are typically closed at resting membrane potential. Their main role seems to be in regulating cell volume (Gründer *et al.*, 1992; Strange *et al.*, 1996; Furukawa *et al.*, 1998; Xiong *et al.*, 1999).

ClC-2 is found in the RPE, and in a ClC-2 knockout mouse, retinal degeneration and testicular atrophy were the only defects (Bösl *et al.*, 2001; Nehrke *et al.*, 2002). It is highly likely that ClC-2 in the RPE plays a vital role in either the regulation of cell volume, pH_{out} and fluid secretion as it does in other epithelia (Cuppoletti *et al.*, 1993; Malinowska *et al.*, 1995). ClC-2, ClC-3, ClC-5 and CFTR are co-expressed in a human foetal RPE cell line (Wills *et al.*, 2000). CFTR and ClC-2 are both activated by PKA (Cid *et al.*, 1995; Tewari *et al.*, 2000). Therefore, ClC-2 may provide an alternative Cl^- conductance when CFTR is defective (Thiemann *et al.*, 1992; Schwiebert *et al.*, 1998; Blaisdell *et al.*, 2000).

1.9 Calcium Channels of the RPE

In cultures of human RPE a variety of peptides, growth factors, amino acids and agonists have been shown to elevate $[Ca^{2+}]_{in}$ via IP_3 generation (Kuriyama *et al.*, 1991, 1992; Feldman and Randolph, 1993; Ammar *et al.*, 1998; Quinn *et al.*, 2001). In addition, Ca^{2+} is required for binding and ingestion of rod outer segments in cultured rat RPE cells and together with PKC plays a role in inhibiting phagocytosis (Hall *et al.*, 1991, 2001, 2002). Resting cytosolic free $[Ca^{2+}]_{in}$ in human cell cultures is estimated to be approximately 70 - 200 nM (Feldman *et al.*, 1991; Kuriyama *et al.*, 1991, 1992) which is significantly lower than the millimolar extracellular concentration. Therefore, there is a favourable electrochemical gradient for Ca^{2+} to enter the RPE and consequently there

are a number of active pumps and transporters that operate against the concentration gradient to maintain $[Ca^{2+}]_{in}$ low.

1.9.1 Na^+/Ca^{2+}-Exchanger and the Ca^{2+}-ATPase Pump

Efflux of Ca^{2+} from the cytosol is in part accomplished by utilising the favourable high extracellular Na^+ concentration maintained by the NaKATPase pump. The sodium-calcium exchanger (NCX) was first identified in heart muscle (Reuter and Seitz, 1968). Three members of this family have been identified. NCX1 is expressed ubiquitously and transports three Na^+ ions out in exchange for one Ca^{2+} ion into the cytosol. The other two types, NCX2 and NCX3 are limited to brain and skeletal muscle. A NCX was identified in the apical membrane fraction of bovine and fish RPE cells (Fijisawa *et al.*, 1993). In man, cardiac NCX1 protein is present in both retina and RPE (Mangini *et al.*, 1997; Loeffler and Mangini, 1998). This exchanger is extremely fast and in the RPE, it would act to rapidly regulate $[Ca^{2+}]_{in}$ when sudden rises in $[Ca^{2+}]_{in}$ occurred by extruding Ca^{2+} from the cytosol.

Another mechanism that moves calcium across the plasma membrane is the (Ca^{2+}-Mg^{2+})-ATPase pump (PMCA) (Kennedy and Mangini, 1996). PMCA uses the energy of ATP hydrolysis to actively transport Ca^{2+} against its concentration gradient to remove Ca^{2+} from the RPE's cytosol (Kennedy and Mangini, 1996).

1.9.2 Voltage-Gated Ca^{2+} Channels (L-type)

The NCX1 and the PMCA provide a route for Ca^{2+} exit the RPE, a means of Ca^{2+} influx is also required. Voltage gated Ca^{2+} channels are found in skeletal muscle, heart, neurons and epithelia. The voltage dependent L-type Ca^{2+} currents were first observed in the heart (Orkand and Niedergerke, 1964). In the heart two types of voltage gated Ca^{2+} channels were identified, the low voltage activated (LVA) or 'transient' T-type channels which are activated by small depolarisations and are rapidly deactivated. The second was the high voltage activated (HVA) channel that activated with large depolarisations and had a slower inactivation. This channel was termed the L-type for 'long' activation (Nowycky *et al.*, 1985).

L-type Ca^{2+} channels are formed by 5 protein subunits (α_1, α_2, β, δ and γ) with the α_1-subunit forming the pore, voltage sensor and binding site for drugs. The α_2 and δ-subunit are linked by a disulphide bond and anchor the channel to the plasma membrane. The α_2 and β-subunits have sites for phosphorylation by kinases. The L-type Ca^{2+} channel is inhibited by dihydropyridines (nifedipine), phenlalklamines (verapamil) and benzothiazepines (dilitazem) (Flockerzi *et al.*, 1986; Rane *et al.*, 1987; Garcia *et al.*, 1990). For further review, see Dolphin, (1995).

The gating of L-type Ca^{2+} currents depends upon V_M with a greater probability of the channel opening as the membrane depolarises. L-type voltage-gated Ca^{2+} channels were first identified in fresh and cultured RPE cells from rat (Ueda and Steinberg, 1993). Strauss has identified that the

L-type Ca^{2+} channels in the RPE are of the neuroendocrine subtype that are found in neurons, neuroendocrine cells, heart and pancreatic islet cells. These L-type channels possess the α_{1D}-subunit and are regulated by both PKC and PTK. This important aspect of the regulation of L-type Ca^{2+} channels would provide a means by which growth factors that activate PTKs could result in an increase in $[Ca^{2+}]_{in}$. Possible growth factors that regulate PTKs would be bFGF (Mergler *et al.*, 1998) or platelet-derived growth factor (PDGF) (Heldin *et al.*, 1989) whose receptors are expressed on the RPE (Yoshida *et al.*, 1992; Bost *et al.*, 1994).

The increased Ca^{2+} conductance found in dystrophic rats may also interfere with phagocytosis (Hall *et al.*, 1991). L-type Ca^{2+} currents in cultured human and rat RPE cells show dual regulation by PTK and PKC, with the level of PKC activation determining whether PTK increases or decreases the L-type Ca^{2+} current (Strauss *et al.*, 1997, 1999, 2000).

L-type Ca^{2+} channels have been recently shown to be involved in generating the sustained Ca^{2+}-signal for the light-rise in mice (Marmorstein *et al.*, 2006). The kinetics of this channel is increased by bestrophin which increases the rate of Ca^{2+} influx (Rosenthal *et al.*, 2006). Furthermore, mice lacking the L-type Ca^{2+} channel's β_4-subunit had a significantly reduced light-rise and also reductions in the c-wave and FOs. Therefore, the L-type Ca^{2+} channel with the β_4-subunit is required to generate a normal light-rise (Marmorstein *et al.*, 2006).

1.10 Electrophysiology of the RPE

The light-evoked responses of the eye may be separated in terms of their time-course with the EOG being the slowest electrical change to be manifested. Figure 1.5 shows some of the commonly recorded electrophysiological measures in relation to the light stimulus. In this study the primarily concern is the effect of ethanol on the ocular standing potential but several other electrical signals are associated with light stimulation of the dark-adapted eye. The 'fast' components that occur in < 1 second form the ERG and the 'slower' components that occur over 10 seconds to 10 minutes and are the c-wave, the FOs and the EOG. The slower components derive from changes in the membrane potentials of the RPE.

Figure 1.5 Light-Evoked Responses of the Eye

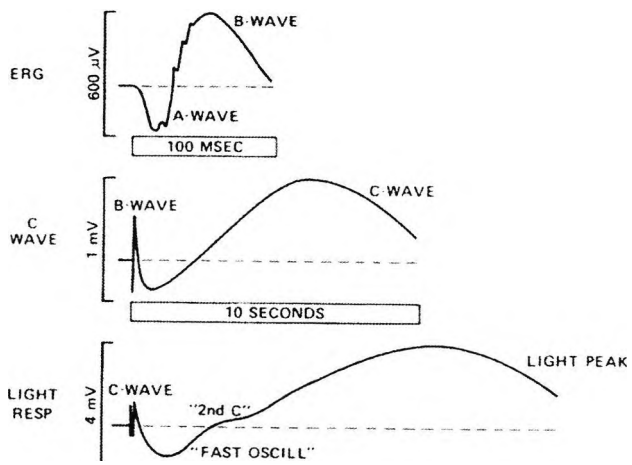

The time course of various responses generated by light. The fastest responses originate in the photoreceptors and neural retina which generate the a- and b-waves of the ERG. The RPE contributes to the generation of the c-wave, FOs and the light-rise of the EOG. Modified from, Marmor and Lurie (1979).

1.10.1 The Fast Components of the ERG

The components of the ERG were originally recorded from frog eyes and were labelled according to their latency. The initial negative change in the ocular potential, the a-wave, the second positive change, the b-wave and the third slower positive waveform the c-wave (Einthoven and Jolly, 1908). Einthoven and Jolly were the first to propose that the ERG was the product of separate underlying processes that arose from different cells in the eye. The underlying waveforms (processes) that contributed to the ERG were uncovered in a series of experiments using ether. The three processes (PI, PII and PIII) were based upon their resistance to abolition by anaesthesia. P1 the first was the most sensitive to anaesthesia and corresponded to the c-wave, PII corresponded to the b-wave and PIII corresponded to both the a-and c-waves (Granit, 1933, 1947). See figure 1.6 overleaf.

Figure 1.6 Processes of the ERG

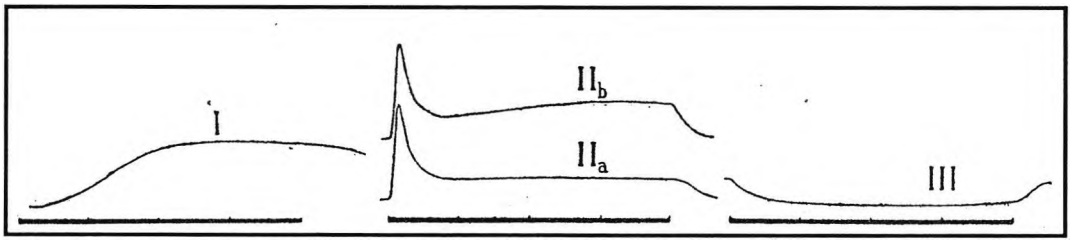

The three 'processes' originally described by Granit (1933) account for the ERG waveform. PI- was the most sensitive to anaesthesia and was responsible for the slowly developing c-wave. PII, the second process was responsible for the b-wave and PIII, the least sensitive to anaesthesia, was responsible for the a-wave and contributed to the c-wave. PIIa and PIIb reflect interspecies differences in their response to ether with some species showing, a rise in PII after PI was initially removed with ether. The dark bar represents light. Reproduced from, Granit (1947).

Figure 1.7 shows an early ERG trace from frog with the negative a-wave followed by the positive b-wave and slower developing c-wave. At light offset, there is a further positive deflection in the trace – the d-wave. The summation of PI, PII and PIII give the recorded ERG waveform.

Figure 1.7 ERG Recording

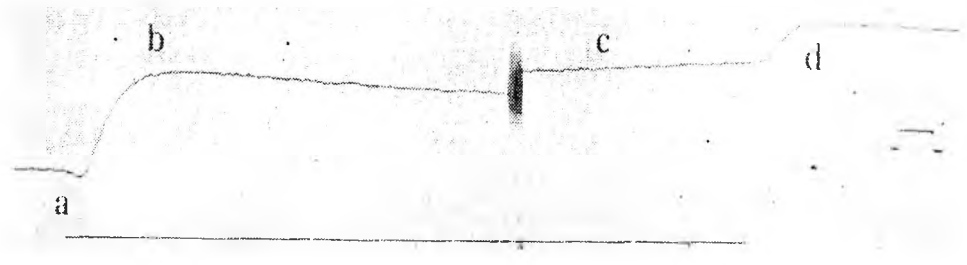

ERG recording from the frog with light stimulus indicated by the black bar below the trace. The recordings were stopped at the smudge in the trace to allow the c-wave to develop (Granit, 1933). The a- and b-waves develop in < 0.4 seconds. The c-wave is present > 1 second later. Reproduced from Granit, (1947).

The analysis of the cellular contribution to each of the ERG components was advanced by, Werner Noell. He used a combination of cytotoxins that selectively affected the RPE and photoreceptors. By selectively injecting these poisons into rabbits, Noell was able to isolate the PI component to the RPE layer (Noell, 1942, 1953).

1.10.2 The ERG Fast Components- Ionic Currents

The early investigators of the ERG realised that the ERG was a composite waveform derived from the neural cells and the RPE whose responses overlap in time to generate the ERG. Alterations in the ionic currents across the membranes of the photoreceptors, bipolar cells, Müller cells and the RPE all contribute to the final changes in the recorded potential across the eye.

The leading negative edge of the ERG a-wave (PIII) is a photoreceptor response. Intra-retinal depth recordings in cat localised the a-wave response to the outer segments of the rods. The b-wave was seen as a current sink in the inner nuclear layer and the c-wave to the RPE layer (Brown and Wiesel, 1959, 1961a, b). Recordings of local membrane currents along the length of the rods showed that the current responsible for the a-wave was maximal at the level of the outer segments (Penn and Hagins, 1969). In the dark, a 'resting' dark current flows out from the inner limb of the rod to the outer segment where it returns. Light causes a decrease in this dark current (Hagins *et al.*, 1970). The first step is the photo-isomerisation of 11-*cis*-retinal to all-*trans*-retinal that permits the activation of opsin from Rh to active Rh^* by a conformational change. Rh^* then binds to the G_t-protein (transducin) which upon dissociation the α-subunit activates cyclic guanosine monophosphate (cGMP) phosphodiesterase that hydrolyses cGMP (Shimoda *et al.*, 1984) resulting in decreased cytosolic cGMP concentration (Fung and Stryer, 1980). The fall in cGMP then results in the dissociation of cGMP from the plasma membrane Na^+, K^+, Ca^{2+} channels causing them to close and the outer segment to hyperpolarise as the cations accumulate outside the membrane and this is recorded as the negative a-wave of the ERG (Bader *et al.*, 1978; Kurkin and Fesenko, 1982; Woodruff *et al.*, 1982; Miller and Laughlin, 1983; Zimmerman *et al.*, 1985; Fesenko *et al.*, 1986).

The inner segments contain two main sources for K^+ regulation and current. Passive K^+ channels (Kx) that maintain the outward K^+ flux in the dark (Yan and Matthews, 1992; Liu and Kourennyi, 2004). To counter the large influx of Na^+ in the dark the inner segment is also rich in the NaKATPase pump (Stirling and Lee, 1980). At light onset the activity of the NaKATPase pump is not affected by changes in the membrane voltage and there is a continued reduction of extracellular K^+ as the pump continues to exchange intracellular Na^+ for K^+ at the inner segment (Matsuura *et al.*, 1978; Fujimoto and Tomita, 1979; Oakley II *et al.*, 1979; Shimazaki and Oakley II, 1984). The rate of the pump slows over time as levels of intracellular Na^+ fall but the immediate result is that there is a fall in sub-retinal K^+ (Oakley II and Steinberg, 1982). The decrease in sub-retinal $[K^+]$ has implications for the generation of the b- and c-waves (Oakley II and Green, 1976).

The b-wave of the ERG (PII) is not related to the RPE and is a bipolar response with some input from the Müller cells. The spatial buffering of K^+ by Müller cells was believed to be the source of the b-wave (Brown and Wiesel, 1961b; Miller and Dowling, 1970; Karwoski and Proenza, 1977; Kline *et al.*, 1978; Newman, 1979). However, in the scotopic mammalian ERG the b-wave is now

thought to be due to depolarisation of the ON-bipolar cells (Xu and Karwoski, 1994; Karwoski and Xu, 1999).

The RPE and Müller cells directly influence the c-wave of the ERG. The fall in sub-retinal K^+ owing to the closing of the dark current in the rods has a major effect on the RPE's apical membrane and the Müller cells. The c-wave is the net result of the apical membrane of the RPE hyperpolarising resulting in an increased TEP seen as a cornea-positive component (PI). The second negative component is due to the hyperpolarisation of the distal end of the Müller cells that generate a slow corneal negative response (PIII) following the a-wave (Karwoski and Proenza, 1977; Newman, 1989). The fall in sub-retinal K^+ results in a change in the driving force for K^+ in the RPE and inward rectifying K_{ir} channels open and K^+ leaves the RPE resulting in a corneal positive change in potential (Oakley II and Green, 1976; Linsenmeier and Steinberg, 1983; Hughes and Takahira, 1996). The net result of the Müller cell hyperpolarisation (negative) and apical membrane of the RPE hyperpolarising so that the TEP gives a positive potential change and contributes to the cornea positive c-wave.

1.11 The Slow Components – The Light-EOG

Two distinct changes in the standing potential have their origins in the RPE's basal membrane conductance. When light-dark cycles are applied at approximately one-minute intervals, there is a fall in the standing potential in light and a rise in the dark intervals. This sequence underlies the FOs of the EOG. When the eye is dark adapted over a 10 – 20 minute interval there is a fall in the standing potential (the dark-trough). When the eye is then illuminated, the standing potential increases slowly and reaches a maximal value at approximately ten minutes following light onset (light-rise). This process underlies the light-EOG.

Griff and Steinberg, (1982), Linsenmeier and Steinberg, (1982), Valeton and van Norren, (1982) used a combination of intra-retinal microelectrodes, combined with reference electrodes sited in the sub-retinal space or retro-ocularly, to prove that the light-rise originated in the RPE. Steinberg noted that the change in the RPE was dependent on stimulus area (Linsenmeier and Steinberg, 1982). The conclusion was that some 'light-rise substance' was generated by light and then diffused from the rods to the RPE: the concentration depended upon the light intensity, and upon whether the substance could diffuse away into the un-illuminated portions of the sub-retinal space. Gallemore *et al.*, (1988) showed that when post photoreceptor signalling was blocked the light-rise was unaffected, thereby demonstrating that the light-rise substance, however it was generated, was released by the rods.

Evidence that the light-rise was mediated by an increase in basolateral Cl^- conductance was shown when four Cl^- channel blockers all abolished the light-rise in chick (Gallemore and Steinberg, 1989). Furthermore, Cl^--sensitive microelectrodes inserted into chick RPE showed a decrease in the intracellular Cl^- activity that matched the light-rise (Gallemore and Steinberg, 1993). Another issue is the role of calcium in regulating the basolateral Cl^- currents that cause

the light-rise. In cat, Hofmann and Niemeyer, (1985) showed the light-rise was reduced by an increase of $[Ca^{2+}]_{out}$ and so Ca^{2+} was presumed to play some role in initiating the light-rise.

In order to quantify the contribution of the apical and basal membranes to the EOG as well as the role of the neural retina in the generation of the light-rise, preparations of intact RPE-retina were mounted in modified Ussing chambers. By introducing a microelectrode into the RPE, it was possible to record V_{Basal} and V_{Apical} differentially by referencing the intracellular electrode to the basal and apical bath electrodes respectively. Griff and Steinberg, (1982), Linsenmeier and Steinberg, (1983) passed current pulses between apical and basal electrodes while monitoring the membrane voltage changes caused across each membrane (ΔV_{Apical} and ΔV_{Basal}). Some of the injected current passes via the paracellular pathway in parallel to the membranes and so the absolute values of the resistance of apical (R_{Apical}) and basal (R_{Basal}) membranes could not be determined. Instead, the ratio of the resistances (the *a*-value) was obtained (equation 1.v).

$$a = \Delta V_{Apical} / \Delta V_{Basal} = R_{Apical} / R_{Basal} \qquad \text{— 1.v}$$

When the *a*-value was analysed with the changes in total tissue resistance then it was possible to determine at which membrane the greatest change in resistance occurred. In lizard (Griff and Steinberg, 1982), cat (Linsenmeier and Steinberg, 1982) and chick (Gallemore *et al.*, 1988; Gallemore and Steinberg, 1989, 1991), V_{Basal} depolarised in response to light with a rise in the *a-value* and a fall in the total tissue resistance. This demonstrated that the change in the standing potential was due to V_{Basal} depolarising at a faster rate than V_{Apical} and that the conductance was greater across the basal membrane as the *a*-value increased.

1.12 Mechanism of the Light-Rise

The basic model of the light-rise is that light releases a substance from the rods that leads to a change in the basolateral membrane chloride conductance. What this substance is, where it may/or may not bind to, and ultimately what second messengers are involved and the nature of the basolateral chloride channel responsible are now beginning to be understood.

The clinical evidence has implicated bestrophin in the generation of the light-rise given that in Best's disease the light-rise is reduced (Cross and Bard, 1974; Barricks, 1977; Weleber, 1989; Pinckers *et al.*, 1996). Marmorstein *et al.*, (2006) have recently proposed a new model for the role of bestrophin based upon two findings in mouse RPE that lack functional bestrophin. Firstly, bestrophin was shown to decrease $[Ca^{2+}]_{in}$ following elevation with ATP from the ER stores. This may have been the result of bestrophin either inhibiting the release or increasing re-uptake of Ca^{2+} by the ER. Alternatively bestrophin could have been acting to inhibit the entry of Ca^{2+} through the L-type Ca^{2+} channel. Secondly the whole cell RPE chloride currents were no different between bestrophin deficient and control mice. This suggested that bestrophin was not the chloride channel responsible for the light-rise but was a modulator of $[Ca^{2+}]_{in}$.

An alternative model places CFTR at the centre for the generation of the light-rise. CFTR is an active transporter of many substrates and ATP is believed to be one of them. CFTR is present at the apical membrane of the RPE. Therefore, in this proposed model, CFTR transports ATP from the RPE into the sub-retinal space. At the apical membrane of the RPE there are purinergic receptors (P_2Y_2) (Sullivan *et al.*, 1997) for ATP and its hydrolysed product adenosine-diphosphate (ADP). Stimulation of the purinergic receptor results in an elevation of $[Ca^{2+}]_{in}$ and this could provide the signal for the light-EOG (Reigada *et al.*, 2005; Reigada and Mitchell, 2005). In conflict with this hypothesis are two abstracts that report that the light-rise is normal in CF which would suggest that CFTR is not directly responsible for the light-rise (Miller *et al.*, 1992; Lara *et al.*, 2003).

1.12.1 The Elusive Light-Rise Substance

The identity of the light-rise substance and receptor has continued to elude all efforts at discovery. The apical membrane of the RPE has various receptors that could conceivably mediate the light-rise. Dopamine was considered a possible candidate for the light-rise substance because dopamine levels increase in the sub-retinal space following light onset (Kramer, 1971). Furthermore, the light-rise was reduced in depressives but elevated in manic depressives (Economou and Stefanis, 1979) suggesting a possible interaction between dopamine levels and the light-rise. However, *in-vitro* studies have been unable conclusively to demonstrate that dopamine is the light-rise substance (Dawis and Niemeyer, 1986; Textorius *et al.*, 1989; Gallemore and Steinberg, 1990; Rudolf and Wioland, 1990)

Evidence for the presence of functional adrenergic, muscarinic, neuropeptidic and purinergic receptors have been identified at the apical membrane of the RPE in a variety of species (Frambach *et al.*, 1990; Crook *et al.*, 1992; Peterson and Miller, 1995; Ammar *et al.*, 1998; Mitchell, 2001; Quinn *et al.*, 2001; Rymer *et al.*, 2001; Collison *et al.*, 2005). However, no ligand for these receptors has been shown to be the light-rise substance. However, ATP is now regarded as a possible candidate (Marmorstein *et al.*, 2006).

1.13 The Fast Oscillation

The FO has received less attention than the light-EOG and is not routinely performed in a clinical setting. However, the FOs have a different origin from the light-rise and are affected differently in diseases of the eye. The main differences are in Best's and RP where the FOs are normal in Best's with an abnormal light-rise and in RP the FOs are affected before the loss of the light-rise associated with the advanced stages of the degeneration (Weleber, 1989; Vaegan and Beaumont, 1996, 2005). Figure 1.8 shows the FOs remaining normal in the absence of a light-rise in Best's disease.

Figure 1.8 EOG and FOs in Best's Disease

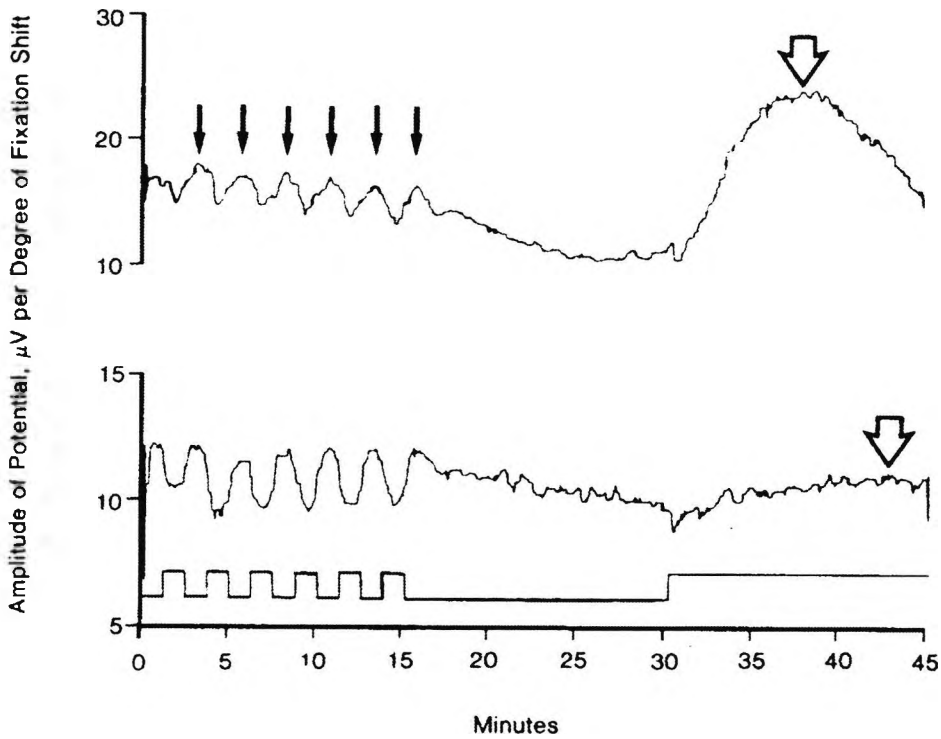

The light-EOG and Fast oscillations in Best's disease. Upper trace shows a normal subject and below an individual with Best's disease. The FOs are recorded at the beginning of the trace and are represented by the dark arrows. The FOs are preserved in both cases. However, the light-rise (open arrow) is absent in Best's. The stimulus (light on or off is represented by the square waves below the lower figure. During the FOs the standing potential falls and rises when the light stimulus is off. In contrast the light-EOG falls during prolonged darkness (15-30) then rises and peaks at approximately 10 minutes once the light is returned. From Weleber, (1989).

For the FOs the first step is the photoreceptor-induced decrease in $[K^+]_{out}$ in the sub-retinal space. The activity of the Na-K-2Cl decreases as $[K^+]_{out}$ is reduced (Joseph and Miller, 1991). Because now the inward Na^+, K^+ and Cl^- flux driven by the apical Na-K-2Cl transporter is

reduced, the intracellular chloride concentration decreases (Gallemore and Steinberg, 1993). Consequently, the CFTR transport of chloride across the basal membrane decreases and this causes a hyperpolarisation of V_{Basal} and a fall in the TEP immediately following light onset. This decrease in the TEP is recorded as the light-trough of the FO.

In mice that are homozygous for Δ508 the FOs are reduced but not abolished which suggests that CFTR is not solely responsible for the FO amplitude. Interestingly the same study found that the amplitude of the light-rise was reduced more in Δ508 homozygote mice than the FOs, (which is not the case in man). The authors suggest that these effects reflect the complex interaction of CFTR with other ionic channels (Wu *et al.*, 2006).

The current model proposes that the light-rise is dependent upon a Ca^{2+}-gated chloride with bestrophin modulating L-type Ca^{2+} currents and possibly reuptake of Ca^{2+} by the ER and that the FOs are dependent in part upon CFTR.

Figure 1.9 with caption on the following page and figure following the description shows the ionic currents in the RPE during a change from darkness to light and the generation of the FOs and some of the possible mechanisms for the light-rise.

Caption to Figure 1.9

A: *In the dark, the sub-retinal [K^+] is maintained by the photoreceptor dark current. The high extracellular apical Na^+ concentration is used to cotransport K^+ and Cl^- ions against their concentration gradients into the RPE. K^+ is recycled at the apical membrane through the voltage gated K^+ channel.*

B: *Representation of the changes in the TEP during the light-trough of the FOs. Immediately following light onset the dark current is reduced and the sub-retinal [K^+] falls. K^+ now moves down its electrochemical gradient through apical voltage-gated K^+ channels into the sub-retinal space so that V_{Apical} hyperpolarises and contributes to the c-wave. However, the reduction in sub-retinal K^+ also slows the transport of Na^+ and Cl^- by the apical Na-K-2Cl cotransporter. Consequently, intracellular [Cl^-] decreases which results in a fall in basolateral Cl^- transport by the cystic fibrosis transmembrane conductance regulator (CFTR). Now the basal membrane hyperpolarises and there is a fall in the TEP. This is seen as the light-trough of the FO.*

C: *The putative light-rise receptor LRR is situated on the apical membrane. In one model, the LRR is purinergic and CFTR activates this receptor through transport of ATP. However, the actual agonist is still to be determined although ATP is suspected. Activation of either LRR or the P_2Y_2 receptor initiates the rise in $[Ca^{2+}]_{in}$ and this is presumed to be the second messenger involved in the light-rise. The source of Ca^{2+} may derive from the endoplasmic reticulum via the generation of inositol triphosphate (IP_3) that binds to the IP_3-R. The increase in $[Ca^{2+}]_{in}$ opens the CaCC and this is the most likely source of the Cl^- current that generates the basolateral depolarisation that results in the light-rise. The exact role that bestrophin plays in the light-rise is still under investigation. However, recent findings have shown that bestrophin can increase the rate of Ca^{2+} entry through the L-type Ca^{2+} channel and also reduces $[Ca^{2+}]_{in}$ following ATP mediated store release but the mechanism is unknown.*

Figure 1.9 Possible Ionic Mechanisms that Alter the EOG Voltage

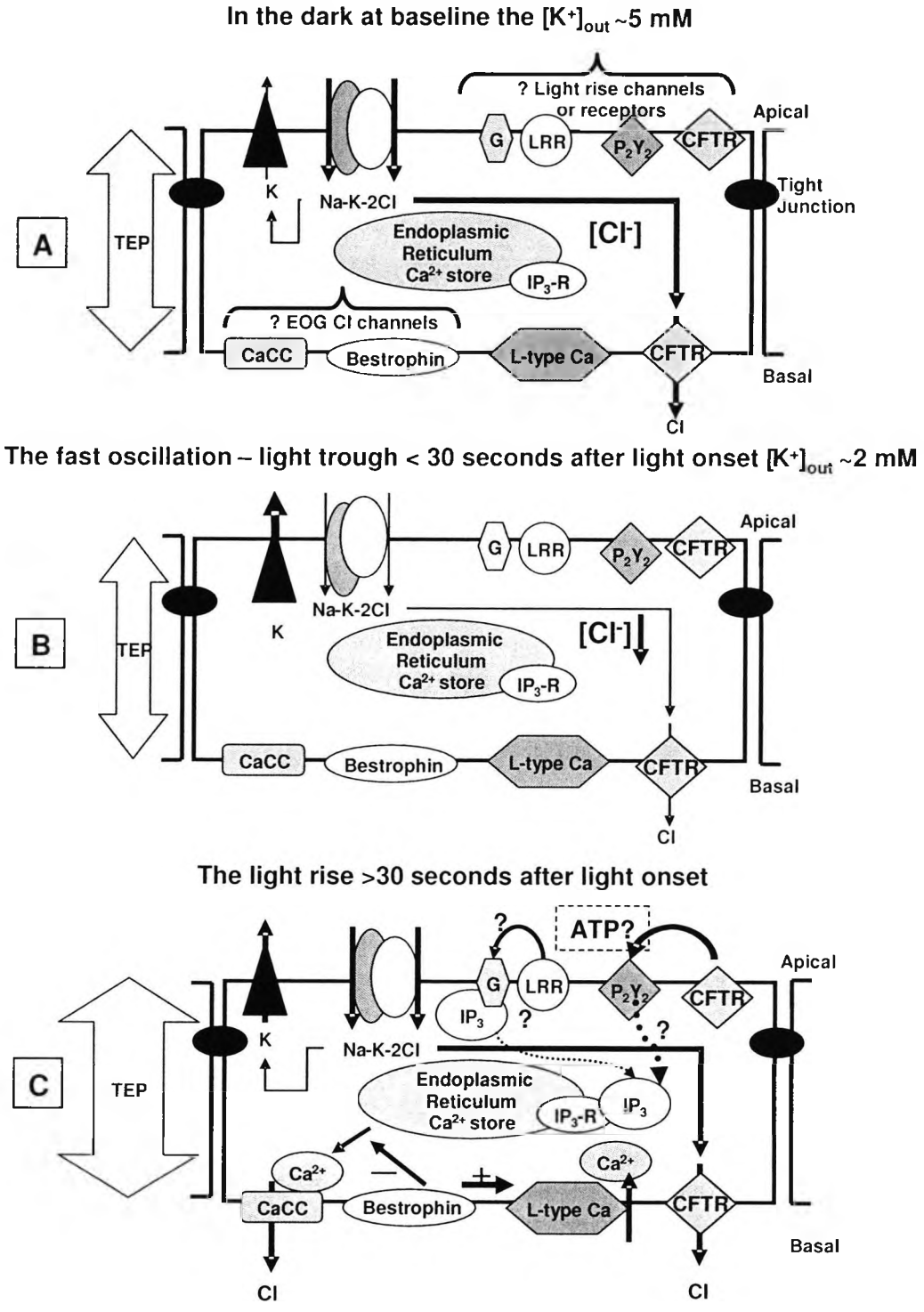

1.13.1 Non-Photic EOGs

The lack of specificity with the light-EOG in its inability to differentiate between photoreceptor or RPE defects has led to the search for other non-photic stimuli that could be used as an alternative means of investigating the RPE directly. The light-rise is decreased by hypoxia and increasing blood pH (hypercapnia) in cat (Linsenmeier *et al.*, 1983). In man, the decrease in the standing potential in response to hypoxia is also seen (Marmor *et al.*, 1985). Intra-venous infusion of a 7% solution of $NaHCO_3$ decreases the standing potential and this response is reduced in diseases affecting the RPE such as RP (Segawa, 1987). However, hypoxia or the sodium bicarbonate EOGs have not become practical clinical tools.

An increase in osmolarity also decreases the ocular standing potential (Madachi-Yamamoto *et al.*, 1984). This hyperosmolar response is reduced in diabetic retinopathy (Kawasaki *et al.*, 1984) but not in central serous retinopathy or extramacular drusen (Gupta and Marmor, 1994, 1995). Acetazolamide (Diamox) also reduces the ocular standing potential (Kawasaki *et al.*, 1986) but this finding has not proven to be a sensitive measure of RPE function (Gupta and Marmor, 1994, 1995).

Ideally, a non-photic stimulus that would alter the standing-potential would be safe and easy to administer to a wide range of patients and be able to detect early RPE dysfunction.

1.14 The Alcohol-EOG

Ethanol is a well-known compound that alters human physiology with its interactions with the central nervous system (CNS) well documented. The electrophysiological effects of ethanol on the ERG in human show that the b- and c-waves increase but there is little or no effect on the a-wave (Ikeda, 1963; Skoog, 1974; Skoog *et al.*, 1975). These findings suggest that the ionic channels of the rods are not involved in generating the alcohol-EOG.

The first study to show that ethanol increased the standing potential of the eye was performed by Skoog, (1975). He found that in man following 400 mg/kg of oral ethanol given after dark adaptation, the ocular standing potential increased. Arden and Wolf (2000a, b) identified the potential clinical relevance of the alcohol-EOG. In their initial studies a basic mechanism was proposed for the interaction between light, alcohol and the RPE. In a series of normal subjects, they noted that very small quantities of alcohol were required to generate a change in the standing potential of the eye with 9 mg/kg being sufficient to generate a 30% increase in the standing potential with saturation occurring at 300 mg/kg (Arden and Wolf, 2000b).

They also noted that the change in the standing potential caused by alcohol had exactly the same time-course and oscillations that are present in the light-EOG. The mimicry of the alcohol-EOG to the light-EOG implied that at least a part of the mechanism was the same. To establish a

model they investigated the interaction of light and alcohol on the standing potential in normal subjects. The principal findings were:

1: When the individual responses to a low oral dose of ethanol and a low dose of light were summed, the resulting EOG was exactly equal to the response when the same low doses of these agents were taken together. That is, low alcohol alone (A) + low light alone (L) = low alcohol and low light together (L+A). When the levels of L and A were increased to near the levels of maximal responses then there was no summation, indicating that under these conditions the change in the standing potential was saturable and that both light and alcohol shared the same final pathway. (See figure 1.10).

Figure 1.10 EOG Summation of Light and Alcohol

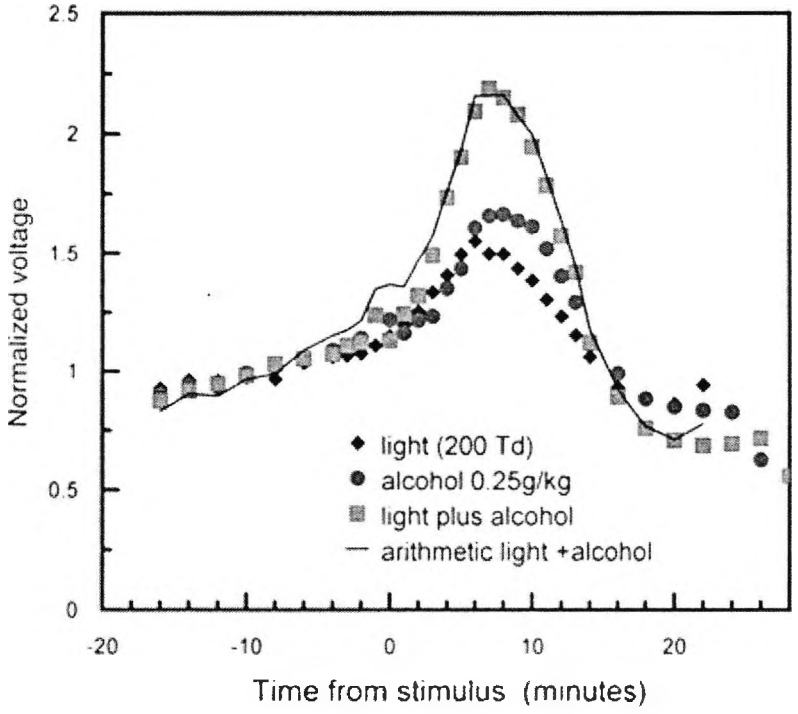

The summation of low levels of alcohol (250 mg/kg) and light (200 Trolands) give the same response amplitude when the two stimulants are taken simultaneously (250 mg/kg alcohol + 200 Trolands of light). This finding suggests that both light and alcohol share the same final saturable pathway. From Arden and Wolf (2000b).

2: When light (or alcohol) was given over a background of either light or alcohol then the interactions were different. Low levels of light or alcohol, when used as a background, reduced the rise in the standing potential when further light or alcohol was given respectively. That is a background of light reduces the light response and a background of alcohol reduced the alcohol response. However, when light was given over a background of low alcohol or alcohol was given over a background of low light then there was no reduction in the response. This implied that light and alcohol did not share the same initial receptor and were agonists for different receptors. See figure 1.11 overleaf.

Figure 1.11 Effects of a Background of Light or Alcohol

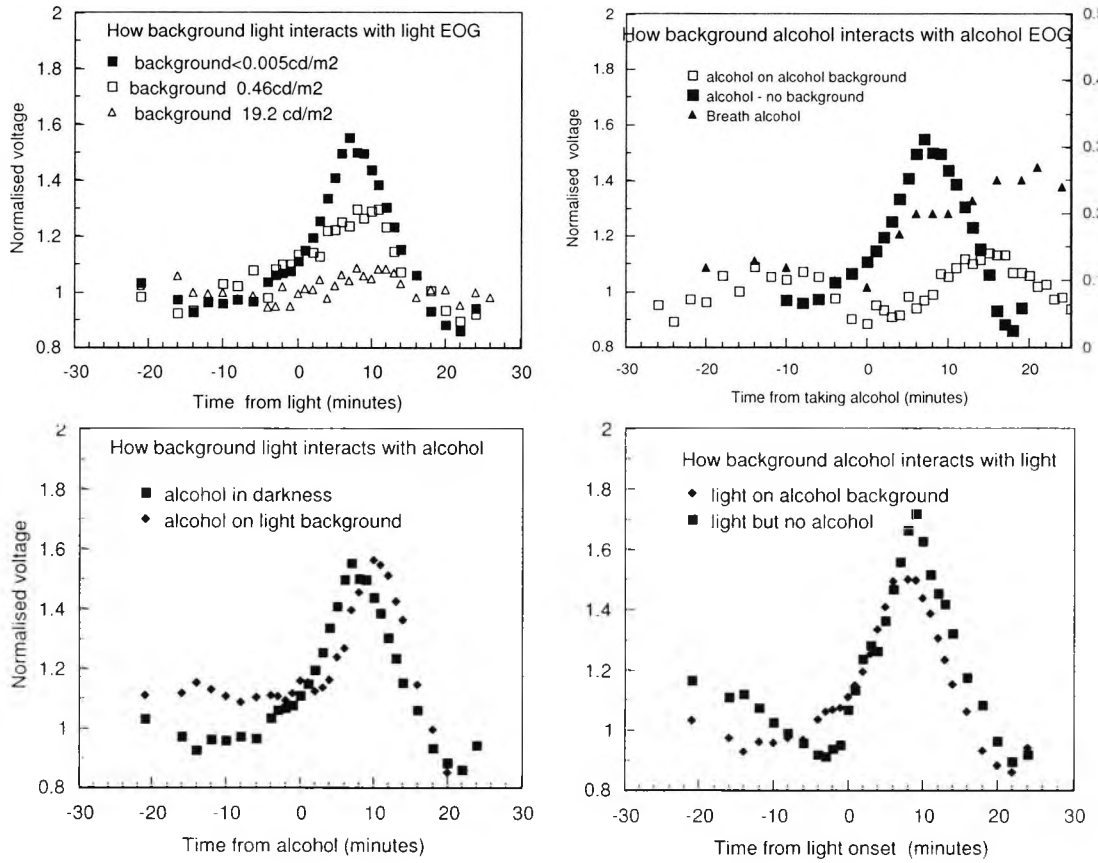

The upper two figures show that a background of either light or alcohol reduces subsequent stimulation with either light or alcohol respectively. In this case, the receptor for light and alcohol are semi-saturated and so subsequent stimulation by the same ligand does not result in a full response. In contrast, when either light or alcohol is present as a background (lower two figures) then there is no interference when alcohol or light is given respectively. This finding suggests that the ethanol and light receptor are different. From, Arden and Constable (2006).

A representation of the model produced by Arden and Wolf (2000 a, b) is shown in figure 1.12 overleaf. The alcohol-EOG is believed to result from ethanol altering the same basolateral chloride conductance that generates the light-rise. The way in which this occurs is unknown but based upon the model the two receptors for light and alcohol are different. It is important to determine the mechanism by which ethanol acts as the alcohol-EOG provides an electrophysiological means of assessing one aspect of RPE function that is independent of any photoreceptor contribution. This is because the alcohol-EOG does not require light and therefore would be a specific test for the RPE.

Figure 1.12 Possible Alcohol-EOG Mechanism

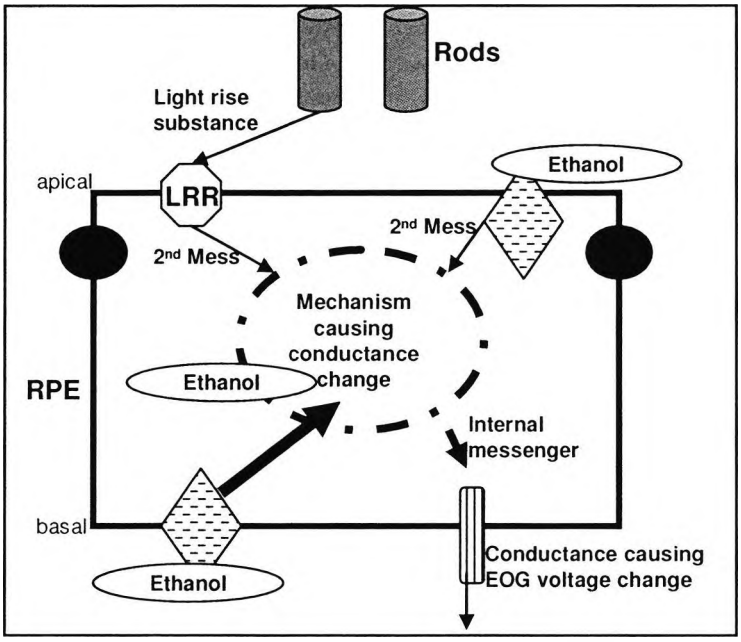

Schematic representation of ethanol's possible interactions with the RPE that could alter the standing potential of the eye as proposed by Arden and Wolf, (2000a, b). Light is believed to release a light-rise substance from the rods that binds to an apical light-rise receptor (LRR). This releases a second messenger that interacts with an intracellular mechanism for generating another messenger that ultimately results in an increase in the basolateral membrane's conductance to Cl^-. Ethanol could act on either an apical or basal membrane receptor or pass through the plasma membrane to act directly on the intracellular generator of the internal messenger. It is important to note that light and ethanol have separate receptors but both converge to increase basolateral Cl^- conductance. Whether they utilise the same internal messenger system is unknown.

1.14.1 The Alcohol-EOG and Retinal Degeneration

The significance of the ethanol induced response on the standing potential of the eye was investigated in a series of patients with RP and compared to the standard light-EOG (Arden and Wolf, 2000a; Arden *et al.*, 2000). In this series of patients, the alcohol-rise of the EOG was reduced more than the small light-rises observed (see figure 1.13 overleaf). This demonstrated that the alcohol-EOG was revealing a different and perhaps more sensitive measure of RPE function than light's interaction with the rods (Arden and Wolf, 2000a; Arden *et al.*, 2000).

Figure 1.13 Alcohol- and Light-EOG in RP

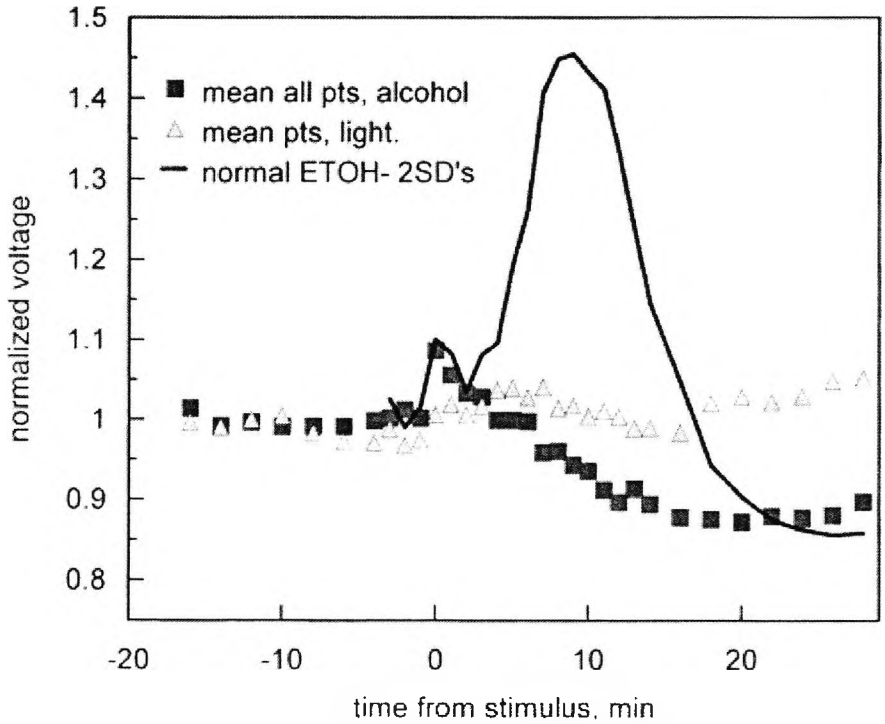

The light-EOG is known to be absent when there is marked retinal degeneration. This is demonstrated in the above figure (△) with an absent light-rise. However, the alcohol-EOG is reduced more than the light-evoked response in RP (■). The solid line shows the normal alcohol-EOG response. From Arden and Wolf (2000a).

A comparison between the light- and alcohol-EOGs in patients with ARMD ranging in severity from mild to severe showed important differences. In this study, Arden and Wolf, (2003) found that the alcohol-rises were also reduced compared to the control group and this reduction was more marked than in the light-rise of the EOG (see figure 1.14 overleaf). These findings may have been attributable to the thickening of Bruch's membrane with age and therefore a limiting the final concentration of ethanol reaching the RPE. Alternatively, it could be that in ARMD and RP the alcohol-EOG is revealing an underlying change in the RPE that is not detected as early with the light-EOG (Arden and Wolf, 2003).

Figure 1.14 Alcohol-EOG in ARMD

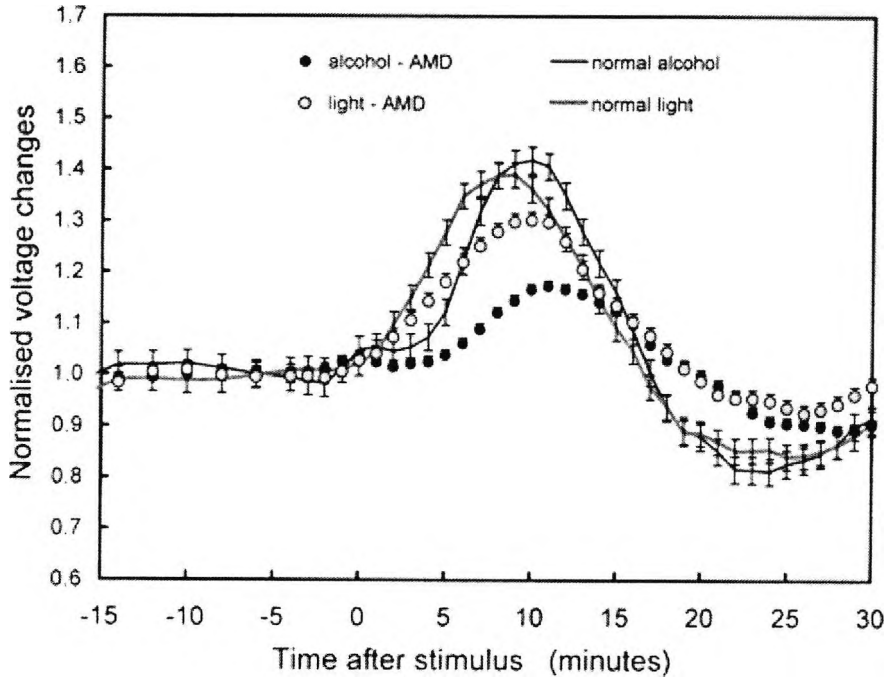

The above figure compares the light-EOG to the alcohol-EOG in a series of patients with ARMD. The alcohol-EOG (●) is affected more than the light-EOG (○) in these patients although both are reduced when compared to the age matched controls. From Arden and Wolf (2003).

The significance of these findings in man is that the alcohol-EOG is identifying a defective RPE pathway that is altered in some way that differs for the light-evoked response. Consequently, an abnormality on the alcohol-EOG would suggest that there is an underlying RPE defect. Thus the pathway or mechanism by which ethanol alters the standing potential of the eye is of interest.

1.15 Animal Investigations into the Alcohol-EOG

One study showed that ethanol applied to the apical surface of bovine RPE increased the TEP and the *a-value* indicating that ethanol was increasing the basolateral membrane conductance (Bialek *et al.*, 1996). This finding would fit with the clinical picture of the alcohol-EOG; in that ethanol acts directly upon an RPE receptor to increase the basolateral Cl^- conductance.

Pautler, (1994), performed more extensive experiments to determine the mechanism of the alcohol-rise in bovine RPE. This study also showed that ethanol increased the TEP when applied to the apical and basal baths of bovine RPE tissue mounted in an Ussing chamber. However, the unexpected finding was that ethanol did not produce the change in TEP if the tissue was dark-adapted and that the response was maximal in green light. The author concluded that ethanol may be acting on a primitive G-protein-coupled 'green light' photopigment that released AA as the second messenger (Pautler, 1994).

The effects of ethanol on the standing potential of the dark-adapted sheep and albino rabbits are similar to those found in man (Knave *et al.*, 1974; Textorius *et al.*, 1985).

1.15.1 Possible Ethanol Receptor(s)

Ethanol has been studied principally concerning its anaesthetic effects and the consequences of chronic ethanol consumption. With relation to the eye, excess alcohol during pregnancy also causes reductions in the rat ERG of the offspring (Katz and Fox, 1991). The most likely sites for the action of ethanol on the RPE would be either a G-protein-coupled receptor or the L-type Ca^{2+} channel.

Modulation of the adrenergic receptors by ethanol and the G-protein-coupled signalling pathways are typically associated with chronic ethanol exposure that results in an up- and down-regulation of proteins (Mochly-Rosen *et al.*, 1988; Gordon *et al.*, 1990; Simonsson *et al.*, 1991; Miles *et al.*, 1993; Pandey, 1996). At high doses > 50 mM adenylate cyclase's catalytic activity is increased (Saito *et al.*, 1985). β-adrenergic receptors are also a site of action with competitive inhibition between ethanol and isoprotenerol demonstrated (Valverius *et al.*, 1987; Bode and Molinoff, 1988). Elevation of cAMP in hepatocytes occurs after chronic ethanol exposure whilst acute exposure decreases cAMP levels (Diehl *et al.*, 1992; Nagy and DeSilva, 1992).

In the limited studies where ethanol has been employed at a physiological level and following acute exposure there is evidence to show that in the nervous system, ethanol (0.001%) potentiates PKC signalling via G proteins in the hippocampus (Lahnsteiner and Hermann, 1995). In the pancreas, low doses of ethanol (0.3 – 30 mM) also increase fluid secretion in the pancreas by mobilising intracellular Ca^{2+} and cAMP (Yamamoto *et al.*, 2003). Arden and Wolf predict that the actual concentration of ethanol to elicit the alcohol-EOG is sub-millimolar and thus represents a novel action of ethanol at low concentrations (Wolf and Arden, 2004).

Ethanol is known to modulate Ca^{2+} currents of the L-type Ca^{2+} channels in a variety of cells, and it either increases or decreases these current depending upon the cell type and the concentration. In rat pinealocytes ethanol (100 mM) inhibits the L-type Ca^{2+} current by 40% (Chik *et al.*, 1992). However at 'low' doses < 120 mM ethanol increases L-type Ca^{2+} currents and inhibits them at concentrations > 120 mM in a neuronal cell line (Belia *et al.*, 1995).

1.16 Summary

The light-EOG is a useful clinical tool for assessing the integrity of the RPE-photoreceptor complex. However, its lack of specificity for either the RPE or photoreceptors has led to a search for non-photic mediators that can alter the ocular standing potential by interacting with the RPE. Alcohol, promises to be one such substance which mimics the light-evoked responses of the eye and is reduced in to a greater extent than the light-EOG in retinal degenerations. The aim of this study is to determine how ethanol interacts with the eye in order to generate the alcohol-EOG.

2 *In vitro* Modelling of the RPE

2.1 Introduction

In order to investigate the underlying mechanism of the alcohol-EOG it was desirable to establish a suitable *in vitro* model of the RPE. One approach was to use cell lines derived from human RPE that either have an inherent ability to undergo indefinite mitosis or to use cell lines that have been transfected with a viral vector that confers immortality. Two RPE cell lines were used in this study, ARPE-19 (Dunn *et al.*, 1996) and D407 (Davis *et al.*, 1995) that are both derived from adult human donors. ARPE-19 has been the most extensively utilised to study human RPE *in vitro*. Of interest was whether through the manipulation of the culture conditions the TER of ARPE-19 could be maintained at a level that would make it possible to use this cell line in the investigation of the alcohol-EOG.

In the developing RPE, secreted retinal factors influence the formation of tight junctions (Rizzolo and Li, 1993; Ban and Rizzolo, 1997, 2000a; Ban *et al.*, 2000). The development of tight junctions in the RPE has been most extensively studied in embryonic chick RPE cells by Rizzolo. His group has determined that that culture conditions, the age of the RPE and the neural retina (from where the secreted factors were isolated) all determine the final TER and paracellular permeability of the monolayer.

These secreted factors differ over time with the more mature embryonic day-14 (E14) retinal factors increasing the TER of chick RPE cells to a greater extent than E7 conditioned retinal medium (Rizzolo and Li, 1993). Further investigation of the source of these factors identified in E7 retina a small < 10 kDa protease resistant growth factor as one component. In E14 retina this small factor was absent but a larger and more potent protease sensitive protein was present with a mass of 49 kDa (Ban and Rizzolo, 2000b). The factors derive from the neural retina although it is not known from which cell type or types they originate. However, the slow changes in the TER over time implied that the factors were altering gene expression in the RPE cells. The addition of fibroblast conditioned medium to the basal compartment with retinal conditioned medium in the apical chamber increased the TER in E14 chick RPE to ~ 230 $\Omega.cm^2$ (Rahner *et al.*, 2004).

The dependence on tight junction formation and secreted retinal factors suggested that the RPE cell lines may also be sensitive to similar factors. Given the anatomical location of the RPE, the most likely source of these factors would be the photoreceptors or bipolar cells (neural retinal factors) or from the Müller cells (glial cells). A less likely but possible source would be from the astrocytes that are found in the inner retina where they contribute to the formation of and maintenance of the inner blood retinal barrier (Gardner *et al.*, 1997; Zhang and Stone, 1997).

In this section, different methods were used to try and enhance the barrier properties of ARPE-19. One was to modify both the cell culture substrate, and to use a defined cell culture medium that replicated some of the likely factors that the RPE would encounter *in situ*. Furthermore, ARPE-19 were grown in co-culture with glial cells whose secreted factors may simulate those of the retinal factors identified as being important in tight junction formation.

2.2 Epithelial Cell Lines

Cell lines are derived from sub-cultures of native cells and provide a means of modelling the behaviour of the parent cell. However, the process of sub-culturing over generations decreases the similarity between the parent and daughter cells. One reason for this de-differentiation may be the lack of particular factors that are present *in situ.* Consequently, cell lines, though providing a useful model, do not exactly replicate the parent cell. Micro-array studies comparing the genetic profile of ARPE-19 cells to primary cultured human and native macula RPE cells (from three elderly donors) display variation. However, the micro-array used in these studies was not specific for RPE gene expression but consisted of an array of genomic human DNA. The gene profile between ARPE-19 and native human RPE cells was closest when the ARPE-19 cells were grown on laminin, collagen IV or fibronectin (Tian *et al.*, 2004).

Foetal human RPE has been shown to retain its phenotype when grown in specialised medium (Hu and Bok, 2001). The RPE with age becomes senescent and difficult to culture without losing the RPE's phenotype. Cultured human RPE cells typically lose their pigmentation and the expression of ionic channels differs to that of native RPE (Ueda and Steinberg, 1995). Cultures of adult donor RPE were attempted but the rate of growth was slow and often the sub-culture was contaminated with non-epithelial cells that quickly overtook the culture. Furthermore, the post mortem delay for adult RPE was at best 28 hours but typically 72-96 hours which compromised the cell's integrity.

2.2.1 ARPE-19

ARPE-19 cells are a spontaneously arising cell line derived from a 19-year-old male donor. The cells were isolated by selective trypsinisation to produce a sub-culture that best resembled the cobblestone morphology of native RPE (Dunn *et al.*, 1996). The mRNA for two specific RPE proteins: cellular retinaldehyde binding protein (CRALBP) and RPE65 were identified by Northern blots and the protein identified using Western blots and immunocytochemistry. When this cell line was grown in reduced serum on laminin coated permeable filters at a density of 1.66×10^5 cells/cm^2 the TER obtained was 35 $\Omega.cm^2$. However, the TER was increased to 90 $\Omega.cm^2$ when the cells were grown in a specialised medium (Bok *et al.*, 1992) defined for human RPE. The chromosomes of this cell line showed a deletion of the long arm on chromosome 8 and a small addition to the long arm of chromosome 19 (Dunn *et al.*, 1996).

ARPE-19 cells have been used to model numerous aspects of native RPE physiology and pathophysiology such as ATP transport via CFTR (Reigada and Mitchell, 2005), the cellular mechanism of ARMD (Higgins *et al.*, 2003; Kim *et al.*, 2003; Amin *et al.*, 2004; Martin *et al.*, 2004; Chen *et al.*, 2005; Miceli and Jazwinski, 2005). They have also been used to model the blood-brain and blood-retinal barriers (Abe *et al.*, 2003; Fukuoka *et al.*, 2003; Toimela *et al.*, 2004). ARPE-19 cells have been used to model fluid transport coupled to taurine transport (Bridges *et al.*, 2001b; El-Sherbeny *et al.*, 2004), the phagocytosis of rod outer segments

(Finnemann *et al.*, 1997; Chowers *et al.*, 2004), cell polarity (Dunn *et al.*, 1998) and oxidative stress (Alizadeh *et al.*, 2001; Weigel *et al.*, 2002, 2003 Garg and Chang, 2003; Bailey *et al.*, 2004; Strunnikova *et al.*, 2004). This cell line has also been shown to rescue photoreceptors following sub-retinal transplantation into the Royal College of Surgeons' (RCS) rat model of retinal degeneration where they restored some visual function (Lund *et al.*, 2001; Wang *et al.*, 2005; Sauve *et al.*, 2006).

ARPE-19 cells were supplied by the European Collection of Animal Cell Cultures (ECACC, Salisbury, UK) at passage 20[2]. Figure 2.1 below shows ARPE-19 cells in culture (passage 33). All cell images in this section were acquired on a Nikon TS120 eclipse phase contrast inverted microscope (Nikon, Kingston, UK) with a 10 x objective, numerical aperture (NA) 0.25 equipped with a digital camera, Spot 221 (Diagnostic Instruments Inc, Livingstone, UK). Images were acquired using Spot software version 3.45 (Diagnostic Instruments Inc) and stored on computer hard drive.

Figure 2.1 ARPE-19 Cells in Culture

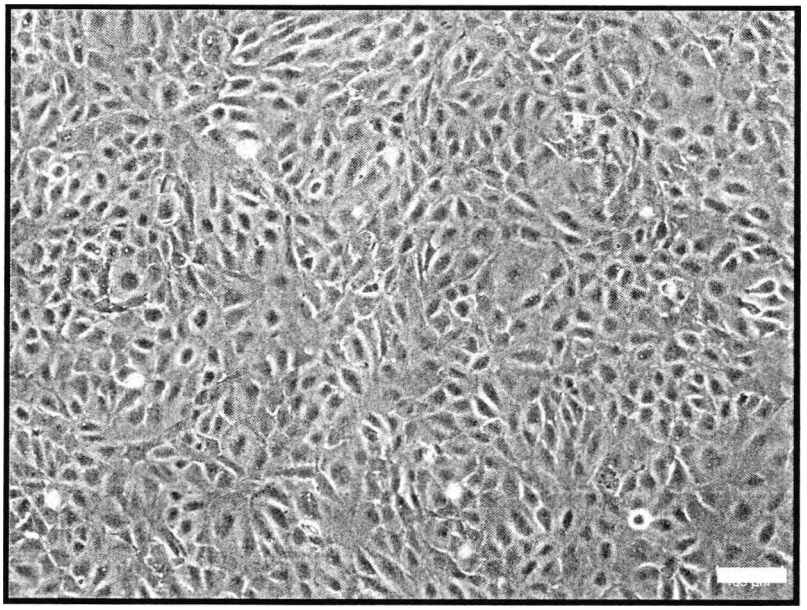

ARPE-19 cells grown under standard culture conditions exhibit an heterologous epithelial morphology. (Scale bar lower right is 100 µm).

2.2.2 D407

D407 is also a spontaneously arising cell line derived from a 12-year-old male donor with the sub-culture established by selective trypsinisation. When originally described, D407 formed tight junctions and some apical microvilli. CRALBP was identified using immunocytochemistry and the D407 cell line retained the ability to phagocytose rod outer segments. The karyotype was normal

[2] Passage number: The passage number is an indication of the number of times the cell has undergone mitosis.

with early passage numbers having 44 ± 2 chromosomes. With increased passaging of the cells (beyond 52) the number of chromosomes identified was 70 ± 4 (near triploid) (Davis *et al.*, 1995).

D407, has similarly been used to model human RPE behaviour including phagocytosis (Mannerstrom *et al.*, 2001), pathogenesis of ARMD (Zhang *et al.*, 2002) and drug delivery (Pitkanen *et al.*, 2003). D407 has not been as extensively studied as ARPE-19 with respect to its gene profile.

The D407 cells were a generous gift of Prof Richard Hunt, University of South Carolina, CA, USA and were supplied at passage 80. Figure 2.2 shows D407 cells in culture at passage 88.

Figure 2.2 D407 Cells in Culture

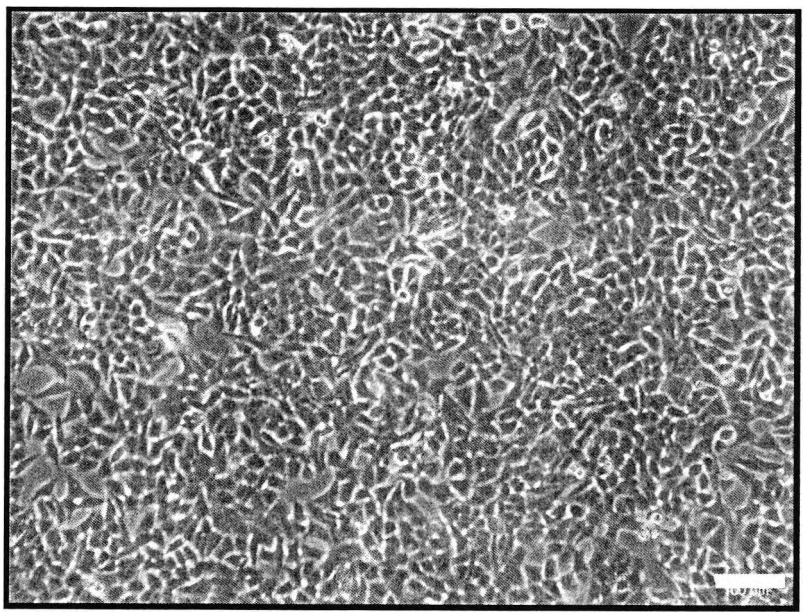

D407 cells exhibit an epithelial morphology when grown in culture. (Scale bar lower right is 100 μm).

2.2.3 ECV304

ECV304 was originally isolated from human umbilical vein and proposed as a potential model for human endothelial cells (Takahashi *et al.*, 1990). However, it was subsequently shown that ECV304 had been incorrectly deposited and was actually the T24 cell line that was derived from human bladder carcinoma cells (Dirks *et al.*, 1999; Brown *et al.*, 2000; Tan *et al.*, 2001; Drexler. *et al.*, 2002). ECV304 was used as a positive control to compare the level of induction in ARPE-19 with another epithelial cell whose increased TER have been well established when grown with the C6 astroglial cell line (Hurst *et al.*, 1998). ECV304 has been used to model the formation of tight junctions in the RPE (Penfold *et al.*, 2000; Tretiach *et al.*, 2004).

ECV304 cells were generously provided by Prof Joan Abbott at King's College London at passage 15. Cells were originally sourced from ECACC. Figure 2.3 shows ECV304 in culture.

Figure 2.3 ECV304 Cells in Culture

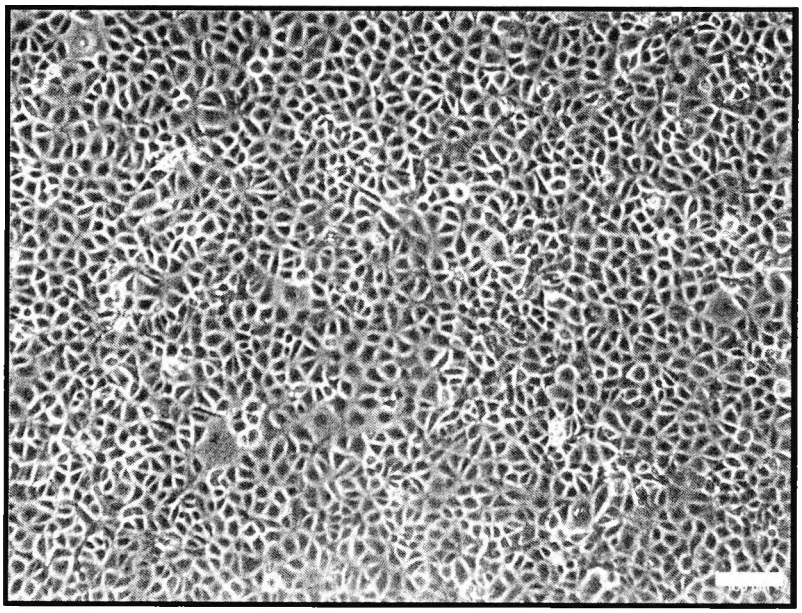

ECV304 cells closely resemble the epithelial cobblestone morphology. (Scale bar lower right is 100 µm).

2.3 Glial Cell Lines: C6 and MIO-M1

The C6 cell line was derived from a rat glial tumour that was induced by the tumourigenic agent N-nitrosomethylurea (Benda *et al.*, 1968). C6 is not of retinal origin but is used to simulate the astrocytes in the blood brain barrier models (Tan *et al.*, 2001). Therefore, C6 cells were used to simulate the astrocytes in the retina as the potential source of secreted retinal factors.

The immortalised human Müller cell line designated MIO-M1 was utilised as a potential source of secreted retinal factors. Factors from the RPE can increase Müller cell proliferation (Jaynes *et al.*, 1995; Jaynes and Turner, 2000). Müller cells can increase the barrier properties of vascular endothelial cells (Tretiach *et al.*, 2005). However, whether there is a potential for Müller cell derived factors to up-regulate tight junctional proteins in the RPE is unknown.

MIO-M1 were derived from a 68 year-old female donor and isolated by cloning cells that expressed Müller cell markers (Limb *et al.*, 2002). MIO-M1 cells were a generous gift of Dr Astrid Limb from the Institute of Ophthalmology and supplied at passage 65. C6 cells were generously provided by Prof Joan Abbott at King's College London at passage 118 and were sourced originally from ECAAC. See figures 2.4 A –C6 cells and 2.4 B –MIO-M1 cells for these cell lines in culture.

Figure 2.4 C6 and MIO-M1 Cells in Culture

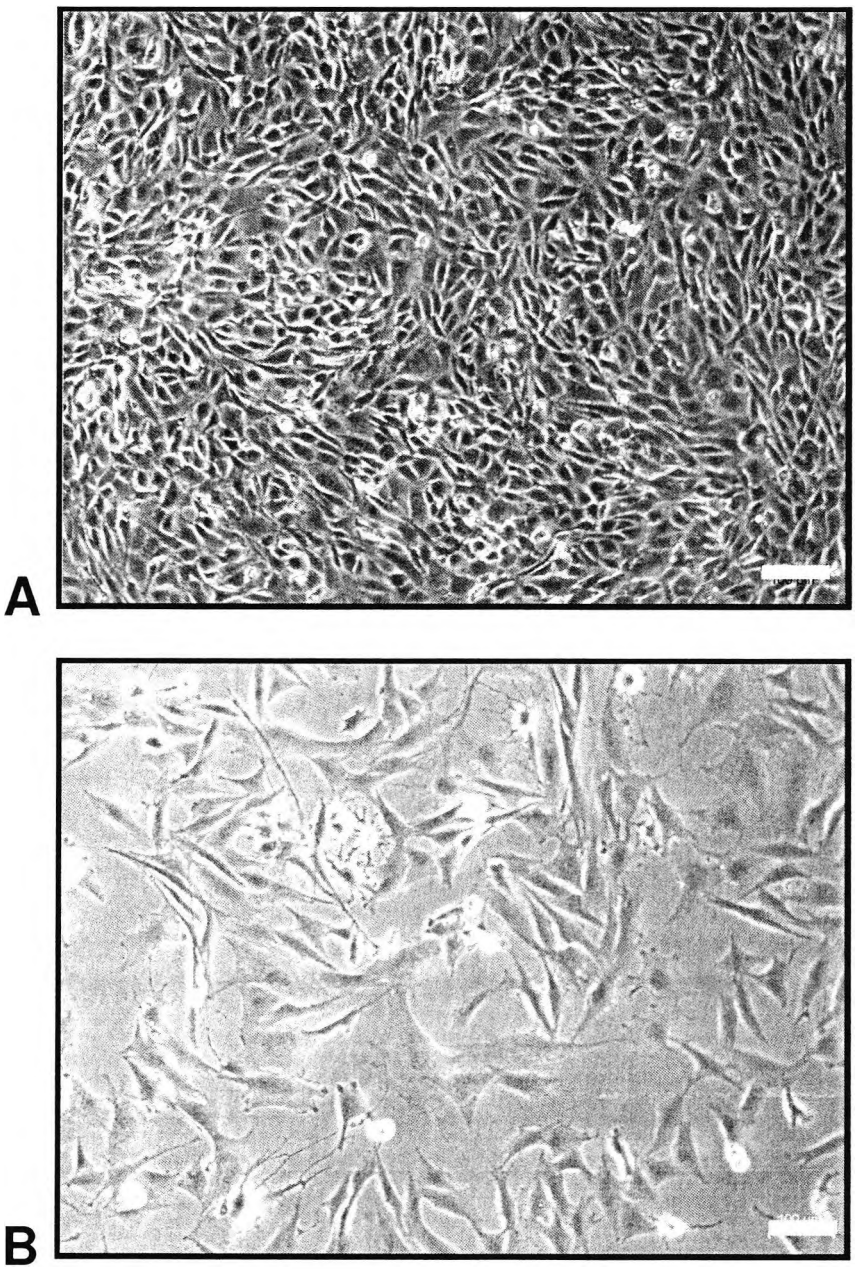

C6 cells are in the upper panel (A) and MIO-M1 cells are on the lower panel (B). Both cell types exhibit a glial-like morphology with extended cell bodies (Scale bars lower right are 100 μm).

2.4 Trans-Epithelial Resistance and Potential

The polarisation of ionic channels in the apical and basal membrane are segregated by the intercellular tight junctions which establishes the TEP and the TER. Table 2.1 below gives reported values of the TEP and TER in primary explants of animal tissue. Table 2.2 (overleaf) gives these values for human RPE in culture and primary explants depending upon age. All animal preparations exhibit a TER of > 100 $\Omega.cm^2$ and human RPE-choroid preparations range from 18 - 480 $\Omega.cm^2$.

The measurements of the TERs are not always comparable across studies with different recording techniques affecting the result. For example, intracellular recordings from a monolayer will give higher values than those obtained in an Ussing chamber. Also the temperature will affect the TER with a low temperature associated with a higher TER such as those taken after allowing the cells to rest outside of the incubator at room temperature before taking a reading (Gonzalez-Mariscal *et al.*, 1984; Luo *et al.*, 2006).

Table 2.1 TEP and TER in Animal RPE

Species	TER ($\Omega.cm^2$)	TEP (mV)	Reference
Bovine	160 - 220	8 - 9	Edelman and Miller, (1991)
Bovine	138 ± 7	6 ± 1	Joseph and Miller, (1991)
Bovine	152 ± 12	5.1 ± 1.1	Miller and Edelman, (1990)
Bovine	100 ± 18	6.0 ± 0.4	Arndt *et al.*, (2001)
Porcine	262 ± 46	3.8 ± 2.5	
Chick[T]	115 ± 5	4.9 ± 0.3	Gallemore *et al.*, (1993)
Chick[Ŧ]	1950 ± 520	5.40 ± 1.20	Kuntz *et al.*, (1994)
Chick	—	8 - 12	Gallemore and Steinberg, (1991)
Bufo	3400 ± 800	23.4 ± 6.4	Griff, (1990)
Rana	134 ± 3	9.9 ± 0.3	la Cour, (1992)
Canine	129 ± 34	4.9 ± 1.7	Quinn and Miller, (1992)
Feline	280 to 420	4.6 to 15.0	

Table of the electrical parameters of the RPE in animal species. The TER is > 100 $\Omega.cm^2$ and the TEPs are > 5 mV. (Ŧ) - denotes trans- tissue resistance (retina-RPE-Bruch's).

Cell cultures derived from human tissue also display variability in the reported TERs and TEPs reported depending upon the age of the RPE and the culture medium. Cultured human RPE are reported to obtain a TER of 70 $\Omega.cm^2$ that can be enhanced by specialised medium. The TEP of adult human RPE is reported to be 0.9 – 3.5 mV and the TER ranges from 36 to 215 $\Omega.cm^2$.

Table 2.2 TEP and TER in Human and Cultured RPE

Human	TER ($\Omega.cm^2$)	TEP (mV)	Reference
Foetal	225 ± 30	1.3 ± 0.2	Hu *et al.*, (1994)
2 years	440 ± 97	6.4 ± 1.5	
21 years	215 ± 38	2.1 ± 0.2	
30 - 69 years	36 — 148	0.9 to 3.5	Quinn and Miller, (1992)
Foetal	18 — 486	0.3 to 4.8	
Adult (Cell Culture)	70 ± 12	0.6 ± 0.2	Hernandez *et al.*, (1995)
Adult (Cell Culture)	444 ± 65	—	Rajasekaran *et al.*, (2003)
Foetal (Cell Culture)	834 ± 31	—	Hu and Bok, (2001)

Table of the electrical parameters of the RPE in human primary explants and cell culture. The TERs are generally > 100 $\Omega.cm^2$ and the TEPs vary from 0.3 to 6.4 mV.

2.4.1 TER in ARPE-19

The majority of studies report a TER of ARPE-19 in the region of 20 – 40 $\Omega.cm^2$ when grown in reduced serum (table 2.3 overleaf). High resistances have been reported when the substrate is altered to porcine lens capsule which induced polarisation and up-regulation of tight junction and basement membrane proteins (Turowski *et al.*, 2004). The report of Bridges *et al.*, (2002) with a TER of 300 $\Omega.cm^2$ is exceptional given the standard conditions in which the cells were cultured. Most recently, the variability in the TERs reported for ARPE-19 seem to derive from the fact that these cells have a mixed phenotype depending upon the culture conditions with only a small percentage of cells retaining completely differentiated epithelial junctional proteins (Luo *et al.*, 2006).

Table 2.3 Published TER for ARPE-19 Cells

TER ($\Omega.cm^2$)	Condition	Author
35	DMEM:F12 1% FBS on laminin	Dunn *et al.*, (1996)
91	Specialised Medium† on laminin	
60 - 80	DMEM:F12 1% and 10% FBS on types I and III collagen	Abe *et al.*, (2003)
30	DMEM:F12 1% FCS uncoated Transwell™	Turowski *et al.*, (2004)
200	DMEM:F12 1% Porcine lens capsule	
40	DMEM:F12 1% FBS on laminin	Geiger *et al.*, (2005)
30	DMEM:F12 1% FCS on Matrigel™	Holtkamp *et al.*, (1998)
300	DMEM:F12 1% FBS on laminin	Bridges *et al.*, (2002)
21 - 28	DMEM:F12 1% FBS on laminin	Luo *et al.*, (2006)
23 - 27	Specialised medium defined for chick	

List or reported TERs for ARPE-19 cells grown on permeable inserts. Most studies report a TER of 30 - 40 $\Omega.cm^2$. (†) = culture medium defined by Bok et al., (1992).

2.5 Co-Culture and Specialised Medium

Co-culturing of cells that exist in close association has been used as a means of replicating the microenvironment *in situ*. Figure 2.5 (overleaf) shows a schematic of the RPE with the potential cells that could secrete factors from the neural retina to induce tight junction formation. Given the extensive use of glial cells to enhance the tight junctions in a variety of epithelial and endothelial cell types (Hurst *et al.*, 1998; Ramsohoye and Fritz, 1998; Chishty *et al.*, 2002) glial cells were employed with the RPE cells in culture. Two cell lines were used to model glial cells in the retina. One was derived from human Müller cells and the other derived from a glioma and replicated the astrocytes in the inner retina. The potential for secreted factors from the outer segments was also possible but this condition was not tested despite the possibility of developing a photoreceptor sub-culture (Saga *et al.*, 1996) given the evidence for glial cell induction of tight junctions.

Figure 2.5 Retinal Factors and the RPE

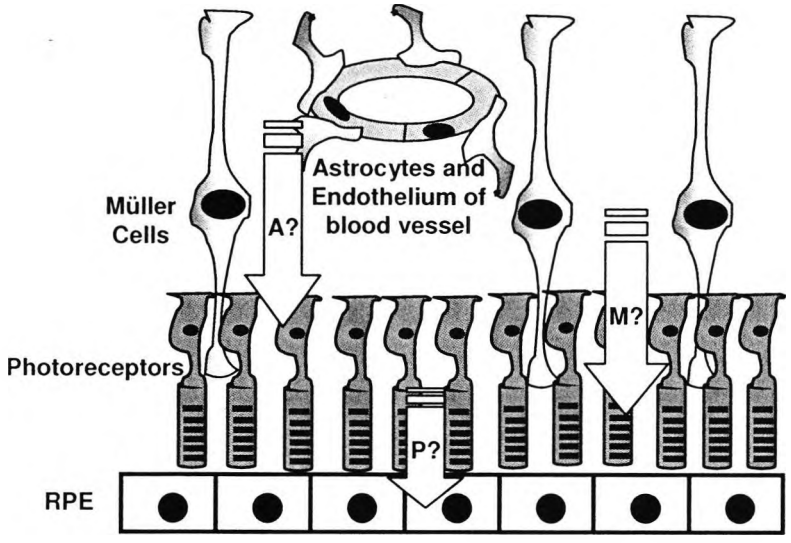

*Schematic representing the possible sources of secreted factors from **1:** astrocytes (A?) in the inner retina. **2:** Müller cells (M?) that extend from the photoreceptors to the inner limiting membrane or **3:** photoreceptors (P?) whose outer segments interdigitate with the apical microvilli of the RPE.*

Glial cell lines when grown in co-culture with epithelial cell lines have been shown to increase the TER. Notably, the co-culture of astroglial cells (C6) with an epithelial cell line (ECV304) induces a high TER (Hurst and Fritz, 1996; Dobbie *et al.*, 1999; Chishty *et al.*, 2002). Conditioned medium from C6 also increases the TER in Madin-Darby Canine Kidney (MDCK) cells (Veronesi, 1996) and endothelial cells (Tontsch and Bauer, 1991; Raub, 1996; Ramsohoye and Fritz, 1998). In the brain, astrocytes serve a similar function to the Müller cells of the retina by spatial buffering of K^+ in the brain (Butt and Kalsi, 2006). Astrocytes also play a role in up-regulating the tight junctions of endothelial cells (Igarashi *et al.*, 1999; Gaillard *et al.*, 2001).

In the co-culture model involving C6 and ECV304 (Hurst and Fritz, 1996; Hurst *et al.*, 1998) the secreted factors from C6 cells are not believed to be proteins but have a mass of < 1000 kDa (Ramsohoye and Fritz, 1998). The factors act by up-regulating intercellular adhesion molecules (Dobbie *et al.*, 1999). The reported TERs of this co-culture model vary between authors with ECV304 cells grown without C6 induction obtaining a TER of 27 - 37 $\Omega.cm^2$. However, in co-culture with C6 the TER is increased to between 80 and 600 $\Omega.cm^2$ (Hurst *et al.*, 1998; Ramsohoye and Fritz, 1998; Dobbie *et al.*, 1999).

Müller cells are also important to the development and maintenance of the inner blood-retinal barrier that is defined by the retinal vascular endothelium (Tretiach *et al.*, 2005). Therefore, in addition to C6 cells we used a human Müller cell line to determine whether secreted factors from this cell line would increase the TER of the RPE cell lines.

The first aim of this study was to determine whether secreted factors from glial cells using MIO-M1 to replicate the Müller cells of the retina or C6 cells to replicate the astrocytes of the inner blood retinal barrier could induce an increase in the TER of the human RPE cell lines.

The second aim was to modfy the culture medium by adding specific cytokines and hormones that have been shown to maintain the RPE phenotype in culture. Several formulations have been used to enhance the differentiation and tight junction formation of RPE cells derived for cell lines, human and chick (Oka *et al.*, 1984; Frambach *et al.*, 1990; Rizzolo and Li, 1993; Rizzolo *et al.*, 1994; Tezel and Del Priore, 1998; Hu and Bok, 2001; Rahner *et al.*, 2004). All of the defined media in one way or another attempt to nurture the RPE in a culture environment that closely resembles that of the *in situ* milieu. Such additions promote the differentiation of the RPE cells by replicating to some extent the likely factors that the RPE would experience *in situ*. Preparations of specialised media (SM) used in this study (SM1, SM2 and SM3) are detailed in Appendix I.

2.5.1 Cytokines, Growth Factors, Supplements and Hormones

The stimuli that maintain the RPE phenotype derive from the close cell-cell interactions of the RPE with itself and the outer retina as well as the circulating hormones and factors that reach the basal membrane of the RPE via the choroid. The maintenance of phenotype is therefore reliant upon mimicking this environment as closely as possible. Several key constituents of these factors and hormones have been identified and form the basis of the specialised media used in this study.

Growth factors or cytokines are extracellular proteins that are mainly involved in stimulating mitosis and are said to be mitogenic. The receptors for growth factors belong to the tyrosine kinase family and are cell surface receptors. Once activated by the growth factor the intracellular kinase domain phosphorlyates intracellular proteins which may alter intracellular signalling pathways or alter gene transcription. For review see Mukherjee *et al.*, (2006).

2.5.1.1 Epidermal Growth Factor

EGF stimulates epithelial growth (Cohen, 1965) and was the first protein to be recognised as a ligand for cell surface tyrosine-specific protein kinases (Waterfield *et al.*, 1982). EGF receptors are found on the RPE (Kociok *et al.*, 1998) and the addition of EGF promotes cell survival via intracellular signalling pathways (Defoe and Grindstaff, 2004). The rate of RPE proliferation is higher with bFGF rather than EGF (Song and Lui, 1990).

2.5.1.2 Fibroblast Growth Factor

There are two analogues of FGFs, the brain-derived acidic form (aFGF) and pituitary basic form (bFGF) (Esch *et al.*, 1985). bFGF receptors are expressed in the RPE (Sternfeld *et al.*, 1989) and in particular the nucleus and cytoplasm (Ishigooka *et al.*, 1992) where bFGF modulates gene

expression and increases proliferation. However, this effect has not been observed in one RPE cell line, D407 (Schwegler *et al.*, 1997; Kaven *et al.*, 2000). Bovine pituitary extract (BPE) is a rich source of bFGF and hormones (Esch *et al.*, 1985) and has been used in RPE culture media (Peng *et al.*, 2003).

2.5.1.3 Insulin

The interaction between insulin and the insulin-like growth factor receptor (IGF)-1 signalling mechanisms are central to cellular metabolism, growth, development, reproduction and longevity (Kimura *et al.*, 1997). Insulin binds to IGF-1, a receptor tyrosine kinase, which once activated leads to the phosphorylation of insulin receptor substrates 1, 2 and Shc (Withers and White, 2000). Insulin is a more potent mitogen in epithelia than fibroblasts (Hollenberg and Cuatrecasas, 1975; Reddan and Wilson-Dziedzic, 1983). The insulin-like growth factor receptor (IGF-R) is found on the RPE (Ocrant *et al.*, 1989) where it is required to maintain retinyl esterase activity (Edwards *et al.*, 1991). However, insulin and IGFs also increases vascular endothelial growth factor (VEGF) production in the RPE and may therefore act to decrease the TER (Punglia *et al.*, 1997; Lu *et al.*, 1999; Treins *et al.*, 2001, 2002).

2.5.1.4 Additional Hormones and Supplements

Ferric (Fe^{3+}) ions are required for cellular metabolism and transferrin transports these ions across the plasma membrane. Transferrin is produced by the RPE and transferrin receptors are also present indicating a role for the RPE in iron transport between the outer retina and choroid (Yefimova *et al.*, 2000).

Sodium selenite is a trace element normally provided in serum and was added to media where serum was omitted. Hydrocortisone, (cortisol) is produced by the adrenal cortex and therefore would be present in the systemic circulation. Hydrocortisone increases epithelial cell proliferation (Andersen *et al.*, 1993) and decreases the production of inflammatory cytokines in the RPE (Chiba *et al.*, 1993).

Putrescine is a polyamide that increases cell migration (motogenesis) in the RPE and the maintenance of the actin cytoskeleton (Yanagihara *et al.*, 1996; Johnson *et al.*, 2002).

Linoleic acid is an essential fatty acid that is present in the plasma membrane. The oxidised product of linoleic acid is cytotoxic and may contribute to RPE damage *in-situ* (Akeo *et al.*, 1999). Oleic acid is a fatty acid also present in the RPE plasma membrane (Wang and Anderson, 1993).

2.5.1.5 All Trans-Retinoic Acid

All *trans*-retinoic acid is essential for the formation of visual pigments (Hubbard and Wald, 1952; Wiggert *et al.*, 1978). The RPE plays a role in the transport of all *trans*-retinoic acid to the photoreceptors (Bok, 1985). At high concentrations (1 μM) retinoic acid promotes the RPE

phenotype in culture (Campochiaro *et al.*, 1991). However, retinoic acid is reported to reduce the rate of differentiation of ARPE-19 cells in culture (Janssen *et al.*, 2000).

Table 2.4 below gives the composition of culture media previously described for the RPE showing the major additions to the base medium. All concentrations are per ml unless otherwise stated.

Table 2.4 Summary of Published Specialised Media per ml

Additive	Hu and Bok, (2001)	Tezel and Del Priore, (1998)	Rizzolo and Li, (1993)
Base Medium	MEM [1]	DMEM:F12	DMEM
Selenious acid	2.6 ng	5 ng	6.3 μg
Hydrocortisone	10 ng	20 nM	18 ng
FCS	1%	—	—
Linoleic acid	0.085 μg	10 μg	—
Oleic acid	—	—	5.3 μg
Insulin	5 μg	100 μg	6.3 μg
Transferrin	5.0 μg	100 μg	6.3 μg
Putrescine	0.3 μg	0.3 μg	—
Tri-iodothyronine (T3)	6.5 pg	10 nM	—
EGF	—	8 ng	—
BSA	—	1 %	1.25 %
FSH	—	0.5 mU	—
bFGF	—	1 ng	—
All *trans*-retinoic acid	—	50 ng	—
Progesterone	—	—	6.6 ng
BPE	—	—	50 μg

Composition of media used in three studies to increase the tight junctions of RPE cells in culture. ([1]) MEM = Eagle's Minimum Essential Medium. BPE = Bovine Pituitary Extract. BSA = Bovine Serum Albumin. FSH = Follicular Stimulating Hormone. In addition to these supplements, bovine retinal extract 0.5% was added by Hu and Bok, (2001) to their SM and 1 retina/ml from E14 chick was added to the medium of Rizzolo and Li (1993).

2.6 Methods

2.6.1 Culturing of Cell Lines

All cells were maintained with 5% CO_2, 95% air mix at 37˚C in the culture media described below and in table 6.5. Culture flasks with a 0.2 μm vented cap with a growth area of 25 cm^2 (T25) or 75 cm^2 (T75) were used (Corning, Schiphol-Rijk, The Netherlands). All cell-culture media were supplied by Sigma, Poole UK unless otherwise stated. Medium was changed every two to four days depending on the cell line and the cells were split in a 1:3 or 1:5 ratio at confluence. Splitting of cells was performed by aspirating the medium and adding either 5 ml or 10 ml of Ca^{2+}-free Hank's Balanced Salt Solution (CFHBSS) to a T25 or T75 flask respectively for five minutes at room temperature. Tight junctions require Ca^{2+} to maintain their integrity and so by adding CFHBSS these tight junctions are weakened (Chu and Grunwald, 1990). The CFHBSS was then removed by aspiration and 200 μl (T25) or 1 ml (T75) of 0.25% (w/v) trypsin with 0.2 g/ml ethylenediaminetetraacetic acid (EDTA) in HBSS was added to the flask and incubated at 37˚C until the cells dissociated. The cells were then resuspended in culture medium and transferred to new flasks and returned to the incubator.

Routine culture of cells was performed using the following media preparations. For ARPE-19 cells they were grown in a 1:1 mixture of Dulbecco's Modified Eagle's Medium (DMEM) and nutrient mixture Ham's F12 with 15 mM N-2-hydroxylpiperazine-N-2-ethanesulphonic acid (HEPES) buffer and supplemented with 10% (vol/vol)[3] heat inactivated Foetal Calf Serum (FCS), 2 mM L-glutamine, 100 μg/ml streptomycin and 100 U/ml penicillin. ECV304 and C6 cells were grown routinely in supplemented medium 199 (M199) with 10 mM HEPES, 2 mM L-glutamine, 100 μg/ml streptomycin and 100 U/ml penicillin. D407 cells were grown in DMEM supplemented with 4.5 g/l glucose, 10% FCS, 2 mM L-glutamine, 100 μg/ml streptomycin and 100 U/ml penicillin. MIO-M1 cells were grown in nutrient mixture Ham's F-10 supplemented with 20 mM HEPES, 20% FCS, 100 U/ml penicillin, 100 μg/ml streptomycin, 0.25 μg/ml amphotericin-B and 2 mM L-glutamine. For all experiments 'under standard conditions' refers to the above culture medium conditions. Whilst 'reduced serum' refers to a reduction of FCS to 1% and all other ingredients remaining unchanged.

[3] All percentage concentrations are vol/vol unless otherwise stated in all sections.

2.6.2 Cell Culture Density

Cell density calculations were performed by centrifuging the cell suspension in culture medium at 1000*g* for ten minutes and re-suspending the pellet in 5 ml of cell culture medium. A 10 μl aliquot of the suspension was then transferred to a glass haematocytometer. The numbers of cells in the central square were counted. The quoted densities are the average of two counts (mean cell count). The cell density/ml is given by equation 2.i.

$$\text{Cell density/ml} = \text{mean cell count} \times 10^4 \qquad \text{— 2.i}$$

The cell density required for plating was then determined per μl and added to each well. Additional culture medium was then added to the well to make up to 0.5 ml (Transwell™) or 0.25 ml (Cellagan™).

Table 2.5 below shows the medium used and the seeding density for cells on inserts for all experiments unless otherwise stated. The range of passage numbers used in experiments is also noted.

Table 2.5 Standard Cell Culture Media and Densities for Cell lines

Cell Line	Medium	Seeding Density (cells/cm^2)	Passage Numbers
ARPE-19	DMEM:F12 +10% FCS	166,000	23 - 33
D407	DMEM with 4.5g/l D-Glucose +10% FCS	80,000	93 - 108
ECV304	M199 with 10% FCS	100,000	17 - 25
C6	M199 with 10% FCS	125,000	130 - 150
MIO-M1	Ham's F10 with 20% FCS	200,000	68 - 85

Culture media for the cell lines used in the modelling of the outer blood retinal barrier and respective seeding densities. All media for ARPE-19, D407, ECV304 and C6 cells were supplemented with 100 µg/ml streptomycin, 100 U/ml penicillin and 2 mM L-glutamine. MIO-M1 culture medium was supplemented with an antibiotic-antimycotic solution to give a final concentration of (100 U/ml Penicillin, 100 µg/ml streptomycin and 0.25 µg/ml amphotericin B) and 2 mM L-glutamine. FCS is heat inactivated Foetal Calf Serum. Passage numbers are given for the cell lines that were used in this study.

2.6.3 Cell Culture Filters

A variety of cell culture inserts and coatings are available to enhance polarisation and tight-junction formation of epithelial cells. Commercial preparations such as Matrigel™ which contains predominantly laminin and collagen IV are available as well as collagen-based filters such as

Cellagan™ or Transwell™ that can be coated to modify the substrate further. The integrity of the substrate is critical for the development of RPE cells in culture (Gullapalli *et al.*, 2005). Various substrates have been used to model the interaction between Bruch's membrane and the RPE including the secreted extracellular matrix from corneal endothelial cells (Campochiaro and Hackett, 1993), porcine lens capsule (Nicolini *et al.*, 2000; Turowski *et al.*, 2004), Descemet's membrane (Thumann *et al.*, 1997), biodegradable synthetic substrates (Hadlock *et al.*, 1999) and amniotic membrane (Capeans *et al.*, 2003; Ohno-Matsui *et al.*, 2005; Stanzel *et al.*, 2005).

Two types of cell-culture insert were used to grow cells on. One was the Transwell™ (Corning) that forms a permeable polyester membrane with 0.2 μm pores and a growth area of 1.12 cm^2. The second type was, Cellagan™ (MP Biomedicals, Oxfordshire, UK) whose filter is collagen based with a growth area of 0.79 cm^2. The pore size is not specified in this proprietary product. Transwell™ inserts contained 0.5 ml of culture medium in the apical chamber and 1.5 ml in the basal chamber with six inserts per well. The Cellagan™ inserts were placed in the wells of a 12 well plate (Nunc, Roskilde, Denmark) with 1.5 ml of culture medium in the basal chamber and 0.25 ml in the apical chamber.

2.6.3.1 Laminin Coating

Laminin, derived from an Engelbreth-Holm-Swarm murine sarcoma was supplied as a stock solution of 1 mg/ml in 50 mM Tris-HCl pH 7.5 (Sigma). Laminin was thawed and kept on ice. The stock solution was diluted with 1 ml of ice-cold PBS such that each 120 μl aliquot contained 60 μg of laminin. Each of the six Transwell™ filters was coated with 20 μl of the aliquot so that each filter had (~ 9 µg laminin/cm^2). In addition to the laminin 100 μl of culture medium was added to ensure an even distribution of laminin by gentle rocking. The filters were then returned to the incubator for thirty minutes. Prior to the addition of cells, any excess fluid was aspirated and the cells plated at the densities listed in table 6.5. Aliquots of laminin were stored at -50˚C until required.

2.6.4 Co-Culture with Glial Cells

Method of glial co-culture is based upon that originally described by Ramsohoye and Fritz, (1998). ARPE-19 and ECV304 cells were grown as described in section 6.4.1 and seeded according to the densities in table 6.5 onto their respective filters. The basal chamber contained either C6 or MIO-M1 cells that were seeded two days earlier in order to attain confluence at an initial density of 1.25 x 10^5 cells/cm^2 or 2 x10^5 cells/cm^2 respectively. Apical chamber medium for ARPE-19 was DMEM:F12 with 1% FCS and antibiotics. ECV304 and C6 were maintained in M199 with 10% FCS and antibiotics and MIO-M1 were maintained in Ham's F10 with 10% FCS and antibiotic-antimycotic solution. See section 6.4.1.

Two experimental configurations were used in order to model the outer blood-retinal barrier. Glial cells (C6 and MIO-M1) were used as a potential source of factors that would up-regulate the

junctional proteins. The glial cells were plated in the basal chamber of a well and the permeable insert placed within the well containing either ECV304 as a positive control or ARPE-19 cells. However, as any retinal factors would presumably act upon the apical surface of the RPE *in situ*, to replicate this situation the conditioned medium from confluent flasks of C6 or MIO-M1 cells was added to the apical side of the cell culture inserts. The aim was to replicate the natural relationship between the retina (and any secreted factors) and the underlying RPE. Cellagan™ filters were used for ECV304 as these filters have been shown to be the most successful for the co-culture model with this cell line (Hurst and Fritz, 1996; Dobbie *et al.*, 1999). Laminin-coated Transwell™ filters for ARPE-19 cells were used given that these inserts have been widely used for ARPE-19 experiments previously (Dunn *et al.*, 1996; Luo *et al.*, 2006).

Figure 2.6 shows the experimental design for the co-culture experiments with the glial cells grown in the basal chamber. Any secreted factors would diffuse to the basal side of the RPE where they would induce a change in the barrier properties.

Figure 2.6 Co-Culture Experimental Configuration

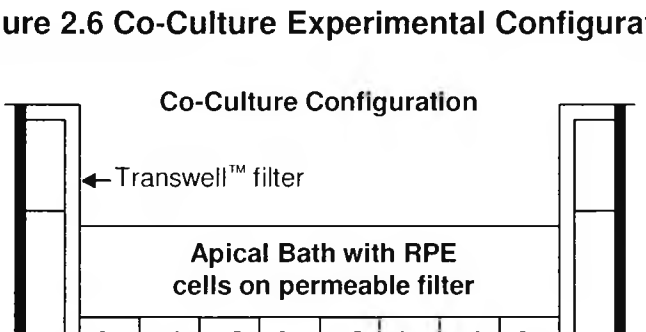

In co-culture experiments glial cells were seeded into the basal chamber of a 6- or 12-well plate and either ARPE-19 or ECV304 cells were seeded onto a permeable support (Transwell™ coated with laminin or Cellagan™) respectively. The filter was removed from the well periodically and the TER measured to assess the barrier properties of the cell monolayer.

2.6.5 Conditioned Media

Media from confluent T75 flasks of two- to three-day old C6 or MIO-M1 cells was removed with a 10 ml pipette and added to a 15 ml centrifuge tube (Corning). The medium was then spun down to remove cells at 1000*g* for 10 minutes. The supranate was collected as 'conditioned medium' and used on the same day. In the initial experiments when M199 was added to the apical side of the ARPE-19 cell line there was a marked acidification of the medium (pH 6.8) within 24 hours. Therefore, a 1:1 dilution of conditioned medium was used with DMEM:F12 with 1% FCS and antibiotics for ARPE-19 cells. With this modification the pH was 7.2 after 24 hours. Conditioned medium was collected from C6 cells at passages 134 -145 and MIO-M1 from cells at passage 78

- 85. ARPE-19 and ECV304 cells grown on Transwell™ and Cellagan™ inserts respectively and the TER measured over time.

2.7 Specialised Media

Defined media used for ARPE-19 cells was based on formulations for the culture of human RPE by Tezel and Del Priore, (1998) and foetal RPE by Frambach et al., (1990). Serum-free medium was prepared according to table 6.6. Stock 500 ml bottles of medium (DMEM:F12) with added nutrients (linoleic acid, putrescine and selenium salt) were stored with HEPES (20 mM), antibiotics, and 2 mM L-glutamine were added. Fresh solution of specialised medium (Denoted SM1, SM2 and SM3) were prepared each day according to the methods described in appendix I. All concentrations are per ml of base medium unless otherwise stated. SM2 is the same as SM1 but with 50 ng/ml of all *trans*-retinoic acid added and 3,3',5-Triiodo-L-thyronine sodium salt (T3) removed. Details of the preparation of the SM can be found in appendix I.

SM3 is based upon that of Rizzolo and Li, (1993). Cells were treated with SM3 as defined in table 2.6 (overleaf) or with two variations of SM3. (The notation SM3/SM3 indicates that SM3 was used in the apical and basal chambers). The first modification to SM3 was to add bFGF and EGF and use this medium in the apical and basal chambers (SM3 + bFGF +EGF). The second modification was to add 50 μg/ml of bovine pituitary extract (BPE) to the SM3 and use this in the basal chamber with SM3 in the apical chamber (SM3/(SM3 + BPE)) as originally described by Peng *et al.*, (2003).

Table 2.6 Specialised Medium Composition per ml

Ingredient	Stock Solution	SM1 DMEM:F12	SM2 DMEM:F12	SM3 DMEM
Insulin	10 mg	100 μg	100 μg	100 μg [Ŧ]
Transferrin	1 mg	5 μg	5 μg	55 μg [Ŧ]
Selenium	5.5 μg	5 ng[§]	5 ng[§]	50 μg [Ŧ]
EGF	100 μg	10 ng	10 ng	—
bFGF	250 μg	1 ng	1 ng	—
Hydrocortisone	50 μM	25 nM	25 nM	50 nM
Progesterone	10 μg	—	—	10 ng
Putrescine	0.1 mg	0.3 μg	0.3 μg	—
Linoleic acid	4.7 μg	10 μg	10 μg	47 ng [Ŧ]
Oleic acid	4.7 μg	—	—	47 ng [Ŧ]
All *trans*-retinoic acid	40 μg	—	50 ng	—
BSA	30% wt/vol	1% wt/vol	1% wt/vol	5 μg [Ŧ]
T3	20 μg	5 ng	—	—
HEPES	1 M	20 mM	20 mM	20 mM

Additives to the base media to make 50 ml of specialised medium used with ARPE-19. ([Ŧ]) indicates components added as pre-defined supplement ITS[+3]. ([§]) Constituents present in DMEM:F12 with added nutrients. T3 is 3,3',5-Triiodo-L-thyronine sodium salt. *See appendix 1 for further details.*

A control group of ARPE-19 cells in reduced serum was always used. From a total of N=6 independent control trials with 5 samples per trial the highest TERs were used as the baseline to compare the experimental conditions against. All TERs developed using the modifications of substrate, co-culture, conditioned medium and specialised media (SM1 and SM2) were compared to this sub-set. The aim of the manipulations in culture conditions was to increase the best TER obtainable with reduced serum by at least two-fold.

2.8 Measuring the Trans Epithelial Resistance

The TER is a sensitive measure of the paracellular permeability formed by the tight junctional proteins (Schneeberger and Lynch, 1992). Additionally, the measurement of electrical resistance permits a rapid, simple and non-destructive method for determining changes in the barrier properties during culture. A high TER was taken as a measure of barrier formation and a low TER taken to indicate low barrier integrity.

The electrical resistance of the cultures was measured using an epithelial voltohmmeter EndOHM™, World Precision Instruments Inc. (WPI, Aston, UK) with a planar electrode chamber (Endohm-12, WPI) for Cellagan™ or (Endohm-24, WPI) for Transwell™ inserts. In the measuring chamber, an isolated square wave alternating current (± 20 μA at 12.5 Hz) flows between concentric, opposing pairs of circular electrodes above and below the membrane (See figures 2.6 and 2.7 (overleaf). The electrodes consist of a voltage-sensing electrode (silver/silver chloride pellet) in the centre surrounded by an annular current electrode made of silver/silver chloride (chamber) and stainless steel (cap).

The TER was determined by the difference of the resistance recorded between a blank filter (R_{Filter}) treated and maintained in identical culture conditions to the inserts containing cells ($R_{Filter + Cells}$). The result was then multiplied by the area of the insert to give the TER in $\Omega.cm^2$. (See equation 2.ii).

$$\mathbf{TER = (R_{(Filter + Cells)} - R_{Filter}) \times area\ of\ filter} \qquad \mathbf{— 2.ii}$$

The EndOHM™ chamber was sterilised with 70% ethanol prior to use. During measurements, the basal chamber contained 2 ml of phosphate buffered saline (PBS) to complete the electrical circuit for Transwell™ or 1 ml for Cellagan™ filters. The apical electrode was adjusted so that it was ~ 1 mm from the cell monolayer when measurements were taken. All measurements were taken within 5 minutes of removing the cells from the incubator. Figures 2.6 shows the EndOHM™ chamber with electrodes and figure 2.7 (overleaf) shows the recording set-up.

Figure 2.6 EndOHM™ Chamber

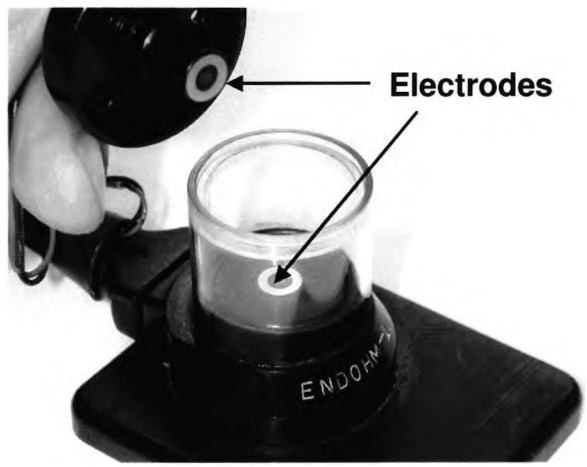

The EndOHM™ chamber consists of an apical and basal voltage and current electrode visible as the concentric rings on the lid and basal chamber into which the insert containing cells or the blank insert was placed with PBS in the lower chamber.

Figure 2.7 EndOHM™ Chamber and Cellagan™ Insert

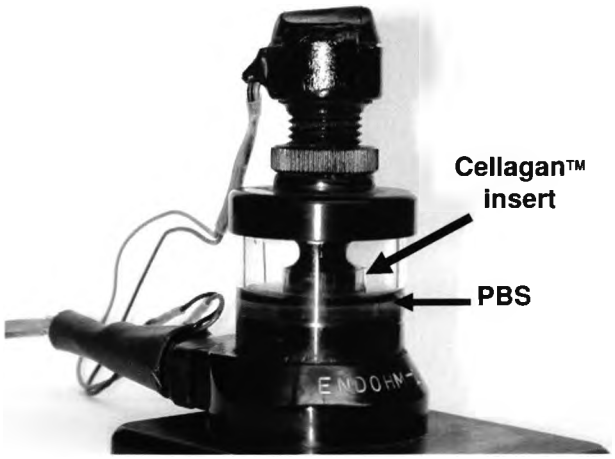

Recording configuration with Cellagan™ insert mounted in the EndOHM™ unit with PBS in the lower chamber.

2.9 Long-Term Storage of Cell Lines

Cells were grown to confluence and culture medium replenished the day before storage. Cells were trypsinised as described (section 2.6.1) and suspended in 10 ml of their culture medium to quench the trypsin. The cell suspension was then centrifuged at 1000*g* for ten minutes. The supranate was aspirated and the cell pellet re-suspended in 1 ml of the freezing medium per 25 cm^2 of the original cell population. Freezing medium contained FCS (95%) and dimethyl sulphoxide (DMSO 5%). Cell suspensions were transferred to cryovials, which were then placed in a Nalgene cryo 1°C freezing container (Nalge, Thorn, UK) and held at -70°C for a minimum of four hours before being stored in the vapour phase of liquid nitrogen. When required, frozen cell suspensions were thawed by removing the vials from the liquid nitrogen and leaving them at room temperature for one minute before rapid thawing in a 37°C water bath. Thawed cell suspensions were transferred to a T25 culture flask and warmed culture medium (1 ml, 37°C) was slowly mixed with the suspension. The culture flask was held at room temperature for a further ten minutes before 3 ml of culture medium was added to the flask. The cells were then returned to the incubator. Culture medium was replaced approximately four hours later, once the cells had begun to settle on the flask.

2.10 Data Analysis

The results are expressed as mean ± standard deviation (SD) unless otherwise stated. Student's unpaired, two-tailed t-tests were used to determine the significant differences between means, where $p < 0.05$ was taken as statistically significant. Statistical calculations were made using Microsoft Excel™.

2.11 Results

2.11.1 D407 and ARPE-19

The results in figure 2.8 (overleaf) show the TER of D407 and ARPE-19 cells over time grown on laminin-coated and uncoated Transwell™ filters. The TER for D407 was not significantly increased on day 7 ($p=0.9274$) or day 21 ($p=0.1437$) when laminin was used as a substrate ($N=5$) compared to the uncoated Transwell™ inserts ($N=6$). However, the effect of laminin coating ($N=5$) significantly increased the mean TER for ARPE-19 compared to the uncoated inserts ($N=3$) on days 7 to 21 ($^{***}p<0.001$). However, by day 24 the difference in the TER was less apparent ($^{*}p=0.0148$) with the ARPE-19 cells grown on laminin coated filters obtaining a TER of 29 ± 2 $\Omega.cm^2$ compared to 24 ± 2 $\Omega.cm^2$ for the ARPE-19 cells grown on uncoated filters. Note that the group is compared to the selected sub-set of TERs from the control groups and so represent the upper limit of the TERs obtained under standard reduced serum culture conditions.

The TERs of ARPE-19 were higher than the D407 cell line and consequently the D407 cells were not pursued any further with respect to their barrier properties.

Figure 2.8 TER of ARPE-19 and D407 on Filters

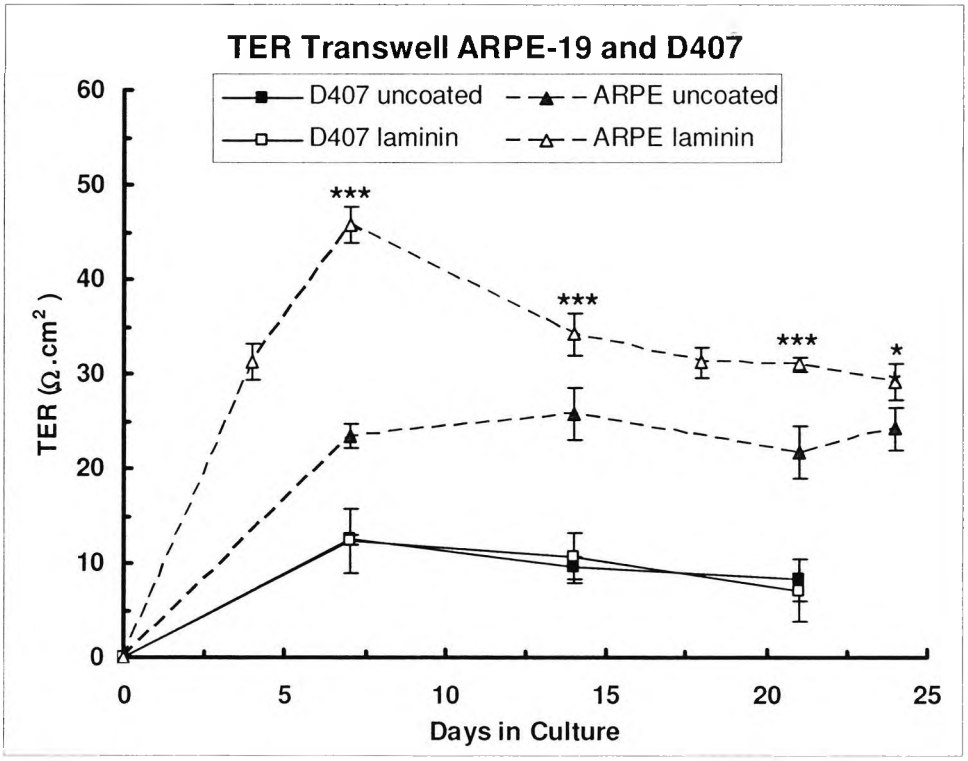

*The TERs over time of ARPE-19 and D407 grown on Transwell™ filters with and without laminin. Results show that the TER was greater for the ARPE-19 cells (N=5) on laminin-coated Transwell™ filters than the uncoated Transwell™ filters. The peak TER was 46 ± 2 Ω.cm² on day 7 (*** p<0.001). On day 24 the TER was still significantly higher (* p=0.0147). The D407 cells (N=9) for laminin-coated or uncoated (N=6) showed no difference in the TER (p=0.9770) with a low peak TER of 12 ± 1 Ω.cm².*

2.12 Co-Culture

2.12.1 ARPE-19 and C6

Figure 2.9 (overleaf) shows the TER of ARPE-19 cells grown in co-culture with C6 cells on laminin-coated Transwell™ filters from three independent trials with N=5, 5 and 11 inserts used respectively. They are compared to the best sub-set of ARPE-19 cells grown in reduced serum on laminin coated Transwell™ filters. Co-culture with C6 cells in the basal compartment decreased the TERs with the mean ± SD peak TER on day 7 for the combined three trials being 25 ± 5 Ω.cm² which is significantly lower (*** p<0.0001) than at day 7 for ARPE-19 cells when grown without C6 cells (46 ± 2 Ω.cm²). A similar difference was evident on days 14 and 21 with the TER of control ARPE-19 cells being 34 ± 2 and 31 ± 1 Ω.cm² respectively compared 18 ± 4 Ω.cm² at the same time points with ARPE-19 grown with C6 cells (*** p<0.001).

Figure 2.9 ARPE-19 and C6 Co-Culture

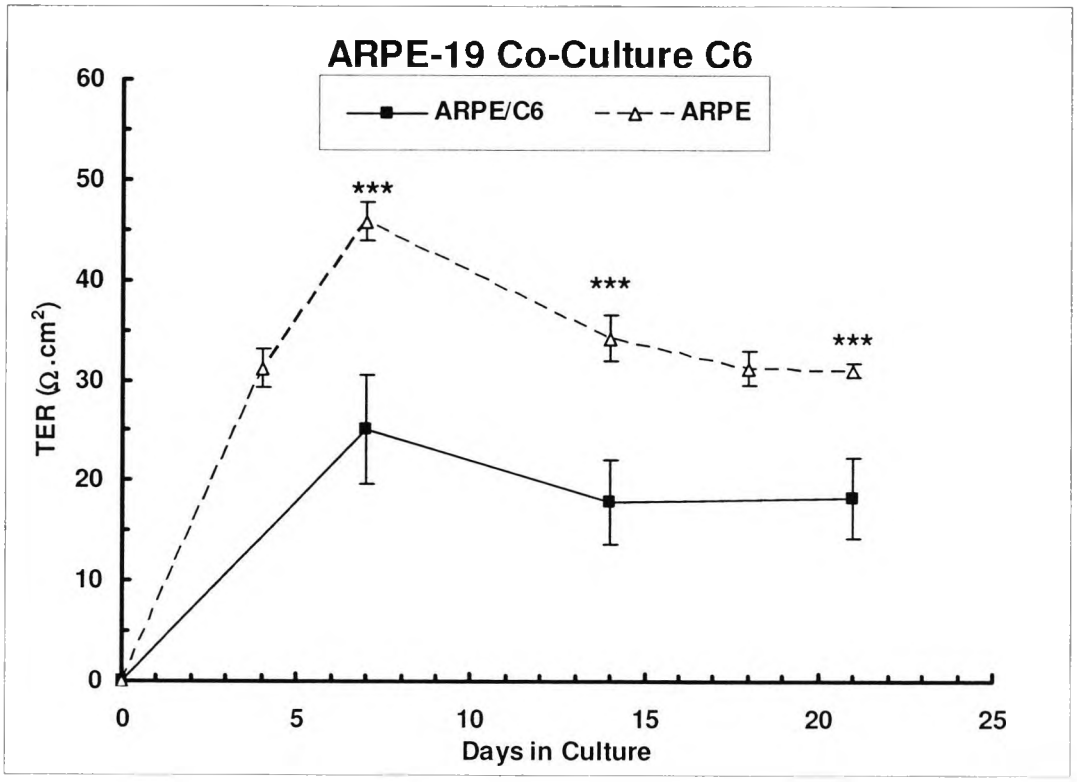

*ARPE-19 cells grown in low serum on laminin-coated Transwell™ filters with C6 cells in the basal compartment. The TER of ARPE-19 cells grown without C6 cells in the basal chamber were significantly higher than the co-culture model (***p<0.001) on days 7- 21 of culture. The ARPE-19/C6 co-culture plot represents the mean ± SD of three independent trials with a total of (N=21) wells compared to (N=5) control of the maximum TERs recorded with ARPE-19 cells.*

2.12.2 ARPE-19 and MIO-M1

Figure 2.10 (overleaf) shows the TER over time of ARPE-19 cells grown in co-culture with MIO-M1 in the basal chamber of Transwell™ filters pre-coated with laminin as previously described. There was a significant decrease in the TER from these three trials over 21 days with the maximal TER being 22 ± 5 $\Omega.cm^2$ on day 21 which was significantly lower (***p<0.001) than the 31 ± 1 $\Omega.cm^2$ obtained at the same time point when ARPE-19 cells were grown alone. The MIO-M1 co-culture plot represents the mean ± SD of three independent trials with N= 5, 5 and 11 samples in the trials respectively.

Figure 2.10 ARPE-19 and MIO-M1 Co-Culture

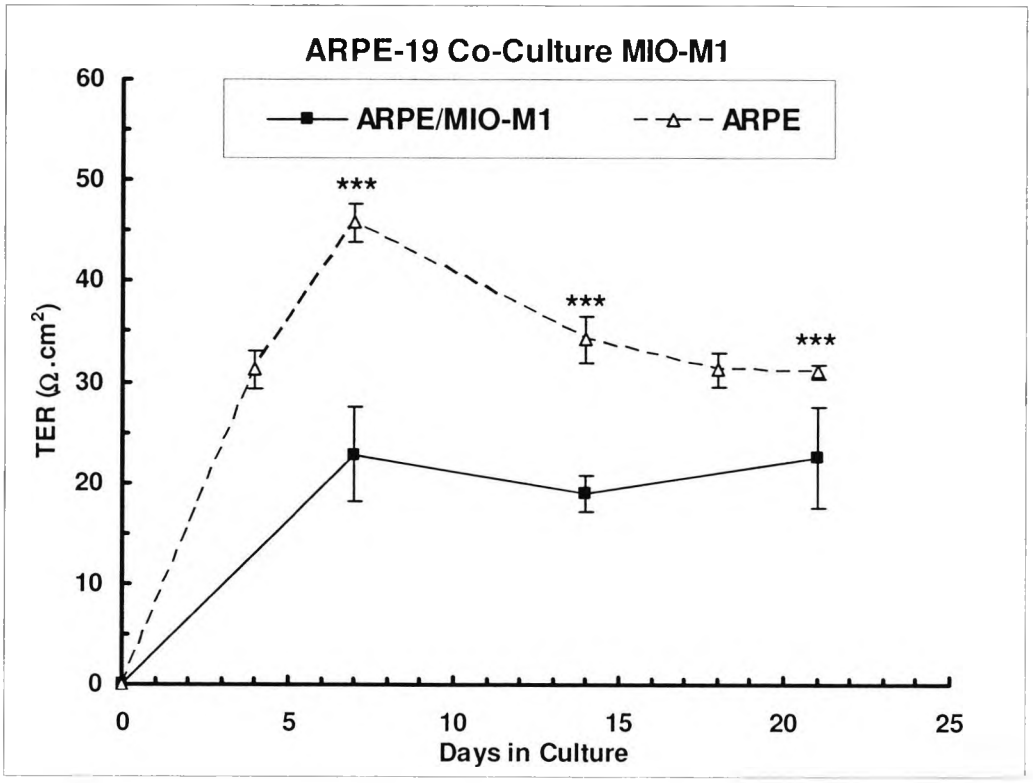

*The TER of ARPE-19 cells grown in co-culture with MIO-M1 cells. Plot of ARPE-19/MIO-M1 co-culture represents the mean ± SD of three independent trials (N=21). The TER of ARPE-19 grown without MIO-M1 was significantly higher than ARPE-19 grown with MIO-M1 cells on after 7- 21 days in culture (***p<0.001).*

2.12.3 ECV304 Co-Culture and Glial Cells

As a positive control, ECV304 cells were grown in co-culture with C6 or MIO-M1 cells. The TER of ECV304 was significantly higher than control ECV304 cells grown on Cellagan™ filters alone under these conditions.

An induction of the TER by C6 and MIO-M1 cells was evident with a significant (***p<0.001) increase demonstrated in the first two weeks of culture. The TER was not sustained and decreased after day 14 but was still significantly higher than the control group on day 24 (*p=0.0432). The MIO-M1 co-culture group represents (N=5 inserts from one trial) with a peak TER of 140 ± 29 $\Omega.cm^2$ on day 14. The C6 co-cultured ECV304 cells reached a peak TER of 76 ± 8 $\Omega.cm^2$ on day 14 (N=6 from one trial). In contrast the control group reached a peak TER of 51 ± 16 $\Omega.cm^2$ on day 14 which represents the TER of two independent trials with N=3 samples in each trial. The MIO-M1 co-culture group had a consistently higher TER than the control group on

days 7 -14 (***p<0.001). The C6 co-culture group's TER was significantly higher on days 7 (***p<0.001), 14 (***p<0.001), 21 (**p=0.0016) and 24 (*p=0.0158) of culture. (See figure 2.11).

Figure 2.11 ECV304 and Glial Cell Co-Culture

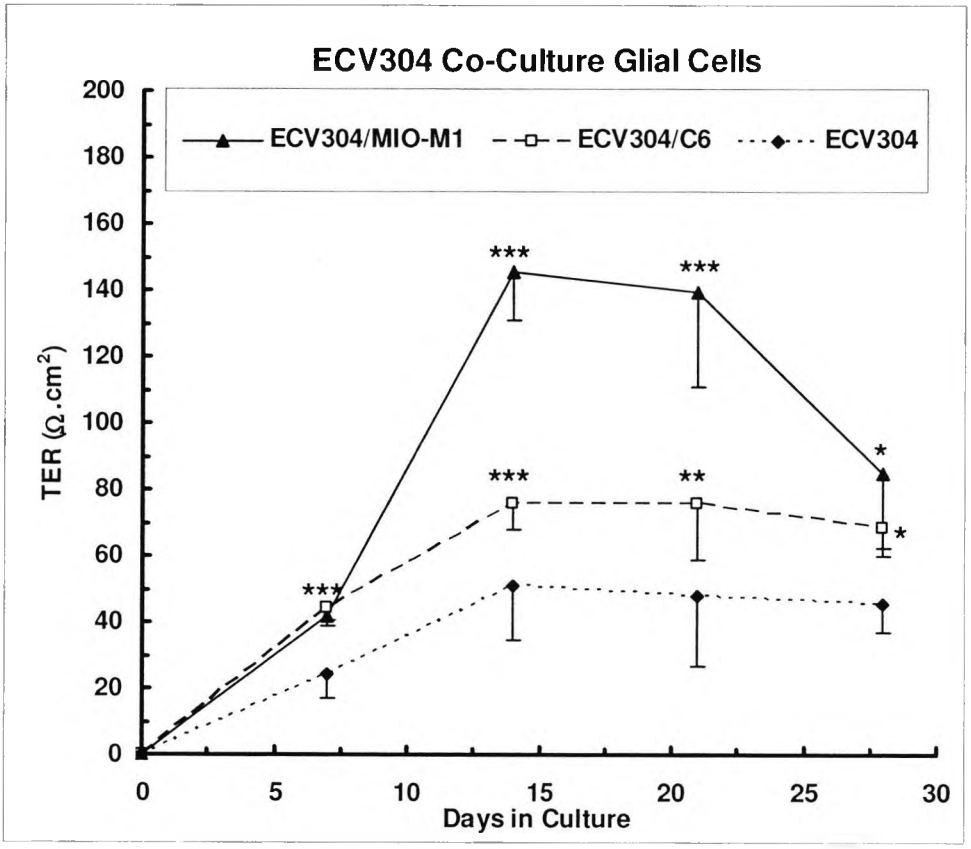

*ECV304 cells grown on Cellagan™ filters with C6 or MIO-M1 cells in the basal chamber induced a rise in the TER compared to ECV304 cells grown alone on Cellagan™ filters. The induction was greater with MIO-M1 cells reaching a TER of 140 ± 29 Ω.cm² on day 14. At the same time point, the ECV304 cells grown with C6 cells had a TER of 76 ± 8 Ω.cm² compared to the control ECV304 cells (51 ± 16 Ω.cm²) on day 14. SD error bars are shown with one arm for clarity. The asterisks represent the p-values as being significant (*** p<0.001, ** p<0.01 and * p<0.05).*

2.13 Glial Cell Conditioned Medium

2.13.1 ARPE-19

C6 or MIO-M1 conditioned medium did not significantly increase the TERs of ARPE-19 cells when grown on laminin coated Transwell™ inserts compared to controls. Figure 2.12 (overleaf) shows the TER from two independent trials with N=5 filters in each trial for C6 or MIO-M1 conditioned medium in the apical chamber compared to the control ARPE-19 cells (N=5 filters). The peak TER of the C6 conditioned medium group was 21 ± 2 Ω.cm² on day 7 which was significantly (***p<0.0001) less than the control group on day 7 (46 ± 2 Ω.cm²). This trend

continued on days 14 and 21 with no increase in the TER observed. The MIO-M1 conditioned medium was also significantly (***p<0.0001) lower on day 7 being 25 ± 3 Ω.cm^2. No difference in the TER was observed on day 14 compared to the control group. On day 21 the MIO-M1 conditioned medium group (25 ± 3 Ω.cm^2) and C6 conditioned medium group (16 ± 5 Ω.cm^2) were both significantly lower (***p<0.001) than the control group's TER of 31 ± 1 Ω.cm^2.

Figure 2.12 ARPE-19 and Glial Cell Conditioned Medium

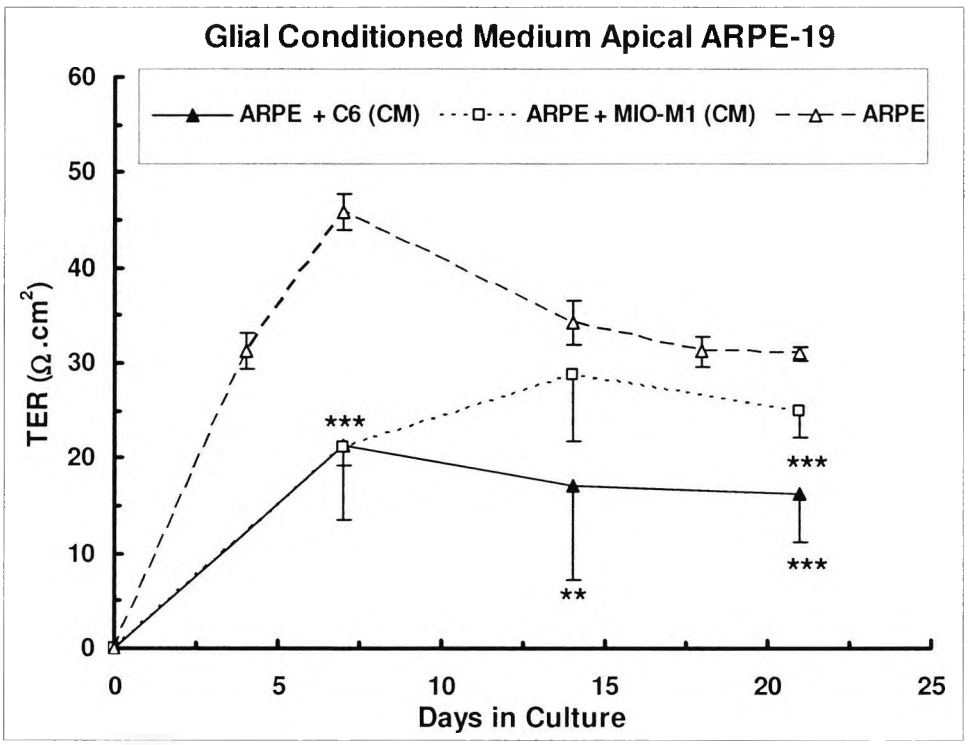

*TER measurements of ARPE-19 cells with C6 or MIO-M1 conditioned medium in the apical chamber of a laminin-coated Transwell™ filters. The TER was significantly reduced on days 7 and 21 (***p<0.001). On day 14 there was no significant difference in the TERs for the MIO-M1 conditioned medium and a significantly lower TER (**p<0.01) with C6 conditioned medium. Conditioned medium plots represent the mean ± SD of two independent trials with N=5 samples in each trial. Control ARPE-19 plot is shown for comparison. The SD error bars are truncated for clarity.*

2.13.2 ECV304

The TER of ECV304 cells was not altered significantly in the first two weeks of culture with C6 or MIO-M1 conditioned medium compared to the control group (figure 2.13 overleaf). All cells were grown on Cellagan™ filters as previously described. The C6 conditioned medium plot represents the mean ± SD of two independent trials with N=4 and N=3 filters used respectively. The MIO-M1 conditioned medium plot represents two independent trials with N=3 and N=5 filters used respectively. The control group is from two trials with N=3 filters in each trial. On day 14 there

was no significant difference in the TER between the groups. The TERs were 39 ±12 $\Omega.cm^2$ for C6 conditioned medium, 34 ± 13 $\Omega.cm^2$ for MIO-M1 conditioned medium and 51 ± 16 $\Omega.cm^2$ for the control group. However, by day 21 the TERs had fallen in the C6 and MIO-M1 conditioned medium groups and were significantly reduced. In the C6 conditioned medium group the TERs were 16 ± 5 $\Omega.cm^2$ ($^{**}p=0.0028$) and for the MIO-M1 conditioned medium group the TER was 17 ± 9 $\Omega.cm^2$ ($^{**}p=0.0031$) compared with the control group's TER at this time (48 ± 21 $\Omega.cm^2$).

Figure 2.13 ARPE-19 and ECV304 with MIO-M1 Conditioned Medium

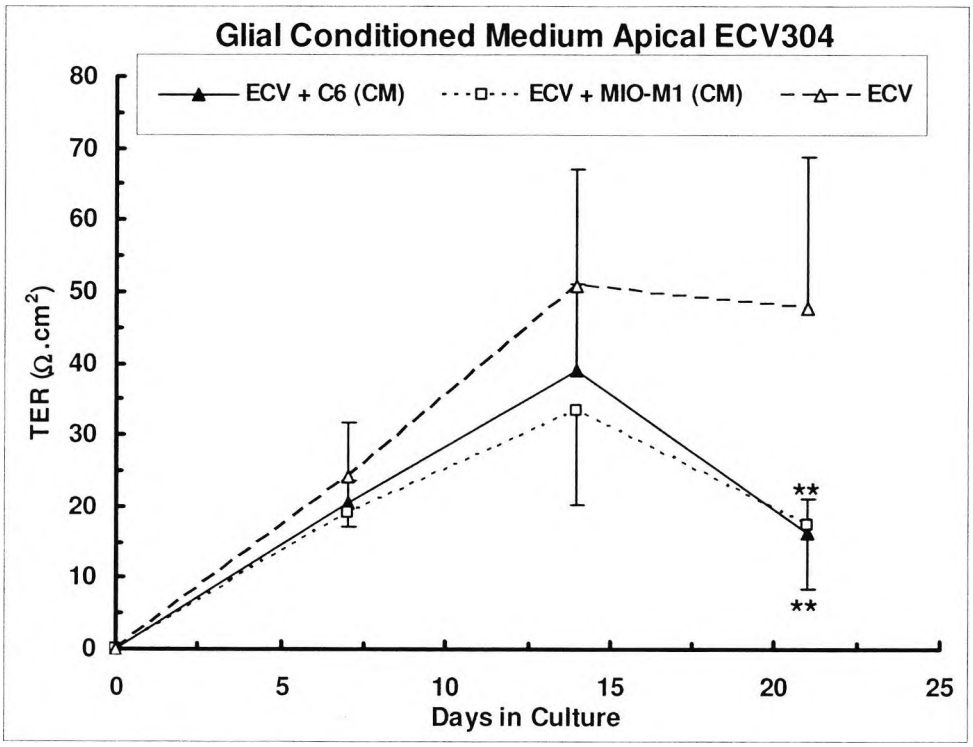

The effects on the TER of ECV304 grown on Cellagan™ filters with either C6 or MIO-M1 conditioned medium (CM) in the apical chamber compared to control ECV304 cells. No significant difference in the TER was apparent until day 21 when the TER of the conditioned medium groups fell ($^{**}p<0.01$). The SD error bars are truncated for clarity.

2.14 Modification of Medium– SM1 and SM2

Results of ARPE-19 cells grown on laminin-coated Transwell™ filters are shown in figure 2.14 (overleaf). High resistances were obtained with SM2 medium containing all *trans*-retinoic acid. The maximal TER recorded was 86 ± 6 $\Omega.cm^2$ after 21 days in culture in SM2. A significant increase in the TER was observed after two weeks of culture in both SM1 and SM2 media ($^{***}p<0.001$). The SM1 group represents the mean ± SD of one trial with N=5 samples and the SM2 group in the mean ± SD of two independent trials with N=5 filters in each trial. The control group shows ARPE-19 cells N=5. The peak TER in SM1 was 58 ± 7 $\Omega.cm^2$ and in SM2 it was 86 ± 6 $\Omega.cm^2$ occurring on day 21 when the TER of the control group was 31 ± 1 $\Omega.cm^2$. SM1

medium produced a significantly (***p<0.001) higher maximal TER of 58 ± 7 Ω.cm^2 than low serum on day 7 (46 ± 2 Ω.cm^2). However, on day 7 the TER of SM1 medium with ARPE-19 cells (33 ± 1 Ω.cm^2) was significantly lower (***p<0.001) than the controls.

Figure 2.14 ARPE-19 and Specialised Media

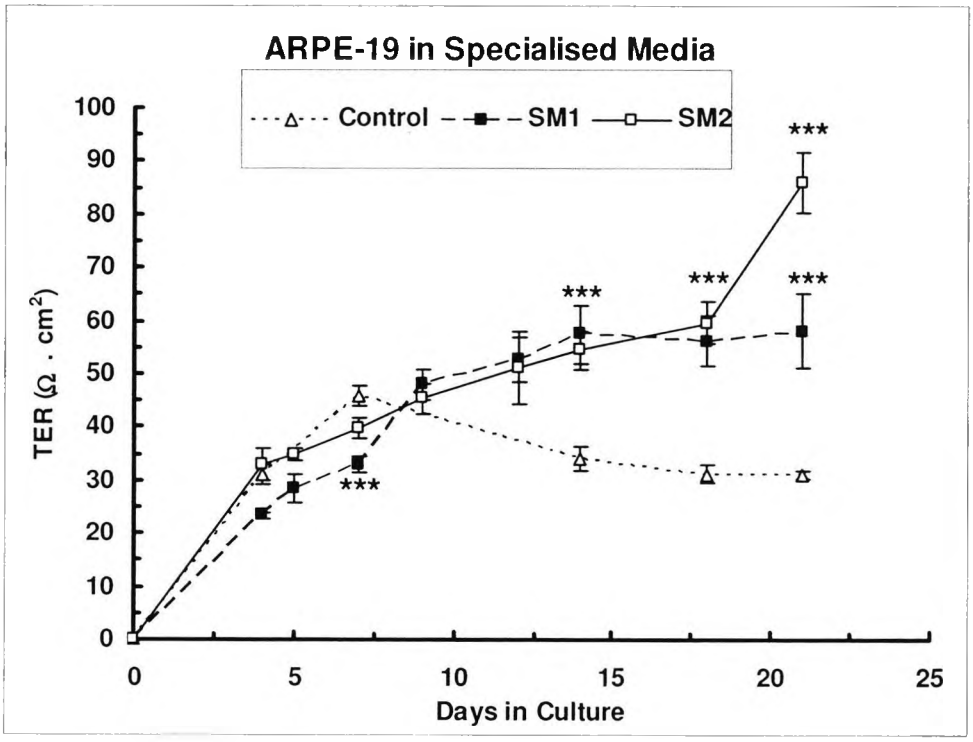

*ARPE-19 in specialised media showed an increase in the TER of > 50 Ω.cm^2 with SM2 showing the greatest effect. The TERs are significantly (***p<0.001) higher than the control ARPE-19 cells grown in reduced serum after two weeks in culture. The peak TER for SM1 was 58 ± 7 Ω.cm^2 on day 21 and for SM2 it was 86 ± 6 Ω.cm^2 on day 21. In comparison, the TER of the control group on day 21 was 31 ± 1 Ω.cm^2.*

2.14.1 SM3

Figure 2.15 (overleaf) shows the results of SM3 medium and modifications to this medium for ARPE-19 cells grown on laminin-coated Transwell™ filters compared to a control group in reduced serum. On day 7 all of the three modifications had a significantly (p<0.001) lower TER than the control group grown in reduced (1%) FCS. Resistances were in (Ω.cm^2) 32 ± 0 control, 27 ± 3 (SM3/SM3), 21 ± 1 (SM3/(SM3 + BPE)) and 26 ± 1 (SM3+ EGF + bFGF). On day 14 the TERs were: control 29 ± 1 Ω.cm^2, (SM3/SM3) 24 ± 2 Ω.cm^2 (p=0.2960), (SM3/(SM3 + BPE)) 21 ± 1 Ω.cm^2 (***p<0.001) and (SM3 + EGF + bFGF) 30 ± 1 Ω.cm^2 (p=0.0166). On day 24 only the TER of SM3 with EGF and bFGF group had a significantly higher (*p=0.0265) TER than the controls of 30 ± 1 Ω.cm^2 compared to 26 ± 3 Ω.cm^2. The SM3/SM3 group had a significantly lower (*p=0.0265) TER on day 24 compared to the controls.

Figure 2.15 ARPE-19 and Rizzolo Specialised Medium Derivatives

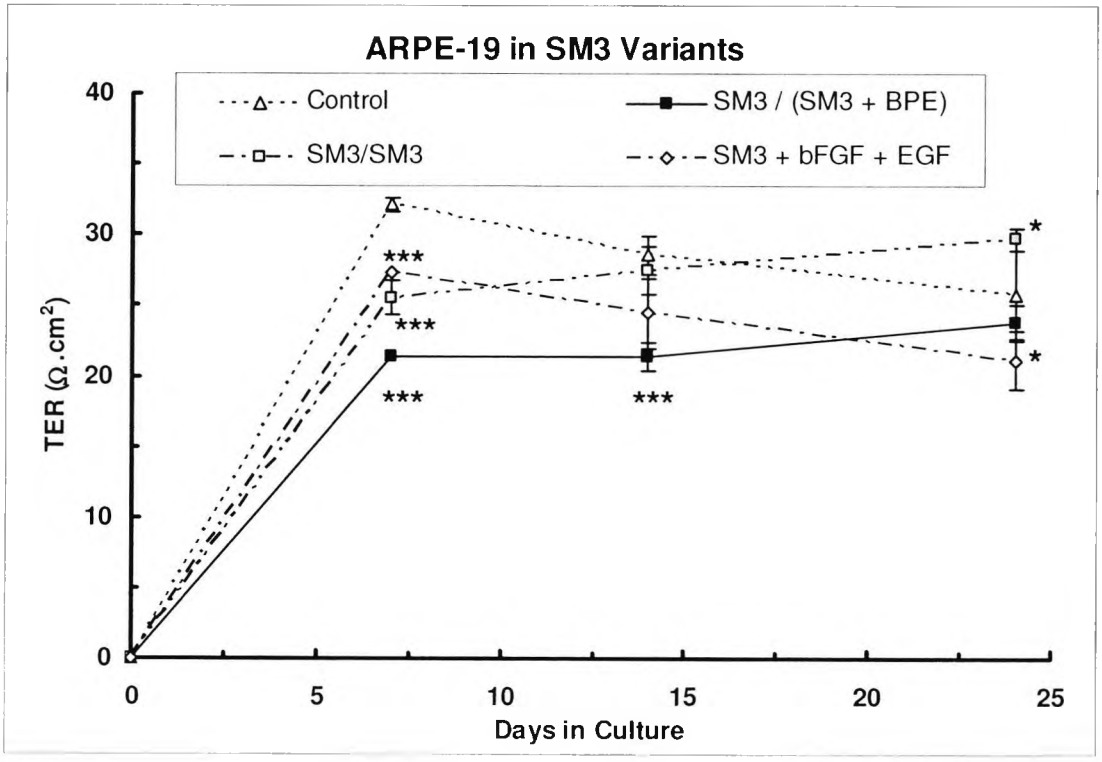

Modifications of SM3 with addition of EGF and bFGF significantly reduced the TER by day 21 of culture ($^{*}p<0.05$). The addition of BPE to SM3 in the basal chamber also reduced the TER in the first 14 days of culture ($^{***}p<0.001$). When SM3 was not modified there was a small increase in the TER compared to the control low serum group on day 24 ($^{*}p<0.05$). Plot shows mean ± SD of N=5 filters from each culture condition.

2.15 Discussion

Early attempts at growing primary human RPE cells were hindered by the loss melanin and the characteristic cobblestone morphology after a few weeks (Tso *et al.*, 1973). It is now well established that cells in culture de-differentiate and lose the characteristics of the parent cell unless maintained under conditions that replicate the *in situ* environment. Primary RPE cultures lose their polarised distribution of ion channels (Rizzolo, 1990), transdifferentiate into non-epithelial cells (Kodama and Eguchi, 1994) and express neuronal voltage-gated Na^+ channels in culture (Botchkin and Matthews, 1994). Primary cultures of porcine, chick and human RPE were attempted in this study but the results were not satisfactory and are not presented owing largely to contamination of the primary culture with non-RPE cells. Typically the RPE is senescent in adulthood (Korte *et al.*, 1994) and therefore the sub-culturing of adult human RPE cells requires modifications to the culture medium and substrate in order to maintain an RPE phenotype. The main objective was to utilise existing human cell lines and try to improve the barrier characteristics by modifying the culture conditions and substrate owing to the difficulty in obtaining large quantities of fresh human donor RPE.

Initial experiments showed that ARPE-19 cells developed a higher TER when grown in reduced serum medium on laminin compared with uncoated Transwell™ filters. The TERs on laminin represented were the mean ± SD of the highest TERs from four control trials. This selected group's TER was similar to that reported by Dunn *et al.*, (1996) of approximately 35 $\Omega.cm^2$. However, not all filters attained this TER and in the control group with the SM3 media variants the TER of reduced serum ARPE-19 cells was approximately 20 - 25 $\Omega.cm^2$. This is probably a true reflection of the variability of this cell line in obtaining a modest TER of 20 – 30 $\Omega.cm^2$ (Luo *et al.*, 2006).

From the control groups a subset of filters was used as a control upper limit with which to judge the effects of the various culture conditions on. In practice, for experimental work the filters with the highest TER would have been selected as the high TER implies the development of tight junctions and polarity. Therefore, taking this level as a baseline was practical. However, the majority of filters with ARPE-19 cells grown in reduced serum had a TER in the range of 20-30 $\Omega.cm^2$. Nonetheless, the results of the modifications to culture conditions did not substantially improve upon the TER in this cell line.

Given the importance of the substrate in modelling, the *in-situ* environment laminin coating was applied in all subsequent experiments. Laminin coating also increases the number of expressed genes in ARPE-19 that are also found in human RPE cells compared to other substrates and is generally used for this cell line (Tian *et al.*, 2004). The TER of ARPE-19 grown in reduced serum was still significantly lower than the TER of native human or primary cultures of human RPE. The D407 cells had an even lower TER than the ARPE-19 cells and the laminin coating had little effect on this parameter. There are no reported TERs for D407 which may reflect the poor ability of this cell line to form a tight barrier.

ECV304 cells when grown in co-culture with C6 glioma cells did show the increase in the TER as previously reported (Hurst *et al.*, 1998; Dobbie *et al.*, 1999). ECV304 also showed an induction by MIO-M1 which suggests that this cell line responds to a factor common to both cell lines.

The likely explanation for the lack of induction by ARPE-19 cells compared with ECV304 may be due to the culture medium (M199) in which the C6 cells were grown. M199 medium differs to DMEM:F12 medium in which ARPE-19 cells are normally grown. M199 contains lower D-glucose 1 gm/l as opposed to 3.15 gm/l in DMEM:F12 which may account for the acidification noted when pure conditioned C6 medium was added to the apical chamber of ARPE-19 cells. It may have been that the glucose in M199 was utilised by the C6 cells in the basal chamber. This would have deprived the ARPE-19 cells of sufficient nutrients to develop tight-junctions. Furthermore, the high serum (10%) in which the C6 cells were grown would have also inhibited tight-junction formation (Chang *et al.*, 1997).

RPE cell proliferation is increased in the presence of glial cells and this is believed to contribute to the formation of epiretinal membranes (Burke and Foster, 1985; Hogg *et al.*, 2002). The factors secreted by the glial cell lines may have increased RPE cell proliferation and migration and decreased the TER owing to the lack of tight junction formation. One additional difference was the substrate on which ECV304 and ARPE-19 were grown. The secreted factors from C6 cells have a mass of < 1000 Da but may not permeate the laminin-coated Transwell™ filters as readily as the Cellagan™ filters.

Furthermore, the ARPE-19 cell line is derived from an adult donor and the induction of tight-junctions has been shown to be sensitive to the timing of the signal. High barrier properties are obtained in foetal and embryonic chick RPE cells but not routinely in adult RPE (Ban and Rizzolo, 2000a; Hu and Bok, 2001). For instance, embryonic E14 chick RPE cells obtain a higher TER than E7 RPE cells grown under the same conditions (Rahner *et al.*, 2004). This coupling of the development of the tight junctions to the developing retina may have also contributed to the lack of increased TER in the adult derived ARPE-19 cells.

The MIO-M1 cell line (Limb *et al.*, 2002) also failed to induce an increase in the TER of the ARPE-19 cell lines when grown in co-culture or when conditioned medium was used. However, the TERs were not as low as with the C6 cell line. The composition of the F10 media also has reduced glucose (1.1g/l) but the rate of growth of the Müller cells was far less than the prolific glioma-derived C6 cell line and so the metabolic demands of the MIO-M1 cells would have been lower.

MIO-M1 cells secrete hepatocyte growth factor (HGF) in the presence of 10% FBS and the HGF also causes secretion of VEGF by MIO-M1 (Hollborn *et al.*, 2004). The RPE secretes HGF and also has the HGF receptor (*c-met*) which is proposed to play a role in the proliferative retinopathy seen in patients where the RPE differentiates into a mesenchymal phenotype (He *et al.*, 1998;

Lashkari *et al.*, 1999; Briggs *et al.*, 2000). HGF increases ECV304 proliferation via the production of sphingosine kinase that regulates a variety of cell functions related to growth, differentiation and angiogenesis (Duan *et al.*, 2004). It is therefore possible that the secretion of HGF by MIO-M1 induced the RPE cells to develop a more mesenchymal and proliferative phenotype and a loss of tight-junctions and the epithelial phenotype. VEGF secretion would be expected to reduce the barrier properties of the ARPE-19 cells as VEGF has been shown to increase permeability in bovine RPE (Hartnett *et al.*, 2003).

In the original description ARPE-19 cells were grown in a specialised medium devised by Bok *et al.*, (1999) with the ARPE-19 cells achieving a TER or 90 $\Omega.cm^2$ (Dunn *et al.*, 1996). The precise formulation of the specialised medium was not specified at the time but this was later published (Hu and Bok, 2001). Other authors have also published specialised media for the culture of foetal and human RPE cells that vary in composition (see table 6.1) (Oka *et al.*, 1984; Rizzolo and Li, 1993; Tezel and Del Priore, 1998; Hu and Bok, 2001). The concentration of some components varies between authors such as insulin 5 - 100 μg/ml, transferrin 5 - 100 μg/ml and the addition of certain growth factors, vitamins and hormones (EGF, bFGF progesterone and all *trans*-retinoic acid). Further modifications have also been made by adding medium that has been conditioned with either bovine or embryonic chick retinas.

Three modifications of the defined media described by Hu and Bok, (2001), Tezel and Del Priore, (1998) and Rizzolo and Li, (1993) were utilised in this study. The composition of SM1 and SM2 varied in the addition of all *trans*-retinoic acid and the removal of 3,3',5-Triiodo-L-thyronine sodium salt (T3). The removal of T3 was based upon the findings of Peng *et al.*, (2003) who found no increase in the TER of embryonic chick RPE cultures with T3. Their rationale for originally considering this hormone was that T3 enhances the epithelial phenotype in RPE cells (Chang *et al.*, 1991) and foetal RPE cells have T3 receptors and therefore T3 may influence the developing RPE (Duncan *et al.*, 1999).

All *trans*-retinoic acid induces a gene in ARPE-19 that appears to contribute to the cytoskeleton (Kutty *et al.*, 2001). All *trans*-retinoic acid has been shown to decrease RPE cell proliferation and de-differentiation in culture (Campochiaro *et al.*, 1991). However, in one report that used a large dose (1 μM) of retinoic acid a delay in differentiation of ARPE-19 cells was reported (Janssen *et al.*, 2000). At 0.1 μM all trans-retinoic acid increases VEGF secretion by ARPE-19 cells (Chen *et al.*, 2005) which is similar to the final concentration of all *trans*-retinoic acid used in the present study 50 ng/ml (0.16 μM). In contrast all *trans*-retinoic acid down-regulates VEGF and up-regulates PEDF and the basement membrane proteins fibronectin and collagen IV in cultured mouse RPE (Uchida *et al.*, 2005). The effect of all *trans*-retinoic acid with the removal of T3 was to increase the TER in the ARPE-19 cells in this study despite the potential for an increased production of VEGF as has been reported (Chen *et al.*, 2005). One explanation may be that the study of Chen *et al.*, (2005) is that the ARPE-19 cells were grown in flasks with reduced serum. Given that substrate, time in culture and cell culture medium all influence the phenotype of ARPE-19 cells the effects of all *trans* retinoic acid may differ depending upon these conditions.

The addition of the above compounds had some effect on the TER of ARPE-19 cells compared to the cells grown under reduced serum conditions. Although the TER did not exceed 100 $\Omega.cm^2$ the results indicate the importance of the culture conditions to the barrier properties of this cell line. There was no advantage in using SM1 medium for growing the ARPE-19 cells. Although the TER was higher at the end of 24 days, the control cells had a similar TER after 7 days. The addition of all *trans*–retinoic acid in SM2 did increase the TER after 24 days in culture to a level that was reported by Dunn *et al.*, (1996) using a more complex formulation. However, the TER was still lower than that reported for cultured human RPE cells and did take a long period of time. The experiments in SM1 and SM2 were not carried on beyond 24 days as the aim was to establish a high TER in a relatively short period of time. Observations of the cells beyond day 17 also revealed that they were clumping and forming small pyramid structures associated with a high proliferation rate and the cells could not be considered a simple monolayer. This may have accounted for the sharp rise in the TER seen in the SM2 group towards the end of the culture period.

Further trials were performed with the media defined by Rizzolo who incorporated BPE. In one trial, the effects of EGF and bFGF were added to SM3 and this group of cells did show a modest increase in the TER compared to controls after 24 days. However, neither of the trials with SM3 produced an enhanced TER in ARPE-19 cells. These results are similar to those reported for embryonic chick RPE cultures (Peng *et al.*, 2003). Recently, Rizzolo has performed the same experiment and obtained a TER of 23 – 27 $\Omega.cm^2$ with SM3 which was consistent with these findings (Luo *et al.*, 2006).

The important adjunct to establishing a tight barrier would appear to be an improved basement membrane such as amniotic membrane and the addition of retinal conditioned medium. The media formulations SM1 and SM2 did enhance the TER in the ARPE-19 cell line; however, they did not exceed 100 $\Omega.cm^2$ or approach the higher TERs reported for foetal RPE cultures. The development of tight junctions in embryonic chick RPE is dependent on the age at which the RPE cells are harvested. The TER of E7 chick RPE cells is less than that of E14 chick RPE cells when grown in retinal conditioned medium (Peng *et al.*, 2003). Adult RPE cultures do not attain the same high TER as foetal RPE and this may be that these cells are senescent and are no longer responsive to signals that would encourage tight junction formation. ARPE-19 cells are derived from an adult and may therefore be less predisposed to forming a tight junction than cells from a younger donor.

Luo *et al.*, (2006) has recently performed a detailed analysis of ARPE-19 and the development of tight junctions *in vitro*. The main conclusion was that ARPE-19 expressed a variety of junctional proteins but that the expression levels varied between cells which prevented a tight epithelial barrier forming. In particular, ARPE-19 cells generally expressed cytotokeratin-18, as does native human RPE, but some also expressed cytokeratin-7 which is not normally found in the RPE. Furthermore, the actin filaments did not form circumferential bands around the apical

surface of the cells under standard conditions. Only after six weeks in culture in SM3 was there an apparent re-organisation of the actin filaments with the upregulation of associated junctional proteins. Claudin expression also varied in type, distribution and quantity amongst the ARPE-19 cell populations. Because the claudins form the intercellular tight junctions this heterogeneity would account for the inability of this cell line to form fully mature tight junctional complexes with an associated rise in the TER.

2.15.1 Summary

The importance of the culture conditions on the TER of ARPE-19 cells was demonstrated by the responses obtained with SM2 medium. The glial induction of ARPE-19 cells was not successful despite an increase in the TER of ECV304 cells. The up-regulation of barrier properties in ARPE-19 may be the limited owing to their adult origin and heterogeneity of expression of junctional proteins that vary with culture conditions.

3 Ussing Chambers

3.1 Introduction

Establishing a suitable *in vitro* model in which to explore the alcohol-EOG was an aim of this part of the study. Previous work has established that bovine RPE responds to ethanol when added to the apical and basal surfaces (Pautler, 1994; Bialek *et al.*, 1996). Furthermore, *in vivo* studies involving sheep (Knave *et al.*, 1974) and albino rabbits (Textorius *et al.*, 1985) have also demonstrated a response similar to the alcohol-EOG in man.

The site of action for ethanol is unknown and may involve the retina, the apical or basal membranes of the RPE or may have an intracellular target or involve any combination of these sites. The most likely of these however would be that ethanol acts upon the basal membrane given that the oral dose would reach this surface initially at the highest concentration. However, Pautler, (1994) added ethanol to both the apical and basal baths simultaneously which meant the location of the ethanol receptor could have been on either side of the RPE. In contrast, Bialek *et al.*, (1996) added ethanol only to the apical side and demonstrated an alcohol response which suggests that an ethanol receptor is localised to the apical membrane. The highly lipophillic nature of ethanol would not exclude it from traversing the basal plasma membrane and interacting with an apical or intracellular receptor. If ethanol only elicited a response from the apical or basal surface or when the retina was in place then this would limit the number of potential targets for ethanol given the different distribution of ionic channels and receptors on the apical and basal plasma membranes of the RPE.

Bovine RPE has some advantages and some disadvantages for this study. The advantages are that bovine eyes are readily obtainable and an ethanol response has been demonstrated in this species. The number of studies utilising bovine preparations has led to a good knowledge of the ionic channels, transporters as well as the intracellular signalling pathways present in this species (Frambach *et al.*, 1989; Miller and Edelman, 1990; Joseph and Miller, 1991; Peterson *et al.*, 1997; Rymer *et al.*, 2001).

The study of Pautler, (1994) into ethanol's interaction with bovine RPE concluded that ethanol was interacting with a primitive light sensitive G-protein coupled receptor. Furthermore, Pautler did not detect any alterations in the intracellular [Ca^{2+}] from bovine eye-cups incubated with 0.5% ethanol which implied that Ca^{2+} was not the intracellular signal utilised by ethanol. However, Ca^{2+} is believed to be central to the light-EOG is also probably involved in the alcohol-EOG given the similarities between the responses (Arden and Wolf, 2000a, b; Marmorstein *et al.*, 2006; Rosenthal *et al.*, 2006). This suggests that the bovine alcohol response may differ to man. Furthermore, the observation of Pautler that the alcohol response was dependent on light also differs to man where the alcohol-EOG is performed on the dark adapted eye (Knave *et al.*, 1974; Skoog *et al.*, 1975; Arden and Wolf, 2000b).

Bialek *et al.*, (1996) found that ethanol increased the basolateral conductance of bovine RPE. In this study the basal membrane depolarised and the TEP increased when 0.1% ethanol was

added to the apical bath. No further investigation was undertaken by the group as to the likely receptor or mechanism that led to these changes.

Rana have similarly been used to investigate the properties of the RPE in a number of studies (Oakley II *et al.*, 1978; Miller and Farber, 1984; Griff *et al.*, 1985; Hughes *et al.*, 1989; la Cour, 1991). One advantage of using frog was that this preparation can be used at room temperature and the delay in post-mortem time could be minimised. No previous studies have investigated the electrophysiological effects of ethanol on the RPE of *Rana*. However, there are also some species differences between man and amphibian with respect to the pharmacology of the basolateral chloride channels.

ARPE-19 cells were also used in an Ussing chamber to investigate the alcohol-EOG.

3.1.1 The Ussing Chamber

The advantages of using an Ussing chamber are that the RPE retains its cell-cell contacts and the interactions between the RPE and the retina may be explored in detail (Ussing, 1953; Voüte and Ussing, 1968). A typical Ussing chamber consists of two chambers that are separated by the epithelium. A voltage and current electrode are placed in the apical and basal baths and the changes in voltage and current are recorded differentially with an amplifier. The chamber design allows for rapid changes of bath solution as well as the addition of agonists or inhibitors to investigate their effects on the TEP and TER (Miller and Steinberg, 1977; Quinn *et al.*, 2001; Rymer *et al.*, 2001).

In this study, the Ussing chamber provides an ideal means to determine the likely pathway by which ethanol acts upon either the retina or the RPE. By monitoring changes in the TEP and the TER over time following the addition of ethanol there should be a rise in the TEP that correlates to the alcohol-rise of the alcohol-EOG and a fall in the TER as the presumed basolateral Cl^- channel opens. Inhibition of the response with drugs would then identify the alcohol-receptor responsible for the alcohol-EOG.

As discussed, the TEP is defined in the RPE as the difference between the basal and apical membrane voltages ($TEP = V_{Basal} - V_{Apical}$). In the RPE, the TEP is positive with V_{Apical} at a more hyperpolarised potential than V_{Basal} at rest. To record the trans-epithelial resistance (TER) a two-second pulse of 4 - 10 mV was applied across the tissue. The instantaneous current (I) is recorded and Ohm's law applied to give the TER which is then multiplied by the area of the tissue to give the TER in $\Omega.cm^2$. In the simplest case that was employed by Pautler (1994) to explore the alcohol-EOG in bovine RPE the TEP increased following the addition of ethanol. In a more advanced configuration, an intracellular electrode may be inserted into the tissue so that the changes in V_M could also be recorded (Bialek *et al.*, 1996).

3.2 Methods

3.2.1 Bovine

Bovine eyes from herds < 30 months old were obtained from an abattoir and transported on ice to the laboratory approximately two to four hours post mortem. The extra-ocular muscles were trimmed. A small ~2 mm incision was initially made with a razor blade at the limbus and then extended to separate the anterior and posterior chambers. The anterior segment and vitreous were removed and the eye-cup filled with buffer at room temperature. An 8 mm diameter disposable biopsy punch (WPI, Aston UK) was used to cut out a 'button' of sclera, choroid, RPE and retina from the non-tapetal mid-periphery of the posterior pole. The button was transferred to buffer where the RPE-choroid was gently removed from the sclera with fine scissors and the retina floated off (in some cases the retina was retained *in situ* for the experiment). The RPE-choroid was then transferred to a piece of trimmed hardened Whatman filter paper grade 541 with 25 - 50 μm pores (Sigma-Aldrich) and held between two circular Lucite plates with an aperture diameter of 4 mm. The plates and tissue were sealed by means of three screws that were tightened gently to avoid damaging the tissue. This insert was used in Ussing chamber 1.

3.2.1.1 Ussing Chamber 1

A modified Ussing chamber (WPI) was used with 5 ml of buffer to each of the apical and basal hemi-chambers. Each half chamber was designed with recessed sections to accommodate the mounted tissue where it was clamped between the two halves. The 4 mm diameter disc of tissue acted as the barrier between the two compartments. Buffer for Ussing chamber 1 (see table 3.1 page 98) was circulated gently through the system by bubbling humidified 5% CO_2 and 95% O_2 into the buffer. The buffer's pH was adjusted to 7.5 ± 0.1 before use by bubbling it with 5% CO_2 and 95% O_2. The buffer's temperature was controlled by circulating water at 38°C through an outer glass jacket that surrounded the buffer as it circulated within the Ussing chamber. The temperature of the buffer inside the Ussing chamber was monitored by a bead thermister placed at the opening of the Ussing chamber's fluid inlet. Stock buffer was kept in a separate circulating water bath at 37°C until being added to the chamber when a fresh preparation was inserted.

An ECV4000 amplifier and pre-amplifier (WPI) was used to record the TEP. Initially a blank insert was placed in the Ussing chamber containing a piece of filter paper described earlier with 5 ml of heated buffer added to the apical and basal baths and voltage electrodes connected. The electrode offset was zeroed after ten minutes with the built-in potentiometer of the amplifier. Electrodes were monitored to ensure no drift was present before the Ussing chamber was opened and the insert containing the preparation added. Tissues with a TEP of > 2 mV were considered viable for all of the bovine experiments (Miller and Edelman, 1990). The ECV4000 also recorded the TER but the sensitivity was too low for these values to be of any practical use

and are not shown. The main reason was that the Ammeter had a resolution of ± 1 μA which did not permit changes in the TER of ~ 5 Ω.cm^2 as reported by Bialek *et al.*, (1996) to be resolved. In the study of Pautler, the TERs were not reported.

Recordings of the TEP were made initially at five-minute intervals for thirty minutes to allow the preparation to stabilise and then at one to two minute intervals once ethanol was added to the apical bath. Ethanol (1 ml of 0.5% vol/vol) was added to the apical bath after the removal of 1 ml of buffer to give a final concentration of 0.1% ethanol in the apical bath.

Electrodes (WPI) were Ag/AgCl pellets with an Agar salt bridge that was prepared by heating 3 grams of agarose in 100 ml of buffer and injecting the heated agar mixture into the casing of the Ag/AgCl pellet and allowing the agar to set. Figure 3.1 shows a schematic of the WPI Ussing chamber system with pre-amplifier.

Figure 3.1 Ussing Chamber 1

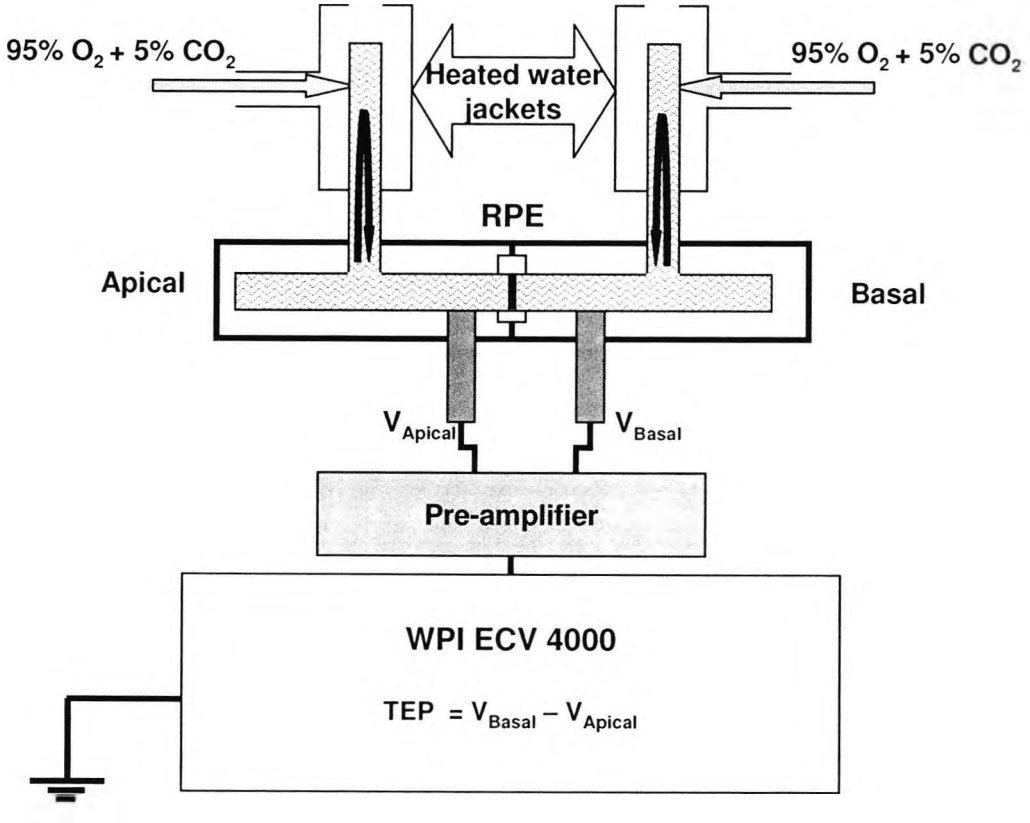

Ussing chamber with glass water jacket heated by circulating water maintained at 38°C. Gentle bubbling of the solution with humidified gas (5% CO_2 + 95 % O_2) circulated the buffer (dark arrows). Baseline potential was set to zero by placing a blank insert into the Ussing chamber and zeroing the potential difference with the potentiometer after five to ten minutes. The blank insert was removed and the one containing the bovine RPE tissue was mounted in the Ussing chamber. The black bar that separates the apical and basal baths indicates the RPE.

3.2.1.2 Ussing Chamber 2

The second chamber consisted of a 100 ml glass reservoir divided with a removable lucite carrier that held the bovine preparation with an aperture diameter of 3 mm. The carrier formed two 50 ml half chambers into each of which a voltage and current electrode were fixed in place. The preparation of the tissue was identical to that described for Ussing chamber 1. However, the carrier was a different design that enabled the tissue to be sealed gently between two interlocking Lucite plates with vacuum grease (Dow Corning, USA) applied lightly around the periphery of the tissue edge. The pressure to seal the two plates together was considerably less than that in Ussing chamber 1 where the tissue was clamped between two discs by means of tightening three screws. In this series, 1 mM glutathione was incorporated into the buffer and the gas switched to (5% CO_2, 10 % O_2 and 85%). Lowered pO_2 and glutathione are reported to increase the longevity of the tissue (Winkler and Giblin, 1983; Miller and Edelman, 1990). The pH was adjusted to 7.5 ± 0.1 before use with 5% CO_2, 10 % O_2 and 85% N_2. For details of buffer, see (table 3.1 page 98). The ionic composition of the buffer was also altered to reduce the $[K^+]$ to 5 mM and increase the $[Ca^{2+}]$ to 1.8 mM and D-glucose to 10 mM (Maminishkis *et al.*, 2002).

Recordings of instantaneous voltage and current were made at thirty-second intervals with a Keithley Multimeter 2700. (Keithley instruments, Ohio, USA) Data was stored in an Excel™ spreadsheet using ExceLinx™ (Keithley) for later analysis. The TER was calculated by dividing the TEP with the instantaneous current and multiplying this resistance by the area of the chamber aperture (0.07 cm^2). Absolute ethanol was added to either the apical or basal bath to give a final concentration of 0.2% or 0.5% ethanol after the electrical parameters were stable. To determine if ethanol may be acting directly upon the retina, 0.2% ethanol was added to the apical bath in preparations with the retina in place. The electrodes were the same as the ones used in Ussing chamber 1. Figure 3.2 overleaf is a schematic of the second Ussing chamber design.

The mean of the voltage and current offset for the preceding five minutes before the preparation was added to the chamber was subtracted from the subsequent recordings with the tissue in place.

Figure 3.2 Ussing Chamber 2

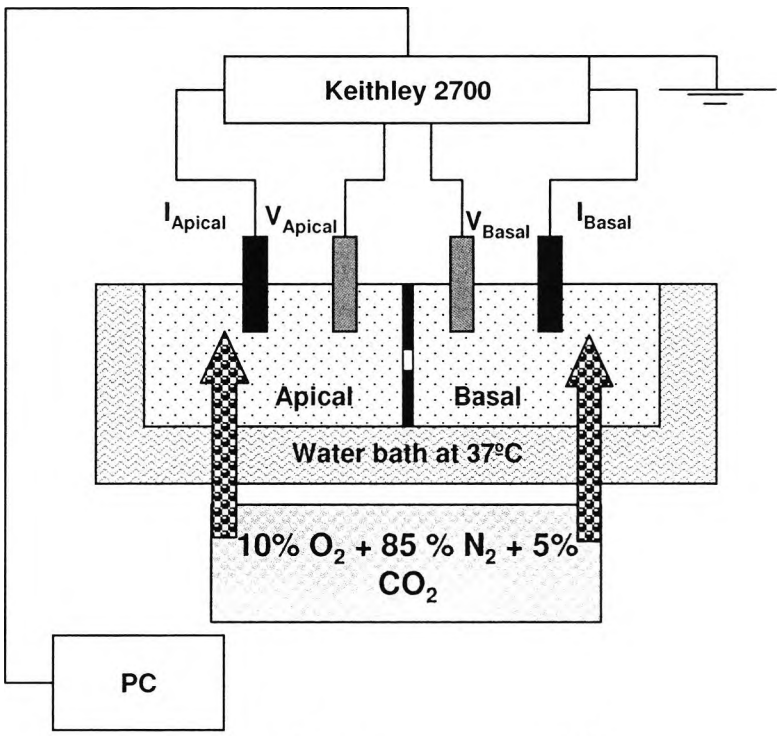

$$TEP = V_{Basal} - V_{Apical} \quad (mV)$$

$$TER = [TEP/(I_{Basal} - I_{Apical})] \times Area \quad (\Omega.cm^2)$$

Schematic representation of the second Ussing chamber used for bovine RPE tissue. The glass Ussing chamber was placed in a water bath maintained at 37˚C. Gas was gently bubbled into the apical and basal baths. Voltage and current electrodes were fixed into the apical and basal baths and the differential instantaneous voltage and current were recorded at 30 second intervals with the Keithley 2700 multimeter. The values were stored on a computer hard drive.

3.2.2 Rana

All animal procedures were performed in accordance with the Association for Research in Vision and Ophthalmology *Statement for the Use of Animals in Ophthalmic and Vision Research.*

Rana Temporaria were pithed before decapitation and the eyes carefully cut away from the head and placed in buffer solution (see table 3.1 page 98) at room temperature. The buffer was pre-gassed with humidified 5% CO_2, 10% O_2 and 85% N_2 to give a pH of 7.5 ± 0.1. Each eye was bisected at the equator with a razor blade and the anterior section discarded. Excess vitreous was removed with absorbent tissue paper and the eye-cup mounted on the lower half of an Ussing chamber. For this experiment one of the half chambers from Ussing chamber 1 was used

with the eye-cup mounted in the central aperture and the earth and active electrodes inserted into the luer fittings.

Electrodes were 3% (w/v) agarose dissolved in the buffer for *Rana* eye-cup experiments. The apical electrode contained a single surgical silk thread (2-0) Mersilk™ (Johnson and Johnson Intl, Brussels, Belgium) that was moistened with buffer. The apical electrode was held in place with a micromanipulator (WPI) and lowered so that tip of the silk thread just made contact with the meniscus of buffer that filled the eye-cup. Additional buffer was added to the eye-cup as required which was typically at five to ten minute intervals. One drop of 0.1% or 0.2% ethanol in buffer was added to the retinal surface with a Pasteur pipette at suitable intervals (~ 20 - 30 minutes). The baseline was established prior to the addition of the eye-cup by lowering the tip of the apical electrode into the basal bath and waiting approximately ten to fifteen minutes for the potential difference to stabilise. This potential was then subtracted from the resulting voltage when the eye-cup was added. Recordings of the differential voltage were made at twenty second intervals using the Keithley 2700 multimeter and stored directly in an Excel™ spreadsheet using ExceLinx™ (Keithley).

In order to establish that the RPE-retina were still functional an EOG was performed on the eye-cup. The light source for the EOG was a 100 W incandescent lamp placed 15 cm from the eye-cup. Background room luminance was 70 cd/m^2 and in darkness 0.01 cd/m^2 and with the lamp switched on the luminance was 530 cd/m^2. (Minolta Chroma meter, CS100, Japan). Figure 3.3 overleaf shows the schematic diagram of the Ussing chamber used to record from the eye-cup.

Figure 3.3 Eye-Cup Chamber for *Rana*

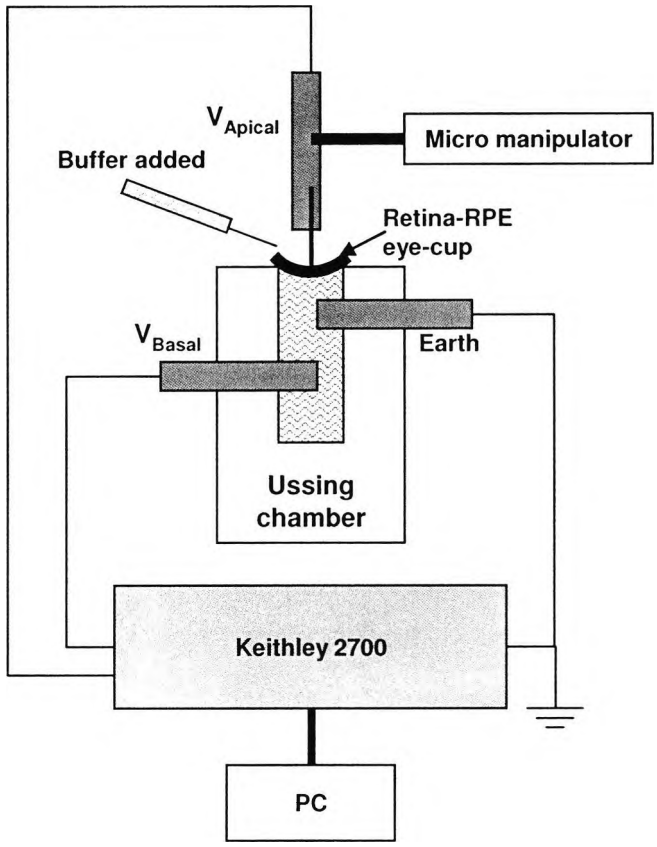

Schematic representation of the modified Ussing chamber used for the Rana eye-cup experiments. The eye-cup was placed in a cylinder with two electrode ports that contacted the buffer. This was one of the half chambers from Ussing chamber 1. The apical electrode contained a silk thread which was gently lowered onto the apical surface of the eye-cup. Buffer and drugs were added periodically with a Pasteur pipette. The eye-cup potential was recorded directly with the Keithley 2700 multimeter and was taken as the difference between V_{Basal} and V_{Apical}.

3.2.3 ARPE-19

ARPE-19 cells were grown under standard culture conditions before being seeded onto laminin coated Transwell™ filters as described in sections 2.6.1 and 2.6.3.1. The serum was reduced to 1% FCS and the TER monitored over time with the EndOHM™ voltohmmeter (as described in section 6.5.1). Constituents of the ARPE-19 buffer are detailed in table 3.1 on page 98. The buffer was prepared and gassed with 10% O_2, 5% CO_2, and 85% N_2 to a pH of 7.4. 25 ml aliquots were then filtered through a 0.22 μM nylon pore (Corning), and stored at 37°C in a water bath.

The inserts were then mounted in an Ussing chamber designed to support the Transwell™ inserts (WPI) containing 5 ml of solution in the apical and basal baths respectively as described in Ussing chamber 1. Voltage electrodes were connected to the board of the Keithley multimeter and voltage differences were recorded at thirty second intervals and stored on an Excel™ spreadsheet using ExceLinx™ (Keithley). Approximately five to ten minutes was required to stabilise the potential difference between the electrodes.

3.3 Buffers and Drug Preparation

All solutions were prepared on the day of the experiment in double distilled water (ddH_2O) using analytical grade chemicals (Sigma-Aldrich). The composition of the buffers are listed in table 3.1.

Table 3.1 Buffer Composition for Ussing Chambers

Solute	Bovine Ussing 1 (mM)	Bovine Ussing 2 (mM)	*Rana* (mM)	ARPE-19 (mM)
NaCl	118.0	120.0	100.0	125.0
KCl	0.8	0.8	1.8	4.8
$MgSO_4$	1.6	1.0	1.0	0.8
$CaCl_2$	1.6	1.8	1.8	1.8
KH_2PO_4	1.2	1.2	0.2	0.2
$NaHCO_3$	25.0	23.0	10.0	10.0
D-Glucose	6.6	10.0	10.0	5.6
Glutathione	—	1.0	—	—
BSA w/v (%)	0.01	0.01	—	—
pH	7.5	7.5	7.5	7.5

List of the ionic composition of buffers used in the Ussing chamber experiments.

3.3.1 Ethanol

Ussing chamber 1: Absolute ethanol was diluted to a 0.5% (vol/vol) working concentration (50 μl ethanol (Analytical Grade): 10 ml of buffer). 1 ml of the apical bath solution was removed and replaced with 1 ml of 0.5% ethanol solution giving a final concentration of 0.1% ethanol in the apical bath.

Ussing chamber 2: With a larger volume in the apical and basal baths of 50 ml it was possible to add absolute ethanol to the bath directly. For 0.2% (vol/vol) 100 μl ethanol was added and for 0.5% (vol/vol) 250 μl of ethanol was added to each bath with an equal volume of buffer removed prior to the addition of ethanol.

Rana: For the *Rana* eye-cup, ethanol (0.1% and 0.2%) was prepared in buffer solution and added to the eye-cup as required.

3.3.2 Epinephrine and Ouabain

Epinephrine hydrochloride (MW 219) and ouabain octahydrate (MW 729) were dissolved in 100 ml of buffer to prepare a working concentration of 1 mM epinephrine and 10 mM ouabain respectively. 50 μl of these stock solutions were added to the apical bath of Ussing chamber 2 with an equal volume removed of circulating buffer (dilution 1:1000). All drugs were kept at 4°C and protected from the light until use.

Epinephrine and ouabain were used to test the viability of the tissues and to ensure that the drugs were reaching the aperture in the Ussing chamber. Circulation of the solutions was also observed by adding sodium fluorescein to the baths with a blank filter.

3.4 Data analysis

The results are expressed as mean ± SD unless otherwise stated. Student's unpaired, two-tailed t-tests were used to determine the significant differences between means, where $p < 0.05$ was taken as statistically significant. Statistical calculations were made using Microsoft Excel™.

3.5 Results

3.5.1 Bovine (Ussing Chamber 1)

From five out of six samples exposed to 0.1% ethanol in the apical bath at t=0 there was no increase in the TEP over time. Figure 3.4 shows the mean ± SEM of the TEP of the samples. Of these, only one showed a rise in the TEP of > 2 mV and is labelled 'response' (open circles).

No significant alteration in the TEP was observed at t=10 minutes compared to t=0 minutes when ethanol was added to the apical bath. The mean ± SD (N=5) of the TEPs at t=0 was 7.5 ± 3.0 mV and at t=10 minutes post ethanol (0.1%) the TEPs were 7.4 ± 2.1 mV (p=0.8396). The responding sample was not included in this analysis. The TEP at t=0 for this sample was 6.9 mV and at t=10 minutes the TEP was 9.2 mV representing a change in the TEP of +2.3 mV.

Figure 3.4 Bovine TEP in Ussing Chamber 1

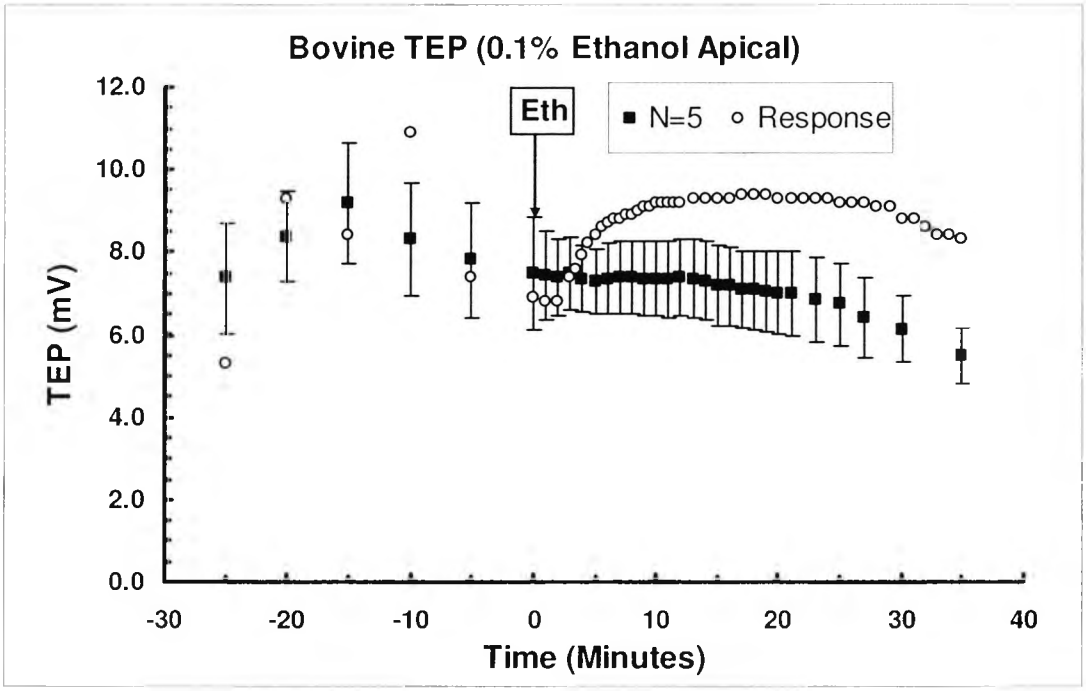

The TEP over time recorded from six bovine RPE preparations mounted in Ussing chamber 1. When 0.1% ethanol was present in the apical bath (arrow), no significant rise in the TEP was observed except from one sample (○). The Filled squares (■) show the mean ± SEM of five samples that did not show any response.

3.5.2 Bovine (Ussing Chamber 2)

In Ussing chamber 2 the preparations could be maintained for longer. Recordings were made of the TEP and the current at thirty-second intervals over time. The trace below (figure 3.5) shows a typical recording over two hours in which the electrical parameters remained stable. In this preparation, absolute ethanol was added to the apical or basal baths to give a final concentration of 0.2% or 0.5%. At the time points indicated by 'wash out' either the apical or basal bath was rapidly exchanged for fresh control buffer by aspiration which occasionally resulted in a shift in the trace. The bath in which ethanol had been added was replaced with control buffer. In the trace below the sample was added at t=8 minutes.

Figure 3.5 Bovine RPE in Ussing Chamber 2 TEP and TER

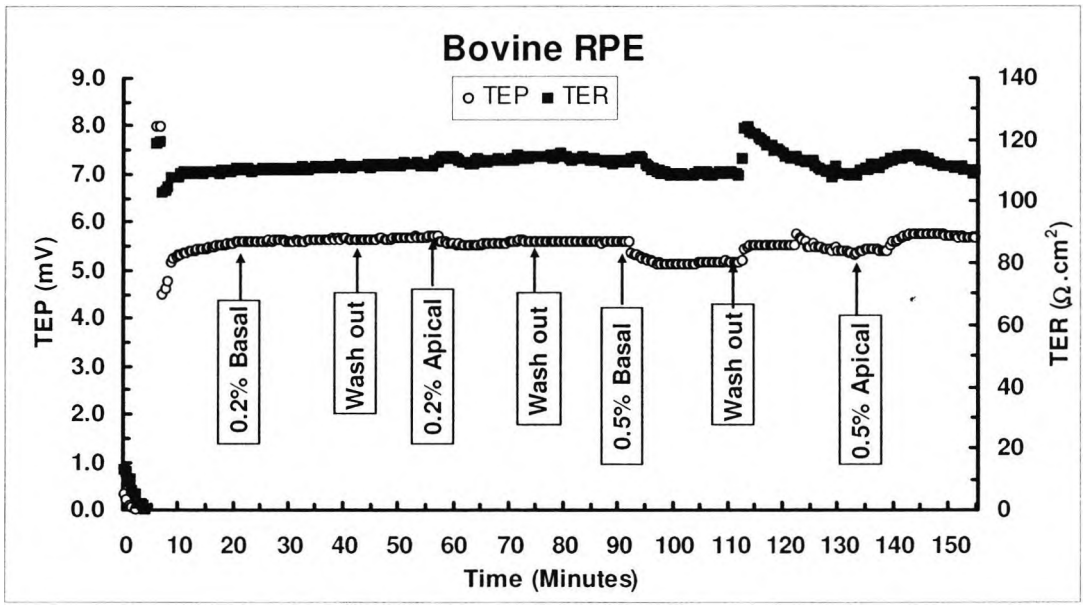

Bovine RPE maintained in Ussing chamber 2 and ethanol applied to the apical or basal baths in (0.2% and 0.5%). The TEP (○) and TER (■), did not change. Wash out indicates the removal of either the apical or basal bath depending upon which side the ethanol had been applied to.

In table 3.2 (overleaf) the mean ± SD of the TEP and TER are summarised for (N=2 and N=3) individual RPE explants with 0.2% and 0.5% ethanol in the apical bath and from 0.2% ethanol in the basal bath (N=3). No changes in either TEP or the TER were observed at 5, 10 or 15 minutes post ethanol dose.

Table 3.2 TEP and TER in Bovine RPE with Ethanol

Time (Min)	0.2% Ethanol Apical RPE (N=2)		0.5% Ethanol Apical RPE (N=3)		0.5% Ethanol Basal RPE (N=3)	
	TEP (mV)	TER ($\Omega.cm^2$)	TEP (mV)	TER ($\Omega.cm^2$)	TEP (mV)	TER ($\Omega.cm^2$)
-5	5.01 ± 0.55	136 ± 39	6.33 ± 2.32	133 ± 32	9.01 ± 2.32	98 ± 32
0	5.04 ± 0.46	132 ± 36	6.23 ± 2.43	133 ± 33	8.91 ± 2.43	98 ± 33
5	5.10 ± 0.46	129 ± 33	6.20 ± 2.46	134 ± 35	8.86 ± 2.46	98 ± 35
10	5.16 ± 0.44	129 ± 32	6.28 ± 2.46	135 ± 36	8.87 ± 2.46	98 ± 36
15	5.17 ± 0.42	138 ± 41	6.27 ± 2.44	136 ± 37	8.86 ± 2.44	97 ± 37

Combined results from the second Ussing chamber with ethanol applied to the apical or basal side of light adapted bovine RPE. No alterations in TEP or TER are evident following ethanol (0.2% or 0.5%) in the apical bath or ethanol (0.5%) in the basal bath at t=0 minutes. All values are mean ± SD.

3.5.3 RPE and Retina

When the retina was retained in the preparation and 0.5% ethanol was added to the apical side no alteration in the TEP or TER was observed at t=5, 10 or 15 minutes after the addition of ethanol. See table 3.3.

Table 3.3 Summary of Bovine RPE-retina with Ethanol

0.5% Ethanol Apical Bath with Bovine RPE-Retina (N=2)		
Time (min)	TEP (mV)	TER ($\Omega.cm^2$)
-5	10.90 ± 2.10	100 ± 8
0	10.97 ± 2.00	100 ± 8
5	11.05 ± 2.18	99 ± 7
10	11.09 ± 2.22	100 ± 8
15	10.95 ± 2.38	98 ± 8

The TEP and TER over time with the RPE-retina intact and mounted in Ussing chamber 2. No changes in the TEP or the TER were observed over this time interval. All values are mean ± SD.

Figure 3.6 shows a trace of Bovine RPE with the retina still *in situ* mounted in Ussing chamber 2 and challenged with 0.5% ethanol from the apical side. The preparation was added at t=10 minutes.

Figure 3.6 Bovine RPE and Retina Ussing Chamber 2

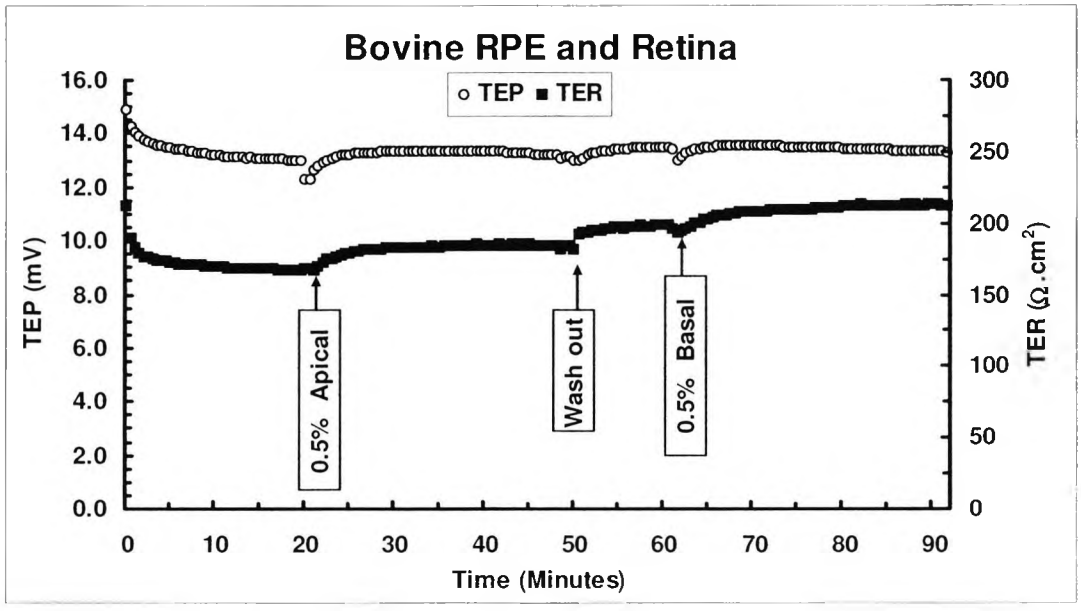

The TEP (○) and the TER (■) did not show any response to 0.5% ethanol in the apical bath. No response was observed when 0.5% ethanol was in the basal bath in this preparation.

3.5.4 Epinephrine and Ouabain

The result shown (figure 3.7 overleaf) is from one sample with epinephrine (1 μM) followed by an interval of sixty minutes in which the apical and basal bath solutions were replaced with buffer before replacing the apical bath with ouabain (10 μM). Epinephrine did increase the TEP slightly from 5.09 mV at t=0 to 5.19 mV at t=30 minutes and the TER fell from 244 $\Omega.cm^2$ at t=0 to 222 $\Omega.cm^2$ at t=30 minutes. These results are consistent with an increase in the basolateral membrane conductance caused by epinephrine from N=1 sample.

The addition of ouabain (figure 3.8 overleaf) also led to slight changes in the electrical parameters with a slight fall in the TEP from 4.24 mV at t=0 to 3.90 mV at t=30 minutes (N=1). The TER increased from 169 $\Omega.cm^2$ at t=0 to 185 $\Omega.cm^2$ at t=30 minutes consistent with the increased tissue resistance caused by the blockade of the apical NaKATPase pump.

Figure 3.7 Epinephrine (1 μM) and Bovine RPE (N=1)

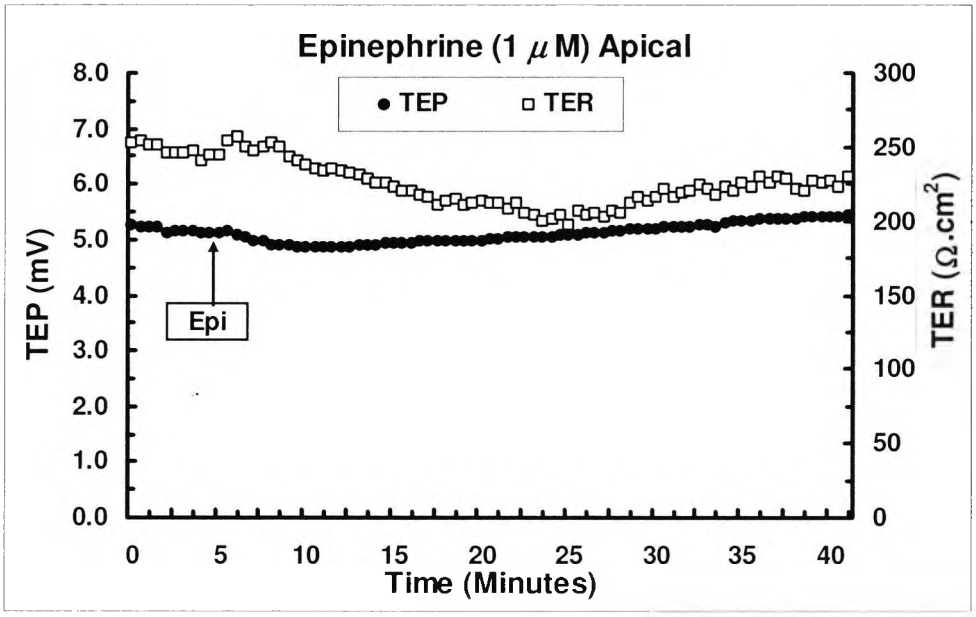

Epinephrine 1 μM final concentration in 50 ml of buffer was exchanged for the control 50 ml buffer at t=5 minutes (Epi). There is a slight increase in the TEP (●) and fall in the TER (□) (N=1).

Figure 3.8 Ouabain (10 μM) and Bovine RPE (N=1)

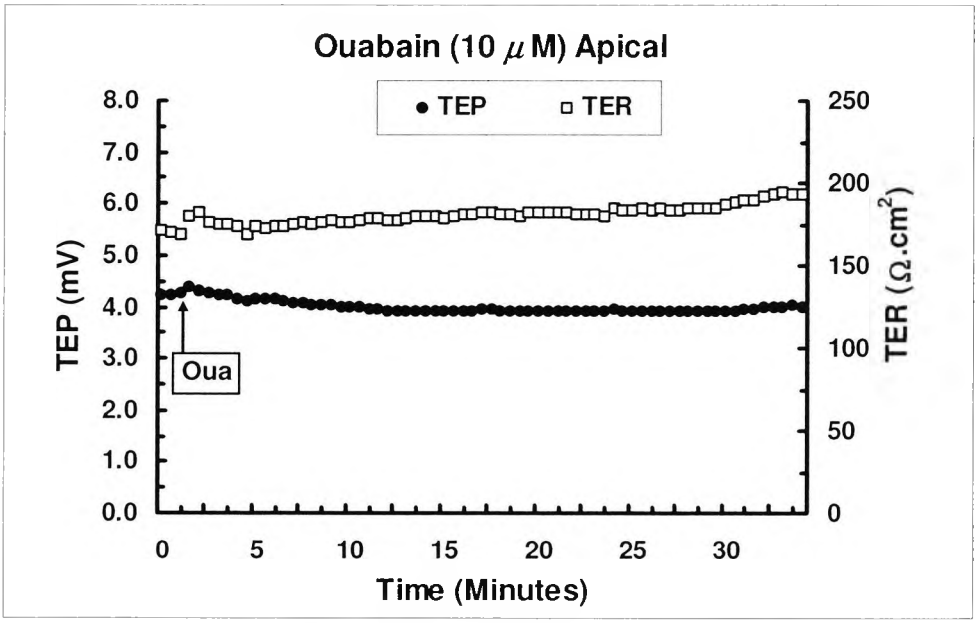

Ouabain 10 μM (Oua) added to the apical bath after one hour of wash out with control buffer following the initial trial with epinephrine. The TEP (●) falls slightly over time and the TER (□) rises slightly when ouabain was added (arrow). (N=1).

3.5.5 Rana

In the preparation shown in figure 3.9 the eye-cup, potential was measured directly following the addition of ethanol as well as a change in luminance to simulate the light-EOG in man. The peak eye-cup potential of 8.5 mV occurred approximately 7 minutes after the eye-cup was mounted in the modified Ussing chamber. Repeated application of 0.1% ethanol did not increase the eye-cup potential. However, when the background luminance was reduced to 0.01 cd/m^2 for ten minutes there was a sharp decrease in the eye-cup potential corresponding to the dark-trough of the EOG in man. Upon re-illumination to 530 cd/m^2 the eye-cup potential rose by 2 mV and peaked 5 minutes after light onset. This response corresponds to the light-rise of the EOG and demonstrates a functional RPE-retina despite the eye-cup potential being 50% less than at the start of the experiments. However, there was still no response to 0.2% ethanol after this period.

Figure 3.9 Rana Eye-Cup Response to Ethanol, Epinephrine and Light (N=1)

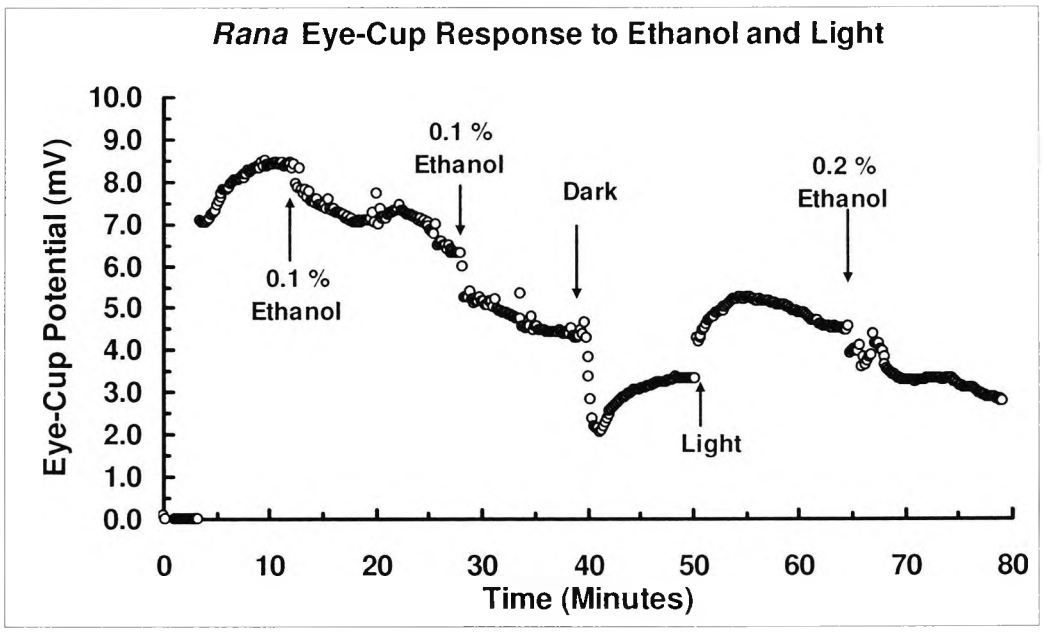

Rana eye-cup potential in response to 0.1% and 0.2% solutions of ethanol showed no increase in the potential. However, a distinct dark-trough and light-rise were evident indicating a functional RPE-retina complex. The small deflections in the trace at approximately 20 and 30 minutes are time points when fresh buffer was added. The eye-cup was added at t=4 minutes once the electrodes were stable. Recording from N=1 eye-cup.

3.5.6 ARPE-19 in Ussing Chamber

Figure 3.10 shows the mean ± SEM of 6 ARPE-19 cells mounted on Transwell™ filters with a mean ± SD TER of 18 ± 2 $\Omega.cm^2$ after one week in culture. The TEPs were small from 0.2 - 0.8 mV which were too low to perform reliable experiments. The mean ± SEM of the TEP at 30 minutes after insertion was 0.43 ± 0.24 mV (N=6).

Figure 3.10 TEP of ARPE-19 cells

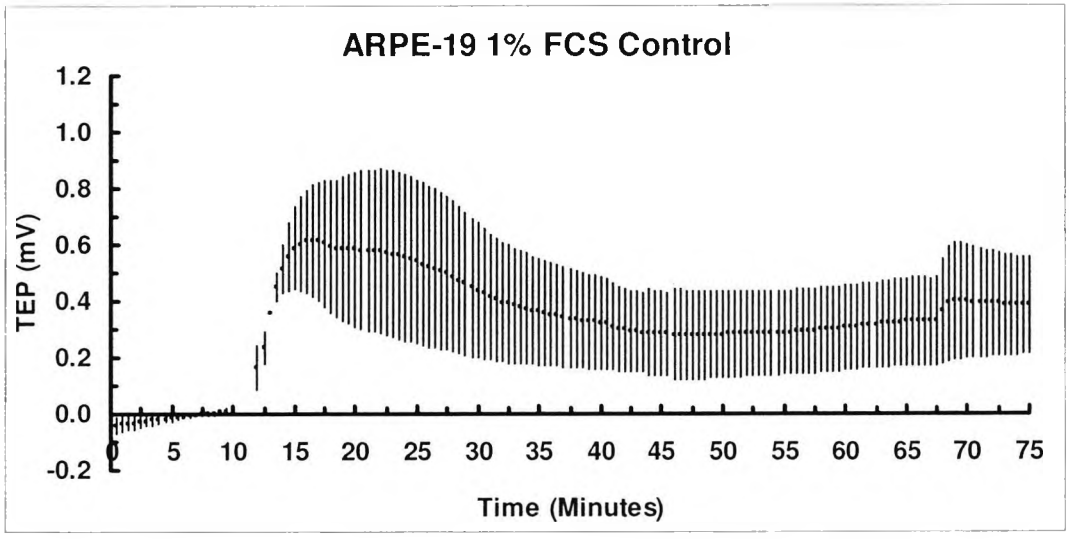

ARPE-19 cells mounted in an Ussing chamber failed to establish a high TEP. Plot shows mean ± SEM of six filters with the TEP recorded at fifteen-second intervals.

3.6 Discussion

The light-EOG has been demonstrated in numerous species besides man such as lizard (Griff and Steinberg, 1982), chick (Gallemore *et al.*, 1988; Gallemore and Steinberg, 1993), cat (Linsenmeier and Steinberg, 1982) and monkey (Valeton and van Norren, 1982). The alcohol-EOG has been demonstrated in man and in sheep (Knave *et al.*, 1974) but is absent in cat (Arden, personal communication). Studies using animal RPE preparations have contributed greatly to our understanding of the RPE's physiology and the interaction of the light-evoked responses generated across the RPE such as the light-rise and c-wave (Steinberg *et al.*, 1970, 1985; Griff and Steinberg).

The TEP and TERs recorded with the Ussing chambers were consistent with previously published work. Bovine RPE typically has a TEP of 6 - 9 mV and a TER of 100 - 200 $\Omega.cm^2$ (Miller and Edelman, 1990; Edelman and Miller, 1991; Joseph and Miller, 1991; Arndt *et al.*, 2001; Rymer *et al.*, 2001; Maminishkis *et al.*, 2002; Hillenkamp *et al.*, 2004a). The response to ethanol in bovine RPE preparations has been previously reported. In one study the effects of ethanol (0.1%) on the TEP and TER were assessed in control experiments carried out in a pharmacological study of the RPE (Bialek *et al.*, 1996). Using intracellular recordings from five cells (2 eyes) the authors reported that when ethanol was added to the apical bath the TEP increased by +1.5 ± 0.3 mV with a depolarisation of V_{Basal} of +3.7 ± 0.9 mV. The TER also fell by -5.4 ± 1.2 $\Omega.cm^2$. These findings are consistent with an action of ethanol to depolarise the basal membrane due to an increase in basolateral conductance that accounts for the fall in tissue resistance.

In a second study using bovine RPE, Pautler (1994) showed that the ethanol response was maximal in green light (λ = 530 nm) and only when the RPE was light-adapted. Pautler found that for a dose of 0.5% ethanol when applied simultaneously to the apical and basal baths in green light the TEP rose by 2.0 ± 0.46 mV (Pautler, 1994). Pautler's findings, though of interest, were not fully completed and would contradict the findings in man where ethanol administered in the dark clearly causes a rise in the ocular standing potential (Skoog *et al.*, 1975; Arden and Wolf, 2000b).

The results from the first Ussing chamber did show a rise in the TEP for one preparation only with a similar change in the TEP as previously reported. In the current study, 0.1% ethanol was used which was lower than the dose used by Pautler. This lower dose was used as in man the estimated concentration of ethanol reaching the RPE is sub millimolar (Wolf and Arden, 2004). The higher doses used by Pautler may explain the more consistent results he observed.

This low number of successful trials with Ussing chamber 1 led to alterations in the buffer composition, the gas and the Ussing chamber design in an effort to obtain more consistent results. The modifications to the buffer and gas were in line with that of Mamishikis et al (2002). The addition of glutathione together with a reduction in pO_2 also increased the longevity of the

tissue. The second Ussing chamber design may have been better with the larger volume of circulating buffer and the tissue was sealed more gently with vacuum grease rather than screws which may have reduced the tissue's edge damage. After one hour in the first Ussing chamber, the TEPs had fallen by approximately 33%. In the second chamber tissues survived for two hours with no reduction in the electrical parameters. The tissue area was reduced to 0.07 cm^2 and the recordings of current to ± 0.01 μA enabled the TER to be calculated with greater accuracy. Ussing chamber 1 had been used for a previous study investigating taurine transport across the RPE and so it is unlikely that ethanol was not reaching the apical surface (Hillenkamp *et al.*, 2004a, b).

When the low ethanol dose of 0.1% was used in the apical chamber, no effects were seen on the TEP or TER. Consequently, the dose was increased to 0.5% in line with that of Pautler but still no responses were apparent when added to either the apical or the basal chambers. When the retina was retained on the RPE, there was similarly no alterations in the TEP or TER by ethanol.

To test the viability of the tissue two drugs were used that are known to alter the electrical parameters of bovine RPE in one sample. Epinephrine at 0.1 μM causes a sharp increase in the TEP of bovine RPE of approximately +2.4 mV with a fall in the TER (Edelman and Miller, 1991). In the trial epinephrine at a concentration of 1 μM did result in a modest increase in the TEP of 0.1 mV and a fall in the TER of 22 $\Omega.cm^2$ over a thirty minute interval. This result suggested that the drug was reaching the tissue but that either the receptors or the intracellular signalling pathway was impaired due to the post mortem delay. Epinephrine is known to act on the RPE via the G-protein coupled α_1-adrenergic receptor resulting in an increase in $[Ca^{2+}]_{in}$ and increased basolateral Cl^- conductance (Edelman and Miller, 1991; Rymer *et al.*, 2001).

Ouabain (0.1 mM) inhibits the apical NaKATPase pump, and in bovine, this results in a decrease in net Na^+ transport across V_{Apical} which depolarises this membrane and results in a fall in the TEP. The results in the preparation also showed a small fall in the TEP consistent with an effect of ouabain at the apical membrane but not of the same magnitude as reported by Miller's group who found that V_{Apical} depolarised at a rate of ~ 9 mV/min (Joseph and Miller, 1991).

The unresponsiveness of the bovine preparations in the second chamber and the inconsistent changes in the first chamber could be the result of several factors. One is that the apical membrane was damaged during the removal of the retina so that the apical receptors were impaired. Secondly, the delay of approximately 4 - 6 hours from the time of slaughter to mounting the tissues in the Ussing chambers was longer than the forty minutes reported elsewhere (Joseph and Miller, 1991; Rymer *et al.*, 2001). The bovine eyes were transported in an ice-box to the laboratory which maintained them at close to 4°C before storage in a refrigerator at 4°C. The experiments were performed over an 8 – 10 hour period and so the actual time from slaughter would have been in some cases greater than 4 hours.

One study into the viability of RPE from porcine recommended that that the eyes be removed immediately following slaughter and the tissue rapidly cooled (Steuer *et al.*, 2004). The time from slaughter to the removal of the eyes and packaging in the ice-box were unknown. The percentage of viable cells in porcine RPE if stored at 4°C after four hours was ~ 80% and therefore, the number of viable cells in the RPE of the bovine preparations would have been also compromised by the delay in receiving the tissue. These factors, despite the satisfactory electrical parameters of the preparations, may have contributed to the lack of responses seen by ethanol and the smaller changes in the TEP observed with epinephrine and ouabain that have been previously reported.

Therefore, in order to decrease the post-mortem time *Rana Temporalia* was investigated. In part, this was to exclude a role of the retina in generating the alcohol-EOG as well as to investigate another species given the lack of consistent responses from the bovine material. The ease of working at room temperature was seen as another advantage. One eye-cup was successfully prepared with a TEP close to the range of previously reported values for *Rana* RPE preparations (typically 11 - 14 mV) (Miller *et al.*, 1978; Miller and Farber, 1984).

From the preparation, no alteration in the eye-cup potential was seen with ethanol. The eye-cup still retained close retina-RPE contact and was not compromised given the clear dark-trough and light-rise that were present. The response that replicated the light-EOG in man demonstrates that the intracellular signalling pathway and cell surface receptors necessary for this response were still functional.

The addition of ethanol to the apical retinal surface did not alter the eye-cup potential and this would imply that either ethanol does not liberate a substance from the retina to alter the standing potential in frog. In man, the bulk of the ethanol dose would arrive at the basolateral side of the RPE owing to the large choroidal supply relative to the inner retina. Therefore, the apical administration of ethanol in this model would be the least likely site of action for ethanol. The role of ethanol on the rod outer segment currents is unlikely given that oral ethanol (750 mg/kg) increases the b-wave slightly but does not alter the a-wave of the ERG (Ikeda, 1963). Therefore, any retinal interactions are distal to the RPE. Furthermore, the studies of Pautler and Bialek have shown a direct action of ethanol on the RPE and so the RPE remains the most likely site of ethanol's action in generating the alcohol-EOG.

One difficulty in using non-human animal species is that differences in the signalling pathways are known to exist between man and bovine and *Rana*. The two major differences identified are in the action of inhibitors on the cAMP gated chloride channels and the chloride transport by cAMP. DIDS inhibits frog and bovine cAMP activated chloride currents but in man DIDS is ineffective at blocking the cAMP current when applied extracellularly (Miller and Edelman, 1990; Anderson and Welsh, 1991; Fujii *et al.*, 1992; Hughes and Segawa, 1993; Bialek and Miller, 1994).

Intracellular signalling is also different in bovine and man with the regulation of $[Ca^{2+}]_{in}$ affected by second messengers at the level of the ER (See Section 1.4). However, cAMP increases basolateral Cl^- conductance in man and depolarises V_{Basal} whilst in bovine cAMP hyperpolarises V_{Basal} indicating a difference between these species in the way that cAMP and Ca^{2+} regulation is controlled at the ER as this response is not seen when the endoplasmic reticulum calcium ATPase (ERCA) pump is inhibited (Peterson *et al.*, 1998; Quinn *et al.*, 2001).

ARPE-19 cells have not been studied in any Ussing chamber configuration. This is undoubtedly due to the low TEP and TER developed when compared to animal tissues. ARPE-19 have been used for transport studies using the same Ussing chamber design but no electrical parameters were reported (Zhang *et al.*, 2006). The low TERs of the ARPE-19 cells now seem likely to be an result of the heterogeneity of this cell line with respect to phenotype and the junctional proteins expressed (Luo *et al.*, 2006).

One additional difficulty with mounting the Transwell™ insert in the Ussing chamber was the need to separate the two half chambers after stabilising the electrode offset with a blank filter. The potential drift encountered with the new buffer although held at the same temperature was of the order of ± 0.1 mV which introduced a large variable error into the measured TEPs. Furthermore, there was potentially damage to the ARPE-19 monolayer at the edges of the insert as the tissue was not clamped into a holder as in the bovine experiments that would induce leak current and a reduced TEP. It was hoped that a method for increasing the TER of ARPE-19 cells through co-culture or by modifications of the culture medium would have been possible. This would have increased the likelihood of obtaining results in an Ussing chamber. However, both cell-culture and the animal explants of RPE tissue failed to provide a suitable model with which to investigate the alcohol-EOG in man.

3.6.1 Summary

The initial Ussing chamber experiments with Bovine RPE did not produce a response when ethanol was added at a concentration similar to those previously used to alter the TEP. A further modification to the chamber and buffer did not produce any responses. The failure of epinephrine and ouabain to alter the TEP and TER significantly indicated that these tissues were not sufficiently viable to produce an ethanol response. In one trial with a *Rana* eye-cup, the lack of an ethanol response may reflect the species difference or that ethanol does not release a substance from the retina in *Rana*. The culture of ARPE-19 cells did not produce a suitable TEP with which to gauge accurately the effects of ethanol on this monolayer under these conditions.

4 Ca^{2+}-Signalling and Ethanol

4.1 Introduction

The RPE's basal membrane has two types of chloride channel that could be responsible for the alcohol-EOG. One is gated by cAMP and the other is gated by Ca^{2+}. The cAMP dependent PKA gated chloride channel is likely to be CFTR and the Ca^{2+}-gated channel could be one of the bestrophin isoforms (hBest 2-3) or a CaCC (Reigada and Mitchell, 2005; Marmorstein *et al.*, 2006). If ethanol can cause a rise in $[Ca^{2+}]_{in}$ by a direct interaction with the RPE then this would favour the model in which a Ca^{2+}-gated chloride channel was responsible for the alcohol-rise. One method to determine changes in $[Ca^{2+}]_{in}$ is to use a fluorescent probe that binds to cytosolic free Ca^{2+}.

Ca^{2+} has long been suspected to be involved in the development of the light-rise (Hofmann and Niemeyer, 1985; Peterson *et al.*, 1997). The standard model was that light liberated the light-rise substance that increased intracellular Ca^{2+} that then gated open bestrophin which was presumed to be the basolateral chloride channel finally responsible for the light-rise. However, recent findings now suggest that this process is more complex and that bestrophin is not necessarily the basolateral chloride channel responsible for the light-rise. However, Ca^{2+} is the intracellular signal that evokes the light-rise (Marmorstein *et al.*, 2006; Rosenthal *et al.*, 2006).

Mutations in the gene encoding bestrophin, (Vitelliform Macular Dystrophy) *VMD2*, are responsible for several maculopathies including Best's disease (Marquardt *et al.*, 1998; Petrukhin *et al.*, 1998). Typically Best's disease has an early age of onset and is characterised by a loss of the light-rise (Thorburn and Nordstrom, 1978; Weleber, 1989; Pinckers *et al.*, 1996; Ponjavic *et al.*, 1999) which has implicated bestrophin in the generation of this response. However, there has been a report of normal light-rises in a family with mutations in *VMD2* suggesting that bestrophin may not be involved in this process (Pollack *et al.*, 2005). Furthermore, adult onset vitelliform macular dystrophy is also caused by mutations in *VMD2* but the light-rise is preserved (Seddon *et al.*, 2001).

The link between bestrophin, Ca^{2+} and the light-rise was made when transfection of hBest1 into HEK 293 cells resulted in a Ca^{2+}-activated chloride current (Sun *et al.*, 2002). Similar findings were observed when bestrophin from *Xenopus*, were also expressed in HEK 293 (Qu *et al.*, 2003). The chloride currents were all reduced when mutated bestrophins were expressed. There are four human homologues of human bestrophin (hBest1-4) with hBest1 displaying a slight rectification (Tsunenari *et al.*, 2003). Of the homologues mutations in hBest1 account for 60% of the clinical cases of Best's disease and consequently the relationship between hBest1 and the light-rise has been closely examined.

The first piece of evidence that bestrophin may not be the chloride channel responsible for the light-rise was that when bestrophin (hBest-1) was over-expressed in rat there was no increase in the light-rise amplitude and it was instead reduced (Marmorstein *et al.*, 2004). In the same study, the authors also found that when mutant bestrophin genes were expressed in rats the light-rises

were reduced, but not abolished as would be predicted if bestrophin was the sole chloride channel responsible for the basolateral membrane depolarisation (Marmorstein *et al.*, 2004).

The second important finding was that the hBest1 isoform increased the kinetics of the L-type Ca^{2+} channel so that the rate of Ca^{2+} entry was greater. Bestrophin also altered the properties of the L-type Ca^{2+} channel so that the membrane voltage at which Ca^{2+} entered the cell was nearer to the resting membrane potential. This implied that bestrophin was important at influencing the timing and the probability of an L-type Ca^{2+} channel opening (Rosenthal *et al.*, 2006).

Finally, the most recent study using mice by Marmorstein *et al.*, (2006) with disrupted *Vmd2* so that they expressed no functional bestrophin and compared the light responses to the wild-type *Vmd2* bestrophin expressing strain. The authors found that inhibition of the L-type Ca^{2+} with nifedipine reduced the light-rise by 35%. This finding supports a role for the L-type Ca^{2+} channel in generating at least a part of the Ca^{2+} signal required for the light-EOG. Furthermore, when the possible light-rise substance, ATP was used to increase $[Ca^{2+}]_{in}$ in RPE cells derived from *Vmd2* null mice, the ATP stimulated $[Ca^{2+}]_{in}$ was found to be five fold higher in the *Vmd2* deficient RPE cells than the control cells expressing bestrophin. This suggested that bestrophin was inhibiting $[Ca^{2+}]_{in}$ through modulation of the L-type-Ca^{2+} channel. A further significant finding was that whole cell chloride currents were not reduced in the *Vmd2* null mice compared to controls. The light-rises of the mice with a defect in the β_4-subunit of the voltage gated Ca^{2+} were slowed compared to controls. It now appears that bestrophin (hBest1) is not the chloride channel responsible for the alterations in basement membrane conductance.

Evidence from Arden and Wolf, (2000a, b) suggests that both the alcohol-EOG and light-EOG share the same final common pathway but signalling starts from different receptors. The model predicts that light and alcohol act on a different initial receptor but the resulting intracellular pathway activated is the same and is saturable (Arden and Wolf, 2000a, b). The simplest hypothesis is that the second messenger system in both cases acts on the same basolateral chloride channel responsible for the light-rise. The most likely candidate for the messenger is Ca^{2+} and so the first step was to determine whether ethanol could alter $[Ca^{2+}]_{in}$ directly in the RPE.

As discussed in the introductory sections 5.10, 5.10.1 and 5.10.2 the cytoplasmic free $[Ca^{2+}]$ is low and is maintained by membrane-bound Ca^{2+} channels and transporters. Within the RPE Ca^{2+} is stored in the ER and melanosomes (Fishman *et al.*, 1977; Ulshafer *et al.*, 1990). If $[Ca^{2+}]_{in}$ generates the alcohol-rise then it may enter the cytosol from these stores or from the extracellular medium. Release of Ca^{2+} from intracellular stores could be mediated by ethanol binding to a G-protein coupled receptor to mediate the release of Ca^{2+} from the ER. Alternatively Ca^{2+} could be entering the cell from the extracellular side via L-type Ca^{2+} channels (Strauss and Wienrich, 1993, 1994; Rosenthal *et al.*, 2006).

There is evidence for ethanol to increase $[Ca^{2+}]_{in}$ through either release from the intracellular stores or by permitting entry from the extracellular pools. Ethanol has been shown to increase $[Ca^{2+}]_{in}$ via L-type Ca^{2+} channels in cultures of rat foetal hypothalamic cells (Simasko *et al.*, 1999) as well as by G-protein coupled receptor activation of adrenergic receptors (Bode and Molinoff, 1988; Hoek *et al.*, 1990) or other receptors coupled to the generation of PLC-β (Hoek and Rubin, 1990). However, ethanol also inhibits L-type Ca^{2+} currents in the neural cell line (Mullikin-Kilpatrick and Treistman, 1994), adult rat hippocampus (Hendricson *et al.*, 2003) and rat pinealocytes (Chik *et al.*, 1992). The experiments were designed to determine if ethanol could act directly upon a suitable RPE cell line and evoke a rise in $[Ca^{2+}]_{in}$ and then to determine the source of the Ca^{2+}.

The majority of studies into ethanol have been undertaken on tissues where chronic alcohol consumption is detrimental, notably the CNS, liver, muscle and heart. Table 4.1 overleaf lists the concentrations used in several studies investigating the effects of ethanol. Typical values are from 25 mM to 250 mM which are higher than the calculated sub millimolar concentration estimated to cause the alcohol-EOG in man (Wolf and Arden, 2004).

Table 4.1 Summary of Published Ethanol Concentrations

Tissue (Animal)	Ethanol Concentration (mM)	Ca^{2+} Effect	Reference
Smooth muscle (dog)	20 - 200	Opens voltage gated Ca^{2+} channel	Yang *et al.*, (2001a)
Skeletal muscle (rabbit)	100 - 400	Inhibits voltage dependent Ca^{2+} efflux	Oz *et al.*, (2001)
Dorsal root ganglia (rat)	40 - 80	Opens large K^+ dependent Ca^{2+} channels	Gruss *et al.*, (2001)
Hippocampus (rat)	25 - 100	Opens large K^+ dependent Ca^{2+} channels	Dopico *et al.*, (1998)
Skeletal muscle (mouse)	20 - 300	Inhibits voltage dependent Ca^{2+} channel	Cofan *et al.*, (2000)
Astrocytes (rat)	25 - 150	Increases $[Ca^{2+}]_{in}$ from ER	Allansson *et al.*, (2001)
Basilar artery muscle (dog)	20 - 200	Increase $[Ca^{2+}]_{in}$ via protein tyrosine kinases	Yang *et al.*, (2001b)
Hepatocytes (rat)	30 - 300	Decreases IP_3 mediated release of Ca^{2+}	Renard-Rooney *et al.*, (1997)

Concentrations of ethanol used in studies investigating changes in $[Ca^{2+}]_{in}$ vary from 25-400 mM which encompasses those used in this study (25 – 250 mM).

4.1.1 Fluo4-AM

There are a number of Ca^{2+} indicators available for the recording of changes in $[Ca^{2+}]_{in}$ associated with intracellular signalling. Fluo-4 (Gee *et al.*, 2000) has an excitation peak of 488 nm and is coupled to an acetoxymethyl (AM) ester that permits the indicator to cross the cell membrane. Within the cell cytoplasm, there are esterases that rapidly cleave the AM ester thereby enabling the hydrophilic fluorescent indicator to bind to intracellular free Ca^{2+}. With fluo indicators (1-4) the fluorescence increases with increasing intracellular $[Ca^{2+}]$ making such probes a powerful tool in detecting changes in $[Ca^{2+}]_{in}$ (Minta *et al.*, 1989). When the fluo-4 chromophore binds to Ca^{2+} there is an increased fluorescent emission at 516 nm. Figure 4.1 shows ARPE-19 cells were loaded with fluo4-AM displaying strong cytoplasmic staining of cytosolic free Ca^{2+}. Other indicators are available such as the fura compounds that have different excitation wavelengths depending upon whether Ca^{2+} is bound or free and an approximately

identical emission for these two states. By alternating between the two excitation wavelengths and measuring the emission it is possible to compensate for photobleaching and also accurately determine the $[Ca^{2+}]_{in}$ (Grynkiewicz *et al.*, 1985).

Figure 4.1 ARPE-19 Loaded with Fluo4-AM

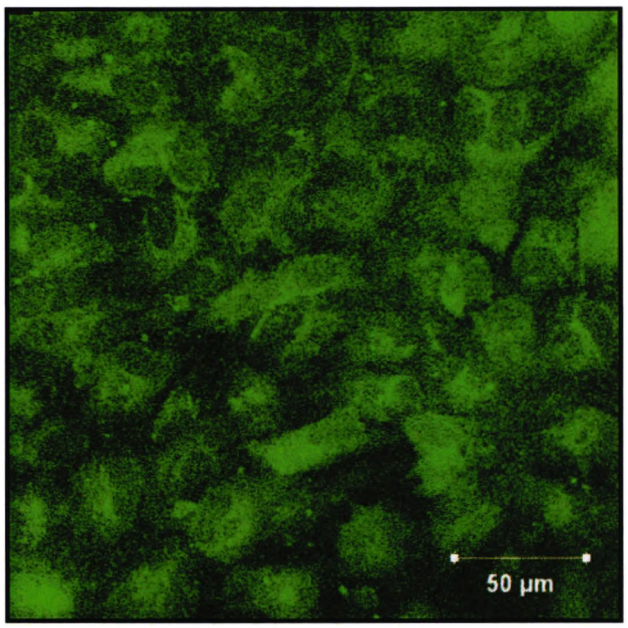

ARPE-19 cells loaded with fluo-4 AM grown to confluence in low serum for two to six weeks. The fluo-4 indicator can be seen in the cell cytoplasm bound to resting cytosolic free Ca^{2+}.

4.1.2 An Appropriate Cell Line

The human RPE cell lines available for this study, ARPE-19, D407 and h1RPE have all been characterised in terms of their expression of RPE-specific proteins (Davis *et al.*, 1995; Dunn *et al.*, 1996; Kanuga *et al.*, 2002). One issue is that ARPE-19 and D407 do not express functional bestrophin (Marmorstein *et al.*, 2000). Given that bestrophin plays a role in Ca^{2+} regulation then the absence of this channel in the cell lines is a problem (Marmorstein *et al.*, 2006). It could be argued that a change of $[Ca^{2+}]_{in}$ in a cell line without functional bestrophin would indicate that bestrophin was unlikely to be the target. ARPE-19 expresses functional CFTR (Wills *et al.*, 2000; Reigada and Mitchell, 2005) whereas the expression is unknown in D407 and h1RPE.

ARPE-19 and D407 have been used to monitor changes in intracellular $[Ca^{2+}]_{in}$ using flura-2 (Reigada and Mitchell, 2005) and fluo-3 (Toimela and Tahti, 2001) respectively. However, it has been shown that a drug transporter, P-glycoprotein (P-gp) is capable of extruding the negatively charged AM ester of Ca^{2+} indicators (Homolya *et al.*, 1993). The study of Homolya identified that the uptake of several AM chromophores, including fluo-3 was 80% less in a P-gp expressing cell line. The uptake was improved when the P-gp competitive inhibitor verapamil was used. P-gp is expressed in human RPE cultures on the apical and basal surfaces *in situ* (Kennedy and

Mangini, 2002) and predominantly on the basal membrane of porcine RPE (Steuer *et al.*, 2005). It was possible that the human RPE cell lines would also express P-gp and this factor may have reduced the loading of the chromphore into the cells. The presence of P-gp activity in either of the cell lines would not necessarily exclude the cell line from future work with Ca^{2+} indicators as P-gp could be inhibited with verapamil to enhance dye uptake. However, verapamil is an L-type Ca^{2+} channel inhibitor (Tytgat *et al.*, 1988; Kuga *et al.*, 1990) and given the involvement of L-type Ca^{2+} in the generation of the light-EOG (Rosenthal *et al.*, 2006) then the inhibition of this channel may have masked any effect of ethanol if the L-type Ca^{2+} channel was a target.

The first step was to determine if a particular human cell line was preferable to use based on whether it expressed P-gp. The next question was to determine whether ethanol could alter $[Ca^{2+}]_{in}$ in this chosen cell line. Finally, to determine whether the source of Ca^{2+} was derived from the intracellular or extracellular pools.

4.2 Methods

4.2.1 Cell Culture

Three human RPE cell lines were studied to determine which of them expressed P-gp. D407 and ARPE-19 have been described in sections (2.2.1 and 2.2.2). In addition to the two spontaneously arising human RPE cell lines ARPE-19 and D407 one additional RPE cell line was utilised. This cell line, h1RPE has recently been developed and is the product of transfecting a fifty-year-old female human donor's RPE with simian virus (SV)40 large T antigen to confer immortalisation. As originally described these cells expressed apical microvilli and tight junctional complexes but lacked pigmentation. The cells expressed mRNA for RPE65 and CRALBP and have been used successfully to restore visual function in the RCS rat (Lund *et al.*, 2001; Kanuga *et al.*, 2002). The presence of bestrophin has not been determined. The h1RPE cell line was a generous gift of Prof John Greenwood, University College London and supplied at passage 20.

As a positive control the Madin Darby Canine Kidney (MDCK) (Gaush *et al.*, 1966) cell line that has been stably transfected with the multi-drug resistance (MDR1) gene and expresses functional P-gp activity was used (Pastan *et al.*, 1988) and denoted MDCK-MDR1. These cells were a generous gift of R. Melarange (GlaxoSmithKline, Ware, UK). MDCK-MDR1 were grown in DMEM with high (4.5 g/l) glucose supplemented with 10% heat inactivated FCS, 100 U/ml penicillin, 100 μg/ml streptomycin and 2 mM L-glutamine; they were used within forty passages of receipt. ARPE-19 and D407 cells were grown under standard conditions as described in section 6.4.1. h1RPE cells were grown in Ham's F10 medium supplemented with 20% FCS, 100 U/ml penicillin, 100 μg/ml streptomycin, 0.25 μg/ml amphotericin B and 2 mM L-glutamine.

4.2.2 Immunocytochemistry

To enhance attachment and growth of the cell lines, glass cover slips (12 mm diameter) were pre-coated with 5 - 10 $\mu g/cm^2$ of mouse collagen type-1 solution and placed in 4-well chambers (Nunc, Roskilde, Denmark) overnight at 37°C. Excess collagen solution was aspirated the next day before cells were seeded at an initial density (cells/$cm^{2)}$) of $5x10^4$ for D407; $1x10^5$ for ARPE-19 and $2x10^5$ for MDCK-MDCK and h1RPE respectively. Cells were grown to confluence under standard conditions. All procedures were carried out at room temperature unless stated otherwise. Cover slips were washed twice in PBS for five minutes and fixed with ice-cold acetone at 4°C for ten minutes to permeabalise the cell membrane. They were then rinsed three times in PBS and blocked in PBS containing 0.5% (wt/vol) BSA and 5% mouse serum for twenty minutes before washing the cover slips again three times for five minutes in PBS. The primary antibody, C219 (ID Labs, Glasgow, UK) recognises an internal epitope of human P-gp (Friedlander *et al.*, 1989); it was added at a dilution of 1:10 in blocking buffer and cells incubated for sixty minutes. Cover slips were washed three times for five minutes in PBS before the secondary antibody

(FITC-conjugated goat anti-mouse; Dako, Glostrup, Denmark) was added (1:200 dilution in blocking buffer) and incubated in the dark for one hour. Cover slips were washed three times in PBS and nuclei counterstained with propidium iodide (1 μg/ml in PBS) for ten seconds before washing again three times in PBS. Cells were imaged with a Zeiss Axiovert 510 laser scanning confocal microscope (Carl Zeiss, Jena, Germany) with dual excitation of 488 nm and 543 nm. They were viewed with a 40x oil immersion lens, NA = 1.3. Images (1024 x1024 pixels) were stored on computer hard drive and viewed with Axiovision 3 (Carl Zeiss, Jena, Germany). Negative controls were incubated with the secondary antibody only.

4.2.3 Intracellular Ca^{2+}

All preparation and recordings were carried out at room temperature unless otherwise stated. The protocol for intracellular Ca^{2+} measurements is a modification of that described by Mangini *et al.*, (1997). ARPE-19 cells were grown in standard culture conditions with passage 24 - 30 used in these experiments. Cells were grown at an initial density of 2 x 10^5 cells/cm^2 on glass coverslips that were pre-coated the day before with 100 μl of FCS and allowed to dry overnight (Kanuga *et al.*, 2002). Cover slips were placed in the wells of 4 well plates (Nunc) and the FCS in the growth medium was reduced to FCS 1%. The medium was changed every four days and the coverslips were used after two to six weeks in culture in the lowered serum to enhance polarisation of the cells (Dunn *et al.*, 1998; Mitchell, 2001).

Coverslips were rinsed in buffer containing (in mM): NaCl, 140; KCl, 4.8; $MgSO_4$; $CaCl_2$, 1.8; KH_2PO_4, 0.2; HEPES, 15; and glucose, 5. For nominally Ca^{2+}-free experiments $CaCl_2$ was omitted and 2 mM Ethylene-bis(oxyethylenenitrilo)tetraacetic acid (EGTA) used. The pH was adjusted to 7.40 with NaOH. Loading buffer was prepared by adding 10 μl of 10 mM stock solution of Fluo4-AM in DMSO (Molecular Probes-Invitrogen, Paisley, UK) and 10 μl of 30% BSA to 10 ml of Ca^{2+}-containing buffer solution. Final concentrations in the loading buffer were 1 μM Fluo4-AM, 0.1% DMSO and 0.03% BSA. 0.5 ml of loading buffer was added to each well in the dark for sixty minutes. Cells were then rinsed twice with Ca^{2+}-containing buffer before being incubated in 0.5 ml of Ca^{2+}-containing buffer at 37°C with 5% CO_2 for forty-five to sixty minutes to allow endogenous proteases to cleave the AM ester from the dye.

The cover slips were then transferred in the dark to a perfusion chamber (Warner, CT, USA) with a volume of approximately 1.5 ml and mounted onto the stage of a Zeiss (LSM510) confocal laser-scanning microscope (Zeiss). The laser enabled single narrow band excitation at 488 nm. The cell monolayer was imaged with a 40x oil immersion lens (NA = 1.3). Fluorescent emission was transferred via a broad band pass filter (λ > 500 nm) and captured with an image intensified charge-coupled device camera at 1 second intervals. Images 512 x 512 pixels were stored on a hard drive. Cytoplasmic areas were analysed with axioviewer 3.0 (Zeiss, Jena, Germany).

After fifteen to thirty seconds the buffer was removed with suction and replaced with either buffer with $CaCl_2$ and ethanol in the following concentrations: 0 mM (N=3 trials with 28 sampled cells),

25 mM (N=2 trials with 22 sampled cells), 50 mM (N=4 trials with 30 sampled cells), 100 mM (N=15 trials with 127 sampled cells) or 250 mM (N=30 with 273 sampled cells). Alternatively the cells were challenged with 250 mM ethanol (N=18 trials with 139 sampled cells) in Ca^{2+}-free buffer to determine whether any responses were present in the absence of extracellular Ca^{2+}. In all trials between thirty and fifty cells were visible in the field of which six to ten were sampled. Fluorescent recordings continued for up to five minutes.

The ratio (R) of change above baseline was calculated using $[(F-F_o)/F_o]$ where F_o is baseline fluorescence taken as the mean fluorescence for the fifteen second interval preceding the ethanol dose, with F being the fluorescence after the dose. The R-value therefore represents the normalised fluorescence. Cells were considered to respond if there was a change in baseline fluorescence of >1.25R (e.g. greater than 25% change in fluorescence above background). See equation 4.i.

$$\mathbf{R = (F - F_o) / F_o} \qquad \mathbf{— 4.i}$$

Where:

R = Ratio of fluorescent change.

F = Fluorescence intensity during recordings at a given time.

F_o = Mean baseline fluorescence emission of the ten second interval prior to recordings.

Limitations of the experimental set-up prevented the addition of ethanol directly to the basal surface of the RPE as the cells were grown on glass cover slips and visualised on an inverted microscope.

4.2.4 Preparation of Drugs and Ethanol

4.2.4.1 Ethanol

Concentrations in this section are reported in mM which is consistent with other publications. Absolute ethanol was diluted to produce a 250 mM stock solution which was then diluted (1 : 2.5) to give 100 mM solution, (1 : 5) to give 50 mM solution and (1 : 10) to give a 25 mM solution. Taking 50 ml/l of absolute ethanol as Molar then a 250 mM solution was prepared by adding 1.25 ml of ethanol to 98.75 ml of Ca^{2+}-free or Ca^{2+}-containing buffer.

4.2.4.2 Calcimycin (A23187)

Calcimycin A23187 (Molecular Weight (MW) = 524) is a Ca^{2+} ionophore that permeabalises the cell membrane enabling Ca^{2+} to enter the cytosol. A23187 (10 mg) was dissolved in 200 μl of DMSO giving a stock solution of 50 μg/μl. 20 μl aliquots were stored at -50°C in the dark. One aliquot was then added to 20 ml of Ca^{2+}-containing buffer to give a final concentration of A23187 (2.5 μg/ml) and 0.1% DMSO (Salceda and Sànchez-Chàvez, 2000).

4.2.4.3 Epinephrine and Nifedipine

Preparation of a 1 mM stock epinephrine solution in Ca^{2+}-containing buffer has been described in section 7.3.2. In these experiments, the 1 mM epinephrine solution was diluted (1:100) to give a final concentration of 10 μM. Nifedipine (MW = 347) has been used in patch clamp studies at a concentration of (1 - 10 μM) to inhibit L-type Ca^{2+} currents in rat RPE cells (Strauss and Wienrich, 1994; Mergler *et al.*, 1998; Rosenthal *et al.*, 2006). Nifedipine (35 mg) was dissolved in 1 ml DMSO to give a working concentration of 100 mM. This solution was serially diluted so that the final concentration of DMSO was kept low. Initially 100 μl of the working 100 mM stock solution was diluted 1:1000 with 100 ml of Ca^{2+}-containing buffer and then 1 ml of this solution was diluted a further 1:100 in Ca^{2+}-containing buffer to give a final concentration of 1 μM Nifedipine and 0.01% DMSO and stored in the dark at 4°C until use.

4.2.5 Estimation of $[Ca^{2+}]_{in}$

The R-value is not linearly related to the $[Ca^{2+}]_{in}$ but indicates a qualitative change in $[Ca^{2+}]_{in}$ over time. Because there is no spectral shift with the fluo indicators upon Ca^{2+}-binding (Minta *et al.*, 1989) a ratiometric approach is impractical without the loading of additional indicators such as fluo-red (Floto *et al.*, 1995).

However, the R-value used here, of the normalised fluorescent, gives a qualitative measure of the change in $[Ca^{2+}]_{in}$ over time compared to the baseline.

An approximation to the change in $[Ca^{2+}]$ after the application of ethanol can be made based upon the fluorescence emission. The standard protocol for calculating the $[Ca^{2+}]_{in}$ using fura indicators is to use the ratio of fluorescence based upon the emission when flura is in 0 mM Ca^{2+} and when it is saturated in high Ca^{2+}. Using equation 4.ii derived by Grynkiewicz *et al.*, (1985).

$$[Ca^{2+}] = K_d \times [(R - R_{min}) / (R_{max} - R)] \times Q \qquad \text{— 4.ii}$$

Where:

$[Ca^{2+}]$ = Concentration of cytosolic Ca^{2+} (nM).

K_d = dissociation constant of the fluorescent indicator (nM).

R_{min} = Ratio of fluorescent emission at the two excitation wavelengths in zero Ca^{2+}.

R_{max} = Ratio of fluorescent emission at the two excitation wavelengths with saturating $[Ca^{2+}]$.

R = Ratio of fluorescent emission at the two excitation wavelengths recorded during the experiment.

Q = Ratio of fluorescence minimum to fluorescence maximum at the excitation wavelength for the flura indicator.

However, fluo indicators do not lend themselves to a ratiometric approach to determine the $[Ca^{2+}]_{in}$. One method of determining the change in fluorescence emission above baseline is to assume that the baseline fluorescence represents the resting $[Ca^{2+}]_{in}$ of the cells. Then the change in fluorescence can be estimated from this baseline concentration. The following derivation is that of Cannell *et al.*, (1994) who used fluo-3 to record alterations in $[Ca^{2+}]_{in}$ in cardiac myocytes based upon the fluorescence only. As *R* represents the fluorescent ratio then equation 4.ii can be rewritten to become equation 4.iii (Grynkiewicz *et al.*, 1985).

$$[Ca^{2+}]_{in} = K_d \times [(F-F_{min}) / (F_{max}-F)] \qquad \text{— 4.iii}$$

Where:

$[Ca^{2+}]_{in}$ = Intracellular Ca^{2+} concentration.

K_d = Dissociation constant.

F = Fluorescence during the recording.

F_{min} = Fluorescence in zero Ca^{2+}.

F_{max} = Fluorescence in saturating Ca^{2+}.

Assuming that F_{min} equals zero for fluo4 so that F_{max} can be estimated from the resting $[Ca^{2+}]_{in}$ in RPE cells. This is assumed to be 153 ± 1.5 nM range (130 – 180 nM) based on measurements from sub-cultured human foetal RPE cells (Kuriyama *et al.*, 1991). Then substituting $F_{min} = 0$ and letting $F = F_{rest}$ (baseline) and solving for F_{max} then equation 4.iii becomes equation 4.iv.

$$F_{max} = F_{rest} \times [(K_d / [Ca^{2+}]_{rest}) + 1] \qquad \text{— 4.iv}$$

The change in $[Ca^{2+}]_{in}$ based upon the fluorescence increase above resting $[Ca^{2+}]$ is then derived by dividing equation 4.iii by F_{rest} and substituting equation 4.iv for F_{max} giving the relative increase in $[Ca^{2+}]_{in}$ – equation 4.v:

$$[Ca^{2+}]_{in} = (K_d \times R) / (K_d / ([Ca^{2+}]_{rest}) - R + 1)) \qquad \text{— 4.v}$$

K_d is the dissociation constant for fluo-4 which is 345 nM and $[Ca^{2+}]_{rest}$ = 153 nM, R is the ratio of baseline fluorescence compared to the fluorescence maximum (i.e. $[(F-F_O)/F_O]$.

After substitution equation, 4.v reduces to equation 4.vi.

$$[Ca^{2+}]_{in} = 345 \times R \times (3.3 - R) \qquad \text{— 4.vi}$$

These assumptions are valid provided that there is minimal bleaching of the dye during the scan. This was achieved by using low laser power of < 10% and using responses that occurred in the first two-minutes. From figure, 4.10 below the fall in fluorescence is approximately 10% over two minutes. The indicator concentration was constant owing to the short experimental time. The confocal microscope provides a uniform path length and the cell monolayer may be assumed to be of uniform thickness (Cannell *et al.*, 1994).

4.3 Data Analysis

Fisher's exact test was used to determine the significance of the proportion of responses between the Ca^{2+}-free and Ca^{2+}-containing buffers responses. A two-sided p-value was used with a p=0.05 taken as the point probability at which the expected and observed results do not differ. Calculations were performed using the *Simple Interactive Statistical Analysis* website at: http://home.clara.net/sisa/index.htm

4.4 Results

4.4.1 Immunocytochemistry

Staining with the P-gp specific antibody C219 revealed strong immunoreactivity in MDCK-MDR1 cells. Plasma membrane staining was evident (figure 4.2A). ARPE-19 cells were negative for P-gp (figure 4.2D). However, h1RPE and D407 showed weak immunoreactivity (figures 4.2B and 4.2C respectively).

In addition to immunocytochemistry, reverse transcriptase polymerase chain reaction (RT-PCR) and a functional assay were performed that also confirmed that ARPE-19 lacked functional P-gp expression. See Constable *et al.*, (2006b).

Figure 4.2 P-gp immunocytochemistry

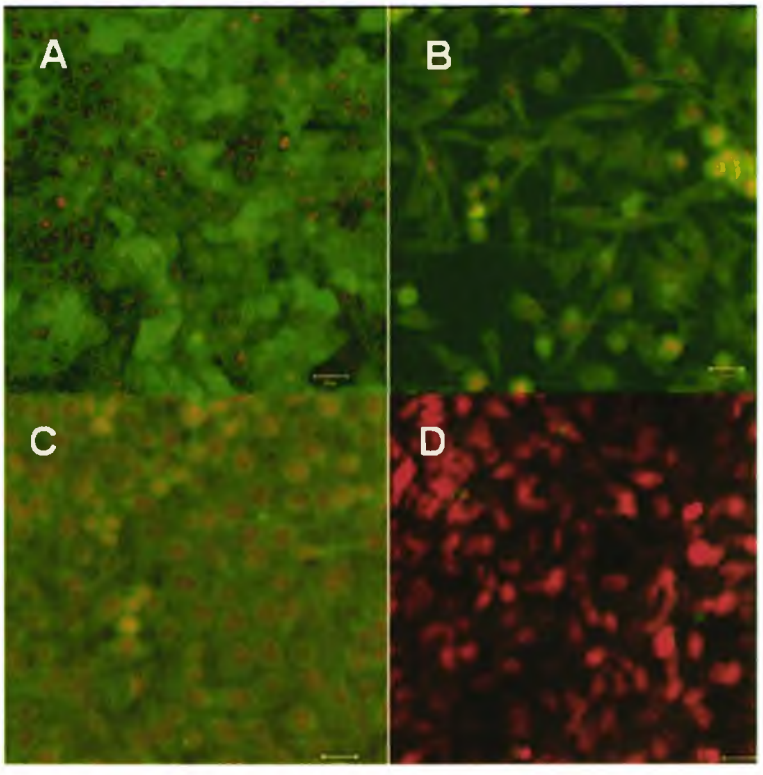

Results of immunocytochemistry show strong staining in the positive control MDCK-MDR1 cell (A). ARPE-19 cells (D) were negative whilst weak staining was evident with h1RPE and D407 cell (B and C respectively). Nuclei are counter stained with propidium iodide. Scale bars 20 µm.

When the primary antibody was omitted there was no immunoreactivity. See figures 4.3 (A-D).

Figure 4.3 Negative Control for P-gp Immunocytochemistry

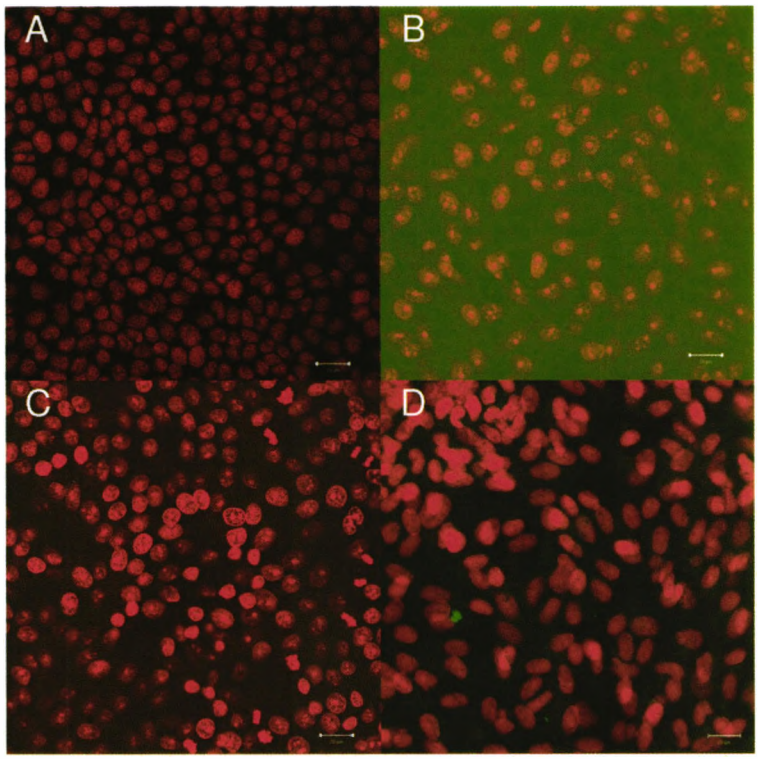

Negative controls in which the primary antibody was omitted were all negative indicating that the secondary antibody did not cross-react with any epitope in these cell lines. Figure A (MDCK-MDR1), B (h1RPE), C (D407) and D (ARPE-19). Nuclei are counter stained with propidium iodide. Scale bars 20 µm.

4.4.2 Calcimycin (A23187) and Epinephrine

A23187 was effective at increasing the $[Ca^{2+}]_{in}$ with a peak occurring at approximately five minutes and an increase of the R-value by a factor 6 which represents the maximal saturated response. These experiments confirmed that the both the recording protocol was capable of visualising changes in $[Ca^{2+}]_{in}$. See figure 4.4.

Figure 4.4 A23187 Response

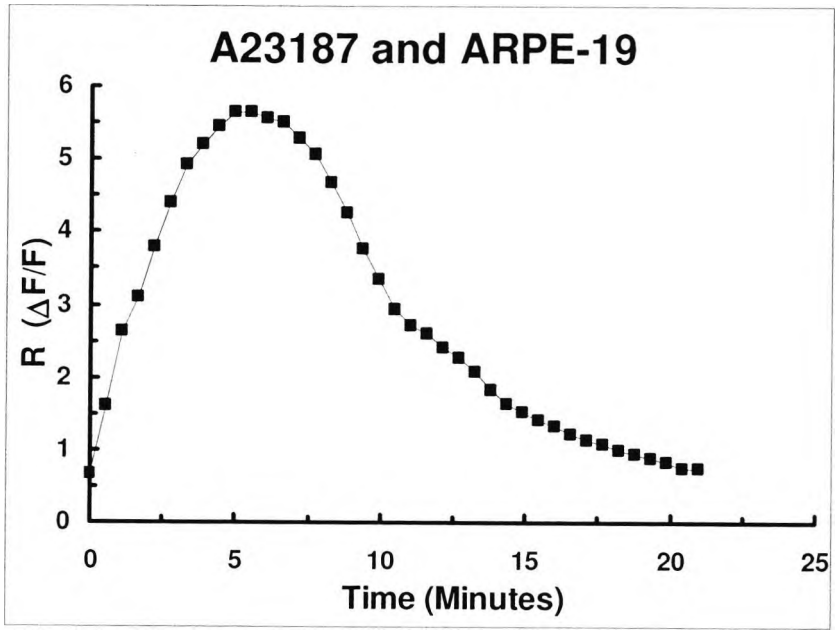

Response from an ARPE-19 cell when the buffer containing 2.5 µg/ml A23187 and 1.8 mM $CaCl_2$ was added at t=0 minutes. A23187 permeabalises the cell membrane permitting extracellular Ca^{2+} to enter the cell. When this occurs, there is a slow rise in fluorescence as the Ca^{2+} binds to the fluo-4 probe.

When 10 μM epinephrine was added to Ca^{2+} containing buffer several cells responded with sharp elevations in $[Ca^{2+}]_{in}$ through the release of Ca^{2+} from intracellular stores. Figure 4.5 shows the mean ± SEM R-values of 10 ARPE-19 cells responding to 10 μM epinephrine in Ca^{2+}-containing buffer.

Figure 4.5 10 µM Epinephrine Response

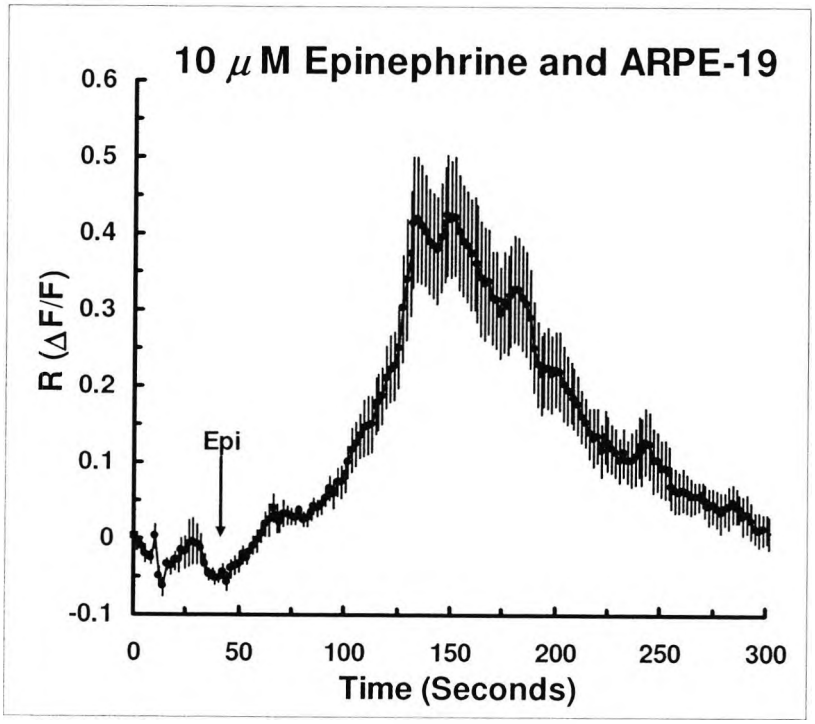

Increase in baseline fluorescence when ARPE-19 cells are challenged with 10 µM epinephrine (Epi) at the arrow. The mean increase in the baseline fluorescence ratio (R) is 0.5. Plot show mean ± SEM of ten sampled cells.

4.4.3 Ethanol Responses in ARPE-19

Figure 4.6 shows transients observed in a group of cells responding to 250 mM ethanol in Ca^{2+}-containing buffer. The onset of each transient was between 17 - 27 seconds with a range of peak R-values from 0.34 to 0.74. Mean responses from the cells are shown in the heavy line. (Ethanol added at the arrow).

Figure 4.6 250 mM Ethanol

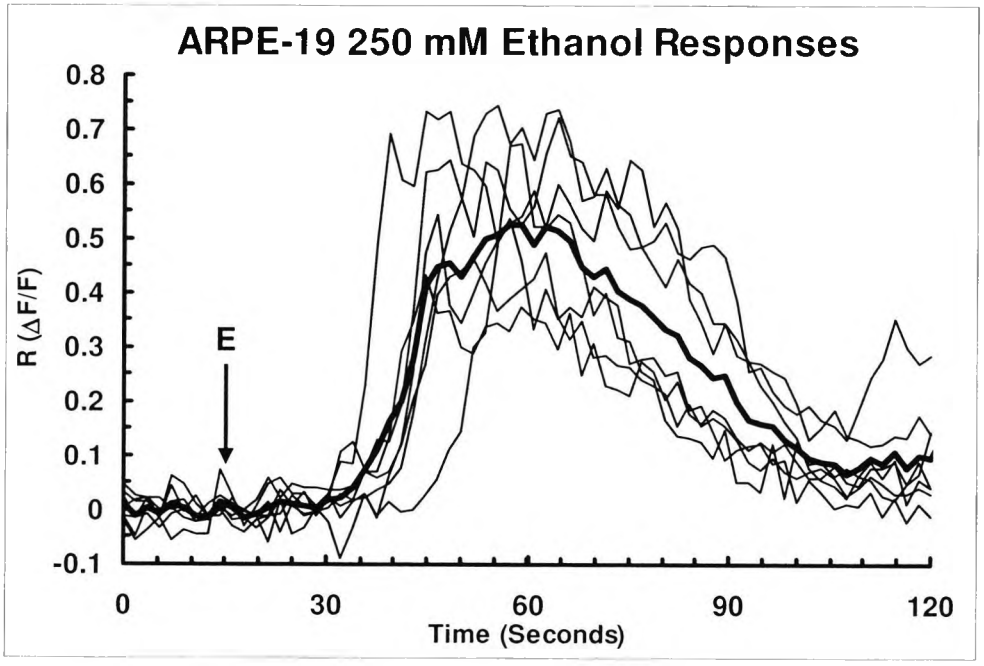

Transients observed in a group of cells in response to 250 mM ethanol in Ca^{2+} containing buffer solution administered at t=15 seconds (E and arrow). The heavy line shows the mean response of the seven cells whose individual traces are shown in the lighter lines.

Figure 4.7 below shows the changes in fluorescence after 100 mM of ethanol in Ca^{2+}-containing buffer was added to the ARPE-19 cells. Ethanol was added at the end of the first row at t=14 seconds. The lower half of the field shows an increase in fluorescence in the third and fourth row that falls back to baseline in the fifth row. The response is over in approximately 40 seconds.

Figure 4.7 Intracellular Ca^{2+}-Transients in ARPE-19 cells (100 mM)

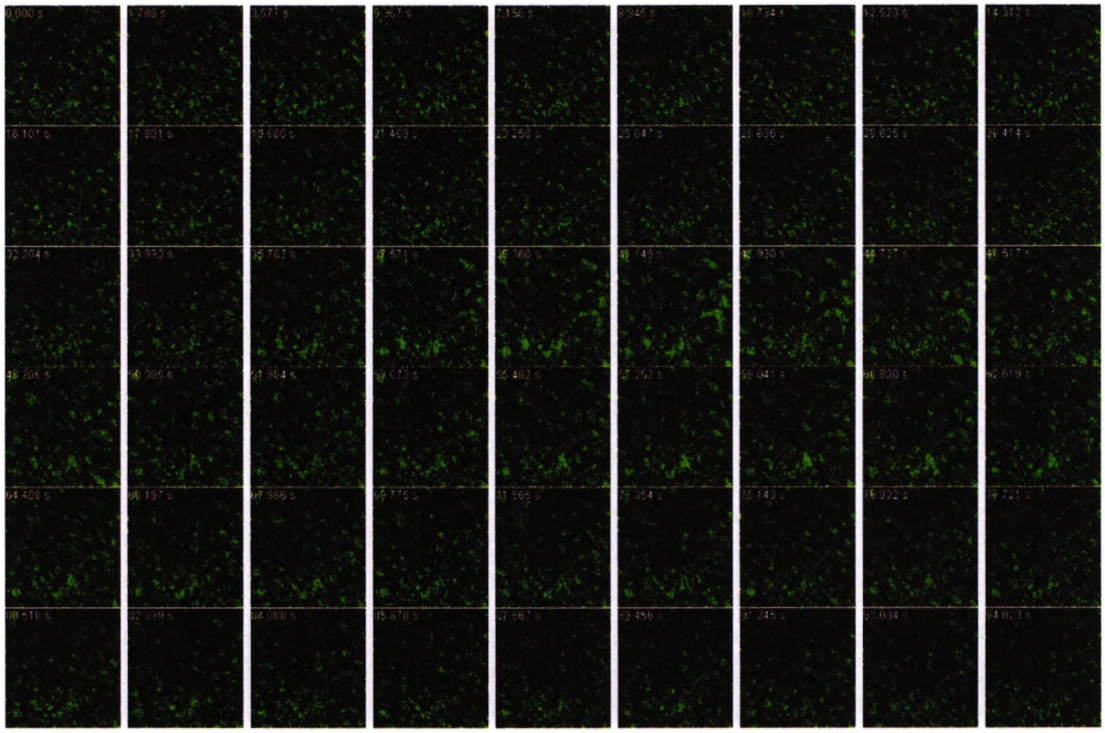

A time series of ARPE-19 cells responding to 100 mM ethanol in Ca^{2+}-containing buffer after it was added at t=14 seconds. (End of the first row). In the third and fourth rows at the bottom of each slide an increased fluorescent signal is apparent from some cells that commences at ~ t=35 seconds and ends at ~ t=76 seconds when the fluorescence has returned to near baseline levels.

In Ca^{2+}-containing buffer with ethanol at doses of 25, 50, 100 and 250 mM increases in $[Ca^{2+}]_{in}$ were present in a total of 7.9% (range 4.6 - 15.8%) cells that were analysed. Cells responded within fifteen to ninety seconds following ethanol exposure and the transients lasted for no longer than sixty seconds. Figure 4.8 (overleaf) shows isolated cell responses to 0, 25, 50, 100 and 250 mM ethanol. The transients are small and not as sharp at the lower doses. Distinct transient elevations were observed at the higher doses. The onset of the transient varies in each cell and is probably an artefact of the time for the ethanol to reach its target. No responses were observed when buffer containing 0 mM ethanol was used from 28 sampled cells in three independent trials.

Figure 4.8 Ethanol (0 – 250 mM)

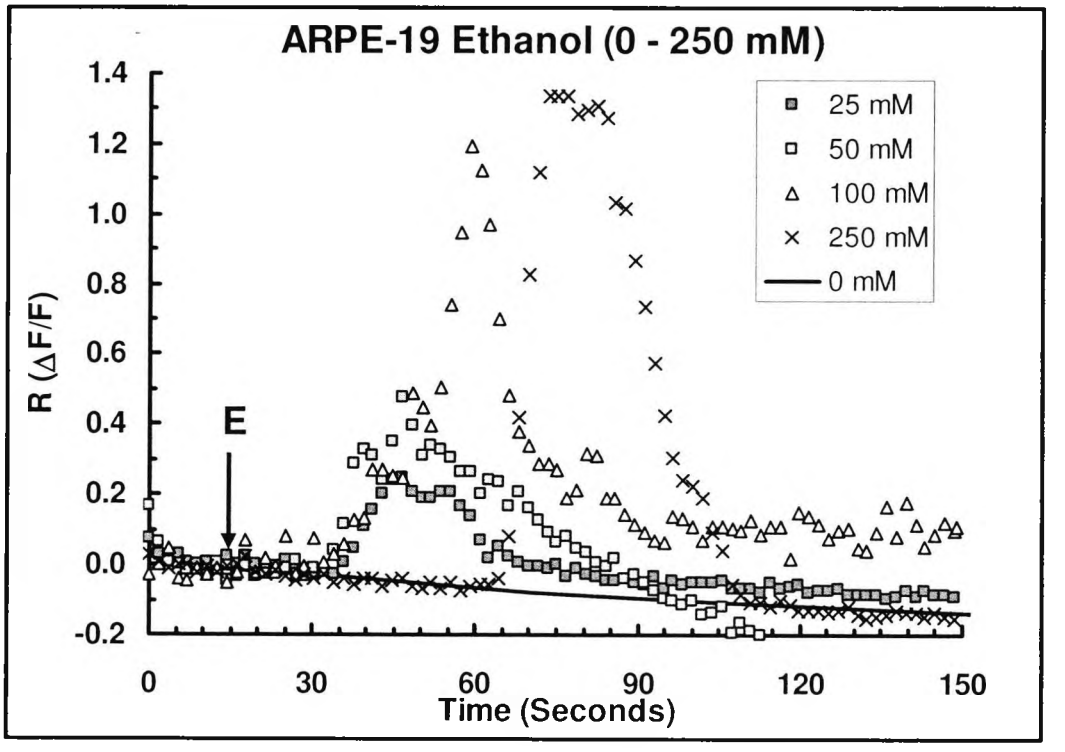

Individual cell responses to ethanol (E) in Ca^{2+}-containing buffer at t=15 seconds. The onset of each response varies and is probably a result of the time for the ethanol to reach its target rather than any physiological effect. Responses lasted no more than 60 seconds. The heavy line shows the mean response of 28 cells (three independent trials) of Ca^{2+}-containing buffer changed at 15 seconds when the ethanol concentration was 0 mM.

Figure 4.9 (overleaf) shows the mean ± SEM responses of 5 cells to 100 mM ethanol (E1) in Ca^{2+}-containing buffer that was repeatable (E2) following washout of ethanol with Ca^{2+}-containing buffer (B) which demonstrating that these responses were not due to solution manipulation. The R-value increases ranged from 0.32 to 0.86 for the first peak and from 0.30 to 0.66 for the second peak.

Figure 4.9 100 mM Ethanol Repeated Response

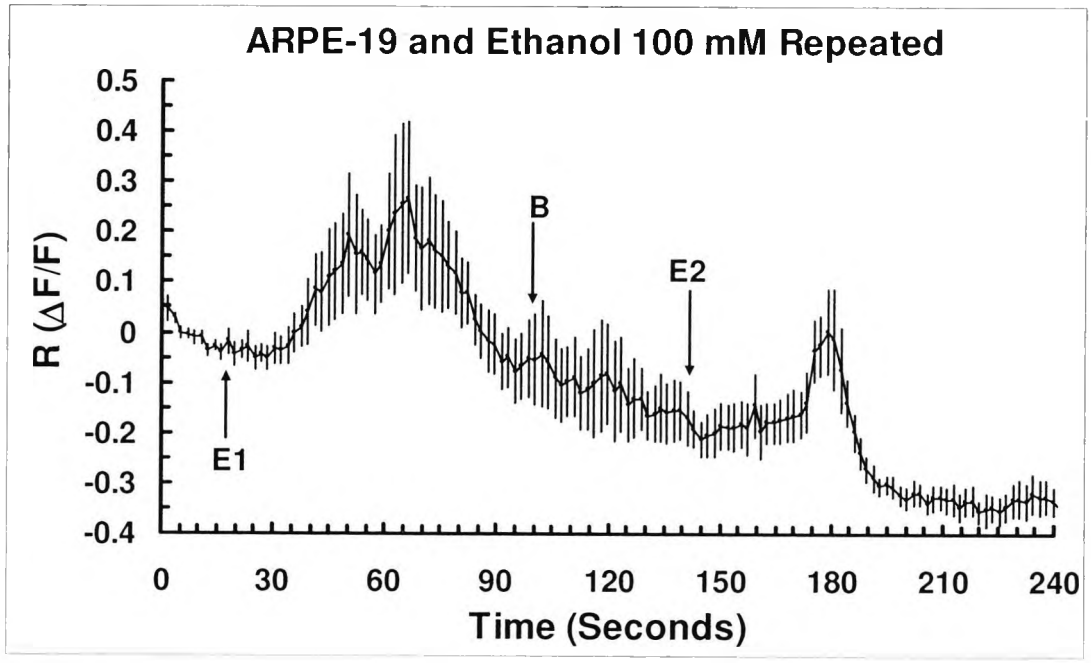

When ethanol (100 mM) in Ca^{2+}-containing buffer to ARPE-19 cells at E1 an increase in intracellular Ca^{2+} was observed before returning towards baseline after sixty seconds. Following wash out at (B) with Ca^{2+}-containing buffer a second dose of ethanol (100 mM) in Ca^{2+}-containing buffer at E2 a second weaker transient was also evident. Trace shows mean ± SEM of five sampled cells.

When Ca^{2+}-free buffer was used with the maximal dose of 250 mM ethanol, no responses were seen in any of the 139 cells sampled from 18 independent trials (figure 4.10 overleaf). The exponential fall in fluorescence is consistent with bleaching of the fluo-4 indicator.

Figure 4.10 Ca^{2+}-Free Responses (250 mM Ethanol)

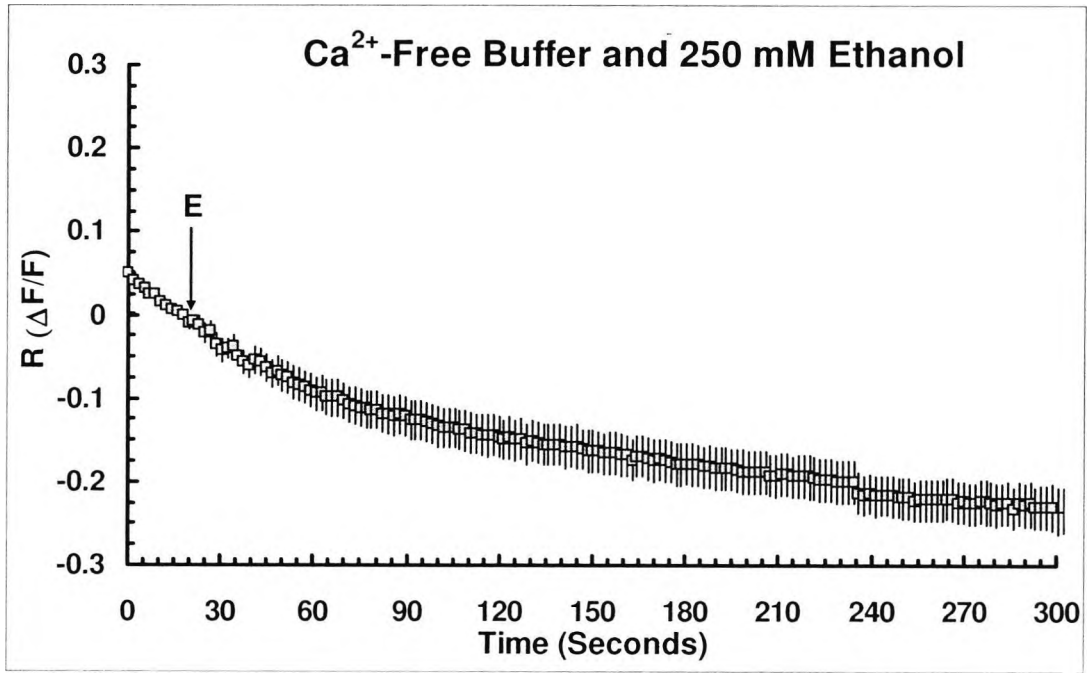

When Ca^{2+} was removed from the extracellular buffer and 250 mM ethanol was present (arrow) then no Ca^{2+} transients were observed from N=18 independent trials (139 cells). Mean ± SEM of the R-value is shown.

To assess whether this difference between the number of responding cells in the Ca^{2+}-free or Ca^{2+}-containing buffer is significant for 250 mM ethanol a frequency table was drawn (Table 4.2). Using Fisher's exact test, the probability that zero responses from 139 sampled cells in Ca^{2+}-free buffer with 250 mM ethanol compared with 12 responses from 261 sampled cells in Ca^{2+}-containing buffer with 250 mM was p = 0.0054 and so the observations in the Ca^{2+}-containing buffer are significantly different to the expected observations in the Ca^{2+}-free buffer (Altman, 1999).

Table 4.2 Frequency of Responses in Ca^{2+}-Free and Ca^{2+}-Containing Buffer

	Responses	No Responses	Total
Ca^{2+}-free	0	139	**139**
Ca^{2+}-containing	12	249	**273**
Total	**12**	**388**	**400**

Frequency of responses in Ca^{2+}-free and Ca^{2+}-containing buffer for 250 mM ethanol.

To calculate the 95% confidence interval that the responses in the Ca^{2+}-containing samples falls outside the zero responses observed in the Ca^{2+}-free experiments the standard error of the two proportions (p_1) for Ca^{2+}-containing (12/273 =0.0440) and (p_2) for Ca^{2+}-free (0/139 = 0.0) was determined and is given by equation 4.vii.

$$\textbf{Standard error } (p_1 - p_2) = \sqrt{((p_1(1-p_1)/n_1) + ((p_2(1-p_2)/n_2))} \qquad \textbf{— 4.vii}$$

Where:

p_1 = proportion of responding cells in Ca^{2+}-containing = 0.0440.

p_2 = proportion of responding cells in Ca^{2+}-free = 0.0.

n_1 = population size in Ca^{2+}-free = 273.

n_2 = population size in Ca^{2+}-containing = 139.

Solving equation 4.vii gives a standard error of 0.0124 and the difference between the proportions is $(p_1 - p_2) = 0.0440$.

The 95% confidence interval is given by equation 4.viii.

$$\textbf{(}p_1 - p_2\textbf{) – 1.96 x (standard error) to (}p_1 - p_2\textbf{) + 1.96 x (standard error)} \qquad \textbf{— 4.viii}$$

Which gives a 95% confidence interval of 0.02 to 0.07 or that 95% of the mean proportion of Ca^{2+}-containing responses fall between 2% and 7% and therefore if a response was present from the Ca^{2+}-free experiments then the proportion of responding cells would fall between this range ($p<0.05$). The zero percentage of responses in the Ca^{2+}-free buffer lies outside this 95% confidence range of this observation occurring by chance alone.

Table 4.3 overleaf lists the number of trials and the percentage of responding cells observed from the number of sampled cells in a field. Each field had at least thirty cells of which typically five to ten were sampled. Note in the Ca^{2+}-free experiments no cells responded from 139 samples.

Table 4.3 Summary of Ethanol Responses

Ethanol Concentration (mM)	Number of Trials	% Responding Cells	Sampled Cells	Mean R ± SEM Response
Ca^{2+} free 250	18	0	139	0
0 with Ca^{2+}	3	0	28	0
25 with Ca^{2+}	2	16	19	0.30 ± 0.03
50 with Ca^{2+}	4	12	25	0.55 ± 0.02
100 with Ca^{2+}	15	16	109	0.56 ± 0.07
250 with Ca^{2+}	32	5	261	0.72 ± 0.08

Summary of $[Ca^{2+}]_{in}$ experiments with ARPE-19 cells. The table illustrates the number of independent trials and percentage of cells responding with a change in baseline fluorescence of > 25% from the total of cells sampled. Mean ± SEM of the responses are shown. The number of cells responding in Ca^{2+}-containing buffer compared with Ca^{2+}-free buffer with 250 mM is significant (p = 0.0054).

Figure 4.11 (overleaf) shows the mean ± SEM of three responding cells to 50 mM ethanol and the effects of 1μM nifedipine. All solutions are in Ca^{2+}-containing buffer. Ethanol (50 mM) was added at fifteen seconds (E50). A rise in the baseline fluorescence was evident with an R-value of 0.3 that lasted for sixty seconds. Following this the Ca^{2+}-containing buffer was replaced (B1) for thirty seconds then buffer containing 1 μM nifedipine with 0.01% DMSO was added (Nif 1 μM) for thirty seconds before being replaced with control buffer (B2) to remove the DMSO. Following a further thirty seconds, the cells were challenged with 100 mM ethanol (E100) but no responses were evident. In contrast, figure 4.9 showed that repeated application of ethanol at 100 mM after a wash out did not abolish the response in the absence of nifedipine.

Figure 4.11 Nifedipine and Ethanol Responses

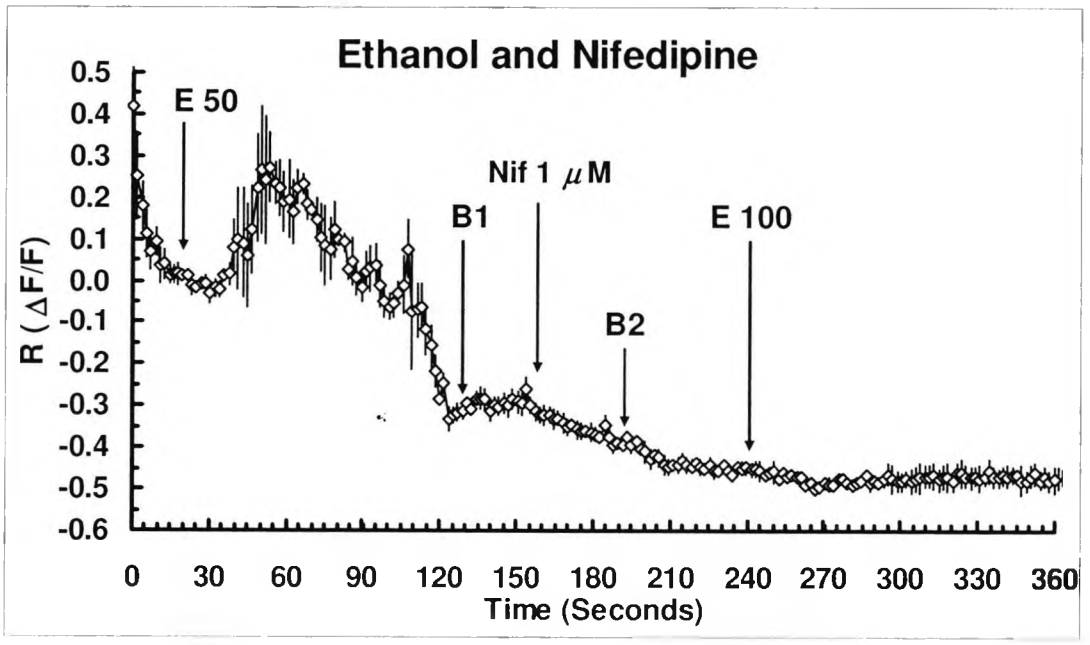

Ethanol response to 100 mM (E100) ethanol following pre-treatment with 1 μM nifedipine (Nif 1 μM) abolished the previous responses obtained with 50 mM ethanol (E50). Trace shows mean ± SEM of three cells' responses with washes indicated where the chamber solution was aspirated (B1 and B2) and replaced with Ca^{2+}-containing buffer.

4.5 Estimation of $[Ca^{2+}]_{in}$

Table 4.4 below gives the estimated change in $[Ca^{2+}]_{in}$ above baseline for the doses of ethanol. The values range from 365 nM to 906 nM and are estimated from the maximum R-value at each concentration used.

Table 4.4 Intracellular $[Ca^{2+}]$ Calculations

Concentration of Ethanol (mM)	$[Ca^{2+}]$ maximum (nM) $[Ca^{2+}]_{free} = 345 \times R \times (3.3 - R)$
25	365
50	529
100	879
250	906
Epinephrine (10 μM) mean of N=10 cells	483

Estimation of $[Ca^{2+}]_{in}$ in the cytosol following ethanol and epinephrine application to ARPE-19 cells. Figures based upon the assumption that resting $[Ca^{2+}]$ = 150 nM and the K_d of fluo-4 is 345 nM. Calculations based on the derived formula: $[Ca^{2+}]_{free} = 345 \times R \times (3.3 - R)$.

4.6 Discussion

The main purpose of the initial study into P-gp expression was to eliminate the cell line that would be least appropriate for work with intracellular fluorescent indicators. This was because the anionic nature of the AM ester makes these probes a substrate for P-gp (Homolya *et al.*, 1993). ARPE-19 was deemed to be the most appropriate cell line to use given that it lacks functional expression of P-gp (Constable *et al.*, 2006b).

ARPE-19 exhibited a rise in $[Ca^{2+}]_{in}$ in response to ethanol. This finding adds some support to the suggestion that the alcohol-EOG (as with the light-EOG) is dependent upon Ca^{2+}-signalling. An unexpected finding was that alcohol apparently acts by increasing inward Ca^{2+} flux although this is consistent with recent findings regarding the origins of the sustained Ca^{2+}-signal being generated by the L-type Ca^{2+} channels (Strauss and Rosenthal, 2005; Rosenthal *et al.*, 2006).

Initial results with the Ca^{2+} ionophore, A23187 indicated that the experimental apparatus was capable of detecting changes in $[Ca^{2+}]_{in}$. Epinephrine has been widely used to evoke changes in RPE membrane voltage and fluid transport in bovine and human RPE (Edelman and Miller, 1991; Quinn *et al.*, 2001; Rymer *et al.*, 2001). In bovine RPE mounted in Ussing chambers loaded with flura-2 and 0.1 μM epinephrine caused a 60% increase in baseline $[Ca^{2+}]_{in}$ which was similar to the results obtained with ARPE-19 cells and 10 μM epinephrine in this study. This would indicate that the cells grown under the conditions were viable and expressed adrenergic receptors and the G-protein coupled signalling pathway required to release Ca^{2+} from the ER.

The changes in $[Ca^{2+}]_{in}$ following ethanol in Ca^{2+}-containing buffer ranged from 365 - 906 nM which are in the range of other modulators of $[Ca^{2+}]_{in}$ previously reported. For instance, ATP stimulation of cultured human RPE cells increases $[Ca^{2+}]_{in}$ by 500 nM (Collison *et al.*, 2005), neuropeptides by 600 nM (Kuriyama *et al.*, 1992) and the synthetic purinergic agonist (INS37217) by 200 nM in bovine RPE (Mitchell, 2001). The calculated change in $[Ca^{2+}]_{in}$ of 483 nM with 10 μM epinephrine is also consistent with those reported for bovine RPE using 0.1 μM (300 - 400 nM) (Rymer *et al.*, 2001). These values indicate that the changes in $[Ca^{2+}]_{in}$ were in the physiological range and not the result of ethanol induced cell damage. This would have produced a broader response with a slower recovery to baseline (Allansson *et al.*, 2001).

The lack of a high number of responding cells is not uncommon in intracellular Ca^{2+} studies. Two similar investigations into the acute action of ethanol to alter $[Ca^{2+}]_{in}$ in cell culture also found some variability in responses. In rat hypothalamic cells Simasko *et al.*, (1999) reported that responses were present in 65% of cells with 170 mM ethanol. However, in rat astrocytes Allansson *et al.*, (2001) found significantly fewer responding cells with the following doses: 25 mM (0%), 50 mM (3%), 100 mM (4%) and 150 mM (1%) which are similar to the percentage of responding cells in this study.

It is likely that only a subset of cells in the culture were capable of responding fully to ethanol. The culture conditions for ARPE-19 are important in determining the phenotype. Substrate, time in culture, medium and the cell line's particular history all influence the final phenotype observed (Tian *et al.*, 2004; Luo *et al.*, 2006).These factors may have contributed to the small clusters of cells that responded. The ability of ARPE-19 to form a confluent monolayer with tight intercellular junctions is difficult to establish owing to the diversity of junctional proteins expressed by these cells (Luo *et al.*, 2006). It is more likely that the cells in culture were not fully polarised and therefore the distribution of the ethanol receptor may have been dispersed throughout the plasma membrane so that in only some cases a response was possible. The culture method used was designed to improve the barrier properties of ARPE-19 and is reported to produce a polarised monolayer (Dunn *et al.*, 1998; Reigada and Mitchell, 2005). However, the more findings of Luo *et al.*, (2006) would suggest that a well established monolayer is difficult to obtain with this cell line.

One further limitation was imposed by the design of the experiment meant that ethanol could only be added to the apical surface because the ARPE-19 cells grown on glass cover slips. The prediction would be, despite the lipophillic nature of ethanol that the main target for ethanol would be on the basolateral surface of the RPE given the low concentrations required to attain this response in man (Arden and Wolf, 2000b; Wolf and Arden, 2004). The lowered working temperature may have also reduced the number of responses that would be expected physiologically. However, a reduced working temperature was desirable to minimise any further loss of fluo4-AM by organic anionic transporters (Mangini *et al.*, 1997).

The alcohol-EOG peaks before maximal breath alcohol and is considered to be a first pass response (Arden and Wolf, 2000b; Marmor and Wu, 2005). Wolf and Arden (2004) modelled the blood serum concentrations based upon a two compartment model of absorption and elimination studied in fasting and non-fasting humans (Welling *et al.*, 1977). The equations derived estimate the blood alcohol concentrations in the range of 0.001 mM to 0.1 mM for oral doses of alcohol in fasting subjects of 5 mg/kg to 226 mg/kg. Therefore, the doses used in these experiments are considerably higher than those that would be expected to generate the alcohol-EOG in man (Wolf and Arden, 2004).

However, ethanol concentrations required to alter $[Ca^{2+}]_{in}$ via Ca^{2+} channels have also been investigated in a number of different preparations with few eliciting responses in the physiological range. In bovine preparations maintained at 37˚C the concentration of ethanol required to alter the TEP was also significantly higher than in man. Pautler (1994) used 0.5% ethanol applied to the apical side, and Bialek *et al.*, (1996) used 0.1% and so the increased dose required for cells maintained at room temperature is not unexpected. The concentrations used in the experiments with ARPE-19 were consistent with similar investigations involving ethanol and intracellular Ca^{2+} signalling. (See table 8.1).

The principal finding that the Ca^{2+}-transients were only present when extracellular Ca^{2+} was present excludes the intracellular stores as the source of Ca^{2+}. No responses were present when Ca^{2+} was removed from the extracellular buffer so this means that the likely candidate for the Ca^{2+}-entry is through a voltage gated Ca^{2+} channel. The most likely candidate would be the L-type Ca^{2+} channel given its role in generating the light-EOG (Marmorstein *et al.*, 2006).

A possible scenario to describe the way in which the light-rise is initiated and sustained would involve a positive feedback between intracellular Ca^{2+} and Cl^- efflux. The assumption is that ATP is the light-rise substance and whether the source is from the rods or the RPE is immaterial at this point. However, the binding of ATP to the apical purinergic receptor initiates a transient increase in $[Ca^{2+}]_{in}$ from the ER. This rise in cytosolic free Ca^{2+} is then able to gate open the basolateral CaCC which increases basolateral Cl^- conductance and depolarises V_{Basal}. The stimulated increase in $[Ca^{2+}]_{in}$ is reduced by the NCX and re-uptake by the ER, PMCA pumps and bestrophin (Kennedy and Mangini, 1996; Mangini *et al.*, 1997; Marmorstein *et al.*, 2006). The depolarisation of V_{Basal} would increase the open probability of the L-type Ca^{2+} channel and permit a sustained slow entry of Ca^{2+} into the RPE. This gradual secondary increase in $[Ca^{2+}]_{in}$ then drives an increasing basolateral Cl^- conductance as the open probability of the L-type Ca^{2+} channel increases with increasing membrane depolarisation. Ultimately the cycle is halted when the basal membrane depolarises to a point to that the L-type Ca^{2+} channel's conductance decreases again. It can be seen that the I-V curve of the L-type Ca^{2+} channel closely resembles that of the EOG with a bell shaped I-V relationship that is similar to the light-rise of the EOG. See figure 1.3 in section 1.7. The role of bestrophin (hBest1) or one of the homologues such as hBest2 has not been fully determined and so how bestrophin would modulate this model is unknown (Marmorstein *et al.*, 2006). The absence of bestrophin (hBest1) results in an elevation of $[Ca^{2+}]_{in}$ following ATP stimulation and it may be that bestrophin, in addition to modulating the L-type Ca^{2+} channel activation kinetics also decreases either the re-uptake of Ca^{2+} into the ER or inhibits the NCX or PMCA pump to slow the extrusion of Ca^{2+}.

One possible route by which ethanol could be elevating $[Ca^{2+}]_{in}$ is by acting upon a chloride channel that then depolarises the membrane so that this initiates an entry of Ca^{2+} through the L-type Ca^{2+} channel. The most likely channel would be the CaCC which is found in native human RPE (Ueda and Steinberg, 1994; Quinn *et al.*, 2001). However, ethanol at 25-100 mM has been shown to inhibit the endogenous CaCC currents in *Xenopus* oocytes (Clayton and Woodward, 2000). CFTR could also be a target but patch a patch clamp study has shown that ethanol does not increase CFTR chloride conductance (Marcet *et al.*, 2004).The most likely candidate is therefore the L-type Ca^{2+} channel on which ethanol acts to elevate $[Ca^{2+}]_{in}$ and initiate the membrane depolarisation through the CaCC rather than requiring the putative light-rise substance (ATP) to do so through release of Ca^{2+} from the ER.

L-type Ca^{2+} channels are found in rat, freshly isolated monkey, adult human and foetal cells that show slow inward Ca^{2+}-currents as the membrane depolarises (Ueda and Steinberg, 1993, 1995; Strauss and Wienrich, 1994). However, the transient nature of the Ca^{2+}-transients recorded in

this study do not resemble the long slow sustained influx of Ca^{2+} associated with the L-type Ca^{2+} channels (Strauss *et al.*, 1999; Xu *et al.*, 2004; Marmorstein *et al.*, 2006). Several factors have been identified that modulate the expression of L-type Ca^{2+} or voltage gated Ca^{2+} channels. The substrate of cultured rat RPE cells alters the type of L-type Ca^{2+} channels expressed. Cells grown on laminin or collagen type IV express the high voltage activated (HVA) L-type and low voltage activated (LVA) T-type Ca^{2+} currents (Strauss and Wienrich, 1994). Given that the Ca^{2+} current through the L-type Ca^{2+} channel is voltage dependent the lack of a sustained influx of Ca^{2+} may have been due to a lack of adequate depolarisation of the ARPE-19 cell following inward Ca^{2+} flux. The dependence of membrane depolarisation would rely upon a CaCC to provide the outward depolarising chloride current. The potential lack of polarity may have meant that the membrane was unable to depolarise sufficiently to maintain the inward Ca^{2+} flux.

Furthermore, differences in the expression of the L-type Ca^{2+} channel subunits have been reported. The L-type Ca^{2+} channels are composed of the α-subunit which forms the pore and two accessory protein subunits, the β and α-δ-subunits that are involved with anchoring the α_1-subunit to the plasma membrane. One report has identified that ARPE-19 cells do not express the $\alpha_2\delta_3$ complex and the same β-subunit as human RPE which may have altered the stability of the channel forming α-subunit pore in the membrane. The α-subunit in both ARPE-19 and the cultured RPE cells also differed slightly (Wimmers *et al.*, 2004). This may be important as the α-subunit is responsible for the binding of inhibitors and agonists to the L-type Ca^{2+} channel and may alter the activation and inactivation kinetics of this channel (Tang *et al.*, 1993; Adams and Tanabe, 1997).

The maintenance of the sustained Ca^{2+} current from L-type Ca^{2+} channels also depends upon phosphorylation of the α_1-subunit. In typical whole cell patch recordings to obtain the sustained Ca^{2+} current the pipette solution is supplemented with ATP to obtain such recordings (Ueda and Steinberg, 1993; Strauss *et al.*, 2000). The ARPE-19 cells, having been maintained in buffer solution at room temperature for one hour and then incubated at 37°C for a further hour may have been depleted of ATP and therefore the regulation of these Ca^{2+}-transients observed differed to those recorded under more physiological conditions.

L-type Ca^{2+} channels are also regulated by protein tyrosine kinases and activate Cl^- currents in rat RPE cells (Strauss *et al.*, 1997, 1999). Tyrosine kinases regulate L-type Ca^{2+} channels through phosphorylation and are regulated by growth factors such as bFGF (Mergler *et al.*, 1998). It is possible that ethanol could activate tyrosine kinases as ethanol is known to alter gene expression and levels of growth factors. Ethanol inhibits fibroblast growth factor (FGF) in low doses and may play a role in ethanol's reported protective role in heart disease by reducing smooth muscle cell growth in arteries (Ghiselli *et al.*, 2003). Similar protective mediated roles for ethanol are ascribed to its role in up-regulating VEGF in the heart in low doses (Gu *et al.*, 2001). Receptors for other growth factors such as bFGF and PDGF could have also been a target for ethanol (Kuriyama *et al.*, 1991). However, these changes were due to the generation of PKC and release of Ca^{2+} from intracellular stores and therefore these receptors are unlikely to be the site

of action of ethanol given the Ca^{2+}-signal was absent when Ca^{2+}-free buffer was used as the extracellular buffer.

There is evidence that ethanol alters the properties of L-type Ca^{2+} channels in the CNS, especially following chronic exposure. L-type Ca^{2+} channels have been shown to be responsible for bradycardia associated with alcohol-withdrawal (Kahkonen and Bondarenko, 2004). L-type Ca^{2+} channels are up-regulated in the PC12 cell line with prolonged ethanol exposure of ethanol that involves an increased activity of PKC_{δ} (Gerstin Jr *et al.*, 1998; Walter *et al.*, 2000). The PC12 cell line is a neuronal model that was derived from a rat pheochromocytoma (tumour) (Greene and Tischler, 1976). It is believed that ethanol increases the levels of PKC_{δ} that then modulates gene transcription for the L-type Ca^{2+} channel α_1-subunit thereby increasing the number of L-type Ca^{2+} channels in response to chronic ethanol consumption.

L-type Ca^{2+} channel currents can be either increased or inhibited by ethanol depending upon the cell type and concentration of ethanol used. Acute ethanol exposure inhibits L-type Ca^{2+} currents in neurons (Wang *et al.*, 1994) and PC12 cells (Mullikin-Kilpatrick and Treistman, 1994). Similarly ethanol also inhibits L-type Ca^{2+} currents in cardio vein myocytes (Chen *et al.*, 2004) and pinealocytes (Chik *et al.*, 1992).

However, ethanol can also increase L-type Ca^{2+} currents in rat hypothalamic cells following acute exposure to ethanol at a dose of 1 - 250 mM (Simasko *et al.*, 1999). This study also found that the majority of the responses were present only when Ca^{2+} was present in the extracellular buffer. The authors also showed that ethanol could increase $[Ca^{2+}]_{in}$ via other members of the voltage gated Ca^{2+} channels (P, Q. T and N). The dual action of ethanol to both increase and decrease L-type Ca^{2+} currents has also been demonstrated in PC12 cells with an increases in $[Ca^{2+}]_{in}$ reported at doses less than 120 mM and an inhibitory effect on $[Ca^{2+}]_{in}$ at doses in the range of 120-160 mM (Belia *et al.*, 1995). Ethanol at very high dose (400 mM) has also been shown to elevate $[Ca^{2+}]_{in}$ by 150 nM with 100 mM ethanol having no effect on $[Ca^{2+}]_{in}$ in PC12 cells (Rabe and Weight, 1987).

It seems likely that ethanol can increase and decrease Ca^{2+} transients in voltage gated Ca^{2+} channels and exerts a dual regulation over these channels by altering intracellular $[Ca^{2+}]$ (Simasko *et al.*, 1999). However, in this study it was not possible to demonstrate conclusively that ethanol was modulating a voltage gated Ca^{2+} channel. The presumption that this is the case rests with the finding that no Ca^{2+} transients were observed in Ca^{2+}-free medium which would exclude the source of Ca^{2+} from the intracellular stores. Secondly the localisation of the L-type Ca^{2+} channel with presumably bestrophin in the basal membrane would mean that it is ideally suited as a ligand for ethanol. It should be remembered that the concentrations in which ethanol inhibits the L-type Ca^{2+} currents are much higher than the sub-millimolar range predicted to evoke the alcohol-EOG in man. It could therefore be that at such low concentrations ethanol is an agonist and at high/chronic levels ethanol is an antagonist of the L-type Ca^{2+} channel. The

result showing that nifedipine abolished the action of ethanol in ARPE-19 cells lends some support to this conclusion although further studies are required.

It is possible that an alternative pathway for Ca^{2+} exists in ARPE-19 cells but our knowledge of Ca^{2+} currents in the RPE is limited and mainly consists of pumps or transporters that remove Ca^{2+} from the cytosol such as the NCX and PMCA (Kennedy and Mangini, 1996; Mangini *et al.*, 1997). However, ethanol at high and chronic levels can inhibit the NCX in brain and this effect if also true at acute levels may result in an elevation of intracellular Ca^{2+} as the exchange rate decreases (Michaelis *et al.*, 1987).

4.6.1 Summary

The *in-vitro* data presented in this section showed that ethanol was capable of directly increasing $[Ca^{2+}]_{in}$ in ARPE-19 and that the source of Ca^{2+} was extracellular. These responses were repeatable and consistently returned to baseline levels. Although the concentrations used were not in the physiologically range thought to generate the alcohol-EOG, these results indicate that ethanol can act directly upon an adult derived human RPE cell line to elevate intracellular Ca^{2+}. The proposal is that this is by activation of the L-type Ca^{2+} channel owing to its location and involvement in generating the light-EOG and the similarity between the alcohol- and light-EOGs.

5 The Electro-Oculogram in Cystic Fibrosis

5.1 Introduction

The main aim of this study was to determine whether CFTR was involved in generating the alcohol-EOG. CF is an autosomal recessive inherited disease in which lung function is primarily affected. The gene involved, CFTR, encodes for the cystic fibrosis transmembrane conductance regulator chloride channel (Li *et al.*, 1988; Riordan *et al.*, 1989; Rommens *et al.*, 1989). The most prevalent Caucasian mutation results in the deletion of phenylalanine at position 508 (Δ508) and thereby renders CFTR incapable of reaching the plasma membrane (Kerem *et al.*, 1989; Riordan *et al.*, 1989; Lemna *et al.*, 1990; Gregory *et al.*, 1991; Puchelle *et al.*, 1992). Heterozygotes for Δ508 are also affected, though typically mildly. However, the genotype is not always correlated to the severity of the phenotype (Sermet-Gaudelus *et al.*, 2002; Rowntree and Harris, 2003). CFTR gating requires ATP binding and hydrolysis and is also regulated by cAMP dependent PKA phosphorylation (Rich *et al.*, 1990; Anderson *et al.*, 1991a, b; Welsh and Smith, 1993). CFTR is not gated by changes in $[Ca^{2+}]_{in}$ and therefore if, as the results on ARPE-19 cells implicate Ca^{2+} as the second messenger, then individuals with CF should have normal alcohol-EOG amplitudes.

CFTR has been identified in both the apical and basal membranes of foetal RPE sheets (Blaug *et al.*, 2003) and the corresponding mRNA in adult human RPE and retina (Miller *et al.*, 1992). CFTR is also present in cultured RPE cells (Weng *et al.*, 2002; Reigada and Mitchell, 2005) and in canine RPE (Loewen *et al.*, 2003). ARPE-19 cells display CFTR activity at the apical membrane (Reigada and Mitchell, 2005) but immunocytochemical studies in native foetal RPE sheets showed a predominantly basolateral localisation (Blaug *et al.*, 2003).

CFTR is not the only cAMP gated chloride channel expressed in the RPE. Members of the voltage gated ClC (Jentsch *et al.*, 1990) chloride family of channels have also been identified. In particular, ClC-2, ClC-3 and ClC-5 mRNA have been identified in cultured human RPE. Immunocytochemistry localised ClC-3 and ClC-5 to the apical membrane and intracellular compartments with no localisation determined for ClC-2 (Wills *et al.*, 2000; Weng *et al.*, 2002). Their likely apical localisation may explain the loss of photoreceptor function in ClC-3 or ClC-2 deficient mice (Bösl *et al.*, 2001; Stobrawa *et al.*, 2001). The possible relationship of these chloride channels to the EOG would depend upon them being localised to the basal membrane as it is an increase in basolateral chloride current that generates the light-rise (Gallemore and Steinberg, 1989) and presumably the alcohol-rise as well (Arden and Wolf, 2000b).

5.1.1 Electro-oculogram

In the standard model of the light-EOG and FO generation, bestrophin is believed to be the Ca^{2+}-gated chloride channel responsible for the light-rise and CFTR is believed to be solely responsible for the FO amplitudes. However, two important recent findings suggest an alternative and more complex generation of both the FOs and the light-rise.

One is that bestrophin is responsible for modulating Ca^{2+} entry through an interaction with the L-type Ca^{2+} channels as previously discussed in section 5.10.2 (Rosenthal *et al.*, 2006).

Furthermore, the hBest1 isoform inhibits the cytosolic Ca^{2+} transient when mouse RPE cells were stimulated with ATP (Marmorstein *et al.*, 2006).

The second relates to the generation of the FOs. In one study, using both CFTR null mice and homozygous mice expressing the Δ508 phenotype were examined. If CFTR was the sole generator of the FOs then this response should have been absent in the null mice and reduced or absent in the Δ508 strain. The light-EOGs should have been normal for both if, as has been previously reported in abstract form in man that the FOs are reduced and the light-EOGs are normal in CF (Miller *et al.*, 1992; Lara *et al.*, 2003). However, the results were not as expected with reductions in the light-rise observed, FOs and c-wave for the Δ508 homozygote strain. The more pronounced finding was that the FOs were still present, though reduced, in the CFTR null mice which indicated that CFTR was not the sole generator of the FOs. One proposed explanation was that the lack of CFTR in the RPE would result in an increased R_{basal} that would decrease the light-evoked responses. The authors proposed that the light-evoked responses generated across the basal membrane are the result of a complex interaction between, bestrophin, L-type Ca^{2+} channels, CFTR and CaCC (Loewen *et al.*, 2003; Wu *et al.*, 2006).

5.1.2 CFTR Interactions with Ionic Channels

CFTR has been implicated in the regulation of other ionic channels as well as the transport of ATP and regulating pH. Although our understanding of the functional role of CFTR in the RPE is still developing (Blaug *et al.*, 2003; Reigada and Mitchell, 2005; Wu *et al.*, 2006). However, the widespread expression of CFTR in secretory epithelia has revealed several secondary regulatory roles in conjunction with chloride transport (Kunzelmann, 2001).

1: Inhibition of the amiloride sensitive epithelial sodium channel (ENaC) is one possible interaction of CFTR. ENaC has been identified in bovine RPE (Golestaneh *et al.*, 2002) and human ciliary epithelium (Rauz *et al.*, 2003). ENaC typically acts to allow the passive entry of Na^+ into the cell that is then pumped out by the NaKATPase pump. CFTR is believed to inhibit ENaC thereby resulting in an excess of extracellular Na^+. The early studies showed that CFTR inhibited ENaC and resulted in an increased extracellular [Na^+] that was characteristic of CF sweat and lung mucosa (Boucher *et al.*, 1986). Co-expression of CFTR with ENaC inhibited the Na^+ currents by 24% (Ismailov *et al.*, 1996) in airway epithelia. The inhibitory action is believed to be due to a direct interaction between CFTR and ENaC (Schreiber *et al.*, 1999). However, more recent models and expression of ENaC in *Xenopus* have failed to demonstrate the inhibitory action of CFTR on ENaC (Mall *et al.*, 1996; Konig *et al.*, 2002; Horisberger, 2003; Nagel *et al.*, 2005).

2: Activation of inward rectifying K^+ (K_{ir}) channels has also been demonstrated by cAMP in the presence of functional CFTR (Loussouarn *et al.*, 1996). The RPE has a large population of mild inward rectifying K^+ channels (Hughes and Takahira, 1998; Yang *et al.*, 2003). Inward rectifying channels typically maintain the membrane potential near to the reversal potential for K^+

and are therefore suited to regulating K^+ homeostasis. In the transition from dark to light the sub-retinal K^+ decreases resulting in a hyperpolarisation of V_{apical} (Oakley II, 1977, 1983; Steinberg *et al.*, 1980; Hughes and Steinberg, 1990; Segawa and Hughes, 1994). This hyperpolarisation is countered in part by the K_{ir} channel increase in conductance and K^+ leaving the RPE (Shimura *et al.*, 2001; Yang *et al.*, 2003). It may be possible that the RPE of CF sufferers would lack the activation of K_{ir} and this would result in a reduced capacity to regulate sub-retinal $[K^+]$ and therefore result in impaired fluid regulation and oedematous retinopathy which is not documented.

3: The regulation of an outward rectifying chloride current (ORCC) by CFTR is well documented but the precise mechanism is still not fully resolved. ORCC are regulated by cAMP and display increasing Cl^- current out of the cell as the membrane depolarises or when the cell volume increases (McCann *et al.*, 1989; Worrell *et al.*, 1989). ORCC currents are absent or small at resting membrane potentials. ORCC currents have been recorded from cultured mouse RPE cells but they were only present in ~ 10% of recordings and uncharacteristically they did not respond to cell swelling or activation of intracellular signalling cascades (Wollmann *et al.*, 2006). The authors did not specify which intracellular signalling cascades they modulated and did not present the data showing that in hyperosmotic extracellular buffer the ORCC were unaltered. These findings differ to the traditional role of ORCC that regulate cell volume following cell swelling such as those found in the ciliary epithelium (Chen *et al.*, 1998).

CFTR was shown to correct the ORCC when it was expressed in bronchial epithelial cells that lacked CFTR (Egan *et al.*, 1992) and ORCC currents were also defective in CF nasal epithelia (Gabriel *et al.*, 1993). The activation of the ORCC by PKA and ATP only occurred in the presence of CFTR in when these ion channels were co-expressed in planar lipid bilayers (Jovov *et al.*, 1995a, b). ATP transported by CFTR can also regulate ORCC currents via the purinergic P_{2U} receptor and this may be the interaction involved in ORCC regulation by CFTR (Schwiebert *et al.*, 1995). A lack of CFTR would therefore result in a decrease in the ORCC currents and reduce the capacity of the RPE to regulate cell volume. However, given that the ORCC currents recorded from the RPE were not always present and did not respond to alterations in the intracellular signalling cascades then the regulation of CFTR on these channels cannot be assumed to be true.

4: In hypotonic solutions, CFTR releases ATP into the extracellular compartment. ATP can then bind to the purinergic receptor P_2Y, which would then cause a rise in $[Ca^{2+}]_{in}$ (Reisin *et al.*, 1994; Prat *et al.*, 1996; Taylor *et al.*, 1998; Walsh *et al.*, 2000; Braunstein *et al.*, 2004). In turn this change of calcium would increase chloride fluxes, (Schwiebert *et al.*, 1995). ATP release from cells has not been universally supported by all investigators (Li *et al.*, 1996; Reddy *et al.*, 1996; Abraham *et al.*, 1997; Grygorczyk and Hanrahan, 1997b) with the possibility that the ATP released from the cell is a result of mechanical disruption of the plasma membrane during patch formation (Grygorczyk and Hanrahan, 1997a). In transfected cells one study suggests that the

amount of ATP released from CFTR is not sufficient to stimulate purinergic activation and that P_2Y_2 receptor activation down-regulates CFTR (Marcet *et al.*, 2003).

The aim is to determine the effect of CF on the alcohol-EOG and whether defective CFTR results in an abnormal alcohol-rise. In using human participants with a known defect in the CFTR gene we were able to avoid the problems inherent in cell culture and animal models which do not perfectly replicate man.

5.2 Methods

All participants provided written, informed consent in accordance with the protocol approved by City University's Senate Research and Ethics Committee and in agreement with the tenets of the 2nd declaration of Helsinki. The mean UK life expectancy for an individual with CF is approximately 29 years and diabetes mellitus is a common complication. Sufferers require medication, and the CF participants in the group were all taking prednisolone 5 mg 1 x day, vitamin supplements, pancreatic enzymes, antibiotics and bronchodilators. One of the CF group had received a lung transplant 18 months previously and was taking the following additional medications: immunmosuppressives (azothioprine 125 mg 1 x day and ciclosporin 250 mg 2 x day); anti-hypertensives (ramipril (ACE inhibitor) 10 mg 1 x day and doxazosin (α_1-agonist) 16 mg 1 x day). This individual was not included in the statistical analysis owing to the potential interactions of the medications with the RPE (López-Jiménez *et al.*, 1997; Garweg *et al.*, 2006). However, this individual's responses are shown in the figures and are labelled 'lung transplant'. Another of the CF participants was an insulin-dependent diabetic and was taking furosemide 40 mg 1 x day and warfarin 6 mg 1 x day. Elevated blood glucose levels have been shown to increase the amplitude of the FOs and therefore this participant took his blood glucose levels at just before performing the FOs (Schneck *et al.*, 2000). The blood glucose levels were normal at 6.0 mmol/l.

Participants were contacted via the United Kingdom CF trust website. All CF volunteers were Caucasians attending specialist CF clinics within the UK, and referred by their consultant physicians. Their genotypes had been assessed for the expression of the 33 known mutations associated with CF. Of the six CF participants, three were homozygous for Δ508 and three were heterozygous for Δ508 with one other unidentified mutation in the CFTR gene. The two female homozygotes ages (Δ508/Δ508) were 18 and 20 years. The male Δ508 homozygote that was post lung transplant was excluded because of his medications. In the all-male heterozygous group (Δ508/?), the ages ranged from 37 - 43 years. The mean age of the CF group was 32 with a SD of ± 11 (N=5). The older age of the heterozygous group may reflect the difference in the severity of these two genotypes.

A control group of normal participants was recruited. The control groups for the tests were not identical with some participants declining either to have mydriasis or to drink alcohol. The mean age for the light-EOG was 41 with a SD of ± 12 (N=6) and ranged from 21 - 54 years with five males and one female. For the alcohol-EOG the mean age was 44 with a SD of ± 8 (N=6) and ranged from 34 - 54 years with four males and two females. For the FOs the mean age was 34 with a SD of ± 11 (N=9) and ranged from 20 - 54 years with seven males and two females. There was no significant difference in age between groups for the light-EOG ($p=0.2063$), FOs ($p=0.6834$) and alcohol-EOG ($p=0.0789$). Binocular motility, colour vision and visual acuity were normal for all subjects. All tests were performed on the same day for each participant.

5.2.1 Electrophysiology

The participants were asked to fast overnight for at least ten hours. Two dim red light-emitting diodes that subtended 30° to the observer were mounted on a uniform white wall. The ceiling and side walls were also illuminated and this provided (approximately) full field illumination. The skin was cleaned and 5 mm diameter gold electrodes with conductive jelly were taped to the skin near the outer canthi of each eye and one reference electrode placed on the forehead (impedance was 3 - 5 kΩ). Electrodes were connected to a digital Keithley 2700 series analogue/digital voltmeter (Keithley) and voltages were sampled every 240 msec whilst the subject executed horizontal saccades at 1 Hz (maintained with the aid of a metronome).

For the alcohol- and light-EOGs, the subjects performed saccades for 10-second intervals when instructed. A period of 26 minutes was allowed for dark adaptation (<0.01 cd/m^2) before either the light (100 cd/m^2) was turned on or alcohol was drunk in order to generate either the light- or alcohol-EOGs respectively. The alcohol was whisky, diluted with water to 7% ethanol at a dose of 110 mg/kg body weight. Recordings were continued for a further 34 minutes. Pupils were dilated with 0.5% tropicamide to at least 7 mm diameter for the light-EOG and FOs only. For the FOs illumination was alternated at one-minute intervals between light and dark with recordings made continuously for ten minutes.

The recordings and measurements of the EOGs deviated from the 1993 International Society for Clinical Electrophysiology of Vision (ISCEV) standard (Marmor and Zrenner, 1993) in the following ways. The pre-adaptation time was longer than the ISCEV standard for the EOGs so that a baseline could be established (Arden and Wolf, 2000a, b; Arden *et al.*, 2000; Arden and Wolf, 2003). The recording of only four oscillations in the FOs was lower than the ISCEV standard recommendations of six but four has been reported to be adequate and it also reduces the test time (Vaegan and Beaumont, 2005). A full Ganzfeld illumination was not used and the recordings were made bitemporally rather than monoculary.

5.2.2 Data Collection and Analysis

The voltmeter was connected via an interface card to a personal computer and voltage difference between each canthal electrode recorded in a spreadsheet with ExceLinx™ (Keithley). The modulus of the voltage difference (v_n) between successive recordings was taken (equation 5.i).

$$\textbf{Potential} = \left| (v_{n+1} - v_n) \right| \qquad \textbf{— 5.i}$$

Where:

Potential = bi-temporal standing potential.

v_{n+1} = Instantaneous $(n + 1)^{th}$ bi-temporal voltage.

v_n = Instantaneous n^{th} bi-temporal voltage.

Most of these voltage differences were very small, because in the $(n+1)^{th}$ and n^{th} episodes, the eyes did not move. However, in some instances they were large, because the eyes repositioned between the two samples. By taking the modulus of the voltages both positive and negative voltage differences were treated identically so that the signal was the same for lateral and medial eye movements. Figure 5.1 shows the actual results with a square wave representing the horizontal eye movements. The portion of the trace is from a FO recording between the dark and light phases. The bi-temporal potential approximates the ocular standing potential and is represented by the amplitude of the square wave (marked by 'A' in figure 5.1). There was some voltage drift between the electrodes, however we were concerned only with the absolute instantaneous difference between the canthal electrodes and so the actual electrode offset was immaterial.

Figure 5.1 Raw Bi-Temporal Trace

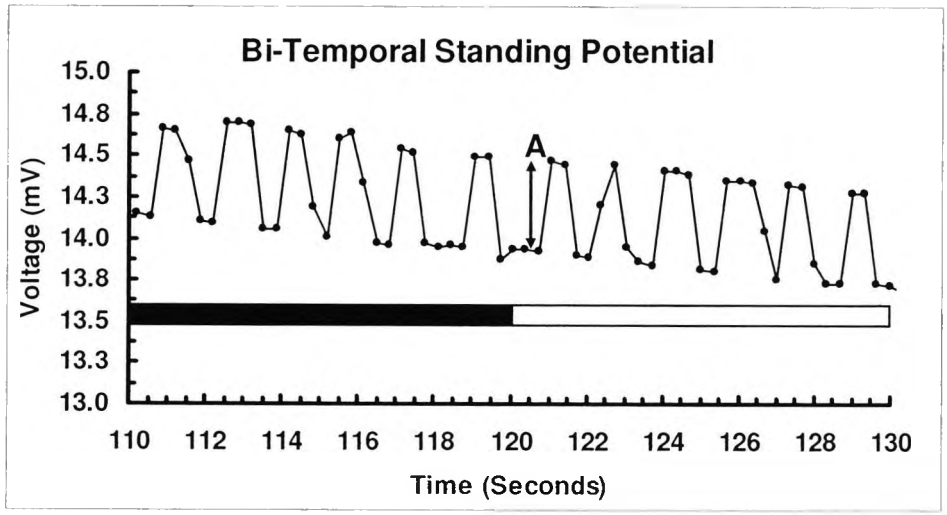

Trace of the bi-temporal potential over time during a recording of the fast oscillations. In order to calculate the amplitude of the standing potential the absolute difference between consecutive data points were calculated and replotted.

5.2.2.1 Calculation of EOG Parameters

The transformed data when plotted describes a curve whose upper boundary represents the change in the ocular standing potential over time in light and dark and in response to alcohol. Figure 5.2 shows the data that represents the alcohol-EOG.

The EOG is typically described in terms of the Arden ratio which represents the light-peak maximum to the dark-trough minimum preceding light onset (Arden and Barrada, 1962; Marmor and Zrenner, 1993). In this study, the EOG voltages were treated differently and three components of the light- and alcohol-EOGs were analysed. Figure 5.2 shows the transformed data from the bi-temporal voltages recorded for the alcohol-EOG. The maximal values at each

time point along the upper limit of the curve were taken as the ocular standing potential at that time. The figure shows that in dark the bi-temporal potential falls and following alcohol at t=26.5 minutes there is a rise in the potential (the alcohol-rise) followed by a second trough.

Figure 5.2 Transformed Data for Alcohol-EOG

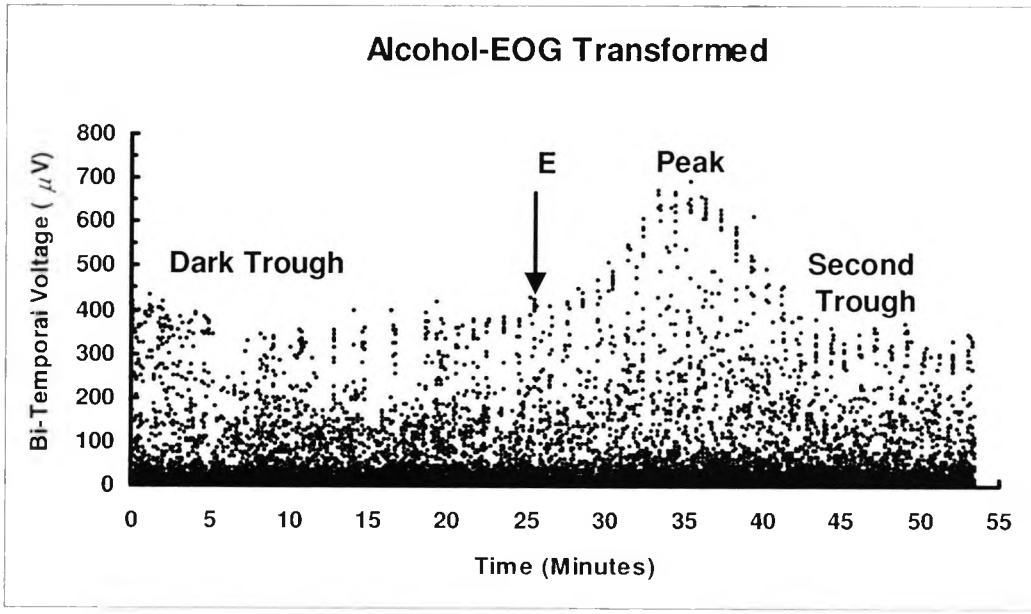

The figure shows the transformed data (equation 5.i) recorded as the bi-temporal potential of a 54 year-old male control ingesting 110 mg/kg of alcohol at 26.5 minutes (arrow labelled E). In the dark, the bi-temporal voltage falls to a 'dark-trough' minimum. After ingestion if alcohol there is a rise, the alcohol-rise that peaks approximately ten minutes later. Subsequently the bi-temporal voltage falls to a second trough minimum. The outline of the curve describes the alcohol-EOG. Values were taken at each time point along the upper limit of the waveform as the bi-temporal voltage.

The EOG voltages were normalised to the ten-minute pre-stimulus baseline voltages. In equation 5.ii the normalised potential (X_N) was equal to the potential at time (T) denoted (X_T) divided by the mean of the measurements made in the 10 minutes prior to the stimulus. These recordings were made at T= 16, 18, 20, 21, 22, 23, 24, 25 and 26 minutes into the pre-adaptation dark period. Light or alcohol was then given at 26.5 minutes.

$$X_N = X_T / (\text{Mean } X_{T\,(16,\,18,\,20,\,21,\,22,\,23,\,24,\,25,\,26)}) \qquad \text{— 5.ii}$$

Where:

X_N = Normalised voltage at time T.

X_T = bi-temporal voltage at time T.

Mean ($X_{T(16....26)}$ = Mean baseline bi-temporal voltage at T = 16^{th},18^{th},20^{th}, 21^{th},22^{th},23^{th},24^{th},25^{th} and the 26^{th} minute.

Subsequently the normalised voltages were smoothed further by weighting each value with 50% of the preceding and the following normalised voltage (equation 5.iii).

Smoothed Voltage = $[X_N + (0.5 \times X_{N-1})) / (X_T + (0.5 \times X_{N+1})] \times 0.5$ — 5.iii

Where:

X_N = the normalised voltage at time T (from equation 5.ii).

X_{N+1} = the normalised voltage value after X_N.

X_{N-1} = the normalised voltage value preceding X_N.

The baseline-normalised voltages were not identical between the CF and the control groups. To correct for this so that the amplitudes of the responses could be compared to an identical baseline the following correction was used. The ratio of the normalised voltages from all subjects in the 10 minute interval preceding the stimulus for the CF group to the same values of the control group were taken.

For the light-EOG the values were for CF = 0.9804 and for the control = 1.0196 and the correction factor was 0.9804/1.0196 = 0.9616. This correction to the baseline was then multiplied through all the normalised voltages for the control group. The corresponding baseline correction factor for the alcohol-EOG was 1.0449.

Figure 5.3 (overleaf) shows a typical light-EOG after transformation and normalisation of the bi-temporal potential. Three parameters were then used to analyse the EOGs between the CF and control group.

1: The time to peak or implicit time of the response from stimulus to the peak voltage.

2: The normalised peak voltage or amplitude of the EOG.

3: The ratio of the peak normalised voltage to the second trough minimum voltage.

Figure 5.3 Electro-Oculogram Parameters

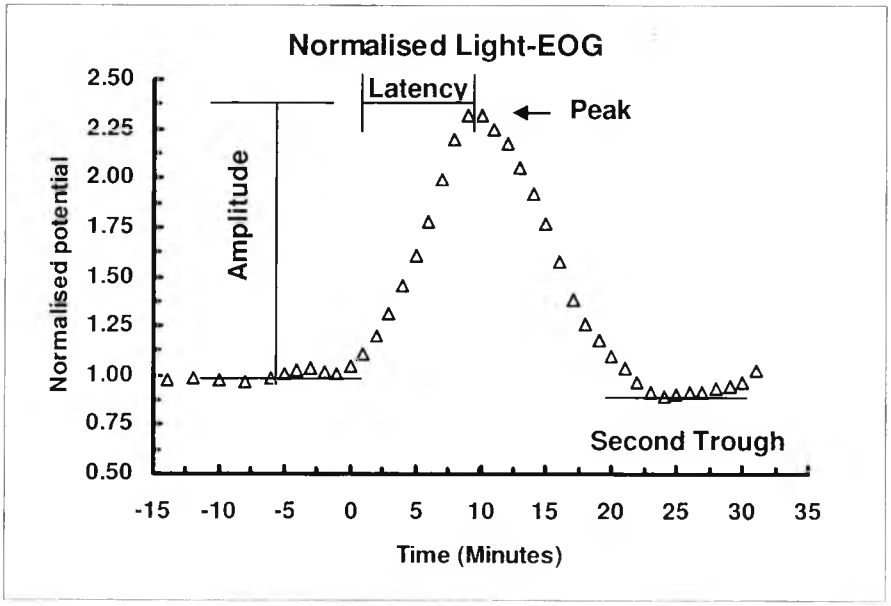

Parameters recorded fro the EOGs included the latency or time from stimulus (either light or alcohol) to the peak voltage. The EOG amplitude was the ratio of the peak voltage to the normalised baseline voltage at t=0 (stimulus onset). The third parameter was the ratio of the peak voltage to the trough minimum voltage after the fall from either light or alcohol and is termed the 'second trough'.

The three EOG parameters recorded were the amplitude of the peak-normalised voltage to the baseline. The latency or implicit time was the interval from stimulus to the peak normalised voltage. The ratio of the peak voltage to the second trough minimum was also recorded. Figure above shows a typical light-EOG recording from a control participant.

5.2.2.2 Calculation of FO Parameters

In the FO the peak voltage occurs in the dark cycle and the minimum occurs in the light cycle so the peak to trough ratio represents the dark-rise maximum : light-trough minimum (DR:LT). The times from dark-rise peak to light-trough minimum were also recorded as the latency of the response. The methods for analysing the FO parameters vary between authors but published values for the DR:LT ratios are listed in table 5.1 (overleaf) with normal values ranging from approximately 1.1 to 1.3.

Table 5.1 Published DR:LT ratios

Author	DR:LT Ratio Mean ± SD	N	Luminance (cd/m^2)	Stimulus Duration (Seconds)
Mergaerts *et al.*, (2001)	1.13 ± 0.01	51	250	60
Miller *et al.*, (1992)	1.26 ± 0.09	15	—	—
Weleber, (1989)	1.22 ± 0.15	8	70	75
Schneck *et al.*, (2000)	1.20 ± 0.03	9	30	60

Reported values of the DR:LT ratio for the fast oscillations in man.

Figure 5.4 overleaf shows the transformed data (equation 5.i) of a FO from a CF participant (Δ508/Δ508). The outline of the transformed data represents the FOs that rise in the dark (black bars) and fall in the light intervals. Recordings were made continuously for ten minutes with each light-dark cycle lasting ten minutes. Values that lay away from the curve were ignored like those in the intervals (180-240) and (420-480) seconds. These were either caused by blinks or in the case with the CF group occasional coughing. A cursor was placed at the dark-rise maximum and the subsequent light-trough minimum as shown in figure 5.4. The ratio of the bi-temporal voltage at the dark-rise maximum to the light-trough minimum was then taken as the DR:LT ratio. The time interval between the maximum and minimum values was taken as the latency.

Figure 5.4 Fast Oscillation Transformed Data

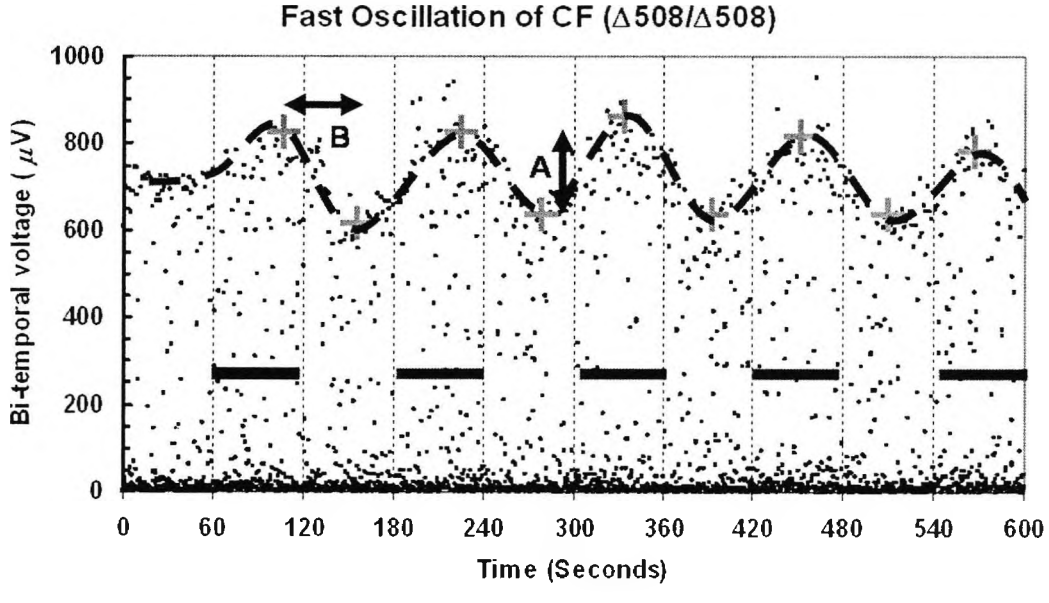

When the differences between successive voltage recordings are made the amplitude of the standing potential is seen to alternate with light and dark (black horizontal bars). Most voltage differences are near to zero, because the eyes were stationary. The extremes represent the EOG voltage change due to the saccades. The ratio of the dark-rise peak : light-trough minimum (DR:LT) represented by the arrow labelled A and the time from peak to trough represented by arrow B were recorded for each individual. Four measurements were taken from each trace for each parameter. The grey crosses in this figure are approximately placed at the values of the dark-rise and light-trough maximums and minimums. To give an indication of the oscillatory waveform a dark dotted line is also shown that follows the upper boundary of the recordings.

5.2.3 Data Analysis

The results are expressed as mean ± standard deviation (SD) unless otherwise stated. Test for equal variance was used (F-test) for all parameters. In this series the DR:LT ratios of the FOs did not have equal variance using the F-distribution ($p<0.0001$). Therefore, this data set was divided into the homozygote and heterozygous groups and a one-way Analysis of Variance (ANOVA) performed with $p<0.05$ as significant using Minitab™ ver 13.32 (Coventry, UK) software. The remaining data were evaluated for a significant difference between means using the Student's unpaired two-tailed t-test. A p-value of <0.05 was taken as statistically significant. A least squares linear regression analysis was performed on the DR:LT ratio and FO latency using Minitab™ software. All other calculations were performed in Excel™.

5.3 Results

5.3.1 Cystic Fibrosis Alcohol- and Light-EOGs

There was no difference in the amplitude of the alcohol-EOG between the CF group and the controls (figure 5.5). The amplitudes were 1.62 ± 0.16 (N=6) controls and 1.67 ± 0.07 (N=5) for the CF group (p=0.8533). The times to peak were: for the controls 9.0 ± 1.4 minutes and for the CF group 7.4 ± 0.9 minutes (p=0.0570) which was 1.6 minutes faster. The one CF individual with an abnormal alcohol-response was receiving immunosuppressive therapy and is also shown but the data were not included in the statistical analysis. This individual's data are labelled as 'CF lung transplant'.

Figure 5.5 Alcohol-EOG in Cystic Fibrosis

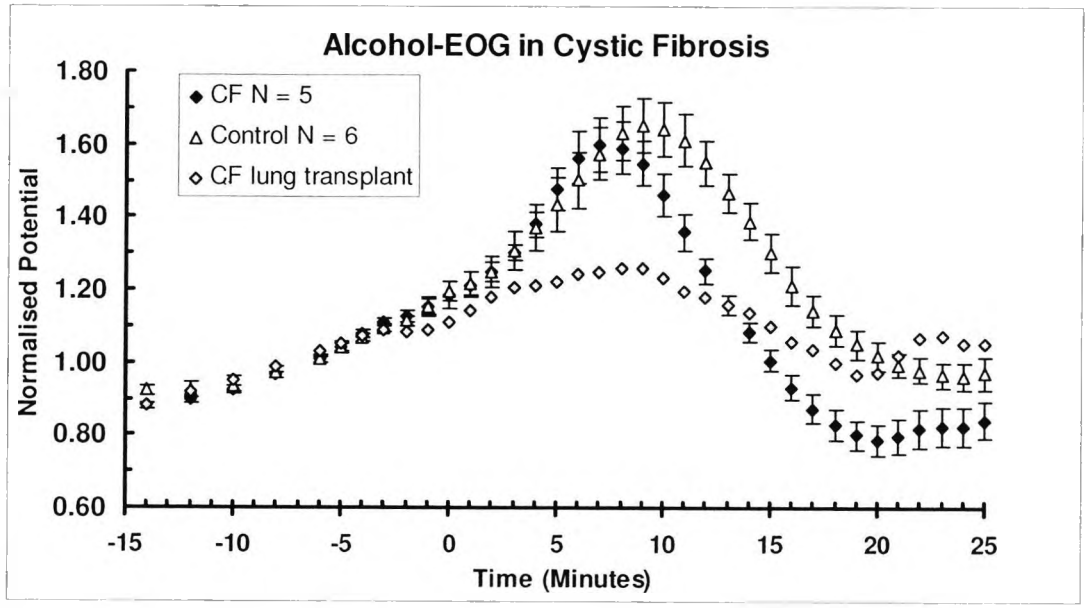

The alcohol-EOG responses to 110 mg/kg of oral alcohol at t=0. The time to peak was significantly faster (p=0.0504) but the amplitudes are similar. One individual who had received a lung transplant showed an abnormal alcohol response which may have been due to an interaction with his systemic medications. Plot shows mean ± SEM.

The amplitude of the light-rise was not significantly different (p=0.8653) between controls (2.01 ± 0.16 N=6) and CF patients (1.93 ± 0.15 N=5). However, there is a significant difference in the timing of the responses with the control group peaking at t = 10.2 ± 0.4 and CF group peaking at t = 8.0 ± 0.6 minutes which is 2.2 minutes faster than in the controls (p<0.0001). See figure 5.6 (overleaf). The lung transplant participant had a normal light-EOG and is also shown in the figure but his data were not included in any analysis.

Figure 5.6 Light-EOG in Cystic Fibrosis

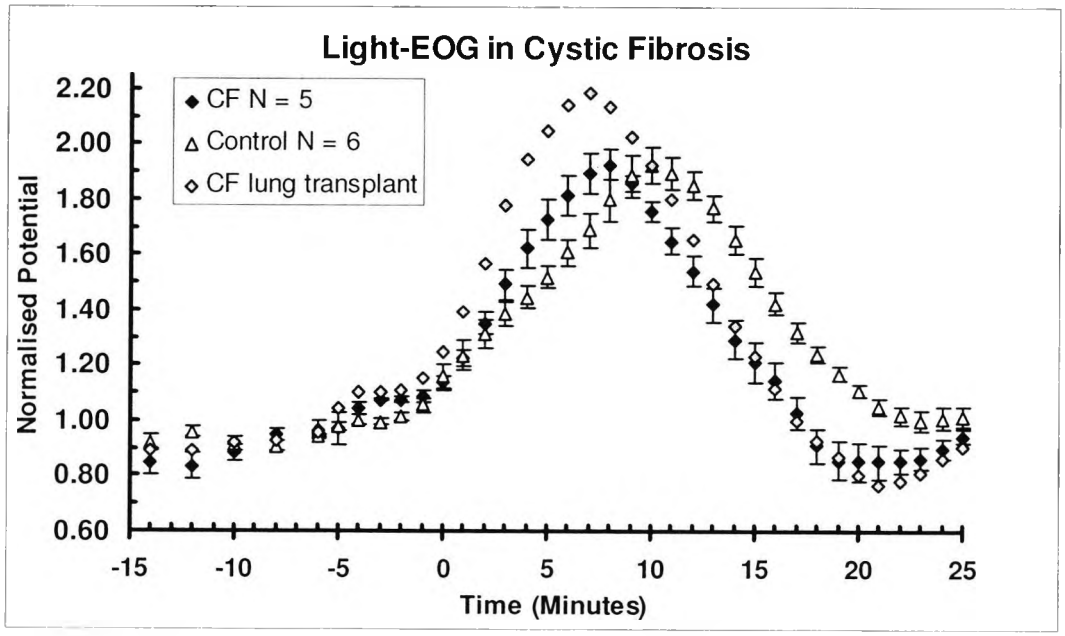

The light-EOG in a series of individuals with CF shows that whilst the amplitude of the response is the same compared to controls, the time to peak is significantly faster ($p<0.0001$) in the CF group. Plot shows mean ± SEM with light on at t=0. The individual who is post transplant is also shown – with a normal light response.

The ratio of the light peak to the second trough normalised voltages for the CF and control group were compared. The alcohol-EOG ratio for the CF group was 2.25 ± 0.23 which was significantly higher ($p=0.0297$) than the control group's ratio of 1.82 ± 0.31. In the light-EOG the ratio was not so significantly ($p=0.0879$) different with the CF group's ratio equal to 2.37 ± 0.42 and the control group's ratio being 1.92 ± 0.38.

5.3.2 Fast Oscillations

Unlike the EOGs the FOs of the Δ508 homozygotes and the Δ508 heterozygotes were significantly different with respect to the amplitudes. One-way ANOVA analysis of the DR:LT ratio and the latency from dark-rise to light-trough revealed the following differences compared to controls (all values are mean ± SD). The Heterozygote's DR:LT ratio was 1.44 ± 0.10 which was significantly ($p<0.001$) greater than the controls with a ratio of 1.29 ± 0.05. Furthermore, the time from the dark-rise to light-trough was significantly slower ($p=0.029$) with the heterozygote's time being 61.8 ± 5.0 seconds and the controls being 57.2 ± 6.5 seconds. By contrast, when the controls were compared to the Δ508 homozygotes then no significant differences were noted in either the DR:LT ratio 1.28 ± 0.09 ($p=0.689$) or the timing 57.8 ± 5.7 seconds ($p=0.827$). When the two CF groups were compared then the heterozygotes had a significantly higher DR:LT ratio ($p=0.0010$) but there was no difference in the timing ($p=0.1070$). A series of representative FOs are shown in figures 5.7(a-c) overleaf. Trace 5.7a shows a control FO whilst traces 5.7b and 5.7c show a homozygote and heterozygote CF sufferer for the Δ508 mutation respectively. All traces began with a one-minute interval of light before dark in which the bi-temporal potential rose. Points that deviated from the curve were ignored.

Figure 5.7a Fast Oscillation - Normal

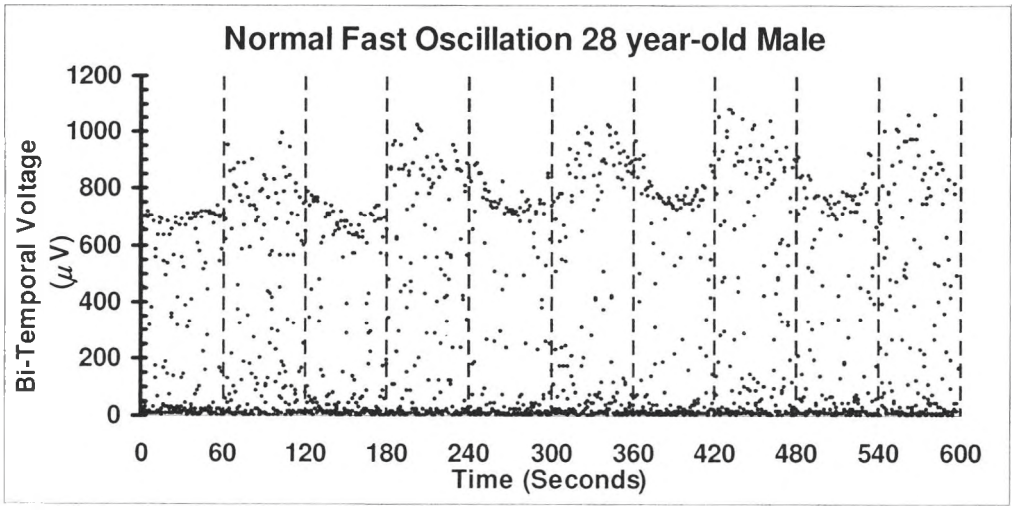

Figure 5.7b Fast Oscillation - Δ508/Δ508

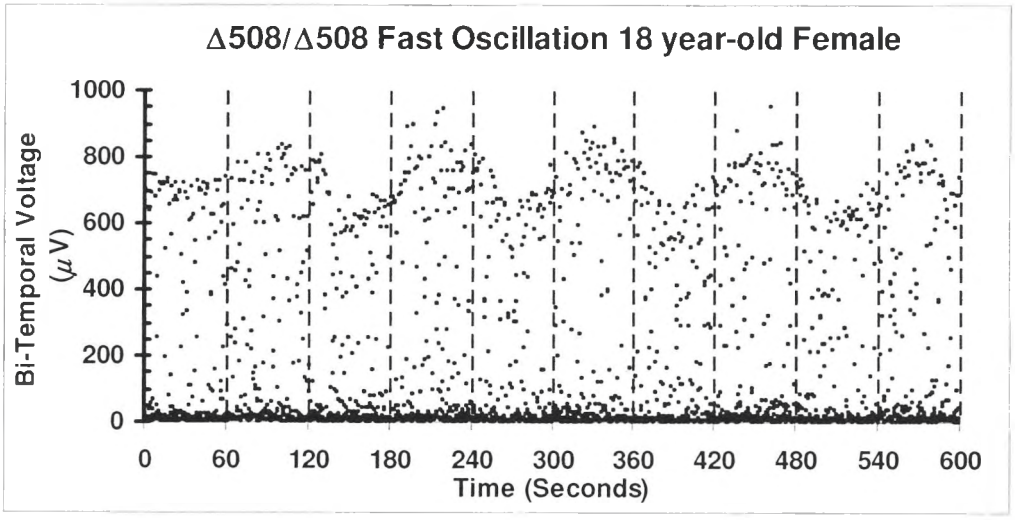

Figure 5.7c Fast Oscillation - Δ508/?

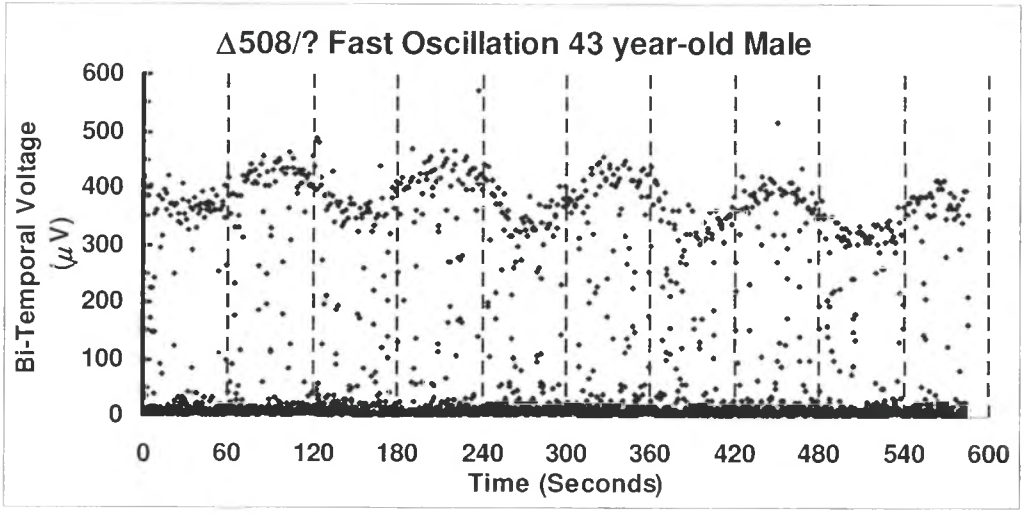

Figure 5.8 shows the DR:LT ratio plotted against the latencies for the FOs. Both the CF and control group results are shown. The DR:LT axis is on the ordinate. A ratio of 1.0 indicates a total absence of FO. In the CF group, the heterozygous group had the highest DR:LT ratios and these were also significantly slower than the control group (open diamond ◊). The homozygous pair are represented by filled black diamonds (♦) and were no different to the controls in either the DR:LT ratio or the timing of the FOs. Only one oscillation from this group was < 1.15 and could be considered abnormal. The lung transplant participant represented by grey diamonds (◊) had two values in the normal range (1.23 and 1.25) and two values that were very low and abnormal (1.12 and 1.02). The controls are represented by crosses (X) in the figure.

Figure 5.8 Linear Regression of DR:LT Vs Latency

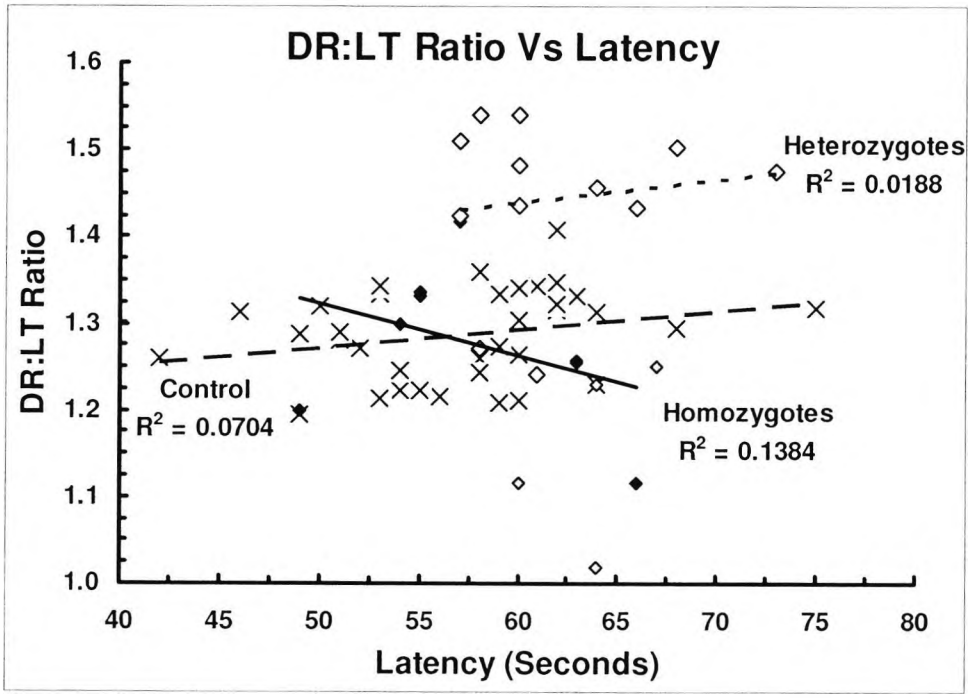

Linear least squares regression plot of the DR:LT ratios against latency from dark-peak to light-trough for control (x) and the CF participants. The CF data points are divided so that the Δ508 homozygotes are indicated by a (♦). The CF Δ508 heterozygotes by a (◊) and the lung transplant individual by a ( ). There is no strong linear relationship between the DR:LT ratio of the FO and the latency from peak to trough. The CF group had a greater variance in the DR:LT than the control group. However, only one value of the DR:LT ratio fell below 1.15. The heterozygotes tended to have a higher DR:LT ratio than the homozygotes. Note axes are truncated.

Equations 5.iv to 5.vi are the least squares linear regression relationships between the DR:LT ratio and the latency for the control and CF groups. There were no strong relationships between the DR:LT amplitude and the timing of the FOs. However, the homozygotes did suggest that in this case the DR:LT amplitude did decrease as the latency increased.

Control	DR:LT ratio = 1.16 + 0.00214 x Latency	(R^2 = 0.0704)	(p=0.124) — 5.iv
Δ508/Δ508	DR:LT ratio = 1.62 - 0.006 x Latency	(R^2 = 0.1384)	(p=0.364) — 5.v
Δ508/?	DR:LT ratio = 1.28 + 0.0026 x Latency	(R^2 = 0.0188)	(p=0.671) — 5.vi

5.4 Discussion

The alcohol- and light-EOGs in patients with CF are both altered with respect to the time to peak. Both responses are shifted to the left with the light-rise being affected to a greater extent than the alcohol-rise. However, the amplitudes are not different and this makes it unlikely that CFTR is the major chloride channel responsible for these responses. The CF group contained both Δ508 homozygotes and heterozygotes. This common mutation renders CFTR incapable of reaching the plasma membrane in any substantial amounts. The significant differences in the time to peak must relate to an interaction between CFTR and the initiation of the light- and alcohol-EOG responses. It was possible that alcohol absorption might be slowed in CF. However because both the light- and alcohol-EOGs have faster onsets then this acceleration must be due to processes occurring within the RPE.

Our current understanding of the origins of the light-rise is incomplete with the putative 'light-rise' substance and its receptor unknown. CFTR has numerous interactions with other ionic channels in epithelia (Greger *et al.*, 1996; Schwiebert *et al.*, 1999; Kunzelmann, 2001) and therefore a similar function may exist in the RPE. This has recently been proposed as a possible explanation for the presence of the FOs in CFTR null mice (Wu *et al.*, 2006). The Δ508 phenotype is variable with individuals that share the same genotype showing different phenotypes (Rowntree and Harris, 2003). Cellular studies on CF lung gene expression indicate that an absence of CFTR results in an upregulation of mRNA that may both improve or hinder the condition. Transcription levels for proteins involved in inflammation, protein trafficking, degradation, cell-cell communication and ion transport are altered in CFTR null mice lung epithelium (Xu *et al.*, 2003). It is therefore likely that there would be some differences in the RPE of CF sufferers that would compensate for a lack of functional CFTR.

Investigations into the role of functional CFTR in the RPE suggest that it contributes to fluid transport in foetal human RPE (Blaug *et al.*, 2003). The study of Blaug *et al.*, (2003) in foetal RPE revealed by immunocytochemistry that CFTR was present at both the apical and basal membranes. The localisation of CFTR in foetal tissue may differ to adult RPE and immunological staining at the apical membrane may not indicate the true proportions of the epitope. The loss of apical processes may reduce the number of CFTR channels that are present during the preparation of the tissue (Rizzolo, 1990). CFTR is presumed to be at the basal membrane based upon the increased fluid secretion noted when levels of PKA were increased and also the loss of the FOs in CF homozygotes reported (Miller *et al.*, 1992).

The study of Blaug *et al* (2003) showed that the FOs were increased in the presence of PKA and that fluid transport also increased. These findings were taken as evidence that CFTR is probably involved in these processes. However, the investigators did not inhibit CFTR with a blocker and so the increase in fluid transport following elevation of PKA may have been due to an alternative chloride channel such as ClC-2 (Jovov *et al.*, 1995b; Tewari *et al.*, 2000). In another study that compared the relative contributions of CFTR and CaCC to fluid regulation in canine RPE

suggested that the contribution of CFTR to fluid regulation was not significant (Loewen *et al.*, 2003). This finding is consistent with the observations that individuals with CF are not prone to a maculopathy which is the case with mutations in bestrophin. CFTR is probably expressed at both the apical and basal membranes, because other studies using bovine and ARPE-19 have demonstrated functional activity of CFTR at the apical membrane (Reigada and Mitchell, 2005).

The closest study investigating ionic fluxes in ocular CF tissue in Ussing chambers are of mouse corneal-conjunctival preparations (Levin and Verkman, 2005; Levin *et al.*, 2006). In these two studies the trans epithelial potentials were higher in the CF mice than in controls and a direct action of CFTR regulating the ENaC sodium currents was not demonstrated. There are no Ussing chamber experiments utilising human Δ508/Δ508 RPE tissue and therefore it is unknown what effects this phenotype would have on the ionic channels and membrane potentials. However, in other tissues lacking CFTR there have been several studies investigating the implications of a functional loss of CFTR. Typically in affected epithelia such as skin and lung the sweat or mucosa respectively are high in NaCl due to poor Cl^- transport (Knowles *et al.*, 1983; Boucher *et al.*, 1986; Joris *et al.*, 1993).

If there was a difference in the TEP in the CF participants compared to the controls then a difference in the amplitudes of the responses would have been apparent in all cases of the EOGs. The voltage changes for the light-EOG occur at the basal membrane with an increased Cl^- conductance (Gallemore and Steinberg, 1989). The FOs arise from a fall in Cl^- conductance across the same membrane following hyperpolarisation. Given that the apical and basal membranes are electrically coupled then a difference in either membrane voltage between the groups would be reflected in a difference in the amplitude of the responses. The light- and alcohol-EOGs had no difference in amplitude. This suggests that the absence of CFTR did not affect the membrane conductance or contribute to the change in the TEP that resulted in the light- and alcohol- rises.

However, the FOs did display a large variance in the amplitudes. This was especially obvious in the Δ508 heterozygotes which suggest that there is an interaction of CFTR with this process. Furthermore, the differences observed in the FO amplitudes compare to the light- and alcohol-EOG rises supports the model in which these two processes originate from different mechanisms (Gallemore and Steinberg, 1989, 1993; Weleber, 1989). That is the EOG amplitudes are generated by a basolateral depolarisation, whereas the FOs are believed to be generated by a basolateral membrane hyperpolarisation. From this small sample, the Δ508 heterozygotes had a larger FO amplitude (DR:LT) compared with the controls and the Δ508 homozygotes. Although both genotypes result in minimal functional CFTR being present at the plasma membrane with heterozygotes having < 50% of normal chloride transport (Sermet-Gaudelus *et al.*, 2005). The variability of the CF phenotype and the alterations in other proteins to compensate for the loss of CFTR may account for the differences observed between the heterozygotes and homozygotes and will be discussed further below.

A direct interaction of ethanol on CFTR conductance can be excluded as patch clamp studies have shown that ethanol does not alter Cl^- currents in both wild-type CFTR and Δ508CFTR (Marcet *et al.*, 2004).

5.4.1 Electro-oculogram

There were two principle differences between the EOGs of the CF and control group. One was that the CF group peaked earlier than the controls. The second was that the fall from peak to the second trough was greater in the CF group than controls. The only similarity between the two groups was that the amplitude of the alcohol- and light-rise was the same.

The interactions of CFTR with Na^+ and K^+ channels are unlikely to modify the voltage change across the RPE during the EOG. This is because the main ion responsible is Cl^- for the EOG waveform (Gallemore and Steinberg, 1989). Given that the alcohol-EOGs had normal amplitudes in CF group, the likely channel responsible for this change is the CaCC which is believed to be responsible for the light-EOG. Alternatives to the CaCC at the basement membrane that could in theory generate the alcohol-EOG in the absence of CFTR would be the ORCC or ClC-2. However, these channels are unlikely to be responsible for the voltage change. The ORCC is only expressed in a small ~ 10% of cultured mouse RPE cells (Wollmann *et al.*, 2006). ClC (chloride channels) are voltage gated channels with nine members identified and are widely expressed throughout the body where they are involved with cell volume regulation, transepithelial transport and the stabilisation of membrane potential in skeletal muscle. They can be modulated by cell sweeling, membrane hyperpolarisation or depolarisation, intracellular pH and $[Ca^{2+}]_{in}$ (Jentsch *et al.*, 1999).

The RPE contains ClC-2 that may have contributed to the alcohol-EOG but the localisation of ClC-2 has not been determined (Weng *et al.*, 2002). However, in guinea pig colon the ClC-2 ion channel is expressed in the plasma membrane where it shows outward voltage dependent chloride currents that increase in response to membrane hyperpolarisation (Catalan *et al.*, 2002). However, the voltage dependence of ClC-2 does not show the same slow voltage dependent inactivation as the L-type Ca^{2+} channel that would be required to decrease the alcohol- and light-EOG waveform (Ueda and Steinberg, 1993).

Both ARPE-19 and bovine RPE do transport ATP across the apical membrane and this transport is inhibited by a CFTR specific antagonist (Reigada and Mitchell, 2005). Therefore, it may be that in CF this pathway is impaired. It has been proposed that ATP may be the light-rise substance (Peterson *et al.*, 1997; Reigada and Mitchell, 2005; Marmorstein *et al.*, 2006). It has been speculated that ATP may derive from the rods and not the RPE owing to the high metabolic rate in the dark that is dramatically reduced at light onset (Arden and Constable, 2006). Thus if purinergic receptors were up-regulated owing to the loss of CFTR-driven ATP transport, then the response of the purinergic receptors may be heightened and result in a faster onset of the light-rise. However, this theory would not explain the faster alcohol-rise times, given no light is

involved. In CF epithelia the mRNA levels of the P_2Y_2 receptors were no different to controls (Ribeiro *et al.*, 2001) which argues against the up-regulation of these receptors to compensate for the lack of Cl^- transport in affected tissues. P_2Y_2 receptors coupeod to a G-protein that when bound to purinergic agonists such as ATP then a rise in intracellular [Ca^{2+}] follows through the generation of IP_3 (Maminishkis *et al.*, (2002).

It is possible that CFTR may alter the CaCC currents to alter the kinetics of the light- and alcohol-EOG responses. An interaction between these two channels has been demonstrated in a number of species. In *Xenopus* oocytes expression of CFTR inhibited the endogenous CaCC current (Kunzelmann *et al.*, 1997). Similarly, CFTR inhibits the CaCC current in bovine pulmonary artery but the Δ508CFTR mutant did not (Wei *et al.*, 1999). Therefore, a loss of inhibition on the CaCC would result in a larger chloride conductance and bigger EOG amplitudes which were not observed.

There were two main differences between the EOGs of the CF and control group. One was the time to peak and the second was in the ratio of the rise to second trough. These two findings could be explained by an interaction with the L-type Ca^{2+} channel based upon the evidence that this channel is also regulated by bestrophin and is central to the generation of the slow Ca^{2+} influx required for the EOG (Marmorstein *et al.*, 2006; Rosenthal *et al.*, 2006). It is well documented that CFTR interacts with other ionic channels (Ando-Akatsuka *et al.*, 2002; Cornejo-Perez and Arreola, 2004; Reddy and Quinton, 2005) and therefore it seems most likely that CFTR also modulates the conductance of ionic channels in the RPE.

The faster onset of the light- and alcohol-EOGs could be explained given the recent findings that show hBest1 increases the kinetics of inward Ca^{2+} flux through the L-type Ca^{2+} channel (Rosenthal *et al.*, 2006). Given the widespread interactions of CFTR with other ionic channels it could be that CFTR also modulates the kinetics of the L-type Ca^{2+} channel. In this possible explanation the absence of CFTR would result in a faster onset of the EOGs because the rate of entry would be regulated by bestrophin. It is important to note that it is only the kinetics and not the total inward Ca^{2+} current that is modulated by bestrophin so that the amplitudes are unaltered. The proposal is that CFTR inhibits the action of bestrophin or directly acts upon the L-type Ca^{2+} channel to reduce the rate of Ca^{2+} entry. In the absence of CFTR this regulation is lost so that the inward Ca^{2+} currents increase faster and this is what results in the earlier peak times of both the light- and alcohol-EOGs.

The CF group had higher ratios for the peak to second trough with this being more pronounced in the alcohol-EOG. It has recently been suggested that the compound waveform of the EOG is not a simple damped oscillation, but a resultant of two separate processes- an initial rise and a delayed fall in the TEP. The evidence was that the ratio peak: second trough varied systematically with the stimulus intensity (Wolf and Arden, 2004). The increased ratios from peak to second trough could be due to either an increase in the positive (depolarising) or an increase in the negative (hyperpolarising) component. The results of the CF EOGs show that

the normalised second negative trough falls below the normalised pre-stimulus baseline and given that the peak amplitudes are the same the likely contributor to the higher ratios is from the negative hyperpolarising component.

The hyperpolarisation could result from several different mechanisms. The simplest is that in the absence of CFTR the basal membrane is more hyperpolarised than normal owing to the reduced Cl^- transport. However, this would imply that the R_{Basal} would be higher and therefore the amplitudes of the light- and alcohol-EOGs should be lower which was not found. The delayed nature of the second trough would suggest that a slow conducting channel is involved. The greater fall from the peak of the EOG response to the second negative trough implies that the inactivation of the inward Ca^{2+}-current could be increased by a stronger deactivation of the L-type Ca^{2+}. If this were the case then the inward Ca^{2+} current is reduced at a faster rate and the signal for the outward Cl^- current through the CaCC is also rapidly reduced. This would then hyperpolarise V_{Basal} and result is a larger decrease in the TEP as shown by the increased ratio of the peak to second trough ratio in CF.

The individual who was taking immunosuppressives following his lung transplant had an abnormal alcohol-response but normal light responses (for CF). It was likely that the medications he was taking could have interfered with the alcohol-rise in this case. Doxazosin is an α_1-antagonist and is a derivative of prazosin (Elliott *et al.*, 1982) that reduces α_1-adrenergic stimulated release of intracellular Ca^{2+} from the ER in foetal RPE (Quinn *et al.*, 2001). If the α_1-receptor was the receptor for ethanol then this would explain the reduced alcohol-EOG as doxazosin would block any agonistic effect of ethanol. However, the ER is not the source of the Ca^{2+} signal in the alcohol-EOG, as suggested by the *in-vitro* Ca^{2+} experiments. Similarly, ramipril acts by suppressing angiotensin II formation and angiotensin receptors are present in human RPE (Wagner *et al.*, 1996). However, activation of the angiotensin receptor results in a release of Ca^{2+} from intracellular stores and not from the extracellular space which would preclude the angiotensin receptor being a site of action of ethanol (Cullinane *et al.*, 2002).

The most likely explanation for a lack of an alcohol-EOG in this individual is that the immunosuppressive agents were altering the physiological response to ethanol in this participant. Azothioprine's mode of action is to inhibit ATP synthesis and down-regulate DNA and mRNA synthesis (Tiede *et al.*, 2003). In relation to the alcohol-EOG, a reduction in ATP may alter Ca^{2+} homeostasis through decreasing the PMCA pump leading to a higher $[Ca^{2+}]_{in}$. Ciclosporin is toxic to the retina and the RPE with visual loss reported from the use of this drug (Kutlay *et al.*, 1997, López-Jiménez *et al.*, 1997). It is feasible that this drug may be cytotoxic to the RPE and that the alcohol-EOG is detecting these early changes before the alterations in the light-evoked changes.

5.4.2 Fast Oscillations

The current model of the FOs is that they result from the fall in sub-retinal potassium following retinal illumination. This causes a decrease in the activity of the apical Na-K-2Cl co-transporter resulting in a decrease in $[Cl^-]_{in}$ (Oakley II and Green, 1976; Linsenmeier and Steinberg, 1984; Gallemore and Steinberg, 1993). Consequently, the basal membrane hyperpolarises as there is less basolateral Cl^- flux and so the TEP falls causing the light-trough of the FO. The FO is normal in Best's but the light-rise is absent indicating that a different mechanism is responsible for the FOs and the light-rise (Weleber, 1989). The FOs have been claimed to be selectively reduced in CF (Miller *et al.*, 1992; Lara *et al.*, 2003), and this has been taken as evidence that CFTR forms (at least part) of the basal chloride conductance. However, the results indicated that the FOs were higher in the CF Δ508 heterozygotes and they were not reduced in the Δ508 homozygotes. The values reported here for the DR:LT ratio in the control group are similar to previous studies that used a similar analysis.

The findings in this study differ in part to those reported in abstract form previously (Miller *et al.*, 1992; Lara *et al.*, 2003) in that the CF group was not composed entirely of homozygotes for Δ508. However, the two individuals that were homozygous had normal FOs with the exception of one value. Differences between the heterozygotes and homozygotes may be attributed to the different trafficking of CFTR protein. In Δ508, homozygotes CFTR does not reach the plasma membrane while in the heterozygous isoform may still retain some function. In a study of CF patients in both homozygous for Δ508 and heterozygous for Δ508 a wide variation between genotype and phenotype was observed (Duguépéroux and De Braekeleer, 2004).

The variability in the CF phenotype has been attributed to the effect of both environmental and other genetic factors such as promoter genes that compensate in part for the mutations in the CFTR gene (Rowntree and Harris, 2003). The larger DR:LT amplitudes and slightly reduced latency may be related to the association of complex alleles. In a complex allele a second mutation in the gene partially compensates for primary mutation. For example, in Δ508 the accompanying mutation R553Q confers stability to the protein so that it retains function by improving the folding and trafficking of CFTR to the plasma membrane (Dork *et al.*, 1991). All of the heterozygotes were pancreatic insufficient with one being a type 1 diabetic and would normally be classified as 'severe' sufferers (Rowntree and Harris, 2003).

There is some evidence that CFTR current is not reduced by lowered intracellular $[Cl^-]$ (Wright *et al.*, 2004) which would mean that our current understanding of the mechanism of the FO's light-trough requires modification. This finding is supported by the observations in mouse models of CF (Wu *et al.*, 2006). There are few alternative Cl^- pathways at the basal membrane that could account for the FOs if they are not caused by CFTR. It has been proposed that the ClC chloride channels could compensate for the lack of CFTR in the lung given that these channels are also gated by PKA. In knock-out mouse models of ClC-2 retinal degeneration occurs indicating a role

for these channels in the RPE (Bösl *et al.*, 2001). However, immunological staining in native human RPE cells shows expression of ClC-3 and ClC-5 at the apical membrane with ClC-2 showing weak expression but the authors did not state whether ClC-2 was present at the apical or basal surface (Weng *et al.*, 2002). The apical localisation of these channels, would suggest that they do not play a role in the generation of the FOs which are the result from hyperpolarisation of the basal membrane (Blaug *et al.*, 2003).

The recent findings in mouse point to a different mechanism underlying the FOs that are not solely dependent upon CFTR (Wu *et al.*, 2006). The authors found that the FO amplitudes were not abolished in either Δ508CFTR expressing or CFTR null mice. The light-rise amplitudes were reduced to a greater extent than the FOs which was unexpected given that CFTR is not thought to be involved in the light-EOG.

The explanation for the findings, as suggested by Wu *et al.*, (2006) is that there is a complex interaction between the ionic channels at the basal membrane and the absence of functional CFTR may lead to disturbances in regulation and transport of ions that are still to be determined (Kunzelmann, 2001). The CFTR currents are believed to contribute only a fraction of the total Cl^- conductance and so the lack of this current may not alter R_{Basal} to a large extent, given that other compensatory mechanisms may be in place in the RPE given the lack of retinal pathology in CF (Loewen *et al.*, 2003).

Given that the origin of the FOs relies upon a fall in sub-retinal $[K^+]$ and a reduced rate of Cl^- transport through the apical Na-K-2Cl cotransporter then it is possible that the Δ508 heterozygote mutations are affecting this pathway. One possible explanation may have been that the regulation of the apical Na-K-2Cl cotransporter was affected in CF which may account for the large DR:LT ratios owing to a more dramatic fall in $[Cl^-]_{in}$. In pancreatic duct cell lines CFTR has been shown to up-regulate Na-K-2Cl. Therefore, in CF there may be less Na-K-2Cl present which would not explain the observations as this would result in a slowing of the decrease in $[Cl^-]$ and a slower and reduced FOs which was not found. A similar study investigating altered gene regulation in Δ508CFTR and control cultures of human airway epithelium did not find any significant differences in gene expression (Zabner *et al.*, 2005). However, another study has found alterations in the transcriptional products in mouse CF airway epithelium (Xu *et al.*, 2003). Furthermore, levels of CaCC homologues are also upregulated in the gut in CF affected epithelia which suggest that some alterations in the expression of ionic channels must occur in CF (Leverkoehne *et al.*, 2006). The compensatory mechanisms of upregulating chloride channels may partly account for the large variability in the phenotypes observed in this condition (Rowntree and Harris, 2003).

There are not many studies investigating the FO amplitudes and in many cases, the authors used different parameters to measure the waveform. The DR:LT value is often reported and values from other publications are listed in table 5.1. The value of the DR:LT ratio of 1.29 ± 0.05 is similar to that of Miller *et al.*, (1992) and Weleber, (1989) with large SDs reported. Elevated

blood glucose levels have been shown to increase the amplitude of the FOs (Schneck *et al.*, 2000) and there may be some unidentified metabolic difference in the RPE of CF to account for the higher FOs.

No relationship between the DR:LT ratio and the latency from dark-rise peak to light-trough minimum was evident. This supports the findings that CFTR is not involved in the oscillations as if defective CFTR was responsible for the interval from peak to trough then it would be expected that those individuals that more severely affected, homozygous participants would have a slower latency than the heterozygotes. Instead, there was no strong linear relationship in either the CF group or control group to the amplitude of the FO and the time-course. There were also no differences in the period of the oscillations from dark-rise to light-trough between the groups. This finding suggests that there are other factors involved in generating the FOs and that CFTR is not directly responsible.

5.4.3 Summary

The main findings are that CFTR does not contribute to the amplitude of the alcohol-EOG. This supports the findings in the previous section that showed Ca^{2+} to be the second messenger responsible for the alcohol-EOG. The results also show that the timing of the slow EOG voltage changes is faster in CF than in controls. This could be explained by a lack of CFTR inhibiting the effect of bestrophin that acts to increase the kinetics of this ion channel. The FOs showed that the amplitudes were higher in the CF Δ508 heterozygotes. The Δ508 homozygous group did not have any significant reduction in the amplitudes which supports recent findings that suggest CFTR is not solely responsible for this response.

6 Conclusions

The initial aim of this study was to establish an *in vitro* model of the RPE that would allow a detailed exploration of the underlying cellular mechanism of the alcohol-EOG. The use of immortalised cell lines has been employed by many researchers to model human RPE behaviour. The RPE in man forms a tight barrier and one aim was to replicate this property in the well characterised human RPE cell line ARPE-19. A variety of experimental approaches were used to enhance the barrier characteristics of these cells, including varying the composition of the culture medium, varying the underlying substrate or growing the cells in the presence of glia (or glial conditioned media). This latter approach was based on evidence from the literature that glial cells can induce barrier tightening in a variety of epithelia e.g., the rat glioma cell line (C6) has been shown to substantially increase the TER in the human epithelial cell line ECV304 (Hurst and Fritz, 1996).

Despite replicating these findings with ECV304, no similar induction of ARPE-19 cells was evident with this or the Müller cell line MIO-M1. A possible explanation was that the ARPE-19 cells were differentiated and not receptive to secreted factors from glial cells. Several reports on chick RPE have shown that both the age of the retina and the RPE determine whether tight junctions will be fully developed (Rizzolo *et al.*, 1994; Ban *et al.*, 2000; Rahner *et al.*, 2004). Since ARPE-19 cells were derived from an adult donor the potential for induction would be reduced compared to an embryonic RPE cell and this may have accounted for the lack of barrier induction in this cell line. Furthermore, a recent study has found that ARPE-19 shows significant phenotypic heterogeneity, including the organisation of its junctional proteins. Although this heterogeneity could be partially overcome by prolonged culture in specialised medium, the ARPE-19 cell line may not have the capacity to form a very tight monolayer (Luo *et al.*, 2006).

A rise in the TER of the ARPE-19 cells was obtained by modifications to the culture medium with growth factor and hormone supplements to a level that has been previously reported (100 $\Omega.cm^2$) using specially defined medium (Dunn *et al.*, 1996). The composition of the specialised media (SM1 and SM2) significantly increased the TER compared to the standard conditions in which ARPE-19 cells are grown. The 100 $\Omega.cm^2$ TER reported by Dunn *et al.*, (1996) was with an optimum cell culture medium and with cells that were of a lower passage number. The recent experiments by Yau *et al.*, (2006) with SM did not attain as high values as those reported here. Disappointingly, when the ARPE-19 cells were mounted in an Ussing chamber the TEP was very low and unsuitable for further detailed work on the origins of the alcohol-EOG using this model.

Bovine and *Rana* RPE have been used to elucidate the mechanisms of fluid transport across the RPE as well as the ionic channels and signalling pathways within the RPE (Miller and Steinberg, 1977; Miller and Edelman, 1990). Bovine RPE has been shown to respond to ethanol (Pautler,

1994; Bialek *et al.*, 1996). Pautler implicated AA and not Ca^{2+} as the signalling mechanism (which is contrary to the findings reported here using the fluo-4 indicator). His results do not show any similarities with the human alcohol-EOG. He showed that in bovine RPE, the effect of alcohol was absent in darkness and maximal in green light. This is contrary to the findings in man. There are species differences between human, bovine and amphibian RPE with respect to the regulation of intracellular second messengers. In human, cAMP increases fluid transport and in bovine the reverse is true (Rymer *et al.*, 2001; Blaug *et al.*, 2003). In amphibian RPE the addition of extracellular DIDS blocks the basolateral cAMP Cl^- current which is not blocked in mammalian RPE (Hughes and Segawa, 1993; Linsdell and Hanrahan, 1996). These species differences, though important when comparing the intracellular signalling pathways and chloride channel functions, were not responsible for the lack of responses in the bovine RPE and *Rana* eye-cup preparations.

Two previous studies have shown a direct effect of ethanol on the RPE of bovine eyes. In the Ussing chamber experiments, attempts were made to obtain a response from bovine RPE with and without the retina in place, and in two different Ussing chamber designs and with modifications to the buffers. The lack of any consistent responses coupled to the poor response to epinephrine and ouabain indicated that the RPE was not viable enough at the time of the experiments despite having stable electrical parameters. This failure is therefore likely to be due to post-mortem deterioration in the tissue obtained in this study.

The experiments with *Rana* were designed to overcome the delay in post mortem time and to provide some insight into whether ethanol was acting via a receptor in the retina or one in the RPE. The results from these experiments indicate that ethanol does not liberate a signalling molecule from the retina to alter the standing potential. The demonstration of a functioning retina-RPE complex was demonstrated by evoking a light-EOG from the eye-cup. However, no alcohol-EOG could be convincingly observed. Although it is possible that there may be a species difference in the response to alcohol, an alternative explanation is that in the *Rana* model the alcohol had to be applied to the inner retinal surface of the eye-cup. In man the bulk of the ethanol dose would arrive via the choroid. If the receptors for alcohol were situated near the choroid, it is possible that the concentration of alcohol diffusing from the retinal surface was too low to evoke a response.

6.1 The Alcohol- and Light-Electro-oculograms

A series of experiments were undertaken based on the hypothesis that a change in intracellular Ca^{2+} generated the alcohol-EOG rise. This was due to the recent evidence in support of Ca^{2+} being crucial to the generation of the light-rise of the EOG.

> **1:** An elevation in $[Ca^{2+}]_{in}$ caused by either an apical purinergic activation by ATP (Reigada and Mitchell, 2005). This rise in $[Ca^{2+}]_{in}$ would then open a basolateral chloride channel.
>
> *Or*
>
> **2:** Bestrophin can both increase the rate of Ca^{2+} through L-type Ca^{2+} channels but can also inhibit Ca^{2+} entry if cytosolic $[Ca^{2+}]_{in}$ is high. Bestrophin is unlikely to the basolateral chloride channel responsible for the light-rise with the CaCC channel now appears to be the most likely candidate (Marmorstein *et al.*, 2006; Rosenthal *et al.*, 2006).

The first hypothesis, postulates that the source of the ATP is the RPE cell, and ATP is transported into the sub-retinal space by CFTR. If so, then in cases where CFTR is non-functional the alcohol- EOG rise should be absent or modified. In the second hypothesis, the basolateral L-type calcium channel is gated by an interaction with bestrophin, which inhibits the sustained increase in $[Ca^{2+}]_{in}$ following the putative light-rise substance increase. The involvement of bestrophin in the light-rise has been accepted given that an absent light-rise is pathognomic of Best's disease (Cross and Bard, 1974; Thorburn and Nordstrom, 1978; Weleber, 1989). However, bestrophin now appears to be a regulator of $[Ca^{2+}]_{in}$ and not the Ca^{2+}-gated chloride channel as originally understood. Bestrophin protein then has two functions. One it can increases the rate of Ca^{2+} entry through the L-type Ca^{2+} (Rosenthal *et al.*, 2006) and secondly, bestrophin inhibits the $[Ca^{2+}]_{in}$ once elevated following ATP stimulation (Marmorstein *et al.*, 2006). ARPE-19 was found to be a the most suitable cell line for $[Ca^{2+}]_{in}$ measurements using fluorescent calcium probes given its lack of functional P-gp (Constable *et al.*, 2006b). The identification of the most suitable cell line was necessary because the possible changes in $[Ca^{2+}]_{in}$ may have been low and sustained over several minutes as the alcohol-rise is. Therefore, it was important to maintain the levels of fluo4 within the cytosol for as long as possible.

The nature of the light-rise substance remains elusive but ATP has been proposed to fulfil this role (Reigada and Mitchell, 2005; Marmorstein *et al.*, 2006). During the dark, the rods consume high quantities of ATP to maintain the dark current by the active NaKATPase pump at the inner segment. At light onset, the non-selective channels in the rod outer segment close rapidly, while the NaKATPase exchange pump continues to operate at high speed for some seconds, causing potassium depletion in the sub-retinal space. It is possible that the production of ATP continues

for a short time so the intracellular ATP concentration of the rod rises and may leak into the sub-retinal space (Uehara *et al.*, 1990). See also Arden and Constable, (2006).

ATP or as it is rapidly degraded to ADP could provide the trigger for the light-rise by releasing Ca^{2+} from the intracellular stores (Peterson *et al.*, 1997; Reigada *et al.*, 2005; Reigada and Mitchell, 2005). This transient rise in $[Ca^{2+}]_{in}$ initiated by the release of ATP from the rods would cause an increase in basolateral Cl^- conductance by the CaCC. This would in turn depolarise the V_{Basal} which would then gate open the voltage dependent L-type Ca^{2+} channels which would provide a sustained inward Ca^{2+} flux resulting in further CaCC currents and a continued depolarisation of V_{Basal} until the L-type Ca^{2+} channels inactivated at as V_{Basal} depolarised further. This mechanism may underlie the process involved in generating the light-rise of the light-EOG.

The alcohol-EOG, however, must have a different origin but share at least some part of the final basolateral pathway outlined for the light-EOG. Intracellular Ca^{2+} recordings showed that ethanol increased intracellular calcium, but only by permitting an increased inward calcium flux. The concentrations of ethanol used were higher than the physiological levels but consistent with other studies. The low number of responding cells may have been due to phenotypic heterogeneity within the ARPE-19 cell line (Wimmers *et al.*, 2004; Luo *et al.*, 2006), or to a lesser extent the lowered working temperature and the experimental limitation of being able to add ethanol only to the apical surface. The demonstration that ethanol could produce sharp rises in intracellular Ca^{2+} in a cell line that is known not to express bestrophin would imply that bestrophin is not an ethanol receptor. The responses generated showed concentration dependence, was repeatable and all of the responses returned to baseline indicating that the responses were not a result of damage to cell membranes.

Given that the L-type Ca^{2+} channel has been directly implicated in the light-EOG it is likely that the same channel mediates calcium entry in response to alcohol. Ethanol has been shown to activate L-type channels in PC12 cells (Belia *et al.*, 1995). However, the question remains as to whether ethanol acts directly upon the channel or upon a separate receptor that regulates the L-type Ca^{2+} channel currents. Two possible second messengers could increase the basolateral Cl^- conductance and result in the alcohol-EOG waveform. One is an elevation of $[Ca^{2+}]_{in}$ and the second is the generation of cAMP dependent PKA.

To help discriminate between the two possible signalling modalities (Ca^{2+} or cAMP dependent PKA) and to avoid the problems of working with a cell line, whose phenotype was likely to be different in some respects to native human RPE, a parallel experiment was conducted using individuals with CF. The premise was that the alcohol-EOG should be normal in CF if Ca^{2+}-signalling is involved and abnormal if cAMP were involved. Elevating levels of cAMP has been observed to increase basolateral Cl^- current associated with the FOs in foetal RPE and if, as in CF, where CFTR is absent or largely defective then these currents would be absent. If CFTR was determining the alcohol-EOG voltage change then these response would be expected to be significantly reduced. If the alcohol-EOGs were normal then Ca^{2+} would be the likely second

messenger and a Ca^{2+}-gated chloride channel the most probably candidate for the generation of the alcohol-EOG.

Although the magnitude of the light- and alcohol-EOGs in CF patients was normal, the time course was more rapid than the control group. CFTR is known to interact directly with a variety of ionic channels (Kunzelmann, 2001; Vankeerberghen *et al.*, 2002). One possible explanation could be that CFTR decreases the activation kinetics of the L-type Ca^{2+} channel so that it acts as a counterbalance to the increased activation kinetics when bestrophin is expressed. Therefore, in the absence of CFTR, the influence of bestrophin would be greater so that the rate of Ca^{2+} entry into the cytosol would be faster. This could account for the corresponding light- and alcohol-rises that peaked earlier, in the CF group than the control group. Because both the light and alcohol responses were affected in a similar way this would also support the model in which the L-type Ca^{2+} channel was the centre piece of both of these responses. It is only the rate and not the total current that is influenced which would alter the magnitude of the response and not the timing.

In CF, the ratios of the peak to second trough were greater in both the light- and alcohol-EOGs than in controls. The EOG waveform has been suggested to be a composite of an apical hyperpolarising and a basal depolarising component (Wolf and Arden, 2004). The results with CF lend some support to this view. The lack of CFTR in the basal membrane is suspected to alter the kinetics of the L-type Ca^{2+} channel and acts to balance the influence of bestrophin. The proposal is that as bestrophin increases the rate of Ca^{2+} entry, CFTR may slow the deactivation of this slow voltage dependent channel. This would mean that in the absence of CFTR the inactivation of the inward Ca^{2+} current is faster and this results in a greater fall from the peak to the trough voltage.

A possible mechanism for both the light- and alcohol-EOGs can be proposed based upon the findings of this study. The L-type Ca^{2+} channel is central to both processes because this channel provides the slow voltage dependent Ca^{2+} influx required to maintain the outward depolarising Cl^- current responsible for the light-EOG. It is presumed that given the similarity between the alcohol- and light-EOG that Cl^- is also the ion responsible for the alcohol-rise.

A proposal for the alcohol-EOG would be that ethanol acts upon the L-type Ca^{2+} be effecting one of the tyrosine kinase effectors. Evidence has been shown that regulation by PKC and PKA can alter the kinetics and activation of this Ca^{2+} channel (Strauss *et al.*, 1997). Furthermore the activation by the cytosolic subtype tyrosine kinase $pp60^{c\text{-}src}$ may be a potential target for ethanol that could activate L-type Ca^{2+} channel currents in the RPE (Strauss *et al.*, 2000).

The alternative basolateral channel through which ethanol could act is the CaCC, but the effects of ethanol on this channel are inhibitory (Clayton and Woodward, 2000). Furthermore, the L-type Ca^{2+} channel is central to the sustained Ca^{2+} signal for generating the light-EOG. It is therefore, plausible given the similar nature of the alcohol- and light-EOGs that this channel is the probable site of ethanol action. If ethanol acted directly upon the L-type Ca^{2+} channel then the rise in

$[Ca^{2+}]_{in}$ would gate open the CaCC and instigate the depolarisation of V_{Basal} through a greater chloride conductance that in turn would sustain the slow Ca^{2+} influx by the L-type Ca^{2+} channel. There is some evidence from the trial using nifedipine that abolished the Ca^{2+} transient when present.

The alternative would be that ethanol may act upon the CaCC directly to increase basolateral chloride conductance that, again, depolarises the L-type Ca^{2+} channel to continue the cycle of chloride efflux, membrane depolarisation, Ca^{2+} influx, chloride efflux until finally V_{Basal} depolarised to such a point that the L-type Ca^{2+} channel was inactivated and the cycle halts and with it the alcohol or light-rise. However, there are no studies which have shown ethanol to increase CaCC currents (Clayton and Woodward, 2000).

A summary of the proposed model for the alcohol-EOG is shown in figure 6.1.

Figure 6.1 Model of Alcohol-EOG

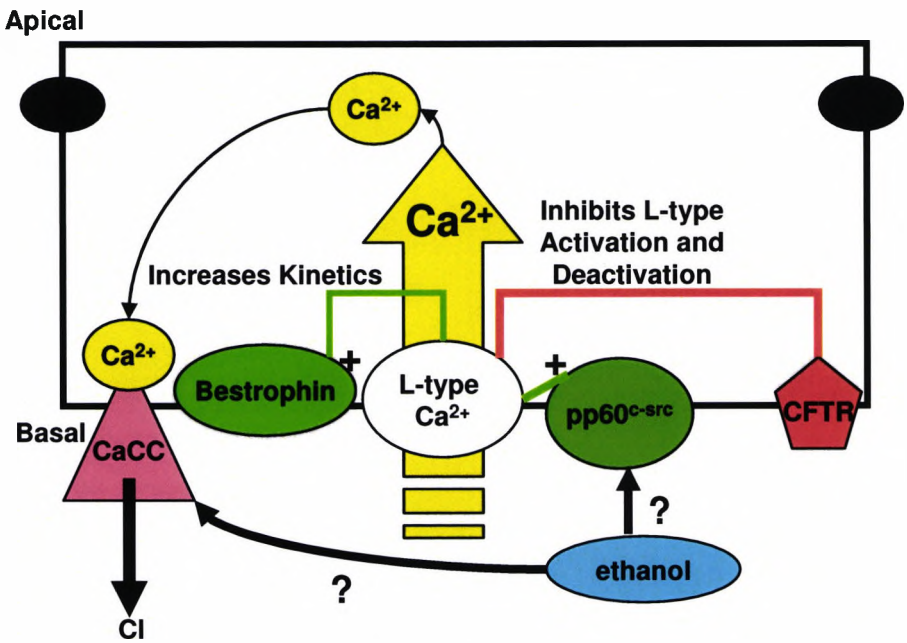

The model of the alcohol-EOG centres on the L-type Ca^{2+} channel. Ethanol activates this channel by modulation of a cytosolic tyrosine kinase that could be of the $pp60^{c\text{-}src}$ sub-type to increase the inward Ca^{2+} conductance. The increased $[Ca^{2+}]_{in}$ then gates open a chloride channel (most likely CaCC), as this channel is presumed to be responsible for the light-rise. It is possible that ethanol gates the CaCC directly which would depolarise the membrane and increase inward Ca^{2+} currents through the L-type Ca^{2+} channel. However, experimental evidence suggests that ethanol inhibits the CaCC currents, but this is yet to be shown in the RPE.. The faster EOGs observed in the CF group may be the result of the loss of the inhibition of CFTR on the Ca^{2+} influx. The absence of CFTR would result in a faster Ca^{2+} conductance by the voltage dependent L-type Ca^{2+} channel. It is also proposed that the inactivation kinetics of the L-type Ca^{2+} channel is also altered so that the fall from peak to second trough is greater with a more hyperpolarising voltage change across the basal membrane being generated.

6.1.1 The Fast Oscillations

Previous work has reported reductions in the amplitude of the FOs in Δ508 CF sufferers (Miller *et al.*, 1992; Lara *et al.*, 2003). The present study has found that the FOs in CF are not universally decreased. One reason for this discrepancy could be that three of the five CF individuals were heterozygotes, while other workers have tested homozygotes only. Heterozygotes in our sample tended to have the higher FO amplitudes. This finding implies that our current understanding of the FOs is incomplete. The lack of a strong linear relationship between the DR:LT amplitude and the timing of the FOs suggest that other factors influence this response. The multiple interactions of CFTR with other ionic channels and the varied phenotype in this condition owing to environmental and genetic factors may account for some of the differences observed between these two groups (Rowntree and Harris, 2003). However, the results do indicate, that in man dysfunctional CFTR does not precipitate a complete loss of the FOs. This conclusion was also found in a recent animal study where the FOs were present even in CFTR null mice (Wu *et al.*, 2006).

6.2 Future Directions

The results provide evidence for intracellular [Ca^{2+}] being the signal required to generate the alcohol-EOG in man. In relation to early retinal degeneration, associated with RP and ARMD this finding suggests that in these diseases Ca^{2+}-signalling is altered and that the alcohol-EOG is capable of detecting these early anomalies before a substantial loss in the light-rise is apparent.

Further experiments are required to show conclusively that the calcium channels are of the L-type. This would be achieved by further work using nifedipine and inhibitors of the intracellular stores (thapsigargin and cyclopiazonic acid). Demonstration that L-type Ca^{2+} channels are present in the monolayers could be performed using immunocytochemistry and the specific subunits determined by RT-PCR. In view of the varied heterogeneity this work would be performed using an animal model such as chick RPE. The use of primary chick RPE explants loaded with fluo4-AM would also be possible to demonstrate that the alcohol is capable of elevating $[Ca^{2+}]_{in}$ in an animal model.

Performing the alcohol-EOG on individuals with Best's disease would indicate whether bestrophin was required to generate the alcohol-EOG. Further studies on individuals with CF would also help clarify the FOs as there appears to be a difference in the amplitudes between the heterozygotes and homozygous groups. It may be that the FOs could be used as a prognostic test in these individuals.

Further work on animal models is required and the most likely candidate is chick where post-mortem time can be minimised. Chick has been used before in Ussing chamber and intracellular

recordings to elucidate the basic mechanism of the light-EOG. Using a similar recording technique the effects on basolateral chloride conductance could be shown with ethanol.

Additional clinical uses of the alcohol-EOG could be assessed in diabetics to determine whether there are any abnormalities that may indicate individuals likely to develop diabetic retinopathy. Drug toxicity may also provide a use for the alcohol-EOG with patients on immunosuppressives.

Demonstrating that nifedipine also suppresses the light-rise in man is another immediate goal and arrangements are currently in progress to perform this study.

7 Appendix 1 Preparation of Solutions

7.1 Cell Culture Additives and Solution Preparation

Typically, 40 ml of specialised medium was prepared to have sufficient for the 12 Transwells™ (36 ml).

Penicillin, Streptomycin and L-Glutamine (G1146): Stock 5 ml solution containing 200 mM L-glutamine, 10,000 U/ml penicillin, and 10 mg/ml streptomycin in 0.9% sodium chloride. Diluted 1:100 in culture medium to give 2 mM L-glutamine, 100 U/ml penicillin and 100 μg/ml streptomycin.

Antibiotic-Antimycotic solution (A5955): Stock solution containing 10,000 units/ml penicillin G, 10 mg/ml streptomycin sulphate and 25 μg/ml amphotericin B. Diluted 1:100 in culture medium to give 100 U/ml penicillin, 100 μg/ml streptomycin and 0.25 μg/ml amphotericin B.

Insulin (I9278): Supplied as stock (5 ml) solution of 10 mg/ml in HEPES. Solution stored at 4°C. Diluted 1:100 when added to base medium to give final concentration of 100 μg/ml.

Transferrin (T8158): Supplied as 1 mg human transferrin dissolved in 1 ml of sterile PBS and 250 μl aliquots stored at – 50°C. Working concentration 1 mg/ml. 5 μl/ml added to SM1 or SM2 on the day of use.

Epidermal Growth Factor (EGF) (E4127): 100 μg of EGF isolated from mouse sub-maxillary glands was diluted in 1 ml of PBS with 1% FCS to give a final working concentration of 100 μg/ml. 25 μl aliquots were stored at -50°C. 0.25 μl/ml was added to specialised media on the day approximately 10 μl to give 10 ng/ml.

Tyrosine sodium salt (3,3',5-Triiodo-L-thyronine sodium salt) (T3) (T5516): 1 mg was dissolved in sterile 1N NaOH and then diluted with 49 ml of DMEM:F12 and stored at 100 μl aliquots at -50°C at a working concentration of 20 μg/ml. 0.25 μl/ml of SM3 was added on the day to give 5 ng/ml.

Putrescine (P6024): 1 mg was dissolved in 10 ml of sterile PBS and stored at room temperature at a working concentration of 100 μg/ml. 3 μl/ml was added to SM1 and SM2 on the day.

Basic fibroblast growth factor (bFGF) (F0291): 25 μg of human bFGF was dissolved in 0.1 ml of sterile PBS. 200 μl aliquots were stored at -50°C with a working concentration of bFGF of 250 μg/ml. 4 μl/ml was added to the specialised media on the day to give a final concentration of 1 ng/ml.

Hydrocortisone (H6909): Supplied as 50 μM sterile solution. Stored at 4°C. 0.5 ml added to 500 ml of base medium to give a final concentration of 25 nM in SM1 and SM2 or 1 ml to SM3 to give 50 nM.

Linoleic acid (L5900): 10 mg dissolved in 10 ml absolute ethanol giving 1 mg/ml. Stored at -50°C and protected from light in 1 ml aliquots. 10 μl/ml added to SM1 and SM2 to give a final concentration of 10 μg/ml.

All *trans*-retinoic acid (R2625): Prepared in the dark. Add 1.5 ml of DMSO to 50 mg of all *trans*-retinoic acid, giving a working concentration of 40 mg/ml (Store at -50°C). Then diluted stock 1:1000 by taking 10 μl of working solution and adding to 10 ml of base medium. Final concentration now 40 μg/ml. Add 62.5 μl to 50 ml of medium to give final concentration of 50 ng/ml. Retinoic acid was added to SM2 only.

Progesterone (P7556): 100 mg was dissolved in 100 ml of sterile ddH_20 giving 1 mg/ml and stored at room temperature. 1 ml was then diluted 1:100 with 99 ml of sterile ddH_2O to give a final working concentration of 10 μg/ml. 1 μl/ml was added to SM3 to give a final concentration of 10 ng/ml.

ITS^{+3} (I2771): Pre-formulated cell culture additive containing insulin 10 mg/l, transferrin 5.5 mg/l, selenium 5 μg/l, BSA 0.5 mg/l, linoleic acid 4.7 μg/ml and oleic acid 4.7 μg/ml. Used as cell culture additive in SM3. Diluted 1:100 with SM3 base media on day of use.

Bovine Serum Albumin (BSA): 30% (wt/vol) solution was prepared by adding 10 gm sterile BSA to 33 ml of DMEM:F12 and stirring with a magnetic rotor (sterilised in absolute ethanol) until dissolved. 5 ml added to SM1 and SM2 base media and stored at 4°C.

Bovine Pituitary Extract (BPE) (P1476): Supplied as ~ 14mg/ml in PBS (2.5 ml) total volume. The BPE solution was added to SM3 base medium (500 ml) to give a final concentration of ~ 70 μg/ml.

7.2 Specialised Media Preparations

7.2.1 SM1 and SM2

DMEM:F12 with added nutrients was used as base medium (500 ml) supplemented with 10 ml of 1 M HEPES (N-(2-Hydroxyethyl)piperazine-N'-(2-ethanesulphonic acid)), 5 ml of L-glutamine, penicillin and streptomycin, 5 ml of insulin solution, 5 ml of 30% BSA and stored at 4°C. Final concentrations in the base medium were 20 mM HEPES, 100 μg/ml streptomycin, 100 U/ml penicillin, 100 μg/ml insulin and 2 mM L-glutamine and 1% BSA.

7.2.2 SM3

Base medium was made using DMEM (500 ml) supplemented with 10 ml of 1M HEPES, 5 ml of penicillin streptomycin L-glutamine solution 5 ml of ITS^{+3} and 100 μl of hydrocortisone giving a final concentration of 20 mM HEPES, 100 μg/ml streptomycin, 100 U/ml penicillin, 100 μg/ml, insulin 100 μg/ml, transferrin 55 μg/ml, selenium 50 μg/ml, BSA 5 μg/ml, linoleic acid 47 ng/ml, oleic acid 47 ng/ml, 50 nM hydrocortisone and 2 mM L-glutamine.

For SM3 two additional modifications were made. One was to add bFGF and EGF to give a final concentration of 1 ng/ml and 10 ng/ml respectively. A second modification was to add bovine pituitary extract (BPE) to SM3 to give a final concentration of 70 μg/ml. Medium was stored at 4°C and extra supplements added from stock solutions as described above to give the final concentrations given in table 7.1.

Table 7.1 SM3 Constituents

Ingredient	SM3 DMEM
Insulin	100 μg/ml ǂ
Transferrin	55 μg/ml ǂ
Selenium	50 μg/ml ǂ
Hydrocortisone	50 nM
Progesterone	10 ng/ml
Linoleic acid	47 ng/ml ǂ
Oleic acid	47 ng/ml ǂ
BSA	5 μg/ml ǂ
HEPES	20 mM

Constituents of SM3. (ǂ) The addition of insulin, transferrin, selenium, linoleic acid, oleic acid and BSA was supplied as ITS^{3+} medium supplement (Sigma). Additions were to add bFGF and EGF or to add BPE to the SM3 base mixture.

8 List of Publications

Publications form work in this thesis

Constable, P. A, Lawrenson, J. G. and Arden, G. B. The electro-oculogram in cystic fibrosis. Doc Ophthalmol. 113: 133-143.

Constable, P. A., Lawrenson, J. G., Dolman, D. E. M., Arden, G. B. and Abbott, N. J. (2006). P-Glycoprotein expression in retinal pigment epithelium cell lines. Exp. Eye Res. 83: 24-30.

Arden, G. B. and Constable, P. A. (2006). The electro-oculogram. Prog. Ret. Eye Res. 25: 207-248.

Conference presentation

Constable, P. A., Lawrenson, J. G. and Arden, G. B. (2005). Role of the cystic fibrosis transmembrane conductance regulator in the electro-oculogram. ISCEV 43rd, Glasgow. UK.

Abstracts and other published work

Constable, P. A., Lawrenson, J. G. and Abbott, N. J. (in press). P-glycoprotein expression and function in the retinal barriers. Ocular Transporters in Ophthalmic Diseases and Drug Delivery. J. Tombran-Tink and C. Barnstable (EDs). Totawa, Humana Press Inc.

Hillenkamp, J., Hussain, A. A., Jackson, T. L., Constable, P. A., Cunningham, J. R. and Marshall, J. (2004). Compartmental analysis of taurine transport to the outer retina in the bovine eye. Invest. Ophthalmol. Vis. Sci. 45: 4099-4105.

Constable, P. A., Lawrenson, J. G., Tarttelin, E. E., Douglas, R. H., Lucas, R. J. (2006). Circadian rhythm in ARPE-19. ISOCB 1st, Cambridge, UK.

Constable, P. A, Lawrenson, J. G. and Arden, G. B. (2005). The ethanol electro-oculogram: A Ca^{2+} mediated response. ISCEV 43rd, Glasgow. UK.

Constable, P. A., Lawrenson, J. G., Dolman, D. E. M., Arden, G. B. and Abbott, N. J. (2004). P-Glycoprotein expression in retinal pigment epithelium cell lines. ARVO Ft Lauderdale, Florida USA.

9 References

Abe, T., Sugano, E., Saigo, Y. and Tamai, M. (2003). Interleukin-1β and barrier function of retinal pigment epithelial cells (ARPE-19): aberrant expression of junctional complex molecules. Invest. Ophthalmol. Vis. Sci. 44: 4097-4104.

Abraham, E. H., Okunieff, P., Scala, S., Vos, P., Oosterveld, M. J. S., Chen, A. Y., Shrivastav;, B., Guidotti;, G., Reddy, M. M., Quinton, P. M., Haws, C., Wine;, J. J., Grygorczyk, R., Tabcharani, J. A., Hanrahan, J. W., Gunderson, K. L., Kopito;, R. R. and Grygorczyk, R. (1997). Cystic fibrosis transmembrane conductance regulator and adenosine triphosphate. Science. 275: 1324-1326.

Adams, B. and Tanabe, T. (1997). Structural regions of the cardiac Ca channel α_{1C} subunit involved in Ca-dependent Inactivation. J. Gen. Physiol. 110: 379-389.

Akeo, K., Miyamoto, H., Okisaka, S. and Hiramitsu, T. (1999). Effects of fluorescent light on growth of bovine retinal pigment epithelial cells *in vitro* incubated with linoleic acid or linoleic acid hydroperoxide. Pigment Cell Res. 12: 199-205.

Alizadeh, M., Wada, M., Gelfman, C. M., Handa, J. T. and Hjelmeland, L. M. (2001). Downregulation of differentiation specific gene expression by oxidative stress in ARPE-19 cells. Invest. Ophthalmol. Vis. Sci. 42: 2706-2713.

Allansson, L., Khatibi, S., Olsson, T. and Hansson, E. (2001). Acute ethanol exposure induces $[Ca^{2+}]_i$ transients, cell swelling and transformation of actin cytoskeleton in astroglial primary cultures. J. Neurochem. 76: 472-479.

Altman, D. G. (1999). Practical statistics for medical research. London, Chapman and Hall/CRC.

Amin, S., Chong, N. H. V., Bailey, T. A., Zhang, J., Knupp, C., Cheetham, M. E., Greenwood, J. and Luthert, P. J. (2004). Modulation of sub-RPE deposits *in vitro*: a potential model for age-related macular degeneration. Invest. Ophthalmol. Vis. Sci. 45: 1281-1288.

Ammar, D. A., Hughes, B. A. and Thompson, D. A. (1998). Neuropeptide Y and the retinal pigment epithelium: receptor subtypes, signaling, and bioelectrical responses. Invest. Ophthalmol. Vis. Sci. 39: 1870-1878.

Andersen, A., Pedersen, H., Bendtzen, K. and Ropke, C. (1993). Effects of growth factors on cytokine production in serum-free cultures of human thymic epithelial cells. Scand. J. Immunol. 38: 233-238.

Anderson, J. M. (2001). Molecular structure of tight junctions and their role in epithelial transport. News Physiol. Sci. 16: 126-130.

Anderson, M. P., Berger, H. A., Rich, D. P., Gregory, R. J., Smith, A. E. and Welsh, M. J. (1991a). Nucleoside triphosphates are required to open the CFTR chloride channel. Cell. 67: 775-784.

Anderson, M. P., Gregory, R. J., Thompson, S., Souza, D. W., Paul, S., Mulligan, R. C., Smith, A. E. and Welsh, M. J. (1991b). Demonstration that CFTR is a chloride channel by alteration of its anion selectivity. Science. 253: 202-205.

Anderson, M. P., Rich, D. P., Gregory, R. J., Smith, A. E. and Welsh, M. J. (1991c). Generation of cAMP-activated chloride currents by expression of CFTR. Science. 251: 679-682.

Anderson, M. P. and Welsh, M. J. (1991). Calcium and cAMP activate different chloride channels in the apical membrane of normal and cystic fibrosis epithelia. Proc. Natl. Acad. Sci. U.S.A. 88: 6003-6007.

Ando-Akatsuka, Y., Abdullaev, I., Lee, E., Okada, Y. and Sabirov, R. (2002). Down-regulation of volume-sensitive Cl^- channels by CFTR is mediated by the second nucleotide-binding domain. Pflügers Archive 445: 177-186.

Arden, G. B. (1962). Alterations in the standing potential of the eye associated with retinal disease. Trans. Ophthalmol. Soc. U.K. 82: 63-72.

Arden, G. B. and Barrada, A. (1962). An analysis of the electrooculograms of a series of normal subjects. Brit. J. Ophthalmol. 46: 468-482.

Arden, G. B., Barrada, A. and Kelsey, J. H. (1962). A new clinical test of retinal function based upon the standing potential of the eye. Brit. J. Ophthalmol. 46: 449-467.

Arden, G. B. and Constable, P. A. (2006). The electro-oculogram. Prog. Ret. Eye Res. 25: 207-248.

Arden, G. B. and Kelsey, J. H. (1962). Changes produced by light in the standing potential of the human eye. J. Physiol. (Lond). 161: 189-204.

Arden, G. B. and Kolb, H. (1966). Antimalarial therapy and early retinal changes in patients with rheumatoid arthritis. Brit. Med. J. 5482: 270-273.

Arden, G. B. and Wolf, J. E. (2000a). The electro-oculographic responses to alcohol and light in a series of patients with retinitis pigmentosa. Invest. Ophthalmol. Vis. Sci. 41: 2730-2734.

Arden, G. B. and Wolf, J. E. (2000b). The human electro-oculogram: interaction of light and alcohol. Invest. Ophthalmol. Vis. Sci. 41: 2722-2729.

Arden, G. B. and Wolf, J. E. (2003). Differential effects of light and alcohol on the electro-oculographic responses of patients with age-related macular disease. Invest. Ophthalmol. Vis. Sci. 44: 3226-3232.

Arden, G. B., Wolf, J. E., Singbartl, F., Berninger, T. E., Rudolph, G. and Kampik, A. (2000). Effect of alcohol and light on the retinal pigment epithelium of normal subjects and patients with retinal dystrophies. Brit. J. Ophthalmol. 84: 881-883.

Arndt, C. F., Sari, A., Ferre, M., Parrat, E., Courtas, D., De Seze, J., Hache, J. and Matran, R. (2001). Electrophysiological effects of corticosteroids on the retinal pigment epithelium. Invest. Ophthalmol. Vis. Sci. 42: 472-475.

Arndt, C. F., Husson, J., Derambure, P., Hache, J. C., Arnaud, B. and Defoort-Dhellemmes, S. (2005). Retinal electrophysiological results in patients receiving lamotrigine monotherapy. Epilepsia. 46: 1055-1060.

Atalla, L. R., Sevanian, A. and Rao, N. A. (1988). Immunohistochemical localization of glutathione peroxidase in ocular tissue. Curr. Eye Res. 8: 1023-1027.

Bader, C. R., MacLeish, P. R. and Schwartz, E. A. (1978). Responses to light of solitary rod photoreceptors isolated from tiger salamander retina. Proc. Natl. Acad. Sci. U.S.A. 75: 3507-3511.

Bailey, T. A., Kanuga, N., Romero, I. A., Greenwood, J., Luthert, P. J. and Cheetham, M. E. (2004). Oxidative stress affects the junctional integrity of retinal pigment epithelial cells. Invest. Ophthalmol. Vis. Sci. 45: 675-684.

Ban, Y. and Rizzolo, L. J. (1997). A culture model of development reveals multiple properties of RPE tight junctions. Mol. Vis. 3.

Ban, Y. and Rizzolo, L. J. (2000a). Differential regulation of tight junction permeability during development of the retinal pigment epithelium. Amer. J. Physiol. 279: C744-750.

Ban, Y. and Rizzolo, L. J. (2000b). Regulation of glucose transporters during development of the retinal pigment epithelium. Dev. Brain Res. 121: 89-95.

Ban, Y., Wilt, S. D. and Rizzolo, L. J. (2000). Two secreted retinal factors regulate different stages of development of the outer blood-retinal barrier. Dev.Brain Res. 119: 259-267.

Barish, M. E. (1983). A transient calcium-dependent chloride current in the immature *Xenopus* oocyte. J. Physiol. (Lond). 342: 309-325.

Barricks, M. E. (1977). Vitelliform lesions developing in normal fundi. Amer. J. Ophthalmol. 83: 324-327.

Belia, S., Mannucci, R., Lisciarelli, M., Cacchio, M. and Fano, G. (1995). Double effect of ethanol on intracellular Ca^{2+} levels in undifferentiated PC12 cells. Cell Signal. 7: 389-395.

Benda, P., Lightbody, J., Sato, G., Levine, L. and Sweet, W. (1968). Differentiated rat glial cell strain in tissue culture. Science. 161: 370-371.

Berridge, M. J., Bootman, M. D. and Roderick, H. L. (2003). Calcium signalling: dynamics, homeostasis and remodelling. Nature Rev. Mol. Cell Biol. 4: 517-529.

Best, F. (1905). Ueber eine hereditaere Maculaaffektion. Augenheilk 13: 199-212. Cited by Pollack, K., Kreuz, F. and Pillunat, L. (2005). Morbus Best mit normalem EOG. Der Ophthalmologe. 102: 891-894.

Bialek, S. and Miller, S. S. (1994). K+ and Cl- transport mechanisms in bovine pigment epithelium that could modulate subretinal space volume and composition. J. Physiol. (Lond). 475: 401-417.

Bialek, S., Quong, J. N., Yu, K. and Miller, S. S. (1996). Nonsteroidal anti-inflammatory drugs alter chloride and fluid transport in bovine retinal pigment epithelium. Amer. J. Physiol. 270: C1175-1189.

Blaisdell, C. J., Edmonds, R. D., Wang, X. T., Guggino, S. and Zeitlin, P. L. (2000). pH-regulated chloride secretion in fetal lung epithelia. Amer. J. Physiol. 278: L1248-L1255.

Blaug, S., Quinn, R., Quong, J., Jalickee, S. and Miller, S. S. (2003). Retinal pigment epithelial function: a role for CFTR? Doc. Ophthalmol. 106: 43-50.

Bode, D. C. and Molinoff, P. B. (1988). Effects of ethanol *in vitro* on the β adrenergic receptor-coupled adenylate cyclase system. J. Pharmacol. Exp. Ther. 246: 1040-1047.

Bok, D. (1985). Retinal photoreceptor-pigment epithelium interactions. Friedenwald lecture. Invest. Ophthalmol. Vis. Sci. 26: 1659-1694.

Bok, D., O'Day, W. and Rodriguez-Boulan, E. (1992). Polarized budding of vesicular stomatitis and influenza virus from cultured human and bovine retinal pigment epithelium. Exp. Eye Res. 55: 853-860.

Bollimuntha, S., Cornatzer, E. and Singh, B. B. (2005). Plasma membrane localization and function of TRPC1 is dependent on its interaction with beta-tubulin in retinal epithelium cells. Vis. Neurosci. 22: 163-170.

Bösl, M. R., Stein, V., Hübner, C., Zdebik, A. A., Jordt, S-E., Mukhopadhyay, A. K., Davidoff, M. S., Holstein, A-F. and Jentsch, T. J. (2001). Male germ cells and photoreceptors, both dependent on close cell–cell interactions, degenerate upon ClC-2 Cl channel disruption. EMBO J. 20: 1289-1299.

Bost, L. M., Aotaki-Keen, A. E. and Hjelmeland, L. M. (1994). Cellular adhesion regulates bFGF gene expression in human retinal pigment epithelial cells. Exp. Eye Res. 58: 545-552.

Botchkin, L. M. and Matthews, G. (1994). Voltage-dependent sodium channels develop in rat retinal pigment epithelium cells in culture. Proc. Natl. Acad. Aci. U.S.A. 91: 4564-4568.

Boucher, R. C., Stutts, M. J., Knowles, M. R., Cantley, L. and Gatzy, J. T. (1986). Na^+ transport in cystic fibrosis respiratory epithelia. Abnormal basal rate and response to adenylate cyclase activation. J. Clin. Invest. 78: 1245-1252.

Braunstein, G. M., Zsembery, A., Tucker, T. A. and Schwiebert, E. M. (2004). Purinergic signaling underlies CFTR control of human airway epithelial cell volume. J. Cystic Fibrosis. 3: 99-117.

Bridges, C. C., El-Sherbeny, A., Ola, M. S., Ganapathy, V. and Smith, S. B. (2002). Transcellular transfer of folate across the retinal pigment epithelium. Curr. Eye Res. 24: 129-138.

Bridges, C. C., Kekuda, R., Wang, H., Prasad, P. D., Mehta, P., Huang, W., Smith, S. B. and Ganapathy, V. (2001a). Structure, function, and regulation of human cystine/glutamate transporter in retinal pigment epithelial cells. Invest. Ophthalmol. Vis. Sci. 42: 47-54.

Bridges, C. C., Ola, M. S., Prasad, P. D., El-Sherbeny, A., Ganapathy, V. and Smith, S. B. (2001b). Regulation of taurine transporter expression by NO in cultured human retinal pigment epithelial cells. Amer. J. Physiol. 281: C1825-1836.

Bridges, C. D., Alvarez, R. A., Fong, S. L., Gonzalez-Fernandez, F., Lam, D. M. and Liou, G. I. (1984). Visual cycle in the mammalian eye. retinoid-binding proteins and the distribution of 11-*cis* retinoids. Vis. Res. 24: 1581-1594.

Briggs, M. C., Grierson, I., Hiscott, P. and Hunt, J. A. (2000). Active scatter factor (HGF/SF) in proliferative vitreoretinal disease. Invest. Ophthalmol. Vis. Sci. 41: 3085-3094.

Brown, J., Reading, S. J., Jones, S., Fitchett, C. J., Howl, J., Martin, A., Longland, C. L., Michelangeli, F., Dubrova, Y. E. and Brown, C. A. (2000). Critical evaluation of ECV304 as a human endothelial cell model defined by genetic analysis and functional responses: a comparison with the human bladder cancer derived epithelial cell line T24/83. Lab. Invest. 80: 37-45.

Brown, K. T. and Wiesel, T. N. (1959). Intraretinal recording with micropipette electrodes in the intact cat eye. J. Physiol. (Lond). 149: 537-562.

Brown, K. T. and Wiesel, T. N. (1961a). Analysis of the intraretinal electroretinogram in the intact cat eye. J. Physiol. (Lond). 158: 229-256.

Brown, K. T. and Wiesel, T. N. (1961b). Localization of the origins of the electroretinogram components by intraretinal recording in the intact cat eye. J. Physiol. (Lond). 158: 257-280.

Burke, J. M., Cao, F., Irving, P. E. and Skumatz, C. M. B. (1999). Expression of E-cadherin by human retinal pigment epithelium: delayed expression *in vitro*. Invest. Ophthalmol. Vis. Sci. 40: 2963-2970.

Burke, J. M. and Foster, S. J. (1985). Induction of DNA synthesis by co-culture of retinal glia and pigment epithelium. Invest. Ophthalmol. Vis. Sci. 26: 636-642.

Burnside, B. and Bost-Usinger, L. (1998). The retinal pigment epithelial cytoskeleton. The Retinal Pigment Epithelium. M. F. Marmor and T. J. Wolfensberger. New York, OUP: 41-67.

Buse, E., Eichmann, T., deGroot, H. and Leker, A. (1993). Differentiation of the mammalian retinal pigment epithelium *in vitro*: influence of presumptive retinal neuroepithelium and head mesenchyme. Anat. Embryol. (Berl). 187: 259-268.

Butt, A. M. and Kalsi, A. (2006). Inwardly rectifying potassium channels (K_{ir}) in central nervous system glia: a special role for Kir4.1 in glial functions. J. Cell Mol. Med. 10: 33-44.

Campochiaro, P. A. and Glaser, B. M. (1986). Mechanisms involved in retinal pigment epithelial cell chemotaxis. Arch. Ophthalmol. 104: 277-280.

Campochiaro, P. A. and Hackett, S. F. (1993). Corneal endothelial cell matrix promotes expression of differentiated features of retinal pigmented epithelial cells: implication of laminin and basic fibroblast growth factor as active components. Exp. Eye Res. 57: 539-547.

Campochiaro, P. A., Hackett, S. F. and Conway, B. P. (1991). Retinoic acid promotes density-dependent growth arrest in human retinal pigment epithelial cells. Invest. Ophthalmol. Vis. Sci. 32: 65-72.

Campochiaro, P. A., Jerdon, J. A. and Glaser, B. M. (1986). The extracellular matrix of human retinal pigment epithelial cells in vivo and its synthesis *in vitro*. Invest. Ophthalmol. Vis. Sci. 27: 1615-1621.

Cannell, M. B., Cheng, H. and Lederer, W. J. (1994). Spatial non-uniformities in $[Ca^{2+}]_i$ during excitation-contraction coupling in cardiac myocytes. Biophys. J. 67: 1942-1956.

Capeans, C., Pineiro, A., Pardo, M., Sueiro-Lopez, C., Blanco, M. J., Dominguez, F. and Sanchez-Salorio, M. (2003). Amniotic membrane as support for human retinal pigment epithelium (RPE) cell growth. Acta. Ophthalmol. Scand. 81: 271-277.

Casaroli-Marano, R. P., Pagan, R. and Vilaro, S. (1999). Epithelial-mesenchymal transition in proliferative vitreoretinopathy: intermediate filament protein expression in retinal pigment epithelial cells. Invest. Ophthalmol. Vis. Sci. 40: 2062-2072.

Catalan, M., Cornejo, I., Figueroa, C. D., Niemeyer, M. I., Sepulveda, F. V. and Cid, L. P. (2002). CIC-2 in guinea pig colon: mRNA, immunolabeling, and functional evidence for surface epithelium localization. Amer. J. Physiol. 283: G1004-1013.

Chang, C. W., Roque, R. S., Defoe, D. M. and Caldwell, R. B. (1991). An improved method for isolation and culture of pigment epithelial cells from rat retina. Curr. Eye Res. 10: 1081-1086.

Chang, C. W., Ye, L., Defoe, D. M. and Caldwell, R. B. (1997). Serum inhibits tight junction formation in cultured pigment epithelial cells. Invest. Ophthalmol. Vis. Sci. 38: 1082-1093.

Chen, J-T., Liang, J-B., Chou, C-L., Shyu, R-C. and Lu, D-W. (2005). Retinoic acid Induces VEGF gene expression in human retinal pigment epithelial cells (ARPE-19). J. Ocular Pharm. Ther. 21: 413-419.

Chen, S., Wan, X. L. and Sears, M. (1998). pI_{Cln} can regulate swelling-induced Cl^- currents in either layer of rabbit ciliary epithelium. Biochem. Biophys. Res. Commun. 246: 59-63.

Chen, Y-C., Chen, S-A., Chen, Y-J., Tai, C-T., Chan, P. and Lin, C-I. (2004). Effect of ethanol on the electrophysiological characteristics of pulmonary vein cardiomyocytes. Eur. J. Pharmacol. 483: 215-222.

Chiba, K., Inada, K. and Sakamoto, S. (1993). Human cultured retinal pigment epithelial cells produce interleukin-6. Nippon Ganka Gakkai Zasshi 97: 29-35.

Chik, C., Liu, Q., Girard, M., Karpinski, E. and Ho, A. (1992). Inhibitory action of ethanol on L-type Ca^{2+} channels and Ca^{2+}- dependent guanosine 3',5'-monophosphate accumulation in rat pinealocytes. Endocrinology. 131: 1895-1902.

Chishty, M., Reichel, A., Begley, D. J. and Abbott, N. J. (2002). Glial induction of blood-brain barrier-Like L-system amino acid transport in the ECV304 cell line. Glia. 39: 99-104.

Chowers, I., Kim, Y., Farkas, R., Gunatilaka, T., Hackam, A., Campochiaro, P., Finnemann, S. and Zack, D. (2004). Changes in retinal pigment epithelial gene expression induced by rod outer segment uptake. Invest. Ophthalmol. Vis. Sci. 45: 2098 - 2106.

Chu, P. G. and Grunwald, G. B. (1990). Identification of an adhesion-associated protein of the retinal pigment epithelium. Invest. Ophthalmol. Vis. Sci. 31: 847-855.

Cid, L., Montrose-Rafizadeh, C., Smith, D., Guggino, W. and Cutting, G. (1995). Cloning of a putative human voltage-gated chloride channel (ClC-2) cDNA widely expressed in human tissues. Hum. Mol. Genet. 4: 407-413.

Clayton, R. and Woodward, J. J. (2000). Effects of ethanol on three endogenous membrane conductances present in *Xenopus laevis* oocytes. Neurochem. Int. 36: 67-74.

Coakley, R. D., Grubb, B. R., Paradiso, A. M., Gatzy, J. T., Johnson, L. G., Kreda, S. M., O'Neal, W. K. and Boucher, R. C. (2003). Abnormal surface liquid pH regulation by cultured cystic fibrosis bronchial epithelium. Proc. Natl. Acad. Sci. U.S.A. 100: 16083-16088.

Cofan, M., Nicolas, J. M., Fernandez-Sola, J., Robert, J., Tobias, E., Sacanella, E., Estruch, R. and Urbano-Marquez, A. (2000). Acute ethanol treatment decreases intracellular

calcium-ion transients in mouse single skeletal muscle fibers *in vitro.* Alcohol Alcohol. 35: 134-138.

Cohen, S. (1965). The stimulation of epidermal proliferation by a specific protein (EGF). Dev. Biol. 12: 394-407.

Colegio, O. R., Itallie, C. V., Rahner, C. and Anderson, J. M. (2003). Claudin extracellular domains determine paracellular charge selectivity and resistance but not tight junction fibril architecture. Amer. J. Physiol. 284: C1346-1354.

Colegio, O. R., Van Itallie, C. M., McCrea, H. J., Rahner, C. and Anderson, J. M. (2002). Claudins create charge-selective channels in the paracellular pathway between epithelial cells. Amer. J. Physiol. 283: C142-147.

Collison, D. J., Tovell, V. E., Coombes, L. J., Duncan, G. and Sanderson, J. (2005). Potentiation of ATP-induced Ca^{2+} mobilisation in human retinal pigment epithelial cells. Exp. Eye Res. 80: 465-475.

Constable, P. A., Lawrenson, J. G. and Arden, G. B. (2006a). The electro-oculogram in cystic fibrosis. Doc. Ophthalmol. 113: 133-143.

Constable, P. A., Lawrenson, J. G., Dolman, D. E. M., Arden, G. B. and Abbott, N. J. (2006b). P-Glycoprotein expression in retinal pigment epithelium cell lines. Exp. Eye Res. 83: 24-30.

Cornejo-Perez, P. and Arreola, J. (2004). Regulation of Ca^{2+}-activated chloride channels by cAMP and CFTR in parotid acinar cells. Biochem. Biophys. Res. Commun. 316: 612-617.

Crawford, B. J. and Vielkind, U. (1985). Location and possible function of fibronectin and laminin in clones of chick retinal pigmented epithelial cells. *In Vitro* Cell Dev. Biol. 21: 79-87.

Crook, R. B., Song, M. K., Tong, L. P., Yabu, J. M., Polansky, J. R. and Lui, G. M. (1992). Stimulation of inositol phosphate formation in cultured human retinal pigment epithelium. Brain Res. 583: 23-30.

Cross, H. E. and Bard, L. (1974). Electro-oculography in Best's macular dystrophy. Amer. J. Ophthalmol. 77: 46-50.

Cullinane, A. B., Leung, P. S., Ortego, J., Coca-Prados, M. and Harvey, B. J. (2002). Renin-angiotensin system expression and secretory function in cultured human ciliary body non-pigmented epithelium. Brit. J. Ophthalmol. 86: 676-683.

Cuppoletti, J., Baker, A. M. and Malinowska, D. H. (1993). Cl^- channels of the gastric parietal cell that are active at low pH. Amer. J. Physiol. 264: C1609-1618.

Cutting, G. R., Kasch, L. M., Rosenstein, B. J., Zielenski, J., Tsui, L-C., Anatonarakis, S. E. and Kazazian Jr, H. H. (1990). A cluster of cystic fibrosis mutations in the first nucleotide-binding fold of the cystic fibrosis conductance regulator protein. Nature. 346: 366-369.

Davis, A. A., Bernstein, P. S., Bok, D., Turner, J., Nachtigal, M. and Hunt, R. C. (1995). A human retinal pigment epithelial cell line that retains epithelial characteristics after prolonged culture. Invest. Ophthalmol. Vis. Sci. 36: 955-964.

Dawis, S. and Niemeyer, G. (1986). Dopamine influences the light peak in the perfused mammalian eye. Invest. Ophthalmol. Vis. Sci. 27: 330-335.

Dean, M. and Allikmets, R. (2001). Complete characterization of the human ABC gene family. J. Bioenerg. Biomembr. 33: 475-479.

Defoe, D. M. and Grindstaff, R. D. (2004). Epidermal growth factor stimulation of RPE cell survival: contribution of phosphatidylinositol 3-kinase and mitogen-activated protein kinase pathways. Exp. Eye Res. 79: 51-59.

Diehl, A. M., Yang, S. Q., Cote, P. and Wand, G. S. (1992). Chronic ethanol consumption disturbs G-protein expression and inhibits cyclic AMP-dependent signaling in regenerating rat liver. Hepatology. 16: 1212-1219.

Dirks, W. G., MacLeod, R. A. and Drexler, H. G. (1999). ECV304 (endothelial) is really T24 (bladder carcinoma): cell line cross- contamination at source. In Vitro Cell Dev. Biol. Anim. 35: 558-559.

Dobbie, M. S., Hurst, R. D., Klein, N. J. and Surtees, R. A. H. (1999). Upregulation of intercellular adhesion molecule-1 expression on human endothelial cells by tumour necrosis factor-α in an *in vitro* model of the blood-brain barrier. Brain Res. 830: 330-336.

Dolphin, A. C. (1995). The G.L. Brown Prize Lecture. Voltage-dependent calcium channels and their modulation by neurotransmitters and G proteins. Exp. Physiol. 80: 1-36.

Dopico, A. M., Anantharam, V. and Treistman, S. N. (1998). Ethanol increases the activity of Ca^{2+}-dependent K^+ (*mslo*) channels: functional interaction with cytosolic Ca^{2+}. J. Pharmacol. Exp. Ther. 284: 258-268.

Dork, T., Wulbrand, U., Richter, T., Neumann, T., Wolfes, H., Wulf, B., Maass, G. and Tummler, B. (1991). Cystic fibrosis with three mutations in the cystic fibrosis transmembrane conductance regulator gene. Hum. Genet. 87: 441-446.

Drexler., H. G., Quentmeier., H., Dirks., W. G. and MacLeod., R. A. F. (2002). Bladder carcinoma cell line ECV304 is not a model system for endothelial cells. In Vitro Cellular Dev. 38: 185-186.

Du Bois Reymond, E. (1849). Untersuchungen über dei thierische Electricität. vol II. Berlin, Reimer Ged. Cited by Arden, G. B. and Constable, P. A. (2006). The electro-oculogram. Prog. Ret. Eye Res. 25: 207-248.

Duan, H-F., Wu, C-T., Lu, Y., Wang, H., Liu, H-J., Zhang, Q-W., Jia, X-X., Lu, Z-Z. and Wang, L-S. (2004). Sphingosine kinase activation regulates hepatocyte growth factor induced migration of endothelial cells. Exp. Cell Res. 298: 593-601.

Duguépéroux, I. and De Braekeleer, M. (2004). Genotype-phenotype relationship for five CFTR mutations frequently identified in western France. J. Cystic Fibrosis. 3: 259-263.

Duncan, K. G., Bailey, K. R., Baxter, J. D. and Schwartz, D. M. (1999). The human fetal retinal pigment epithelium: A target tissue for thyroid hormones. Ophthalmic. Res. 31: 399-406.

Dunn, K. C., Aotaki-Keen, A. E., Putkey, F. R. and Hjelmeland, L. M. (1996). ARPE-19, a human retinal pigment epithelial cell line with differentiated properties. Exp. Eye Res. 62: 155-169.

Dunn, K. C., Marmorstein, A. D., Bonilha, V. L., Rodriguez-Boulan, E., Giordano, F. and Hjelmeland, L. M. (1998). Use of the ARPE-19 cell line as a model of RPE polarity: basolateral secretion of FGF5. Invest. Ophthalmol. Vis. Sci. 39: 2744-2749.

Economou, S. G. and Stefanis, C. N. (1979). Electrooculographic (EOG) findings in manic-depressive illness. Acta. Psychiatr. Scand. 60: 155-162.

Edelman, J. L. and Miller, S. S. (1991). Epinephrine stimulates fluid absorption across bovine retinal pigment epithelium. Invest. Ophthalmol. Vis. Sci. 32: 3033-3040.

Edwards, R. B., Adler, A. J. and Claycomb, R. C. (1991). Requirement of insulin or IGF-1 for the maintenance of retinyl ester synthetase activity by cultured retinal pigment epithelial cells. Exp. Eye Res. 52: 51-57.

Egan, M., Flotte, T., Afione, S., Solow, R., Zeitlin, P. L., Carter, B. J. and Guggino, W. B. (1992). Defective regulation of outwardly rectifying Cl^- channels by protein kinase A corrected by insertion of CFTR. Nature. 358: 581-584.

Eggermont, J. (2004). Calcium-activated chloride channels: (un)known, (un)loved? Proc. Amer. Thorac. Soc. 1: 22-27.

Einthoven, W. and Jolly, W. (1908). The form and magnitude of the electrical response of the eye to stimulation by light at various intensities. Q. J. Exp. Physiol. 1: 373-416. Cited by Arden, G. B. and Constable, P. A. (2006). The electro-oculogram. Prog. Ret. Eye Res. 25: 207-248.

El-Sherbeny, A., Naggar, H., Miyauchi, S., Ola, M. S., Maddox, D. M., Martin, P. M., Ganapathy, V. and Smith, S. B. (2004). Osmoregulation of taurine transporter function and expression in retinal pigment epithelial, ganglion, and muller cells. Invest. Ophthalmol. Vis. Sci. 45: 694-701.

Elliott, H. L., Meredith, P. A., Sumner, D. J., McLean, K. and Reid, J. L. (1982). A pharmacodynamic and pharmacokinetic assessment of a new alpha-adrenoceptor antagonist, doxazosin (UK33274) in normotensive subjects. Br. J. Clin. Pharmacol. 13: 699-703.

Esch, F., Baird, A., Ling, N., Ueno, N., Hill, F., Denoroy, L., Klepper, R., Gospodarowicz, D., Bohlen, P. and Guillemin, R. (1985). Primary structure of bovine pituitary basic fibroblast growth factor (FGF) and comparison with the amino-terminal sequence of bovine brain acidic FGF. Proc. Natl. Acad. Aci. U.S.A. 82: 6507-6511.

Feldman, E. L. and Randolph, A. E. (1993). Peptides stimulate phosphoinositide hydrolysis in human retinal pigment epithelium. Invest. Ophthalmol. Vis. Sci. 34: 431-437.

Feldman, E. L., Randolph, A. E., Johnston, G. C., DelMonte, M. A. and Greene, D. A. (1991). Receptor-coupled phosphoinositide hydrolysis in human retinal pigment epithelium. J. Neurochem. 56: 2094-2100.

Fesenko, E. E., Kolesnikov, S. S. and Lyubarsky, A. L. (1986). Direct action of cGMP on the conductance of retinal rod plasma membrane. Biochim. Biophys. Acta. 856: 661-671.

Fijisawa, K., Ye, J. and Zadunaisky, J. A. (1993). A Na^+/Ca^{2+} exchange mechanism in apical membrane vesicles of the retinal pigment epithelium. Curr. Eye Res. 12: 261-270.

Finnemann, S. C., Bonilha, V. L., Marmorstein, A. D. and Rodriguez-Boulan, E. (1997). Phagocytosis of rod outer segments by retinal pigment epithelial cells requires αvβ5

integrin for binding but not for internalization. Proc. Natl. Acad. Sci. U.S.A. 94: 12932-12937.

Fischmeister, R. and Hartzell, H. C. (2005). Volume sensitivity of the bestrophin family of chloride channels. J. Physiol. (Lond). 562: 477-491.

Fisher, S. K. and Linberg, K. A. (1975). Intercellular junctions in the early human embryonic retina. J. Ultrastruct. Res. 51: 69-78.

Fishman, M. L., Oberc, M. A., Hess, H. H. and Engel, W. K. (1977). Ultrastructural demonstration of calcium in retina, retinal pigment epithelium and choroid. Exp. Eye Res. 24: 341-353.

Flockerzi, V., Oeken, H. J., Hofmann, F., Pelzer, D., Cavalie, A. and Trautwein, W. (1986). Purified dihydropyridine-binding site from skeletal muscle t-tubules is a functional calcium channel. Nature. 323: 66-68.

Floto, R. A., Mahaut-Smith, M. P., Somasundaram, B. and Allen, J. M. (1995). IgG-induced Ca^{2+} oscillations in differentiated U937 cells; a study using laser scanning confocal microscopy and co-loaded fluo-3 and fura-red fluorescent probes. Cell Calcium. 18: 377-389.

Forsman, K., Graff, C., Nordstrom, S., Johansson, K., Westermark, E., Lundgren, E., Gustavson, K. H., Wadelius, C. and Holmgren, G. (1992). The gene for Best's macular dystrophy is located at 11q13 in a Swedish family. Clin. Genet. 42: 156-159.

Frambach, D. A., Fain, G. L., Farber, D. B. and Bok, D. (1990). Beta adrenergic receptors on cultured human retinal pigment epithelium. Invest. Ophthalmol. Vis. Sci. 31: 1767-1672.

Frambach, D. A., Valentine, J. L. and Weiter, J. J. (1989). Furosemide-sensitive Cl transport in bovine retinal pigment epithelium. Invest. Ophthalmol. Vis. Sci. 30: 2271-2274.

Francis, P. J., Marinescu, A., Fitzke, F. W., Bird, A. C. and Holder, G. E. (2005). Acute zonal occult outer retinopathy: towards a set of diagnostic criteria. Br. J. Ophthalmol. 89: 70-73.

Friedlander, M. L., Bell, D. R., Leary, J. and Davey, R. A. (1989). Comparison of western blot analysis and immunocytochemical detection of P-glycoprotein in multidrug resistant cells. J. Clin. Pathol. 42: 719-722.

Fuchs, U., Kivela, T. and Tarkkanen, A. (1991). Cytoskeleton in normal and reactive human retinal pigment epithelial cells. Invest. Ophthalmol. Vis. Sci. 32: 3178-3186.

Fujii, S., Gallemore, R. P., Hughes, B. A. and Steinberg, R. H. (1992). Direct evidence for a basolateral Cl^- conductance in the toad retinal pigment epithelium. Amer. J. Physiol. 262: C374-383.

Fujimoto, M. and Tomita, T. (1979). Reconstruction of the slow PIII from the rod potential. Invest. Ophthalmol. Vis. Sci. 18: 1091-1093.

Fukuoka, Y., Strainic, M. and Medof, M. E. (2003). Differential cytokine expression of human retinal pigment epithelial cells in response to stimulation by C5a. Clin. Exp. Immunol. 131: 248-253.

Fung, B-K. K. and Stryer, L. (1980). Photolyzed rhodopsin catalyzes the exchange of GTP for bound GDP in retinal rod outer segments. Proc. Natl. Acad. Sci. U.S.A. 77: 2500-2504.

Furukawa, T., Ogura, T., Katayama, Y. and Hiraoka, M. (1998). Characteristics of rabbit ClC-2 current expressed in *Xenopus* oocytes and its contribution to volume regulation. Amer. J. Physiol. 274: C500-512.

Gabriel, S. E., Clarke, L. L., Boucher, R. C. and Stutts, M. J. (1993). CFTR and outward rectifying chloride channels are distinct proteins with a regulatory relationship. Nature. 363: 263-266.

Gaillard, P. J., Voorwinden, L. H., Nielsen, J. L., Ivanov, A., Atsumi, R., Engman, H., Ringbom, C., de Boer, A. G. and Breimer, D. D. (2001). Establishment and functional characterization of an *in vitro* model of the blood-brain barrier, comprising a co-culture of brain capillary endothelial cells and astrocytes. Eur. J. Pharm. Sci. 12: 215-222.

Gallemore, R. P., Griff, E. R. and Steinberg, R. H. (1988). Evidence in support of a photoreceptoral origin for the "light-peak substance". Invest. Ophthalmol. Vis. Sci. 29: 566-571.

Gallemore, R. P., Hernandez, E., Tayyanipour, R., Fujii, S. and Steinberg, R. H. (1993). Basolateral membrane Cl^- and K^+ conductances of the dark-adapted chick retinal pigment epithelium. J. Neurophysiol. 70: 1656-1668.

Gallemore, R. P., Hughes, B. A. and Miller, S. S. (1998). Light induced responses in the retinal pigment epithelium. The retinal pigment epithelium: function and disease. M. F. Marmor and T. J. Wolfensberger. Oxford, OUP: 175-198.

Gallemore, R. P., Hughes, B. A. and Miller, S. S. (1997). Retinal pigment epithelial transport mechanisms and their contributions to the electroretinogram. Prog. Ret. Eye Res. 16: 509-566.

Gallemore, R. P. and Steinberg, R. H. (1989). Effects of DIDS on the chick retinal pigment epithelium. II. mechanism of the light peak and other responses originating at the basal membrane. J. Neurosci. 9: 1977-1984.

Gallemore, R. P. and Steinberg, R. H. (1990). Effects of dopamine on the chick retinal pigment epithelium. Membrane potentials and light-evoked responses. Invest. Ophthalmol. Vis. Sci. 31: 67-80.

Gallemore, R. P. and Steinberg, R. H. (1991). Cobalt increases photoreceptor-dependent responses of the chick retinal pigment epithelium. Invest. Ophthalmol. Vis. Sci. 32: 3041-3052.

Gallemore, R. P. and Steinberg, R. H. (1993). Light-evoked modulation of basolateral membrane Cl^- conductance in chick retinal pigment epithelium: the light peak and fast oscillation. J. Neurophysiol. 70: 1669-1680.

Garcia, M. L., King, V. F., Shevell, J. L., Slaughter, R. S., Suarez-Kurtz, G., Winquist, R. J. and Kaczorowski, G. J. (1990). Amiloride analogs inhibit L-type calcium channels and display calcium entry blocker activity. J. Biol. Chem. 265: 3763-3771.

Gardner, T. W., Lieth, E., Khin, S. A., Barber, A. J., Bonsall, D. J., Lesher, T., Rice, K. and Brennan, W. A., Jr. (1997). Astrocytes increase barrier properties and ZO-1 expression in retinal vascular endothelial cells. Invest. Ophthalmol. Vis. Sci. 38: 2423-2427.

Garg, T. K. and Chang, J. Y. (2003). Oxidative stress causes ERK phosphorylation and cell death in cultured retinal pigment epithelium: Prevention of cell death by AG126 and 15-deoxy-delta 12, 14-PGJ_2. BMC. Ophthalmol. 3: 5-20.

Garweg, J., Wegmann-Burns, M. and Goldblum, D. (2006). Effects of daunorubicin, mitomycin C, azathioprine and cyclosporin A on human retinal pigmented epithelial, corneal endothelial and conjunctival cell lines. Graefe's Arch. Clin. Exp. Ophthalmol. 244: 382-389.

Gaush, C. R., Hard, W. L. and Smith, T. F. (1966). Characterization of an established line of canine kidney cells (MDCK). Proc. Soc. Exp. Biol. Med. 122: 931-935.

Gee, K. R., Brown, K. A., Chen, W. N. U., Bishop-Stewart, J., Gray, D. and Johnson, I. (2000). Chemical and physiological characterization of fluo-4 Ca^{2+}-indicator dyes. Cell Calcium. 27: 97-106.

Geiger, R. C., Waters, C. M., Kamp, D. W. and Glucksberg, M. R. (2005). KGF prevents oxygen-mediated damage in ARPE-19 cells. Invest. Ophthalmol. Vis. Sci. 46: 3435-3442.

Gerstin Jr, E. H., McMahon, T., Dadgar, J. and Messing, R. O. (1998). Protein kinase Cδ mediates ethanol-induced up-regulation of L-type calcium channels. J. Biol. Chem. 273: 16409-16414.

Ghiselli, G., Chen, J., Kaou, M., Hallak, H. and Rubin, R. (2003). Ethanol inhibits fibroblast growth factor-induced proliferation of aortic smooth muscle cells. Arterioscler. Thromb. Vasc. Biol. 23: 1808-1813.

Gilman, A. G. (1987). G Proteins: transducers of receptor-generated signals. Annu. Rev. Biochem. 56: 615-649.

Glenney Jr, J. R. (1992). Tyrosine-phosphorylated proteins: mediators of signal transduction from the tyrosine kinases. Biochem. Biophys. Acta. 1134: 113-127.

Golestaneh, N., Picaud, S. and Mirshahi, M. (2002). The mineralocorticoid receptor in rodent retina: ontogeny and molecular identity. Mol. Vis. 9: 221-225.

Gomez, A., Cedano, J., Oliva, B., Pinol, J. and Querol, E. (2001). The gene causing the Best's macular dystrophy (BMD) encodes a putative ion exchanger. DNA Seq. 12: 431-435.

Gonzalez-Mariscal, L., Chavez de Ramirez, B. and Cereijido, M. (1984). Effect of temperature on the occluding junctions of monolayers of epithelioid cells (MDCK). J. Membr. Biol. 79: 175-184.

Goodenough, D. A. (1974). Bulk isolation of mouse hepatocyte gap junctions: characterization of the principal protein, connexin. J. Cell Biol. 61: 557-563.

Gordon, A. S., Nagy, L., Mochly-Rosen, D. and Diamond, I. (1990). Chronic ethanol-induced heterologous desensitization is mediated by changes in adenosine transport. Biochem. Soc. Symp. 56: 117-136.

Granit, R. (1933). The components of the retinal action potential in mammals and their relation to the discharge in the optic nerve. J. Physiol. (Lond). 77: 207-239.

Granit, R. (1947). The components of the vertebrate electroretinogram. Sensory mechanisms of the retina. G. Cumberlege. London, OUP: 38-69.

Greene, L. A. and Tischler, A. S. (1976). Establishment of a noradrenergic clonal line of rat adrenal pheochromocytoma cells which respond to nerve growth factor. Proc. Natl. Acad. Sci. U.S.A. 73: 2428-2428.

Greger, R., Mall, M., Bleich, M., Ecke, D., Warth, R., Riedemann, N. and Kunzelmann, K. (1996). Regulation of epithelial ion channels by the cystic fibrosis transmembrane conductance regulator. J. Mol. Med. 74: 527-534.

Gregory, R. J., Rich, D. P., Cheng, S. H., Souza, D. W., Paul, S., Manavalan, P., Anderson, M. P., Welsh, M. J. and Smith, A. E. (1991). Maturation and function of cystic fibrosis transmembrane conductance regulator variants bearing mutations in putative nucleotide-binding domains 1 and 2. Mol. Cell Biol. 11: 3886-3893.

Griff, E. R. (1990). Response properties of the toad retinal pigment epithelium. Invest. Ophthalmol. Vis. Sci. 31: 2353-2360.

Griff, E. R., Shirao, Y. and Steinberg, R. H. (1985). Ba2+ unmasks K+ modulation of the Na+-K+ pump in the frog retinal pigment epithelium. J. Gen. Physiol. 86: 853-876.

Griff, E. R. and Steinberg, R. H. (1982). Origin of the light peak: *in vitro* study of *Gekko gekko*. J. Physiol. (Lond). 331: 637-652.

Gründer, S., Thiemann, A., Pusch, M. and Jentsch, T. J. (1992). Regions involved in the opening of CIC-2 chloride channel by voltage and cell volume. Nature. 360: 759-762.

Gruss, M., Henrich, M., Konig, P., Hempelmann, G., Vogel, W. and Scholz, A. (2001). Ethanol reduces excitability in a subgroup of primary sensory neurons by activation of BKCa channels. Eur. J. Neurosci. 14: 1246-1256.

Grygorczyk, R. and Hanrahan, J. W. (1997a). CFTR-independent ATP release from epithelial cells triggered by mechanical stimuli. Amer. J. Physiol. 272: C1058-1066.

Grygorczyk, R. and Hanrahan, J. W. (1997b). Cystic fibrosis transmembrane conductance regulator and adenosine triphosphate. Science. 275: 1325-1326.

Grynkiewicz, G., Poenie, M. and Tsien, R. (1985). A new generation of Ca^{2+} indicators with greatly improved fluorescence properties. J. Biol. Chem. 260: 3440-3450.

Gu, J-W., Elam, J., Sartin, A., Li, W., Roach, R. and Adair, T. H. (2001). Moderate levels of ethanol induce expression of vascular endothelial growth factor and stimulate angiogenesis. Amer. J Physiol. 281: R365-372.

Gullapalli, V. K., Sugino, I. K., Van Patten, Y., Shah, S. and Zarbin, M. A. (2005). Impaired RPE survival on aged submacular human Bruch's membrane. Exp. Eye Res. 80: 235-248.

Gupta, L. Y. and Marmor, M. F. (1994). Sequential recording of photic and nonphotic electro-oculogram responses in patients with extensive extramacular drusen. Doc. Ophthalmol. 88: 49-55.

Gupta, L. Y. and Marmor, M. F. (1995). Electrophysiology of the retinal pigment epithelium in central serous chorioretinopathy. Doc. Ophthalmol. 91: 101-107.

Hadlock, T., Singh, S., Vacanti, J. P. and McLaughlin, B. J. (1999). Ocular cell monolayers cultured on biodegradable substrates. Tissue Eng. 5: 187-196.

Hagins, W. A., Penn, R. D. and Yoshikami, S. (1970). Dark current and photocurrent in retinal rods. J. Biophys. 10: 380-412.

Hall, M. O., Abrams, T. A. and Mittag, T. W. (1991). ROS ingestion by RPE cells is turned off by increased protein kinase C activity and by increased calcium. Exp. Eye Res. 52: 591-598.

Hall, M. O., Obin, M. S., Prieto, A. L., Burgess, B. L. and Abrams, T. A. (2002). Gas6 binding to photoreceptor outer segments requires γ-carboxyglutamic acid (Gla) and Ca^{2+} and is required for OS phagocytosis by RPE cells *in vitro*. Exp. Eye Res. 75: 391-400.

Hall, M. O., Prieto, A. L., Obin, M. S., Abrams, T. A., Burgess, B. L., Heeb, M. J. and Agnew, B. J. (2001). Outer segment phagocytosis by cultured retinal pigment epithelial cells requires Gas6. Exp. Eye Res. 73: 509-520.

Harding, G. F., Robertson, K., Spencer, E. L. and Holliday, I. (2002). Vigabatrin; its effect on the electrophysiology of vision. Doc. Ophthalmol. 104: 213-229.

Hartnett, M. E., Lappas, A., Darland, D., McColm, J. R., Lovejoy, S. and D'Amore, P. A. (2003). Retinal pigment epithelium and endothelial cell interaction causes retinal pigment epithelial barrier dysfunction via a soluble VEGF-dependent mechanism. Exp. Eye Res. 77: 593-599.

Hartzell, H. C. and Qu, Z. (2003). Chloride currents in acutely isolated *Xenopus* retinal pigment epithelial cells. J. Physiol. (Lond). 549: 453-469.

He, P. M., He, S., Garner, J. A., Ryan, S. J. and Hinton, D. R. (1998). Retinal pigment epithelial cells secrete and respond to hepatocyte growth factor. Biochem. Biophys. Res. Commun. 249: 253-257.

Heldin, C. H., Ernlund, A., Rorsman, C. and Ronnstrand, L. (1989). Dimerization of B-type platelet-derived growth factor receptors occurs after ligand binding and is closely associated with receptor kinase activation. J. Biol. Chem. 264: 8905-8912.

Hendricson, A. W., Thomas, M. P., Lippmann, M. J. and Morrisett, R. A. (2003). Suppression of L-type voltage-gated calcium channel-dependent synaptic plasticity by ethanol: analysis of miniature synaptic currents and dendritic calcium transients. J. Pharmacol. Exp. Ther. 307: 550-558.

Hernandez, E. V., Hu, J. G., Frambach, D. A. and Gallemore, R. P. (1995). Potassium conductances in cultured bovine and human retinal pigment epithelium. Invest. Ophthalmol. Vis. Sci. 36: 113-122.

Hidajat, R. R., McLay, J. L., Goode, D. H. and Spearing, R. L. (2004). EOG as a monitor of desferrioxamine retinal toxicity. Doc. Ophthalmol. 109: 273-278.

Higgins, G. T., Wang, J. H., Dockery, P., Cleary, P. E. and Redmond, H. P. (2003). Induction of angiogenic cytokine expression in cultured RPE by ingestion of oxidized photoreceptor outer segments. Invest. Ophthalmol. Vis. Sci. 44: 1775-1782.

Hillenkamp, J., Hussain, A. A., Jackson, T. L., Constable, P. A., Cunningham, J. R. and Marshall, J. (2004a). Compartmental analysis of taurine transport to the outer retina in the bovine eye. Invest. Ophthalmol. Vis. Sci. 45: 4099-4105.

Hillenkamp, J., Hussain, A. A., Jackson, T. L., Cunningham, J. R. and Marshall, J. (2004b). Taurine uptake by human retinal pigment epithelium: implications for the transport of small solutes between the choroid and the outer retina. Invest. Ophthalmol. Vis. Sci. 45: 4529-4534.

Himpens, B., Stalmans, P., Gomez, P., Malfait, M. and Vereecke, J. (1999). Intra- and intercellular Ca^{2+} signaling in retinal pigment epithelial cells during mechanical stimulation. FASEB. J. 13: S63-68.

Ho, T. C. and Del Priore, L. V. (1997). Reattachment of cultured human retinal pigment epithelium to extracellular matrix and human Bruch's membrane. Invest. Ophthalmol. Vis. Sci. 38: 1110-1118.

Hodgkin, A. L. and Huxley, A. F. (1952a). The components of membrane conductance in the giant axon of *Loligo*. J. Physiol. (Lond). 116: 473-496.

Hodgkin, A. L. and Huxley, A. F. (1952b). Currents carried by sodium and potassium ions through the membrane of the giant axon of *Loligo*. J. Physiol. (Lond). 116: 449-472.

Hodgkin, A. L. and Huxley, A. F. (1952c). The dual effect of membrane potential on sodium conductance in the giant axon of *Loligo*. J. Physiol. (Lond). 116: 497-506.

Hoek, J. B. and Rubin, E. (1990). Alcohol and membrane-associated signal transduction. Alcohol Alcohol. 25: 143-156.

Hoek, J. B., Taraschi, T. F., Higashi, K., Rubin, E. and Thomas, A. P. (1990). Phospholipase C activation by ethanol in rat hepatocytes is unaffected by chronic ethanol feeding. J. Biochem. 272: 59-64.

Hofmann, H. and Niemeyer, G. (1985). Calcium blocks selectively the EOG-light peak. Doc. Ophthalmol. 60: 361-368.

Hogg, P. A., Grierson, I. and Hiscott, P. (2002). Direct comparison of the migration of three cell types involved in epiretinal membrane formation. Invest. Ophthalmol. Vis. Sci. 43: 2749-2757.

Hollborn, M., Krausse, C., Iandiev, I., Yafai, Y., Tenckhoff, S., Bigl, M., Schnurrbusch, U. E., Limb, G. A., Reichenbach, A., Kohen, L., Wolf, S., Wiedemann, P. and Bringmann, A. (2004). Glial cell expression of hepatocyte growth factor in vitreoretinal proliferative disease. Lab Invest. 84: 963-972.

Hollenberg, M. D. and Cuatrecasas, P. (1975). Insulin and epidermal growth factor. Human fibroblast receptors related to deoxyribonucleic acid synthesis and amino acid uptake. J. Biol. Chem. 250: 3845-3853.

Hollenberg, M. J. and Burt, W. L. (1969). The fine structure of Bruch's membrane in the human eye. Can. J. Ophthalmol. 4: 296-306.

Hollenberg, M. J. and Spira, A. W. (1972). Early development of the human retina. Can. J. Ophthalmol. 7: 472-491.

Hollyfield, J. G. and Witkovsky, P. (1974). Pigmented retinal epithelium involvement in photoreceptor development and function. J. Exp. Zool. 189: 357-378.

Holtkamp, G. M., Van Rossem, M., de Vos, A. F., Willekens, B., Peek, R. and Kijlstra, A. (1998). Polarized secretion of IL-6 and IL-8 by human retinal pigment epithelial cells. Clin. Exp. Immunol. 112: 34-43.

Homolya, L., Hollo, Z., Germann, U., Pastan, I., Gottesman, M. and Sarkadi, B. (1993). Fluorescent cellular indicators are extruded by the multidrug resistance protein. J. Biol. Chem. 268: 21493-21496.

Horisberger, J-D. (2003). ENaC-CFTR interactions: the role of electrical coupling of ion fluxes explored in an epithelial cell model. Pflügers. Archiv. 445: 522-528.

Hu, J. and Bok, D. (2001). A cell culture medium that supports the differentiation of human retinal pigment epithelium into functionally polarized monolayers. Mol. Vis. 7: 14-19.

Hu, J. G., Gallemore, R. P., Bok, D., Lee, A. Y. and Frambach, D. A. (1994). Localization of NaK ATPase on cultured human retinal pigment epithelium. Invest. Ophthalmol. Vis. Sci. 35: 3582-3588.

Hubbard, R. and Wald, G. (1952). Cis-trans isomers of vitamin A and retinene in the rhodopsin system. J. Gen. Physiol. 36: 269-315.

Hughes, B. A., Adorante, J. S., Miller, S. S. and Lin, H. (1989). Apical electrogenic $NaHCO_3$ cotransport. A mechanism for HCO_3 absorption across the retinal pigment epithelium. J. Gen. Physiol. 94: 125-150.

Hughes, B. A., Miller, S. S. and Machen, T. E. (1984). Effects of cyclic AMP on fluid absorption and ion transport across frog retinal pigment epithelium. measurements in the open-circuit state. J. Gen. Physiol. 83: 875-899.

Hughes, B. A. and Segawa, Y. (1993). cAMP-activated chloride currents in amphibian retinal pigment epithelial cells. J. Physiol. (Lond). 466: 749-766.

Hughes, B. A. and Steinberg, R. H. (1990). Voltage-dependent currents in isolated cells of the frog retinal pigment epithelium. J. Physiol. (Lond). 428: 273-297.

Hughes, B. A. and Takahira, M. (1996). Inwardly rectifying K+ currents in isolated human retinal pigment epithelial cells. Invest. Ophthalmol. Vis. Sci. 37: 1125-1139.

Hughes, B. A. and Takahira, M. (1998). ATP-dependent regulation of inwardly rectifying K+ current in bovine retinal pigment epithelial cells. Amer. J. Physiol. 275: C1372-1383.

Hurst, R. D. and Fritz, I. B. (1996). Properties of an immortalised vascular endothelial/glioma cell co-culture model of the blood-brain barrier. J. Cell Physiol. 167: 81-88.

Hurst, R. D., Heales, S. J. R., Dobbie, M. S., Barker, J. E. and Clark, J. B. (1998). Decreased endothelial cell glutathione and increased sensitivity to oxidative stress in an *in vitro* blood-brain barrier model system. Brain Res. 802: 232-240.

Igarashi, Y., Utsumi, H., Chiba, H., Yamada-Sasamori, Y., Tobioka, H., Kamimura, Y., Furuuchi, K., Kokai, Y., Nakagawa, T., Mori, M. and Sawada, N. (1999). Glial cell line-derived neurotrophic factor induces barrier function of endothelial cells forming the blood-brain barrier. Biochem. Biophys. Res. Commun. 261: 108-112.

Ikeda, H. (1963). Effects of ethyl alcohol on the evoked potential of the human eye. Vis. Res. 3: 155-169.

Irschick, E. U., Haas, G., Geiger, M., Singer, W., Ritsch-Marte, M., Konwalinka, G., Frick, M., Gottinger, W. and Huemer, H. P. (2006). Phagocytosis of human retinal pigment epithelial cells: evidence of a diurnal rhythm, involvement of the cytoskeleton and interference of antiviral drugs. Ophthalmic Res. 38: 164-174.

Ishigooka, H., Aotaki-Keen, A. E. and Hjelmeland, L. M. (1992). Subcellular localization of bFGF in human retinal pigment epithelium *in vitro*. Exp. Eye Res. 55: 203-214.

Ismailov, I. I., Awayda, M. S., Jovov, B., Berdiev, B. K., Fuller, C. M., Dedman, J. R., Kaetzel, M. A. and Benos, D. J. (1996). Regulation of epithelial sodium channels by the cystic fibrosis transmembrane conductance regulator. J. Biol. Chem. 271: 4725-4732.

Janssen, J. J., Kuhlmann, E. D., van Vugt, A. H., Winkens, H. J., Janssen, B. P., Deutman, A. F. and Driessen, C. A. (2000). Retinoic acid delays transcription of human retinal pigment neuroepithelium marker genes in ARPE-19 cells. Neuroreport. 11: 1571-1579.

Jaynes, C. D., Sheedlo, H. J., Agarwal, N., O' Rourke, K. and E. Turner, J. (1995). Müller and retinal pigment epithelial (RPE) cell expression of NGFI-A and c-fos mRNA in response to medium conditioned by the RPE. Mol. Brain Res. 32: 329-337.

Jaynes, C. D. and Turner, J. E. (2000). Isolation of a retinal pigment epithelial cell-derived fraction which promotes Müller cell proliferation. Brain Res. 120: 267-271.

Jentsch, T. J., Friedrich, T. and Schriever, A. (1999). ClC Chloride Channels. Chloride Channels. R. Kozlowski. Oxford, Isis Medical Media Ltd: 200.

Jentsch, T. J., Steinmeyer, K. and Schwarz, G. (1990). Primary structure of *Torpedo marmorata* chloride channel isolated by expression cloning in *Xenopus* oocytes. Nature. 348: 510-514.

Johnson, D. A., Fields, C., Fallon, A., Fitzgerald, M. E., Viar, M. J. and Johnson, L. R. (2002). Polyamine-dependent migration of retinal pigment epithelial cells. Invest. Ophthalmol. Vis. Sci. 43: 1228-1233.

Jones, T. W. (1833). Notice relative to the pigmentum nigrum of the eye. Edin. Med. Surg. J. 40: 77-83. *Cited by* Wolfensberger, T. J. (1998). The Historical Discovery of the Retinal Pigment Epithelium. The retinal pigment epithelium: function and disease. M. F. Marmor and T. J. Wolfensberger. New York, OUP: 745.

Jordt, S-E. and Jentsch, T. J. (1997). Molecular dissection of gating in the ClC-2 chloride channel. EMBO J. 16: 1582-1592.

Joris, L., Dab, I. and Quinton, P. M. (1993). Elemental composition of human airway surface fluid in healthy and diseased airways. Amer. Rev. Respir. Dis. 148: 1633-1637.

Joseph, D. P. and Miller, S. S. (1991). Apical and basal membrane ion transport mechanisms in bovine retinal pigment epithelium. J. Physiol. (Lond). 435: 439-463.

Jovov, B., Ismailov, I. I. and Benos, D. J. (1995a). Cystic fibrosis transmembrane conductance regulator is required for protein kinase A activation of an outwardly rectified anion channel purified from bovine tracheal epithelia. J. Biol. Chem. 270: 1521-1528.

Jovov, B., Ismailov, I. I., Berdiev, B. K., Fuller, C. M., Sorscher, E. J., Dedman, J. R., Kaetzel, M. A. and Benos, D. J. (1995b). Interaction between cystic fibrosis transmembrane conductance regulator and outwardly rectified chloride channels. J. Biol. Chem. 270: 29194-29200.

Kahkonen, S. and Bondarenko, B. B. (2004). L-type Ca^{2+} channels mediate cardiovascular symptoms of alcohol withdrawal in humans. Prog. Neuro-Psych. Biolog. Psych. 28: 45-48.

Kanuga, N., Winton, H. L., Beauchene, L., Koman, A., Zerbib, A., Halford, S., Couraud, P. O., Keegan, D., Coffey, P., Lund, R. D., Adamson, P. and Greenwood, J. (2002). Characterization of genetically modified human retinal pigment epithelial cells developed for *in vitro* and transplantation studies. Invest. Ophthalmol. Vis. Sci. 43: 546-555.

Kartner, N., Hanrahan, J. W., Jensen, T. J., Naismith, A. L., Sun, S. Z., Ackerley, C. A., Reyes, E. F., Tsui, L-C., Rommens, J. M. and Bear, C. E. (1991). Expression of the cystic fibrosis gene in non-epithelial invertebrate cells produces a regulated anion conductance. Cell. 64: 681-691.

Karwoski, C. J. and Proenza, L. M. (1977). Relationship between Muller cell responses, a local transretinal potential, and potassium flux. J. Neurophysiol. 40: 244-259.

Karwoski, C. J. and Xu, X. (1999). Current source-density analysis of light-evoked field potentials in rabbit retina. Vis. Neurosci. 16: 369-377.

Kasahara, E., Lin, L-R., Ho, Y-S. and Reddy, V. N. (2005). SOD2 protects against oxidation-induced apoptosis in mouse retinal pigment epithelium: implications for age-related macular degeneration. Invest. Ophthalmol. Vis. Sci. 46: 3426-3434.

Katz, L. M. and Fox, D. A. (1991). Prenatal ethanol exposure alters scotopic and photopic components of adult rat electroretinograms. Invest. Ophthalmol. Vis. Sci. 32: 2861-2872.

Kaven, C. W., Spraul, C. W., Zavazava, N. K., Lang, G. K. and Lang, G. E. (2000). Growth factor combinations modulate human retinal pigment epithelial cell proliferation. Curr. Eye Res. 20: 480-487.

Kawasaki, K., Mukoh, S., Yonemura, D., Fujii, S. and Segawa, Y. (1986). Acetazolamide-induced changes of the membrane potentials of the retinal pigment epithelial cell. Doc. Ophthalmol. 63: 375-381.

Kawasaki, K., Yonemura, D. and Madachi-Yamamoto, S. (1984). Hyperosmolarity response of ocular standing potential as a clinical test for retinal pigment epithelium activity diabetic retinopathy. Doc. Ophthalmol. 58: 375-384.

Kennedy, B. G. and Mangini, N. J. (1996). Plasma membrane calcium-ATPase in cultured human retinal pigment epithelium. Exp. Eye Res. 63: 547-556.

Kennedy, B. G. and Mangini, N. J. (2002). P-glycoprotein expression in human retinal pigment epithelium. Mol. Vis. 8: 422-430.

Kerem, B-S., Rommens, J. M., Buchanan, J. A., Markiewicz, D., Cox, T. K., Chakravarti, A., Buchwald, M. and Tsui, L-C. (1989). Identification of the cystic fibrosis gene: genetic analysis. Science. 245: 1073-1080.

Kim, M. H., Chung, J., Yang, J. W., Chung, S. M., Kwag, N. H. and Yoo, J. S. (2003). Hydrogen peroxide-induced cell death in a human retinal pigment epithelial cell line, ARPE-19. Korean J. Ophthalmol. 17: 19-28.

Kimura, K. D., Tissenbaum, H. A., Liu, Y. and Ruvkun, G. (1997). *daf-2*, an insulin receptor-like gene that regulates longevity and diapause in *Caenorhabditis elegans*. Science. 277: 942-946.

Kishi, H., Mishima, H. K. and Yamashita, U. (2000). Involvement of the protein kinase pathway in melanin synthesis by chick retinal pigment epithelial cells. Cell Biol. Int. 24: 79-83.

Kline, R. P., Ripps, H. and Dowling, J. E. (1978). Generation of b-wave currents in the skate retina. Proc. Natl. Acad. Sci. U.S.A. 75: 5727-5731.

Klyne, M. A. and Ali, M. A. (1981). Microtubules and 10 nm-filaments in the retinal pigment epithelium during the diurnal light-dark-cycle. Cell Tissue Res. 214: 397-405.

Knave, B., Persson, H. E. and Nilsson, S. E. G. (1974). A comparative study on the effects of barbituate and ethyl alcohol on the retinal functions with specific reference to the c-wave of the electroretinogram and the standing potential of the sheep eye. Acta. Ophthalmol. Scand. 52: 254 -259.

Knowles, M. R., Stutts, M. J., Spock, A., Fischer, N., Gatzy, J. T. and Boucher, R. C. (1983). Abnormal ion permeation through cystic fibrosis respiratory epithelium. Science. 221: 1067-1070.

Kociok, N., Heppekausen, H., Schraermeyer, U., Esser, P., Thumann, G., Grisanti, S. and Heimann, K. (1998). The mRNA expression of cytokines and their receptors in cultured iris pigment epithelial cells: a comparison with retinal pigment epithelial cells. Exp. Eye Res. 67: 237-250.

Kodama, R. and Eguchi, G. (1994). The loss of gap junctional cell-to-cell communication is coupled with dedifferentiation of retinal pigmented epithelial cells in the course of transdifferentiation into the lens. Int. J. Dev. Biol. 38: 357-364.

Kojima, S., Rahner, C., Peng, S. and Rizzolo, L. J. (2002). Claudin 5 is transiently expressed during the development of the retinal pigment epithelium. J. Membr. Biol. 186: 81-88.

Konari, K., Sawada, N., Zhong, Y., Isomura, H., Nakagawa, T. and Mori, M. (1995). Development of the blood-retinal barrier *in vitro*: formation of tight junctions as revealed by occludin and ZO-1 correlates with the barrier function of chick retinal pigment epithelial cells. Exp. Eye Res. 61: 99-108.

Konig, J., Schreiber, R., Mall, M. and Kunzelmann, K. (2002). No evidence for inhibition of ENaC through CFTR-mediated release of ATP. Biochim. Biophys. Acta. 1565: 17-28.

Kopelman, H., Corey, M., Gaskin, K., Durie, P., Weizman, Z. and Forstner, G. (1988). Impaired chloride secretion, as well as bicarbonate secretion, underlies the fluid secretory defect in the cystic fibrosis pancreas. Gastroenterology. 95: 349-355.

Korte, G. E., Perlman, J. I. and Pollack, A. (1994). Regeneration of mammalian retinal pigment epithelium. Int. Rev. Cytol. 152: 223-263.

Kramer, S. G. (1971). Dopamine: A retinal neurotransmitter. I. Retinal uptake, storage, and light-stimulated release of H3-dopamine in vivo. Invest. Ophthalmol. Vis. Sci. 10: 438-452.

Kris, C. (1958). Corneo-fundal potential variations during light and dark adaption. Nature. 182: 1027-1028.

Kuga, T., Sadoshima, J., Tomoike, H., Kanaide, H., Akaike, N. and Nakamura, M. (1990). Actions of Ca^{2+} antagonists on two types of Ca^{2+} channels in rat aorta smooth muscle cells in primary culture. Circ. Res. 67: 469-480.

Kuntz, C. A., Crook, R. B., Dmitriev, A. and Steinberg, R. H. (1994). Modification by cyclic adenosine monophosphate of basolateral membrane chloride conductance in chick retinal pigment epithelium. Invest. Ophthalmol. Vis. Sci. 35: 422-433.

Kunzelmann, K. (2001). CFTR: interacting with everything? News Physiol. Sci. 16: 167-170.

Kunzelmann, K., Mall, M., Briel, M., Hipper, A., Nitschke, R., Ricken, S. and Greger, R. (1997). The cystic fibrosis transmembrane conductance regulator attenuates the endogenous Ca^{2+} activated Cl^- conductance of *Xenopus* oocytes. Pflügers Archiv. 435: 178-181.

Kuriyama, S., Ohuchi, T., Yoshimura, N. and Honda, Y. (1991). Growth factor-induced cytosolic calcium ion transients in cultured human retinal pigment epithelial cells. Invest. Ophthalmol. Vis. Sci. 32: 2882-2890.

Kuriyama, S., Yoshimura, N., Ohuchi, T., Tanihara, H., Ito, S. and Honda, Y. (1992). Neuropeptide-induced cytosolic Ca^{2+} transients and phosphatidylinositol turnover in cultured human retinal pigment epithelial cells. Brain Res. 579: 227-233.

Kurkin, S. A. and Fesenko, E. E. (1982). Action of cyclic nucleotides on the cytoplasmic membrane conductance of the rod outer segment in the retina. Dokl. Akad. Nauk. SSSR. 262: 1269-1272.

Kutlay, S., Savas, S., Yalcin, P., Ataman, S. and Ergin, S. (1997). Central nervous system toxicity of cyclosporin A treatment in rheumatoid arthritis. Rheumatology. 36: 397-399.

Kutty, R. K., Kutty, G., Samuel, W., Duncan, T., Bridges, C. C., El-Sherbeeny, A., Nagineni, C. N., Smith, S. B. and Wiggert, B. (2001). Molecular characterization and developmental expression of NORPEG, a novel gene induced by retinoic acid. J. Biol. Chem. 276: 2831-2840.

la Cour, M. (1991). pH homeostasis in the frog retina: the role of $Na+:HCO_3-$ co-transport in the retinal pigment epithelium. Acta. Ophthalmol. Scand. 69: 496-504.

la Cour, M. (1992). Cl^- transport in frog retinal pigment epithelium. Exp. Eye Res. 54: 921-931.

la Cour, M., Baekgaard, A. and Zeuthen, T. (1997). Antibodies against a furosemide binding protein from Ehrlich ascites tumour cells inhibit Na+, K+, Cl- co-transport in frog retinal pigment epithelium. Acta. Ophthalmol. Scand. 75: 405-408.

Lahnsteiner, E. and Hermann, A. (1995). Acute action of ethanol on rat hippocampal CA1 neurons: effects on intracellular signaling. Neuroscie. Lett. 191: 153-156.

Lam, R. W., Beattie, C. W., Buchanan, A., Remick, R. A. and Zis, A. P. (1991). Low electrooculographic ratios in patients with seasonal affective disorder. Amer. J. Psychiat. 148: 1526-1529.

Lara, W. C., Jordan, B. L., Hope, G. M., Dawson, W. W., Foster, R. A. and Kaushal, S. (2003). Fast oscillations of the electro-oculogram in cystic fibrosis. Invest. Ophthalmol. Vis. Sci. 44: #4957 ARVO Abstract.

Lashkari, K., Rahimi, N. and Kazlauskas, A. (1999). Hepatocyte growth factor receptor in human RPE cells: implications in proliferative vitreoretinopathy. Invest. Ophthalmol. Vis. Sci. 40: 149-156.

Lawden, M. C., Eke, T., Degg, C., Harding, G. F. A. and Wild, J. M. (1999). Visual field defects associated with vigabatrin therapy. J. Neurol. Neurosurg. Psychiatry. 67: 716-722.

Lemna, W. K., Feldman, G. L., Kerem, B., Fernbach, S. D., Zevkovich, E. P., O'Brien, W. E., Riordan, J. R., Collins, F. S., Tsui, L. C. and Beaudet, A. L. (1990). Mutation analysis for heterozygote detection and the prenatal diagnosis of cystic fibrosis. N. Engl. J. Med. 322: 291-296.

Leverkoehne, I., Holle, H., Anton, F. and Gruber, A. (2006). Differential expression of calcium-activated chloride channels (CLCA) gene family members in the small intestine of cystic fibrosis mouse models. Histochem. Cell Biol. 126: 239-250.

Levin, M. H., Kim, J. K., Hu, J. and Verkman, A. S. (2006). Potential difference measurements of ocular surface Na^+ absorption analyzed using an electrokinetic model. Invest. Ophthalmol. Vis. Sci. 47: 306-316.

Levin, M. H. and Verkman, A. S. (2005). CFTR-regulated chloride transport at the ocular surface in living mice measured by potential differences. Invest. Ophthalmol. Vis. Sci. 46: 1428-1434.

Li, C., Ramjeesingh, M. and Bear, C. E. (1996). Purified cystic fibrosis transmembrane conductance regulator (CFTR) does not function as an ATP channel. J. Biol. Chem. 271: 11623-11626.

Li, M., McCann, J. D., Liedtket, C. M., Nairn, A. C., Greengard, P. and Welsh, M. J. (1988). Cyclic AMP-dependent protein kinase opens chloride channels in normal but not cystic fibrosis airway epithelium. Nature. 331: 358-360.

Lin, H. and Clegg, D. O. (1998). Integrin alphavbeta5 participates in the binding of photoreceptor rod outer segments during phagocytosis by cultured human retinal pigment epithelium. Invest. Ophthalmol. Vis. Sci. 39: 1703-1712.

Limb, G. A., Salt, T. E., Munro, P. M. G., Moss, S. E. and Khaw, P. T. (2002). *In vitro* characterization of a spontaneously immortalized human müller cell line (MIO-M1). Invest. Ophthalmol. Vis. Sci. 43: 864-869.

Linsdell, P. (2006). Mechanism of chloride permeation in the cystic fibrosis transmembrane conductance regulator chloride channel. Exp. Physiol. 91: 123-129.

Linsdell, P. and Hanrahan, J. W. (1996). Disulphonic stilbene block of cystic fibrosis transmembrane conductance regulator Cl^- channels expressed in a mammalian cell line and its regulation by a critical pore residue. J. Physiol. (Lond). 496: 687-693.

Linsenmeier, R. A., Mines, A. and Steinberg, R. H. (1983). Effects of hypoxia and hypercapnia on the light peak and electroretinogram of the cat. Invest. Ophthalmol. Vis. Sci. 24: 37-46.

Linsenmeier, R. A. and Steinberg, R. H. (1982). Origin and sensitivity of the light peak in the intact cat eye. J. Physiol. (Lond). 331: 653-673.

Linsenmeier, R. A. and Steinberg, R. H. (1983). A light-evoked interaction of apical and basal membranes of retinal pigment epithelium: c-wave and light peak. J. Neurophysiol. 50: 136-147.

Linsenmeier, R. A. and Steinberg, R. H. (1984). Delayed basal hyperpolarization of cat retinal pigment epithelium and its relation to the fast oscillation of the dc electroretinogram. J. Gen. Physiol. 83: 213-232.

Liu, X-D. and Kourennyi, D. E. (2004). Effects of tetraethylammonium on K_x channels and simulated light response in rod photoreceptors. Annals Biomed. Engin. 32: 1428-1442.

Loeffler, K. U. and Mangini, N. J. (1998). Immunohistochemical localization of Na^+/Ca^{2+} exchanger in human retina and retinal pigment epithelium. Graefe's Arch. Clin. Exp. Ophthalmol. 236: 929-933.

Loewen, M. E., Smith, N. K., Hamilton, D. L., Grahn, B. H. and Forsyth, G. W. (2003). CLCA protein and chloride transport in canine retinal pigment epithelium. Amer. J. Physiol. 285: C1314-1321.

López-Jiménez, J., Sánchez, A., Fernández, C. S., Gutiérrez, C., Herrera, P. and Odriozola, J. (1997). Cyclosporine-induced retinal toxic blindness. Bone Marrow Transplant. 20: 243-245.

Loussouarn, G., Demolombe, S., Mohammad-Panah, R., Escande, D. and Baro, I. (1996). Expression of CFTR controls cAMP-dependent activation of epithelial K^+ currents. Amer. J. Physiol. 271: C1565-1573.

Lu, K. H., Patterson, A. P., Wang, L., Marquez, R. T., Atkinson, E. N., Baggerly, K. A., Ramoth, L. R., Rosen, D. G., Liu, J., Hellstrom, I., Smith, D., Hartmann, L., Fishman, D., Berchuck, A., Schmandt, R., Whitaker, R., Gershenson, D. M., Mills, G. B. and Bast, R. C., Jr. (2004). Selection of potential markers for epithelial ovarian cancer with gene expression arrays and recursive descent partition analysis. Clin. Cancer Res. 10: 3291-3300.

Lu, M., Amano, S., Miyamoto, K., Garland, R., Keough, K., Qin, W. and Adamis, A. P. (1999). Insulin-induced vascular endothelial growth factor expression in retina. Invest. Ophthalmol. Vis. Sci. 40: 3281-3286.

Lund, R. D., Adamson, P., Sauve, Y., Keegan, D. J., Girman, S. V., Wang, S., Winton, H., Kanuga, N., Kwan, A. S., Beauchene, L., Zerbib, A., Hetherington, L., Couraud, P. O., Coffey, P. and Greenwood, J. (2001). Subretinal transplantation of genetically

modified human cell lines attenuates loss of visual function in dystrophic rats. Proc. Natl. Acad. Sci. U.S.A. 98: 9942-9947.

Luo, Y., Zhuo, Y., Fukuhara, M. and Rizzolo, L. J. (2006). Effects of culture conditions on heterogeneity and the apical junctional complex of the ARPE-19 cell line. Invest. Ophthalmol. Vis. Sci. 47: 3644-3655.

Lytton, J., Westlin, M. and Hanley, M. (1991). Thapsigargin inhibits the sarcoplasmic or endoplasmic reticulum Ca- ATPase family of calcium pumps. J. Biol. Chem. 266: 17067-17071.

Madachi-Yamamoto, S., Yonemura, D. and Kawasaki, K. (1984). Hyperosmolarity response of ocular standing potential as a clinical test for retinal pigment epithelium activity. Normative data. Doc. Ophthalmol. 57: 153-162.

Malinowska, D. H., Kupert, E. Y., Bahinski, A., Sherry, A. M. and Cuppoletti, J. (1995). Cloning, functional expression, and characterization of a PKA-activated gastric Cl^- channel. Amer. J. Physiol. 268: C191-200.

Mall, M., Hipper, A., Greger, R. and Kunzelmann, K. (1996). Wild type but not ΔF508 CFTR inhibits Na^+ conductance when coexpressed in *Xenopus* oocytes. FEBS Letters. 381: 47-52.

Maminishkis, A., Jalickee, S., Blaug, S. A., Rymer, J., Yerxa, B. R., Peterson, W. M. and Miller, S. S. (2002). The $P2Y_2$ receptor agonist INS37217 stimulates RPE fluid transport *in vitro* and retinal reattachment in rat. Invest. Ophthalmol. Vis. Sci. 43: 3555-3566.

Mangini, N. J., Haugh-Scheidt, L., Valle, J. E., Cragoe, E. J., Jr., Ripps, H. and Kennedy, B. G. (1997). Sodium-calcium exchanger in cultured human retinal pigment epithelium. Exp. Eye Res. 65: 821-834.

Mannerstrom, M., Maenpaa, H., Toimela, T., Salminen, L. and Tahti, H. (2001). The phagocytosis of rod outer segments is inhibited by selected drugs in retinal pigment epithelial cell cultures. Pharmacol. Toxicol. 88: 27-33.

Marcet, B., Becq, F., Norez, C., Delmas, P. and Verrier, B. (2004). General anaesthetic octanol and related compounds activate wild-type and del508 cystic fibrosis chloride channels. Br. J. Pharmacol. 141: 905-914.

Marcet, B., Chappe, V., Delmas, P., Gola, M. and Verrier, B. (2003). Negative regulation of CFTR activity by extracellular ATP Involves P_2Y_2 receptors in CFTR-expressing CHO cells. J. Membr. Biol. 194: 21-32.

Marchant, D., Gogat, K., Boutboul, S., Péquignot, M., Sternberg, C., Dureau, P., Roche, O., Uteza, Y., Hache, J. C., Puech, B., Puech, V., Dumur, V., Mouillon, M., Munier, F. L., Schorderet, D. F., Marsac, C., Dufier, J. L. and Abitbol, M. (2001). Identification of novel VMD2 gene mutations in patients with best vitelliform macular dystrophy. Hum. Mut. 17: 235-235.

Marmor, M. and Wu, K. (2005). Alcohol- and light-induced electro-oculographic responses: variability and clinical utility. Doc. Ophthalmol. 110: 227-236.

Marmor, M. F. (1991). Clinical electrophysiology of the retinal pigment epithelium. Doc. Ophthalmol. 76: 301-313.

Marmor, M. F. (1998). Structure, function, and disease of the retinal pigment epithelium. The retinal pigment epithelium: function and disease. M. F. Marmor and T. J. Wolfensberger. New York, OUP: 3-9.

Marmor, M. F., Donovan, W. J. and Gaba, D. M. (1985). Effects of hypoxia and hyperoxia on the human standing potential. Doc. Ophthalmol. 60: 347-352.

Marmor, M. F. and Lurie, M. (1979). Light induced responses of the retinal pigment epithelium. The retinal pigment epithelium. K. Zinn and M. F. Marmor. Cambridge MA, Harvard University Press: 226-244.

Marmor, M. F. and Zrenner, E. (1993). Standard for clinical electro-oculography. International society for clinical electrophysiology of vision. Doc. Ophthalmol. 85: 115-124.

Marmorstein, A. D., Marmorstein, L. Y., Rayborn, M., Wang, X., Hollyfield, J. G. and Petrukhin, K. (2000). Bestrophin, the product of the Best vitelliform macular dystrophy gene (VMD2), localizes to the basolateral plasma membrane of the retinal pigment epithelium. Proc. Natl. Acad. Sci. U.S.A. 97: 12758-12763.

Marmorstein, A. D., Stanton, J. B., Yocom, J., Bakall, B., Schiavone, M. T., Wadelius, C., Marmorstein, L. Y. and Peachey, N. S. (2004). A model of best vitelliform macular dystrophy in rats. Invest. Ophthalmol. Vis. Sci. 45: 3733-3739.

Marmorstein, L. Y., Wu, J., McLaughlin, P., Yocom, J., Karl, M. O., Neussert, R., Wimmers, S., Stanton, J. B., Gregg, R. G., Strauss, O., Peachey, N. S. and Marmorstein, A. D. (2006). The light peak of the electroretinogram is dependent on voltage-gated calcium channels and antagonized by bestrophin (Best-1). J. Gen. Physiol. 127: 577-589.

Marquardt, A., Stohr, H., Passmore, L., Kramer, F., Rivera, A. and Weber, B. (1998). Mutations in a novel gene, *VMD2*, encoding a protein of unknown properties cause juvenile-onset vitelliform macular dystrophy (Best's disease). Hum. Mol. Genet. 7: 1517-1525.

Marrs, J. A., Andersson-Fisone, C., Jeong, M. C., Cohen-Gould, L., Zurzolo, C., Nabi, I. R., Rodriguez-Boulan, E. and Nelson, W. J. (1995). Plasticity in epithelial cell phenotype: modulation by expression of different cadherin cell adhesion molecules. J. Cell Biol. 129: 507-519.

Martin, G., Schlunck, G., Hansen, L. L. and Agostini, H. T. (2004). Differential expression of angioregulatory factors in normal and CNV-derived human retinal pigment epithelium. Graefes Arch. Clin. Exp. Ophthalmol. 242: 321-326.

Matsuura, T., Miller, W. H. and Tomita, T. (1978). Cone-specific c-wave in the turtle retina. Vis. Res. 18: 767-775.

McCann, J. D., Li, M. and Welsh, M. J. (1989). Identification and regulation of whole-cell chloride currents in airway epithelium. J. Gen. Physiol. 94: 1015-1036.

McKay, B. S. and Burke, J. M. (1994). Separation of phenotypically distinct subpopulations of cultured human retinal pigment epithelial cells. Exp. Cell Res. 213: 85-92.

McKechnie, N. M., Boulton, M., Robey, H. L., Savage, F. J. and Grierson, I. (1988). The cytoskeletal elements of human retinal pigment epithelium: *in vitro* and *in vivo*. J. Cell Sci. 91 (Pt 2): 303-312.

Mergaerts, F., Daems, E., Van Malderen, L. and Spileers, W. (2001). Recording of the fast oscillations in the human electro-oculogram. Doc. Ophthalmol. 103: 63-72.

Mergler, S., Steinhausen, K., Wiederholt, M. and Strauss, O. (1998). Altered regulation of L-type channels by protein kinase C and protein tyrosine kinases as a pathophysiologic effect in retinal degeneration. FASEB. J. 12: 1125-1134.

Miceli, M. V. and Jazwinski, S. M. (2005). Nuclear gene expression changes due to mitochondrial dysfunction in ARPE-19 cells: implications for age-related macular degeneration. Invest. Ophthalmol. Vis. Sci. 46: 1765-1773.

Michaelis, M. L., Michaelis, E. K., Nunley, E. W. and Galton, N. (1987). Effects of chronic alcohol administration on synaptic membrane Na^+ - Ca^{2+} exchange activity. Brain Res. 414: 239-244.

Miledi, R. (1982). A calcium-dependent transient outward current in *Xenopus laevis* oocytes. Proc. Natl. Acad. Sci. U.S.A. 215: 491-497.

Miles, M. F., Barhite, S., Sganga, M. and Elliott, M. (1993). Phosducin-like protein: an ethanol-responsive potential modulator of guanine nucleotide-binding protein function. Proc. Natl. Acad. Sci. U.S.A. 90: 10831-10835.

Miller, R. F. and Dowling, J. E. (1970). Intracellular responses of the Müller (glial) cells of mudpuppy retina: their relation to b-wave of the electroretinogram. J. Neurophysiol. 33: 323-341.

Miller, S. S. and Farber, D. (1984). Cyclic AMP modulation of ion transport across frog retinal pigment epithelium. measurements in the short-circuit state. J. Gen. Physiol. 83: 853-874.

Miller, S. S. and Edelman, J. L. (1990). Active ion transport pathways in the bovine retinal pigment epithelium. J. Physiol. (Lond). 424: 283-300.

Miller, S. S., Rabin, J., Strong, T., Iannuzzi, M. C., Adams, A. J., Collins, F. S., Reenstra, W. and Mc Cray Jr, P. (1992). Cystic fibrosis (CF) gene product is expressed in retina and retinal pigment epithelium. Invest. Ophthalmol. Vis. Sci. 33: #1597 ARVO Abstract.

Miller, S. S. and Steinberg, R. H. (1977). Active transport of ions across frog retinal pigment epithelium. Exp. Eye Res. 25: 235-248.

Miller, S. S. and Steinberg, R. H. (1979). Potassium modulation of taurine transport across the frog retinal pigment epithelium. J. Gen. Physiol. 74: 237-259.

Miller, S. S., Steinberg, R. H. and Oakley II, B. (1978). The electrogenic sodium pump of the frog retinal pigment epithelium. J. Membr. Biol. 44: 259-279.

Miller, W. H. and Laughlin, S. B. (1983). Light-mediated cyclic GMP hydrolysis controls important aspects of kinetics of retinal rod voltage response. Biophys. Struct. Mech. 9: 269-276.

Minta, A., Kao, J. and Tsien, R. (1989). Fluorescent indicators for cytosolic calcium based on rhodamine and fluorescein chromophores. J. Biol. Chem. 264: 8171-8178.

Mitchell, C. H. (2001). Release of ATP by a human retinal pigment epithelial cell line: potential for autocrine stimulation through subretinal space. J. Physiol. (Lond). 534: 193-202.

Mitchell, R. H. (1982a). Inositol lipid metabolism in dividing and differentiating cells. Cell Calcium. 3: 429-440.

Mitchell, R. H. (1982b). Stimulated inositol lipid metabolism: an introduction. Cell Calcium. 3: 285-294.

Mitsuda, S., Yoshii, C., Ikegami, Y. and Araki, M. (2005). Tissue interaction between the retinal pigment epithelium and the choroid triggers retinal regeneration of the newt *Cynops pyrrhogaster*. Dev. Biol. 280: 122-132.

Miyaguchi, K. (2000). Ultrastructure of the zonula adherens revealed by rapid-freeze deep-etching. J. Struct. Biol. 132: 169-178.

Mochly-Rosen, D., Chang, F. H., Cheever, L., Kim, M., Diamond, I. and Gordon, A. S. (1988). Chronic ethanol causes heterologous desensitization of receptors by reducing alpha s messenger RNA. Nature. 333: 848-850.

Mondini, C. (1790). Commentationes Bononienses. Cited by Wolfensberger, T. J. (1998). The Historical Discovery of the Retinal Pigment Epithelium. The retinal pigment epithelium: function and disease. M. F. Marmor and T. J. Wolfensberger. New York, OUP: 13-22.

Mukherjee, S., Tessema, M. and Wandinger-Ness, A. (2006). Vesicular trafficking of tyrosine kinase receptors and associated proteins in the regulation of signaling and vascular function. Circ. Res. 98: 743-756.

Mullikin-Kilpatrick, D. and Treistman, S. N. (1994). Ethanol inhibition of L-type Ca^{2+} channels in PC12 cells: role of permeant ions. Eur. J. Pharmacol. 270: 17-25.

Mund, M. L., Rodrigues, M. M. and Fine, B. S. (1972). Light and electron microscopic observations on the pigmented layers of the developing human eye. Amer. J. Ophthalmol. 73: 167-182.

Nagel, G., Barbry, P., Chabot, H., Brochiero, E., Hartung, K. and Grygorczyk, R. (2005). CFTR fails to inhibit the epithelial sodium channel ENaC expressed in *Xenopus laevis* oocytes. J. Physiol. (Lond). 564: 671-682.

Nagy, L. E. and DeSilva, S. E. (1992). Ethanol increases receptor-dependent cyclic AMP production in cultured hepatocytes by decreasing G_i-mediated inhibition. Biochem. J. 286 (Pt. 3): 681-686.

Nash, M. S. and Osborne, N. N. (1996). Cell surface receptors associated with the retinal pigment epithelium: the adnylate cyclase and phospholipase C signal transduction pathways. Prog. Retin. Eye Res. 15: 501-546.

Nehrke, K., Arreola, J., Nguyen, H-V., Pilato, J., Richardson, L., Okunade, G., Baggs, R., Shull, G. E. and Melvin, J. E. (2002). Loss of hyperpolarization-activated Cl^- current in salivary acinar cells from *Clcn2* knockout mice. J. Biol. Chem. 277: 23604-23611.

Nernst, W. (1888). Zur Kinetik der in Lösung befindlichen Körper: Theorie der Diffusion. Z. Phys. Chem: 613-637. Cited by Hille B, in *Ion channels of excitable membranes (Third Edition)*. 2001, Sinauer Associates, Inc: Sunderland (MA).

Newman, E. A. (1979). *B*-wave currents in the frog retina. Vis. Res. 19: 227-234.

Newman, E. A. (1989). Potassium conductance block by barium in amphibian Müller cells. Brain Res. 498: 308-314.

Nicolini, J., Kiilgaard, J. F., Wiencke, A. K., Heegaard, S., Scherfig, E., Prause, J. U. and la Cour, M. (2000). The anterior lens capsule used as support material in RPE cell-transplantation. Acta. Ophthalmol. Scand. 78: 527-531.

Nilius, B. and Droogmans, G. (2003). Amazing chloride channels: an overview. Acta. Physiol. Scand. 177: 119-147.

Noell, W. K. (1942). Studies on the electrophysiology and metabolism of the retina. project #21-1201-0004. Randolf field Texas, U.S.A.F school of aviation medicine.

Noell, W. K. (1953). Experimentally induced toxic effects on structure and function of visual cells and pigment epithelium. Amer. J. Ophthalmol. 36: 103-116.

Nowycky, M. C., Fox, A. P. and Tsien, R. W. (1985). Three types of neuronal calcium channel with different calcium agonist sensitivity. Nature. 316: 440-443.

Oakley II, B. (1977). Potassium and the photoreceptor-dependent pigment epithelial hyperpolarization. J. Gen. Physiol. 70: 405-425.

Oakley II, B. (1983). Effects of maintained illumination upon $[K^+]_O$ in the subretinal space of the isolated retina of the toad. Vis. Res. 23: 1325-1337.

Oakley II, B., Flaming, D. G. and Brown, K. T. (1979). Effects of the rod receptor potential upon retinal extracellular potassium concentration. J. Gen. Physiol. 74: 713-737.

Oakley II, B. and Green, D. G. (1976). Correlation of the light-induced changes in retinal extracellular potassium concentration with c-wave of the electroretinogram. J. Neurophysiol. 39: 1117-1133.

Oakley II, B., Miller, S. S. and Steinberg, R. H. (1978). Effect of intracellular potassium upon the electrogenic pump of frog retinal pigment epithelium. J. Membr. Biol. 44: 281-307.

Oakley II, B. and Steinberg, R. H. (1982). Effects of maintained illumination upon $[K^+]_O$ in the subretinal space of the frog retina. Vis. Res. 22: 767-773.

Ocrant, I., Valentino, K. L., King, M. G., Wimpy, T. H., Rosenfeld, R. G. and Baskin, D. G. (1989). Localization and structural characterization of insulin-like growth factor receptors in mammalian retina. Endocrinology. 125: 2407-2413.

Ohno-Matsui, K., Ichinose, S., Nakahama, K., Yoshida, T., Kojima, A., Mochizuki, M. and Morita, I. (2005). The effects of amniotic membrane on retinal pigment epithelial cell differentiation. Mol. Vis. 11: 1-10.

Oka, M. S., Landers, R. A. and Bridges, C. D. (1984). A serum-free defined medium for retinal pigment epithelial cells. Exp. Cell Res. 154: 537-547.

Orkand, R. K. and Niedergerke, R. (1964). Heart action-potential dependence on external calcium and sodium ions. Science. 146: 1176-1177.

Owaribe, K., Kartenbeck, J., Rungger-Brandle, E. and Franke, W. W. (1988). Cytoskeletons of retinal pigment epithelial cells: interspecies differences of expression patterns indicate independence of cell function from the specific complement of cytoskeletal proteins. Cell Tissue Res. 254: 301-315.

Owaribe, K., Kodama, R. and Eguchi, G. (1981). Demonstration of contractility of circumferential actin bundles and its morphogenetic significance in pigmented epithelium *in vitro* and in vivo. J. Cell Biol. 90: 507-514.

Owaribe, K., Sugino, H. and Masuda, H. (1986). Characterization of intermediate filaments and their structural organization during epithelium formation in pigmented epithelial cells of the retina *in vitro*. Cell Tissue Res. 244: 87-93.

Oz, M., Tchugunova, Y. B. and Dunn, S. M. J. (2001). Direct inhibition of voltage-dependent Ca^{2+} fluxes by ethanol and higher alcohols in rabbit T-tubule membranes. Eur. J. Pharmacol. 418: 169-176.

Pandey, S. C. (1996). Acute and chronic ethanol consumption effects on the Immunolabeling of $G_{q/11}\alpha$ subunit protein and phospholipase C isozymes in the rat brain. J. Neurochem. 67: 2355-2361.

Pastan, I., Gottesman, M., Ueda, K., Lovelace, E., Rutherford, A. and Willingham, M. (1988). A retrovirus carrying an MDR1 cDNA confers multidrug resistance and polarized expression of P-glycoprotein in MDCK cells. Proc. Natl. Acad. Sci. U.S.A. 85: 4486-4490.

Pautler, E. L. (1994). Photosensitivity of the isolated pigment epithelium and arachidonic acid metabolism: preliminary results. Curr. Eye Res. 13: 687-695.

Pearson, R. A., Catsicas, M., Becker, D. L., Bayley, P., Luneborg, N. L. and Mobbs, P. (2004). Ca^{2+} signalling and gap junction coupling within and between pigment epithelium and neural retina in the developing chick. Eur. J. Neurosci. 19: 2435-2445.

Pearson, R. A., Dale, N., Llaudet, E. and Mobbs, P. (2005). ATP released via Gap junction hemichannels from the pigment epithelium regulates neural retinal progenitor proliferation. Neuron. 46: 731-744.

Penfold, P. L., Wen, L., Madigan, M. C., Gillies, M. C., King, N. J. C. and Provis, J. M. (2000). Triamcinolone acetonide modulates permeability and intercellular adhesion molecule-1 (ICAM-1) expression of the ECV304 cell line: implications for macular degeneration. Clin. Exp. Immunol. 121: 458-465.

Peng, S., Rahner, C. and Rizzolo, L. J. (2003). Apical and basal regulation of the permeability of the retinal pigment epithelium. Invest. Ophthalmol. Vis. Sci. 44: 808-817.

Penn, R. D. and Hagins, W. A. (1969). Signal transmission along retinal rods and the origin of the electroretinographic a-wave. Nature. 223: 201-205.

Peterson, W. M., Meggyesy, C., Yu, K. and Miller, S. S. (1997). Extracellular ATP activates calcium signaling, ion, and fluid transport in retinal pigment epithelium. J. Neurosci. 17: 2324-2337.

Peterson, W. M. and Miller, S. S. (1995). Identification and functional characterization of a dual GABA/taurine transporter in the bullfrog retinal pigment epithelium. J. Gen. Physiol. 106: 1089-1122.

Peterson, W. M., Quong, J. N. and Miller, S. S. (1998). Mechanism of fluid transport in retinal pigment epithelium. The Third Great Basin Visual Science Symposium on Retinal Research., Utah.

Petrukhin, K., Koisti, M. J., Bakall, B., Li, W., Xie, G., Marknell, T., Sandgren, O., Forsman, K., Holmgren, G., Andreasson, S., Vujic, M., Bergen, A. A., McGarty-Dugan, V., Figueroa, D., Austin, C. P., Metzker, M. L., Caskey, C. T. and Wadelius, C. (1998). Identification of the gene responsible for Best macular dystrophy. Nat. Genet. 19: 241-247.

Philp, N. J. and Nachmias, V. T. (1985). Components of the cytoskeleton in the retinal pigmented epithelium of the chick. J. Cell Biol. 101: 358-362.

Philp, N. J. and Nachmias, V. T. (1987). Polarized distribution of integrin and fibronectin in retinal pigment epithelium. Invest. Ophthalmol. Vis. Sci. 28: 1275-1280.

Philp, N. J., Yoon, M. Y. and Hock, R. S. (1990). Identification and localization of talin in chick retinal pigment epithelial cells. Exp. Eye Res. 51: 191-198.

Pinckers, A., Cuypers, M. H. and Aandekerk, A. L. (1996). The EOG in Best's disease and dominant cystoid macular dystrophy (DCMD). Ophthalmic. Genet. 17: 103-108.

Pitkanen, L., Ruponen, M., Nieminen, J. and Urtti, A. (2003). Vitreous is a barrier in nonviral gene transfer by cationic lipids and polymers. Pharm. Res. 20: 576-583.

Pollack, K., Kreuz, F. and Pillunat, L. (2005). Morbus Best mit normalem EOG. Der Ophthalmologe. 102: 891-894.

Ponjavic, V., Eksandh, L., Andreasson, S., Sjostrom, K., Bakall, B., Ingvast, S., Wadelius, C. and Ehinger, B. (1999). Clinical expression of Best's vitelliform macular dystrophy in Swedish families with mutations in the bestrophin gene. Ophthalmic. Genet. 20: 251-257.

Prat, A. G., Reisin, I. L., Ausiello, D. A. and Cantiello, H. F. (1996). Cellular ATP release by the cystic fibrosis transmembrane conductance regulator. Amer. J. Physiol. 270: C538-545.

Puchelle, E., Gaillard, D., Ploton, D., Hinnrasky, J., Fuchey, C., Boutterin, M. C., Jacquot, J., Dreyer, D., Pavirani, A. and Dalemans, W. (1992). Differential localization of the cystic fibrosis transmembrane conductance regulator in normal and cystic fibrosis airway epithelium. Amer. J. Respir. Cell Mol. Biol. 5: 485-491.

Punglia, R. S., Lu, M., Hsu, J., Kuroki, M., Tolentino, M. J., Keough, K., Levy, A. P., Levy, N. S., Goldberg, M. A., D'Amato, R. J. and Adamis, A. P. (1997). Regulation of vascular endothelial growth factor expression by insulin-like growth factor I. Diabetes. 46: 1619-1626.

Qu, Z., Fischmeister, R. and Hartzell, C. (2004). Mouse bestrophin-2 Is a bona fide Cl^- channel: identification of a residue important in anion binding and conduction. J. Gen. Physiol. 123: 327-340.

Qu, Z. and Hartzell, C. (2004). Determinants of anion permeation in the second transmembrane domain of the mouse bestrophin-2 chloride channel. J. Gen. Physiol. 124: 371-382.

Qu, Z., Wei, R. W., Mann, W. and Hartzell, H. C. (2003). Two bestrophins cloned from *Xenopus laevis* oocytes express Ca^{2+}-activated Cl currents. J. Biol. Chem. 278: 49563-49572.

Quinn, R. H. and Miller, S. S. (1992). Ion transport mechanisms in native human retinal pigment epithelium. Invest. Ophthalmol. Vis. Sci. 33: 3513-3527.

Quinn, R. H., Quong, J. N. and Miller, S. S. (2001). Adrenergic receptor activated ion transport in human fetal retinal pigment epithelium. Invest. Ophthalmol. Vis. Sci. 42: 255-264.

Rabe, C. S. and Weight, F. F. (1987). Effects of ethanol on neurotransmitter release and intracellular free calcium in PC12 cells. J. Pharmacol. Exp. Ther. 244: 417-422.

Rahner, C., Fukuhara, M., Peng, S., Kojima, S. and Rizzolo, L. J. (2004). The apical and basal environments of the retinal pigment epithelium regulate the maturation of tight junctions during development. J. Cell Sci. 117: 3307-3318.

Rajasekaran, S. A., Hu, J., Gopal, J., Gallemore, R., Ryazantsev, S., Bok, D. and Rajasekaran, A. K. (2003). Na,K-ATPase inhibition alters tight junction structure and permeability in human retinal pigment epithelial cells. Amer. J. Physiol. 284: C1497-1507.

Ramsohoye, P. V. and Fritz, I. B. (1998). Preliminary characterization of glial-secreted factors responsible for the induction of high electrical resistances across endothelial monolayers in a blood-brain barrier model. Neurochem. Res. 23: 1545-1551.

Rane, S. G., Holz $4^{th.}$ G. G. and Dunlap, K. (1987). Dihydropyridine inhibition of neuronal calcium current and substance P release. Pflügers Arch. 409: 361-366.

Raub, T. J. (1996). Signal transduction and glial cell modulation of cultured brain microvessel endothelial cell tight junctions. Amer. J. Physiol. 271: C495-503.

Rauz, S., Walker, E. A., Hughes, S. V., Coca-Prados, M., Hewison, M., Murray, P. I. and Stewart, P. M. (2003). Serum- and glucocorticoid-regulated kinase isoform-1 and epithelial sodium channel subunits in human ocular ciliary epithelium. Invest. Ophthalmol. Vis. Sci. 44: 1643-1651.

Reddan, J. R. and Wilson-Dziedzic, D. (1983). Insulin growth factor and epidermal growth factor trigger mitosis in lenses cultured in a serum-free medium. Invest. Ophthalmol. Vis. Sci. 24: 409-416.

Reddy, M. M. and Quinton, P. M. (2005). ENaC activity requires CFTR channel function independently of phosphorylation in sweat duct. J. Membr. Biol. 207: 23-33.

Reddy, M. M., Quinton, P. M., Haws, C., Wine, J. J., Grygorczyk, R., Tabcharani, J. A., Hanrahan, J. W., Gunderson, K. L. and Kopito, R. R. (1996). Failure of the cystic fibrosis transmembrane conductance regulator to conduct ATP. Science. 271: 1876-1879.

Redzic, Z. B., Isakovic, A. J., Misirlic Dencic, S. T., Popadic, D. and Segal, M. B. (2006). Uneven distribution of nucleoside transporters and intracellular enzymatic degradation prevent transport of intact [^{14}C] adenosine across the sheep choroid plexus epithelium as a monolayer in primary culture. Cerebrospinal Fluid Res. 3: 4.

Reigada, D., Lu, W., Zhang, X., Friedman, C., Pendrak, K., McGlinn, A., Stone, R. A., Laties, A. M. and Mitchell, C. H. (2005). Degradation of extracellular ATP by the retinal pigment epithelium. Amer. J. Physiol. 289: C617-624.

Reigada, D. and Mitchell, C. H. (2005). Release of ATP from retinal pigment epithelial cells involves both CFTR and vesicular transport. Amer. J. Physiol. 288: C132-140.

Reisin, I., Prat, A., Abraham, E., Amara, J., Gregory, R., Ausiello, D. and Cantiello, H. (1994). The cystic fibrosis transmembrane conductance regulator is a dual ATP and chloride channel. J. Biol. Chem. 269: 20584-20591.

Renard-Rooney, D. C., Seitz, M. B. and Thomas, A. P. (1997). Inhibition of hepatic inositol 1,4,5-trisphosphate receptor function by ethanol and other short chain alcohols. Cell Calcium. 21: 387-398.

Renner, A. B., Tillack, H., Kraus, H., Kramer, F., Mohr, N., Weber, B. H. F., Foerster, M. H. and Kellner, U. (2005). Late onset is common in Best macular dystrophy associated with *VMD2* gene mutations. Ophthalmology. 112: 586-592.

Reuter, H. and Seitz, N. (1968). The dependence of calcium efflux from cardiac muscle on temperature and external ion composition. J. Physiol. (Lond). 195: 45-70.

Ribeiro, C. P., Paradiso, A. M. and Boucher, R. C. (2001). Upregulation of the apical endoplasmic reticulem network in CF human airway epithelia. Pediatr. Pulmonol: S22:235.

Rich, D. P., Anderson, M. P., Gregory, R. J., Seng, C. H., Paul, S., Jefferson, D. M., McCann, J. D., Klinger, K. W., Smith, A. E. and Welsh, M. J. (1990). Expression of cystic fibrosis transmembrane conductance regulator corrects defective chloride channel regulation in cystic fibrosis airway epithelial cells. Nature. 347: 358-363.

Riordan, J. R. (2005). Assembly of functional CFTR chloride channels. Ann. Rev. Physiol. 67: 701-718.

Riordan, J. R., Rommens, J. M., Kerem, B-S., Alon, N., Rozmahel, R., Grzelczak, Z., Zielenski, J., Lok, S., Plavsic, N., Chou, J-L., Drumm, M. L., Iannuzzi, M. C., Collins, F. S. and Tsui, L-C. (1989). Identification of the cystic fibrosis gene: cloning and characterization of complementary DNA. Science. 245: 1066-1073.

Rizzolo, L. J. (1990). The distribution of Na+,K(+)-ATPase in the retinal pigmented epithelium from chicken embryo is polarized in vivo but not in primary cell culture. Exp. Eye Res. 51: 435-446.

Rizzolo, L. J. (2006). Tissue interactions that regulate tight junctions of the RPE. ISCOB 1st, Cambridge.

Rizzolo, L. J. and Li, Z. (1993). Diffusible, retinal factors stimulate the barrier properties of junctional complexes in the retinal pigment epithelium. J. Cell Sci. 106: 859-867.

Rizzolo, L. J. and Joshi, H. C. (1993). Apical orientation of the microtubule organizing center and associated γ-tubulin during the polarization of the retinal pigment epithelium *in vivo*. Dev. Biol. 157: 147-156.

Rizzolo, L. J., Zhou, S. and Li, Z. Q. (1994). The neural retina maintains integrins in the apical membrane of the RPE early in development. Invest. Ophthalmol. Vis. Sci. 35: 2567-2576.

Robey, H. L., Hiscott, P. S. and Grierson, I. (1992). Cytokeratins and retinal epithelial cell behaviour. J. Cell Sci. 102: 329-340.

Rodbell, M., Birnbaumer, L., Pohl, S. L. and Krans, H. M. (1971). The glucagon-sensetive adenyl cyclase system in plasma membranes of rat liver. V. An obligatory role of guanylnucleotides in glucagon action. J. Biol. Chem. 246: 1877-1882.

Rommens, J. M., Iannuzzi, M. C., Kerem, B., Drumm, M. L., Melmer, G., Dean, M., Rozmahel, R., Cole, J. L., Kennedy, D., Hidaka, N., Zsiga, M., Buchwald, M., Riordan, J. R., Tsui, L-C. and Collins, F. S. (1989). Identification of the cystic fibrosis gene: chromosome walking and jumping. Science. 245: 1059-1065.

Rosenthal, R., Bakall, B., Kinnick, T., Peachey, N., Wimmers, S., Wadelius, C., Marmorstein, A. and Strauss, O. (2006). Expression of bestrophin-1, the product of the *VMD2* gene, modulates voltage-dependent Ca^{2+} channels in retinal pigment epithelial cells. FASEB. J. 20: 178-180.

Rosenthal, R., Malek, G., Salomon, N., Peill-Meininghaus, M., Coeppicus, L., Wohlleben, H., Wimmers, S., Bowes Rickman, C. and Strauss, O. (2005). The fibroblast growth factor receptors, FGFR-1 and FGFR-2, mediate two independent signalling pathways in human retinal pigment epithelial cells. Biochem. Biophys. Res. Commun. 337: 241-247.

Rosenthal, R. and Strauss, O. (2002). Ca^{2+}-channels in the RPE. Adv. Exp. Med. Biol. 514: 225-235.

Rowntree, R. K. and Harris, A. (2003). The phenotypic consequences of *CFTR* Mutations. Ann. Human Genet. 67: 471-485.

Rudolf, G. and Wioland, N. (1990). Effects of intravitreal and intravenous administrations of dopamine on the standing potential and the light peak in the intact chicken eye. Curr. Eye Res. 9: 1077-1082.

Rymer, J., Miller, S. S. and Edelman, J. L. (2001). Epinephrine-induced increases in $[Ca^{2+}]_{(in)}$ and KCl-coupled fluid absorption in bovine RPE. Invest. Ophthalmol. Vis. Sci. 42: 1921-1929.

Saga, T., Scheurer, D. and Adler, R. (1996). Development and maintenance of outer segments by isolated chick embryo photoreceptor cells in culture. Invest. Ophthalmol. Vis. Sci. 37: 561-573.

Saito, T., Lee, J. M. and Tabakoff, B. (1985). Ethanol's effects on cortical adenylate cyclase activity. J. Neurochem. 44: 1037-1044.

Salceda, R. and Sànchez-Chàvez, G. (2000). Calcium uptake, release and ryanodine binding in melanosomes from retinal pigment epithelium. Cell Calcium. 27: 223-229.

Sauve, Y., Pinilla, I. and Lund, R. D. (2006). Partial preservation of rod and cone ERG function following subretinal injection of ARPE-19 cells in RCS rats. Vis. Res. 46: 1459-1472.

Schafer, D. A., Mooseker, M. S. and Cooper, J. A. (1992). Localization of capping protein in chicken epithelial cells by immunofluorescence and biochemical fractionation. J. Cell Biol. 118: 335-346.

Schlessinger, J. and Ullrich, A. (1992). Growth factor signaling by receptor tyrosine kinases. Neuron. 9: 383-391.

Schneck, M. E., Fortune, B. and Adams, A. J. (2000). The fast oscillation of the electrooculogram reveals sensitivity of the human outer retina/retinal pigment epithelium to glucose level. Vis. Res. 40: 3447-3453.

Schneeberger, E. E. and Lynch, R. D. (1992). Structure, function, and regulation of cellular tight junctions. Amer. J. Physiol. 262: L647-661.

Schreiber, R., Hopf, A., Mall, M., Greger, R. and Kunzelmann, K. (1999). The first-nucleotide binding domain of the cystic-fibrosis transmembrane conductance regulator is important for inhibition of the epithelial Na^+ channel. Proc. Natl. Acad. Aci. U.S.A. 96: 5310-5315.

Schwegler, J. S., Knorz, M. C., Akkoyun, I. and Liesenhoff, H. (1997). Basic, not acidic fibroblast growth factor stimulates proliferation of cultured human retinal pigment epithelial cells. Mol. Vis. 3: 10.

Schwiebert, E. M., Benos, D. J., Egan, M. E., Stutts, M. J. and Guggino, W. B. (1999). CFTR Is a conductance regulator as well as a chloride channel. Physiol. Rev. 79: 145-166.

Schwiebert, E. M., Cid-Soto, L. P., Stafford, D., Carter, M., Blaisdell, C. J., Zeitlin, P. L., Guggino, W. B. and Cutting, G. R. (1998). Analysis of ClC-2 channels as an alternative pathway for chloride conduction in cystic fibrosis airway cells. Proc. Natl. Acad. Sci. U.S.A. 95: 3879-3884.

Schwiebert, E. M., Egan, M. E., Hwang, T. H., Fulmer, S. B., Allen, S. S., Cutting, G. R. and Guggino, W. B. (1995). CFTR regulates outwardly rectifying chloride channels through an autocrine mechanism involving ATP. Cell. 81: 1063-1073.

Seagle, B-L. L., Rezai, K. A., Kobori, Y., Gasyna, E. M., Rezaei, K. A. and Norris, J. R., Jr. (2005). Melanin photoprotection in the human retinal pigment epithelium and its correlation with light-induced cell apoptosis. Proc. Natl. Acad. Sci. U.S.A. 102: 8978-8983.

Seddon, J. M., Afshari, M. A., Sharma, S., Bernstein, P. S., Chong, S., Hutchinson, A., Petrukhin, K. and Allikmets, R. (2001). Assessment of mutations in the Best macular dystrophy (VMD2) gene in patients with adult-onset foveomacular vitelliform dystrophy, age-related maculopathy, and bull's-eye maculopathy. Ophthalmology. 108: 2060-2067.

Segawa, Y. (1987). Electrical response of the retinal pigment epithelium to sodium bicarbonate (II). Clinical use for electrophysiological evaluation of the retinal pigment epithelium activity. J. Juzen Med. Soc. 96: 1022-1041.

Segawa, Y. and Hughes, B. A. (1994). Properties of the inwardly rectifying K+ conductance in the toad retinal pigment epithelium. J. Physiol. (Lond). 476: 41-53.

Seidler, N. W., Jona, I., Vegh, M. and Martonosi, A. (1989). Cyclopiazonic acid is a specific inhibitor of the Ca^{2+}-ATPase of sarcoplasmic reticulum. J. Biol. Chem. 264: 17816-17823.

Sermet-Gaudelus, I., Dechaux, M., Vallee, B., Fajac, A., Girodon, E., Nguyen-Khoa, T., Marianovski, R., Hurbain, I., Bresson, J. L., Lenoir, G. and Edelman, A. (2005). Chloride transport in nasal ciliated cells of cystic fibrosis heterozygotes. Amer. J. Respir. 171: 1026-1031.

Sermet-Gaudelus, I., Vallée, B., Urbin, I., Torossi, T., Marianovski, R., Fajac, A., Feuillet, M-N., Bresson, J-L., Lenoir, G., Bernaudin, J. F. and Edelman, A. (2002). Normal function of the cystic fibrosis conductance regulator protein can be associated with homozygous ΔF508 mutation. Pediatr. Res. 52: 628-635.

Shimazaki, H. and Oakley II, B. (1984). Reaccumulation of $[K^+]_o$ in the toad retina during maintained illumination. J. Gen. Physiol. 84: 475-504.

Shimoda, Y., Hurley, J. B. and Miller, W. H. (1984). Rod light response augmented by active phosphodiesterase. Proc. Natl. Acad. Sci. U.S.A. 81: 616-619.

Shimura, M., Yuan, Y., Chang, J. T., Zhang, S., Campochiaro, P. A., Zack, D. J. and Hughes, B. A. (2001). Expression and permeation properties of the K^+ channel $Kir_{7.1}$ in the retinal pigment epithelium. J. Physiol. (Lond). 531: 329-346.

Sigal, E. (1991). The molecular biology of mammalian arachidonic acid metabolism. Amer. J. Physiol. 260: L13-28.

Simasko, S. M., Boyadjieva, N., De, A. and Sarkar, D. K. (1999). Effect of ethanol on calcium regulation in rat fetal hypothalamic cells in culture. Brain Res. 824: 89-96.

Simonsson, P., Rodriguez, F. D., Loman, N. and Alling, C. (1991). G proteins coupled to phospholipase C: molecular targets of long-term ethanol exposure. J. Neurochem. 56: 2018-2026.

Skoog, O-K. (1974). The c-wave of the human d.c. registered erg. III. effects of ethyl alcohol on the c-wave. Acta. Ophthalmol. (Copenh). 52: 913-923.

Skoog, O-K., Textorius, O. and Nilsson, S. E. G. (1975). Effects of ethyl alcohol on the directly recorded standing potential of the human eye. Acta. Ophthalmol. (Copenh). 53: 710-720.

Smith-Thomas, L. C., Richardson, P. S., Rennie, I. G., Palmer, I., Boulton, M., Sheridan, C. and MacNeil, S. (2000). Influence of pigment content, intracellular calcium and cyclic AMP on the ability of human retinal pigment epithelial cells to contract collagen gels. Curr. Eye Res. 21: 518-529.

Smrcka, A. V., Hepler, J. R., Brown, K. O. and Sternweis, P. C. (1991). Regulation of polyphosphoinositide-specific phospholipase C activity by purified Gq. Science. 251: 804-807.

Song, M. K. and Lui, G. M. (1990). Propagation of fetal human RPE cells: preservation of original culture morphology after serial passage. J. Cell Physiol. 143: 196-203.

Spat, A., Bradford, P. G., McKinney, J. S., Rubin, R. P. and Putney Jr, J. W. (1986). A saturable receptor for ^{32}P-inositol-1,4,5-triphosphate in hepatocytes and neutrophils. Nature. 319: 514-516.

Stanzel, B. V., Espana, E. M., Grueterich, M., Kawakita, T., Parel, J-M., Tseng, S. C. G. and Binder, S. (2005). Amniotic membrane maintains the phenotype of rabbit retinal pigment epithelial cells in culture. Exp. Eye Res. 80: 103-112.

Starita, C., Hussain, A. A., Patmore, A. and Marshall, J. (1997). Localization of the site of major resistance to fluid transport in Bruch's membrane. Invest. Ophthalmol. Vis. Sci. 38: 762-767.

Steinberg, R., Schmidt, R. and Brown, K. (1970). Intracellular responses to light from cat pigment epithelium: origin of the electroretinogram c-wave. Nature. 227: 728-730.

Steinberg, R. H., Linsenmeier, R. A. and Griff, E. R. (1983). Three light-evoked responses of the retinal pigment epithelium. Vis. Res. 23: 1315-1323.

Steinberg, R. H., Linsenmeier, R. A. and Griff, E. R. (1985). Retinal pigment epithelial cell contributions to the electroretinogram and electrooculogram. Prog. Retin. Eye Res. 4: 33-66.

Steinberg, R. H., Oakley II, B. and Niemeyer, G. (1980). Light-evoked changes in $[K^+]_O$ in retina of intact cat eye. J. Neurophysiol. 44: 897-921.

Sternfeld, M. D., Robertson, J. E., Shipley, G. D., Tsai, J. and Rosenbaum, J. T. (1989). Cultured human retinal pigment epithelial cells express basic fibroblast growth factor and its receptor. Curr. Eye Res. 8: 1029-1037.

Steuer, H., Jaworski, A., Elger, B., Kaussmann, M., Keldenich, J., Schneider, H., Stoll, D. and Schlosshauer, B. (2005). Functional characterization and comparison of the outer blood-retina barrier and the blood-brain barrier. Invest. Ophthalmol. Vis. Sci. 46: 1047-1053.

Steuer, H., Jaworski, A., Stoll, D. and Schlosshauer, B. (2004). *In vitro* model of the outer blood-retina barrier. Brain Res. Prot. 13: 26-36.

Stevenson, B. R., Siliciano, J. D., Mooseker, M. S. and Goodenough, D. A. (1986). Identification of ZO-1: a high molecular weight polypeptide associated with the tight junction (zonula occludens) in a variety of epithelia. J. Cell Biol. 103: 755-766.

Stirling, C. E. and Lee, A. (1980). [^{3}H]ouabain autoradiography of frog retina. J. Cell Biol. 85: 313-324.

Stobrawa, S. M., Breiderhoff, T., Takamori, S., Engel, D., Schweizer, M., Zdebik, A. A., Bösl, M. R., Ruether, K., Jahn, H. and Draguhn, A. (2001). Disruption of ClC-3, a chloride channel expressed on synaptic vesicles, leads to a loss of the hippocampus. Neuron. 29: 185-196.

Strange, K., Emma, F. and Jackson, P. S. (1996). Cellular and molecular physiology of volume-sensitive anion channels. Amer. J. Physiol. 270: C711-730.

Strauss, O. (2005). The retinal pigment epithelium in visual function. Physiol. Rev. 85: 845-881.

Strauss, O., Buss, F., Rosenthal, R., Fischer, D., Mergler, S., Stumpff, F. and Thieme, H. (2000). Activation of neuroendocrine L-type channels (α1D subunits) in retinal pigment epithelial cells and brain neurons by $pp60^{c\text{-}src}$. Biochem. Biophys. Res. Commun. 270: 806-810.

Strauss, O., Mergler, S. and Wiederholt, M. (1997). Regulation of L-type calcium channels by protein tyrosine kinase and protein kinase C in cultured rat and human retinal pigment epithelial cells. FASEB. J. 11: 859-867.

Strauss, O. and Rosenthal, R. (2005). Funktion des Destrophins. Der Ophthalmologe. 102: 122-126.

Strauss, O., Steinhausen, M., Mergler, S., Stumpff, F. and Wiederholt, M. (1999). Involvement of protein tyrosine kinase in the InsP3-induced activation of Ca^{2+}-dependent Cl^- currents in cultured cells of the rat retinal pigment epithelium. J. Membr. Biol. 169: 141-153.

Strauss, O. and Wienrich, M. (1993). Cultured retinal pigment epithelial cells from RCS rats express an increased calcium conductance compared with cells from non-dystrophic rats. Pflügers Arch 425: 68-76.

Strauss, O. and Wienrich, M. (1994). Ca^{2+}-conductances in cultured rat retinal pigment epithelial cells. J. Cell Physiol. 160: 89-96.

Strunnikova, N., Zhang, C., Teichberg, D., Cousins, S. W., Baffi, J., Becker, K. G. and Csaky, K. G. (2004). Survival of retinal pigment epithelium after exposure to prolonged oxidative injury: a detailed gene expression and cellular analysis. Invest. Ophthalmol. Vis. Sci. 45: 3767-3777.

Sullivan, D. M., Erb, L., Anglade, E., Weisman, G. A., Turner, J. T. and Csaky, K. G. (1997). Identification and characterization of P2Y2 nucleotide receptors in human retinal pigment epithelial cells. J. Neurosci. Res. 49: 43-52.

Sun, H., Tsunenari, T., Yau, K-W. and Nathans, J. (2002). The vitelliform macular dystrophy protein defines a new family of chloride channels. Proc. Natl. Acad. Sci. U.S.A. 99: 4008-4013.

Tada, M. and Inui, M. (1983). Regulation of calcium transport by the ATPase-phospholamban system. J. Mol. Cell Cardiol. 15: 565-575.

Tada, M. and Kadoma, M. (1989). Regulation of the Ca^{2+} pump ATPase by cAMP-dependent phosphorylation of phospholamban. Bioessays. 10: 157-163.

Takahashi, K., Sawasaki, Y., Hata, J., Mukai, K. and Goto, T. (1990). Spontaneous transformation and immortalization of human endothelial cells. In Vitro Cell Dev. Biol. 26: 265-274.

Tan, K. H., Dobbie, M. S., Felix, R. A., Barrand, M. A. and Hurst, R. D. (2001). A comparison of the induction of immortalized endothelial cell impermeability by astrocytes. Neuroreport. 12: 1329-1334.

Tang, S., Yatani, A., Bahinski, A., Mori, Y. and Schwartz, A. (1993). Molecular localization of regions in the L-type calcium channel critical for dihydropyridine action. Neuron. 11: 1013-1021.

Taylor, A. L., Kudlow, B. A., Marrs, K. L., Gruenert, D. C., Guggino, W. B. and Schwiebert, E. M. (1998). Bioluminescence detection of ATP release mechanisms in epithelia. Amer. J. Physiol. 275: C1391-C1406.

Tewari, K. P., Malinowska, D. H., Sherry, A. M. and Cuppoletti, J. (2000). PKA and arachidonic acid activation of human recombinant ClC-2 chloride channels. Amer. J. Physiol. 279: C40-50.

Textorius, O., Nilsson, S. E. and Andersson, B. E. (1989). Effects of intravitreal perfusion with dopamine in different concentrations on the DC electroretinogram and the standing potential of the albino rabbit eye. Doc. Ophthalmol. 73: 149-162.

Textorius, O., Welinder, E. and Nilsson, S. E. G. (1985). Combined effects of DL-α-aminoadipic acid with sodium iodate, ethyl alcohol, or light stimulation on the ERG *c*-wave and on the standing potential of the albino rabbit eyes. Doc. Ophthalmol. 60: 393-400.

Tezel, T. H. and Del Priore, L. V. (1998). Serum-free media for culturing and serial-passaging of adult human retinal pigment epithelium. Exp. Eye Res. 66: 807-815.

Tezel, T. H., Del Priore, L. V. and Kaplan, H. J. (2004). Reengineering of aged Bruch's membrane to enhance retinal pigment epithelium repopulation. Invest. Ophthalmol. Vis. Sci. 45: 3337-3348.

Theischen, M., Bornfeld, N., Becher, R., Kellner, U. and Wessing, A. (1993). Hexadecylphosphocholine may produce reversible functional defects of the retinal pigment epithelium. Ger. J. Ophthalmol. 2: 113-115.

Thiemann, A., Grunder, S., Pusch, M. and Jentsch, T. J. (1992). A chloride channel widely expressed in epithelial and non-epithelial cells. Nature. 356: 57-60.

Thorburn, W. and Nordstrom, S. (1978). EOG in a large family with hereditary macular degeneration. (Best's vitelliform macular dystrophy) identification of gene carriers. Doc. Ophthalmol. 56: 455-464.

Thumann, G., Schraermeyer, U., Bartz-Schmidt, K. U. and Heimann, K. (1997). Descemet's membrane as membranous support in RPE/IPE transplantation. Curr. Eye Res. 16: 1236-1238.

Tian, J., Ishibashi, K. and Handa, J. T. (2004). The expression of native and cultured RPE grown on different matrices. Physiol. Genomics. 17: 170-182.

Tiede, I., Fritz, G., Strand, S., Poppe, D., Dvorsky, R., Strand, D., Lehr, H. A., Wirtz, S., Becker, C., Atreya, R., Mudter, J., Hildner, K., Bartsch, B., Holtmann, M., Blumberg, R., Walczak, H., Iven, H., Galle, P. R., Ahmadian, M. R. and Neurath, M. F. (2003). CD28-dependent Rac1 activation is the molecular target of azathioprine in primary human CD4+ T lymphocytes. J. Clin. Invest. 111: 1133-1145.

Toimela, T., Maenpaa, H., Mannerstrom, M. and Tahti, H. (2004). Development of an *in vitro* blood-brain barrier model-cytotoxicity of mercury and aluminum. Toxicol. Appl. Pharmacol. 195: 73-82.

Toimela, T. A. and Tahti, H. (2001). Effects of mercuric chloride exposure on the glutamate uptake by cultured retinal pigment epithelial cells. Toxicol. In Vitro. 15: 7-12.

Tontsch, U. and Bauer, H-C. (1991). Glial cells and neurons induce blood-brain barrier related enzymes in cultured cerebral endothelial cells. Brain Res. 539: 247-253.

Treins, C., Giorgetti-Peraldi, S., Murdaca, J., Semenza, G. L. and Van Obberghen, E. (2002). Insulin stimulates hypoxia-inducible factor 1 through a phosphatidylinositol 3-kinase/target of rapamycin-dependent signaling pathway. J. Biol. Chem. 277: 27975-27981.

Treins, C., Giorgetti-Peraldi, S., Murdaca, J. and Van Obberghen, E. (2001). Regulation of vascular endothelial growth factor expression by advanced glycation end products. J. Biol. Chem. 276: 43836-43841.

Tretiach, M., Madigan, M. C. and Gillies, M. C. (2004). Conditioned medium from mixed retinal pigmented epithelium and Muller cell cultures reduces *in vitro* permeability of retinal vascular endothelial cells. Brit. J. Ophthalmol. 88: 957-961.

Tretiach, M., Madigan, M. C., Wen, L. and Gillies, M. C. (2005). Effect of Müller cell co-culture on *in vitro* permeability of bovine retinal vascular endothelium in normoxic and hypoxic conditions. Neurosci. Lett. 378: 160-165.

Tso, M. O., Albert, D. and Zimmerman, L. E. (1973). Organ culture of human retinal pigment epithelium and choroid: a model for the study of cytologic behavior of RPE *in vitro*. Invest. Ophthalmol. Vis. Sci. 12: 554-566.

Tsukahara, I., Ninomiya, S., Castellarin, A., Yagi, F., Sugino, I. K. and Zarbin, M. A. (2002). Early attachment of uncultured retinal pigment epithelium from aged donors onto Bruch's membrane explants. Exp. Eye Res. 74: 255-266.

Tsunenari, T., Nathans, J. and Yau, K-W. (2006). Ca^{2+}-activated Cl^- current from human bestrophin-4 in excised membrane patches. J. Gen. Physiol.: 749-754.

Tsunenari, T., Sun, H., Williams, J., Cahill, H., Smallwood, P., Yau, K-W. and Nathans, J. (2003). Structure-function analysis of the bestrophin family of anion channels. J. Biol. Chem. 278: 41114-41125.

Turksen, K., Aubin, J. E., Sodek, J. and Kalnins, V. I. (1984). Changes in the distribution of laminin, fibronectin, type IV collagen and heparan sulfate proteoglycan during colony formation by chick retinal pigment epithelial cells *in vitro.* Coll. Relat. Res. 4: 413-426.

Turksen, K., Aubin, J. E., Sodek, J. and Kalnins, V. I. (1985). Localization of laminin, type IV collagen, fibronectin, and heparan sulfate proteoglycan in chick retinal pigment epithelium basement membrane during embryonic development. J. Histochem. Cytochem. 33: 665-671.

Turksen, K., Opas, M. and Kalnins, V. I. (1989). Cytoskeleton, adhesion, and extracellular matrix of fetal human retinal pigmented epithelial cells in culture. Ophthalmic. Res. 21: 56-66.

Turowski, P., Adamson, P., Sathia, J., Zhang, J. J., Moss, S. E., Aylward, G. W., Hayes, M. J., Kanuga, N. and Greenwood, J. (2004). Basement membrane-dependent modification of phenotype and gene expression in human retinal pigment epithelial ARPE-19 cells. Invest. Ophthalmol. Vis. Sci. 45: 2786-2794.

Tytgat, J., Vereecke, J. and Carmeliet, E. (1988). Differential effects of verapamil and flunarizine on cardiac L-type and T-type Ca channels. Naunyn-Schmiedeberg's Arch. Pharmacol. 6: 690-692.

Uchida, H., Hayashi, H., Kuroki, M., Uno, K., Yamada, H., Yamashita, Y., Tombran-Tink, J., Kuroki, M. and Oshima, K. (2005). Vitamin A up-regulates the expression of thrombospondin-1 and pigment epithelium-derived factor in retinal pigment epithelial cells. Exp. Eye Res. 80: 23-30.

Ueda, Y. and Steinberg, R. H. (1993). Voltage-operated calcium channels in fresh and cultured rat retinal pigment epithelial cells. Invest. Ophthalmol. Vis. Sci. 34: 3408-3418.

Ueda, Y. and Steinberg, R. H. (1994). Chloride currents in freshly isolated rat retinal pigment epithelial cells. Exp. Eye Res. 58: 331-342.

Ueda, Y. and Steinberg, R. H. (1995). Dihydropyridine-sensitive calcium currents in freshly isolated human and monkey retinal pigment epithelial cells. Invest. Ophthalmol. Vis. Sci. 36: 373-380.

Uehara, F., Matthes, M. T., Yasumura, D. and LaVail, M. M. (1990). Light-evoked changes in the interphotoreceptor matrix. Science. 248: 1633-1636.

Ulshafer, R. J., Allen, C. B. and Rubin, M. L. (1990). Distributions of elements in the human retinal pigment epithelium. Arch. Ophthalmol. 108: 113-117.

Unwin, P. N. and Ennis, P. D. (1984). Two configurations of a channel-forming membrane protein. Nature. 307: 609-613.

Ussing, H. H. (1953). Transport through biological membranes. Ann. Rev. Physiol. 15: 1-20.

Vaegan and Beaumont, P. (1996). Relationships between EOG parameters and their sensitivity to disease. Proc 36th ISCEV Symposium, Tübingen.

Vaegan and Beaumont, P. (2005). The fast oscillation of the electroculogram Is a rapidly recorded independent parameter, sensitive to and specific for retinitis pigmentosa. Invest. Ophthalmol. Vis. Sci. 46: #515 ARVO abstract.

Valeton, J. M. and van Norren, D. (1982). Intraretinal recordings of slow electrical responses to steady illumination in monkey: isolation of receptor responses and the origin of the light peak. Vis. Res. 22: 393-399.

Valverius, P., Hoffman, P. L. and Tabakoff, B. (1987). Effect of ethanol on mouse cerebral cortical beta-adrenergic receptors. Mol. Pharmacol. 32: 217-222.

van der Schaft, T. L., de Bruijn, W. C., Mooy, C. M. and de Jong, P. T. (1993). Basal laminar deposit in the aging peripheral human retina. Graefes Arch. Clin. Exp. Ophthalmol. 231: 470-475.

van Itallie, C. M. and Anderson, J. M. (2006). Claudins and epithelial paracellular transport. Ann. Rev. Physiol. 68: 403-429.

Vankeerberghen, A., Cuppens, H. and Cassiman, J-J. (2002). The cystic fibrosis transmembrane conductance regulator: an intriguing protein with pleiotropic functions. J. Cystic Fibrosis. 1: 13-29.

Vergani, P., Lockless, S. W., Nairn, A. C. and Gadsby, D. C. (2005). CFTR channel opening by ATP-driven tight dimerization of its nucleotide-binding domains. Nature. 433: 876-880.

Veronesi, B. (1996). Characterization of the MDCK cell line for screening neurotoxicants. Neurotoxicology. 17: 433-443.

Voüte, C. L. and Ussing, H. H. (1968). Some morphological aspects of active sodium transport. The epithelium of the frog skin. J. Cell Biol. 36: 625-638.

Wagner, J., Jan Danser, A. H., Derkx, F. H., de Jong, T. V., Paul, M., Mullins, J. J., Schalekamp, M. A. and Ganten, D. (1996). Demonstration of renin mRNA, angiotensinogen mRNA, and angiotensin converting enzyme mRNA expression in the human eye: evidence for an intraocular renin-angiotensin system. Br J Ophthalmol 80: 159-163.

Walsh, D. E., Harvey, B. J. and Urbach, V. (2000). CFTR regulation of intracellular calcium in normal and cystic fibrosis human airway epithelia. J. Membr. Biol. 177: 209-219.

Walter, H. J., McMahon, T., Dadgar, J., Wang, D. and Messing, R. O. (2000). Ethanol regulates calcium channel subunits by protein kinase C δ-dependent and -independent mechanisms. J. Biol. Chem. 275: 25717-25722.

Wang, N. and Anderson, R. E. (1993). Transport of 22:6n-3 in the plasma and uptake into retinal pigment epithelium and retina. Exp. Eye Res. 57: 225-233.

Wang, S., Lu, B., Wood, P. and Lund, R. D. (2005). Grafting of ARPE-19 and schwann cells to the subretinal space in RCS rats. Invest. Ophthalmol. Vis. Sci. 46: 2552-2560.

Wang, X., Wang, G., Lemos, J. and Treistman, S. (1994). Ethanol directly modulates gating of a dihydropyridine-sensitive Ca^{2+} channel in neurohypophysial terminals. J. Neurosci. 14: 5453-5460.

Wang, Z., Dillon, J. and Gaillard, E. R. (2006). Antioxidant properties of melanin in retinal pigment epithelial cells. Photochem. Photobiol. 82: 474-479.

Waterfield, M. D., Mayes, E. L., Stroobant, P., Bennet, P. L., Young, S., Goodfellow, P. N., Banting, G. S. and Ozanne, B. (1982). A monoclonal antibody to the human epidermal growth factor receptor. J. Cell Biochem. 20: 149-161.

Waters, C., Pyne, S. and Pyne, N. J. (2004). The role of G-protein coupled receptors and associated proteins in receptor tyrosine kinase signal transduction. Sem. Cell Dev. Biol. 15: 309-323.

Wei, L., Vankeerberghen, A., Cuppens, H., Eggermont, J., Cassiman, J. J., Droogmans, G. and Nilius, B. (1999). Interaction between calcium-activated chloride channels and the cystic fibrosis transmembrane conductance regulator. Pflügers Archiv. Eur. J. Physiol. 438: 635-641.

Weigel, A. L., Handa, J. T. and Hjelmeland, L. M. (2002). Microarray analysis of $H_2O_2^-$, HNE^-, or tBH-treated ARPE-19 cells. Free Radic. Biol. Med. 33: 1419-1432.

Weigel, A. L., Ida, H., Boylan, S. A. and Hjelmeland, L. M. (2003). Acute hyperoxia-induced transcriptional response in the mouse RPE/choroid. Free Radic. Biol. Med. 35: 465-474.

Weleber, R. G. (1989). Fast and slow oscillations of the electro-oculogram in best's macular dystrophy and retinitis pigmentosa. Arch. Ophtalmol. 107: 530-537.

Welling, P. G., Lyons, L. L., Elliot, R. and Amidon, G. L. (1977). Pharmacokinetics of alcohol following single low doses to fasted and nonfasted subjects. J. Clin. Pharmacol. 17: 199-206.

Welsh, M. J. and Smith, A. E. (1993). Molecular mechanisms of CFTR chloride channel dysfunction in cystic fibrosis. Cell. 73: 1251-1254.

Weng, T. X., Godley, B. F., Jin, G. F., Mangini, N. J., Kennedy, B. G., Yu, A. S. and Wills, N. K. (2002). Oxidant and antioxidant modulation of chloride channels expressed in human retinal pigment epithelium. Amer. J. Physiol. 283: C839-849.

White, M. M. and Miller, C. (1979). A voltage-gated anion channel from the electric organ of *Torpedo californica*. J. Biol. Chem. 254: 10161-10166.

Wiggert, B., Bergsma, D. R., Helmsen, R. and Chader, G. J. (1978). Vitamin A receptors. Retinoic acid binding in ocular tissues. Biochem. J. 169: 87-94.

Wills, N. K., Weng, T., Mo, L., Hellmich, H. L., Yu, A., Wang, T., Buchheit, S. and Godley, B. F. (2000). Chloride channel expression in cultured human fetal RPE cells: response to oxidative stress. Invest. Ophthalmol. Vis. Sci. 41: 4247-4255.

Wimmers, S., Coeppicus, L. and Strauss, O. (2004). Cloning and molecular characterization of L type Ca^{2+} channels in the retinal pigment epithelium. Invest. Ophthalmol. Vis. Sci. 45: #3688 ARVO Abstract.

Winkler, B. S. and Giblin, F. J. (1983). Glutathione oxidation in retina: effects on biochemical and electrical activities. Exp. Eye Res. 36.

Withers, D. J. and White, M. (2000). Perspective: The Insulin signaling system- a common link in the pathogenesis of type 2 diabetes. Endocrinology. 141: 1917-1921.

Wolf, J. E. and Arden, G. B. (2004). Two components of the human alcohol electro-oculogram. Doc. Ophthalmol. 109: 123-130.

Wollmann, G., Lenzner, S., Berger, W., Rosenthal, R., Karl, M. O. and Strauss, O. (2006). Voltage-dependent ion channels in the mouse RPE: comparison with Norrie disease mice. Vis. Res. 46: 688-698.

Woodruff, M. L., Fain, G. L. and Bastian, B. L. (1982). Light-dependent ion influx into toad photoreceptors. J. Gen. Physiol. 80: 517-536.

Worrell, R. T., Butt, A. G., Cliff, W. H. and Frizzell, R. A. (1989). A volume-sensitive chloride conductance in human colonic cell line T84. Amer. J. Physiol. 256: C1111-1119.

Wright, A. M., Gong, X., Verdon, B., Linsdell, P., Mehta, A., Riordan, J. R., Argent, B. E. and Gray, M. A. (2004). Novel regulation of cystic fibrosis transmembrane conductance regulator (CFTR) channel gating by external chloride. J. Biol. Chem. 279: 41658-41663.

Wu, J., Marmorstein, A. D. and Peachey, N. S. (2006). Functional abnormalities in the retinal pigment epithelium of CFTR mutant mice. Exp. Eye Res. 83: 424-428.

Wu, Y., Singh, S., Georgescu, M-M. Birge, R. B. (2005). A role for Mer tyrosine kinase in αvβ5 integrin-mediated phagocytosis of apoptotic cells. J. Cell Sci. 118: 539-553.

Xiong, H., Li, C., Garami, E., Wang, Y., Ramjeesingh, M., Galley, K. and Bear, C. E. (1999). ClC-2 activation modulates regulatory volume decrease. J. Membr. Biol. 167: 215-221.

Xu, T. H., Ding, J. and Shi, Y. L. (2004). Toosendanin increases free-Ca^{2+} concentration in NG108-15 cells via L-type Ca^{2+} channels. Acta. Pharmacol. Sin. 25: 597-601.

Xu, X. and Karwoski, C. J. (1994). Current source density analysis of retinal field potentials. II. pharmacological analysis of the b-wave and M-wave. J. Neurophysiol. 72: 96-105.

Xu, Y., Clark, J. C., Aronow, B. J., Dey, C. R., Liu, C., Wooldridge, J. L. and Whitsett, J. A. (2003). Transcriptional adaptation to cystic fibrosis transmembrane conductance regulator deficiency. J. Biol. Chem. 278: 7674-7682.

Yamamoto, A., Ishiguro, H., Ko, S. B. H., Suzuki, A., Wang, Y., Hamada, H., Mizuno, N., Kitagawa, M., Hayakawa, T. and Naruse, S. (2003). Ethanol induces fluid hypersecretion from guinea-pig pancreatic duct cells. J. Physiol. (Lond). 551: 917-926.

Yan, K. and Matthews, G. (1992). Blockers of potassium channels reduce the outward dark current in rod photoreceptor inner segments. Vis. Neurosci. 8: 479-481.

Yanagihara, Miura, Moriwaki, Shiraki, Imamura, Kaida and Miki (2001). Hepatocyte growth factor promotes epithelial morphogenesis and occludin linkage to the cytoskeleton in cultured retinal pigment epithelial cells. Graefe's Arch. Clin. Exp. Ophthalmol. 239: 619-627.

Yanagihara, N., Moriwaki, M., Shiraki, K., Miki, T. and Otani, S. (1996). The involvement of polyamines in the proliferation of cultured retinal pigment epithelial cells. Invest. Ophthalmol. Vis. Sci. 37: 1975-1983.

Yang, D., Pan, A., Swaminathan, A., Kumar, G. and Hughes, B. A. (2003). Expression and localization of the inwardly rectifying potassium channel $Kir_{7.1}$ in native bovine retinal pigment epithelium. Invest. Ophthalmol. Vis. Sci. 44: 3178-3185.

Yang, Y., Janich, S., Cohn, J. and Wilson, J. (1993). The common variant of cystic fibrosis transmembrane conductance regulator is recognized by hsp70 and degraded in a pre-golgi nonlysosomal compartment. Proc. Natl. Acad. Sci. U.S.A. 90: 9480-9484.

Yang, Z-W., Wang, J., Zheng, T., Altura, B. T. and Altura, B. M. (2001a). Importance of extracellular Ca^{2+} and intracellular Ca^{2+} release in ethanol-induced contraction of cerebral arterial smooth muscle. Alcohol. 24: 145-153.

Yang, Z-W., Wang, J., Zheng, T., Altura, B. T., Altura, B. M. and Hurn, P. D. (2001b). Ethanol-induced contractions in cerebral arteries : role of tyrosine and mitogen-activated protein kinases. Stroke. 32: 249-257.

Yefimova, M. G., Jeanny, J-C., Guillonneau, X., Keller, N., Nguyen-Legros, J., Sergeant, C., Guillou, F. and Courtois, Y. (2000). Iron, ferritin, transferrin, and transferrin receptor in the adult rat retina. Invest. Ophthalmol. Vis. Sci. 41: 2343-2351.

Yoshida, M., Tanihara, H. and Yoshimura, N. (1992). Platelet-derived growth factor gene expression in cultured human retinal pigment epithelial cells. Biochem. Biophys. Res. Commun. 189: 66-71.

Young, R. W. and Bok, D. (1969). Participation of the retinal pigment epithelium in rod outer segment renewal process. J. Cell Biol. 42: 392-403.

Zabner, J., Scheetz, T. E., Almabrazi, H. G., Casavant, T. L., Huang, J., Keshavjee, S. and McCray, P. B., Jr. (2005). CFTR ΔF508 mutation has minimal effect on the gene expression profile of differentiated human airway epithelia. Amer. J. Physiol. 289: L545-553.

Zhang, D., Lai, M. C., Constable, I. J. and Rakoczy, P. E. (2002). A model for a blinding eye disease of the aged. Biogerontology 3: 61-66.

Zhang, N., Kannan, R., Okamoto, C. T., Ryan, S. J., Lee, V. H. L. and Hinton, D. R. (2006). Characterization of brimonidine transport in retinal pigment epithelium. Invest. Ophthalmol. Vis. Sci. 47: 287-294.

Zhang, Y. and Stone, J. (1997). Role of astrocytes in the control of developing retinal vessels. Invest. Ophthalmol. Vis. Sci. 38: 1653-1666.

Zimmerman, A. L., Yamanaka, G., Eckstein, F., Baylor, D. A. and Stryer, L. (1985). Interaction of hydrolysis-resistant analogs of cyclic GMP with the phosphodiesterase and light-sensitive channel of retinal rod outer segments. Proc. Natl. Acad. Sci. U.S.A. 82: 8813-8817.

10 Publications

ARTICLE IN PRESS

Available online at www.sciencedirect.com

SCIENCE DIRECT®

Progress in Retinal and Eye Research ▮ (▮▮▮▮) ▮▮▮–▮▮▮

Progress in RETINAL AND EYE RESEARCH

www.elsevier.com/locate/prer

The electro-oculogram

Geoffrey B. Arden*, Paul A. Constable

Department of Optometry and Visual Science, Henry Wellcome Laboratories for Visual Sciences, City University, London, UK

Abstract

The retinal pigment epithelium (RPE) lying distal to the retina regulates the extracellular environment and provides metabolic support to the outer retina. RPE abnormalities are closely associated with retinal death and it has been claimed several of the most important diseases causing blindness are degenerations of the RPE. Therefore, the study of the RPE is important in Ophthalmology. Although visualisation of the RPE is part of clinical investigations, there are a limited number of methods which have been used to investigate RPE function. One of the most important is a study of the current generated by the RPE. In this it is similar to other secretory epithelia. The RPE current is large and varies as retinal activity alters. It is also affected by drugs and disease. The RPE currents can be studied in cell culture, in animal experimentation but also in clinical situations. The object of this review is to summarise this work, to relate it to the molecular membrane mechanisms of the RPE and to possible mechanisms of disease states.

Contents

Abbreviations: ARMD, Age-related macular degeneration; AZOOR, Acute zonal occult outer retinopathy; CaCC, Calcium-activated Cl^- channel; CF, Cystic fibrosis; CFTR, Cystic fibrosis transmembrane conductance regulator; cAMP, Cyclic adenosine monophosphate; cGMP, Cyclic guanosine monophosphate; DAG, Diacylglycerol; DIDS, 4, 4′-diisothiocyanostilbene-2, 2′-disulphonic acid; DPC, Diphenylamine-2-carboxylic acid; DR:LT, Dark rise: light trough; ER, Endoplasmic reticulum; ERCA, Endoplasmic reticulum calcium ATPase pump; EOG, Electro-oculogram; ERG, Electroretinogram; ERP, Early receptor potential; FO, Fast oscillation; IP_3, Inositol 1, 4, 5-triphosphate; IP_3-R, the IP_3 receptor; ISCEV, International Society for Clinical Electrophysiology of Vision; NCX, Sodium–calcium exchanger; NBD, Nucleotide binding domain; PMCA, Plasma membrane calcium ATPase pump; PKA(C), Protein kinase A(C); PTK, Protein tyrosine kinase; RCS, Royal College of Surgeon's; RP, Retinitis pigmentosa; RPE, Retinal pigment epithelium; TEP, Trans-epithelial potential; TER, Trans-epithelial resistance; V_M, Membrane voltage

*Corresponding author. Tel.: +44 207 040 8863; fax: +44 207 040 8355.
E-mail address: g.arden@city.ac.uk (G.B. Arden).

1350-9462/$ - see front matter © 2005 Elsevier Ltd. All rights reserved.
doi:10.1016/j.preteyeres.2005.11.001

1. Introduction

The retinal pigmented epithelium (RPE) is an electrically polarised pigmented epithelial monolayer that lies posterior to the photoreceptors where it plays a central role in maintaining the outer retina (Strauss, 2005). The RPE's functions include transporting retinol to the outer segments, phagocytosing shed photoreceptor outer segments (Besharse and Defoe, 1998) the transport of fluid and metabolites, and the regulation of the contents of the RPE cytosol and the subretinal space (Adorante and Miller, 1990; Bialek and Miller, 1994; Bialek et al., 1996; Lin et al., 1992; Rymer et al., 2001). Furthermore, the RPE forms a part of the outer blood retinal barrier by virtue of its tight-junctional complexes. It contains a number of potential drug transporters that are of medical interest and also excludes potentially harmful xenobiotics from the subretinal space (Kennedy and Mangini, 2002; Steuer et al., 2005). The RPE is responsible for the corneo-fundal standing potential (Kühne and Steiner, 1881) and the change in this voltage across the human eye evoked by change of illumination forms the basis of the clinical electro-oculogram (EOG) (Arden and Kelsey, 1962a; Kris, 1958). The light-EOG has also been recorded in other species: lizard (Griff and Steinberg, 1982), chicken (Gallemore et al., 1988), mouse (Kikawada, 1968), rat (Arden and Ikeda, 1964), rabbit (Ogawa, 1967), cat (Linsenmeier and Steinberg, 1982), primate (Valeton and van Norren, 1982). The light rise of the EOG results from the release of a substance, termed the "light rise" or "light peak" substance from the photoreceptors (the chemical composition of which is unknown) that interacts either directly or indirectly with the RPE (Gallemore et al., 1988). There is indirect evidence (see Section 9) that this substance causes an increase in the intracellular concentration of calcium ($[Ca^{2+}]_{in}$) within the RPE which in turn opens a basolateral ionic Cl^- channel, thus depolarising the basal membrane (Gallemore et al., 1988, 1993; Gallemore and Steinberg, 1989b) and leading to the characteristic light rise of the EOG (Gallemore and Steinberg, 1993). However, the exact nature of the basolateral Cl^- channel has not been determined, but is believed to be bestrophin (Hartzell et al., 2005b; Marmorstein et al., 2004; Strauss and Rosenthal, 2005).

The light rise of the light-EOG is a slow complex change. Following dark adaptation, the return to light causes an increase in the ocular standing potential that peaks at ~7–10 min. Following this the voltage decreases to a trough at ~22 min. Smaller and slower ripples occur for over 2 h. The amplitude of the rise is dependent upon the

duration of the previous period in darkness (see Section 13) up to a duration of 22 min. This is not the only effect of light on the RPE. When the period of light and dark intervals is ~1 min an induced oscillation—the fast oscillation (FO) of the standing potential occurs at the stimulus frequency. The FO has an opposite sense to the light rise. Immediately following retinal illumination there is a fall in the standing potential and a light trough develops that begins to rise ~30 s after light onset. The FOs are believed to be a function of the alteration of basolateral Cl^- channel transport following a fall in subretinal $[K^+]_{out}$ (Blaug et al., 2003). The FOs provides insights into inherited dystrophies (Weleber, 1989) and potentially RPE function as well (Schneck et al., 2000).

Whilst the EOG provides useful information about the integrity of the photoreceptor-RPE complex in acquired and inherited retinal degenerations, the test in itself is not specific for RPE function. Therefore, investigators have employed alternative means to detect early changes in RPE physiology. The EOG changes in response to acetazolamide (Kawasaki et al., 1986), mannitol (Kawasaki et al., 1977; Shirao and Steinberg, 1987) hypoxia and hyperoxia (Marmor et al., 1985) have all been explored as potentially suitable non-photic stimuli that directly affect the RPE. In man, alcohol apparently initiates the same voltage changes and series of intracellular events that cause the light-induced change in the RPE (Arden and Wolf, 2000a; Skoog et al., 1975) and may provide an additional method of detecting early RPE dysfunction (Arden and Wolf, 2003; Arden et al., 2000). Alcohol-induced changes similar to those seen in man have been observed in dark-adapted sheep in vivo (Knave et al., 1974) and alcohol changes the voltage (in vitro) of light-adapted bovine RPE (Pautler, 1994), but the mechanisms remain unclear.

Our intention is to provide a background for the understanding of the ionic channels within the RPE and how alterations in them cause the changes in RPE membrane potential that produce the clinical EOG currents. To this end we discuss the basic biophysics of cell membranes and the electrophysiological techniques of measuring the ionic currents. In addition we will review practical aspects of the EOG, because as a non-invasive technique it can be used to investigate not only membrane properties of the RPE, but also the functioning of the subretinal space and photoreceptors in disease states and can provide information unrelated to changes of visual sensation and supplemental to those of modern imaging techniques. For these reasons, the EOG is a tool often used in clinical research on the retina.

2. Discovery and the first analyses

The potential voltage difference that occurs between the cornea and fundus was discovered by Du Bois Reymond (1849). He showed that it persisted for long periods in the isolated eye. Kühne and Steiner (1881) and de Haas (1901) also measured the voltages after removing successively cornea, iris, lens vitreous and retina. Only when the RPE had been damaged did the potential vanish, and this localised the source of the current production to the RPE. Although illumination was known to affect the potential recorded between the cornea and fundus (Himstedt and Nagel, 1902) the capillary electrometers used in early work were not sufficiently sensitive or stable to analyse the changes in detail (Einthoven, 1893). With the advent of electronic amplification, the sensitivity problem was solved, but the amplifiers were unstable, and required condenser-coupling, so slow changes were not amplified. In the 1940s, Noell was able to employ systems both stable and sensitive (DC amplification) and could follow the slow changes; he related the c-wave of the electroretinogram (ERG) to the later and still slower responses. He used poisons that selectively damaged the RPE, as demonstrated by histological changes caused. He found that azide, acting on the RPE transiently increased the "standing potential" and the c-wave of the ERG, while iodate, that damaged the RPE selectively, not only caused a fall in the standing potential but also reduced the azide increase, and reduced the c-wave. Faster changes caused by illumination—i.e. other components of the ERG—were less affected (Noell, 1942, 1952, 1953a, b).

3. Development of current fields round the eyes

The RPE consists of a layer of cells connected by tight junctions, so that the resistance to current flowing across the membrane in the spaces between the cells (the paracellular resistance) is 10 times greater than the transmembrane resistance itself (Brindley and Hamasaki, 1963; Miller and Steinberg, 1977a, b). Therefore, voltage developed across the RPE implies that at its origin current will flow at each point normal to the surface, and the return paths are through the paracellular resistance. Because the RPE follows the curvature of the globe, the current flow at each point can be split (formally) into three vectors. One is in the optic axis, and two at other axes at right angles to it, pointing medially or vertically. At the fundus, nearly all the current flows in the radial vector (in the optic axis). At other positions, there will be current vectors flowing in the optic axis and also vectors in the lateral, medial, superior, and inferior directions will be developed. Because of the approximately spherical shape of the eye non-radial current vectors will approximately cancel. For example, in the nasal part of the RPE, there will be a temporally directed vector, which will cancel with the nasally directed vector from the temporal part of the RPE. Hence the net current flow will be due to the vector in the optic axis and appears to be a dipole in the optic axis, with the cornea positive and the fundus negative. This explains the name given to the potential recorded across the eye, the corneo-fundal potential. The current flowing from such a dipole will spread symmetrically in all directions about the optic

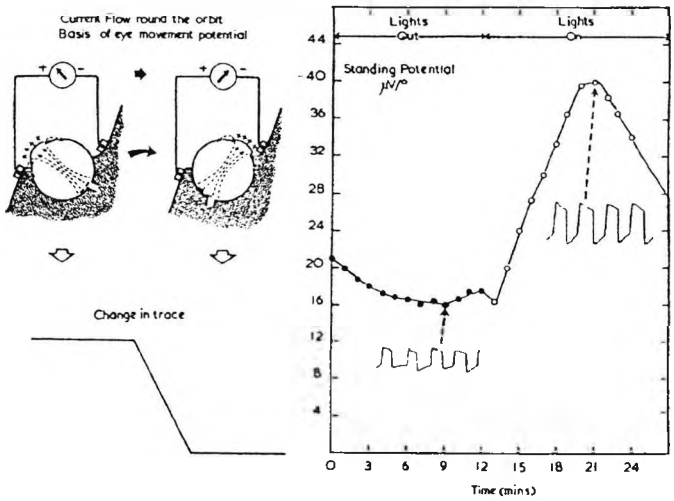

Fig. 1. The generation of the light rise by the corneo-fundal standing potential. From Arden (1962).

axis. Therefore, as the eye moves, the voltages recorded between relatively distant skin electrodes will vary with the angle of rotation of the eye. This is shown in Fig. 1, which illustrates how the magnitude of the responses to fixed eye movements can be used to measure the magnitude of the current produce by the RPE. This simple view of the eye movement potential suggests that abnormalities in the posterior pole will cause larger changes to the current than changes near the equator and that recorded voltage will vary with the sine of the angle moved. However, neither of these suppositions is correct. One reason for this is that the cells of the RPE (which generate the voltage) form a syncitium so damage to some of the RPE cell causes similar voltage changes over a large area. Another is that for the relatively small displacements associated with rapid saccades, it is difficult to be certain whether a linear or sine relation holds between voltage change and angular displacement. The ease with which eye motion could be recorded led to attempts to use the EOG for eye-movement recordings. However, difficulties were found in calibrating such a system, because the apparent magnitude of the dipole was not constant (Aserinsky, 1955; Francois et al., 1955; Kolder, 1959; Miles, 1940; Taumer et al., 1974; ten Doesschate and ten Doesschate, 1955). It became apparent that one of the factors modifying the voltage was light. The first complete description of the human light–dark sequence was due to Kris (1958) but an analysis of the nature of the response and the recognition of its clinical utility is usually attributed to Arden (Arden, 1962; Arden and Barrada, 1962; Arden et al., 1962; Arden and Kelsey, 1962a) (Fig. 1) who showed that a small reduction in light intensity provoked a decrease in voltage, the dark trough, which was not related to the preceding light level, although the change from dark to light caused a transient rise of voltage (the light peak) the magnitude of which was linearly related to the logarithm of retinal illumination.

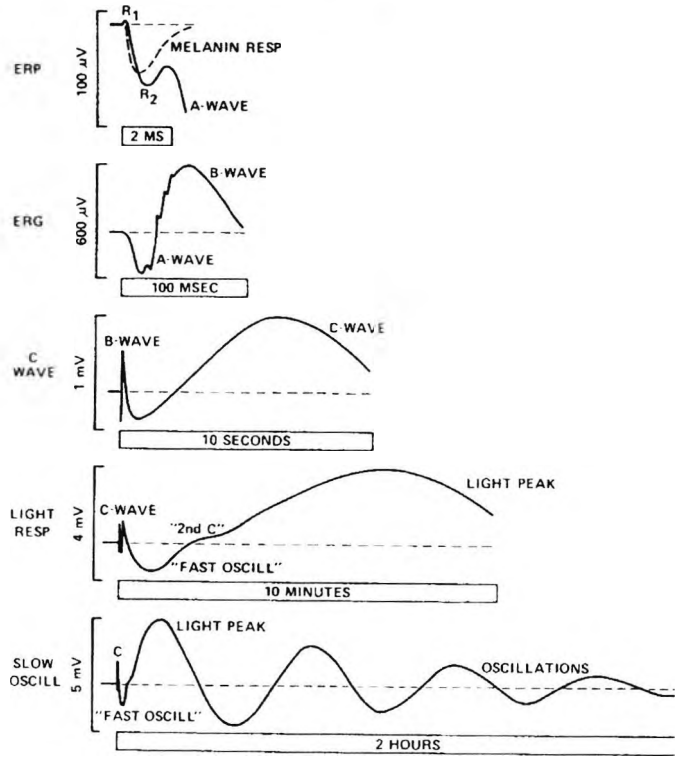

Fig. 2. Voltage changes resulting from photic stimulation of the eye recorded using different timescales, as indicated on each trace. The early receptor potential (ERP) is produced by a conformational change in the outer limb membrane that occurs when visual pigments absorb light. The ERG a- and b-waves are produced mainly by changes in photoreceptor dark current and the hyperpolarising rod bipolars. The c-wave is the result of the RPE's apical membrane hyperpolarisation in response to a decrease in subretinal $[K^+]$ and occurs after the faster ERG components generated in the neural retina. The fast oscillation trough occurs approximately 30 s after light onset and is due to the RPE's basal membrane hyperpolarising. The slow oscillation that is recorded as the EOG peaks at ~8 min is due to the RPE basal membrane depolarising. After the peak of the light rise, the transepithelial potential continues to fluctuate for several hours but these changes have not been investigated systematically. Printed with permission of Marmor and Lurie (1979).

4. The full picture of the DC ERG

The full sequence of the voltage changes is shown in Fig. 2. The electroretinographic a- and b-waves occur in about 0.1 s: following this there is a slower c-wave. Following this sequence, there is a slow cornea-negative swing, the after negativity, followed by a "second c-wave" and then a still slower and larger increase of voltage, the "light rise". These changes have been observed in a number of different mammals. There are species differences. In man, even though light continues, this increase in the corneo-fundal potential is not maintained, but after a peak at 8 min sinks to a trough level at 22 min. If a light-adapted eye is placed in darkness, the potential falls to a level nearly identical to the lowest level reached at the 22–24 min trough. Following this trough, in light or in darkness, further slow rhythmic changes in voltage are seen that may persist for 2 h or more. For reviews on this topic see Marmor and Lurie (1979) and Steinberg et al. (1985).

5. Concepts of membrane voltage

Since the original description of the human EOG, work in animals, isolated eyes and isolated RPE preparations has resulted in a great deal of information about the nature of the ionic channels, cotransporters and pumps in the apical and basal surfaces of the RPE. Because the RPE is a secretory epithelium this knowledge is fundamental to our understanding of how fluid is transported across the epithelium. The development of the EOG likewise can be explained by the regulation or "gating" of these ionic channels by "second messengers"—pathways that link membrane mechanisms to intracellular changes. The methods employed include a variety of electrophysiological techniques that have each provided valuable insights into the membrane voltage (V_M) changes of the RPE, and the ionic channels involved in generating the clinical waveform of the EOG.

The V_M results from the difference in ionic concentrations across the plasma membrane and the relative permeability of the membrane to the ions in the intra and extracellular spaces. Alterations in the permeability or conductance of the membrane to the ions by the gating of ionic channels leads to a change in V_M as ionic currents pass across the membrane. Therefore, we will discuss the basic biophysics of ions and ionic channels and the forces that are involved in generating ionic currents that lead to changes in V_M. For a more detailed account of these underlying principals see the following texts Hille (2001), Sakmann and Neher (1995) from which the following section is summarised.

5.1. The passage of ions through membranes and the membrane potential

The phospholipid bilayer of the cell membrane is practically impermeable to ions; therefore any passage of ions across the membrane occurs in small specialised regions, via protein-containing ionic channels, pumps and cotransporters. Many ionic channels are specifically shaped (and charged) to permit the selective passage of a few types of ions, which will tend to move from a region of high concentration to one of a lower concentration (i.e. down their concentration gradient).[1]

Since ions are electrically charged, their movement through ionic channels causes a change in the charge across the lipid bilayer. For example, as positively charged potassium ions move out of a cell, the interior becomes negatively charged with respect to the exterior and so V_M hyperpolarises. This change in voltage eventually opposes the movement of the ions and an equilibrium is established approximating the Nernst equilibrium potential (Nernst, 1888) (see Eq. (1)).

$$E_X = RT/zF \ln\{[X]_{out}/[X]_{in}\}, \quad (1)$$

where E_X is the equilibrium potential (volts) of ion X; $[X]_{out}$ the concentration of ion X outside cell, $[X]_{in}$ is concentration of ion X inside the cell, R the gas constant ($8.314\,J\,K^{-1}\,mol^{-1}$), T the absolute temperature, F the Faraday's constant ($96{,}500\,C\,mol^{-1}$); z the valence of ion or charge, i.e.: $Cl^- = -1$, $Ca^{2+} = +2$.

Other physical properties of ionic channels as well as the membrane voltage will influence the resting V_M. Because potassium (K^+) channels have a 10^3 times higher permeability to K^+ than Na^+ (these are the only two cations present in relatively high concentration) and sodium channels in the resting state do not have a high permeability, the resting potential of cell membranes such as those of neurones approximates the potassium equilibrium potential. In the RPE the intracellular K^+ activity is ~90 mM and the subretinal $[K^+]$ varies from 2–5 mM which would give a Nernst potential for V_{Apical} between −77 and −101 mM at 37 °C. In human RPE, V_{Apical} ranges from −35 to −63 mV have been reported (Quinn and Miller, 1992), showing that other ionic channels contribute to V_M.

Cell membranes are not simple permeable membranes. The ionic channels have properties that constrain ionic currents and maintain V_M by holding some ions away from equilibrium. It has been shown that single channels change their state frequently, opening and closing very rapidly. The conductance depends upon the proportion of time the channel remains in the same state. If the open state occurs most of the time, the particular ion involved can move toward its equilibrium potential. Therefore, stimuli which change the channel state are said to "gate" it. Opening of the ionic channels allows these ions to move towards their equilibrium potential thus generating ionic currents and a change in V_M.[2]

[1] Even though Na^+ ions have a smaller atomic radius than K^+ they do not pass easily through potassium channels (Doyle et al., 1998). Interactions within the pore between ions and amino acids determine the preferential permeability of one ion above another for each channel type. However, most Cl^- ionic channels are not as selective (Linsdell et al., 1997a) with some displaying cation permeability (Qu and Hartzell, 2000). The significance of permeability and conductance of an ion is different. The permeability of an ion relates to how easily an ion enters the pore whilst the conductance indicates how easily the ion traverses the channel. This depends upon the difference between the free energy of the ion in solution compared to that in the pore (Dawson et al., 1999; Smith et al., 1999).

[2] The behaviour of ions in a pore or channel may be complex. Ions are associated with water molecules, and may interact with each other, and also with charged amino-acids in the cell membrane surface proteins and the negative charge of the phospholipid bilayer all interact with the ions inside a cell and form stable complexes reducing their availability to traverse through an ion channel or pore. Therefore, predictions about ionic behaviour in a dilute solution differ to the actual situation and compensation can be made for some of these interactions by using the ionic "activities" instead of molar concentration (Blum, 1980; Debye and Hückel, 1923; Roberts and Stokes, 1965). Furthermore, when a large difference exists between the intra and extracellular concentrations of an ion such as Ca^{2+} where intracellular free concentrations are 10^3 times lower than extracellular levels (Feldman et al., 1991) the electrochemical gradient is unfavourable for Ca^{2+} to exit the cell and so the ionic current varies as a non linear function of V_M as defined by the

5.2. Maintenance of membrane potential

In the RPE, which is a secretory epithelium, the passage of a cation is often accompanied by the passage of an anion, so that apart from electrical current flow, net movement of salts, acids or alkalis develops and with it the movement of water is induced across the membrane. Any imbalance in such processes, if they continued indefinitely, would alter the composition of the cell. Therefore, there are various active and passive regulatory mechanisms that act to prevent long-term alterations in the cytosolic environment in addition to the mechanisms that transport water ions and other solutes across the epithelium.

One ubiquitous transporter in epithelia is the ouabain-inhibitable Na–K–ATPase pump that is present in the apical membrane of the RPE (Hu et al., 1994; Rizzolo, 1990). This pump utilises the energy of ATP hydrolysis to move three Na^+ ions out of the cell in exchange for two K^+ ions that enter. This pump is the main way in which the cytosol concentration is kept rich in potassium and low in sodium. It only contributes ~10 mV to V_{Apical} in the frog (Miller et al., 1978). The constant fluid elimination from the subretinal space results in an adhesive force between the RPE and retina. Inhibition of the Na–K–ATPase activity by ouabain reduces the adhesive forces between the tissues (Frambach et al., 1989). Even bicarbonate transport requires the activity of Na–K–ATPase because this pump establishes the sodium gradient which serves to uptake bicarbonate and thus establishes the driving forces for bicarbonate movement across the basolateral membrane. Numerous transporters have been localised in the RPE plasma membrane. They operate by coupling ions, amino acids or metabolites in exchange for another compound thereby regulating cell pH, osmolarity and cell volume, as well as transporting metabolic wastes or nutrients across the membrane (Adorante and Miller, 1990; Lin et al., 1992, 1994; Miller and Steinberg, 1977a, 1979; Peterson and Miller, 1995). One example is the bumetanide- and furosemide-inhibitable Na–K–2Cl cotransporter (la Cour et al., 1997; Xu et al., 1994), that regulates cell volume (Adorante and Miller, 1990) but does not contribute to the membrane potential as there is no net movement of charge across the membrane. For reviews see Flatman (2002) and Haas and Forbush (2000). Another very important function of this cotransporter is that it is the only means whereby Cl^- can be moved from subretinal space to the basal surface of the RPE. Sodium ions move with the Cl^-, and this accounts for most of the fluid flow. In contrast, an antiporter or exchanger, exchanges one ionic species for another across the membrane. Thus the Na^+–H^+ antiporter exchanges one Na^+ ion for a proton to counteract the electrogenic Na^+–HCO_3^- cotransporter which enables control of intracellular pH (Hughes et al., 1989; Lin and Miller, 1991).

A further mechanism of fluid transport is controlled by aquaporins of which 11 mammalian types have been identified. Their discovery is recent (Agre et al., 1993) and their regulation is complex. These channels may be associated with intracellular vacuoles, which "traffic" (i.e. move to and fuse with the membranes) under the influence of cyclic adenosine monophosphate (cAMP) or associated with Na–K–ATPase on the plasma membrane in the choroid plexus (Nielsen et al., 1993) to regulate water movement. Their properties in the RPE are not fully understood although they are essential for water transport (Ruiz and Bok, 1996; Stamer et al., 2003) (for review see King et al., 2004). More conventional ionic channels along with transporters also play a role in the movement of ions and water across membranes and the quantity per unit time varies, as the epithelium carries out its functions. The mechanisms by which specialised membrane proteins regulate the movement of charged ions and water are of interest, both on their own account and because of any change in relationship to disease. Because transport is associated with electrochemical phenomena, electrophysiology provides insights into these mechanisms.

V_M may also influence the conductance of an ionic channel so that the gating is voltage dependent. In this case, the ionic current will be zero when the equilibrium potential equals the membrane potential so that Ohm's law ($E = I/g$) can be rewritten (Eq. (3)) to account for the membrane potential.

$$I_X = g_X(V_M - E_X). \tag{3}$$

where I_X is the ionic current of ion X; g_X is the conductance of ion X across the membrane (reciprocal of resistance); V_M is the membrane potential and E_X is the Nernst equilibrium potential for ion X (Hodgkin et al., 1952).

This relationship holds when the current versus voltage (I–V) relation is linear and the intercept is at zero. The conductance (g) is dependent solely upon the difference in ionic concentrations across the membrane as described by the Nernst potential and is independent of V_M. However, for many RPE membrane channels the probability that the channel is open is greatly influenced by membrane voltage. Therefore, it is of interest to determine how these currents vary with V_M.

(*footnote continued*)
Goldman–Hodgkin–Katz current equation (Goldman, 1943; Hodgkin and Katz, 1949).

In practice, determining the equilibrium point for a complex system of ionic channels is handled well by the Goldman–Hodgkin–Katz voltage equation which states that at equilibrium the sum of all ionic currents will be zero. However, the permeability (P) of an ion is governed by the thickness of the membrane and the concentration difference of the ion as it passes through the membrane. Assuming then that ions act independently through the membrane and the electric field of the membrane is constant. Then the reversal potential (E_{rev}) is dependent upon the sum of the permeabilities multiplied by the Nernst potentials of the ions (Eq. (2))

$$E_{rev} = RT/zF \cdot \ln\left\{\sum_{n}^{n}[P \cdot ([X_i^+]_{out}/[X_i^+]_{in})] + \sum_{n}^{n}[P \cdot ([X_i^-]_{in}/[X_i^-]_{out})]\right\} \tag{2}$$

5.3. Voltage clamp and rectification

Although the original analysis of nerve fibre membrane activity was carried out with quite large electrodes in giant nerve fibres, the advent of intracellular recordings with glass micro-pipettes extended this to mammalian cells (Hodgkin and Huxley, 1952a–c; Hodgkin et al., 1952; Hodgkin and Katz, 1949; Ling and Gerard, 1949a c). Further advances were made when a second electrode was placed within the cell so that V_M could be controlled and held constant by an external current (Cole, 1949; Marmont, 1949). Utilising this technique of voltage clamp, the membrane current could be plotted as a function of voltage.

The membrane current (I) was the sum of the ionic current (I_i) that depends upon the conductance of the ionic channels and the local capacity currents that occur when there is a change in the ionic density (charge) between the inner and outer surface of the membrane (Eq. (4)).

$$I = C_m(\delta V/\delta t) + I_i. \quad (4)$$

To isolate I_i the investigators inserted two electrodes into the axon. One electrode recorded the membrane potential whilst the other injected current into the axon to control the local V_M in a series of fixed steps. It was now possible to record I_i directly and determine the direction of I_i at holding potentials that depolarised (or hyperpolarised) the axon over a wide range—from its resting V_M to the reverse potential at the peak of the action potential. The V_M under these two conditions corresponded to the equilibrium potentials of K^+ and Na^+, respectively, and alteration of the intracellular or extracellular ionic composition confirmed that the resting and active membrane potentials changed as though the activity of these two ions controlled V_M under these two conditions (Hodgkin and Huxley, 1952a c).

Such experiments cannot be carried out in the RPE without modifications, and the methods of analysis are discussed below. In practice, even in squid giant axon, there are technical difficulties, for example, when the voltage step begins, the current charges up membrane capacitances, and therefore a transient current is seen that requires nulling by a fast feedback amplifier.

6. Methods for analysing membrane mechanisms

6.1. The Ussing chamber

This consists of two independent half chambers which when joined seal an epithelium between them, creating an apical and basal bath in which recordings can be made of currents and voltage across the tissue (frog skin was the first to be investigated). The resistivity across the RPE is high ($\sim 2000\,\Omega\,cm^2$) because tight junctions between cells create an obstruction to the passage of most ions between the cells (Joseph and Miller, 1991). Consequently, (almost) all current must flow through apical and basal surfaces of the epithelial cells. To record the trans-epithelial resistance (TER) a 2-s pulse of 4–10 mV is applied across the tissue. The instantaneous current (I) is recorded and Ohm's law applied to give the TER. There is also a trans-epithelial potential (TEP), because apical and basal membranes have differing voltages (due to the different ionic channels they contain) and the $TEP = V_{Basal} - V_{Apical}$ (Levi and Ussing, 1949). The advantages of using an Ussing chamber are that the RPE retains its cell–cell contacts and the interactions between the RPE and the retina may be explored in detail. With specific drugs, the intracellular signalling pathways can be modified so that a detailed picture of RPE physiology can be constructed. Hans Ussing introduced the short-circuit procedure in which the TEP was held at zero volts by applying a current. When the ionic composition of the fluid on both sides of the epithelium is identical and there is no net voltage difference across it, then the electrochemical gradient across the apical and basal membranes must be the same. Therefore, any current and voltage changes across the preparation (or at either the apical or basal membranes) must be due to the active electrogenic transporters (Ussing, 1953; Ussing and Zerahn, 1951; Voûte and Ussing, 1968) (Fig. 3). The short-circuit current is therefore an indication of the contribution of active processes (transporters) to ion and water movement. In contrast, the open-circuit current is the current that results from the electrochemical driving forces across ionic channels plus a contribution from the active transporters.

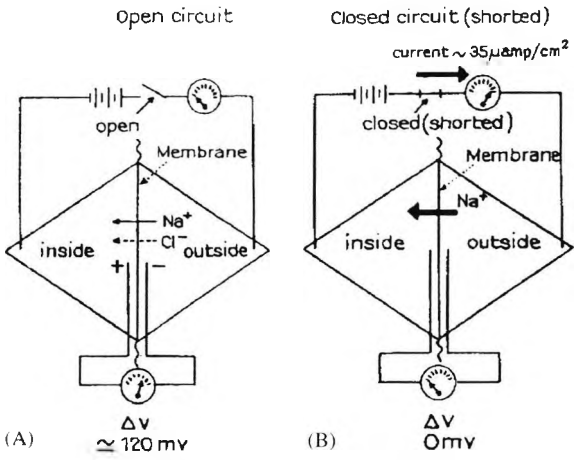

Fig. 3. Open- and closed-circuit recording in an Ussing chamber. In the open circuit a TEP is recorded that is due to the net difference between the voltages across apical and basal RPE membranes *plus* the voltage caused by any ionic current flowing extracellularly between the cells. In the short-circuit condition the TEP is held at zero by an applied current. When the apical and basal baths have identical ionic concentrations and the potential across the tissue is zero the electrochemical driving force upon sodium and potassium channels will be the same for both membranes and a negligibly small current should flow through such channels. However, the current resulting from active transport of ions will continue. This current is "backed off" by the applied current, and in RPE is the net efflux of Na^+ produced by the electrogenic Na–K–ATPase transporter. From Voûte and Ussing (1968). Reprinted with permission from the Journal of Cell Biology.

For work in mammalian RPE preparations at 37 °C, a modified Kreb's solution perfuses the apical and basal sides of the tissue. The chamber design allows for rapid changes of bath solution as well as the addition of agonists or inhibitors to investigate their effects on V_M (Miller and Steinberg, 1977a; Linsenmeier and Steinberg, 1983). Changes in the TEP can be caused by either alterations in V_{Basal} or V_{Apical}. A depolarisation of V_{Basal} causes the rise in the TEP observed in the light rise of the EOG (Gallemore and Steinberg, 1989b) and the c-wave of the ERG is associated with a hyperpolarisation of V_{Apical} (Oakley and Green, 1976).

The RPE can be modelled as an electrical circuit as in Fig. 4 (Miller and Farber, 1984). In the short-circuit state when the TEP = 0 mV, the resulting current is equal to i_{PUMP} and in bovine preparations this current is due to the active transport of Cl^- and HCO_3^- from the retinal to the choroidal surfaces and Na^+ in the opposite direction. Experiments in the open- and closed-circuit states using intracellular microelectrodes combined with radioactive flux measurements have shown how the changes in ionic fluxes accompany alterations in net fluid transport (Joseph and Miller, 1991; Kenyon et al., 1997; Miller and Edelman, 1990).

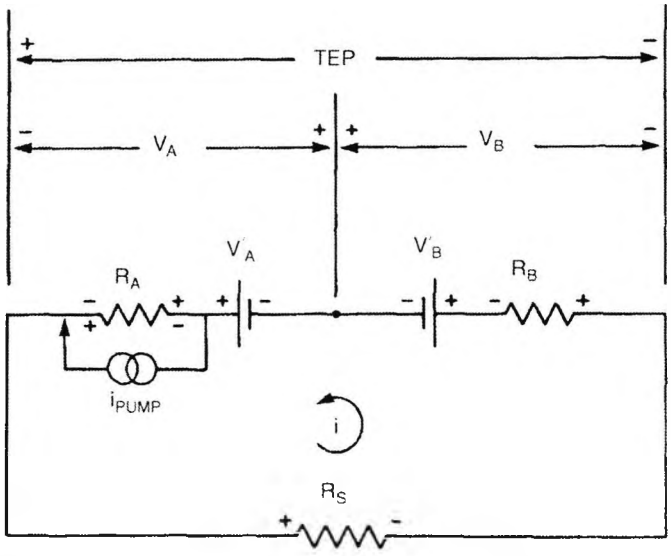

Fig. 4. The electrical circuit model of the RPE of Miller and Farber (1984) in which the apical and basal membranes are electrically coupled by a finite shunt resistance R_S that represents the paracellular resistance of the tight junctional complexes and edge tissue damage. The apical and basal membrane voltages (V_{Apical}) and (V_{Basal}) are represented by two batteries V_{Apical} and V_{Basal} in series with the apical and basal membrane resistances (R_{Apical}) and (R_{Basal}), respectively. At the apical membrane, an active transport current represented by i_{PUMP} is independent of membrane voltage. As the potential across the apical membrane is greater than that of the basal membrane (owing to the differences in ionic channels and conductances of each membrane) a shunt current (i) flowing from the apical to basal membrane, depolarises the apical membrane and hyperpolarises the basal membrane. Reprinted with permission of the Journal of General Physiology.

6.1.1. Fluid transport

Microelectrode studies of amphibian and mammalian RPE preparations have provided insights into the bulk movement of solutes and fluid. In light, the movement is from the subretinal space to the choroid (absorption) (Bialek and Miller, 1994; Edelman et al., 1994b; Hughes et al., 1984; Sellner, 1986; Tsuboi and Pederson, 1988) and in darkness the process reverses—from choroid to retina (secretion) (Edelman et al., 1994a, b). In mammalian, avian and amphibian species the apical membrane of the RPE contains the electroneutral Na–K–2Cl cotransporter, the Na–K–ATPase electrogenic pump and a large K^+ conductance (Miller and Edelman, 1990) that work together to control subretinal space and RPE cell-volume (Adorante, 1995; Adorante and Miller, 1990; Lin et al., 1992).

One method to determine the direction of ionic fluxes is to measure the net movement of trace amounts of radioactive isotopes from the apical to basal and basal to apical surface of the RPE mounted in an Ussing chamber in the open- and closed-circuit states. In the open circuit, the difference in unidirectional fluxes gives the net solute flux and the direction of fluid transport. In the closed-circuit state, the contribution to the ionic flux is that of the active transporters alone (Edelman et al., 1994a; Hughes et al., 1984; Miller and Farber, 1984; Rymer et al., 2001).

To record the minute volume changes over time, a rate of 4–6 $\mu l/h/cm^2$ (Hughes et al., 1984), a modified chamber was made from a water impermeable plastic in which each half chamber was sealed except for a small cannula that connected it to a vertical column of the bathing Kreb's solution. A capacitance probe was placed above each meniscus and as fluid flowed from either the apical or basal baths through the RPE the air gap above each meniscus changed and thus altered the capacitance as a direct function of fluid transport (Hughes et al., 1984; Miller et al., 1982; Peterson et al., 1997). For further details on these techniques see Gallemore et al. (1997) and Marmor (1990).

Application of ouabain to the apical but not basolateral membrane of frog RPE led to a rapid depolarisation of the apical membrane followed by a slower decrease in the TEP. This suggested that an apical Na–K–ATPase pump was present and potentially played a role in fluid regulation owing to its regulation of V_{Apical} (Miller et al., 1978; Miller and Steinberg, 1977a). However, later experiments showed that the Na–K–ATPase pump was not the main transporter involved with bulk fluid movement and in fact fluid transport was more sensitive to external HCO_3^- (Hughes et al., 1984). Furthermore, a role for intracellular second messengers such as cAMP was implicated as fluid absorption was reduced in its presence (Hughes et al., 1984, 1987, 1988). At the basolateral membrane a pH sensitive Cl^-–HCO_3^- antiporter was identified in frog that exchanged intracellular HCO_3^- for extracellular Cl^- (Lin and Miller, 1994). This system provided a means of coupling fluid transport to changes in pH_{in}. The TEP also provides a driving force for the passive transport of Na^+ ions via the paracellular pathway resulting in a net movement of NaCl

in light (Bialek and Miller, 1994; Tsuboi and Pederson, 1988). At the apical membrane, the increased HCO_3^- influx maintains V_{Apical} at a more hyperpolarised potential than V_{Basal} (Hughes et al., 1989).

In isolated frog eyecups, pH sensitive microelectrodes were used to record the changes in pH at different retinal depths in response to changes of light and dark. It was found that in light the pH of the subretinal space increased slightly (Borgula et al., 1989). This change could be attributed to either to a decrease in photoreceptor activity accompanying the decrease in dark current (Hagins et al., 1970) or a decrease in the activity of the apical $Na^+ \sim 2HCO_3^-$ cotransporter, leading to mild alkalisation of the subretinal space (Lin and Miller, 1991).

The direction of fluid transport is largely determined by alterations in subretinal $[K^+]_{out}$ (Oakley, 1983; Oakley and Green, 1976; Oakley and Steinberg, 1982). In darkness photoreceptors are active, and sodium flows into the outer limbs. It is expelled by a Na–K–ATPase exchange pump in the inner limb. Therefore a "dark current" circulates along the rod axis. In light, the outer limb sodium channels close, and the rod hyperpolarises. The pump continues for some time, depleting the subretinal space of potassium (Brown and Pinto, 1974; Korenbrot and Cone, 1972; Penn and Hagins, 1969; Sillman et al., 1969; Toyoda et al., 1969). This causes a hyperpolarisation of the apical RPE membrane that is one component of the c-wave of the ERG. The apical membrane potassium channel, the electroneutral Na–K–2Cl cotransporter and the electrogenic $Na^+ \sim HCO_3^-$ cotransporter respond to changes in subretinal $[K^+]_{out}$. When the dark current is present and the subretinal $[K^+]_{out}$ is ~5 mM then V_{Apical} is largely maintained by the potassium concentration gradient across it, and under these conditions, the $Na^+ \sim HCO_3^-$ cotransporter is active passing sodium and bicarbonate into the cell down the favourable electrochemical gradient: the sodium is then pumped out again, in exchange for potassium (there is also an apical Na^+–H^+ that also regulates pH_{in} (Lin et al., 1992; Zadunaisky et al., 1989). The net result is a mild alkalinisation of the RPE cytosol. This elevated pH_{in} stimulates the *basolateral* Cl^-–HCO_3^- exchanger which causes an enhanced basal flux of Cl^- into the RPE. Chloride ions then exit through the apical membrane (la Cour, 1991a, b). Light onset results in decreased potassium in the subretinal space and therefore the apical surface of the RPE hyperpolarises. The hyperpolarisation reduces the entry of negative ions like HCO_3^- into the RPE, (Oakley, 1977) resulting in a decrease of pH_{in} and a decrease in the exchange rate of the basolateral Cl^-–HCO_3^- (Tsuboi and Pederson, 1988; Bialek and Miller, 1994). This explains how changes in retinal illumination alter the direction of fluid transport (Edelman et al., 1994a, b; Lin and Miller, 1991, 1994). See Fig. 5 which represents work mainly on amphibian RPE preparations. For further reviews of RPE fluid transport and the equivalent circuit derivations, see Gallemore et al. (1997) and Steinberg et al. (1983, 1985).

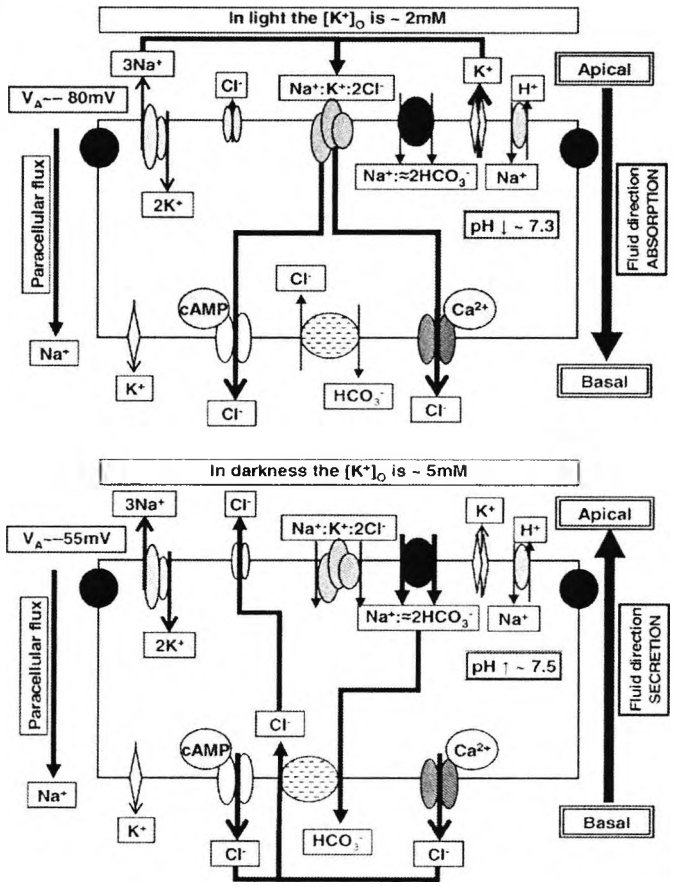

Fig. 5. Schematic representations of the ionic fluxes in the RPE during light (top) and in dark (bottom). In light, there is steady state absorption of fluid and salts from in the retina to choroid maintained by the apical active Na–K–ATPase pump that extrudes Na^+ against its electrochemical gradient. Arrows approximate the relative contribution of each channel to ionic fluxes. The apical Na–K–2Cl cotransporter uses the energy from the Na^+ gradient to return Cl^- into the cell against its electrochemical gradient. At the basolateral membrane, Cl^- leaves via chloride channels (two types are shown in the diagram). *In light*, the intracellular pH is ≈7.3 because the apical membrane Na^+–H^+ antiporter exchanges sodium for hydrogen ions, and the influx of HCO_3^- decreases as the apical membrane hyperpolarises creating an unfavourable electrochemical gradient for HCO_3^-. *In darkness*, when the rod dark current is restored there is a rise in subretinal $[K^+]$ and the apical membrane depolarises. This apical depolarisation then increases the influx of sodium and bicarbonate by the $Na^+ \sim 2HCO_3^-$ cotransporter and as a result the cell interior alkalises to pH ≈7.5. The elevated intracellular $[HCO_3^-]$ then activates the basolateral Cl^-–HCO_3^- antiporter that reverses the direction of net fluid movement from absorption to secretion by returning Cl^- ions back to the subretinal space. Figure based upon those of Hartzell and Qu (2003), Quinn and Miller (1992).

Whilst the Ussing chamber and intracellular recordings provided valuable insights into the mechanisms involved in regulation of cell pH, the volume of the subretinal space and the principal transporters involved in these activities, the underlying kinetics and properties of these ionic channels required a different technique that enabled recordings to be made from single cells and isolated populations of ionic channels in which the intra and extracellular environment can be controlled.

6.2. Patch clamp

Hodgkin's and Huxley's work on the squid giant axon enabled them to record membrane voltage and current, and also to control both the internal and external ionic composition. This was not possible with *small* cells until the development of the patch clamp technique (Hamill et al., 1981; Hamill and Sakmann, 1981; Neher and Sakmann, 1976; Neher et al., 1978; Sigworth and Neher, 1980). A glass micropipette with a tip diameter of 0.5–1 μm is heated (fire polished) in a microforge until its tip is smooth. It is filled with a solution that mimics the intracellular ionic composition and then advanced to the cell membrane, which adheres to the glass so that the resistance between the interior of the pipette and the extracellular fluid rises to $>100\,M\Omega$. If suction is applied to the pipette, the resistance may rise to 10^9–$10^{11}\,\Omega$. This is known as the *cell-attached* configuration. A second (reference or bath) electrode is placed in the bath surrounding the cell: usually it is a Ag/AgCl pellet connected via an agar–salt bridge.

If the cell membrane in the microelectrode tip contains channels or other ionic transporters the resistance of the patch is less than between microelectrode and the bath. The total membrane resistance of the rest of the cell is very much lower, and therefore the voltage between microelectrode and bath approximates to the membrane voltage minus a liquid junction potential between microelectrode tip and bath fluid (due to the different ionic compositions) that must be determined experimentally or calculated (Barry and Lynch, 1991; Neher, 1992; Ng and Barry, 1994). Any small current flowing causes a relatively large voltage change inside the patch electrode. Thus the current of single channels can be monitored.

When V_M is held or clamped at a range of hyperpolarising and depolarising voltages for 50–250 ms the membrane current changes and stabilises, and after 1–2 s another "holding potential" can be applied. Software does this automatically and provides a plot of the *I–V* curve. The slope indicates the instantaneous conductance at each of the voltage steps. An ion channel giving a simple linear current/voltage relationship over the entire range of membrane voltage has an Ohmic *I–V* curve. An example of such an ionic channel is the cystic fibrosis transmembrane conductance regulator (CFTR) (Riordan et al., 1989; Rommens et al., 1989) located at the apical and basal membranes of foetal RPE (Blaug et al., 2003). Rectifying channels have non-Ohmic *I–V* curves. An inward rectifying channel is one in which a hyperpolarising voltage produces a greater inward current than the outward current produced by an equivalent depolarising step. Therefore, in such an *I–V* curve the slope is greater at membrane voltages more negative than the resting membrane voltage. An example is the K^+_{Vir} channel found in the apical membranes of the RPE (Hughes and Takahira, 1996). The outward rectifying currents have the reverse characteristic. The conductance increases for depolarising membrane steps more than it decreases for hyperpolarising voltages steps. An example is the K^+ outward rectifier identified in human (Hughes et al., 1995) and bovine RPE (Takahira and Hughes, 1997).[3]

7. Origins of the light rise

The slow rise in the TEP in animal preparations is related to the light rise in the human light-EOG. It is caused by a depolarisation of the basal membrane of the RPE, so the net difference between basal and apical membrane voltages increases. This slow rise must be produced by a "second messenger" within the cytosol of the RPE. Therefore, for the light rise the entire sequence must be that the retina liberates a chemical (referred to as the "light substance") that, binding to a receptor in the apical membrane of the RPE, liberates an internal "second messenger". The second messenger causes the increase in basal Cl^- conductance. The light-EOG is shown in Fig. 1.

[3]Once a GΩ seal is formed in the *cell-attached* mode there are several possible manipulations of the cell membrane in which to explore the ionic channels and their properties (Hamill and Sakmann, 1981; Hamill et al., 1981). In whole cell recordings suction is applied to the microelectrode to break the patch, which then makes a low-resistance pathway to the cell interior. Then, in small cells the total average response of all the ionic channels in the cell membrane can be recorded. However, cytosolic signalling molecules are diluted by mixing with the solution in the micropipette, and the pipette solution cannot be easily modified (Lapointe and Szabo, 1987; Soejima and Noma, 1984; Tang et al., 1990).

The *perforated whole cell* configuration better maintains intracellular contents. The micropipette contains nystatin (Horn and Marty, 1988) or amphotericin B (Rae et al., 1991). These substances form small pores within the cell membrane through which large molecules and organelles cannot pass. This configuration that has been widely used to examine the currents in amphibian, mammalian and cultured RPE cells (Hartzell and Qu, 2003; Hughes and Segawa, 1993; Hughes and Steinberg, 1990; Hughes and Takahira, 1998; Mergler et al., 1998; Rosenthal and Strauss, 2002; Sheu and Wu, 2003; Strauss et al., 1993, 1997, 1999, 2000; Strauss and Wienrich, 1993, 1994; Takahira and Hughes, 1997; Ueda and Steinberg, 1994, 1995; Valtink et al., 1999; Wen et al., 1993, 1994; Weng et al., 2002; Wills et al., 2000). Manipulation of the pipette and bath solutions can be used to isolate specific ionic currents in the whole cell. For example, addition of $BaCl_2$ to the bath solution will intensify Ca^{2+} currents and the addition of CsCl and tetraethylammonium inhibits K^+ currents (Ueda and Steinberg, 1993, 1995).

Alternative configurations can be made once the seal has been established. In the *inside-out* configuration after the patch has formed, the pipette is withdrawn, so that the membrane is torn from the cell. The bath fluid becomes equivalent to the intracellular environment and can be modified (Hamill and Sakmann, 1981; Hamill et al., 1981). The small excised patch contains only a few channels and when these open and close large proportionate changes in total membrane conductance occur. Therefore, the characteristics of the ionic channels can be investigated fully.

Once the microelectrode has made contact with the surface of the cell, suction applied slowly allows the cell membrane to balloon into the tip. Eventually the tip becomes sealed in such a way that the inside of the cell membrane faces the pipette solution. The pipette is then withdrawn, and separated from the rest of the cell membrane. The outer membrane surface now faces the bath forming the *outside-out* configuration. Direct activation of ionic channels by agonists added to the bath is made easier but this configuration is difficult to achieve unless the cell is attached firmly so that enough force can be applied to remove the patch from the cell membrane (Hamill and Sakmann, 1981; Hamill et al., 1981).

The most notable contributions are by Roy Steinberg and Sheldon Miller and their collaborators (Bialek et al., 1995; Gallemore et al., 1988; Gallemore and Steinberg, 1989a, b, 1993; Griff and Steinberg, 1982, 1984; Joseph and Miller, 1991; Linsenmeier and Steinberg, 1982, 1983, 1984; Oakley and Steinberg, 1982; Valeton and van Norren, 1982).

7.1. *What cells initiate the response?*

Griff and Steinberg (1982), Linsenmeier and Steinberg (1982), Valeton and van Norren (1982) used a combination of intra-retinal microelectrodes, combined with reference electrodes sited in the subretinal space or retro-ocularly, to prove that the light rise originated in the RPE (see Fig. 6). Previously it had been supposed that much of the voltage change could develop in the retina. The mechanism of production was investigated by measuring the spectral sensitivity of the process. There was a simple relationship

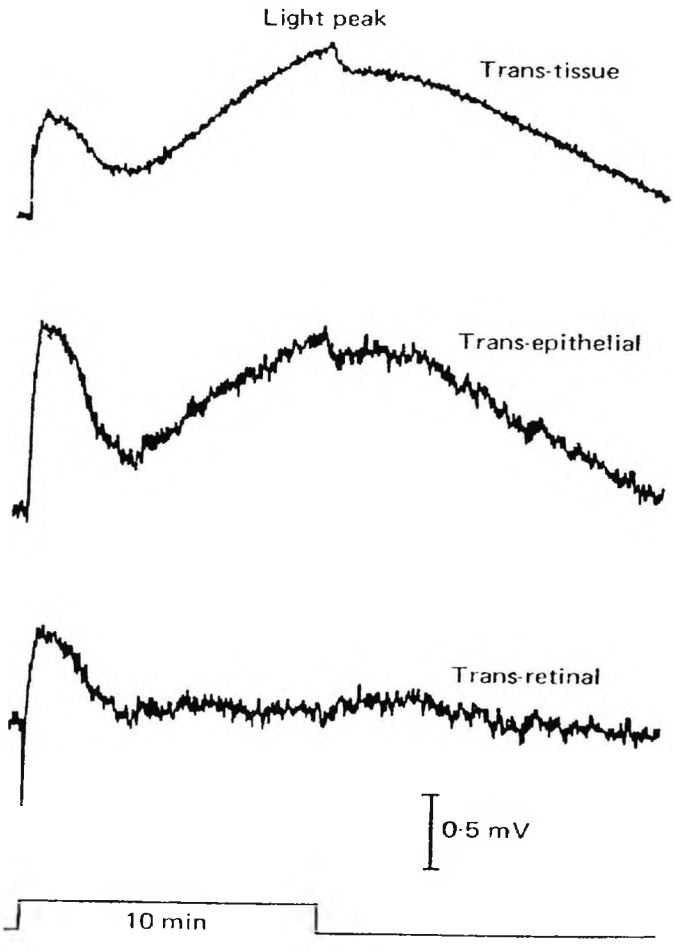

Fig. 6. Intracellular microelectrode recordings from the RPE in a retina–RPE preparation of Gecko. Voltages across the apical and basal faces of the RPE are recorded separately by extracellular electrodes placed in the subretinal space or in choroidal side of the RPE. These electrodes also recorded the TEP. The light rise potential develops across the RPE (middle trace) with no contribution to the potential by the retina (lower trace). From Griff and Steinberg (1982). Reprinted with permission of the Journal of Physiology.

to light intensity, and blue green light being most effective, showing that the light that was being absorbed by the rods. Similar results in man had been described by Arden and Kelsey (1962b). But how then could the rods influence the RPE? Steinberg noted that the change in the RPE was dependent on stimulus area (Linsenmeier and Steinberg, 1982). The obvious explanation was that some substance generated by light, moved from the rods to the RPE: the concentration depended upon the light intensity, and also upon whether the substance could diffuse away into unilluminated portions of the subretinal space. Such experiments did not prove that the light rise substance was generated in photoreceptors: the light rise might be produced as a post-synaptic result of rod activity, as was proposed by Gouras and Gunkel (1963), who found that in central retinal vein occlusion, the light-EOG was reduced. However, Gallemore et al. (1988) showed that when postreceptoral activity was blocked the light rise was unaffected thereby demonstrating that the light rise substance, however it was generated, was released by the rods. The absence of the light rise in patients with early retinal dystrophies also provides evidence that the light rise substance is generated in rods (Arden, 1962).

7.2. *RPE involvement and the basolateral membrane*

In order to quantify the contribution of the apical and basal membranes to the EOG as well as the role of the neural retina in the generation of the light rise, preparations of intact RPE–retina were mounted in modified Ussing chambers. The resistance across the tissue fell during the light peak. By introducing a microelectrode into the RPE it was possible to record V_{Basal} and V_{Apical} differentially by referencing the intracellular electrode to the basal and apical bath electrodes, respectively. Griff and Steinberg (1982) were able to show that during the light peak, net membrane voltage decreased, but the basal membrane depolarised more than the apical membrane, increasing the TEP. However, these observations did not prove which membrane caused the light rise. Griff and Steinberg (1982), Linsenmeier and Steinberg (1983) passed current pulses between apical and basal electrodes while monitoring the membrane voltage changes caused across each membrane (ΔV_{Apical} and ΔV_{Basal}). Some of the injected current passes via the paracellular pathway in parallel to the membranes and so the absolute values of the resistance of apical and basal membranes could not be determined. Instead, the ratio of the resistances (the a-value) was obtained (Eq. (5)).

$$a = \Delta V_{\text{Apical}}/\Delta V_{\text{Basal}} = R_{\text{Apical}}/R_{\text{Basal}} \quad (5)$$

when the a-value is taken together with the changes in total tissue resistance then it is possible to determine at which membrane the greatest change in resistance occurs. In lizard (Griff and Steinberg, 1982), cat (Linsenmeier and Steinberg, 1983) and chick (Gallemore et al., 1988; Gallemore and Steinberg, 1989b, 1991), V_{Basal} depolarises

in response to light with a rise in conductance, but the voltage change across the apical membrane was not accompanied by a change of conductance. Today it is technically possible to measure the paracellular resistance directly, without the contribution of "edge effects" (Gitter et al., 1997).

7.3. Chloride channels

The depolarisation of the basal membrane could be achieved either by a negative ion exiting the cell or a positive ion entering the cell. Evidence that the light rise was mediated by an increase in basolateral Cl^- conductance was shown when four Cl^- channel blockers all abolished the light rise in chick (Gallemore and Steinberg, 1989b). Furthermore, Cl^- sensitive microelectrodes inserted into chick RPE showed a decrease in the intracellular Cl^- activity that matched the light rise (Gallemore and Steinberg, 1993). Therefore, negative Cl^- ions leaving through the basolateral membrane must cause the light rise. From this it follows that the light rise substance must initiate the release of some second messenger within the RPE that in its turn modulates basolateral membrane Cl^- conductance.

However, the identity of the Cl^- channels responsible for the EOG and FOs has not been fully resolved, but with the advent of new compounds that are able to selectively block chloride channels, this should soon be accomplished. It should be noted that different species might have different types of Cl^- channel, which may not all respond in the same way to the second messengers. Another issue is the role of calcium in regulating the basolateral Cl^- currents that cause the light rise Hofmann and Niemeyer (1985) showed that the light rise was reduced by an increase of $[Ca^{2+}]_{out}$ and so Ca^{2+} is presumed to play some role in initiating the light rise. CFTR is not directly affected by Ca^{2+} and as the amplitude of the light rise is normal in cystic fibrosis (CF) this Cl^- channel is not thought to be directly involved in the light rise (Miller et al., 1992; Lara et al., 2003). It is likely that the Cl^- channel responsible for the light rise is gated by Ca^{2+} and current evidence suggests that bestrophin is the channel responsible (see below).

8. Signalling pathways

The study of fluid transport in Ussing chambers along with microelectrode recordings and patch clamp experiments has yielded a large understanding of the ionic currents found within the RPE (Gallemore et al., 1997). Regulation of the ionic channels and gating by second messengers is fundamental to the generation of the light-EOG and FOs and so we will briefly outline the key signalling pathways and messengers that are involved in ionic channel gating. For a detailed review of second messenger signalling pathways in the RPE see Nash and Osborne (1996).

8.1. G-proteins

One way in which a cell communicates with the external environment is via special membrane-spanning proteins that combine with particular chemicals (ligands) in the extracellular fluid. The communication is via an enzyme cascade that amplifies the signal. The intracellular terminals are associated with specialised *G*-proteins, (often distinguished by a subscript, e.g. G_s or G_q) which dissociate from the receptor when it binds to the extracellular signal. The receptor binds extracellularly, often to a single ligand which can be an ion, organic odorant, amine, peptide, protein, lipid or nucleotide. In the olfactory receptors in the nose, the receptor binds to odoriferous substances (Breer, 2003) and in the photoreceptor, rhodopsin, the receptor molecule, absorbs a photon of light. The first suggestion that a conformational change in a protein could lead to a sequence of biochemical changes in the eye was due to Wald (1968), who postulated that the cis–trans isomerisation of rhodopsin by a photon could initiate phototransduction. The binding of the ligand to the receptor initiates the first enzymic step, the activation of *G*-proteins (for review see Kristiansen (2004)) which consist of heterotrimeric isomers (proenzymes) ($G_{\alpha\beta\gamma}$) (Cabrera-Vera et al., 2003; Gilman, 1987; Pierce et al., 2002) that dissociate into G_α and $G_{\beta\gamma}$ complexes. The dissociated fragments are active enzymes, which are capable of acting synergistically or as antagonists to rapidly alter the activity of ionic channels and intracellular signalling molecules. For example, G_s is coupled to the β-adrenergic receptor which when stimulated causes its dissociation into an active enzyme, whose function is to transform another proenzyme, membrane bound adenylate cyclase (AC) (Rodbell et al., 1971) into a fully active enzyme that forms cAMP utilising ATP as a substrate (Friedman et al.,1987). Generation of cAMP then activates protein kinase-A (PKA) that is able to phosphorylate proteins and ionic channels and thereby modulate their function (Anderson et al., 1991c). Another example is photoexcited rhodopsin which complexes with the *G*-protein (transducin) that then activates membrane bound phosphodiesterases. The latter catalyses the hydrolysis of cyclic guanosine monophosphate (cGMP) to GMP which closes down outer segment cation channels (Fung et al., 1981; Fung and Stryer, 1980).

A different but equally important intracellular transduction pathway is provided by G_q which activates phospholipase C-β (Smrcka et al., 1991) through hydrolysis of the plasma membrane phospholipid phosphatidylinositol-4,5-bisphosphate, (Mitchell, 1982a, b) into inositol 1,4,5-triphosphate (IP_3) and diacylglycerol (DAG) which then act as second messengers to raise $[Ca^{2+}]_{in}$ which then modulates the activity of ionic channels either directly or through the activation of protein kinase-C (PKC). The conductance of some ionic channels changes when they are phosphorylated by PKC (Strauss et al., 1997). IP_3 binds to a receptor on the endoplasmic reticulum (ER) to release intracellular Ca^{2+} (see below). DAG is also involved in the

release of the polyunsaturated fatty acid arachidonic acid from the plasma membrane which is metabolised into second messengers (Piomelli and Greengard, 1990; Shimizu and Wolfe, 1990; Sigal, 1991).

8.2. *Protein tyrosine kinases*

One additional means of ionic channel control is through protein tyrosine kinases (PTKs) that are membrane-bound proteins that act as enzymes by directly phosphorylating tyrosine residues in intracellular target proteins after extracellular activation by growth factors such as epidermal growth factor, insulin or pigment-derived growth factor (Glenney, 1992; Schlessinger and Ullrich, 1992). Integration of PTKs and *G*-protein signalling pathways provides an alternative means by which *G*-protein activation and signalling pathways can interact with PTKs to modulate cell physiology (Waters et al., 2004). Of interest in this review are the non-receptor tyrosine kinases that belong to the *src* protein family and lack an extracellular binding domain but retain an intracellular tyrosine kinase catalytic domain. These PTKs also play a role in the regulation of Ca^{2+} channels and homeostasis and will be discussed later (Strauss et al., 1997, 2000; van der Heyden et al., 2005).

9. Ionic channels of the RPE involved in the EOG

9.1. *The calcium activated chloride channel*

A rise in intracellular calcium $[Ca^{2+}]_{in}$ is believed to generate the light rise by gating open a basolateral calcium-activated chloride channel (CaCC). It should be noted that evidence for Ca^{2+} being the intracellular second messenger is indirect, and based upon normal light rises in CF with abnormal FOs (Lara et al., 2003; Miller et al., 1992). In the artificially perfused cat eye a reduction in the light rise occurs when extracellular $[Ca^{2+}]$ is increased, although the FOs and c-wave are unchanged (Hofmann and Niemeyer, 1985). The abnormal FOs in CF implicates cAMP and CFTR in the generation of this response. Therefore, the presence of a normal light rise in CF suggests the ionic mechanisms are different for the FOs and light rise (Blaug et al., 2003). Furthermore, the FOs are normal in Best's with a reduction in the light rise which further suggests that the light rise and FOs have a different underlying mechanism with presumably different basolateral ionic channels responsible (Weleber, 1989). (See below for the differential effect of abnormalities of bestrophin on the light rise and FOs for additional evidence).

CaCCs were first identified in *Xenopus* oocytes where a rise in $[Ca^{2+}]_{in}$ following fertilisation led to a depolarisation of the oocytes that prevented further entry of sperm (Barish, 1983; Miledi, 1982). CaCC is crucial for fluid regulation in the RPE (Peterson et al., 1997; Rymer et al., 2001) as it is in the genesis of many other secretions such as saliva (Melvin et al., 2005) and tears (Mircheff, 1989). A partially inhibitable CaCC current by 4,4′-diisothiocyanostilbene-2,2′-disulphonic acid (DIDS) was first identified in neo-natal rat RPE (Ueda and Steinberg, 1994). However, these currents were short-lived and not always recordable indicating that they were probably dependent upon a compound that was lost during the whole-cell recordings (Botchkin and Matthews, 1993).

In cultures of normal rat RPE, the CaCC currents were stimulated by release of Ca^{2+} from the ER stores via IP_3. To avoid depletion of calcium stores in rat RPE, PTKs initiate an influx of Ca^{2+} from the extracellular space via a voltage gated L-type Ca^{2+} channel which is described below (Strauss et al., 1997, 1999).[4] CaCC currents have been reported in *Xenopus* but display different activation and kinetics (Hartzell and Qu, 2003; Strauss et al., 1999). CaCCs are also sensitive to pH_{in} and may help to buffer extracellular acidification by HCO_3^- conductance (Zhang et al., 1992).

Bovine and human foetal RPE monolayers mounted in Ussing chambers all show an increased basolateral Cl^- conductance following elevation of $[Ca^{2+}]_{in}$ provoked by adrenergic agonists, epinephrine and isoprotenerol (Quinn et al., 2001; Rymer et al., 2001), synthetic or ATP purinergic agonists (Maminishkis et al., 2002; Peterson et al., 1997), and the non-steroidal anti-inflammatory drug, niflumic acid (but not flufenamic acid) (Bialek et al., 1996). Whether Ca^{2+} binds directly to the protein or acts via calmodulin-dependent protein kinase remains to be determined. All these agents stimulate a DIDS-sensitive increase in basolateral Cl^- conductance. The Cl^- channel blockers available show some tissue specificity, with glibenclamide and flufenamic acid showing no inhibition of CaCC and CFTR in rat cerebral arteries (Doughty et al., 1998). Generally, the permeability sequence of CaCC obtained from smooth muscle, endothelial cells, lacrimal glands and *Xenopus* oocytes is $SCN^- > NO_3^- > I^- > Br^- > Cl^- > F^-$ (Cornejo-Perez and Arreola, 2004; Evans and Marty, 1986; Large and

[4]In the RCS rat (Bourne et al., 1938; Bourne and Gruneberg, 1939) where the RPE fails to phagocytose rod outer limbs and a retinal degeneration results, it has been shown that this calcium channel is abnormal (Edwards and Szamier, 1977; Gal et al., 2000). Its regulation is altered allowing a greater inward Ca^{2+} current (Strauss and Wienrich, 1993). This may be an important cause of the inability to phagocytose rod outer segments (Hall et al., 1991, 2002; Heth et al., 1995; Mergler et al., 1998; Rodriguez de Turco et al., 1992; Salceda, 1992). The chloride channel blockers, niflumic and flufenamic acid, and DIDS and SITS all modify the kinetics of voltage gated K^+ channels in myocytes (Wang et al., 1997). Mefenamic and flufenamic acids also activate a K^+ conductance in smooth muscle cells of the gut (Farrugia et al., 1993). Flufenamic and niflumic acids also activate large-conductance Ca^{2+}-gated K^+ channels (Gribkoff et al., 1996; Ottolia and Toro, 1994) and these drugs blockers also inhibit nonselective cation channels (Chen et al., 1993; Gogelein et al., 1990). In mast cells separate membrane Ca^{2+} and Cl^- currents were inhibited by DIDS whilst only the Cl^- current was inhibited with niflumic acid (Reinsprecht et al., 1995). The interactions of the various Cl^- channel blockers with other ionic channels has made interpretations of Cl^- channel function difficult and often high doses of these drugs are required to have an effect (Frings et al., 2000; Hartzell et al., 2005a; Jentsch et al., 2002; Qu and Hartzell, 2000).

Wang, 1996; Nilius et al., 1997; Qu and Hartzell, 2000). This is the same as the sequence for bestrophin (Qu et al., 2004) which also generates calcium-dependent Cl^- currents (Qu et al., 2003; Sun et al., 2002; Tsunenari et al., 2003).

9.2. Bestrophin—a CaCC?

Best's vitelliform macular dystrophy is an inherited autosomal dominant disease with a variable age of onset from childhood to adulthood (Renner et al., 2005) and is characterised by a central vitelliform (poached egg) lesion at the macula. The retina over the lesion becomes damaged, leading to loss of visual acuity. However, the underlying fundamental process is found throughout the entire retina because the light rise of the EOG is absent (Barricks, 1977; Cross and Bard, 1974; Deutman, 1969; Francois et al., 1967; Renner et al., 2005; Thorburn and Nordstrom, 1978).[5]

The gene responsible for Best's (VMD2) has been identified (Forsman et al., 1992; Marchant et al., 2001; Marquardt et al., 1998; Petrukhin et al., 1998; Stöhr et al., 2002; Stone et al., 1992; White et al., 2000; Yoder et al., 1988). It codes for a protein, designated bestrophin, which is specifically expressed in the basal surface of the human, porcine and macaque RPE (Marmorstein et al., 2000). Cultured foetal human RPE cells express bestrophin when grown in specifically defined medium (Hu and Bok, 2001) while the human ARPE-19 (Dunn et al., 1996) and D407 (Davis et al., 1995) and rat (RPE-J) (Nabi et al., 1993) RPE cell lines are positive at the messenger level for bestrophin. The protein was not detected using western blots in these cell lines (Marmorstein et al., 2000).

Bestrophin was predicted to form an ionic exchanger based upon the amino acid sequence (Gomez et al., 2001). Transfection of one of several isoforms of human bestrophin (hBest1) into cell lines demonstrated anionic currents with mutant bestrophin inhibiting wild-type bestrophin currents that were activated by $[Ca^{2+}]_{in}$ (Qu et al., 2003, 2004; Sun et al., 2002; Tsunenari et al., 2003). Hartzell et al. (2005a, b) demonstrated that site-directed mutagenesis of bestrophin pores altered their SCN^- conductance. Expression of mouse bestrophin (mBest2) into mammalian cell lines also demonstrated that the product of mBest2 formed a Cl^- channel whose permeability and anion selectivity could be altered by mutations that strongly suggested that bestrophin was a Cl^- channel (Pusch, 2004; Qu and Hartzell, 2004).

[5]There are a few caveats to be made: Whilst similar lesions occur in 'pseudovitelliform dystrophy' there is no significant reduction in the light-EOG (Epstein and Rabb, 1980; Kingham and Lochen, 1977; Marmor, 1979; Sabates et al., 1982; Theischen et al., 1997). Furthermore, some individuals with VMD2 and vitelliform lesions have normal light-EOGs (Pollack et al., 2005). Histopathological studies in Best's reveal abnormalities of the RPE, neovascularisation, photoreceptor degeneration and accumulation of lipofuscin and melanolipofuscin but these do not pinpoint the fundamental cause of the disease (Frangieh et al., 1982; O'Gorman et al., 1988; Weingeist et al., 1982).

Two human bestrophin homologues investigated (hBest1 and hBest2) have different permeability sequences. They show a high permeability for NO_3^- that suggests bestrophin is also permeable to bicarbonate ions (Sun et al., 2002). *I–V* curves for four human bestrophin proteins have different characteristics with hBest2 and hBest4 being almost linear and hBest3 shows strong inward rectification and hBest1 has moderate outward rectification (Sun et al., 2002; Tsunenari et al., 2003).

The way bestrophin might regulate the light rise is not completely determined (some bestrophin mutations can produce phenotypes that are different to classical Best's disease). In addition to the calcium activation described above, there are also phosphorylation sites that may regulate gating (Marmorstein et al., 2002). In one study mutant versions of bestrophin were expressed in basal membrane of RPE following subretinal injections of an adenovirus vector into rats. The authors found that while wild type increased the light rise, the constructs from Best's (W93C and R218C) selectively reduced (and changed the time course of) the light rise, and could thus serve as a model for Best's disease. There were no significant effects on the FOs or ERG components, but detailed analysis of the sensitivity to light revealed some differences between the rat model and human patients (Marmorstein et al., 2004). The likely candidate for the light rise Cl^- channel is bestrophin. Two bestrophin genes cloned into *Xenopus laevis* oocytes express Ca^{2+}-activated Cl^- currents (Qu et al., 2003, 2004; Qu and Hartzell, 2004).

The molecular identity of this "ionic channel" is unknown despite the fact that the basic voltage dependence, anion selectivity and kinetics of this family of channels has been described (Eggermont, 2004; Qu et al., 2003). Recent evidence suggests that bestrophin regulates Ca^{2+} entry into the RPE via an L-type Ca^{2+} channel (Rosenthal et al., 2005; Strauss and Rosenthal, 2005) and this mediated influx of Ca^{2+} may act directly upon bestrophin or a separate CaCC to increase basolateral Cl^- conductance. There are reports of normal light rises in Best's which further complicate this issue (Lorenz and Preising, 2005; Pollack et al., 2005). This issue will finally be resolved with the demonstration that the light rise is absent in a knock-out animal model of Best's. However, the animal studies to date support the model in which bestrophin is the basolateral Cl^- channel responsible for the light rise (Hartzell et al., 2005b; Marmorstein et al., 2000, 2004; Pinckers et al., 1996; Ponjavic et al., 1999; Pusch, 2004; Qu et al., 2003, 2004). Recent evidence suggests that bestrophin also plays a role in volume regulation with decreasing current in response to hyperosmotic solution (Fischmeister and Hartzell, 2005).

For further reviews on the molecular identity and electrophysiology of Cl^- channels, see Begenisich and Melvin (1998), Fuller and Benos (2000), Hartzell et al. (2005a, b), Jentsch et al. (2002), Nilius and Droogmans (2003), Pusch (2004).

10. Calcium channels of the RPE

Calcium plays an important role in intracellular signalling sequences (second messengers). In cultures of human RPE a variety of peptides, growth factors, amino acids and agonists have been shown to elevate $[Ca^{2+}]_{in}$ via IP_3 generation and release of intracellular Ca^{2+} stores (Ammar et al., 1998; Feldman and Randolph, 1993; Fragoso and Lopez-Colome, 1999; Kuriyama et al., 1991, 1992; Quinn et al., 2001). In addition, Ca^{2+} is required for binding and ingestion of outer rod segments in cultured rat RPE cells and together with PKC plays a role in inhibiting phagocytosis (Hall et al., 1991, 2001, 2002). Thus Ca^{2+} homeostasis is vital for the RPE and the regulation of free cytosolic $[Ca^{2+}]_{in}$ is the responsibility of channels, pumps and transporters located on the plasma membrane and intracellular organelles. Resting cytosolic free $[Ca^{2+}]_{in}$ in human cell cultures is estimated to be ~70–200 nM (Feldman and Randolph, 1993; Feldman et al., 1991; Kuriyama et al., 1991, 1992) which is significantly lower than the millimolar extracellular concentration. However, the total $[Ca^{2+}]_{in}$ in the RPE cell is higher due to storage in both the ER and in melanosomes (Hess, 1975; Salceda and Riesgo-Escovar, 1990; Salceda and Sánchez-Chávez, 2000). Ion selective microelectrode recordings in isolated cat RPE–retina show that the $[Ca^{2+}]_{out}$ in the subretinal space decreases during illumination with the restoration depending upon the RPE (Gallemore et al., 1994; Livsey et al., 1990). Concurrently, the volume of the subretinal space increases and during darkness must be reduced, a process critically dependent upon $[Ca^{2+}]_{in}$ (Li et al., 1994a, b). The sequence appears to be that the rise in the volume of the subretinal space deforms the RPE's membrane which leads to "Ca^{2+} signalling" via gap-junctions in normal rat RPE cell cultures. It is of interest that in the Royal College of Surgeon's (RCS) rat RPE cultures (Himpens et al., 1999; Stalmans and Himpens, 1997) such signalling is reduced. Elevation of $[Ca^{2+}]_{in}$ stimulates fluid transport from the subretinal space by increasing basolateral Cl^- transport (Maminishkis et al., 2002; Mitchell, 2001; Peterson et al., 1997; Rymer et al., 2001). For further reviews on Ca^{2+} channels in the RPE, see Rosenthal and Strauss (2002).

10.1. Na^+/Ca^{2+}-exchanger and Ca^{2+}-ATPase pump

Efflux of Ca^{2+} from the cytosol is in part accomplished by utilising the favourable high extracellular Na^+ concentration maintained by the Na–K–ATPase exchanger. The sodium–calcium exchanger (NCX) was first identified in heart (Reuter and Seitz, 1968) and the squid axon (Baker et al., 1969). Three members of this family have been identified. NCX1 is expressed ubiquitously and transports 3 Na^+ for 1 Ca^{2+} while NCX2 and NCX3 are limited to brain and skeletal muscle. An NCX was identified in the apical membrane fraction of bovine and fish RPE cells and is inhibited by bepridil (Fijisawa et al., 1993). One proposed function of the NCX is the regulation of Ca^{2+} concentration in the subretinal space following light onset. In man, cardiac NCX1 is present in both retina and RPE although localisation to the apical or basal membranes in the RPE was not possible (Loeffler and Mangini, 1998; Mangini et al., 1997). This exchanger is extremely fast and efficient and in heart muscle is responsible for the ending of contraction by reducing cytosolic calcium. In the RPE it could cause equally important and rapid changes, particularly since the RPE expresses voltage-dependent Ca^{2+} channels, but to date there have been no further studies investigating the its role in the RPE despite its role in Ca^{2+} homeostasis.

Another mechanism that moves calcium across the plasma membrane is the (Ca^{2+}–Mg^{2+})-ATPase pump (PMCA) (Kennedy and Mangini, 1996). PMCA hydrolyses ATP to actively transport Ca^{2+} against the concentration gradient and thus, removes Ca^{2+} from the RPE's cytosol and thereby helps to maintain Ca^{2+} homeostasis in the cytosol. It is not known whether PMCA in RPE is localised to apical or basal surfaces of the RPE (Kennedy and Mangini, 1996). There may be several isoforms of this channel (Johnson et al., 1995). For further reviews, see Philipson and Nicoll (1993) and Quednau et al. (2004).

10.2. Voltage-gated Ca^{2+} channels (L-type)

Whilst NCX1 and the PMCA provide a means of Ca^{2+} exit from the RPE cell a means of Ca^{2+} influx is also required. Voltage-dependent L-type Ca^{2+} currents with a very long time constant of de-activation (L = "long") were first observed in the heart (Orkand and Niedergerke, 1964). The inactivation maintains long depolarising responses and provides a means for sustained Ca^{2+} entry into the RPE down the favourable electrochemical gradient. L-type Ca^{2+} channels are blocked by 1,4-dihydropyrimidines such as nifedipine, phenylalkylamines and benzothiazepines. They are formed by five protein subunits (α_1, α_2, β, δ and γ) with the α_1 subunit forming the pore and defining the type (Knaus et al., 1990). See Catterall (2000) and Perez-Reyes and Schneider (1995) for further details.

Such voltage-gated Ca^{2+} channels were first recorded in fresh and cultured RPE cells from normal and dystrophic rats (< 17 days post natal) (Ueda and Steinberg, 1993). Whole cell Ca^{2+} currents were inhibited with nifedipine or cobalt and displayed strong inward currents when the membrane was depolarised. Similar L-type Ca^{2+} currents were observed in freshly isolated human, monkey and cultured foetal but not subcultures of human RPE cells (Ueda and Steinberg, 1995). These channels belong to the neuroendocrine subtype (Strauss et al., 2000). Cultured cells from RCS rats displayed an increased Ca^{2+} conductance and a depolarised V_M compared to normal rat RPE cells (Strauss and Wienrich, 1993). The reduced V_M would affect the activation of apical voltage-dependent K^+ channels (Hughes and Takahira, 1996) that are essential for fluid regulation of the subretinal space. The increased Ca^{2+} conductance may interfere with phagocytosis (Hall

et al., 1991). The L-type Ca^{2+} channels in RCS rats show altered regulation by PTKs and PKC (Mergler et al., 1998). L-type Ca^{2+} currents in cultured human and rat RPE cells show dual regulation by PTK and PKC, with the level of PKC activation determining whether PTK increases or decreases the L-type Ca^{2+} current (Strauss et al., 1997, 1999, 2000). This dual regulation was proposed as a potential role for L-type Ca^{2+} channel autoregulation of RPE by growth factors (Strauss et al., 1997). The altered integration of PTK and PKC in RCS rat RPE cells may underlie the retinal degeneration in this strain (Mergler et al., 1998). Strauss's group have identified that it is the membrane bound protein tyrosine kinase (pp60c-src) expressed in cultured RPE cells (Koh, 1992) that opens L-type Ca^{2+}-channels in cultured rat RPE cells by phosphorylation with the pore forming α_{1D} subunit (Strauss et al., 2000).

10.3. Internal Ca^{2+} stores

Owing to the multiple functions of free Ca^{2+} within the cell the $[Ca^{2+}]_{in}$ must be finely controlled, and the sequestration of calcium or the mobilisation of calcium stores is one mechanism by which this may be achieved. Ca^{2+} is stored within the ER and its regulation is important in considering the generation of the light rise. The conductance of ionic channels changes in less than a millisecond, and pumps and transporters respond in the time scale of seconds. In considering events with the duration of the EOG internal calcium changes are very likely to be important because they are related to the slow activation of second messenger signalling pathways at the inner surface membrane. Calcium is sequestrated in the ER, and its slow release could account for more of the delay in initiating the EOG light rise. Once released Ca^{2+} could gate open the basolateral Cl^- channel responsible for the light rise. Whilst there is no direct evidence that the ER is the source of Ca^{2+} the clinical evidence on the nature of the EOG demands that a totally intracellular mechanism determines the current and voltage changes (Arden and Wolf, 2000a).

Uptake of calcium into the ER is regulated by a calcium–ATPase pump (ERCA).[6] This is inactivated by the binding of a small unphosphorylated protein, phospholamban (Kirchberger et al., 1975). This is an extremely important point in the regulatory control of Ca^{2+}. The phosphorylation of phospholamban by various kinases operated on by second messengers exerts fine control over cytosolic free calcium.

Ca^{2+} release from the ER is dependent upon IP_3-R that forms an ionic Ca^{2+} channel. This is another example of the way the RPE is influenced by the extracellular fluid. The sequence is that when receptors on the RPE membrane combine with their specific targets, either a *G*-protein or tyrosine kinase is activated, and this in turn changes a pro-enzyme to a fully active isoform of phospholipase C (Nash and Osborne, 1996). This lipase hydrolyses the membrane-bound phospholipid (PIP_2) and IP_3 and DAG are formed. IP_3 can move in the cytosol to the ER where it binds to a receptor that opens a Ca^{2+} channel and Ca^{2+} is released into the cytosol. This release cuts short the activity of IP_3-R by negative feedback. For further reviews, see Bosanac et al. (2004), Berridge (1993), Ferris and Snyder, (1992).

11. Cystic fibrosis transmembrane conductance regulator

CF is a genetic disorder caused by several of the over 1000 mutations that have been identified in the gene encoding for CFTR (Rich et al., 1990). The gene responsible for CFTR has been localised to q31–q32 on the 7th chromosome (Riordan et al., 1989; Rommens et al., 1989). The intracellular portion of CFTR consists of two nucleotide binding domains (NBD1 and NBD2) separated by a large polar regulatory domain with nine sites for phosphorylation by PKA and seven sites for phosphorylation by PKC (Riordan et al., 1989). CFTR could be considered to be an ATP-gated Cl^- channel. CFTR is found in foetal RPE (Blaug et al., 2003), its' mRNA in adult RPE (Miller et al., 1992) where it transports Cl^- (Knowles et al., 1983). Only a fraction of the mutations cause known changes in function.[7] The predominant

[6]The calcium pump in the ER is inhibited by thapsigargin (Lytton et al., 1991) and/or cyclopiazonic acid (Kennedy and Mangini, 1996; Rymer et al., 2001; Seidler et al., 1989). These drugs deplete Ca^{2+} stores by inhibiting reuptake and are widely used to study Ca^{2+} regulation in the RPE (Kennedy and Mangini, 1996; Rymer et al., 2001). Physiologically, ERCA is inhibited by phospholamban in its unphosphorylated state (Tada and Kadoma, 1989). Phosphorylation of phospholamban by PKA-dependent cAMP thus provides a means of control of $[Ca^{2+}]$. Thus, the control of free calcium is regulated by cAMP and by $[Ca^{2+}]_{in}$ itself. Much of this work has been carried out in heart and skeletal muscle (Simmerman and Jones, 1998) as well as the RPE (Peterson et al., 1997; Rymer et al., 2001). Melanosomes also store calcium (Salceda and Riesgo-Escovar, 1990; Salceda and Sánchez-Chávez, 2000) of the RPE. Melanin granules in the RPE have many important functions which are still under investigation although melanin does help to protect the RPE from oxidative stress, lipofuscin accumulation and the degradation of rod outer segments. Melanosomes act as a further reservoir for intracellular Ca^{2+} (Drager, 1985; Panessa and Zadunaisky, 1981). Uptake of Ca^{2+} by melanosomes is independent of ATP and probably relies upon a Ca^{2+}–H^+ exchanger. See reviews by Peters and Schraermeyer (2001) and Schraermeyer and Heimann (1999) for further details.

[7]The gene for CFTR is found on chromosome 7 that encodes for a protein, CFTR, consisting of 1480 amino acids forming two transmembrane spanning regions of six α-helixes, with minimal exposure to the extracellular space. Various classes of malformation occur. Class I results in the malformation of CFTR so that it does not reach the Golgi apparatus. In class II, the protein cannot leave the ER and consequently there is an absence or severe depletion of CFTR at the plasma membrane. In class III, the gating of the channel is affected with the channel failing to open following cAMP stimulation (Logan et al., 1994). In class IV the conductance of the pore formed by the protein is reduced (Ashcroft, 2000; Sheppard et al., 1993; Welsh and Smith, 1993). CFTR belongs to the large ATP-binding cassette family of transporters that actively transport a variety of substrates and ions (Higgins, 1992; Stefkova et al., 2004). The frequency of CFTR mutations varies between ethnic groups and countries

mutation (Δ508) in Caucasian CF is a deletion of phenylalanine in NBD1 (Cutting et al., 1990; Lemna et al., 1990) that results in a CFTR unable to reach the plasma membrane (Puchelle et al., 1992). Therefore it is degraded before reaching the Golgi (Yang et al., 1993). The sequence of ATP-binding, hydrolysis and the interaction of the R-domain and how these components interact to regulate gating of CFTR have been debated by various authors (Aleksandrov et al., 2002; Anderson et al., 1991a; Baukrowitz et al., 1994; Gadsby and Nairn, 1999; Gunderson and Kopito, 1995; Winter and Welsh, 1997). Evidence now suggests that when ATP binds to NBD2 the two NBDs become protonated and form a dimer and this opens the pore. Hydrolysis of ATP at NBD2 closes the pore and disrupts the dimer (Vergani et al., 2005). Gating of CFTR has recently been reviewed by Riordan (2005) and Linsdell (2006). Phosphorylation of the regulatory domain by PKA is also required to prime the channel for opening (Li et al., 1988). CFTR currents are non-rectifying when Cl^- concentrations are symmetrical across the membrane (Anderson et al., 1991b,c; Kartner et al., 1991). The halide permeability sequence is now thought to be $I^- > Br^- > Cl^- > F^-$ (Tabcharani et al., 1997).

11.1. Role of CFTR in the RPE

Functional CFTR has not been demonstrated directly in adult human RPE. However, CFTR protein is expressed in cultured adult human RPE cells (Weng et al., 2002) as well as in the transfected human RPE foetal cell line (Wills et al., 2000). It has been localised to the basal and apical membranes in primary human foetal RPE explants (Blaug et al., 2003) and its mRNA identified in both retina and RPE from donor human and bovine eyes (Miller et al., 1992). It is also functionally expressed in the human RPE cell line, ARPE-19 (Reigada and Mitchell, 2005). CFTR is thought to play a role in fluid regulation by the RPE by because it can transport Cl^- (Blaug et al., 2003). However, the bulk of fluid regulation in the RPE is performed by calcium-gated Cl^- channels and the aquaporins, and if CFTR was significantly involved in fluid regulation then it would be expected that CF individuals would be prone to macula oedema (Loewen et al., 2003) which is not observed. However, CFTR could produce current and voltage changes across the RPE and transport molecules through the membrane which could affect other conductances as well as potentially playing a role in the regulation of pH.[8]

11.1.1. Ionic channel interactions

CFTR has numerous interactions with other ionic channels in epithelia and therefore a similar function may exist in the RPE. Control epithelia (from the nose, lung and cell line models) "absorb" less sodium than in affected epithelia lacking CFTR. These effects have been demonstrated to be due to a direct inhibitory action of CFTR on an amiloride sensitive epithelial Na^+ channels (Boucher et al., 1986; Ismailov et al., 1996; Stutts et al., 1995). Activation of inward rectifying K^+ channels has also been demonstrated by cAMP in the presence of functional CFTR (Loussouarn et al., 1996). Furthermore, regulation of an outward rectifying anion channel by CFTR has been demonstrated in planar lipid bilayers (Jovov et al., 1995). In hypotonic solutions, CFTR releases ATP into the extracellular compartment. ATP can then bind to the purinergic receptor P_2Y, which would then cause a rise in $[Ca^{2+}]_{in}$ (Braunstein et al., 2004; Prat et al., 1996; Reisin

(*footnote continued*)
and individuals with identical genotypes may not have similar phenotypes, indicating a role for environmental factors in determining the final severity of CF (Dugueperoux and De Braekeleer, 2004; Estivill et al., 1997).

Blocking of CFTR currents has proven difficult with organic compounds. Whilst DIDS inhibit CFTR currents in a voltage-dependent manner when applied to the cytoplasmic face, they are ineffective when applied to the extracellular face (Anderson et al., 1991b; Cliff and Frizzell, 1990; Linsdell and Hanrahan, 1996). Partial inhibition is possible with millimolar concentrations of diphenylamine-2-carboxylic acid (DPC) and flufenamic acid from the extracellular surface (McCarty et al., 1993). However, the blockage is voltage dependent and not complete. Native but not synthetic scorpion toxin when applied to the cytoplasmic face is an effective blocker, independent of voltage (Fuller et al., 2004). Substrates of the closely related 'multidrug resistance protein' such as taurolithocholate-3-sulphate and β-estradiol also block CFTR currents in a voltage-dependent manner when applied to the cytoplasmic surface (Linsdell and Hanrahan, 1999) and glibenclamide has similar effects (Sheppard and Robinson, 1997) apparently obstructing the open pore (Zhang et al., 2004). However, glibenclamide also inhibits K^+ channels (Yamazaki and Hume, 1997). In contrast, $CFTR_{inh}$-172 is a small thiazolidinone molecule that blocks CFTR by prolonging the mean channel closed time independently of membrane voltage. It is suspected to exert its action by binding to NBD1 (Ma et al., 2002; Muanprasat et al., 2004; Taddei et al., 2004) and has been used to study CFTR in an RPE cell line (Reigada and Mitchell, 2005).

[8]CFTR has a major role in regulating the intracellular pH as well as the pH of the mucosal membranes of the gut (Kopelman et al., 1988). In the gut the mechanism is accomplished by CFTR maintaining a favourable $[Cl^-]_{out}$ which maintains the $Cl^-_{in}/HCO^-_{3\,out}$ exchanger to regulate pH_{in} (Jetten et al., 1989; Paradiso et al., 2003; Simpson et al., 2005) whilst in the lungs CFTR apparently controls a direct HCO_3^- conductance (Coakley et al., 2003), which accounts for the acidic nature of the airway mucosa in CF sufferers. CFTR demonstrates mild permeability to HCO_3^- under non-physiological conditions (Gray et al., 1990; Linsdell et al., 1997b). Whole cell recordings of voltage, current and intracellular pH_{in} from CFTR protein expressed in *Xenopus* oocytes show a switch of conductance from Cl^- only to HCO_3^- and Cl^- when $[Cl^-]_{out}$ is reduced to 0–10 mM (Shcheynikov et al., 2004). This switch may help to control pH_{out} when there are rapid changes in $[Cl^-]_{out}$. In the pancreas, CFTR is inhibited by reduction in $[HCO_3^-]_{out}$ (O'Reilly et al., 2000). In amphibian RPE pH_{in} is the main contributor to fluid transport that stimulates a basolateral HCO_3^-/Cl^- exchanger (Lin and Miller, 1994). Whether CFTR plays a role in regulating pH_{in} in mammalian RPE is unknown. But it has properties that would enable it to regulate intracellular pH: it transports carbonate and chloride ions, to regulate extracellular pH in a variety of epithelia (Akiba et al., 2005; Anderson et al., 1991c; Hug et al., 2003; Paradiso et al., 2003; Poulsen et al., 1994; Ulrich, 2000, Wang et al., 2005). Although in amphibians the RPE chloride conductance is DIDS-sensitive, there may be a species difference that renders mammalian chloride conductance insensitive to DIDS applied from the extracellular space (Hughes and Segawa, 1993; Linsdell and Hanrahan, 1996). In this case CFTR could account for (some) portion of the EOG.

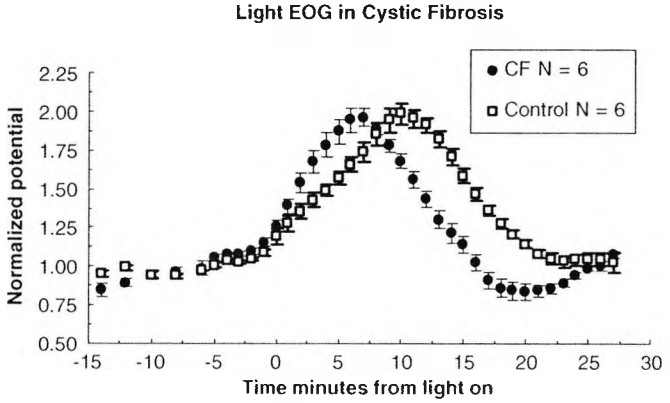

Fig. 7. Preliminary findings of the light-EOG in a group of individuals with CF ($N = 6$) and controls ($N = 6$). Light was 100 cd/m^2 with dilated pupils at $t = 0$. Graphs are mean ± SEM. Three were homozygous and three were heterozygous for Δ508. The amplitude of the light rise is normal, however the time to peak is significantly faster ($p < 0.001$) than normal. Data normalised to the mean voltage of the 10 min preceding the stimulus. The absolute peak value = 1.98 ± 0.07 for controls and 1.96 ± 0.06 for CF patients.

et al., 1994; Taylor et al., 1998). In turn this change of calcium would increase Cl^- fluxes, (Schwiebert et al., 1995). This may be a general means of regulating cell volume. Findings on work using bovine RPE and a human RPE cell line also suggest that CFTR increases ATP in the subretinal space following activation (Mitchell, 2001; Reigada and Mitchell, 2005).

The mechanism by which CFTR facilitates release or transports ATP across the membrane has not been fully resolved. ATP release from cells has not been universally supported by all investigators (Abraham et al., 1997; Grygorczyk and Hanrahan, 1997b; Li et al., 1996; Reddy et al., 1996) with the possibility that the ATP released from the cell is a result of mechanical disruption of the plasma membrane during patch formation (Grygorczyk and Hanrahan, 1997a).

If CFTR played an important role in generating the light rise, then individuals with CF should have a reduced response which is not the case (Lara et al., 2003; Miller et al., 1992) (see also Fig. 7 showing the normal light rise amplitude in a group of individuals with CF). However, we observed an altered time course of the light rise in this group of CF volunteers comprising three heterozygous and three homozygotes for the Δ508 mutation. This may implicate CFTR in determining the time course of the light-EOG and therefore a role for CFTR in the light rise cannot be excluded. One alternative explanation could be that another Cl^- transporter is up-regulated when CFTR is defective and therefore takes over its function. For further reviews in CFTR's interactions, see Kunzelmann (2001) and Schwiebert et al. (1999).

11.2. CIC chloride channels

These channels are very common and various subgroupings have been described. CIC-2 is found in the RPE, and in a CIC-2 knockout mouse, retinal degeneration and testicular atrophy were the only defects (Bösl et al., 2001; Nehrke et al., 2002). It is highly likely that CIC-2 in the RPE plays a vital role in either the regulation of cell volume, pH_{out} and fluid secretion as it does in other epithelia (Cuppoletti et al., 1993; Furukawa et al., 1998; Malinowska et al., 1995). CIC-2, CIC-3, CIC-5 and CFTR are co-expressed in human foetal RPE cell line (Wills et al., 2000) and as CFTR and CIC-2 are activated by PKA (Anderson et al., 1991a; Cid et al., 1995; Tewari et al., 2000) CIC-2 may provide an alternative Cl^- conductance when CFTR is defective (Blaisdell et al., 2000; Cid et al., 1995; Jordt and Jentsch, 1997; Schwiebert et al., 1998; Thiemann et al., 1992). However, this proposal is not supported by recent evidence. In a doubly deficient mouse, with both CFTR and CIC-2 disrupted, the colonic epithelial Cl^- currents were not reduced (Zdebik et al., 2004) casting doubt on the role of CIC-2 as a rescue channel for CFTR.[9]

12. Channel changes associated with the clinical EOG

12.1. The fast oscillation

The FO is normal in Best's whilst it is abnormal in retinitis pigmentosa (RP) and therefore the generation of the light rise and the FOs are different (Sandbach and Vaegan, 2003; Vaegan, 1993; Vaegan and Beaumont, 1996, 2005; Weleber, 1989) (see Fig. 8). One model attributes the difference as indicating that the light rise is dependent upon the bestrophin Cl^- channel and the FOs relying on CFTR (Blaug et al., 2003; Miller et al., 1992).

[9]CIC Cl^- channels were first identified in the electric organ of the *Torpedo* ray (White and Miller, 1979) since named (CIC-0) (Jentsch et al., 1990). A further nine CIC channels have been identified in mammals. They activate slowly at hyperpolarising voltage and conduct anions preferentially in the sequence, $Cl^- \geq Br^- > I^-$ (Thiemann et al., 1992). The diversity of CIC-2 distribution implies that it has a key role to play in epithelial and non-epithelial cells. CIC-2 is activated by acidification of the extracellular space (Jordt and Jentsch, 1997) and is typically closed at resting membrane potential. Its main role seems to be in regulating cell volume (Furukawa et al., 1998; Gründer et al., 1992; Strange et al., 1996; Xiong et al., 1999).The X-ray structure of CIC channels has been described in prokaryotes (Dutzler et al., 2002) with the channel comprising 18 α-helixes running anti-parallel with the positive N terminus orientated towards the centre creating a domain to increase anion binding and gated closed by glutamate residues that mimic Cl^- (Dutzler, 2004). CIC Cl^- channels have two pores that are identical in structure that open in bursts with each pore fluctuating between open and closed (Hanke and Miller, 1983; Miller, 1982). The gating and selectivity of CIC Cl^- channels is still unresolved, although structural models have been ascertained for bacterial CIC channels (Pirruccello et al., 2002).

CIC-2, CIC-5 and CIC-3 mRNA and immunocytochemical techniques have identified these channels in a transfected human foetal RPE cell line (Wills et al., 2000). The electrophysiology of the different types of CIC channel is not identical. CIC-2 has slight inward rectification in the range from −180 to 50 mV that is slowly activated both by hyperpolarisation, extracellular acidification, PKA and arachidonic acid (Cuppoletti et al., 1993; Tewari et al., 2000). CIC-2 is blocked by DPC and 9-anthracene-carboxlic acid (Gründer et al., 1992; Thiemann et al., 1992).

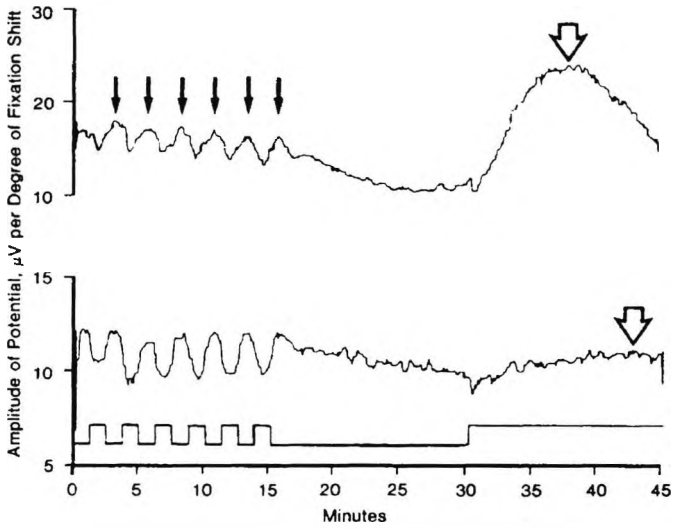

Fig. 8. Upper trace showing normal fast oscillations (arrows) and light rise (broad arrow). Lower trace shows the absence of the light rise in Best's macular dystrophy. From Weleber (1989). Reprinted with permission of Archives of Ophthalmology.

Figs. 9A and B show recordings of the FOs from a normal and Δ508 homozygous volunteers. It can be seen that the standing potential rises in the dark and falls in the light. The minimum occurs 30–45 s after light onset and then the standing potential begins to rise once more and with repeated dark–light periods a series of oscillations can be established.

The model which is generally accepted at the time of writing may not be complete but the first step is the photoreceptor-induced decrease in $[K^+]_{out}$ in the subretinal space. This opens voltage-gated potassium channels in the apical membrane of the RPE (and also in the Müller cells) that results in the c-wave of the ERG (Linsenmeier and Steinberg, 1983). The activity of the Na–K–2Cl exchanger decreases as $[K^+]_{out}$ is reduced (Joseph and Miller, 1991). Because now the inward flux caused by the Na–K–2Cl transporter is reduced, the intracellular Cl^- activity decreases (Gallemore and Steinberg, 1993). Consequently, the CFTR Cl^- current also decreases and therefore the basal membrane of the RPE hyperpolarises, leading to a

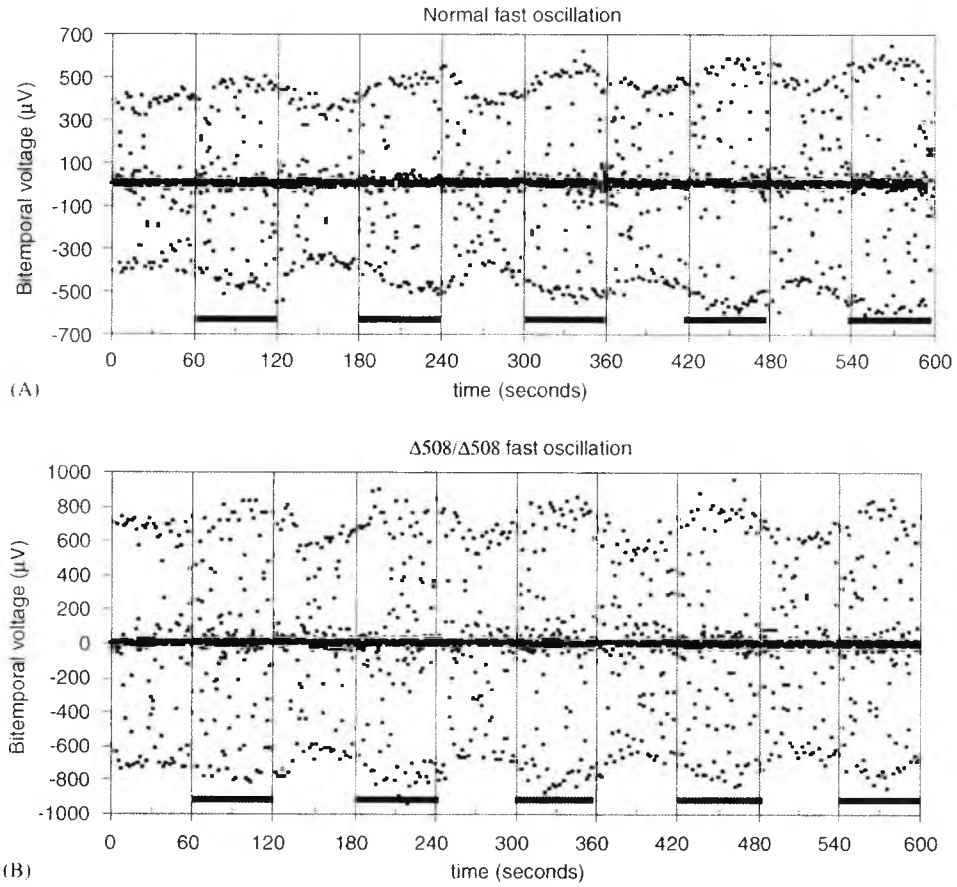

Fig. 9. (A) The fast oscillation (FO) recorded in a 20-year old female over 10 min with alternating periods of light and dark at 1 min intervals. We used bi-temporal skin electrodes with alternating periods of light (100 cd/m^2) and dark (0.01 cd/m^2) at 1 min intervals. Saccades were performed at 1 Hz and the unfiltered raw bi-temporal voltages were sampled continuously at 4 Hz using a simple digital voltmeter. The first 60 s was in light. When the illumination is reduced (dark bar) there is a rise in the standing potential (dark rise) that peaks at ~30 s. When illumination is restored there is a decrease in the standing potential leading to the "light trough" that reaches a minimum after ~30 s and then begins to rise. In this study, we took the mean of four dark–light cycles of the peak-trough voltages giving the dark rise : light trough ratio (DR:LT). In this individual the DR:LT ratio was 1.29 ± 0.06 (mean ± SD). (B) The FO recorded in an 18-year old female with the Δ508/Δ508 genotype for CF. Mean ratio of the DR:LT was 1.35 ± 0.05 (mean ± SD). Note the similarity between A and B, although the Δ508 mutation has been associated with a reduced FO (see text).

fall in the TEP following light onset and this generates the light trough of the FO of the EOG. This model is based upon the work of Blaug et al. (2003) who used human foetal RPE sheets mounted in an Ussing chamber where CFTR expression was demonstrated to support the role of CFTR in the FO light trough. When the effect of light was simulated by reducing the apical bath K^+ level from 5 to 2 mM, in the absence of cAMP, V_{Apical} and V_{Basal} change together with V_{Apical} hyperpolarising at a greater rate than V_{Basal} so the TEP transiently increases, as a "mock c-wave" develops. In the next phase, V_{Basal} hyperpolarises at a greater rate than V_{Apical} and so the TEP falls which is a result of a reduction in $[Cl^-]_{in}$ due to a reduced flux through the Na–K–2Cl cotransporter (Joseph and Miller, 1991). In a tissue treated to increase cAMP levels, the same procedure causes the same sequence but there is a dramatic increase in the magnitude and time course of the FO trough which suggests that CFTR is involved in generating the FO. This model is supported by the reports that in CF the amplitudes of the FO are reduced and delayed whilst the light-EOG remains normal (Lara et al., 2003; Miller et al., 1992). Whilst Blaug could show that elevating intracellular cAMP increased the amplitude of the FOs in foetal RPE sheets where the mRNA and immunocytochemical evidence supported the presence of CFTR he was at that time unable to block these changes using a specific CFTR inhibitor. Therefore, these changes may have been due to another Cl^- channel that is also gated by elevations in cAMP such as CIC-2 (Bösl et al., 2001; Cuppoletti et al., 2000).

However, there is also evidence against this model. Reduction of intracellular Cl^- $[Cl^-]_{in}$ does *not* affect wild type-CFTR or Δ508CFTR Cl^- currents whilst in transfected cell lines the reduction of $[Cl^-]_{out}$ reduces chloride current (Wright et al., 2004). In addition, the reduction of the FO reported in CFTR may not be universal. None of a small group ($N = 3$) of individuals homozygous for Δ508 mutations showed reduced FOs whilst a slight delay was observed (Constable et al., 2005)—see Fig. 9. There are clearly some contradictions regarding CFTR, ATP and the light rise. Certainly CFTR mediates release of ATP at the apical membrane from bovine and human RPE cell lines (Reigada and Mitchell, 2005) and that stimulation of P_2Y_2 receptors by ATP elevates $[Ca^{2+}]_{in}$ (Collison et al., 2005; Peterson et al., 1997; Sullivan et al., 1997). It is also the case that the rise in $[Ca^{2+}]_{in}$ opens the basolateral Cl^- channel involved in the slower light rise of the EOG. Therefore, this model predicts that the light rise will be affected when CFTR is defective or absent which is not the case (Lara et al., 2003; Miller et al., 1992) and Fig. 7 above. Therefore, we must conclude that this simple model is incomplete. However, all three assumptions are well supported by data but further work will be required to determine precisely the role that CFTR plays in the light rise and FOs. Fig. 10 illustrates the current model of the FO generation and the light rise.

13. The elusive light rise substance

Our current understanding of the light rise is basically the model produced by Steinberg: light liberates a substance from the rods that binds to a receptor in the apical surface of the RPE. More recent work has added that second signalling systems inside the cytosol produce a rise in intracellular $[Ca^{2+}]$ which in turn increases the basolateral Cl^- conductance demonstrated by Steinberg. The identity of the substance, the means by which it increases $[Ca^{2+}]_{in}$ and whether the ultimate basolateral Cl^- channel is bestrophin or CaCC is unknown. Ethanol can generate a sequence of slow changes to the human EOG that are identical to that produced by light, implying that the time course is generated internally within the RPE. Light and alcohol produced current changes that share a final common pathway, again supporting the idea that the light rise is mediated via a Ca^{2+} pathway (and see below).

Work on the membrane and cytosol characteristics of RPE cells has mostly been carried out in tissue culture and in various animal models that show some species differences. Therefore, any link between changes in the membrane properties associated with a particular agent and the light rise is speculative, unless a selective blocking agent can be found, that, used in vivo, affects the EOG in predictable ways (Eggermont, 2004; Nilius and Droogmans, 2003). Another difficulty encountered is the difference between RPE cells of different species. For example, with elevation of intracellular cAMP in bovine preparations (Rymer et al., 2001) and chick (Kuntz et al., 1994) there is a decrease in basolateral Cl^- conductance whilst in human foetal RPE (Quinn et al., 2001) as well as whole cell recordings from cultured human RPE (Weng et al., 2002) basolateral Cl^- conductance increases. In frog RPE, cAMP-activated Cl^- currents are inhibited by extracellular DIDS (Hughes and Segawa, 1993) unlike the comparable mammalian cAMP activated Cl^- current generated by CFTR (Linsdell and Hanrahan, 1996; Schultz et al., 1999).

Whilst the RCS rat model of retinal degeneration have provided valuable insights into the regulation of Ca^{2+} currents that closely resemble human (Mergler et al., 1998; Ueda and Steinberg, 1994, 1995) there is some dispute about the identity of bestrophin as the Ca^{2+} activated Cl^- channel involved in the generation of the light rise (Marmorstein et al., 2004; Pollack et al., 2005; Strauss and Rosenthal, 2005). Until a demonstrable knock-out animal model of the light rise can be associated with bestrophin and then restored, the question as to whether bestrophin is the CaCC responsible for the light rise will remain in doubt (Qu et al., 2004; Qu and Hartzell, 2004; Rosenthal et al., 2005; Strauss and Rosenthal, 2005). Although evidence is now stronger that bestrophin is a CaCC and not a modulator of a separate Cl^- channel (Fischmeister and Hartzell, 2005; Hartzell et al., 2005b).

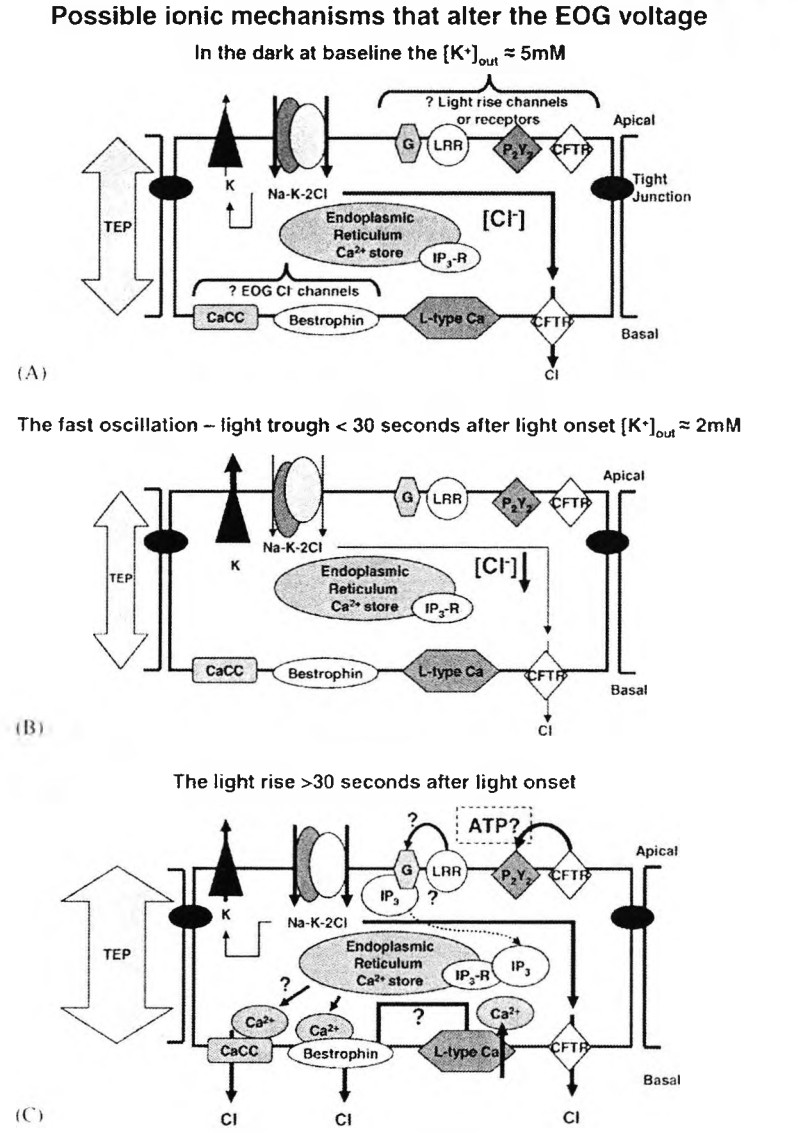

Fig. 10. Schematic representations of the ionic channels and signalling molecules involved in the generation of the fast oscillation (FO) and the light rise in man. At the apical membrane, the possible ionic channels and receptors involved in initiating or generating the light evoked responses are grouped together. These are: a proposed light rise receptor (LRR) that may be coupled to a *G*-protein or the purinergic receptor (P_2Y_2). At the basal membrane the chloride channels that have been proposed for altering V_{Basal} are grouped together. The light rise Cl^- channel may be either a CaCC or bestrophin. However, the mechanism may be more complex, and the channel may interact with a basolateral Ca^{2+} channel (possibly an L-type) to elevate $[Ca^{2+}]_{in}$. There are several possible mechanisms that have been proposed and we are still unsure as to the exact nature of the intermediary steps between light onset and the final depolarisation of V_{Basal} that generates the light rise. (A) The upper figure shows the RPE cell in the dark where subretinal $[K^+]$ is maintained by the photoreceptor dark current. This high $[K^+]$ provides a favourable concentration gradient for the entry of Na^+, K^+ and Cl^- ions via the apical cotransporter. (B) In light, the dark current is not present and the subretinal $[K^+]$ falls. The RPE K^+ now moves down its electrochemical gradient through apical voltage-gated K^+ channels into the subretinal space. The Na–K–2Cl cotransporter has a reduced transport and so intracellular $[Cl^-]$ falls owing to the transiently decreased subretinal $[K^+]$. This then reduces the active transport of Cl^- ions by the cystic fibrosis transmembrane conductance regulator (CFTR) so the basal membrane hyperpolarises and causes a fall in the TEP. This is seen as the light trough of the FO. (C) Some possible pathways for the generation of the light rise. The putative light rise receptor LRR is situated on the apical membrane. The diagram suggests that LRR is satisfied by ATP. This may be provided by CFTR releasing ATP. Alternatively, the source of ATP may originate from the rods. Activation of either LRR or the P_2Y_2 receptor initiates the rise in $[Ca^{2+}]_{in}$ and this is presumed to be the second messenger involved in the light rise (see text). The source of Ca^{2+} may derive from the endoplasmic reticulum via the generation of inositol triphosphate (IP_3) that binds to the IP_3-R receptor. An alternative hypothesis is that the source of Ca^{2+} derives from an interaction of bestrophin with an L-type Ca^{2+} channel that facilitates the entry of Ca^{2+} across the basolateral membrane. In this model bestrophin is not the basolateral Cl^- channel responsible but a distinct CaCC is finally responsible for the light rise. The multiple steps in the generation of the light rise accounts for its slow onset of ~60 s with a peak at ~8 min.

13.1. Some possible candidates

At the apical membrane of the RPE there are various receptors that could conceivably mediate the light rise. Dopamine was considered a possible candidate for the light rise substance because the light rise was reduced in depressives but elevated in manic depressives (Economou and Stefanis, 1979). However, in vitro

studies have been unable to conclusively demonstrate that dopamine is the light rise substance (Dawis and Niemeyer, 1986; Gallemore and Steinberg, 1990; Rudolf and Wioland, 1990; Textorius et al., 1989) despite dopamine increasing in the subretinal space following light onset (Kramer, 1971).

Adrenergic, muscarinic, neuropeptidic and purinergic receptors have been identified at the apical membrane of the RPE in a variety of species and in cell culture (Ammar et al., 1998; Collison et al., 2005; Crook et al., 1992; Frambach et al., 1990; Mitchell, 2001; Peterson et al., 1997; Quinn et al., 2001; Rymer et al., 2001) and despite their potential to elevate $[Ca^{2+}]_{in}$ no definitive light rise receptor or substance has been found. However, the purinergic receptor (P_2Y_2) (Sullivan et al., 1997) with ATP as the agonist has recently been postulated to be involved (Reigada and Mitchell, 2005).

We speculate that ATP may be the light rise substance although the source may not be from the RPE as originally modelled (Reigada and Mitchell, 2005). In light, ATP is released by glial cells (Newman, 2003) that could diffuse towards the RPE. Alternatively, when ATP is degraded to adenosine, in the presence of ATP adenosine receptors on the RPE might evoke a rise in $[Ca^{2+}]_{in}$ (Collison et al., 2005). Another possibility is that ATP released from photoreceptors could be the light rise substance (Uehara et al., 1990). Because the rods consume very large amounts of ATP (Hagins, 1972) to develop the dark current the oxygen tension in the inner limbs falls to zero in darkness. The lactate profile across rat retina does not alter significantly and the rate of production is virtually unaltered when going from light to darkness (Winkler et al., 2003). Consequently, any store of ATP in the rod must be very small. However, when illuminated, the non-selective channels in the outer rod limb close very rapidly, while the Na–K–ATPase exchange pump continues to operate at high speed for some seconds, causing potassium depletion in the subretinal space. It soon stops, but it is plausible that the production of ATP continues for an additional further period so the intracellular ATP concentration of the rod rises: ATP then escaping into the subretinal space could provide the trigger for the light rise. This idea is attractive because it explains certain peculiarities of the EOG which have been known for many years (Arden, 1962; Arden and Kelsey, 1962b). For example, dark adaptation must precede the light rise, but the relation between the duration of preceding darkness and the size of the light rise does not conform to either psychophysical threshold changes or densitometric measures of rhodopsin regeneration. Again, although the rods produce the signal that influences the RPE, rod function can be normal when the EOG is reduced. With the multitude of integration sites for cross-talk between signalling molecules and receptors (Nash and Osborne, 1996) a more complex picture of the light rise will undoubtedly evolve as our understanding of the RPE–retina complex increases.

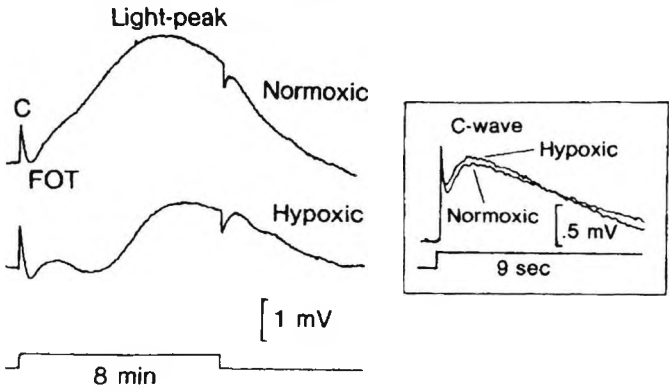

Fig. 11. Hypoxia decreases the light rise in cat (Linsenmeier and Steinberg, 1986). Reprinted with the permission of Investigative Ophthalmology and Visual Science.

14. Physiological characteristics and pharmacology of the light-EOG

The pharmacology of the DC potential, its relation to neurotransmitters and its reliance on changes in metabolism have been investigated by several authors. The slow light peak is extremely sensitive to anoxia (Kreienbuhl and Niemeyer, 1985; Linsenmeier et al., 1983, 1987; Linsenmeier and Steinberg, 1986; Steinberg, 1987). Fig. 11 shows that in mild experimental hypoxia, which does not affect the ERG, the light rise is markedly reduced and similar clinical findings have been reported. (Arden, 1962; Arden et al., 1962; Arden and Kelsey, 1962a; Niemeyer and Steinberg, 1984). Small changes in pH and pCO_2 also dramatically reduce the amplitude of the slow changes in potential caused by light. In view of the complex acid–base regulatory systems described above, it is not surprising that CO_2 and acidification exert differential effects on the TEP and consequently the corneo-fundal standing potential (Dawis et al., 1985; Niemeyer and Steinberg, 1984).

Acetazolamide (Kawasaki et al., 1986; Madachi-Yamamoto et al., 1984a) and changes in osmolarity (Kawasaki et al., 1984; Madachi-Yamamoto et al., 1984b) cause a slow reduction in the EOG voltages, and these findings are the basis on which clinical tests have been developed (see below). In addition, the potentials are influenced by biogenic amines and other substances (Bialek et al., 1996; Dawis and Niemeyer, 1986; Edelman and Miller, 1991; Joseph and Miller, 1992; Rymer et al., 2001; Textorius et al., 1989). Recently, it has been shown that ethyl alcohol affects the human corneo-fundal potential (Arden and Wolf, 2000a, b; Arden et al., 2000; Skoog et al., 1975; Wolf and Arden, 2004). Also at very low dosage non-steroidal anti-inflammatory drugs alter the TEP in isolated porcine and bovine preparations (Arndt et al., 2001; Bialek et al., 1996), and, in doses higher than clinically advisable, they affect the human EOG (Arden, unpublished).

Table 1
Some values reported for the FO ratio of the dark: light amplitudes with luminance

Author	Dark rise : light trough ratio	N	Luminance (cd/m^2)	Stimulus duration (s)
Vaegan (personal communication)	1.16±0.08	58	200	60
Mergaerts et al. (2001)	1.13±0.01	51	250	60
Miller et al. (1992)	1.26±0.09	15	—	—
Weleber (1989)	1.22±0.15	8	70	75
Schneck et al. (2000)	1.20±0.03	9	30	60
Constable et al. (2005)	1.28±0.05	8	100	60

Original units have been converted to cd/m^2 and rounded off. There is some variation between authors that may be a result of differing analysis of the FOs (see text).

14.1. Practical considerations in recording the fast oscillation

The FO is an important test that is rapid to perform and should be conducted in conjunction with the light-EOG. The reason is that the FOs and light rise are often selectively affected as in RP and Best's (Sandbach and Vaegan, 2003; Vaegan, 1993; Vaegan and Beaumont, 2005; Weleber, 1989) (see Fig. 8). Furthermore, a normal FO in the presence of an abnormal light rise may give the clinician greater confidence in the results obtained. In small studies, the FO is reported to be reduced in retinal vein occlusion (Rohde et al., 1981), rod monochromatism (Thaler et al., 1986), gyrate atrophy, pathologic myopia and Goldmann Favre syndrome (Vaegan and Beaumont, 2005). There is some variation between different authors' practices when measurements of the FO are reported. The International Society for Clinical Electrophysiology of Vision (ISCEV) standard for the FO recommendations are (1) six light–dark cycles lasting 120–160 s each should be employed (2) the average peak to trough ratio be used, and (3) the average latency or phase shift of the peaks should be recorded and (4) the absolute magnitude of the standing potential in the troughs (in microvolts per degree of visual angle) be recorded (Marmor and Zrenner, 1993). These recommendations are not always followed. Two large studies by Mergaerts et al. (2001) and Vaegan and Beaumont (2005) investigated the nature of the FO in man. Both found that the FO amplitudes were independent of age, sex and that four cycles of light and dark was sufficient to evaluate the FO parameters. The former investigators recorded the difference between maximum in dark and minimum in light as 69.6±5.3 μV, and the ratio dark/light 1.112±0.013 (Mergaerts et al., 2001). Another method of analysis has been to fit a sine wave to the data and determine the period and amplitude of the variation (Weleber, 1989). In a small study, Thaler et al. (1982) found a linear relationship between FO amplitudes and luminance (8–955 cd/m^2). The duration of the preceding dark adaptation had no effect on the amplitude. The results of various investigations into the normal dark rise: light trough (DR:LT) ratios are shown below in Table 1. Vaegan and colleagues have investigated the FO amplitudes in a large series of normals ($N = 58$) and found the lower limit of normal (5% point) to be 1.05 (Sandbach and Vaegan, 2003). The lower mean values reported by Mergaerts et al. (2001), and Vaegan may be attributed to the data analysis where the authors averaged to total amplitudes in the light and dark intervals rather than measuring the peak to trough ratio which yields an approximately normal value between 1.2 and 1.3 (Constable et al., 2005; Miller et al., 1992; Schneck et al., 2000; Weleber, 1989). The brighter backgrounds used by some authors is also unlikely to be the cause of the lower ratios as the FO increases with light intensity and therefore the ratios should be constant (Thaler et al., 1982).

The FOs can be easily recorded as part of the clinical light-EOG procedure. The level of retinal illumination that precedes the standard test is usually uncontrolled. The FOs can be recorded confidently using a minimum of three cycles of light/dark, each lasting 2 min (Vaegan and Beaumont, 2005). If a determination of the FOs is carried out before the 12 min of dark adaptation that precedes the EOG, the FO measurement will ensure a constant level of light adaptation from which the EOG itself can be measured. This should reduce variability in the light rise and the time penalty incurred is small (Vaegan and Beaumont, 2005).

The amplitude of the FO can be increased by raised blood glucose levels; however, whether this change differs in diabetics and non-diabetics is still to be evaluated but may represent the sensitivity of the FO to RPE metabolism (Schneck et al., 2000). Given the relative ease of recording the FO and its specificity for RP this procedure would appear to be a useful adjunct to the light-EOG (Vaegan and Beaumont, 1996).

15. Recording the EOG

An ISCEV standard (currently under review) gives recommendations for standard clinical tests (Marmor and Zrenner, 1993). The eye movement potential is easily recorded with skin electrodes placed one on either side of the eye. The voltage varies considerably depending upon how close the electrodes are placed to the eye, but 12–30 μV per degree is usual. Rapid saccadic eye movements may be

made over 30°, so the voltage change recorded to such eye movements is ~1 mV. This relatively large signal makes the EOG test technically undemanding. Eye movements >30° are not desirable, because they tend to be carried out in two or more saccades, making measurement of the voltage difficult or impossible with AC recording techniques. Horizontal eye movements should be made, because otherwise, artefactual voltages associated with lid elevation may also be recorded. Direct recording of the DC voltage between the two electrodes is possible, but changes in polarisation of the electrodes, and slow changes in skin potentials occur, and interpretation of such slow voltage changes without eye movement is impossible in clinical conditions. With AC-coupled amplifiers, recording eye movement voltages, any type of surface electrode can be used, including disposable Ag/AgCl pads, or gold cup electrodes. It is desirable to lightly abrade the skin on which the electrodes are placed, to reduce contact resistance below 5 kΩ.

The eye movements can be made in any way convenient. Some workers have advocated that the subject is given two (red) fixation points and asked to look left and right between them, at any convenient rate. Other workers expose only one fixation point at a time, and alternate the fixation points at a suitable rate which should be constant throughout the test. Patients are most comfortable with between one and two eye movements per second. More elaborate schemes have been proposed. For example, a number of closely spaced fixation points have been used, lit sequentially, and the subject is asked to follow the moving spot. The fixation points are so spaced that the angle of gaze varies sinusoidally with time. The amplitude of the voltage change can be determined precisely by a suitable software package (Fourier analyser). In the authors' experience, the simplest method is preferable.

15.1. Technical difficulties

These are very rare with the EOG. In a very few cases, patients may find difficulty in making standard eye movements. These include cases of ophthalmoplegia, or nystagmus (muscle paralyses, Parkinsonism, myasthenia). In certain of these cases, the patient may attempt to compensate by moving the head, not the eye. Such problems can usually be overcome by providing a solid, comfortable head rest, and encouraging the patient to relax the neck muscles. When the patient is first instructed about how to do the test, the clinician should always observe the patient to make sure that satisfactory eye movements are made. In many commercial devices, the patients' eye movements can be observed through an inbuilt infrared camera, so compliance can be checked on the video monitor. This is desirable, and may be included in future standards. If there is local central or peripheral disease, the fixation points may be easy to see in darkness, but become invisible against a brightly illuminated background, unless the fixation point is surrounded by an (unilluminated) opaque black area. In some patients with very poor vision, it may be necessary to make extreme eye movements if the fixation targets cannot be seen. It has been suggested that in such cases, eye movements of uniform angle can be made with the aid of proprioception: the patient can be seated in a chair with arms, on which the elbows can rest, and the forearms are placed vertically. The patient is encouraged to move his eyes toward the position of one thumb, and then toward the other. It is also possible to have a small buzzer behind each fixation point (with two different tones) to aid the subject in making eye movements of constant amplitude. Finally, if the eye movements displace the electrodes, an artefactual voltage can be recorded. These may occur when passive rotations of the eye are induced to obtain EOGs in small animals or if electrodes on the bridge of the nose are improperly secured. In man, using amplifiers of band pass 0.3–100 Hz alternating saccades give a saw-tooth response. Measurement of the peak-to-peak amplitude of the saw-tooth is easy, and many software packages contain horizontal cursors which can be set, by eye, to pass through the average peak voltage or the average trough voltage. The human visual system is good at making such judgements and disregarding any artefactual voltage or incomplete movements that may occur. All subjects can continue making eye movements for about 10 s, at minute intervals, without fatigue or discomfort. The record derived from such recordings is completely suitable for experimental work. In clinical situations it is common either to make records at 2 min intervals, or to make only a few measurements (for example, with totally blind patients). The aim is to determine the lowest level to which the voltage sinks in darkness (the dark trough) and the peak in subsequent illumination (the light peak). For further details, consult the ISCEV standard (Marmor and Zrenner, 1993).

The magnitude of the ratio of these voltages (often called the Arden ratio) gives an index of the change in RPE voltage which is the end result of the test. However, it is desirable to provide more detail, and various schemes have been proposed to provide standard traces, without the need for measurement and graph drawing. Often records are made on a very slow chart recorder (or its virtual equivalent) so the individual eye movements merge, and the average excursion during the 10 s or so of eye movement during each minute can be visualised as a thick line, and a graph of 20 or more consecutive lines shows the slow change in waveform. In clinical tests, it is important to specify the degree of dark adaptation and the intensity of the subsequent light adaptation because these influence the final ratio obtained. Some workers advocate a prolonged pre-test period during which, in constant dim illumination, the voltage becomes steady. This is desirable, but adds to the duration of the test and is not commonly employed. After this, the subject is put in complete darkness for 12–16 min. This is sufficient time to determine that the voltage has begun to rise from the dark trough level. The time in the dark should be fixed, because, when the light is

turned on, there is a relationship between the dark period and the size of the subsequent rise, although after only 8 min of darkness light rise reaches about 80% of the maximal value obtained with 22 min dark adaptation. The relation between amplitude and time in the dark is approximately exponential (Arden and Kelsey, 1962b).

The light rise response is derived from the entire retina, and therefore a Ganzfeld illumination with "white" light is required. Ganzfeld bowls are recommended, but (especially in view of the eye movements) ad hoc large field viewing (e.g. diffusely and evenly illuminated white walls, floor and ceiling) may suffice. It is important to adjust illumination to compensate for individual variation and individual change in pupil size with illumination. Two alternatives are available: If a very bright light is to be used, then "saturated" responses are obtained, and changes in pupillary diameter compensate for any change in illumination. Alternatively, the pupils may be dilated, and the illumination reduced to obtain a standard retinal illumination. The ISCEV standard recommends 100 cd/m^2 with 7 mm diameter dilated pupils.

Even though much information is available from various manufacturers, it is desirable to establish clinic normal values of the light peak/dark trough ratio. For most centres, the mean value will be 2.2 (220%) with the lower limit of normal ~1.8. This can be strongly affected by small levels of background light in the dark and several labs using total darkness and 15 min dark adaptation report the 5% lower limits of normal as ~2.05. Artifactually, high and low ratios can occur when the whole EOG amplitude is small. The standard therefore requires the report to also say if the absolute sizes of the dark trough and light peak are in normal limits. There is some evidence (see below) that very large values (>3) occur when the TEP is low, but the change in basal conductance is normal: These high values may also indicate an abnormality.

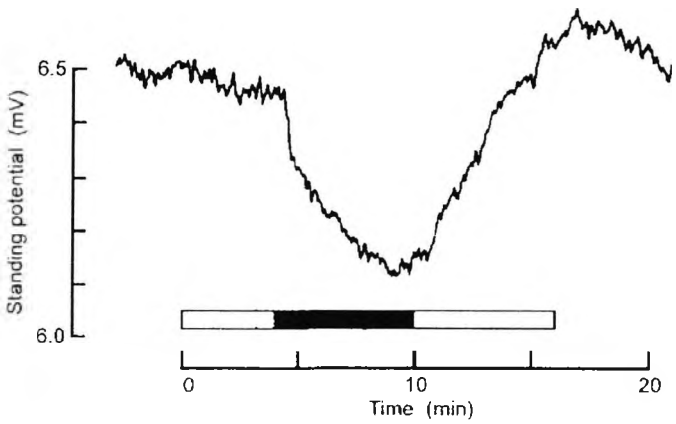

Fig. 12. Sodium bicarbonate (1.4%) infusions in cat causes a decrease in the ocular standing potential. From Segawa et al. (1997). Reprinted with permission of the Japanese Journal of Ophthalmology.

16. Non-photic responses

16.1. Hyperosmolarity, acetazolamide and bicarbonate tests

The light-EOG test depends on the integrity of the retina, the subretinal space and the RPE, and is thus affected by a wide range of pathological processes. The recorded current is generated by large regions of the retina–RPE, and is often normal when localised lesions develop (Gupta and Marmor, 1995). These factors decrease the value of the test. It was hoped that the sensitivity of the test to widespread pathologies could make it useful as a screening test, but other clinical methods (such as fundoscopy, angiography, electroretinography, field testing) provide more detailed information more quickly. A desire to improve the EOG, and obtain a test specific for the RPE has driven workers to investigate non-photic EOGs. In these tests, after a period of recording during which a stable baseline is established, a chemical is infused i.v. It is advisable to set up a venous line before the test begins, and to incorporate a two-way tap in the line so normal saline can be infused during the pre-test period, and the change in infusion made without the subject's knowledge. Otherwise changes of recorded voltage due to anxiety, may affect the test. Recording continues until the decrease in the voltage reaches a lower level. With hyperosmolarity (Kawasaki et al., 1986; Madachi-Yamamoto et al., 1984a) and bicarbonate (Gallemore et al., 1998; Segawa et al., 1997) the infusion causes a reduction in EOG voltage until a trough is reached after 8–10 min (Figs. 12 and 13). With hyperosmolar solutions, a rather slower fall occurs

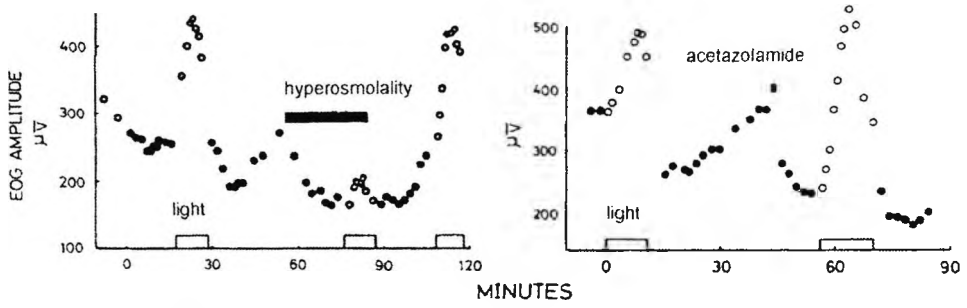

Fig. 13. Hyperosmolality and acetazolamide responses. Note the light rise peak is the same whether acetazolamide has been given or not. Modified from Kawasaki et al. (1977), Madachi-Yamamoto et al. (1984a). Reprinted with permission.

(Gallemore et al., 1998; Madachi-Yamamoto et al., 1984b; Marmor, 1989). Following the trough, the potential may increase slightly if the infusion continues.

The quantity of acetazolamide recommended is 8–10 mg/kg, given by slow intravenous infusion in a period of 1 min and causes a slow decrease in the standing potential. Hyperosmolar solutions used consist of 0.9% normal saline with 25% w/v mannose added, or 15% mannose plus 10% fructose (1400 mOsmolar). The aim is to increase tissue osmolarity by 15–20 mOsmolar. In the bicarbonate test, 0.9% saline, to which sodium bicarbonate, 7% w/v, was added is infused at the rate of 0.83 mg/kg/min. The use of several agents can be combined in a sequence to reduce the number of tests (Gallemore et al., 1998; Gupta and Marmor, 1994, 1995; Leon et al., 1990; Madachi-Yamamoto et al., 1984b; Pinckers et al., 1994).

16.2. Mechanisms and usefulness

During the hyperosmolarity trough the light rise is abolished. However, following administration of acetazolamide the light rise is unaffected so the two tests must provoke different retinal–RPE mechanisms (Gupta and Marmor, 1995; Marmor, 1989). Although experimental work on isolated epithelia has indicated that the hyperpolarisation of the basal membrane may account for the decrease in voltage associated with these agents, the precise mode of action is unknown, so any abnormality detected is merely phenomenological.

There are various reported differences between the light-EOG and the chemically induced changes. Some are of interest in terms of pathology. In Best's disease, the light-EOG is "flat", but the acetazolamide response continues normally (Gupta and Marmor, 1995; Madachi-Yamamoto et al., 1984b; Weleber, 1989) (Fig. 13). Since acetazolamide affects carbonic anhydrase in the RPE, and can enter via the choroidal circulation, this lends some support to the mechanism proposed for the alcohol-EOG (see below). It has been reported (Leon et al., 1990) in a small series of patients with retinal degenerations (particularly X-linked RP) that the response to hyperosmolarity and acetazolamide is more greatly reduced than is the case for the ERG or the light rise. Pinckers et al. (1994) reported that in age-related macular degeneration (ARMD) the acetazolamide response continues normally until choroidal neovascularisation appears. However, in advanced cases of RP, the acetazolamide response is often normal (Gallemore et al., 1998).

Hyperosmolarity EOGs also show abnormality in choroidal neovascular disease but not in ARMD without neovascularisation (Shirao et al., 1997).

17. The alcohol-EOG

In animal experiments (Skoog et al., 1975), and in man (Arden and Wolf, 2000a), a rise in the eye movement voltage occurs after giving alcohol. Unlike the other agents used to produce non-photic EOGs, alcohol can be given by mouth. It also has important differences from the results with the chemically provoked changes described above. Only recently has there been a comparison of the nature and time course of the changes caused by light and the change caused by alcohol. After allowing for the time taken for alcohol to pass from the gullet to the capillaries, both light and alcohol appear to provoke exactly the same complex prolonged voltage changes (within the limit of the experimental precision) (Arden and Wolf, 2000a). Both light and alcohol evoke a rise of voltage to a peak, with a subsequent fall to a trough, and then a second smaller peak. The time for alcohol to travel from the mouth, through the gut and circulation to the eye is minimally 2 min, and the alcohol peaks and troughs are delayed from the light-evoked responses by exactly this interval. It seems that the responses to both agents must be caused in the same manner and by the same mechanisms.

For low doses, the responses of light and alcohol sum. For high doses, light and alcohol "occlude"—i.e. when both agents are given, the response is only very slightly bigger than when each is given alone. These observations imply that the increase in voltage caused by light and by alcohol share a final common pathway. The dose response curves for the "peak" and "trough" alcohol responses are however quite different (Wolf and Arden, 2005). The latter require ~20 times less alcohol than the peak (the implications are discussed below). The quantity of alcohol required to produce minimal changes in the EOG is very small indeed—about 1 gm infused i.v. over ~20 s or 12 mg/kg taken orally in a 7% v/v solution. When alcohol is taken by mouth in this way, the blood level rises slowly for about 15 min, but the RPE voltage changes are determined by the blood levels in the first few minutes. A standard dose that produces acceptable voltage changes is 226 mg/kg, 20% v/v. With this, the peak blood level never exceeds 80 mg/100 ml and by the end of the test is <40 mg/100 ml, a level widely considered as lower than that which reduces motor efficiency and judgement. The effective minimal blood alcohol concentration causing any voltage change is too small to be measurable with standard tests. This suggests that there is an amplifier between the RPE mechanisms that generate the voltage changes, and the mechanisms that detect the changes in the alcohol composition of the tissues.

Alcohol is known to act on a variety of tissues, including the central nervous system and a number of biochemical pathways have been described (Allansson et al., 2001; Dildy-Mayfield et al., 1992; Ma et al., 2001; Sepúlveda and Mata, 2004). Very few experiments on the physiological effects alcohol have employed such low doses as those that appear effective in the eye.

It is unlikely that CFTR plays a role in the generation of the alcohol-EOG as alcohol does not activate CFTR currents (Marcet et al., 2004). Preliminary findings in our department show that the alcohol-EOG is normal in individuals who are homo- and heterozygous for Δ508 (Fig. 14) (Constable et al., 2005). Furthermore, ethanol

(100 mM) is capable of raising $[Ca^{2+}]_{in}$ in a human RPE cell line (ARPE-19) (Dunn et al., 1996) (Fig. 15) suggesting a direct action of ethanol on the RPE and as such the alcohol-EOG is a sensitive test for RPE function as originally proposed by Arden and Wolf (2000a).

So far, it has been shown that the increase in voltage caused by alcohol response is absent in all cases of RP (Arden and Wolf, 2000b). However the slow fall may persist, even in heterozygotes for X-linked RP (see Fig. 16 (Arden and Wolf, unpublished)). Since ERGs and fundal appearances in such persons are often very nearly normal, and very rarely seriously depressed, the results shown in Fig. 16 may be of significance especially where genetic screens may not be available. It may also have some bearing on pathogenesis because the implication is that the genetic abnormality is expressed in the RPE even in cases where the retinal damage is very small. The alcohol-EOG is also abnormal in ARMD, in a series where the light-EOG test is much less affected (Arden and Wolf, 2003) (Fig. 17).

If, as our preliminary findings suggest, the alcohol-EOG is mediated via a rise in $[Ca^{2+}]_{in}$ then Ca^{2+} homeostasis must be affected in early RP and ARMD and the alcohol-EOG is able to detect such changes before advanced retinal degeneration is apparent. It will be of interest to see in what other cases the alcohol-EOG is also abnormal.

17.1. Relationship between alcohol and light-EOG

The EOG appears to be dose dependent: there is an approximate linear relationship between the logarithm of retinal illumination and the magnitude of the light peak that extends over 3.5 decadic units. More recently, the same has been observed of the dose dependency of the

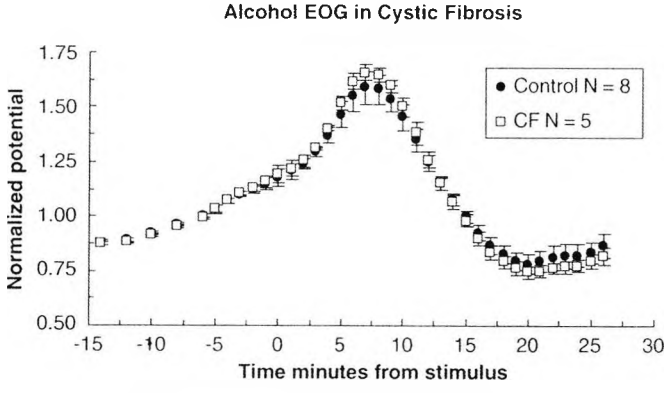

Fig. 14. Preliminary findings a group of individuals with CF ($N = 5$) and controls ($N = 8$) showing normal ethanol responses. Ethanol dose was 110 mg/kg administered orally at $t = 0$. Graphs are mean ± SEM. Two were homozygous and three were heterozygous for Δ508. Data normalised to the mean voltage of the 10 min preceding the stimulus. The absolute peak value = 1.59 ± 0.08 for controls and 1.66 ± 0.04 for CF patients. Compare with Fig. 7, where the light-EOGs of the same groups show differences between controls and CF patients.

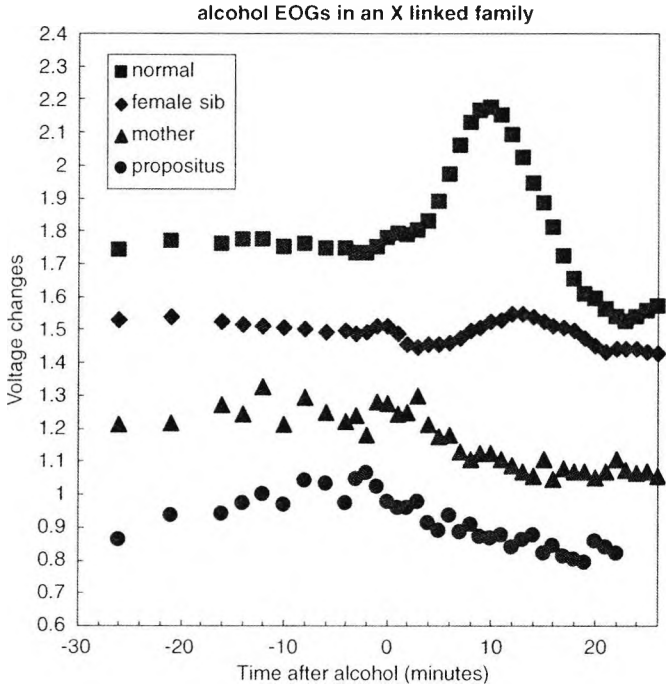

Fig. 16. Alcohol-EOGs in an X-linked family. The propositus is male, and has a severe retinal degeneration. The mother and female sibs are carriers, with normal retinal function, but their EOGs are grossly abnormal. (Arden and Wolf, unpublished).

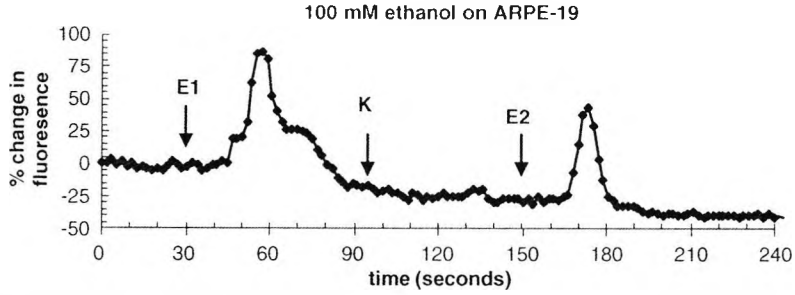

Fig. 15. Response of ARPE-19 cells to 100 mM ethanol loaded with the $[Ca^{2+}]_{in}$ sensitive dye, fluo-4AM. Recordings were made at room temperature in Kreb's solution containing Ca^{2+}. Ethanol 100 mM in Kreb's was added at 30 s (E1) and replaced with Kreb's at 90 s (K) and then challenged again with 100 mM ethanol in Kreb's (E2). The ordinate shows the rise in $[Ca^{2+}]_{in}$ from a single cell expressed as a percentage change in fluorescence from baseline. Note the sharp transient increase and the slower decay.

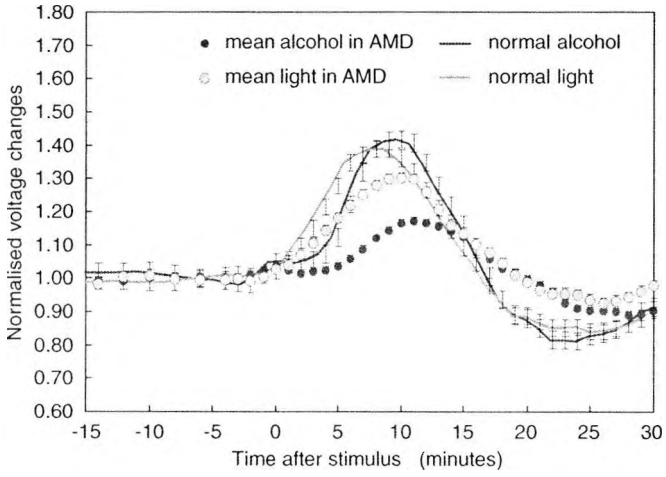

Fig. 17. Comparison of the light- and alcohol-EOGs in normal subjects and patients with ARMD. The standard errors are shown, but they are so low that the loss of the peak response of the light-EOG in patients must be significant, and the additional loss of the alcohol-EOG is also significant. Note that the normalised values are averaged for each minute's records. Compare with Figs. 7 and 14 (from Arden and Wolf, 2003). Reprinted with permission of Investigative Ophthalmology and Visual Science.

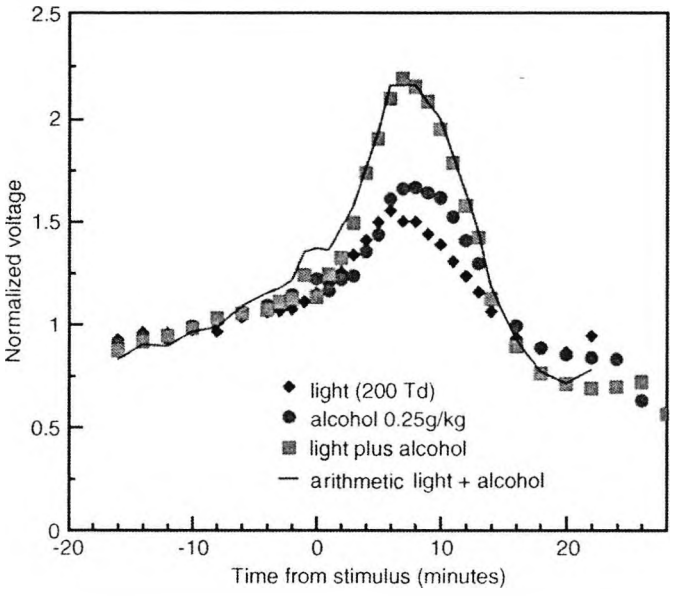

Fig. 18. Alcohol and light: When low light levels and small quantities of alcohol are given, the effects on the EOG are a simple summation (from Arden and Wolf, 2000a). Reprinted with permission of Investigative Ophthalmology and Visual Science.

response to alcohol. It is natural to consider that alcohol may liberate the "light rise substance" but this is not so, because the effects of light and alcohol do not interact as they must do if that were to be the case. Fig. 18 shows that when illumination is increased during the "alcohol rise", the voltage produced by light simply sums with the voltage change produced by alcohol. However, for each agent by itself, there is a pronounced effect of prior stimulation. A prior (low) illumination level suppresses the response to a large step increase of illumination (Fig. 19).

In addition, the presence of a low concentration of alcohol in the blood prevents the development of an "alcohol rise". However, the alcohol response is scarcely affected by illumination, and the light response is scarcely affected by established blood alcohol concentrations. The time course of the production of the "light rise substance" is unknown, but the very similar prolonged responses produced by alcohol can be mimicked by the brief injection of a bolus of alcohol, which rapidly disappears from the circulation. The simplest way of accounting for these findings is that the mechanism that causes the change in potential of the RPE (in this case the depolarisation of the basolateral surface) is a slow intracellular generator within the RPE cells, and a trigger mechanism activates the generator. Extracellular change (of the light substance or alcohol) operates the trigger mechanisms, which then rapidly become desensitised. The triggers release two types of "second messengers" which activate the generator. The implication is that the RPE is responsible for the time course of the EOG, and the voltage–time relationship is not dependent on slow changes in photoreceptors. The work on alcohol has also emphasised the difference between the peak and trough processes in the EOG. The dose–response relationship for peak and trough are different (see above) so that the trough:peak ratio alters systematically with dose (Wolf and Arden, 2004). Moreover, work on the responses of patients with RP show that the positive peak vanishes even in retinas with some preserved rod function, while the fall in voltage remains (Arden and Wolf, 2000b) (Fig. 20). One simple explanation of the fact that positive and negative changes can be separate is that they occur at opposite faces of the RPE. All the agents that provoke non-photic falls in potential might be operating on apical mechanisms, while the alcohol-induced rise, like the light rise seems to occur at the basal surface. A mechanism on the RPE apical surface is apparently a "receptor" for epinephrine, at micromolar concentration (Joseph and Miller, 1992). No such receptor has been demonstrated for alcohol, which is also apparently active at less than micromolar concentration in the RPE. It has been suggested that the alcohol abnormality in ARMD may be the result of a barrier between the RPE and the choroid that prevents entry of alcohol to the sites where it can affect the RPE. This may be of significance in the pathology of ARMD, but has little diagnostic possibility, even though early cases of ARMD show reduction and delay in the alcohol-peak, unless there is a direct and simple relationship between the degree of alcohol-EOG abnormality and the severity of ARMD.

18. Mathematical modelling

In the absence of information about mechanisms, attempts have been made to construct mathematical models that would describe the time course of the EOG changes (Homer and Kolder, 1966; Taumer et al., 1976). These authors treated the changes as a damped oscillation.

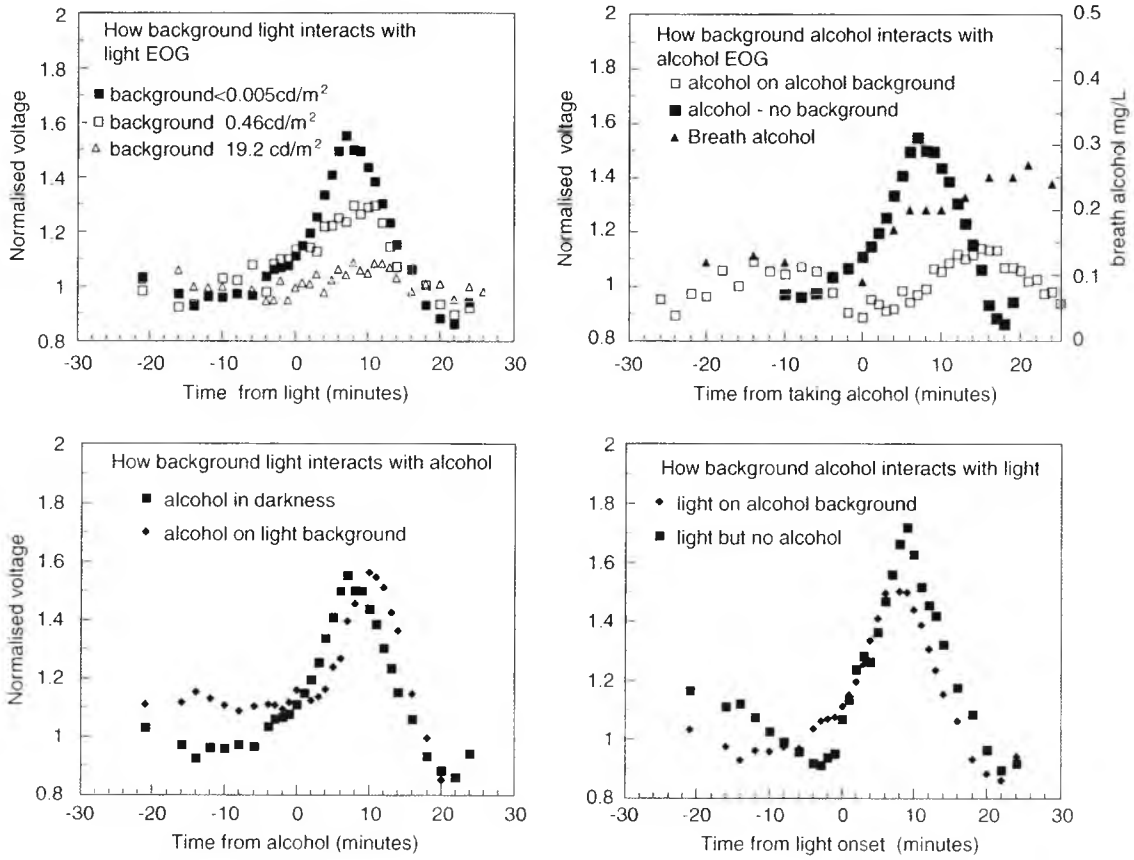

Fig. 19. While backgrounds of low-level light prevent the appearance of a light-induced EOG, and low levels of alcohol inhibit the response to a further dose of alcohol, alcohol has almost no effect on the light rise, and light has almost no effect on the alcohol-induced increase of voltage. The "receptors" for the light rise substance and the receptors (if present) for alcohol must therefore be independent (from Arden and Wolf, 2000a). Reprinted with the permission of Investigative Ophthalmology and Visual Science.

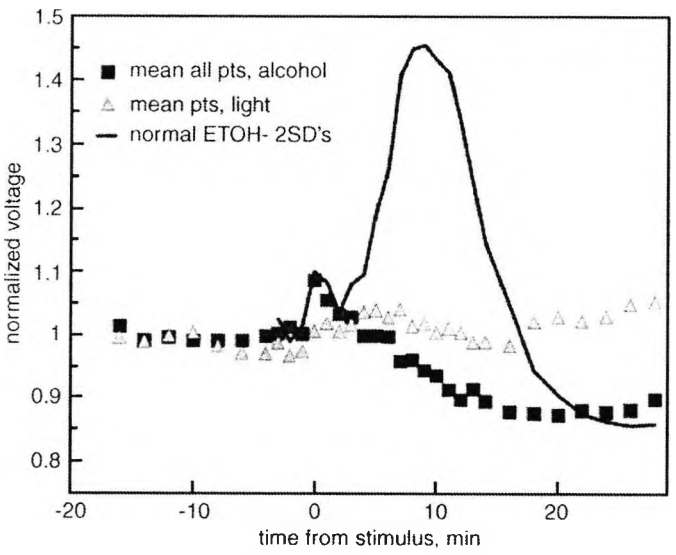

Fig. 20. The average normal alcohol-EOG (full line) is compared to the results in 17 patients with retinitis pigmentosa (squares). The triangles show the same patients' responses to light. It is evident that while the alcohol rise has been lost, a slower fall still occurs. From Arden and Wolf (2000b). Reprinted with permission of Investigative Ophthalmology and Visual Science.

In view of the descriptions above, which indicate that the early rise and the subsequent fall are produced by different mechanisms, it would be expected that the models would be complex, and in fact a number of free parameters have to be introduced before the model predictions correspond to experimental observations—Taumer et al. (1976) indicate that nine free parameters are required to model the EOG.

19. Clinical findings of general interest in the last 10 years

In acute zonal occult outer retinopathy (AZOOR), Francis et al. (2005) used the light-EOG to demonstrate the presence of RPE disturbances and thus help distinguish this condition, commenting "Electrophysiological testing can help avoid lengthy, costly, and potentially invasive investigations" which could be used as a motto by anyone investigating any puzzling defect of vision. The EOG abnormality appears diagnostic in this condition—the only instance (apart from Best's) where this is the case. EOGs are abnormal in cases of Best's associated with mutations of the VMD2 gene, a condition which although genetic have an onset as late as the 4th decade (Renner et al.,

2005)—though see Pollack et al. (2005) and others above for caveats.

Vigabatrin retinopathy has been reported to cause a considerable change to the EOG in many patients, and this is taken as evidence that this drug can alter RPE function (Arndt et al., 1999; Coupland et al., 2001; Harding et al., 2000a, b, 2002; Hardus et al., 2001; Ravindran et al., 2001). The frequency of abnormality is greater than that of the ERG, and is much less in patients on vigabatrin who do not have field defects. If field defects reverse, the EOG abnormality may remain. However, cases have been reported with normal EOGs, and the value of carrying out EOGs in patients under treatment remains undetermined. The antiepileptic drug, lamotrigine has also been associated recently with reduced EOG amplitudes (Arndt et al., 2005).

The prognosis for patients with ARMD treated by a 360° retinotomy and macular translocation is related to the EOG findings. A decreased dark trough is an unfavourable indicator for the return of visual acuity (Luke et al., 2003). Several workers have noticed that in type 1 neurofibromatosis (Lubinski et al., 2001) and in ocular complications associated with interferon alpha (Crochet et al., 2004) a decrease in the absolute value of the EOG voltage indicates damage resulting in loss of vision. In some cases, this may lead to an elevated light–dark ratio. The simplest explanation of this finding is that the absolute voltage depends upon (V_{Basal}–V_{Apical}), and as V_{Apical} is hyperpolarised with respect to V_{Basal}. The change with light depends only on the change in V_{Basal}, and if this is normal the Arden ratio will appear to increase. In conditions where the TEP is reduced but the ratio is normal, it is likely that the recorded voltage is reduced because of a decrease in paracellular resistance. When the absolute value of the voltage is low and the light rise is also reduced, the underlying mechanism maintaining the TEP is likely to be faulty.

It has been reported that malignant melanomata of the posterior uveal tract cause abnormalities in the EOG (Brink et al., 1990), and in a large multicentre study this finding was claimed to be of use in distinguishing between naevi, other forms of retinal detachment, and metastasis into the eye (Spadea et al., 1994, 2002). However, malignant choroidal melanomata have been observed with normal EOGs (McCormick et al., 1996). The EOG has been reported as abnormal in cases of desferrioxamine toxicity (Haimovici et al., 2002; Hidajat et al., 2004), not surprising in view of the effect in reducing the rate of dark adaptation (Arden, 1986). However, other methods of assessing toxicity have been reported (Arden et al., 1984; Davies et al., 1983). A number of authors have emphasised the utility of the EOG in experimental studies involving the genotyping of various retinal degenerations (and especially the carrier states of these conditions), from RP, Usher's syndrome, Best's, helicoidal peripapillary chorioretinal degeneration, neuronal ceroid lipofuscinosis, senior syndrome, choroideremia, butterfly dystrophy and Stargardt's disease (Pojda-Wilczek et al., 2004).

Abnormalities have been reported in multiple evanescent white dot syndrome and in immunodeficiency syndromes (Eysteinsson et al., 1998; Greenstein et al., 2001; Gupta and Marmor, 1995; Harrison and van Heuven, 1999; Jarc-Vidmar et al., 2001; Jurklies et al., 2001; Lafaut et al., 2001; Lim et al., 1999; Miyake et al., 1996; Pinckers et al., 1994, 1996; Ponjavic et al., 1999; Seddon et al., 2001; Stavrou et al., 1996; Theischen et al., 1997; Walter et al., 1994, 1999). In some (e.g. Eysteinsson et al., 1998), it has been reported that in cases of pigmentary disturbance or in degenerations with symptoms occurring delayed to late in life, EOG disturbances are more frequent and profound than are ERG disturbances.

20. Future directions

The identification and roles of the various Cl^- channels in the RPE and how each relates to the generation of the EOG and FOs will become possible when suitable animal models of Best's disease become available. The development of specific mammalian Cl^- channel blockers has already begun to reveal the role of CFTR in the RPE and with further developments the RPE's Cl^- channels' contribution to the EOG components will become clearer. From the clinical point of view, the number of conditions where EOGs have diagnostic value are increasing, and now that it is possible to compare membrane changes evoked (by light) from the retinal surface with those evoked by alcohol acting from the choroidal surface, EOG analysis may serve to produce further information about the pathology of retinal and RPE degenerations.

Acknowledgements

The authors would like to thank Dr. Olaf Strauss, Dr. Claire Mitchell, Dr. Janet Wolf and Dr. Vaegan for helpful comments and reviewing parts of this manuscript. This work was funded by grants from the British Retinitis Pigmentosa Society UK, the College of Optometrists UK and the South Devon and Cornwall Institute for the blind.

References

Abraham, E.H., Okunieff, P., Scala, S., Vos, P., Oosterveld, M.J.S., Chen, A.Y., Shrivastav, B., Guidotti, G., Reddy, M.M., Quinton, P.M., Haws, C., Wine, J.J., Grygorczyk, R., Tabcharani, J.A., Hanrahan, J.W., Gunderson, K.L., Kopito:, R.R., Grygorczyk, R., 1997. Cystic fibrosis transmembrane conductance regulator and adenosine triphosphate. Science 275, 1324–1326.

Adorante, J.S., 1995. Regulatory volume decrease in frog retinal pigment epithelium. Am. J. Physiol. 268, C89–C100.

Adorante, J.S., Miller, S.S., 1990. Potassium-dependent volume regulation in retinal pigment epithelium is mediated by Na,K,Cl cotransport. J. Gen. Physiol. 96, 1153–1176.

Agre, P., Preston, G.M., Smith, B.L., Jung, J.S., Raina, S., Moon, C., Guggino, W.B., Nielsen, S., 1993. Aquaporin CHIP: the archetypal molecular water channel. Am. J. Physiol. 265, F463–F476.

Akiba, Y., Jung, M., Ouk, S., Kaunitz, J.D., 2005. A novel small molecule CFTR inhibitor attenuates HCO_3^- secretion and duodenal ulcer

formation in rats. Am. J. Physiol. Gastrointest. Liver Physiol. 289, 753–759.

Aleksandrov, L., Aleksandrov, A.A., Chang, X-B., Riordan, J.R., 2002. The first nucleotide binding domain of cystic fibrosis transmembrane conductance regulator is a site of stable nucleotide interaction, whereas the second is a site of rapid turnover. J. Biol. Chem. 277, 15419–15425.

Allansson, L., Khatibi, S., Olsson, T., Hansson, E., 2001. Acute ethanol exposure induces $[Ca^{2+}]_i$ transients, cell swelling and transformation of actin cytoskeleton in astroglial primary cultures. J. Neurochem. 76, 472–479.

Ammar, D.A., Hughes, B.A., Thompson, D.A., 1998. Neuropeptide Y and the retinal pigment epithelium: receptor subtypes, signaling, and bioelectrical responses. Invest. Ophthalmol. Vis. Sci. 39, 1870–1878.

Anderson, M.P., Berger, H.A., Rich, D.P., Gregory, R.J., Smith, A.E., Welsh, M.J., 1991a. Nucleoside triphosphates are required to open the CFTR chloride channel. Cell 67, 775–784.

Anderson, M.P., Gregory, R.J., Thompson, S., Souza, D.W., Paul, S., Mulligan, R.C., Smith, A.E., Welsh, M.J., 1991b. Demonstration that CFTR is a chloride channel by alteration of its anion selectivity. Science 253, 202–205.

Anderson, M.P., Rich, D.P., Gregory, R.J., Smith, A.E., Welsh, M.J., 1991c. Generation of cAMP-activated chloride currents by expression of CFTR. Science 251, 679–682.

Arden, G.B., 1962. Alterations in the standing potential of the eye associated with retinal disease. Trans. Ophthalmol. Soc. UK 82, 63–72.

Arden, G.B., 1986. Desferrioxamine administered intravenously by infusion causes a reduction in the electroretinogram in rabbits anaesthetized with urethane. Hum. Toxicol. 5, 229–236.

Arden, G.B., Barrada, A., 1962. An analysis of the electrooculograms of a series of normal subjects. Br. J. Ophthalmol. 46, 468–482.

Arden, G.B., Ikeda, H., 1964. Electrical responses of eyes of rats with inherited retinal degeneration. In: Graymore, C.N. (Ed.), Biochemistry of the Retina. Academic Press, London.

Arden, G.B., Kelsey, J.H., 1962a. Changes produced by light in the standing potential of the human eye. J. Physiol. 161, 189–204.

Arden, G.B., Kelsey, J.H., 1962b. Some observations on the relationship between the standing potential of the human eye and bleaching and regeneration of visual purple. J. Physiol. 161, 205–226.

Arden, G.B., Wolf, J.E., 2000a. The human electro-oculogram: interaction of light and alcohol. Invest. Ophthalmol. Vis. Sci. 41, 2722–2729.

Arden, G.B., Wolf, J.E., 2000b. The electro-oculographic responses to alcohol and light in a series of patients with retinitis pigmentosa. Invest. Ophthalmol. Vis. Sci. 41, 2730–2734.

Arden, G.B., Wolf, J.E., 2003. Differential effects of light and alcohol on the electro-oculographic responses of patients with age-related macular disease. Invest. Ophthalmol. Vis. Sci. 44, 3226–3232.

Arden, G.B., Barrada, A., Kelsey, J.H., 1962. A new clinical test of retinal function based upon the standing potential of the eye. Br. J. Ophthalmol. 46, 449–467.

Arden, G.B., Wonke, B., Kennedy, C., Huehns, E.R., 1984. Ocular changes in patients undergoing long-term desferrioxamine treatment. Br. J. Ophthalmol. 68, 873–877.

Arden, G.B., Wolf, J.E., Singbartl, F., Berninger, T.E., Rudolph, G., Kampik, A., 2000. Effect of alcohol and light on the retinal pigment epithelium of normal subjects and patients with retinal dystrophies. Br. J. Ophthalmol. 84, 881–883.

Arndt, C.F., Derambure, P., Defoort-Dhellemmes, S., Hache, J.C., 1999. Outer retinal dysfunction in patients treated with vigabatrin. Neurology 52, 1201–1205.

Arndt, C.F., Sari, A., Ferre, M., Parrat, E., Courtas, D., De Seze, J., Hache, J., Matran, R., 2001. Electrophysiological effects of corticosteroids on the retinal pigment epithelium. Invest. Ophthalmol. Vis. Sci. 42, 472–475.

Arndt, C.F., Husson, J., Derambure, P., Hache, J.C., Arnaud, B., Defoort-Dhellemmes, S., 2005. Retinal electrophysiological results in patients receiving lamotrigine monotherapy. Epilepsia 46, 1055–1060.

Aserinsky, E., 1955. Effect of illumination and sleep on the amplitude of the electrooculogram. Arch. Ophthalmol. 53, 542–546.

Ashcroft, F.M., 2000. Ion Channels and Disease. Academic Press, San Diego, p. 481.

Baker, P.F., Blaustein, M.P., Hodgkin, A.L., Steinhardt, R.A., 1969. The influence of calcium on sodium efflux in squid axons. J. Physiol. 200, 431–458.

Barish, M.E., 1983. A transient calcium-dependent chloride current in the immature *Xenopus* oocyte. J. Physiol. 342, 309–325.

Barricks, M.E., 1977. Vitelliform lesions developing in normal fundi. Am. J. Ophthalmol. 83, 324–327.

Barry, P.H., Lynch, J.W., 1991. Liquid junction potentials and small cell effects in patch-clamp analysis. J. Membr. Biol. 121, 101–117.

Baukrowitz, T., Hwang, T-C., Nairn, A.C., Gadsby, D.C., 1994. Coupling of CFTR Cl^- channel gating to an ATP hydrolysis cycle. Neuron 12, 473–482.

Begenisich, T., Melvin, J.E., 1998. Regulation of chloride channels in secretory epithelia. J. Membr. Biol. 163, 77–85.

Berridge, M.J., 1993. Inositol trisphosphate and calcium signalling. Nature 361, 315–325.

Besharse, J.C., Defoe, D., 1998. The role of retinal pigment epithelium in photoreceptor turnover. In: Marmor, M.F., Wolfensberger, T.J. (Eds.), The Retinal Pigment Epithelium: Function and Disease. Oxford University Press, New York, pp. 152–172.

Bialek, S., Miller, S.S., 1994. K^+ and Cl^- transport mechanisms in bovine pigment epithelium that could modulate subretinal space volume and composition. J. Physiol. 475, 401–417.

Bialek, S., Joseph, D.P., Miller, S.S., 1995. The delayed basolateral membrane hyperpolarization of the bovine retinal pigment epithelium: mechanism of generation. J. Physiol. 484, 53–67.

Bialek, S., Quong, J.N., Yu, K., Miller, S.S., 1996. Nonsteroidal anti-inflammatory drugs alter chloride and fluid transport in bovine retinal pigment epithelium. Am. J. Physiol. 270, C1175–C1189.

Blaisdell, C.J., Edmonds, R.D., Wang, X.T., Guggino, S., Zeitlin, P.L., 2000. pH-regulated chloride secretion in fetal lung epithelia. Am. J. Physiol. 278, L1248–L1255.

Blaug, S., Quinn, R., Quong, J., Jalickee, S., Miller, S.S., 2003. Retinal pigment epithelial function: a role for CFTR? Doc. Ophthalmol. 106, 43–50.

Blum, L., 1980. Primitive electrolytes in the mean spherical approximation. Theor. Chem. Adv. Persp. 5, 1–66.

Borgula, G.A., Karwoski, C.J., Steinberg, R.H., 1989. Light-evoked changes in extracellular pH in frog retina. Vision Res. 29, 1069–1077.

Bosanac, I., Michikawa, T., Mikoshiba, K., Ikura, M., 2004. Structural insights into the regulatory mechanism of IP_3 receptor. Biochim. Biophys. Acta. 1742, 89–102.

Bösl, M.R., Stein, V., Hübner, C., Zdebik, A.A., Jordt, S-E., Mukhopadhyay, A.K., Davidoff, M.S., Holstein, A-F., Jentsch, T.J., 2001. Male germ cells and photoreceptors, both dependent on close cell–cell interactions, degenerate upon ClC-2 Cl^- channel disruption. EMBO. J. 20, 1289–1299.

Botchkin, L.M., Matthews, G., 1993. Chloride current activated by swelling in retinal pigment epithelium cells. Am. J. Physiol. 265, C1037–C1045.

Boucher, R.C., Stutts, M.J., Knowles, M.R., Cantley, L., Gatzy, J.T., 1986. Na^+ transport in cystic fibrosis respiratory epithelia. Abnormal basal rate and response to adenylate cyclase activation. J. Clin. Invest. 78, 1245–1252.

Bourne, M.C., Gruneberg, H., 1939. Degeneration of the retina and cataract, a new recessive gene in the rat. J. Hered. 30, 130–136.

Bourne, M.C., Campbell, D.A., Tansley, K., 1938. Hereditary degeneration of the rat retina. Br. J. Ophthalmol. 22, 613–622.

Braunstein, G.M., Zsembery, A., Tucker, T.A., Schwiebert, E.M., 2004. Purinergic signaling underlies CFTR control of human airway epithelial cell volume. J. Cystic Fibrosis 3, 99–117.

Breer, H., 2003. Olfactory receptors: molecular basis for recognition and discrimination of odors. Anal. Bio. Chem. 377, 427–433.

Brindley, G.S., Hamasaki, D.I., 1963. The properties and nature of the R membrane of the frog's eye. J. Physiol. 167, 599–606.

Brink, H.M., Pinckers, A.J., Verbeek, A.M., 1990. The electro-oculogram in uveal melanoma. A prospective study. Doc. Ophthalmol. 75, 329–334.

Brown, J.E., Pinto, L.H., 1974. Ionic mechanism for the photoreceptor potential of the retina of *Bufo marinus*. J. Physiol. 236, 575–591.

Cabrera-Vera, T.M., Vanhauwe, J., Thomas, T.O., Medkova, M., Preininger, A., Mazzoni, M.R., Hamm, H.E., 2003. Insights into G protein structure, function, and regulation. Endocr. Rev. 24, 765–781.

Catterall, W.A., 2000. Structure and regulation of voltage-gated Ca^{2+} channels. Ann. Rev. Cell. Dev. Biol. 16, 521–555.

Cid, L., Montrose-Rafizadeh, C., Smith, D., Guggino, W., Cutting, G., 1995. Cloning of a putative human voltage-gated chloride channel (CIC-2) cDNA widely expressed in human tissues. Hum. Mol. Genet. 4, 407–413.

Cliff, W.H., Frizzell, R.A., 1990. Separate Cl^- conductances activated by cAMP and Ca^{2+} in Cl^- secreting epithelial cells. Proc. Natl. Acad. Sci. USA 87, 4956–4960.

Coakley, R.D., Grubb, B.R., Paradiso, A.M., Gatzy, J.T., Johnson, L.G., Kreda, S.M., O'Neal, W.K., Boucher, R.C., 2003. Abnormal surface liquid pH regulation by cultured cystic fibrosis bronchial epithelium. Proc. Natl. Acad. Sci. USA 100, 16083–16088.

Cole, K.S., 1949. Dynamic electrical characteristics of the squid axon membrane. Arch. Sci. Physiol. 3, 253–258.

Collison, D.J., Tovell, V.E., Coombes, L.J., Duncan, G., Sanderson, J., 2005. Potentiation of ATP-induced Ca^{2+} mobilisation in human retinal pigment epithelial cells. Exp. Eye Res. 80, 465–475.

Constable, P.A., Lawrenson, J.G., Arden, G.B., 2005. Role of the cystic fibrosis transmembrane conductance regulator in the electro-oculogram. Paper presented at the Proceedings of the 43rd ISCEV Symposium; Glasgow.

Cornejo-Perez, P., Arreola, J., 2004. Regulation of Ca^{2+}-activated chloride channels by cAMP and CFTR in parotid acinar cells. Biochem. Biophys. Res. Commun. 316, 612–617.

Coupland, S.G., Zackon, D.H., Leonard, B.C., Ross, T.M., 2001. Vigabatrin effect on inner retinal function. Ophthalmology 108, 1493–1496.

Crochet, M., Ingster-Moati, I., Even, G., Dupuy, P., 2004. Retinopathy caused by interferon alpha associated with ribavirin therapy and the importance of the electro-oculogram. J. Fr. Ophthalmol. 27, 257–262.

Crook, R.B., Song, M.K., Tong, L.P., Yabu, J.M., Polansky, J.R., Lui, G.M., 1992. Stimulation of inositol phosphate formation in cultured human retinal pigment epithelium. Brain Res. 583, 23–30.

Cross, H.E., Bard, L., 1974. Electro-oculography in Best's macular dystrophy. Am. J. Ophthalmol. 77, 46–50.

Cuppoletti, J., Baker, A.M., Malinowska, D.H., 1993. Cl^- channels of the gastric parietal cell that are active at low pH. Am. J. Physiol. 264, C1609–C1618.

Cuppoletti, J., Tewari, K.P., Sherry, A.M., Malinowska, D.H., 2000. Activation of human ClC-2 Cl^- channels: implications for cystic fibrosis. Clin. Exp. Pharmacol. Physiol. 27, 896–900.

Cutting, G.R., Kasch, L.M., Rosenstein, B.J., Zielenski, J., Tsui, L.-C., Anatonarakis, S.E., Kazazian Jr., H.H., 1990. A cluster of cystic fibrosis mutations in the first nucleotide-binding fold of the cystic fibrosis conductance regulator protein. Nature 346, 366–369.

Davies, S.C., Marcus, R.E., Hungerford, J.L., Miller, M.H., Arden, G.B., Huehns, E.R., 1983. Ocular toxicity of high-dose intravenous desferrioxamine. Lancet 23, 2.

Davis, A.A., Bernstein, P.S., Bok, D., Turner, J., Nachtigal, M., Hunt, R.C., 1995. A human retinal pigment epithelial cell line that retains epithelial characteristics after prolonged culture. Invest. Ophthalmol. Vis. Sci. 36, 955–964.

Dawis, S., Niemeyer, G., 1986. Dopamine influences the light peak in the perfused mammalian eye. Invest. Ophthalmol. Vis. Sci. 27, 330–335.

Dawis, S., Hofmann, H., Niemeyer, G., 1985. The electroretinogram, standing potential, and light peak of the perfused cat eye during acid-base changes. Vision Res. 25, 1163–1177.

Dawson, D.C., Smith, S.S., Mansoura, M.K., 1999. CFTR: mechanism of anion conduction. Physiol. Rev. 79, 47–75.

Debye, P., Hückel, E., 1923. Zur theorie der elektrolyte II. das grenzgesetz für die elektrische leitfähigkeit. Phys. Z. 24, 305–325.

de Haas, H.K., 1901. Lichtprikkelsen retinastroomen in hun quantitatief verbund (dissertation) quoted by Kohlrausch, A. Electrichev Erscheinungen in Auge. In: Handbuch der normalen und pathologischen Physiologie, vol. XII, Springer, Berlin, University of Leiden, Leiden,1931, pp. 1394–1426.

Deutman, A.F., 1969. Electro-oculography in families with vitelliform dystrophy of the fovea. Detection of the carrier state. Arch. Ophthalmol. 81, 305–316.

Dildy-Mayfield, J.E., Machu, T., Leslie, S.W., 1992. Ethanol and voltage- or receptor-mediated increases in cytosolic Ca^{2+} in brain cells. Alcohol 9, 63–69.

Doughty, J.M., Miller, A.L., Langton, P.D., 1998. Non-specificity of chloride channel blockers in rat cerebral arteries: block of the L-type calcium channel. J. Physiol. 507, 433–439.

Doyle, D.A., Cabral, J.M., Pfuetzner, R.A., Kuo, A., Gulbis, J.M., Cohen, S.L., Chait, B.T., MacKinnon, R., 1998. The structure of the potassium channel: molecular basis of K^+ conduction and selectivity. Science 280, 69–77.

Drager, U.C., 1985. Calcium binding in pigmented and albino eyes. Proc. Natl. Acad. Sci. USA 82, 6716–6720.

Du Bois Reymond, E., 1849. Untersuchungen über dei thierische electricität, vol II. Reimer Ged, Berlin.

Duguépéroux, I., De Braekeleer, M., 2004. Genotype–phenotype relationship for five CFTR mutations frequently identified in western France. J. Cystic Fibrosis 3, 259–263.

Dunn, K.C., Aotaki-Keen, A.E., Putkey, F.R., Hjelmeland, L.M., 1996. ARPE-19, a human retinal pigment epithelial cell line with differentiated properties. Exp. Eye Res. 62, 155–169.

Dutzler, R., 2004. The structural basis of ClC chloride channel function. Trends Neurosci. 27, 315–320.

Dutzler, R., Campbell, E.B., Cadene, M., Chait, B.T., MacKinnon, R., 2002. X-ray structure of a ClC chloride channel at 3.0 Å reveals the molecular basis of anion selectivity. Nature 415, 276–277.

Economou, S.G., Stefanis, C.N., 1979. Electrooculographic (EOG) findings in manic-depressive illness. Acta. Psychiatr. Scand. 60, 155–162.

Edelman, J.L., Miller, S.S., 1991. Epinephrine stimulates fluid absorption across bovine retinal pigment epithelium. Invest. Ophthalmol. Vis. Sci. 32, 3033–3040.

Edelman, J.L., Lin, H., Miller, S.S., 1994a. Acidification stimulates chloride and fluid absorption across frog retinal pigment epithelium. Am. J. Physiol. 266, C946–C956.

Edelman, J.L., Lin, H., Miller, S.S., 1994b. Potassium-induced chloride secretion across the frog retinal pigment epithelium. Am. J. Physiol. 266, C957–C966.

Edwards, R.B., Szamier, R.B., 1977. Defective phagocytosis of isolated rod outer segments by RCS rat retinal pigment epithelium in culture. Science 197, 1001–1003.

Eggermont, J., 2004. Calcium-activated chloride channels: (un)known, (un)loved? Proc. Am. Thorac. Soc. 1, 22–27.

Einthoven, W.W., 1893. Nieuwe methoden voor clinisch onderzoek. Ned. T. Geneesk. 29, 263–286.

Epstein, G.A., Rabb, M.F., 1980. Adult vitelliform macular degeneration: diagnosis and natural history. Br. J. Ophthalmol. 64, 733–740.

Estivill, X., Bancells, C., Ramos, C., 1997. Geographic distribution and regional origin of 272 cystic fibrosis mutations in European populations. Hum. Mutat. 10, 135–154.

Evans, M.G., Marty, A., 1986. Calcium-dependent chloride currents in isolated cells from rat lacrimal glands. J. Physiol. 378, 437–460.

Eysteinsson, T., Jonasson, F., Jonsson, V., Bird, A.C., 1998. Helicoidal peripapillary chorioretinal degeneration: electrophysiology and psychophysics in 17 patients. Br. J. Ophthalmol. 82, 280–285.

Farrugia, G., Rae, J., Szurszewski, J., 1993. Characterization of an outward potassium current in canine jejunal circular smooth muscle and its activation by fenamates. J. Physiol. 468, 297–310.

Feldman, E.L., Randolph, A.E., 1993. Peptides stimulate phosphoinositide hydrolysis in human retinal pigment epithelium. Invest. Ophthalmol. Vis. Sci. 34, 431–437.

Feldman, E.L., Randolph, A.E., Johnston, G.C., DelMonte, M.A., Greene, D.A., 1991. Receptor-coupled phosphoinositide hydrolysis in human retinal pigment epithelium. J. Neurochem. 56, 2094–2100.

Ferris, C.D., Snyder, S.H., 1992. Inositol 1,4,5-triphosphate-activated calcium channels. Ann. Rev. Physiol. 54, 469–488.

Fijisawa, K., Ye, J., Zadunaisky, J.A., 1993. A Na^+/Ca^{2+} exchange mechanism in apical membrane vesicles of the retinal pigment epithelium. Curr. Eye Res. 12, 261–270.

Fischmeister, R., Hartzell, H.C., 2005. Volume sensitivity of the bestrophin family of chloride channels. J. Physiol. 562, 477–491.

Flatman, P.W., 2002. Regulation of Na–K–2Cl cotransport by phosphorylation and protein–protein interactions. Biochim. Biophys. Acta. 1566, 140–151.

Forsman, K., Graff, C., Nordstrom, S., Johansson, K., Westermark, E., Lundgren, E., Gustavson, K.H., Wadelius, C., Holmgren, G., 1992. The gene for Best's macular dystrophy is located at 11q13 in a Swedish family. Clin. Genet. 42, 156–159.

Fragoso, G., Lopez-Colome, A.M., 1999. Excitatory amino acid-induced inositol phosphate formation in cultured retinal pigment epithelium. Vis. Neurosci. 16, 263–269.

Frambach, D.A., Roy, C.E., Valentine, J.L., Weiter, J.J., 1989. Precocious retinal adhesion is affected by furosemide and ouabain. Curr. Eye Res. 8, 553–556.

Frambach, D.A., Fain, G.L., Farber, D.B., Bok, D., 1990. Beta adrenergic receptors on cultured human retinal pigment epithelium. Invest. Ophthalmol. Vis. Sci. 31, 1767–1772.

Francois, J., Verriest, G., de Rouck, A., 1955. Modification of the amplitude of the human electro-oculogram by light and dark adaption. Br. J. Ophthalmol. 39, 398–408.

Francois, J., De Rouck, A., Fernandez-Sasso, D., 1967. Electro-oculography in vitelliform degeneration of the macula. Arch. Ophthalmol. 77, 726–733.

Francis, P.J., Marinescu, A., Fitzke, F.W., Bird, A.C., Holder, G.E., 2005. Acute zonal occult outer retinopathy: towards a set of diagnostic criteria. Br. J. Ophthalmol. 89, 70–73.

Frangieh, G.T., Green, W.R., Fine, S.L., 1982. A histopathologic study of Best's macular dystrophy. Arch. Ophthalmol. 100, 1115–1121.

Friedman, Z., Hackett, S.F., Campochiaro, P.A., 1987. Characterization of adenylate cyclase in human retinal pigment epithelial cells in vitro. Exp. Eye Res. 44, 471–479.

Frings, S., Reuter, D., Kleene, S.J., 2000. Neuronal Ca^{2+}-activated Cl^- channels—homing in on an elusive channel species. Prog. Neurobiol. 60, 247–289.

Fuller, C.M., Benos, D.J., 2000. Electrophysiological characteristics of the Ca^{2+}-activated Cl^- channel family of anion transport proteins. Clin. Exp. Pharmacol. Physiol. 27, 906–910.

Fuller, M.D., Zhang, Z-R., Cui, G., Kubanek, J., McCarty, N.A., 2004. Inhibition of CFTR channels by a peptide toxin of scorpion venom. Am. J. Physiol. 287, C1328–C1341.

Fung, B.-K.K., Stryer, L., 1980. Photolyzed rhodopsin catalyzes the exchange of GTP for bound GDP in retinal rod outer segments. Proc. Natl. Acad. Sci. USA 77, 2500–2504.

Fung, B-K.K., Hurley, J.B., Stryer, L., 1981. Flow of information in the light-triggered cyclic nucleotide cascade of vision. Proc. Natl. Acad. Sci. USA 78, 152–156.

Furukawa, T., Ogura, T., Katayama, Y., Hiraoka, M., 1998. Characteristics of rabbit ClC-2 current expressed in *Xenopus* oocytes and its contribution to volume regulation. Am. J. Physiol. 274, C500–C512.

Gadsby, D.C., Nairn, A.C., 1999. Control of CFTR channel gating by phosphorylation and nucleotide hydrolysis. Physiol. Rev. 79, 77–107.

Gal, A., Li, Y., Thompson, D.A., Weir, J., Orth, U., Jacobson, S.G., Apfelstedt-Sylla, E., Vollrath, D., 2000. Mutations in MERTK, the human orthologue of the RCS rat retinal dystrophy gene, cause retinitis pigmentosa. Nat. Genet. 26, 270–271.

Gallemore, R.P., Steinberg, R.H., 1989a. Effects of DIDS on the chick retinal pigment epithelium. I. Membrane potentials, apparent resistances, and mechanisms. J. Neurosci. 9, 1968–1976.

Gallemore, R.P., Steinberg, R.H., 1989b. Effects of DIDS on the chick retinal pigment epithelium. II. Mechanism of the light peak and other responses originating at the basal membrane. J. Neurosci. 9, 1977–1984.

Gallemore, R.P., Steinberg, R.H., 1990. Effects of dopamine on the chick retinal pigment epithelium. Membrane potentials and light-evoked responses. Invest. Ophthalmol. Vis. Sci. 31, 67–80.

Gallemore, R.P., Steinberg, R.H., 1991. Cobalt increases photoreceptor-dependent responses of the chick retinal pigment epithelium. Invest. Ophthalmol. Vis. Sci. 32, 3041–3052.

Gallemore, R.P., Steinberg, R.H., 1993. Light-evoked modulation of basolateral membrane Cl^- conductance in chick retinal pigment epithelium: the light peak and fast oscillation. J. Neurophysiol. 70, 1669–1680.

Gallemore, R.P., Griff, E.R., Steinberg, R.H., 1988. Evidence in support of a photoreceptoral origin for the "light-peak substance". Invest. Ophthalmol. Vis. Sci. 29, 566–571.

Gallemore, R.P., Hernandez, E., Tayyanipour, R., Fujii, S., Steinberg, R.H., 1993. Basolateral membrane Cl^- and K^+ conductances of the dark-adapted chick retinal pigment epithelium. J. Neurophysiol. 70, 1656–1668.

Gallemore, R.P., Li, J.D., Govardovskii, V.I., Steinberg, R.H., 1994. Calcium gradients and light-evoked calcium changes outside rods in the intact cat retina. Vis. Neurosci. 11, 753–761.

Gallemore, R.P., Hughes, B.A., Miller, S.S., 1997. Retinal pigment epithelial transport mechanisms and their contributions to the electroretinogram. Prog. Ret. Eye Res. 16, 509–566.

Gallemore, R.P., Maruiwa, F., Marmor, M.F., 1998. Clinical electrophysiology of the retinal pigment epithelium. In: Marmor, M.F., Wolfensberger, T.J. (Eds.), The Retinal Pigment Epithelium. Oxford University Press, Oxford, pp. 199–223 (Chapter 10).

Gilman, A.G., 1987. G-proteins: transducers of receptor-generated signals. Annu. Rev. Biochem. 56, 615–649.

Gitter, A.H., Bertog, M., Schulzke, J.-D., Fromm, M., 1997. Measurement of paracellular epithelial conductivity by conductance scanning. Pflüger's Arch. 434, 830–840.

Glenney Jr., J.R., 1992. Tyrosine-phosphorylated proteins: mediators of signal transduction from the tyrosine kinases. Biochem. Biophys. Acta. 1134, 113–127.

Gogelein, H., Dahlem, D., Englert, H.C., Lang, H.J., 1990. Flufenamic acid, mefenamic acid and niflumic acid inhibit single non-selective cation channels in the rat exocrine pancreas. FEBS. Lett. 268, 79–82.

Goldman, D.E., 1943. Potential, impedance, and rectification in membranes. J. Gen. Physiol. 27, 37–60.

Gomez, A., Cedano, J., Oliva, B., Pinol, J., Querol, E., 2001. The gene causing the Best's macular dystrophy (BMD) encodes a putative ion exchanger. DNA Seq. 12, 431–443.

Gouras, P., Gunkel, R.D., 1963. The EOG in chloroquine and other retinopathies. Arch. Ophthalmol. 70, 629–639.

Gray, M.A., Pollard, C.E., Harris, A., Coleman, L., Greenwell, J.R., Argent, B.E., 1990. Anion selectivity and block of the small-conductance chloride channel on pancreatic duct cells. Am. J. Physiol. 259, C752–C761.

Greenstein, V.C., Seiple, W., Liebmann, J., Ritch, R., 2001. Retinal pigment epithelial dysfunction in patients with pigment dispersion syndrome: implications for the theory of pathogenesis. Arch. Ophthalmol. 119, 1291–1295.

Gribkoff, V., Lum-Ragan, J., Boissard, C., Post-Munson, D., Meanwell, N., Starrett, J.J., Kozlowski, E., Romine, J., Trojnacki, J., Mckay, M., Zhong, J., Dworetzky, S., 1996. Effects of channel modulators on cloned large-conductance calcium-activated potassium channels. Mol. Pharmacol. 50, 206–217.

Griff, E.R., Steinberg, R.H., 1982. Origin of the light peak: in vitro study of *Gekko gekko*. J. Physiol. 331, 637–652.

Griff, E.R., Steinberg, R.H., 1984. Changes in apical [K^+] produce delayed basal membrane responses of the retinal pigment epithelium in the gecko. J. Gen. Physiol. 83, 193–211.

Gründer, S., Thiemann, A., Pusch, M., Jentsch, T.J., 1992. Regions involved in the opening of CIC-2 chloride channel by voltage and cell volume. Nature 360, 759–762.

Grygorczyk, R., Hanrahan, J.W., 1997a. CFTR-independent ATP release from epithelial cells triggered by mechanical stimuli. Am. J. Physiol. 272, C1058–C1066.

Grygorczyk, R., Hanrahan, J.W., 1997b. Cystic fibrosis transmembrane conductance regulator and adenosine triphosphate. Science 275, 1325–1326.

Gunderson, K.L., Kopito, R.R., 1995. Conformational states of CFTR associated with channel gating: the role of ATP binding and hydrolysis. Cell 82, 231–239.

Gupta, L.Y., Marmor, M.F., 1994. Sequential recording of photic and nonphotic electro-oculogram responses in patients with extensive extramacular drusen. Doc. Ophthalmol. 88, 49–55.

Gupta, L.Y., Marmor, M.F., 1995. Electrophysiology of the retinal pigment epithelium in central serous chorioretinopathy. Doc. Ophthalmol. 91, 101–107.

Haas, M., Forbush III, B., 2000. The Na–K–Cl cotransporter of secretory epithelia. Ann. Rev. Physiol. 62, 515–534.

Hagins, W.A., 1972. The visual process: excitatory mechanisms in the primary receptor cells. Ann. Rev. Biophys. Bioeng. 1, 131–158.

Hagins, W.A., Penn, R.D., Yoshikami, S., 1970. Dark current and photocurrent in retinal rods. J. Biophys. 10, 380–412.

Haimovici, R., D'Amico, D.J., Gragoudas, E.S., Sokol, S., 2002. The expanded clinical spectrum of deferoxamine retinopathy. Ophthalmology 109, 164–171.

Hall, M.O., Abrams, T.A., Mittag, T.W., 1991. ROS ingestion by RPE cells is turned off by increased protein kinase C activity and by increased calcium. Exp. Eye Res. 52, 591–598.

Hall, M.O., Prieto, A.L., Obin, M.S., Abrams, T.A., Burgess, B.L., Heeb, M.J., Agnew, B.J., 2001. Outer segment phagocytosis by cultured retinal pigment epithelial cells requires Gas6. Exp. Eye Res. 73, 509–520.

Hall, M.O., Obin, M.S., Prieto, A.L., Burgess, B.L., Abrams, T.A., 2002. Gas6 binding to photoreceptor outer segments requires γ-carboxyglutamic acid (Gla) and Ca^{2+} and is required for OS phagocytosis by RPE cells in vitro. Exp. Eye Res. 75, 391–400.

Hamill, O.P., Sakmann, B., 1981. A cell-free method for recording single channel currents from biological membranes. J. Physiol. 288, 509–528.

Hamill, O.P., Marty, A., Neher, E., Sakmann, B., Sigworth, F.J., 1981. Improved patch-clamp techniques for high-resolution current recording from cells and cell-free membrane patches. Pflügers Arch. 391, 85–100.

Hanke, W., Miller, C., 1983. Single chloride channels from *Torpedo* electroplax. Activation by protons. J. Gen. Physiol. 82, 25–45.

Harding, G.F., Wild, J.M., Robertson, K.A., Lawden, M.C., Betts, T.A., Barber, C., Barnes, P.M., 2000a. Electro-oculography, electroretinography, visual evoked potentials, and multifocal electroretinography in patients with vigabatrin-attributed visual field constriction. Epilepsia 41, 1420–1431.

Harding, G.F.A., Wild, J.M., Robertson, K.A., Rietbrock, S., Martinez, C., 2000b. Separating the retinal electrophysiologic effects of vigabatrin: treatment versus field loss. Neurology 55, 347–352.

Harding, G.F., Robertson, K., Spencer, E.L., Holliday, I., 2002. Vigabatrin: its effect on the electrophysiology of vision. Doc. Ophthalmol. 104, 213–229.

Hardus, P., Verduin, W.M., Berendschot, T.T.J.M., Kamermans, M., Postma, G., Stilma, J.S., van Veelen, C.W.M., 2001. The value of electrophysiology results in patients with epilepsy and vigabatrin associated visual field loss. Acta. Ophthalmol. 79, 169–174.

Harrison, J.M., van Heuven, W.A., 1999. Retinal pigment epithelial dysfunction in human immunodeficiency virus-infected patients with cytomegalovirus retinitis. Ophthalmology 106, 790–797.

Hartzell, H.C., Qu, Z., 2003. Chloride currents in acutely isolated *Xenopus* retinal pigment epithelial cells. J. Physiol. 549, 453–469.

Hartzell, H.C., Putzier, I., Arreola, J., 2005a. Calcium-activated chloride channels. Ann. Rev. Physiol. 67, 719–758.

Hartzell, H.C., Qu, Z., Putzier, I., Artinian, L., Chien, L.-T., Cui, Y., 2005b. Looking chloride channels straight in the eye: bestrophins, lipofuscinosis, and retinal degeneration. Physiology 20, 292–302.

Hess, H.H., 1975. The high calcium content of retinal pigmented epithelium. Exp. Eye Res. 21, 471–479.

Heth, C.A., Marescalchi, P.A., Ye, Y., 1995. IP_3 generation increases rod outer segment phagocytosis by cultured royal college of surgeons retinal pigment epithelium. Invest. Ophthalmol. Vis. Sci. 36, 981–989.

Hidajat, R.R., Mc Lay, J.L., Goode, D.H., Spearing, R.L., 2004. EOG as a monitor of desferrioxamine retinal toxicity. Doc. Ophthalmol. 109, 273–278.

Higgins, C.F., 1992. ABC transporters: from microorganisms to man. Annu. Rev. Cell Biol. 8, 67–113.

Hille, B., 2001. Ion Channels of Excitable Membranes, third ed. Sinauer Associates, Inc, Sunderland (MA).

Himpens, B., Stalmans, P., Gomez, P., Malfait, M., Vereecke, J., 1999. Intra- and intercellular Ca^{2+} signaling in retinal pigment epithelial cells during mechanical stimulation. FASEB. J. 13, S63–S68.

Himstedt, F., Nagel, W.A., 1902. Fest. d. Univ Freiburg z 50jahr.Reg-Jubil. SR. Kgl Hocheit dl.l Grosshertzogs Freidrich von Baden. pp. 262–263. In: Handbuch der normalen und pathologischen Physiologie, vol. 12, Springer, Berlin, 1931, pp. 1394–1426 (Quoted by Kohlrausch A Electrichev Erscheinungen in Auge).

Hodgkin, A.L., Katz, B., 1949. The effect of sodium ions on the electrical activity of the giant axon of the squid. J. Physiol. 116, 424–448.

Hodgkin, A.L., Huxley, A.F., 1952a. The components of membrane conductance in the giant axon of *Loligo*. J. Physiol. 116, 473–496.

Hodgkin, A.L., Huxley, A.F., 1952b. Currents carried by sodium and potassium ions through the membrane of the giant axon of *Loligo*. J. Physiol. 116, 449–472.

Hodgkin, A.L., Huxley, A.F., 1952c. The dual effect of membrane potential on sodium conductance in the giant axon of *Loligo*. J. Physiol. 116, 497–506.

Hodgkin, A.L., Huxley, A.F., Katz, B., 1952. Measurement of current–voltage relations in the membrane of the giant axon of *Loligo*. J. Physiol. 116, 424–448.

Hofmann, H., Niemeyer, G., 1985. Calcium blocks selectively the EOG-light peak. Doc. Ophthalmol. 60, 361–368.

Homer, L.C., Kolder, H., 1966. Mathematical model of oscillations in the human corneo-retinal potential. Pflügers Arch. 287, 197–202.

Horn, R., Marty, A., 1988. Muscarinic activation of ionic currents measured by a new whole-cell recording method. J. Gen. Physiol. 92, 145–159.

Hu, J.G., Bok, D., 2001. A cell culture medium that supports the differentiation of human retinal pigment epithelium into functionally polarized monolayers. Mol. Vis. 7, 14–19.

Hu, J.G., Gallemore, R.P., Bok, D., Lee, A.Y., Frambach, D.A., 1994. Localization of NaK ATPase on cultured human retinal pigment epithelium. Invest. Ophthalmol. Vis. Sci. 35, 3582–3588.

Hug, M.J., Tamada, T., Bridges, R.J., 2003. CFTR and bicarbonate secretion to epithelial cells. News Physiol. Sci. 18, 38–42.

Hughes, B.A., Segawa, Y., 1993. cAMP-activated chloride currents in amphibian retinal pigment epithelial cells. J. Physiol. 466, 749–766.

Hughes, B.A., Steinberg, R.H., 1990. Voltage-dependent currents in isolated cells of the frog retinal pigment epithelium. J. Physiol. 428, 273–297.

Hughes, B.A., Takahira, M., 1996. Inwardly rectifying K^+ currents in isolated human retinal pigment epithelial cells. Invest. Ophthalmol. Vis. Sci. 37, 1125–1139.

Hughes, B.A., Takahira, M., 1998. ATP-dependent regulation of inwardly rectifying K^+ current in bovine retinal pigment epithelial cells. Am. J. Physiol. 275, C1372–C1383.

Hughes, B.A., Miller, S.S., Machen, T.E., 1984. Effects of cyclic AMP on fluid absorption and ion transport across frog retinal pigment

epithelium. Measurements in the open-circuit state. J. Gen. Physiol. 83, 875–899.

Hughes, B.A., Miller, S.S., Farber, D.B., 1987. Adenylate cyclase stimulation alters transport in frog retinal pigment epithelium. Am. J. Physiol. 252, C385–C395.

Hughes, B.A., Miller, S.S., Joseph, D.P., Edelman, J.L., 1988. cAMP stimulates the Na^+–K^+ pump in frog retinal pigment epithelium. Am. J. Physiol. 254, C84–C98.

Hughes, B.A., Adorante, J.S., Miller, S.S., Lin, H., 1989. Apical electrogenic $NaHCO_3$ cotransport. A mechanism for HCO_3 absorption across the retinal pigment epithelium. J. Gen. Physiol. 94, 125–150.

Hughes, B.A., Takahira, M., Segawa, Y., 1995. An outwardly rectifying K^+ current active near resting potential in human retinal pigment epithelial cells. Am. J. Physiol. 269, C179–C187.

Ismailov, I.I., Awayda, M.S., Jovov, B., Berdiev, B.K., Fuller, C.M., Dedman, J.R., Kaetzel, M.A., Benos, D.J., 1996. Regulation of epithelial sodium channels by the cystic fibrosis transmembrane conductance regulator. J. Biol. Chem. 271, 4725–4732.

Jarc-Vidmar, M., Popovic, P., Hawlina, M., Brecelj, J., 2001. Pattern ERG and psychophysical functions in Best's disease. Doc. Ophthalmol. 103, 47–61.

Jentsch, T.J., Steinmeyer, K., Schwarz, G., 1990. Primary structure of *Torpedo marmorata* chloride channel isolated by expression cloning in *Xenopus* oocytes. Nature 348, 510–514.

Jentsch, T.J., Stein, V., Weinreich, F., Zdebik, A.A., 2002. Molecular structure and physiological function of chloride channels. Physiol. Rev. 82, 503–568.

Jetten, A.M., Yankaskas, J.R., Stutts, M.J., Willumsen, N.J., Boucher, R.C., 1989. Persistence of abnormal chloride conductance regulation in transformed cystic fibrosis epithelia. Science 244, 1472–1475.

Johnson, J.A., Grande, J.P., Roche, P.C., Campbell, R.J., Kumar, R., 1995. Immuno-localization of the calcitriol receptor, calbindin-D28k and the plasma membrane calcium pump in the human eye. Curr. Eye Res. 14, 101–108.

Jordt, S.-E., Jentsch, T.J., 1997. Molecular dissection of gating in the ClC-2 chloride channel. EMBO. J. 16, 1582–1592.

Joseph, D.P., Miller, S.S., 1991. Apical and basal membrane ion transport mechanisms in bovine retinal pigment epithelium. J. Physiol. 435, 439–463.

Joseph, D.P., Miller, S.S., 1992. Alpha-1-adrenergic modulation of K and Cl transport in bovine retinal pigment epithelium. J. Gen. Physiol. 99, 263–290.

Jovov, B., Ismailov, I.I., Benos, D.J., 1995. Cystic fibrosis transmembrane conductance regulator is required for protein kinase A activation of an outwardly rectified anion channel purified from bovine tracheal epithelia. J. Biol. Chem. 270, 1521–1528.

Jurklies, B., Weismann, M., Kellner, U., Zrenner, E., Bornfeld, N., 2001. Klinische Befunde bei autosomal-rezessivem Syndrom der Blauzapfenhypersensitivität. Der Ophthal. 98, 285–293.

Kartner, N., Hanrahan, J.W., Jensen, T.J., Naismith, A.L., Sun, S.Z., Ackerley, C.A., Reyes, E.F., Tsui, L.-C., Rommens, J.M., Bear, C.E., 1991. Expression of the cystic fibrosis gene in non-epithelial invertebrate cells produces a regulated anion conductance. Cell 64, 681–691.

Kawasaki, K., Mukoh, S., Yonemura, D., Fujii, S., Segawa, Y., 1986. Acetazolamide-induced changes of the membrane potentials of the retinal pigment epithelial cell. Doc. Ophthalmol. 63, 375–381.

Kawasaki, K., Yamamato, S., Yonemura, D., 1977. Electrophysiological approach to clinical test for the retinal pigment epithelium. Nippon Ganka Gakkai Zasshi 81, 1303–1312.

Kawasaki, K., Yonemura, D., Madachi-Yamamoto, S., 1984. Hyperosmolarity response of ocular standing potential as a clinical test for retinal pigment epithelium activity diabetic retinopathy. Doc. Ophthalmol. 58, 375–384.

Kennedy, B.G., Mangini, N.J., 1996. Plasma membrane calcium-ATPase in cultured human retinal pigment epithelium. Exp. Eye Res. 63, 547–556.

Kennedy, B.G., Mangini, N.J., 2002. P-glycoprotein expression in human retinal pigment epithelium. Mol. Vis. 8, 422–430.

Kenyon, E., Maminishkis, A., Joseph, D.P., Miller, S.S., 1997. Apical and basolateral membrane mechanisms that regulate pH_i in bovine retinal pigment epithelium. Am. J. Physiol. 273, C456–C472.

Kikawada, N., 1968. Variations in the corneo-retinal standing potential of the vertebrate eye during light and dark adaptations. Jpn. J. Physiol. 18, 687–702.

King, L.S., Kozono, D., Agre, P., 2004. From structure to disease: the evolving tale of aquaporin biology. Nat. Rev. Mol. Cell Biol. 5, 687–698.

Kingham, J.D., Lochen, G.P., 1977. Vitelliform macular degeneration. Am. J. Ophthalmol. 84, 526–531.

Kirchberger, M.A., Tada, M., Katz, A.M., 1975. Phospholamban: a regulatory protein of the cardiac sarcoplasmic reticulum. Rec. Adv. Stud. Cardiac. Struct. Metab. 5, 103–115.

Knaus, H.-G., Scheffauer, F., Romanin, C., Schindler, H.-G., Glossmann, H., 1990. Heparin binds with high affinity to voltage-dependent L-type Ca^{2+} channels. Evidence for an agonistic action. J. Biol. Chem. 265, 11156–11166.

Knave, B., Persson, H.E., Nilsson, S.E.G., 1974. A comparative study on the effects of barbituate and ethyl alcohol on the retinal functions with specific reference to the c-wave of the electroretinogram and the standing potential of the sheep eye. Acta Ophthalmol. 52, 254–259.

Knowles, M.R., Stutts, M.J., Spock, A., Fischer, N., Gatzy, J.T., Boucher, R.C., 1983. Abnormal ion permeation through cystic fibrosis respiratory epithelium. Science 221, 1067–1070.

Koh, S.W., 1992. The pp60$^{c\text{-}src}$ in retinal pigment epithelium and its modulation by vasoactive intestinal peptide. Cell Biol. Int. Rep. 16, 1003–1014.

Kolder, H., 1959. Spontane und experimentelle anderungen des bestandspotenzials der menschlichen auges. Pflügers Arch. 268, 258–272.

Kopelman, H., Corey, M., Gaskin, K., Durie, P., Weizman, Z., Forstner, G., 1988. Impaired chloride secretion, as well as bicarbonate secretion, underlies the fluid secretory defect in the cystic fibrosis pancreas. Gastroenterology 95, 349–355.

Korenbrot, J.I., Cone, R.A., 1972. Dark ionic flux and the effects of light in isolated rod outer segments. J. Gen. Physiol. 60, 20–45.

Kramer, S.G., 1971. Dopamine: a retinal neurotransmitter. I. Retinal uptake, storage, and light-stimulated release of H3-dopamine in vivo. Invest. Ophthalmol. Vis. Sci. 10, 438–452.

Kreienbuhl, B., Niemeyer, G., 1985. Standing potential and c-wave during changes in pO_2 and flow in the perfused cat eye. Doc. Ophthalmol. 60, 353–360.

Kris, C., 1958. Corneo-fundal potential variations during light and dark adaption. Nature 182, 1027–1028.

Kristiansen, K., 2004. Molecular mechanisms of ligand binding, signaling, and regulation within the superfamily of G-protein-coupled receptors: molecular modeling and mutagenesis approaches to receptor structure and function. Pharm.Ther. 103, 21–80.

Kühne, W., Steiner, J., 1881. Über electrische vorgange im sehorgane. Untersuch. Univ. Heidelberg 4, 64–160.

Kuntz, C.A., Crook, R.B., Dmitriev, A., Steinberg, R.H., 1994. Modification by cyclic adenosine monophosphate of basolateral membrane chloride conductance in chick retinal pigment epithelium. Invest. Ophthalmol. Vis. Sci. 35, 422–433.

Kunzelmann, K., 2001. CFTR: interacting with everything? News Physiol. Sci. 16, 167–170.

Kuriyama, S., Ohuchi, T., Yoshimura, N., Honda, Y., 1991. Growth factor-induced cytosolic calcium ion transients in cultured human retinal pigment epithelial cells. Invest. Ophthalmol. Vis. Sci. 32, 2882–2890.

Kuriyama, S., Yoshimura, N., Ohuchi, T., Tanihara, H., Ito, S., Honda, Y., 1992. Neuropeptide-induced cytosolic Ca^{2+} transients and phosphatidylinositol turnover in cultured human retinal pigment epithelial cells. Brain Res. 579, 227–233.

la Cour, M., 1991a. Kinetic properties and Na^+ dependence of rheogenic Na^+-HCO_3^- co-transport in frog retinal pigment epithelium. J. Physiol. 439, 59–72.

la Cour, M., 1991b. pH homeostasis in the frog retina: the role of Na^+:HCO_3^- cotransport in the retinal pigment epithelium. Acta Ophthalmol. 69, 496–504.

la Cour, M., Baekgaard, A., Zeuthen, T., 1997. Antibodies against a furosemide binding protein from Ehrlich ascites tumour cells inhibit Na^+, K^+, Cl^- co-transport in frog retinal pigment epithelium. Acta. Ophthalmol. 75, 405–408.

Lafaut, B., Loeys, B., Leroy, B., Spileers, W., Laey, J.D., Kestelyn, P., 2001. Clinical and electrophysiological findings in autosomal dominant vitreoretinochoroidopathy: report of a new pedigree. Graefe's Arch. Clin. Exp. Ophthalmol. 239, 575–582.

Lapointe, J.Y., Szabo, G., 1987. A novel holder allowing internal perfusion of patch-clamp pipettes. Pflügers Arch. 410, 212–216.

Lara, W.C., Jordan, B.L., Hope, G.M., Dawson, W.W., Foster, R.A., Kaushal, S., 2003. Fast oscillations of the electro-oculogram in cystic fibrosis. Invest. Ophthalmol. Vis. Sci. 44 (ARVO abstract 4957).

Large, W.A., Wang, Q., 1996. Characteristics and physiological role of the Ca^{2+}-activated Cl^- conductance in smooth muscle. Am. J. Physiol. 271, C435–C454.

Leon, J.A., Arden, G.B., Bird, A.C., 1990. The standing potential in Best's macular dystrophy: baseline and drug induced responses. Invest. Ophthalmol. Vis. Sci. 31 (supplement 497).

Lemna, W.K., Feldman, G.L., Kerem, B., Fernbach, S.D., Zevkovich, E.P., O'Brien, W.E., Riordan, J.R., Collins, F.S., Tsui, L.C., Beaudet, A.L., 1990. Mutation analysis for heterozygote detection and the prenatal diagnosis of cystic fibrosis. N. Engl. J. Med. 322, 291–296.

Levi, H., Ussing, H.H., 1949. Resting potential and ion movements in the frog skin. Nature 164, 928.

Li, C., Ramjeesingh, M., Bear, C.E., 1996. Purified cystic fibrosis transmembrane conductance regulator (CFTR) does not function as an ATP channel. J. Biol. Chem. 271, 11623–11626.

Li, J.D., Gallemore, R.P., Dmitriev, A., Steinberg, R.H., 1994a. Light-dependent hydration of the space surrounding photoreceptors in chick retina. Invest. Ophthalmol. Vis. Sci. 35, 2700–2711.

Li, J.D., Govardovskii, V.I., Steinberg, R.H., 1994b. Light-dependent hydration of the space surrounding photoreceptors in the cat retina. Vis. Neurosci. 11, 743–752.

Li, M., McCann, J.D., Liedtket, C.M., Nairn, A.C., Greengard, P., Welsh, M.J., 1988. Cyclic AMP-dependent protein kinase opens chloride channels in normal but not cystic fibrosis airway epithelium. Nature 331, 358–360.

Lim, J.I., Kokame, G.T., Douglas, J.P., 1999. Multiple evanescent white dot syndrome in older patients. Am. J. Ophthalmol. 127, 725–728.

Lin, H., Miller, S.S., 1991. pH_i regulation in frog retinal pigment epithelium: two apical membrane mechanisms. Am. J. Physiol. 261, C132–C142.

Lin, H., Miller, S.S., 1994. pH_i-dependent Cl-HCO_3 exchange at the basolateral membrane of frog retinal pigment epithelium. Am. J. Physiol. 266, C935–C945.

Lin, H., Kenyon, E., Miller, S.S., 1992. Na-dependent pH_i regulatory mechanisms in native human retinal pigment epithelium. Invest. Ophthalmol. Vis. Sci. 33, 3528–3538.

Lin, H., la Cour, M., Andersen, M.V., Miller, S.S., 1994. Proton–lactate cotransport in the apical membrane of frog retinal pigment epithelium. Exp. Eye Res. 59, 679–688.

Ling, G., Gerard, R.W., 1949a. The influence of stretch on the membrane potential of the striated muscle fiber. J. Cell Physiol. 34, 397–405.

Ling, G., Gerard, R.W., 1949b. The membrane potential and metabolism of muscle fibers. J. Cell Physiol. 34, 413–438.

Ling, G., Gerard, R.W., 1949c. The normal membrane potential of frog sartorius fibers. J. Cell Physiol. 34, 383–396.

Linsdell, P., 2006. Mechanism of chloride permeation in the cystic fibrosis transmembrane conductance regulator chloride channel. Exp. Physiol. 91, 123–129.

Linsdell, P., Hanrahan, J.W., 1996. Disulphonic stilbene block of cystic fibrosis transmembrane conductance regulator Cl^- channels expressed in a mammalian cell line and its regulation by a critical pore residue. J. Physiol. 496, 687–693.

Linsdell, P., Hanrahan, J.W., 1999. Substrates of multidrug resistance-associated proteins block the cystic fibrosis transmembrane conductance regulator chloride channel. Br. J. Pharmacol. 126, 1471–1477.

Linsdell, P., Tabcharani, J.A., Hanrahan, J.W., 1997a. Multi-ion mechanism for ion permeation and block in the cystic fibrosis transmembrane conductance regulator chloride channel. J. Gen. Physiol. 110, 365–377.

Linsdell, P., Tabcharani, J.A., Rommens, J.M., Hou, Y-X., Chang, X-B., Tsui, L-C., Riordan, J.R., Hanrahan, J.W., 1997b. Permeability of wild-type and mutant cystic fibrosis transmembrane conductance regulator chloride channels to polyatomic anions. J. Gen. Physiol. 110, 355–364.

Linsenmeier, R.A., Steinberg, R.H., 1982. Origin and sensitivity of the light peak in the intact cat eye. J. Physiol. 331, 653–673.

Linsenmeier, R.A., Steinberg, R.H., 1983. A light-evoked interaction of apical and basal membranes of retinal pigment epithelium: c-wave and light peak. J. Neurophysiol. 50, 136–147.

Linsenmeier, R.A., Steinberg, R.H., 1984. Delayed basal hyperpolarization of cat retinal pigment epithelium and its relation to the fast oscillation of the dc electroretinogram. J. Gen. Physiol. 83, 213–232.

Linsenmeier, R.A., Steinberg, R.H., 1986. Mechanisms of hypoxic effects on the cat DC electroretinogram. Invest. Ophthalmol. Vis. Sci. 27, 1385–1394.

Linsenmeier, R.A., Mines, A., Steinberg, R., 1983. Effects of hypoxia and hypercapnia on the light peak and electroretinogram of the cat. Invest. Ophthalmol. Vis. Sci. 24, 37–46.

Linsenmeier, R.A., Smith, V.C., Pokorny, J., 1987. The light rise of the electrooculogram during hypoxia. Clin. Vis. Sci. 2, 111–116.

Livsey, C.T., Huang, B., Xu, J., Karwoski, C.J., 1990. Light-evoked changes in extracellular calcium concentration in frog retina. Vision Res. 30, 853–861.

Loeffler, K.U., Mangini, N.J., 1998. Immunohistochemical localization of Na^+/Ca^{2+} exchanger in human retina and retinal pigment epithelium. Graefe's Arch. Clin. Exp. Ophthalmol. 236, 929–933.

Loewen, M.E., Smith, N.K., Hamilton, D.L., Grahn, B.H., Forsyth, G.W., 2003. CLCA protein and chloride transport in canine retinal pigment epithelium. Am. J. Physiol. 285, C1314–C1321.

Logan, J., Hiestand, D., Daram, P., Huang, Z., Muccio, D.D., Hartman, J., Haley, B., Cook, W.J., Sorscher, E.J., 1994. Cystic fibrosis transmembrane conductance regulator mutations that disrupt nucleotide binding. J. Clin. Invest. 94, 228–236.

Lorenz, B., Preising, M.N., 2005. Morbus best. ein überblick zur pathologie und deren ursachen. Der Ophthalmol. 102, 111–115.

Loussouarn, G., Demolombe, S., Mohammad-Panah, R., Escande, D., Baro, I., 1996. Expression of CFTR controls cAMP-dependent activation of epithelial K^+ currents. Am. J. Physiol. 271, C1565–C1573.

Lubinski, W., Zajaczek, S., Sych, Z., Penkala, K., Palacz, O., Lubinski, J., 2001. Electro-oculogram in patients with neurofibromatosis type 1. Doc. Ophthalmol. 103, 91–103.

Luke, C., Altenheld, N., Aisenbury, S., Luke, M., Bartz-Schmidt, K.U., Walter, P., Kirchhoff, B., 2003. Electro-oculographic findings after 360 degrees retinotomy and macular translocation for subfoveal choroidal neovascularisation in age-related degeneration. V. Graefes Arch. Clin. Exp. Ophthalmol. 241, 710–715.

Lytton, J., Westlin, M., Hanley, M., 1991. Thapsigargin inhibits the sarcoplasmic or endoplasmic reticulum Ca–ATPase family of calcium pumps. J. Biol. Chem. 266, 17067–17071.

Ma, W., Pancrazio, J.J., Andreadis, J.D., Shaffer, K.M., Stenger, D.A., Li, B.S., Zhang, L., Barker, J.L., Maric, D., 2001. Ethanol blocks cytosolic Ca^{2+} responses triggered by activation of $GABA_A$ receptor/Cl^- channels in cultured proliferating rat neuroepithelial cells. Neuroscience 104, 913–922.

Ma, T., Thiagarajah, J.R., Yang, H., Sonawane, N.D., Folli, C., Galietta, L.J.V., Verkman, A.S., 2002. Thiazolidinone CFTR inhibitor identified by high-throughput screening blocks cholera toxin-induced intestinal fluid secretion. J. Clin. Invest. 110, 1651–1658.

Madachi-Yamamoto, S., Yonemura, D., Kawasaki, K., 1984a. Diamox response of ocular standing potential as a clinical test for retinal pigment epithelium activity. Normal subjects. Nippon Ganka Gakkai Zasshi 88, 1267–1272.

Madachi-Yamamoto, S., Yonemura, D., Kawasaki, K., 1984b. Hyperosmolarity response of ocular standing potential as a clinical test for retinal pigment epithelium activity. Normative data. Doc. Ophthalmol. 57, 153–162.

Malinowska, D.H., Kupert, E.Y., Bahinski, A., Sherry, A.M., Cuppoletti, J., 1995. Cloning, functional expression, and characterization of a PKA-activated gastric Cl^- channel. Am. J. Physiol. 268, C191–C200.

Maminishkis, A., Jalickee, S., Blaug, S.A., Rymer, J., Yerxa, B.R., Peterson, W.M., Miller, S.S., 2002. The P_2Y_2 receptor agonist INS37217 stimulates RPE fluid transport in vitro and retinal reattachment in rat. Invest. Ophthalmol. Vis. Sci. 43, 3555–3566.

Mangini, N.J., Haugh-Scheidt, L., Valle, J.E., Cragoe Jr., E.J., Ripps, H., Kennedy, B.G., 1997. Sodium–calcium exchanger in cultured human retinal pigment epithelium. Exp. Eye Res. 65, 821–834.

Marcet, B., Becq, F., Norez, C., Delmas, P., Verrier, B., 2004. General anaesthetic octanol and related compounds activate wild-type and del508 cystic fibrosis chloride channels. Br. J. Pharmacol. 141, 905–914.

Marchant, D., Gogat, K., Boutboul, S., Péquignot, M., Sternberg, C., Dureau, P., Roche, O., Uteza, Y., Hache, J.C., Puech, B., Puech, V., Dumur, V., Mouillon, M., Munier, F.L., Schorderet, D.F., Marsac, C., Dufier, J.L., Abitbol, M., 2001. Identification of novel VMD2 gene mutations in patients with Best vitelliform macular dystrophy. Hum. Mutat. 17, 235.

Marmont, G., 1949. Studies on the axon membrane: a new method. J. Cell Physiol. 34, 351–382.

Marmor, M.F., 1979. "Vitelliform" lesions in adults. Ann. Ophthalmol. 11, 1705–1712.

Marmor, M.F., 1989. Clinical electrophysiologic tests for evaluating the retinal pigment epithelium. In: Zingirian, M., Piccolino, F.C. (Eds.), The Retinal Pigment Epithelium. Kugler and Gherdini, Amsterdam.

Marmor, M.F., 1990. Control of subretinal fluid: experimental and clinical studies. Eye 4, 340–344.

Marmor, M.F., Lurie, M., 1979. Light induced responses of the retinal pigment epithelium. In: Zinn, K., Marmor, M.F. (Eds.), The Retinal Pigment Epithelium. Harvard University Press, Cambridge (MA), pp. 226–244.

Marmor, M.F., Zrenner, E., 1993. Standard for clinical electro-oculography. International society for clinical electrophysiology of vision. Doc. Ophthalmol. 85, 115–124.

Marmor, M.F., Donovan, W.J., Gaba, D.M., 1985. Effects of hypoxia and hyperoxia on the human standing potential. Doc. Ophthalmol. 60, 347–352.

Marmorstein, A.D., Marmorstein, L.Y., Rayborn, M., Wang, X., Hollyfield, J.G., Petrukhin, K., 2000. Bestrophin, the product of the Best vitelliform macular dystrophy gene (VMD2), localizes to the basolateral plasma membrane of the retinal pigment epithelium. Proc. Natl. Acad. Sci. USA 97, 12758–12763.

Marmorstein, L.Y., McLaughlin, P.J., Stanton, J.B., Yan, L., Crabb, J.W., Marmorstein, A.D., 2002. Bestrophin interacts physically and functionally with protein phosphatase 2A. J. Biol. Chem. 277, 30591–30597.

Marmorstein, A.D., Stanton, J.B., Yocom, J., Bakall, B., Schiavone, M.T., Wadelius, C., Marmorstein, L.Y., Peachey, N.S., 2004. A model of Best vitelliform macular dystrophy in rats. Invest. Ophthalmol. Vis. Sci. 45, 3733–3739.

Marquardt, A., Stöhr, H., Passmore, L., Kramer, F., Rivera, A., Weber, B., 1998. Mutations in a novel gene, VMD2, encoding a protein of unknown properties cause juvenile-onset vitelliform macular dystrophy (Best's disease). Hum. Mol. Genet. 7, 1517–1525.

McCormick, S.A., Gentile, R.C., Odom, J.V., Farber, M., 1996. Normal electro-oculograms in two patients with malignant melanoma of the choroid. Doc. Ophthalmol. 92, 167–172.

Melvin, J.E., Yule, D., Shuttleworth, T., Begenisich, T., 2005. Regulation of fluid and electrolyte secretion in salivary gland acinar cells. Ann. Rev. Physiol. 67, 445–469.

Mergaerts, F., Daems, E., Van Malderen, L., Spileers, W., 2001. Recording of the fast oscillations in the human electro-oculogram. Doc. Ophthalmol. 103, 63–72.

Mergler, S., Steinhausen, K., Wiederholt, M., Strauss, O., 1998. Altered regulation of L-type channels by protein kinase C and protein tyrosine kinases as a pathophysiologic effect in retinal degeneration. FASEB. J. 12, 1125–1134.

Miledi, R., 1982. A calcium-dependent transient outward current in *Xenopus laevis* oocytes. Proc. Natl. Acad. Sci. USA 215, 491–497.

Miles, W.R., 1940. Modification of the human eye potential by light and dark adaption. Science 91, 456.

Miller, C., 1982. Open-state substructure of single chloride channels from *Torpedo* electroplax. Philos. Trans. R. Soc. Lond. B. 299, 401–411.

Miller, S.S., Edelman, J.L., 1990. Active ion transport pathways in the bovine retinal pigment epithelium. J. Physiol. 424, 283–300.

Miller, S.S., Farber, D., 1984. Cyclic AMP modulation of ion transport across frog retinal pigment epithelium. Measurements in the short-circuit state. J. Gen. Physiol. 83, 853–874.

Miller, S.S., Steinberg, R.H., 1977a. Active transport of ions across frog retinal pigment epithelium. Exp. Eye Res. 25, 235–248.

Miller, S.S., Steinberg, R.H., 1977b. Passive ionic properties of frog retinal pigment epithelium. J. Membr. Biol. 36, 337–372.

Miller, S.S., Steinberg, R.H., 1979. Potassium modulation of taurine transport across the frog retinal pigment epithelium. J. Gen. Physiol. 74, 237–259.

Miller, S.S., Steinberg, R.H., Oakley II, B., 1978. The electrogenic sodium pump of the frog retinal pigment epithelium. J. Membr. Biol. 44, 259–279.

Miller, S.S., Hughes, B.A., Machen, T.E., 1982. Fluid transport across retinal pigment epithelium is inhibited by cyclic AMP. Proc. Natl. Acad. Sci. USA 79, 2111–2115.

Miller, S.S., Rabin, J., Strong, T., Iannuzzi, M.C., Adams, A.J., Collins, F.S., Reenstra, W., Mc Cray Jr., P., 1992. Cystic fibrosis (CF) gene product is expressed in retina and retinal pigment epithelium. Invest. Ophthalmol. Vis. Sci. 33 (ARVO abstract 1597).

Mircheff, A.K., 1989. Lacrimal fluid and electrolyte secretion: a review. Curr. Eye Res. 8, 607–617.

Mitchell, C.H., 2001. Release of ATP by a human retinal pigment epithelial cell line: potential for autocrine stimulation through subretinal space. J. Physiol. 534, 193–202.

Mitchell, R.H., 1982a. Inositol lipid metabolism in dividing and differentiating cells. Cell Calcium 3, 429–440.

Mitchell, R.H., 1982b. Stimulated inositol lipid metabolism: an introduction. Cell Calcium 3, 285–294.

Miyake, Y., Horiguchi, M., Suzuki, S., Kondo, M., Tanikawa, A., 1996. Electrophysiological findings in patients with Oguchi's disease. Jpn. J. Ophthalmol. 40, 511–519.

Muanprasat, C., Sonawane, N.D., Salinas, D., Taddei, A., Galietta, L.J.V., Verkman, A.S., 2004. Discovery of glycine hydrazide pore-occluding CFTR Inhibitors: mechanism, structure-activity analysis, and in vivo efficacy. J. Gen. Physiol. 124, 125–137.

Nabi, I., Mathews, A., Cohen-Gould, L., Gundersen, D., Rodriguez-Boulan, E., 1993. Immortalization of polarized rat retinal pigment epithelium. J. Cell Sci. 104, 37–49.

Nash, M.S., Osborne, N.N., 1996. Cell surface receptors associated with the retinal pigment epithelium: the adenylate cyclase and phospholipase C signal transduction pathways. Prog. Retin. Eye Res. 15, 501–546.

Neher, E., 1992. Correction for liquid junction potentials in patch clamp experiments. Methods Enzymol. 207, 123–131.

Neher, E., Sakmann, B., 1976. Single-channel currents recorded from membrane of denervated frog muscle fibres. Nature 260, 799–802.

Neher, E., Sakmann, B., Steinbach, J.H., 1978. The extracellular patch clamp: a method for resolving currents through individual open channels in biological membranes. Pflügers Arch. 375, 219–228.

Nehrke, K., Arreola, J., Nguyen, H-V., Pilato, J., Richardson, L., Okunade, G., Baggs, R., Shull, G.E., Melvin, J.E., 2002. Loss of hyperpolarization-activated Cl^- current in salivary acinar cells from *Clcn2* knockout mice. J. Biol. Chem. 277, 23604–23611.

Nernst, W., 1888. Zur kinetik der in lösung befindlichen körper: theorie der diffusion. Z. Phys. Chem. 613–637.

Newman, E.A., 2003. Glial cell inhibition of neurons by release of ATP. J. Neurosci. 23, 1659–1666.

Ng, B., Barry, P.H., 1994. Measurement of additional ionic mobilities for use in junction potential corrections in patch-clamping and other electrophysiological measurements. Proc. Aust. Neurosci. Soc. 5, 141.

Nielsen, S., Smith, B., Christensen, E., Agre, P., 1993. Distribution of the aquaporin CHIP in secretory and resorptive epithelia and capillary endothelia. Proc. Natl. Acad. Sci. USA 90, 7275–7279.

Niemeyer, G., Steinberg, R.H., 1984. Differential effects of pCO_2 and pH on the ERG and light peak of the perfused cat eye. Vision Res. 24, 275–280.

Nilius, B., Droogmans, G., 2003. Amazing chloride channels: an overview. Acta Physiol. 177, 119–147.

Nilius, B., Prenen, J., Szucs, G., Wei, L., Tanzi, F., Voets, T., Droogmans, G., 1997. Calcium-activated chloride channels in bovine pulmonary artery endothelial cells. J. Physiol. 498, 381–396.

Noell, W.K., 1942. Studies on the electrophysiology and metabolism of the retina. Project #21-1201-0004. USAF School of Aviation Medicine, Randolf Field, Texas.

Noell, W.K., 1952. Azide sensitive potentials across the eye bulb. Am. J. Ophthalmol. 170, 217–238.

Noell, W.K., 1953a. Electrophysiologic study of the retina during metabolic impairment. Am. J. Ophthalmol. 35, 126–133.

Noell, W.K., 1953b. Experimentally induced toxic effects on structure and function of visual cells and pigment epithelium. Am. J. Ophthalmol. 36, 103–116.

Oakley II, B., 1977. Potassium and the photoreceptor-dependent pigment epithelial hyperpolarization. J. Gen. Physiol. 70, 405–425.

Oakley II, B., 1983. Effects of maintained illumination upon $[K^+]_O$ in the subretinal space of the isolated retina of the toad. Vision Res. 23, 1325–1337.

Oakley II, B., Green, D.G., 1976. Correlation of the light-induced changes in retinal extracellular potassium concentration with c-wave of the electroretinogram. J. Neurophysiol. 39, 1117–1133.

Oakley II, B., Steinberg, R.H., 1982. Effects of maintained illumination upon $[K^+]_O$ in the subretinal space of the frog retina. Vision Res. 22, 767–773.

Ogawa, K., 1967. Experimental studies on the EOG of the rabbit eyes affected with administration of sodium l-glutamate. Nippon Ganka Gakkai Zasshi 71, 1466–1476.

O'Gorman, S., Flaherty, W.A., Fishman, G.A., Berson, E.L., 1988. Histopathologic findings in Best's vitelliform macular dystrophy. Arch. Ophthalmol. 106, 1261–1268.

O'Reilly, C., Winpenny, J., Argent, B., Gray, M., 2000. Cystic fibrosis transmembrane conductance regulator currents in guinea pig pancreatic duct cells: inhibition by bicarbonate ions. Gastroenterology 118, 1187–1196.

Orkand, R.K., Niedergerke, R., 1964. Heart action-potential dependence on external calcium and sodium ions. Science 146, 1176–1177.

Ottolia, M., Toro, L., 1994. Potentiation of large conductance K_{Ca} channels by niflumic, flufenamic, and mefenamic acids. J. Biophys. 67, 2272–2279.

Panessa, B.J., Zadunaisky, J.A., 1981. Pigment granule: a calcium reservoir in the vertebrate eye. Exp. Eye Res. 32, 593–604.

Paradiso, A.M., Coakley, R.D., Boucher, R.C., 2003. Polarized distribution of HCO_3^- transport in human normal and cystic fibrosis nasal epithelia. J. Physiol. 548, 203–218.

Pautler, E.L., 1994. Photosensitivity of the isolated pigment epithelium and arachidonic acid metabolism: preliminary results. Curr. Eye Res. 13, 687–695.

Penn, R.D., Hagins, W.A., 1969. Signal transmission along retinal rods and the origin of the electroretinographic a-wave. Nature 223, 201–205.

Perez-Reyes, E., Schneider, T., 1995. Molecular biology of calcium channels. Kidney Int. 48, 1111–1124.

Peters, S., Schraermeyer, U., 2001. Charakteristika und Funktionen des Melanins im retinalen Pigmentepithel. Der Ophthalmol. 98, 1181–1185.

Peterson, W.M., Miller, S.S., 1995. Identification and functional characterization of a dual GABA/taurine transporter in the bullfrog retinal pigment epithelium. J. Gen. Physiol. 106, 1089–1122.

Peterson, W.M., Meggyesy, C., Yu, K., Miller, S.S., 1997. Extracellular ATP activates calcium signaling, ion, and fluid transport in retinal pigment epithelium. J. Neurosci. 17, 2324–2337.

Petrukhin, K., Koisti, M.J., Bakall, B., Li, W., Xie, G., Marknell, T., Sandgren, O., Forsman, K., Holmgren, G., Andreasson, S., Vujic, M., Bergen, A.A., McGarty-Dugan, V., Figueroa, D., Austin, C.P., Metzker, M.L., Caskey, C.T., Wadelius, C., 1998. Identification of the gene responsible for Best macular dystrophy. Nat. Genet. 19, 241–247.

Philipson, K.D., Nicoll, D.A., 1993. Molecular and kinetic aspects of sodium-calcium exchange. Int. Rev. Cytol. 137C, 199–227.

Pierce, K.P., Premont, R.T., Lefkowitz, R.J., 2002. Seven-transmembrane receptors. Nat. Rev. Mol. Cell Biol. 3, 639–650.

Pinckers, A., van Aarem, A., Brink, H., 1994. The electrooculogram in heterozygote carriers of Usher syndrome, retinitis pigmentosa, neuronal ceroid lipofuscinosis, senior syndrome and choroideremia. Ophthal. Genet. 15, 25–30.

Pinckers, A., Cuypers, M.H., Aandekerk, A.L., 1996. The EOG in Best's disease and dominant cystoid macular dystrophy (DCMD). Ophthal. Genet. 17, 103–108.

Piomelli, D., Greengard, P., 1990. Lipoxygenase metabolites of arachidonic acid in neuronal transmembrane signalling. Trends Pharmacol. Sci. 11, 367–373.

Pirruccello, M.M., Grigorieff, N., Mindell, J.A., 2002. Electron diffraction of a bacterial ClC-type chloride channel. Novartis Found. Symp. 245, 193–203.

Pojda-Wilczek, D., Makowiecka-Obidzinska, K., Herba, E., 2004. Electroretinogram and electrooculogram in a family with Stargardt's disease. Klin. Oczna. 106, 540–541.

Pollack, K., Kreuz, F.R., Pillunat, L.E., 2005. Morbus Best mit normalen EOG. Fallvorstellung einer familiären Makuladystrophie. Der Ophthalmol. 102, 891–894.

Ponjavic, V., Eksandh, L., Andreasson, S., Sjostrom, K., Bakall, B., Ingvast, S., Wadelius, C., Ehinger, B., 1999. Clinical expression of Best's vitelliform macular dystrophy in Swedish families with mutations in the bestrophin gene. Ophthal. Genet. 20, 251–257.

Poulsen, J., Fischer, H., Illek, B., Machen, T., 1994. Bicarbonate conductance and pH regulatory capability of cystic fibrosis transmembrane conductance regulator. Proc. Natl. Acad. Sci. USA 91, 5340–5344.

Prat, A.G., Reisin, I.L., Ausiello, D.A., Cantiello, H.F., 1996. Cellular ATP release by the cystic fibrosis transmembrane conductance regulator. Am. J. Physiol. 270, C538–C545.

Puchelle, E., Gaillard, D., Ploton, D., Hinnrasky, J., Fuchey, C., Boutterin, M.C., Jacquot, J., Dreyer, D., Pavirani, A., Dalemans, W., 1992. Differential localization of the cystic fibrosis transmembrane conductance regulator in normal and cystic fibrosis airway epithelium. Am. J. Respir. 5, 485–491.

Pusch, M., 2004. Ca^{2+}-activated chloride channels go molecular. J. Gen. Physiol. 123, 323–325.

Qu, Z., Hartzell, H.C., 2000. Anion permeation in Ca^{2+}-activated Cl^- channels. J. Gen. Physiol. 116, 825–844.

Qu, Z., Hartzell, C., 2004. Determinants of anion permeation in the second transmembrane domain of the mouse bestrophin-2 chloride channel. J. Gen. Physiol. 124, 371–382.

Qu, Z., Wei, R.W., Mann, W., Hartzell, H.C., 2003. Two bestrophins cloned from *Xenopus laevis* oocytes express Ca^{2+}-activated Cl^- currents. J. Biol. Chem. 278, 49563–49572.

Qu, Z., Fischmeister, R., Hartzell, C., 2004. Mouse bestrophin-2 is a bona fide Cl^- channel: identification of a residue important in anion binding and conduction. J. Gen. Physiol. 123, 327–340.

Quednau, B., Nicoll, D., Philipson, K., 2004. The sodium/calcium exchanger family SLC8. Pflügers Arch. 447, 543–548.

Quinn, R.H., Miller, S.S., 1992. Ion transport mechanisms in native human retinal pigment epithelium. Invest. Ophthalmol. Vis. Sci. 33, 3513–3527.

Quinn, R.H., Quong, J.N., Miller, S.S., 2001. Adrenergic receptor activated ion transport in human fetal retinal pigment epithelium. Invest. Ophthalmol. Vis. Sci. 42, 255–264.

Rae, J., Cooper, K., Gates, P., Watsky, M., 1991. Low access resistance perforated patch recordings using amphotericin B. J. Neurosci. Methods 37, 15–26.

Ravindran, J., Blumbergs, P., Crompton, J., Pietris, G., Waddy, H., 2001. Visual field loss associated with vigabatrin: pathological correlations. J. Neurol. Neurosurg. Psychiatr. 70, 787–789.

Reddy, M.M., Quinton, P.M., Haws, C., Wine, J.J., Grygorczyk, R., Tabcharani, J.A., Hanrahan, J.W., Gunderson, K.L., Kopito, R.R., 1996. Failure of the cystic fibrosis transmembrane conductance regulator to conduct ATP. Science 271, 1876–1879.

Reigada, D., Mitchell, C.H., 2005. Release of ATP from retinal pigment epithelial cells involves both CFTR and vesicular transport. Am. J. Physiol. 288, C132–C140.

Reinsprecht, M., Rohn, M.H., Spadinger, R.J., Pecht, I., Schindler, H., Romanin, C., 1995. Blockade of capacitive Ca^{2+} influx by Cl^- channel blockers inhibits secretion from rat mucosal-type mast cells. Mol. Pharmacol. 47, 1014–1020.

Reisin, I., Prat, A., Abraham, E., Amara, J., Gregory, R., Ausiello, D., Cantiello, H., 1994. The cystic fibrosis transmembrane conductance regulator is a dual ATP and chloride channel. J. Biol. Chem. 269, 20584–20591.

Renner, A.B., Tillack, H., Kraus, H., Kramer, F., Mohr, N., Weber, B.H.F., Foerster, M.H., Kellner, U., 2005. Late onset is common in Best macular dystrophy associated with VMD2 gene mutations. Ophthalmology 112, 586–592.

Reuter, H., Seitz, N., 1968. The dependence of calcium efflux from cardiac muscle on temperature and external ion composition. J. Physiol. 195, 45–70.

Rich, D.P., Anderson, M.P., Gregory, R.J., Cheng, S.H., Paul, S., Jefferson, D.M., McCann, J.D., Klinger, K.W., Smith, A.E., Welsh, M.J., 1990. Expression of cystic fibrosis transmembrane conductance regulator corrects defective chloride channel regulation in cystic fibrosis airway epithelial cells. Nature 347, 358–363.

Riordan, J.R., 2005. Assembly of functional CFTR chloride channels. Ann. Rev. Physiol. 67, 701–718.

Riordan, J.R., Rommens, J.M., Kerem, B.-S., Alon, N., Rozmahel, R., Grzelczak, Z., Zielenski, J., Lok, S., Plavsic, N., Chou, J.-L., Drumm, M.L., Iannuzzi, M.C., Collins, F.S., Tsui, L.-C., 1989. Identification of the cystic fibrosis gene: cloning and characterization of complementary DNA. Science 245, 1066–1073.

Rizzolo, L.J., 1990. The distribution of Na^+, $K(^+)$-ATPase in the retinal pigmented epithelium from chicken embryo is polarized in vivo but not in primary cell culture. Exp. Eye Res. 51, 435–446.

Roberts, R.A., Stokes, R.H., 1965. Electrolyte Solutions. Butterworths, London, pp. 571.

Rodbell, M., Birnbaumer, L., Pohl, S.L., Krans, H.M., 1971. The glucagon-sensetive adenyl cyclase system in plasma membranes of rat liver. V. An obligatory role of guanylnucleotides in glucagon action. J. Biol. Chem. 246, 1877–1882.

Rodriguez de Turco, E.B., Gordon, W.C., Bazan, N.G., 1992. Light stimulates in vivo inositol lipid turnover in frog retinal pigment epithelial cells at the onset of shedding and phagocytosis of photoreceptor membranes. Exp. Eye Res. 55, 719–725.

Rohde, N., Taumer, R., Bleckmann, H., 1981. Examination of the fast oscillation of the corneoretinal potential under clinical conditions. Graefes. Arch. Klin. Exp. Ophthalmol. 217, 79–90.

Rommens, J.M., Iannuzzi, M.C., Kerem, B., Drumm, M.L., Melmer, G., Dean, M., Rozmahel, R., Cole, J.L., Kennedy, D., Hidaka, N., Zsiga, M., Buchwald, M., Riordan, J.R., Tsui, L.-C., Collins, F.S., 1989. Identification of the cystic fibrosis gene: chromosome walking and jumping. Science 245, 1059–1065.

Rosenthal, R., Bakall, B., Kinnick, T., Peachey, N., Wimmers, S., Wadelius, C., Marmorstein, A., Strauss, O., 2005. Expression of bestrophin-1, the product of the VMD2 gene, modulates voltage-dependent Ca^{2+} channels in retinal pigment epithelial cells. FASEB J., in press.

Rosenthal, R., Strauss, O., 2002. Ca^{2+}-channels in the RPE. Adv. Exp. Med. Biol. 514, 225–235.

Rudolf, G., Wioland, N., 1990. Effects of intravitreal and intravenous administrations of dopamine on the standing potential and the light peak in the intact chicken eye. Curr. Eye Res. 9, 1077–1082.

Ruiz, A., Bok, D., 1996. Characterization of the 3′ UTR sequence encoded by the AQP-1 gene in human retinal pigment epithelium. Biochim. Biophys. Acta 1282, 174–178.

Rymer, J., Miller, S.S., Edelman, J.L., 2001. Epinephrine-induced increases in $[Ca^{2+}]_{in}$ and KCl-coupled fluid absorption in bovine RPE. Invest. Ophthalmol. Vis. Sci. 42, 1921–1929.

Sabates, R., Pruett, R.C., Hirose, T., 1982. Pseudovitelliform macular degeneration. Retina 2, 197–205.

Sakmann, B., Neher, E., 1995. Single-Channel Recording. Plenum Press, New York.

Salceda, R., 1992. Zymosan induced $45Ca^{2+}$ uptake by retinal pigment epithelial cells. Curr. Eye Res. 11, 195–201.

Salceda, R., Riesgo-Escovar, J.R., 1990. Characterization of calcium uptake in chick retinal pigment epithelium. Pigment Cell Res. 3, 141–145.

Salceda, R., Sánchez-Chávez, G., 2000. Calcium uptake, release and ryanodine binding in melanosomes from retinal pigment epithelium. Cell Calcium 27, 223–229.

Sandbach, J., Vaegan, 2003. The fast oscillation of the electroculogram (EOG) is a rapidly recorded parameter, sensitive to and specific for retinitis pigmentosa. Paper presented at the Proceedings of the 41st ISCEV Symposium, Nagoya, Japan.

Schlessinger, J., Ullrich, A., 1992. Growth factor signaling by receptor tyrosine kinases. Neuron 9, 383–391.

Schneck, M.E., Fortune, B., Adams, A.J., 2000. The fast oscillation of the electrooculogram reveals sensitivity of the human outer retina, retinal pigment epithelium to glucose level. Vision Res. 40, 3447–3453.

Schraermeyer, U., Heimann, K., 1999. Current understanding on the role of retinal pigment epithelium and its pigmentation. Pigment Cell Res. 12, 219–236.

Schultz, B.D., Singh, A.K., Devor, D.C., Bridges, R.J., 1999. Pharmacology of CFTR chloride channel activity. Physiol. Rev. 79, 109–144.

Schwiebert, E.M., Egan, M.E., Hwang, T.H., Fulmer, S.B., Allen, S.S., Cutting, G.R., Guggino, W.B., 1995. CFTR regulates outwardly rectifying chloride channels through an autocrine mechanism involving ATP. Cell 81, 1063–1073.

Schwiebert, E.M., Cid-Soto, L.P., Stafford, D., Carter, M., Blaisdell, C.J., Zeitlin, P.L., Guggino, W.B., Cutting, G.R., 1998. Analysis of ClC-2 channels as an alternative pathway for chloride conduction in cystic fibrosis airway cells. Proc. Natl. Acad. Sci. USA 95, 3879–3884.

Schwiebert, E.M., Benos, D.J., Egan, M.E., Stutts, M.J., Guggino, W.B., 1999. CFTR is a conductance regulator as well as a chloride channel. Physiol. Rev. 79, 145–166.

Seddon, J.M., Afshari, M.A., Sharma, S., Bernstein, P.S., Chong, S., Hutchinson, A., Petrukhin, K., Allikmets, R., 2001. Assessment of mutations in the Best macular dystrophy (VMD2) gene in patients with adult-onset foveomacular vitelliform dystrophy, age-related maculopathy, and bull's-eye maculopathy. Ophthalmology 108, 2060–2067.

Segawa, Y., Shirao, Y., Kawasaki, K., 1997. Retinal pigment epithelial origin of bicarbonate response. Jpn. J. Ophthalmol. 41, 231–234.

Seidler, N.W., Jona, I., Vegh, M., Martonosi, A., 1989. Cyclopiazonic acid is a specific inhibitor of the Ca^{2+}-ATPase of sarcoplasmic reticulum. J. Biol. Chem. 264, 17816–17823.

Sellner, P.A., 1986. The movement of organic solutes between the retina and pigment epithelium. Exp. Eye Res. 43, 631–639.

Sepúlveda, M.R., Mata, A.M., 2004. The interaction of ethanol with reconstituted synaptosomal plasma membrane Ca^{2+}-ATPase. Biochim. Biophys. 1665, 75–80.

Shcheynikov, N., Kim, K.H., Kim, K-M., Dorwart, M.R., Ko, S.B.H., Goto, H., Naruse, S., Thomas, P.J., Muallem, S., 2004. Dynamic control of cystic fibrosis transmembrane conductance regulator Cl^-/HCO_3^- selectivity by external Cl^-. J. Biol. Chem. 279, 21857–21865.

Sheppard, D.N., Robinson, K., 1997. Mechanism of glibenclamide inhibition of cystic fibrosis transmembrane conductance regulator Cl^- channels expressed in a murine cell line. J. Physiol. 503, 333–346.

Sheppard, D.N., Rich, D.P., Ostedgaard, L.S., Gregory, R.J., Smith, A.E., Welsh, M.J., 1993. Mutations in CFTR associated with mild-disease-form Cl^- channels with altered pore properties. Nature 362, 160–164.

Sheu, S.J., Wu, S.N., 2003. Mechanism of inhibitory actions of oxidizing agents on calcium-activated potassium current in cultured pigment epithelial cells of the human retina. Invest. Ophthalmol. Vis. Sci. 44, 1237–1244.

Shimizu, T., Wolfe, L.S., 1990. Arachidonic acid cascade and signal transduction. J. Neurochem. 55, 1–15.

Shirao, Y., Steinberg, R.H., 1987. Mechanisms of effects of small hyperosmotic gradients on the chick RPE. Invest. Ophthalmol. Vis. Sci. 28, 2015–2025.

Shirao, Y., Ushimura, S., Kawasaki, K., 1997. Differentiation of neovascular maculopathies by nonphotic electro-oculogram responses. Jpn. J. Ophthalmol. 41, 174–179.

Sigal, E., 1991. The molecular biology of mammalian arachidonic acid metabolism. Am. J. Physiol. 260, L13–L28.

Sigworth, C.F., Neher, E., 1980. Single Na^+ channel currents observed in cultured rat muscle cells. Nature 287, 447–449.

Sillman, A.J., Ito, H., Tomita, T., 1969. Studies on the mass receptor potential of isolated frog retina. II. On the basis of the ionic mechanism. Vision Res. 9, 1443–1451.

Simmerman, H.K.B., Jones, L.R., 1998. Phospholamban: protein structure, mechanism of action, and role in cardiac function. Physiol. Rev. 78, 921–947.

Simpson, J.E., Gawenis, L.R., Walker, N.M., Boyle, K.T., Clarke, L.L., 2005. Chloride conductance of CFTR facilitates basal Cl^-/HCO_3^- exchange in the villous epithelium of intact murine duodenum. Am. J. Physiol. Gastrointest. 288, 1241–1251.

Skoog, O.K., Textorius, O., Nilsson, S.E.G., 1975. Effects of ethyl alcohol on the directly recorded standing potential of the human eye. Acta Ophthalmol. 53, 710–720.

Smith, S.S., Steinle, E.D., Meyerhoff, M.E., Dawson, D.C., 1999. Cystic fibrosis transmembrane conductance regulator: physical basis for lyotropic anion selectivity patterns. J. Gen. Physiol. 114, 799–818.

Smrcka, A.V., Hepler, J.R., Brown, K.O., Sternweis, P.C., 1991. Regulation of polyphosphoinositide-specific phospholipase C activity by purified G_q. Science 251, 804–807.

Soejima, M., Noma, A., 1984. Mode of regulation of the ACh-sensitive K-channel by the muscarinic receptor in rabbit atrial cells. Pflügers Arch. 400, 424–431.

Spadea, L., D'Amico, M., Dragani, T., Balestrazzi, E., 1994. Electro-oculographic changes after local excision of uveal melanoma. Doc. Ophthalmol. 86, 239–245.

Spadea, L., Bianco, G., Magni, R., Rinaldi, G., Ponte, F., Brancato, R., Ravalico, G., Balestrazzi, E., 2002. Electro-oculographic abnormality in eyes with uveal melanoma. Eur. J. Ophthalmol. 12, 419–423.

Stalmans, P., Himpens, B., 1997. Confocal imaging of Ca^{2+} signaling in cultured rat retinal pigment epithelial cells during mechanical and pharmacologic stimulation. Invest. Ophthalmol. Vis. Sci. 38, 176–187.

Stamer, W.D., Bok, D., Hu, J., Jaffe, G.J., McKay, B.S., 2003. Aquaporin-1 channels in human retinal pigment epithelium: role in transepithelial water movement. Invest. Ophthalmol. Vis. Sci. 44, 2803–2808.

Stavrou, P., Good, P.A., Broadhurst, E.J., Bundey, S., Fielder, A.R., Crews, S.J., 1996. ERG and EOG abnormalities in carriers of X-linked retinitis pigmentosa. Eye 10, 581–589.

Stefkova, J., Poledne, R., Hubacek, J.A., 2004. ATP-binding cassette (ABC) transporters in human metabolism and diseases. Physiol. Rev. 53, 235–243.

Steinberg, R.H., 1987. Monitoring communications between photoreceptors and pigment epithelial cells: effects of "mild" systemic hypoxia. Friedenwald lecture. Invest. Ophthalmol. Vis. Sci. 28, 1888–1904.

Steinberg, R.H., Linsenmeier, R.A., Griff, E.R., 1983. Three light-evoked responses of the retinal pigment epithelium. Vision Res. 23, 1315–1323.

Steinberg, R.H., Linsenmeier, R.A., Griff, E.R., 1985. Retinal pigment epithelial cell contributions to the electroretinogram and electrooculogram. Prog. Retin. Eye Res. 4, 33–66.

Steuer, H., Jaworski, A., Elger, B., Kaussmann, M., Keldenich, J., Schneider, H., Stoll, D., Schlosshauer, B., 2005. Functional characterization and comparison of the outer blood–retina barrier and the blood–brain barrier. Invest. Ophthalmol. Vis. Sci. 46, 1047–1053.

Stöhr, H., Marquardt, A., Nanda, I., Schmid, M., Weber, B.H., 2002. Three novel human VMD2-like genes are members of the evolutionary highly conserved RFP-TM family. Eur. J. Hum. Genet. 10, 281–284.

Stone, E.M., Nichols, B.E., Streb, L.M., Kimura, A.E., Sheffield, V.C., 1992. Genetic linkage of vitelliform macular degeneration (Best's disease) to chromosome 11q13. Nat. Genet. 1, 246–250.

Strange, K., Emma, F., Jackson, P.S., 1996. Cellular and molecular physiology of volume-sensitive anion channels. Am. J. Physiol. 270, C711–C730.

Strauss, O., 2005. The retinal pigment epithelium in visual function. Physiol. Rev. 85, 845–881.

Strauss, O., Rosenthal, R., 2005. Funktion des bestrophins. Der Ophthalmol. 102, 122–126.

Strauss, O., Wienrich, M., 1993. Cultured retinal pigment epithelial cells from RCS rats express an increased calcium conductance compared with cells from non-dystrophic rats. Pflügers Arch. 425, 68–76.

Strauss, O., Wienrich, M., 1994. Ca^{2+}-conductances in cultured rat retinal pigment epithelial cells. J. Cell. Physiol. 160, 89–96.

Strauss, O., Richard, G., Wienrich, M., 1993. Voltage-dependent potassium currents in cultured human retinal pigment epithelial cells. Biochem. Biophys. Res. Commun. 191, 775–781.

Strauss, O., Mergler, S., Wiederholt, M., 1997. Regulation of L-type calcium channels by protein tyrosine kinase and protein kinase C in cultured rat and human retinal pigment epithelial cells. FASEB. J. 11, 859–867.

Strauss, O., Steinhausen, M., Mergler, S., Stumpff, F., Wiederholt, M., 1999. Involvement of protein tyrosine kinase in the $InsP_3$-induced activation of Ca^{2+}-dependent Cl^- currents in cultured cells of the rat retinal pigment epithelium. J. Membr. Biol. 169, 141–153.

Strauss, O., Buss, F., Rosenthal, R., Fischer, D., Mergler, S., Stumpff, F., Thieme, H., 2000. Activation of neuroendocrine L-type channels (α1D subunits) in retinal pigment epithelial cells and brain neurons by pp60c-src. Biochem. Biophys. Res. Commun. 270, 806–810.

Stutts, M.J., Canessa, C.M., Olsen, J.C., Hamrick, M., Cohn, J.A., Rossier, B.C., Boucher, R.C., 1995. CFTR as a cAMP-dependent regulator of sodium channels. Science 269, 847–850.

Sullivan, D.M., Erb, L., Anglade, E., Weisman, G.A., Turner, J.T., Csaky, K.G., 1997. Identification and characterization of P_2Y_2 nucleotide receptors in human retinal pigment epithelial cells. J. Neurosci. Res. 49, 43–52.

Sun, H., Tsunenari, T., Yau, K.-W., Nathans, J., 2002. The vitelliform macular dystrophy protein defines a new family of chloride channels. Proc. Natl. Acad. Sci. USA 99, 4008–4013.

Tabcharani, J.A., Linsdell, P., Hanrahan, J.W., 1997. Halide permeation in wild-type and mutant cystic fibrosis transmembrane conductance regulator chloride channels. J. Gen. Physiol. 110, 341–354.

Tada, M., Kadoma, M., 1989. Regulation of the Ca^{2+} pump ATPase by cAMP-dependent phosphorylation of phospholamban. Bioessays 10, 157–163.

Taddei, A., Folli, C., Zegarra-Moran, O., Fanen, P., Verkman, A.S., Galietta, L.J.V., 2004. Altered channel gating mechanism for CFTR inhibition by a high-affinity thiazolidinone blocker. FEBS Lett. 558, 52–56.

Takahira, M., Hughes, B.A., 1997. Isolated bovine retinal pigment epithelial cells express delayed rectifier type and M-type K^+ currents. Am. J. Physiol. 273, C790–C803.

Tang, J.M., Wang, J., Quandt, F.N., Eisenberg, R.S., 1990. Perfusing pipettes. Pflügers Arch. 416, 347–350.

Taumer, R., Hennig, J., Pernice, D., 1974. The ocular dipole—a damped oscillator stimulated by the speed of change of illumination. Vision Res. 14, 637–645.

Taumer, R., Rohde, N., Pernice, D., 1976. The slow oscillation of the retinal potential: a biochemical feedback stimulated by the activity of rods and cones. Bibl. Ophthalmol. 85, 40–56.

Taylor, A.L., Kudlow, B.A., Marrs, K.L., Gruenert, D.C., Guggino, W.B., Schwiebert, E.M., 1998. Bioluminescence detection of ATP release mechanisms in epithelia. Am. J. Physiol. 275, C1391–C1406.

ten Doesschate, G., ten Doesschate, J., 1955. The influence of the state of adaptation on the steady potential of the human eye. Aeromed. Acta 4, 138–150.

Tewari, K.P., Malinowska, D.H., Sherry, A.M., Cuppoletti, J., 2000. PKA and arachidonic acid activation of human recombinant ClC-2 chloride channels. Am. J. Physiol. 279, C40–C50.

Textorius, O., Nilsson, S.E., Andersson, B.E., 1989. Effects of intravitreal perfusion with dopamine in different concentrations on the DC electroretinogram and the standing potential of the albino rabbit eye. Doc. Ophthalmol. 73, 149–162.

Thaler, A.R., Lessel, M.R., Heilig, P., 1986. Light induced oscillations of the standing potential in achromatopsia. Doc. Ophthalmol. 63, 333–336.

Thaler, A.R.G., Lesseln, M.R., Heilig, P., Scheiber, V., 1982. The fast oscillation of the electro-oculogram influence of stimulus intensity and adaption time on amplitude and peak latency. Ophthal. Res. 14, 210–214.

Theischen, M., Schilling, H., Steinhorst, U.H., 1997. EOG bei adulter vitelliformer Makuladegeneration (AVMD), schmetterlingsförmiger Patterndystrophie und Morbus Best. Der Ophthalmol. 94, 230–233.

Thiemann, A., Grunder, S., Pusch, M., Jentsch, T.J., 1992. A chloride channel widely expressed in epithelial and non-epithelial cells. Nature 356, 57–60.

Thorburn, W., Nordstrom, S., 1978. EOG in a large family with hereditary macular degeneration. (Best's vitelliform macular dystrophy) identification of gene carriers. Doc. Ophthalmol. 56, 455–464.

Toyoda, J-I., Nosaki, H., Tomita, T., 1969. Light-induced resistance changes in single photoreceptors of *Necturus* and *Gekko*. Vision Res. 969, 453–463.

Tsuboi, S., Pederson, J., 1988. Volume flow across the isolated retinal pigment epithelium of cynomolgus monkey eyes. Invest. Ophthalmol. Vis. Sci. 29, 1652–1655.

Tsunenari, T., Sun, H., Williams, J., Cahill, H., Smallwood, P., Yau, K.-W., Nathans, J., 2003. Structure-function analysis of the bestrophin family of anion channels. J. Biol. Chem. 278, 41114–41125.

Ueda, Y., Steinberg, R.H., 1993. Voltage-operated calcium channels in fresh and cultured rat retinal pigment epithelial cells. Invest. Ophthalmol. Vis. Sci. 34, 3408–3418.

Ueda, Y., Steinberg, R.H., 1994. Chloride currents in freshly isolated rat retinal pigment epithelial cells. Exp. Eye Res. 58, 331–342.

Ueda, Y., Steinberg, R.H., 1995. Dihydropyridine-sensitive calcium currents in freshly isolated human and monkey retinal pigment epithelial cells. Invest. Ophthalmol. Vis. Sci. 36, 373–380.

Uehara, F., Matthes, M.T., Yasumura, D., LaVail, M.M., 1990. Light-evoked changes in the interphotoreceptor matrix. Science 248, 1633–1636.

Ulrich, C., 2000. Bicarbonate secretion and CFTR: continuing the paradigm shift. Gastroenterology 118, 1258–1261.

Ussing, H.H., 1953. Transport through biological membranes. Ann. Rev. Physiol. 15, 1–20.

Ussing, H.H., Zerahn, K., 1951. Active transport of sodium as the source of electric current in the short-circuited isolated frog skin. Acta Physiol. 23, 110–127.

Vaegan, 1993. Independence of the fast oscillation of the electroculogram from the Arden ratio and the dark trough. Paper presented at the Proceedings of the 33rd ISCEV Symposium, Athens, Greece.

Vaegan, Beaumont, P., 1996. Relationships between EOG parameters and their sensitivity to disease. Paper presented at the Proceedings of the 36th ISCEV Symposium, Tübingen.

Vaegan, Beaumont, P., 2005. The fast oscillation of the electroculogram is a rapidly recorded independent parameter, sensitive to and specific for retinitis pigmentosa. Invest. Ophthalmol. Vis. Sci. 46, ARVO E-Abstract 515.

Valeton, J.M., van Norren, D., 1982. Intraretinal recordings of slow electrical responses to steady illumination in monkey: isolation of receptor responses and the origin of the light peak. Vision Res. 22, 393–399.

Valtink, M., Engelmann, K., Strauss, O., Kruger, R., Loliger, C., Ventura, A.S., Richard, G., 1999. Physiological features of primary cultures and subcultures of human retinal pigment epithelial cells before and after cryopreservation for cell transplantation. Graefes Arch. Clin. Exp. Ophthalmol. 237, 1001–1006.

van der Heyden, M.A.G., Wijnhoven, T.J.M., Opthof, T., 2005. Molecular aspects of adrenergic modulation of cardiac L-type Ca^{2+} channels. Cardio. Res. 65, 28–39.

Vergani, P., Lockless, S.W., Nairn, A.C., Gadsby, D.C., 2005. CFTR channel opening by ATP-driven tight dimerization of its nucleotide-binding domains. Nature 433, 876–880.

Voûte, C.L., Ussing, H.H., 1968. Some morphological aspects of active sodium transport. The epithelium of the frog skin. J. Cell Biol. 36, 625–638.

Wald, G., 1968. Molecular basis of visual excitation. Science 162, 230.

Walter, P., Brunner, R., Heimann, K., 1994. Atypical presentations of Best's vitelliform macular degeneration: clinical findings in seven cases. Ger. J. Ophthalmol. 3, 440–444.

Walter, P., Widder, R.A., Lüke, C., Königsfeld, P., Brunner, R., 1999. Electrophysiological abnormalities in age-related macular degeneration. Graefe's Arch. Clin. Exp. Ophthalmol. 237, 962–968.

Wang, H.-S., Dixon, J.E., McKinnon, D., 1997. Unexpected and differential effects of Cl^- channel blockers on the Kv4.3 and Kv4.2 K^+ channels: implications for the study of the I_{to2} current. Circ. Res. 81, 711–718.

Wang, Y., Lam, C.S., Wu, F., Wang, W., Duan, Y., Huang, P., 2005. Regulation of CFTR channels by bicarbonate-sensitive soluble adenylyl cyclase in human airway epithelial cells. Am. J. Physiol. 289, 1241–1251.

Waters, C., Pyne, S., Pyne, N.J., 2004. The role of G-protein coupled receptors and associated proteins in receptor tyrosine kinase signal transduction. Semin. Cell Dev. Biol. 15, 309–323.

Weingeist, T.A., Kobrin, J.L., Watzke, R.C., 1982. Histopathology of Best's macular dystrophy. Arch. Ophthalmol. 100, 1108–1114.

Weleber, R.G., 1989. Fast and slow oscillations of the electro-oculogram in Best's macular dystrophy and retinitis pigmentosa. Arch. Ophthalmol. 107, 530–537.

Welsh, M.J., Smith, A.E., 1993. Molecular mechanisms of CFTR chloride channel dysfunction in cystic fibrosis. Cell 73, 1251–1254.

Wen, R., Lui, G.M., Steinberg, R.H., 1993. Whole-cell K^+ currents in fresh and cultured cells of the human and monkey retinal pigment epithelium. J. Physiol. 465, 121–147.

Wen, R., Lui, G.M., Steinberg, R.H., 1994. Expression of a tetrodotoxin-sensitive Na^+ current in cultured human retinal pigment epithelial cells. J. Physiol. 476, 187–196.

Weng, T.X., Godley, B.F., Jin, G.F., Mangini, N.J., Kennedy, B.G., Yu, A.S., Wills, N.K., 2002. Oxidant and antioxidant modulation of

chloride channels expressed in human retinal pigment epithelium. Am. J. Physiol. 283, C839–C849.

White, K., Marquardt, A., Weber, B.H., 2000. VMD2 mutations in vitelliform macular dystrophy (Best disease) and other maculopathies. Hum. Mutat. 15, 301–330.

White, M.M., Miller, C., 1979. A voltage-gated anion channel from the electric organ of *Torpedo californica*. J. Biol. Chem. 254, 10161–10166.

Wills, N.K., Weng, T., Mo, L., Hellmich, H.L., Yu, A., Wang, T., Buchheit, S., Godley, B.F., 2000. Chloride channel expression in cultured human fetal RPE cells: response to oxidative stress. Invest. Ophthalmol. Vis. Sci. 41, 4247–4255.

Winkler, B.S., Pourcho, R.G., Starnes, C., Slocum, J., Slocum, N., 2003. Metabolic mapping in mammalian retina: a biochemical and ^{3}H-2-deoxyglucose autoradiographic study. Exp. Eye Res. 77, 327–337.

Winter, M.C., Welsh, M.J., 1997. Stimulation of CFTR activity by its phosphorylated R domain. Nature 389, 294–296.

Wolf, J.E., Arden, G.B., 2004. Two components of the human alcohol electro-oculogram. Doc. Ophthalmol. 109, 123–130.

Wright, A.M., Gong, X., Verdon, B., Linsdell, P., Mehta, A., Riordan, J.R., Argent, B.E., Gray, M.A., 2004. Novel regulation of cystic fibrosis transmembrane conductance regulator (CFTR) channel gating by external chloride. J. Biol. Chem. 279, 41658–41663.

Xiong, H., Li, C., Garami, E., Wang, Y., Ramjeesingh, M., Galley, K., Bear, C.E., 1999. ClC-2 activation modulates regulatory volume decrease. J. Membr. Biol. 167, 215–221.

Xu, J., Lytle, C., Zhu, T., Payne, J., Benz Jr., E., Forbush III, B., 1994. Molecular cloning and functional expression of the bumetanide-sensitive Na–K–Cl cotransporter. Proc. Natl. Acad. Sci. USA 91, 2201–2205.

Yamazaki, J., Hume, J.R., 1997. Inhibitory effects of glibenclamide on cystic fibrosis transmembrane regulator, swelling-activated, and Ca^{2+}-activated Cl^- channels in mammalian cardiac myocytes. Circ. Res. 81, 101–109.

Yang, Y., Janich, S., Cohn, J., Wilson, J., 1993. The common variant of cystic fibrosis transmembrane conductance regulator is recognized by hsp70 and degraded in a pre-Golgi nonlysosomal compartment. Proc. Natl. Acad. Sci. USA 90, 9480–9484.

Yoder, F.E., Cross, H.E., Chase, G.A., Fine, S.L., Freidhoff, L., Machan, C.H., Bias, W.B., 1988. Linkage studies of Best's macular dystrophy. Clin. Genet. 34, 26–30.

Zadunaisky, J.A., Kinne-Saffran, E., Kinne, R., 1989. A Na/H exchange mechanism in apical membrane vesicles of the retinal pigment epithelium. Invest. Ophthalmol. Vis. Sci. 30, 2332–2340.

Zdebik, A.A., Cuffe, J.E., Bertog, M., Korbmacher, C., Jentsch, T.J., 2004. Additional disruption of the ClC-2 Cl^- channel does not exacerbate the cystic fibrosis phenotype of cystic fibrosis transmembrane conductance regulator mouse models. J. Biol. Chem. 279, 22276–22283.

Zhang, G.H., Cragoe Jr., E.J., Melvin, J.E., 1992. Regulation of cytoplasmic pH in rat sublingual mucous acini at rest and during muscarinic stimulation. J. Membr. Biol. 129, 311–321.

Zhang, Z.R., Zeltwanger, S., McCarty, N.A., 2004. Steady-state interactions of glibenclamide with CFTR: evidence for multiple sites in the pore. J. Membr. Biol. 199, 15–28.

Available online at www.sciencedirect.com
SCIENCE DIRECT®
ELSEVIER
Experimental Eye Research xx (2006) 1–7
EXPERIMENTAL EYE RESEARCH
www.elsevier.com/locate/yexer

P-Glycoprotein expression in human retinal pigment epithelium cell lines

Paul A. Constable [a,*], John G. Lawrenson [a,b], Diana E.M. Dolman [b], Geoffrey B. Arden [a], N. Joan Abbott [b]

[a] *Department of Optometry and Visual Science, Henry Wellcome Laboratories for Vision Sciences, Applied Vision Research Centre, City University, Northampton Square, London EC1V 0HB, UK*
[b] *Wolfson Centre for Age-Related Diseases, King's College London, London, UK*

Received 20 May 2005; accepted in revised form 21 October 2005

Abstract

P-Glycoprotein (P-gp), an active efflux transporter encoded by the MDR1 gene, has recently been identified in the human and pig retinal pigment epithelium (RPE) in situ. Efflux pumps such as P-gp are major barriers to drug delivery in several tissues. We wished to establish whether human RPE cell lines express P-gp under the culture conditions recommended for each cell line so as to determine their suitability as in vitro models for predicting drug transport across the outer blood–retinal barrier. Three human RPE cell lines, ARPE19, D407 and h1RPE were investigated. Reverse transcriptase–polymerase chain reaction (RT-PCR) was carried out to determine the expression of MDR1 mRNA. Immunocytochemistry using the P-gp-specific antibody C219 was undertaken to investigate the presence of P-gp protein in each cell type. Uptake of rhodamine 123, a P-gp substrate, in the presence or absence of pre-treatment with a P-gp inhibitor, verapamil, was measured in each cell line to determine functional expression of P-gp. For all experiments, MDCK cells stably transfected with the human MDR1 gene (MDCK-MDR1) were used as a positive control. ARPE19 cells were consistently negative for P-gp as assessed by RT-PCR and immunocytochemistry. By contrast, RT-PCR of D407 and h1RPE samples yielded weak bands corresponding to MDR1; P-gp protein expression, as demonstrated by C219 immunoreactivity, was also present. Rhodamine uptake after treatment with verapamil was significantly greater in D407 and MDCK-MDR1, indicating functional expression of P-gp in these two cell lines. No evidence of functional P-gp was found in ARPE19 and h1RPE. In conclusion, D407 and h1RPE cells express P-gp, though functional activity was demonstrable only in D407 cells. ARPE19 cells do not express P-gp. Of these human RPE cells lines D407 could be considered as a suitable model for in vitro drug transport studies, particularly those involving P-gp substrates, without modification of their usual culture conditions.

Keywords: P-glycoprotein; retinal pigment epithelium; cell lines; drug transport

1. Introduction

Drug delivery to the retina is constrained by the presence of a blood–retinal barrier (BRB), which regulates the permeation of substances from the blood into retinal tissue. The BRB is formed by tight junctions (zonulae occludentes) between endothelial cells that make up the walls of retinal blood vessels (inner BRB) and similarly between retinal pigment epithelial cells (RPE) that form a barrier between the choroid and neural retina (outer BRB). The BRB is thus composed of effective cellular barriers that restrict the passive influx of most substances, with the exception of small lipid soluble molecules (Cunha-Vaz, 2004).

Efflux transport systems provide further barriers to drug penetration, by actively removing drugs from the retina and transferring them back into the systemic circulation. P-glycoprotein (P-gp) is a well-characterised efflux transporter that is strongly expressed by retinal vascular endothelial cells (Greenwood, 1992) and has recently been identified in human RPE (Kennedy and Mangini, 2002) and on the basolateral

* Corresponding author. Tel.: +44 207 040 3988; fax: +44 207 040 8494.
E-mail address: p.a.constable@city.ac.uk (P.A. Constable).

0014-4835/$ - see front matter © 2006 Elsevier Ltd. All rights reserved.
doi:10.1016/j.exer.2005.10.029

membrane of pig RPE (Steuer et al., 2005). P-gp displays broad substrate specificity, including the cardiac glycoside digoxin, vinca alkaloids (vincristine and vinblastine), HIV protease inhibitors (saquinavir and ritonavir), corticoids (dexamethasone and hydrocortisone), immunosuppressants (cyclosporin A) and antibiotics (erythromycin, gramicidin D and valinomycin) (reviewed by Schinkel and Jonker, 2003).

The increased pace of discovery of candidate drug molecules requires a high-throughput quantitative screen to predict tissue penetration, and cell-based in vitro models are being increasingly used for this purpose (Gumbleton and Audus, 2001). Although retinal drug delivery is a rapidly emerging field (Duvvuri et al., 2003) few studies have evaluated suitable in vitro models. The aim of the present study was to determine whether RPE cell lines derived from human express P-gp when grown under culture conditions recommended by the original authors.

Three human RPE cell lines were studied. The ARPE19 cell line is a well-established model of human RPE that exhibits many characteristics of native human RPE (Dunn et al., 1996, 1998; Mitchell, 2001). Like ARPE19, D407 cells arose spontaneously and have been used to model the outer BRB (Mannerstrom et al., 2002) and they also maintain characteristics of human RPE (Davis et al., 1995). The newly immortalised RPE cell line, h1RPE, is the result of transfection of human RPE cells with a SV40 large T antigen and therefore one might expect the phenotype to be closest to that of primary human RPE cells; these cells have been shown to retain many biochemical and morphological features of the human RPE in situ (Greenwood et al., 1996; Kanuga et al., 2002). The ARPE19 and h1RPE cell lines have been successfully used to attenuate visual loss, by transplantation into the sub-retinal space of an animal model of inherited retinal degeneration, the Royal College of Surgeons (RCS) rat (Lund et al., 2001).

We studied expression of MDR1 (P-gp) mRNA by RT-PCR and of P-gp protein by immunocytochemistry. Functional P-gp expression was investigated by uptake of the P-gp substrate rhodamine 123 by RPE cells in the presence and absence of pre-treatment with the P-gp inhibitor verapamil.

2. Materials and methods

2.1. Cell culture

Three human RPE cell lines were studied: D407 (Davis et al., 1995), ARPE19 (Dunn et al., 1996) and h1RPE (Kanuga et al., 2002). Madin Darby Canine Kidney (MDCK) cells, which do not express P-gp, and MDCK-MDR1, which have been transfected with full-length human MDR1 and express functional P-gp (Pastan et al., 1988), were used as controls. MDCK and MDCK-MDR1 cells were kindly provided by R. Melarange, GlaxoSmithKline, Ware, UK; D407 cells were a generous gift from Dr Richard Hunt, University of South Carolina Medical School, Colombia, SC, USA; ARPE19 cells were supplied by the American Type Culture Collection (ATCC, Manassas, VA, USA), and h1RPE were a generous gift of Prof. John Greenwood (Institute of Ophthalmology, University College London, UK). The ARPE19 cell line retains many features of human RPE including mild pigmentation, the expression of RPE65 and cellular retinaldehyde-binding protein (CRALBP). ARPE19 has a diploid karyotype but has apparent alterations in chromosome 8 and 19 (Dunn et al., 1996). D407 also arose spontaneously and express CRALBP but are non-pigmented. The karyotype above passage 52 shows a near triploid modal chromosome number (Davis et al., 1995). h1RPE is a transfected cell line and maintains a stable phenotype expressing RPE65 and CRALBP as well as exhibiting polarity but lacking pigmentation (Lund et al., 2001; Kanuga et al., 2002). The cells used in this study exhibited cobblestone morphology similar to that of RPE cells in situ.

ARPE19 cells were grown in a 1:1 mixture of Dulbecco's modified Eagle's medium and Ham's F12 (DMEM:F12) (Gibco-Invitrogen, Paisley, UK) supplemented with 10% (vol/vol) heat inactivated foetal calf serum (FCS), 100 U/ml penicillin, 100 μg/ml streptomycin and 2 mM Glutamax (Gibco-Invitrogen). Cells were used at passage 24–30. D407 cells were grown in DMEM with high (4.5 g/l) glucose (Gibco-Invitrogen) supplemented with 10% heat inactivated FCS, 100 U/ml penicillin, 100 μg/ml streptomycin and 2 mM Glutamax; they were used at passage 85–97. h1RPE cells were grown in Ham's F10 with 20% heat inactivated FCS, 100 U/ml penicillin, 100 μg/ml streptomycin, 100 μg/ml amphotericin-B and 2 mM glutamine. Cells were used at passage 22–33. MDCK and MDCK-MDR1 cells were grown in the same medium as D407 cells and used within 40 passages of receipt. The time from seeding to reaching confluence varied between the cell lines with h1RPE cells taking 2–3 days longer than the other cell lines used. Therefore these cells were seeded earlier so that all cell lines reached confluence on the same day and all experiments were then performed 1–2 days post confluence. Cells were passaged upon reaching confluence (5 min at room temperature in calcium- and magnesium-free Hank's balanced salt solution, followed by 0.25% trypsin-EDTA solution) at a 1:4 split. Cells were maintained in a humidified incubator at 37 °C with 5% CO_2/95% air.

All chemicals were supplied by Sigma, Poole, UK unless otherwise specified.

2.2. RT-PCR

Total RNA was extracted from cells grown in flasks with RNABee (Biogenesis, Poole, UK) according to the manufacturer's protocol. Purity and concentration were determined by ultraviolet spectrophotometry. 1 μg of total RNA from each sample was reversed transcribed in a total volume of 20 μl containing oligo $d(T)_{15}$ primer, RNasin and reverse transcriptase (all from Promega, Southampton, UK). Primers were designed to detect MDR1 (accession number AF016535) (5′-CGAAACCGTATCAGTCCTCG-3′; 5′-CTTGAGTCTGAGAGACCACC-3′; corresponding to the nucleotide sequences 3099–3118 and 3652–3671 respectively) and β-actin (5′-ATCGTGGGCCGCCCTAGGCAC-3′; 5′-TGGCCTTAGGGTTCAGAGGGGC-3′; 1343–1363 and 1652–1673, respectively (Oddiah et al., 1998). They were synthesised by Sigma Genosys

(Pampisford, UK). Reverse transcriptase was omitted from the negative controls. The reverse transcription reaction was carried out at 42 °C for 60 min then 99 °C for 5 min. Amplification was performed with 2.5 μl cDNA in a total volume of 25 μl containing: magnesium-free reaction buffer (Promega), 1.5 mM $MgCl_2$ (Promega), 0.1 mM of each primer, 0.5 mM dNTPs (Bioline, London, UK) and 0.625 U Taq DNA polymerase (Promega). PCR was performed in a thermal cycler (GeneAmp 9700; Applied Biosystems, Warrington, UK), with 5 min at 94 °C for denaturing, followed by 30 cycles of 30 s at 94 °C, 30 s at 55 °C, 30 s at 72 °C, with a final 7 min at 72 °C. For each sample, a negative control was included to check for absence of genomic DNA. PCR products were subjected to gel electrophoresis (1% agarose stained with 5 μg/ml ethidium bromide) together with a size marker (Hyperladder 1; Bioline). The expected product size was 554 bp for MDR1 and 243 bp for β-actin. The PCR products were cloned into the pCR2.1 vector by means of the Original TA Cloning Kit (Invitrogen). Plasmids were isolated with the Sigma GenElute Plasmid Miniprep Kit and the identity of the inserts confirmed by sequencing (Molecular Biology Unit, King's College London).

2.3. Immunocytochemistry

To enhance attachment and growth of the cell lines, glass cover slips (12 mm diameter) were pre-coated with 5–10 μg/cm^2 of mouse collagen type-1 solution and placed in 4-well chambers (Nunc, Roskilde, Denmark) overnight at 37 °C. Excess collagen solution was aspirated the next day before cells were seeded at 5×10^4 D407; 1×10^5 ARPE19; and 2×10^5 MDCK-MDR1 and h1RPE cells/cm^2. Cells were grown to confluence in their respective media. All procedures were carried out at room temperature unless stated otherwise. Cover slips were washed twice in phosphate-buffered saline (PBS) for 5 min and fixed with ice-cold acetone at 4 °C for 10 min. They were rinsed three times in PBS and blocked in PBS containing 0.5% (wt/vol) bovine serum albumin and 5% (vol/vol) mouse serum for 20 min before they were washed thoroughly three times for 5 min in PBS. The antibody C219 (ID Labs, Glasgow, UK) recognizes an internal epitope of human P-gp; it was added at a dilution of 1:10 in blocking buffer and cells incubated for 60 min. Cover slips were washed three times for 5 min in PBS before the secondary antibody (FITC-conjugated goat anti-mouse; Dako, Glostrup, Denmark) was added (1:200 dilution in blocking buffer) and incubated in the dark for 1 h. Cover slips were washed three times in PBS and nuclei counterstained with propidium iodide (1 μg/ml in PBS) before they were washed three times in PBS and mounted with fluorescent mounting medium (DAKO). Cells were imaged with a Zeiss Axiovert 510 laser scanning confocal microscope (Carl Zeiss, Jena, Germany) with dual excitation of 488 nm and 543 nm at appropriate magnification. They were viewed with a 40× oil immersion lens. Images (1024 × 1024 pixels) were stored on computer hard drive and viewed with Axiovision ver. 3 (Carl Zeiss, Jena, Germany). Negative controls (not shown) were incubated with the secondary antibody only.

2.4. Rhodamine 123 uptake assay

Cells were seeded at the densities noted above into 24-well plates (Nunc) and grown to confluence in their respective recommended media. Rhodamine 123 was diluted from 20 mM stock in ethanol to 20 μM in buffer. The buffer was, in mM: NaCl 140; KCl 4.8; $MgSO_4$ 1.0; $CaCl_2$ 1.8; KH_2PO_4 0.2; HEPES 15; and glucose 5.0 adjusted to pH 7.40 with NaOH. One plate was designated for treatment with verapamil in DMSO diluted in buffer to give a final concentration of 50 μM verapamil and 0.125% DMSO (vol/vol). The second plate was treated with buffer containing 0.125% DMSO (vol/vol) and acted as a control. In each plate 4 wells were pooled to give 1 sample. One sample from 4 wells was used as the spectrophotometric blank and a separate sample from 4 wells for protein assay.

All experiments were conducted independently in triplicate with 5 samples per experiment. Cells were washed in buffer briefly to remove all medium then 0.5 ml of buffer containing either verapamil or DMSO was added to the test or control plate respectively. Plates were incubated for 40 min at 37 °C before solutions were aspirated and replaced with 0.5 ml of buffer containing 20 μM rhodamine 123. The cells were incubated for a further 60 min at 37 °C before being washed three times quickly with ice-cold buffer to stop the reaction. Cells were then lysed in Triton-X (1% vol/vol) in buffer (0.5 ml per well) for 90 min at room temperature in the dark.

Cell lysates pooled from 4 wells (2 ml) were used for absorbance measurements or were stored at −55 °C for protein assay. The absorbance spectrum for rhodamine 123 was determined by spectrophotometry (Shimadzu, Kyoto, Japan) and gave a peak at 501 nm. Total absorbance at 501 nm was determined in an Ultraspec® II spectrometer (LKB Biochrom Ltd, Cambridge, UK).

Total protein for each cell line was determined for each run using the BCA protein assay kit according to the manufacturer's instructions (Pierce, Tattenhall, UK). Bovine serum albumin (BSA) standards were diluted from 2 mg/ml stock. 100 μl of standards and 100 μl of cell lysate was added in triplicate to a 96-well plate (Nunc) and 100 μl working reagent was added to each well. The samples were incubated at 37 °C for 30 min before total absorbance was read in a plate reader (Multiskan Ascent®, Thermo, Basingstoke, UK). Total protein per 100 μl was determined for each cell line in each of the three runs.

Rhodamine 123 uptake was normalised per μg of protein for each cell line in each of the runs and was expressed as Abs_{501}/μg protein. Statistical analysis was by Student's *t*-test, with $P < 0.05$ taken as significant.

3. Results

3.1. RT-PCR

RT-PCR was performed on samples of parent MDCK cells and MDCK cells stably transfected with MDR1 (MDCK-MDR1). A strong band of the size expected for the MDR1

amplification product (554 bp) was seen in the MDCK-MDR1 cells but only a very faint band for MDR1 was detected in the parent line (Fig. 1). However, β-actin amplified strongly in both cell types; there were no bands in the negative controls (reverse transcriptase omitted from the RT reaction; results not shown), indicating that genomic DNA was not present.

Samples of the RPE cell lines were screened for MDR1 mRNA; an example of a gel is shown in Fig. 2a. Amplification products of the expected size were seen with h1RPE cells in 2 out of 4 independent samples and in D407 cells (4 out of 5 independent samples), although the bands, when present, were faint. No bands were detected for ARPE19 cells in 5 independent samples. MDCK-MDR1 cells were always run as a positive control. All RPE cell samples showed positive bands for β-actin (Fig. 2b), but reactions in which reverse transcriptase was omitted yielded no bands (results not shown).

Sequencing of the amplified products confirmed that they were identical to published data for human MDR1.

3.2. Immunocytochemistry

Staining with the P-gp specific antibody C219 revealed strong immunoreactivity in MDCK-MDR1 cells. Plasma membrane staining was evident, but P-gp was also expressed in the cytoplasm (Fig. 3a). For RPE cells, ARPE19 cells were consistently negative for P-gp (Fig. 3d). However, h1RPE and D407 showed weak immunoreactivity that appeared to be heterogeneously distributed throughout the cell (Fig. 3b,c respectively).

3.3. Rhodamine uptake assay

Rhodamine 123 enters cells passively but can be extruded from the cytosol by P-gp. The inhibition of P-gp with verapamil prevents the extrusion and therefore rhodamine 123 accumulates in the cytosol. Such an increase in intracellular rhodamine 123 can be clearly seen for the positive control (MDCK-MDR1) (Fig. 4). Of the human RPE cell lines, only D407 showed a significant difference in uptake ($P < 0.01$) between verapamil treated and control (see Fig. 4), indicating functional expression of P-gp. An absence of P-gp activity is demonstrated by no difference in cytosolic rhodamine 123 levels when verapamil is used to block P-gp. This was the case for both ARPE19 and h1RPE7, despite the fact that P-gp was detected in h1RPE7 at both mRNA and protein levels.

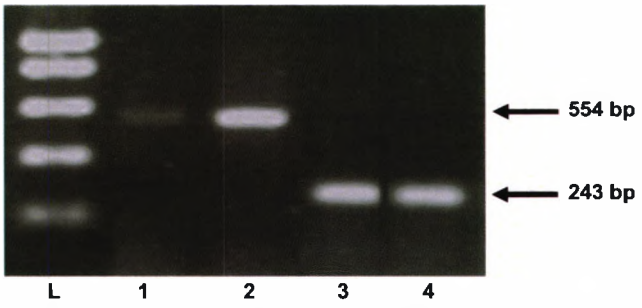

Fig. 1. MDR1 and β-actin mRNA expression in MDCK and MDCK-MDR1 cells: gel of PCR amplification products. Strong bands of the expected size for MDR1 (554 bp) were seen in the MDR1-transfected cells (lane 2), but only very weak bands in the parent cell line (lane 1). Bands for β-actin (expected product size 243 bp) were seen in both cell types (lanes 3 and 4, MDCK and MDCK-MDR1 respectively). L size marker.

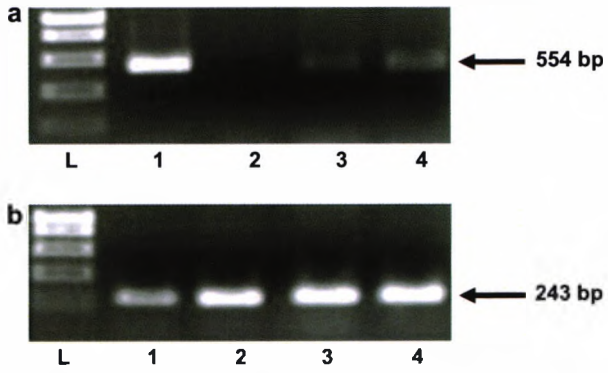

Fig. 2. Expression of mRNA for MDR1 and β-actin in RPE cell lines: an example of a gel of PCR amplification products. (a) Bands for MDR1 (expected size 554 bp) were faint for h1RPE (lane 3) and D407 (lane 4) cells, but ARPE19 (lane 2) cells were negative. A sample of MDR1-MDCK cells was included as a positive control (lane 1). (b) All samples show bands of the size expected for β-actin (243 bp. L size marker).

4. Discussion

Rapid advances in the understanding of the molecular pathogenesis of retinal disease have highlighted the need for targeted drug delivery. Several strategies have been developed to overcome the poor penetration of drugs into the retina. Intravitreal injections are routinely performed to circumvent the BRB. However, repeat injections are necessary to maintain therapeutic drug levels and a number of complications are associated with this invasive procedure (Morlet et al., 1993). Intravitreal implants can maintain drug concentrations over longer periods, although they still require surgical placement (Jaffe et al., 1998; Velez and Whitcup, 1999). Whilst recent studies have highlighted the trans-scleral route as an attractive non-invasive method for delivering drugs to the choroid and retina (Ambati and Adamis, 2002), the RPE remains a significant permeability barrier. The capacity of the RPE to transport drugs has been largely unexplored, despite developments in transporter-targeted drug delivery in other tissues (Mizuno et al., 2003).

The recent description of P-gp expression in the human RPE in situ (Kennedy and Mangini, 2002) has significant implications for retinal drug delivery. Studies have shown that P-gp is an important impediment to the influx of certain hydrophobic drugs across the blood–brain barrier (Kusuhara and Sugiyama, 2001). Several brain capillary endothelial cell lines that stably express P-gp have proven to be useful tools for the study of drug transport and P-gp activity in particular (Begley et al., 1996; Pham et al., 2000). Since immortalised RPE cell lines retain many of the morphological, biochemical and functional characteristics of RPE cells in vivo (Lund et al., 2001;

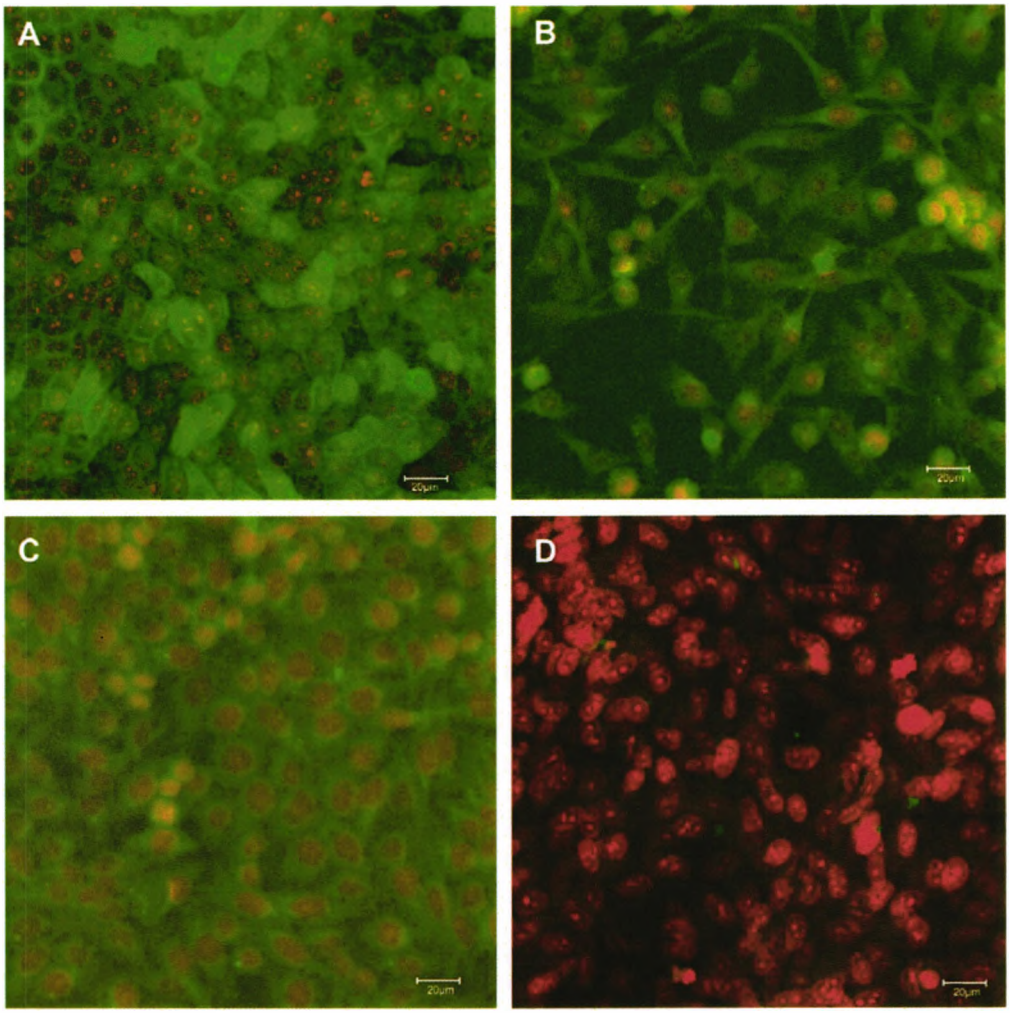

Fig. 3. Results of immunocytochemistry show strong staining in the positive control MDCK-MDR1 cells (a). ARPE19 cells (d) were negative whilst weak staining was evident with h1RPE and D407 cells (b and c respectively). Negative controls (not shown) in which the primary antibody was omitted were immunonegative. Scale bar 20 μm.

Kanuga et al., 2002), it is of significance to establish whether these cells express P-gp to determine their suitability for future drug-transport studies.

The well-characterised human RPE cell line, ARPE19, consistently lacked P-gp expression by RT-PCR, C219 immunocytochemistry and rhodamine 123 uptake assay. This is significant given that ARPE19 have previously been shown to express the closely related transporter, multidrug resistance-associated protein (MRP) (Aukunuru et al., 2001). However, these proteins are frequently not co-expressed in other cells. For example, the rat brain endothelial cell lines, GPNT and RBE4, show strong P-gp activity despite lacking MRP1 (Regina et al., 1998, 1999).

The spontaneously immortalised RPE cell line D407 has been previously shown to express MDR1 mRNA, and Western blots confirmed protein expression (Kennedy and Mangini, 2002). The present study was able to identify a faint MDR1 message in most of the cultures tested, P-gp immunoreactivity was weak, which may be due to the higher passage number (86–97) used in this study compared to Kennedy and Mangini's (57–58) (Kennedy and Mangini, 2002). However, we were able, for the first time, to demonstrate functional P-gp expression in this cell line.

The h1RPE cell line arose following a SV40 large T cell antigen transformation of human RPE primary cultures (Kanuga et al., 2002). These cells express a number of RPE markers including: RPE-65, CRALBP, ZO-1, β-catenin, and brain-derived neurotrophic factor (BDNF). However, P-gp expression in h1RPE cells was variable and the rhodamine uptake assay failed to demonstrate significant P-gp activity.

Cell culture conditions have been shown to significantly influence P-gp expression in a variety of cell types (Tatsuta et al., 1994; Hirsch-Ernst et al., 1995; Lechardeur et al., 1995; Regina et al., 1998; Gaillard et al., 2000). Although Kennedy and Mangini (2002) were able to show constitutive P-gp expression in human RPE primary cultures, an earlier study found that, although mRNA for MDR1 was present, P-gp protein was only detected after pre-treating the cells with the anti-mitotic agent daunomycin (Esser et al., 1998). These data raise the possibility that P-gp can be upregulated in suitable RPE cell lines by appropriate selection of substrate,

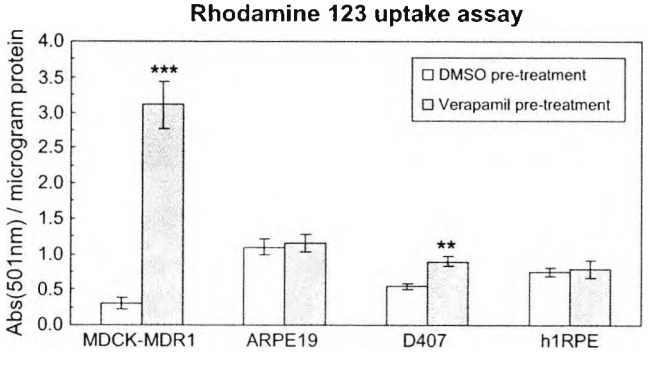

Fig. 4. Rhodamine 123 accumulation in verapamil-treated (open bars) and control (shaded bars) cells. The significant difference seen with MDCK-MDR1 cells indicates functional P-gp activity. Of the human RPE cell lines only D407 shows significant activity; ARPE19 and h1RPE showed no significant difference in accumulation between treated and control cells, indicating no P-gp activity. Bar graphs represent means of $n = 15$ samples from 3 independent runs. Data are mean ± SEM; $n = 15$ samples from 3 independent experiments. ($^{**}P < 0.01$, $^{***}P < 0.001$).

varying the composition of the culture medium and/or pre-treating the cells with anti-mitotic or cell differentiation agents.

In conclusion, D407 has the potential to be used to incorporate P-gp mediated transport into an overall permeability screen of candidate drugs across the RPE.

Acknowledgements

Preliminary results were presented in abstract form at the 2004 annual meeting of the Association for Research in Vision and Ophthalmology, Ft Lauderdale, FL. PC is supported by a Scholarship from the College of Optometrists UK, DD is supported by the Wellcome Trust, UK. This work was funded by the British Retinitis Pigmentosa Society, UK. The authors would like to thank Dr David Begley for comments on the manuscript.

References

Ambati, J., Adamis, A.P., 2002. Transscleral drug delivery to the retina and choroid. Prog. Retin. Eye Res. 21, 145–151.

Aukunuru, J.V., Sunkara, G., Bandi, N., Thoreson, W.B., Kompella, U.B., 2001. Expression of multidrug resistance-associated protein (MRP) in human retinal pigment epithelial cells and its interaction with BAPSG, a novel aldose reductase inhibitor. Pharm. Res. 18, 565–572.

Begley, D.J., Lechardeur, D., Chen, Z.-D., Rollinson, C., Bardoul, M., Roux, F., Scherman, D., Abbott, N.J., 1996. Functional expression of P-glycoprotein in an immortalised cell line of rat brain endothelial cells, RBE4. J. Neurochem. 67, 988–995.

Cunha-Vaz, J., 2004. The blood-retinal barriers system. Basic concepts and clinical evaluation. Exp. Eye Res. 78, 715–721.

Davis, A.A., Bernstein, P.S., Bok, D., Turner, J., Nachtigal, M., Hunt, R.C., 1995. A human retinal pigment epithelial cell line that retains epithelial characteristics after prolonged culture. Invest. Ophthalmol. Vis. Sci. 36, 955–964.

Dunn, K.C., Aotaki-Keen, A.E., Putkey, F.R., Hjelmeland, L.M., 1996. ARPE-19, a human retinal pigment epithelial cell line with differentiated properties. Exp. Eye Res. 62, 155–169.

Dunn, K.C., Marmorstein, A.D., Bonilha, V.L., Rodriguez-Boulan, E., Giordano, F., Hjelmeland, L.M., 1998. Use of the ARPE-19 cell line as a model of RPE polarity: basolateral secretion of FGF5. Invest. Ophthalmol. Vis. Sci. 39, 2744–2749.

Duvvuri, S., Majumdar, S., Mitra, A.K., 2003. Drug delivery to the retina: challenges and opportunities. Expert Opin. Biol. Ther. 3, 45–56.

Esser, P., Tervooren, D., Heimann, K., Kociok, N., Bartz-Schmidt, K.U., Walter, P., Weller, M., 1998. Intravitreal daunomycin induces multidrug resistance in proliferative vitreoretinopathy. Invest. Ophthalmol. Vis. Sci. 39, 164–170.

Gaillard, P., van der Sandt, I., Voorwinden, L., Vu, D., Nielsen, J., de Boer, A., Breimer, D., 2000. Astrocytes increase the functional expression of P-glycoprotein in an in vitro model of the blood-brain barrier. Pharm. Res. 17, 1198–2005.

Greenwood, J., 1992. Characterization of a rat retinal endothelial cell culture and the expression of P-glycoprotein in brain and retinal endothelium in vitro. J. Neuroimmunol. 39, 123–132.

Greenwood, J., Pryce, G., Devine, L., Male, D., dos Santos, W., Calder, V., Adamson, P., 1996. SV40 large T immortalised cell lines of the rat blood-brain and blood-retinal barriers retain their phenotypic and immunological characteristics. J. Neuroimmunol. 71, 51–63.

Gumbleton, M., Audus, K., 2001. Progress and limitations in the use of in vitro cell cultures to serve as a permeability screen for the blood-brain barrier. J. Pharm. Sci. 90, 1681–1698.

Hirsch-Ernst, K.I., Ziemann, C., Schmitzsalue, C., Foth, H., Kahl, G.F., 1995. Modulation of P-glycoprotein and mdr1b mRNA expression by growth factors in primary rat hepatocyte culture. Biochem. Biophys. Res. Commun. 215, 179–185.

Jaffe, G., Yang, C., Wang, X., Cousins, S., Gallemore, R., Ashton, P., 1998. Intravitreal sustained-release cyclosporine in the treatment of experimental uveitis. Ophthalmology 105, 46–56.

Kanuga, N., Winton, H.L., Beauchene, L., Koman, A., Zerbib, A., Halford, S., Couraud, P.O., Keegan, D., Coffey, P., Lund, R.D., Adamson, P., Greenwood, J., 2002. Characterization of genetically modified human retinal pigment epithelial cells developed for in vitro and transplantation studies. Invest. Ophthalmol. Vis. Sci. 43, 546–555.

Kennedy, B.G., Mangini, N.J., 2002. P-glycoprotein expression in human retinal pigment epithelium. Mol. Vis. 8, 422–430.

Kusuhara, H., Sugiyama, Y., 2001. Efflux transport systems for drugs at the blood-brain barrier and blood-cerebrospinal fluid barrier (part 2). Drug Discov. Today 6, 206–212.

Lechardeur, D., Schwartz, B., Paulin, D., Scherman, D., 1995. Induction of blood–brain barrier differentiation in a rat brain-derived endothelial cell line. Exp. Cell Res. 220, 161–170.

Lund, R.D., Adamson, P., Sauve, Y., Keegan, D.J., Girman, S.V., Wang, S., Winton, H., Kanuga, N., Kwan, A.S., Beauchene, L., Zerbib, A., Hetherington, L., Couraud, P.O., Coffey, P., Greenwood, J., 2001. Subretinal transplantation of genetically modified human cell lines attenuates loss of visual function in dystrophic rats. Proc. Natl. Acad. Sci. U.S.A. 98, 9942–9947.

Mannerstrom, M., Zorn-Kruppa, M., Diehl, H., Engelke, M., Toimela, T., Maenpaa, H., Huhtala, A., Uusitalo, H., Salminen, L., Pappas, P., Marselos, M., Mantyla, M., Mantyla, E., Tahti, H., 2002. Evaluation of the cytotoxicity of selected systemic and intravitreally dosed drugs in the cultures of human retinal pigment epithelial cell line and of pig primary retinal pigment epithelial cells. Toxicol. In Vitro 16, 193–200.

Mitchell, C.H., 2001. Release of ATP by a human retinal pigment epithelial cell line: potential for autocrine stimulation through subretinal space. J. Physiol. 534, 193–202.

Mizuno, N., Niwa, T., Yotsumoto, Y., Sugiyama, Y., 2003. Impact of drug transporter studies on drug discovery and development. Pharmacol. Rev. 55, 425–461.

Morlet, N., Young, S., Strachan, D., Coroneo, M., 1993. Technique of intravitreal injection. Aust. N.Z. J. Ophthalmol. 21, 130–131.

Oddiah, D., Anand, P., McMahon, S.B., Rattray, M., 1998. Rapid increase of NGF, BDNF and NT-3 mRNAs in inflamed bladder. Neuroreport 9, 1455–1458.

Pastan, I., Gottesman, M., Ueda, K., Lovelace, E., Rutherford, A., Willingham, M., 1988. A retrovirus carrying an MDR1 cDNA confers multidrug resistance and polarized expression of P-glycoprotein in MDCK cells. Proc. Natl. Acad. Sci. U.S.A. 85, 4486–4490.

Pham, Y., Regina, A., Farinotti, R., Couraud, P., Wainer, I., Roux, F., Gimenez, F., 2000. Interactions of racemic mefloquine and its enantiomers with P-glycoprotein in an immortalised rat brain capillary endothelial cell line, GPNT. Biochem. Biophys. Acta 1524, 212–219.

Regina, A., Koman, A., Piciotti, M., El Hafny, B., Center, M., Bergmann, R., Couraud, P., Roux, F., 1998. Mrp1 multidrug resistance-associated protein and P-glycoprotein expression in rat brain microvessel endothelial cells. J. Neurochem. 71, 705–715.

Regina, A., Romero, I., Greenwood, J., Adamson, P., Bourre, J., Couraud, P., Roux, F., 1999. Dexamethasone regulation of P-glycoprotein activity in an immortalized rat brain endothelial cell line, GPNT. J. Neurochem. 73, 1954–1963.

Schinkel, A.H., Jonker, J.W., 2003. Mammalian drug efflux transporters of the ATP binding cassette (ABC) family: an overview. Adv. Drug Deliv. Rev. 55, 3–29.

Steuer, H., Jaworski, A., Elger, B., Kaussmann, M., Keldenich, J., Schneider, H., Stoll, D., Schlosshauer, B., 2005. Functional characterization and comparison of the outer blood–retina barrier and the blood–brain barrier. Invest. Ophthalmol. Vis. Sci. 46, 1047–1053.

Tatsuta, T., Naito, M., Mikami, K., Tsuruo, T., 1994. Enhanced expression by the brain matrix of P-glycoprotein in brain capillary endothelial cells. Cell Growth Differ. 5, 1145–1152.

Velez, G., Whitcup, S.M., 1999. New developments in sustained release drug delivery for the treatment of intraocular disease. Br. J. Ophthalmol. 83, 1225–1229.

Doc Ophthalmol
DOI 10.1007/s10633-006-9023-z

ORIGINAL PAPER

Light and alcohol evoked electro-oculograms in cystic fibrosis

Paul A. Constable · John G. Lawrenson · Geoffrey B. Arden

Received: 4 April 2006 / Accepted: 16 August 2006

Abstract Cystic fibrosis (CF) is caused by a defect in the cystic fibrosis transmembrane conductance regulator (CFTR) which is a chloride channel. CFTR is expressed in the retinal pigment epithelium (RPE) where it is believed to be important in generating the fast oscillations (FOs) and potentially contributing to the light-electro-oculogram (EOG). The role of CFTR in the alcohol-EOG is unknown. We recruited six individuals with CF (three homozygotes for Δ508 and three heterozygous for Δ508) and recorded the light- and alcohol-EOGs as well as the FOs and compared them to a control group. The results showed that in the CF group the amplitude of the alcohol- and light-EOGs were normal. However, the time to peak of the light- and alcohol-rises were significantly faster than in the control group. We conclude that CFTR is not primarily responsible for the alcohol- or light-rises but is involved in altering the timing of these responses. The FOs showed differences between the homozygotes, heterozygotes and the controls. The amplitudes were significantly higher and the time to the dark troughs were significantly slower in the heterozygote group compared to both controls and the homozygotes. In contrast, the homozygotes did not differ in either amplitude or the timing of the FOs compared to the controls.

Keywords Alcohol · Cystic fibrosis · Electro-oculogram · Fast oscillation · Retinal pigment epithelium

P. A. Constable (✉) · J. G. Lawrenson · G. B. Arden
Department of Optometry and Visual Science, Henry Wellcome Laboratories for Vision Sciences, City University, London, UK
e-mail: p.a.constable@city.ac.uk

Introduction

Cystic fibrosis (CF) is a disease in which lung function is primarily affected. It is inherited recessively. The gene involved, cystic fibrosis transmembrane conductance regulator (CFTR), encodes for the cystic fibrosis transmembrane conductance regulator chloride channel [1–3]. The most prevalent Caucasian mutation results in the deletion of phenylalanine at position 508 (Δ508) and thereby renders CFTR incapable of reaching the plasma membrane [1, 4–8]. Heterozygotes for Δ508 are also affected, though typically mildly. However, the genotype is not always correlated to the severity of the phenotype [9, 10]. CFTR gating requires ATP binding and hydrolysis and is also regulated by cAMP dependent protein kinase-A (PKA) phosphorylation [11–15].

CFTR has been identified in both the apical and basal membranes of foetal RPE sheets [16] and the corresponding mRNA has been identified in adult human RPE and retina [17], in cultured

RPE cells [18, 19] and canine RPE [20]. Although vision is normal in CF, two abstracts have found that the FOs are reduced whilst the light-EOG is normal [17, 21]. However, in Δ508 homozygous mice and in CFTR null mice the FOs are still present which suggests that the FOs are not solely dependent on CFTR [22]. One possible role for CFTR in the RPE is fluid regulation [16] although its contribution is probably minimal [20]. CFTR also transports ATP into the sub-retinal space. This potentially could contribute to the light-rise if ATP binds to an apical purinergic receptor which would then increase the intracellular calcium concentration ($[Ca^{2+}]_{in}$). In turn the raised $[Ca^{2+}]_{in}$ could increase the basolateral chloride conductance associated with the light-rise of the EOG [18].

The main aim of this study was to determine whether CFTR was involved in generating the alcohol-EOG. Alcohol has been shown to alter the ocular standing potential in vivo in ovine [23] and in bovine RPE preparations in vitro [24, 25]. A slight increase in the human ERG b-wave has been reported, but alcohol does not appear to alter the retinal responses in any other way [26] and is thus most likely to be acting directly upon the RPE. Human studies [27, 28] show that oral doses of alcohol causes a rise in the ocular standing potential that mimics the light-rise of the EOG. A proposed model is that ethanol acts on a different initial receptor to the 'light-rise' substance but both ethanol and light share the same common final basolateral membrane chloride channel [27, 29]. Determining whether CFTR is involved or not in the alcohol-EOG is important as the alcohol-EOG has been shown to be more sensitive than the light-EOG in detecting early RPE dysfunction in retinitis pigmentosa and age related macular degeneration [29, 30]. Such a finding would implicate CFTR in these retinal diseases.

The current understanding of the generation of the light-rise is that light liberates an as yet unidentified substance from the rods that binds to an RPE receptor that initiates a rise in $[Ca^{2+}]_{in}$. The elevated $[Ca^{2+}]_{in}$ causes a basolateral chloride channel to open thereby depolarising the basal membrane, and generating the light-rise [31–34]. The basolateral chloride channel responsible for the light-rise is believed to be bestrophin based on clinical findings [35–37]. However, new findings now suggest that bestrophin regulates Ca^{2+} entry into the RPE, and that the basolateral chloride channel is in fact a Ca^{2+}-gated chloride channel and not bestrophin [38, 39]. Our current understanding of the light-evoked responses and the chloride channels involved and how they interact is becoming more complex and the interactions between the basolateral chloride channels appears to be more involved than previously believed. For review, see [40].

The light-EOG requires functioning RPE and photoreceptor complex to generate the light rise. One limitation of the light-EOG is that an absent light response does not discriminate between dysfunction of the photoreceptors or the RPE [41]. The clinical utility of the light- and alcohol-EOGs have been further questioned by the variability in the responses [42, 43]. It has been a long held hope that a sensitive and clinically viable electrophysiological measure of RPE function would be found. Given the close association between the light- and alcohol-EOGs, an understanding of the mechanism of the alcohol-EOG may lead to other substances being used to provide such a test.

Methods

All participants provided written informed consent in accordance with the protocol approved by City University's Senate Research and Ethics Committee and in agreement with the tenets of the 2nd declaration of Helsinki.

Participants

The mean UK life expectancy for an individual with CF is ~29 years and diabetes mellitus is a common complication. Sufferers require medication, and the patients in our group were all taking prednisolone 5 mg 1× day, vitamin supplements, pancreatic enzymes, antibiotics and nebulisers. One of the CF group had received a lung transplant 18 months previously and was taking the following additional medications: immunmosuppressives (azathioprine 125 mg 1× day and

cyclosporine 250 mg 2× day); anti-hypertensives (ramipril (ACE inhibitor) 10 mg 1× day and doxazosin (α_1-agonist) 16 mg 1× day). This individual's results were not incorporated into the statistical analysis owing to the potential for these medications to disrupt the RPE [44, 45]. However, this individual's responses are shown in the figures and are labelled as 'lung transplant'. Another of the CF participants was an insulin dependent diabetic and was also taking furosemide 40 mg 1× day and warfarin 6 mg 1× day. His blood glucose levels at the time of recording the FOs were normal at 6.0 mmol/l. Elevated blood glucose levels have been shown to increase the amplitude of the FOs [46].

Volunteers were contacted via the United Kingdom CF trust website. All CF volunteers were Caucasians attending specialist CF clinics within the UK, and referred by their consultant physicians. Their genotypes were known with each individual having been screened for the 33 alleles known to be associated with CF. There are other genetic and environmental factors that contribute to the final CF phenotype with some heterogeneity observed in the phenotype, even amongst individuals with the same genotype [8, 10]. Of the five CF participants included in this study, two were homozygous for Δ508 (Δ508/Δ508) and three were heterozygous for Δ508 with one other unidentified allele (Δ508/?). The female pair of homozygotes ages were 18 and 20 years. In the all-male heterozygous group, the ages ranged from 37 to 43 years. The mean age of the CF group was 32 with a SD of ±11 (N = 5). The older age of the heterozygous group may reflect the difference in the severity of these two genotypes.

A control group of normal participants was recruited. The control groups for the tests were not identical with some participants declining either to have mydriasis or to drink alcohol. The mean age for the light-EOG was 41 with a SD of ±12 (N = 6) and ranged from 21 to 54 years with five males and one female. For the alcohol-EOG the mean age was 44 with a SD of ±8 (N = 6) and ranged from 34 to 54 years with four males and two females. For the FOs the mean age was 34 with a SD of ±11 (N = 9) and ranged from 20 to 54 years with seven males and two females. There was no significant difference in age between groups for the light-EOG (p = 0.2063), FOs (p = 0.6834) and alcohol-EOG (p = 0.0789). Binocular motility, visual acuity and colour vision were normal for all subjects. All tests were performed on the same day for each participant.

Electrophysiology

All procedures were identical for the CF and control participants. The participants were asked to fast overnight for at least 10 h. Two dim red LEDs that subtended 30° to the observer were mounted on a uniform white wall. The ceiling and side walls were also illuminated and we believe this provides (approximately) full field illumination. The skin was cleaned and 5 mm diameter gold electrodes filled with conductive jelly were taped to the skin near the outer canthi of each eye and one reference electrode was placed on the forehead (electrode impedance was 3–5 kΩ). Electrodes were connected to a digital voltmeter (Keithley 2700) (Keithley Instruments, Ohio, USA) and voltages were sampled every 240 ms whilst the subject executed horizontal saccades at 1 Hz (maintained with the aid of a metronome). For the alcohol- and light-EOGs, the subject performed saccades for 10 s when instructed. A period of 26 min was allowed for dark adaptation (< 0.01 cd/m^2) before either the light (100 cd/m^2) was turned on or alcohol was drunk in order to generate either the light- or alcohol-EOGs, respectively. The alcohol was whisky, diluted with water to 7% ethanol (vol/vol) at a dose of 110 mg/kg body weight. Recordings were continued for a further 34 min. Pupils were dilated with 0.5% tropicamide to at least 7 mm diameter for the light-EOG and FOs only. For the FOs illumination was altered at 60 s intervals and recordings made continuously for 10 min.

Instrumentation

The voltmeter was connected via an interface card to a PC and voltage difference between each canthal electrode recorded in a spreadsheet with ExceLINX^{TM} (Keithley). The modulus of the voltage difference between successive recordings $|(v_{n-1} - v_n)|$ was then taken. Most of these voltage differences were very small, because in the

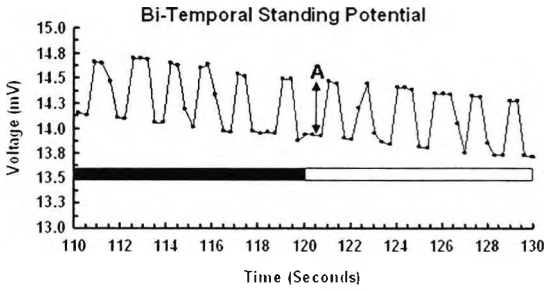

Fig. 1 Trace of the standing potential over time between dark and light indicated by the bars. The amplitude of the standing potential at a given time was taken as the difference in voltage between consecutive data points as the eyes executed horizontal saccades and is indicated by the arrow labelled (A). The absolute voltage differences were then plotted as in Fig. 2

$(n-1)$th and nth episodes, the eyes did not move. However, in some instances they were large, because the eyes repositioned between the two samples. By taking the modulus of the voltages both positive and negative voltage differences were treated identically – i.e., the signal was the same for lateral and medial eye movements. Figure 1 shows the actual results and Fig. 2 the results after the transformation. The upper boundary of the points can be seen to describe a curve which varies as the light/dark condition changes.

For the light- and alcohol-EOGs the mean standing potential for the preceding 10 min interval before stimulus was used to normalise the data points (see appendix 1) [27]. Time to peak and the absolute maxima of the light peak were compared between the CF groups and controls. In addition, the ratio of the light peak to the second trough that follows the peak was also measured [47]. In the FO the peak voltage occurs in the dark cycle and the minimum occurs in the light cycle so the peak to trough ratio represents the dark-rise maxima:light-trough minima (DR:LT). The times from dark-rise peak to light-trough minima were also recorded. A total of four measurements were taken from each individual's trace.

The recordings and measurements of the EOGs deviated from the 1993 ISCEV standard [48] in the following ways. The pre-adaptation time was longer than the ISCEV standard for the EOGs so that a baseline could be established [27, 29, 30]. The recording of only four oscillations in the FOs was lower than the ISCEV standard recommendations of six but four has been reported to be adequate and it also reduces the test

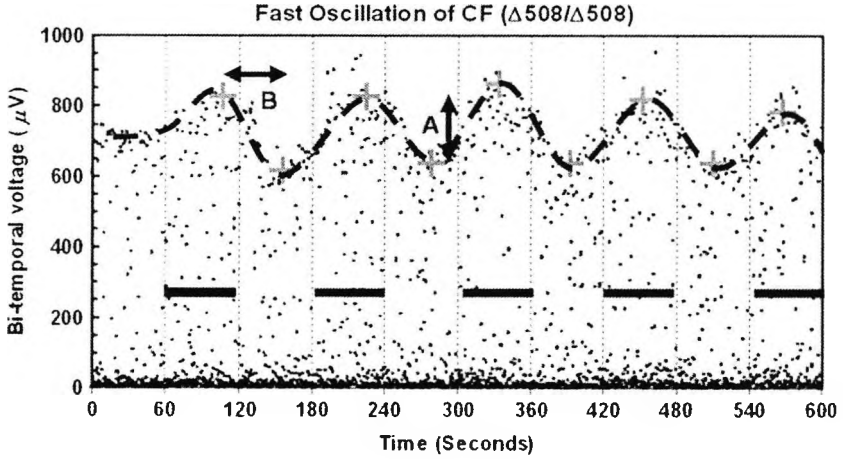

Fig. 2 The transformation of taking the absolute voltage differences between successive data points (as shown in Fig. 1). When plotted the voltage differences describe a curve that alters in relation to light and dark and approximates the ocular standing potential. The figure above shows the FO for a Δ508/Δ508 homozygote. The dark-rise:light-trough ratio (DR:LT) is represented by the magnitude of arrow (A) with the time from peak to trough represented by arrow (B). From each trace four values were recorded. The intervals in dark are represented by black bars. The heavy dotted line is drawn here to indicate the oscillations and grey crosses approximate the DR peak and LT minumum. Points that were distant from this line were not used and represented artefacts such as blinks or coughs from the participants and are evident in the 180–240 and 420–480 s intervals

time [49]. We did not use a Ganzfeld bowl and we recorded bi-temporally.

Statistics

The results are expressed as mean ± SD unless otherwise stated. Test for equal variance was used (F-test) for all parameters. Student's unpaired two-tailed t-test was used for the EOG results. 1-way ANOVA was performed on the FO parameters. Least squares linear regression analysis was performed on the DR:LT ratio and FO latency. A p-value of <0.05 was taken as statistically significant. Statistical calculations were performed using Minitab™ software (Minitab™, Coventry, UK).

Results

There was no difference in the amplitude of the alcohol-EOG between the CF group and the controls (Fig. 3). The amplitudes were 1.62 ± 0.16 ($N = 6$) for controls and 1.67 ± 0.07 ($N = 5$) for the CF group ($p = 0.8533$). The times to peak were: for the controls 9.0 ± 1.4 min and for the CF group 7.4 ± 0.9 min ($p = 0.0504$) which was 1.6 min faster.

The amplitude of the light-rise was not significantly different ($p = 0.8653$) between controls (2.01 ± 0.16 $N = 6$) and CF patients (1.93 ± 0.15 $N = 5$). However, there is a significant difference in the timing of the responses with the control

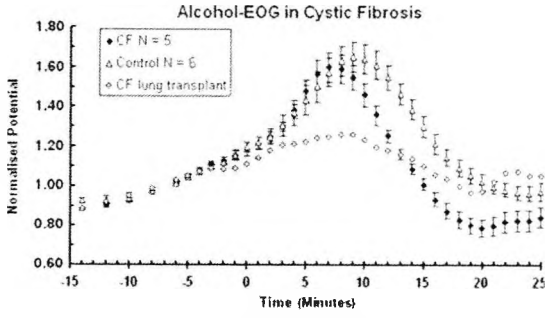

Fig. 3 The alcohol-EOG responses to 110 mg/kg of oral alcohol at $t = 0$. The time to peak was significantly faster ($p = 0.0504$) but the amplitudes are not different. One individual who had received a lung transplant showed an abnormal alcohol response. Plot shows mean ± SEM

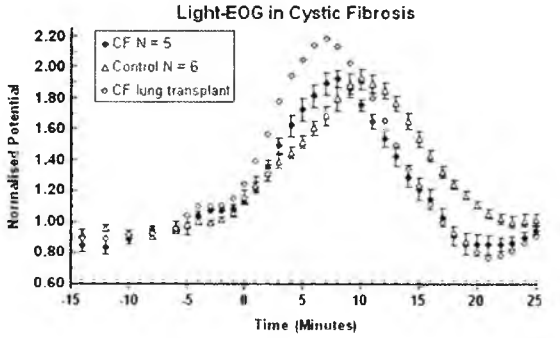

Fig. 4 The light-EOG in a series of individuals with CF shows that whilst the amplitude of the response is the same compared to controls, the time to peak is significantly faster ($p < 0.0001$) in the CF group. Plot shows mean ± SEM with light on at $t = 0$. The individual who is post transplant is also shown – with a normal light response

group peaking at $t = 10.2 \pm 0.4$ and CF group peaking at $t = 8.0 \pm 0.6$ min ($p < 0.0001$) (see Fig. 4). The lung transplant participant is shown and his light-EOG was normal but his alcohol-EOG was reduced.

The ratio of the light peak to the second trough normalised voltages for the CF and control group were compared. The alcohol-EOG ratio for the CF group was 2.25 ± 0.23 which was significantly higher ($p = 0.0297$) than the control group's ratio of 1.82 ± 0.31. In the light-EOG the ratio was not significantly so ($p = 0.0879$) different. The CF group's ratio was 2.37 ± 0.42 compared to the control group's ratio of 1.92 ± 0.38.

Cystic fibrosis fast oscillations

Unlike the EOGs the FOs of the Δ508 homozygotes and the Δ508 heterozygotes were significantly different with respect to the amplitudes. One-way ANOVA analysis of the DR:LT ratio and the latency from dark-rise to light-trough revealed the following differences compared to controls (all values are mean ± SD). The Heterozygote's DR:LT ratio was 1.44 ± 0.10 which was significantly ($p < 0.001$) greater than the controls with a ratio of 1.29 ± 0.05. Furthermore, the time from the dark-rise to light-trough was significantly slower ($p = 0.029$) with the heterozygote's time being 61.8 ± 5.0 s and the controls being 57.2 ± 6.5 s. By contrast, when the controls were compared to the Δ508 homozygotes then no

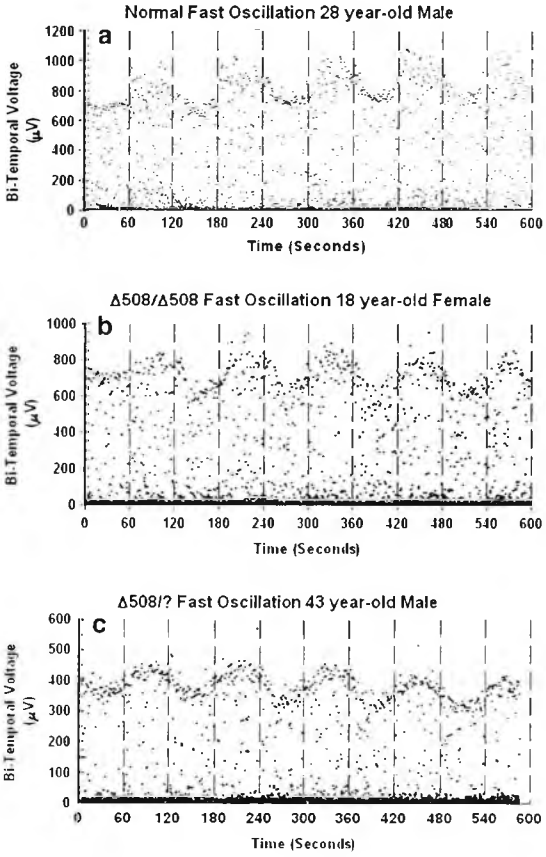

Fig. 5 Representative traces of the fast oscillations from control and the CF participants. (**a**) Shows a control FO with Figs. (**b**) and (**c**) showing the normal amplitudes also seen in the homozygote and heterozygote CF participants with Δ508 mutations. respectively. All traces began with a one minute interval of light before dark in which the standing potential is seen to rise

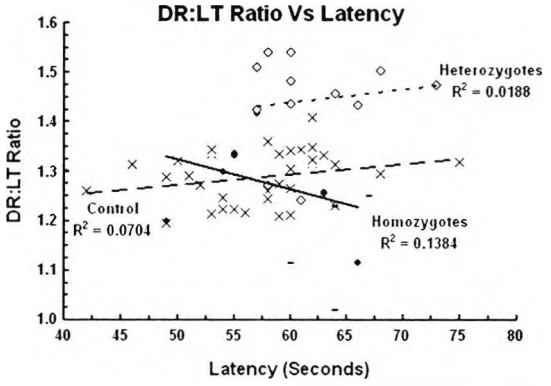

Fig. 6 Regression plot of the DR:LT ratios against latency from dark-peak to light-trough for control (*x*) and the CF participants. The CF data points are divided so that the Δ508 homozygotes are indicated by a (♦). The CF Δ508 heterozygotes by a (◇) and the lung transplant individual by a (-). There is no strong linear relationship between the DR:LT ratio and the timing of the FOs. However, the homozygotes show a negative relationship between the DR:LT amplitude and the timing. There was only one value from an included homozygote of the DR:LT ratio that fell below 1.15. The heterozygotes had a significantly higher and slower response than the controls and had a higher DR:LT ratio than the heterozygotes. No differences were observed between homozygotes and the controls. Note axes are truncated

significant differences were noted in either the DR:LT ratio 1.28 ± 0.09 (p = 0.689) or the timing 57.8 ± 5.7 s (p = 0.827). When the two CF groups were compared then the heterozygotes had a significantly higher DR:LT ratio (p = 0.0010) but there was no difference in the timing (p = 0.1070) (see Fig. 5).

Figure 6 shows the DR:LT ratio plotted against the latencies for the FOs. Both the CF and control group results are shown. The DR:LT axis is on the ordinate. A ratio of 1.0 indicates a total absence of FO. In the CF group, the heterozygous group had the highest DR:LT ratios and these were also significantly slower than the control group. The heterozygotes are indicated by unfilled diamonds (◇). The homozygous pair are represented by filled black diamonds (♦) and were no different to the controls in either the DR:LT ratio or the timing of the FOs. Only one oscillation from this group was < 1.15 and could be considered abnormal. The lung transplant participant represented by black line (-) had two values in the normal range (1.23 and 1.25) and two values that were very low and abnormal (1.12 and 1.02). The controls are represented by crosses in the figure.

Equations 1–3 are the least squares linear regression relationships between the DR:LT ratio and the latency for the control and CF groups. There were no strong relationships between the DR:LT amplitude and the timing of the FOs. However, the homnozygotes did suggest that in this case the DR:LT amplitude did decrease as the time increased.

Control DR:LT ratio = $1.16 + 0.00214 \times$ Time
($R^2 = 0.0704$ $p = 0.124$) (1)

Δ508/Δ508 DR:LT ratio = $1.62 - 0.006 \times$ Time
($R^2 = 0.1384$ $p = 0.364$) (2)

Δ508/? DR:LT ratio = $1.28 + 0.0026 \times$ Time
($R^2 = 0.0188$ $p = 0.671$). (3)

Discussion

The alcohol- and light-EOGs in patients with CF are both altered with respect to the time to peak. Both responses are shifted to the left with the light-rise being affected to a greater extent than the alcohol-rise. However, the amplitudes are not different and this makes it unlikely that CFTR is the major chloride channel responsible for these responses. The CF group contained both Δ508 homozygotes and heterozygotes. This common mutation renders CFTR incapable of reaching the plasma membrane in any substantial amounts. The significant differences in the time to peak must relate to an interaction between CFTR and the initiation of the light- and alcohol-EOG responses. It was possible, a priori, that alcohol absorption might be slowed in CF. However, because both the light- and alcohol-EOGs have faster onsets then this acceleration must be due to processes occurring in the RPE.

Each participant only agreed to attend on one occasion and as the alcohol-EOG was always performed first in the morning (after fasting over-night). It is possible that the relatively less stable baseline of the alcohol-EOG is due to this sequencing effect- for example, any initial anxiety that affected the baseline would have vanished after the patient had breakfast, and was ready to record a light-EOG. Any possible anxiety would affect the first test baseline values more than for the subsequent light tests. This may account for the relatively less stable baseline in the alcohol-EOG. The one individual who had a lung transplant had a reduced alcohol-EOG, normal light-EOG and a borderline reduced FO response. These differences may be in part due to his systemic medications, azathioprine and cyclosporine that are reported to be toxic to the RPE and can cause visual loss [44, 45]. The alcohol-EOG has been claimed to be a more sensitive measure of RPE function than the light-EOG with greater loss apparent in ARMD. It could be that in this case the alcohol-EOG is also detecting early RPE dysfunction before the light-EOG is affected [30]. Therefore, this participant was not included in the statistical treatment.

Our current understanding of the origins of the light-rise is incomplete with the putative 'light-rise' substance and its receptor unknown. Furthermore, the nature of the basolateral chloride channel is also uncertain. The absence of the EOG light-rise in Best's disease was taken as evidence that bestrophin was the Ca^{2+}-gated chloride channel responsible for the light-rise. More recently it has been demonstrated that bestrophin alters the kinetics and activation of L-type Ca^{2+} channels and regulate $[Ca^{2+}]_{in}$ following purinergic stimulation [38, 39]. For review, see [50]. CFTR is known to interact with a variety of ionic channels [51, 52] regulating both outward-rectifying Cl^- channels [53], epithelial Na^+ channels [54] as well as having a regulatory role in pH through the transport of HCO_3 [55]. The numerous interactions of CFTR with ionic channels could alter the ionic fluxes in the RPE when CFTR is absent. In CF, the sweat and lung mucosa is high in NaCl due to poor Cl^- transport [56]. If similar changes occur in the RPE then the electrochemical gradients may be altered which may influence the timing of the light- and alcohol-rises observed.

It has recently been suggested that the compound waveform of the EOG is not a simple damped oscillation, but a resultant of two separate processes – an initial rise and a delayed fall in the trans epithelial potential of the RPE [47]. The evidence was that the ratio peak: second trough varied systematically with the stimulus intensity. The observations of this paper show that in this small group there is a statistically significant correlation in the CF group between the size of the alcohol peak EOG results and the subsequent trough. But there is no significant difference

between the positive light- and alcohol-rises of the control and CF groups. This suggests that there may be an increased negative component in the CF group. A similar result was found in the light EOG, but was not statistically significant.

CFTR has been implicated in generating the light-rise through transport of ATP [18] and we cannot exclude a role for CFTR in generating a component of the light-rise. However, the normal amplitudes of the light-rise in CF would suggest that CFTR is not central to this response. Our findings corroborate earlier reports that the light-rise amplitude is normal [17, 21] in CF and therefore this channel is not responsible for the changes in the TEP associated with these responses.

The FO is the result of a fall in sub-retinal potassium following retinal illumination. This causes a decrease in the activity of the apical NaK2Cl co-transporter resulting in a decrease in $[Cl^-]_{in}$ [57–59]. Consequently, the basal membrane hyperpolarises as there is less basolateral Cl^- flux and so the TEP falls causing the light-trough of the FO. The FO is normal in Best's but the light-rise is absent indicating that a different mechanism is responsible for the FOs and the light-rise [35]. The FOs have been claimed to be selectively reduced in CF [17, 21], and this has been taken as evidence that CFTR forms (at least part) of the basal chloride conductance. However, our result is that the FOs are not reduced in CF and there is a larger amplitude in the heterozygous individuals and they also display a slowed timing of the response. This finding may be related to the influence of complex alleles that partially compensate for the Δ508 mutation. All of the heterozygotes were pancreatic insufficient (one was a type 1 diabetic) and would normally be classified as 'severe' sufferers. In a complex allele, a second mutation in the gene partially compensates for primary mutation. In Δ508, the accompanying mutation R553Q confers stability to the protein so that it retains function by improving the folding and trafficking of CFTR to the plasma membrane [60]. There are also suspected to be promoter genes and environmental factors that all determine the final CF phenotype that may influence the levels of functional CFTR in the RPE [10].

The homozygotes did not show any difference in the DR:LT ratio or the timing of the response which is counter to previous reports. However, there was a tendency for the slower timing of the FOs to be associated with a smaller DR:LT ratio. This would be expected if CFTR was responsible for the FOs and certainly, in the group who are severely affected then CFTR does appear to participate in the response. One recent finding in mouse has also demonstrated that in CFTR, null mice the FOs are still present and therefore it is likely that an alternative mechanism that does not rely solely on CFTR is generating the FOs [22]. Our findings support this contention in that, the FOs are not absent in either Δ508 homozygotes or heterozygotes but the resulting actual mechanism is likely to involve a more complex interaction of CFTR and the basal membrane Cl^- channels. The numerous interactions of CFTR with other ionic channels coupled with the potential regulation by other genetic and environmental factors may limit the ability to establish the precise role of CFTR in man except in the Δ508 homozygotes or by using animal models.

The results indicate that CFTR is not involved in generating the alcohol- and light-rises. This finding supports the original hypothesis of Arden and Wolf [27, 29] who predicted an overlap of these responses with respect to their final common pathway. The findings of this study show that both the alcohol- and light-EOG are affected in a similar way when the Δ508 mutation is present. However, how the alcohol- and light-EOGs are generated is still not fully understood but a defect in CFTR alters the timing of the response in a similar way. Therefore, it is likely that a part of the alcohol- and light-EOGs generation is similar.

CFTR is most likely interacting with other ionic channels to modulate the time-course of the light- and alcohol-responses in man but does not appear to be responsible for the alterations in the RPE's electrical potential in relation to light or alcohol. Further work on individuals with Best's disease should enable a clearer picture of the chloride channel responsible for the alcohol-EOG.

Acknowledgements We thank Prof. D. Geddes and Dr. D. Empey who provided information about the CF

patients. This work was funded by the British Retinitis Pigmentosa Society and PC is supported by grants from the College of Optometrists, UK and the South Devon and Cornwell Institute for the Blind. Parts of this work were presented at the LXIIIth ISCEV Symposium, Glasgow, 2005.

Appendix A

The EOG voltages were normalised to the 10-min pre-stimulus baseline voltages. In Eq. A1 the normalised potential (V_N) was equal to the potential at time (T) denoted (V_T) divided by the mean of the measurements made in the 10 min prior to the stimulus. These recordings were made at T = 16, 18, 20, 21, 22, 23, 24, 25 and 26 min into the pre-adaptation period. Light or alcohol was then given at 26.5 min.

$$V_N = V_T/(\text{Mean}V_{T(16,18,20,21,22,23,24,25,26)}) \quad \text{(A1)}$$

where:
V_N = Normalised voltage at time T.
V_T = bi-temporal voltage at time T.
Mean ($V_{T(16...26)}$) = Mean baseline bi-temporal voltage at T = 16th, 18th, 20th, 21th, 22th, 23th, 24th, 25th and the 26th min.

Subsequently the normalised voltages were smoothed further by weighting each value with 50% of the preceding and the following normalised voltage (Eq. A2).

$$\text{Smoothed Voltage} = [(V_N + (0.5 \times V_{N-1}))/ (V_N + (0.5 \times V_{N+1})] \times 0.5 \quad \text{(A2)}$$

where:
V_N = the normalised voltage at time T (from Eq. A1).
V_{N+1} = the normalised voltage value after V_N
V_{N-1} = the normalised voltage value preceding V_N.

The baseline-normalised voltages were not identical between the CF and the control groups. To correct for this so that the amplitudes of the responses could be compared to an identical baseline the following correction was used. The ratio of the normalised voltages from all subjects in the 10 min interval preceding the stimulus for the CF group to the same values of the control group were taken.

For the light-EOG the values were for CF = 0.9804 and for the control = 1.0196 and the correction factor was 0.9804/1.0196 = 0.9616. This correction to the baseline was then multiplied through all the normalised voltages for the control group. The corresponding baseline correction factor for the alcohol-EOG was 1.0449.

References

1. Riordan JR, Rommens JM, Kerem B-S et al (1989) Identification of the cystic fibrosis gene: cloning and characterization of complementary DNA. Science 245:1066–1073
2. Rommens JM, Iannuzzi MC, Kerem B et al (1989) Identification of the cystic fibrosis gene: chromosome walking and jumping. Science 245:1059–1065
3. Li M, McCann JD, Liedtket CM et al (1988) Cyclic AMP-dependent protein kinase opens chloride channels in normal but not cystic fibrosis airway epithelium. Nature 331:358–360
4. Kerem B-S, Rommens JM, Buchanan JA et al (1989) Identification of the cystic fibrosis gene: Genetic analysis. Science 245:1073–1080
5. Lemna WK, Feldman GL, Kerem B et al (1990) Mutation analysis for heterozygote detection and the prenatal diagnosis of cystic fibrosis. N Engl J Med 322:291–296
6. Gregory RJ, Rich DP, Cheng SH et al (1991) Maturation and function of cystic fibrosis transmembrane conductance regulator variants bearing mutations in putative nucleotide-binding domains 1 and 2. Mol Cell Biol 11:3886–3893
7. Puchelle E, Gaillard D, Ploton D et al (1992) Differential localization of the cystic fibrosis transmembrane conductance regulator in normal and cystic fibrosis airway epithelium. Am J Respir Cell Mol Biol 5:485–491
8. McCormick J, Green MW, Mehta G et al (2002) Demographics of the UK cystic fibrosis population: implications for neonatal screening. Eur J Hum Genet 10:583–590
9. Sermet-Gaudelus I, Vallée B, Urbin I et al (2002) Normal function of the cystic fibrosis conductance regulator protein can be associated with homozygous ΔF508 mutation. Pediatr Res 52:628–635
10. Rowntree RK, Harris A (2003) The phenotypic consequences of CFTR mutations. Ann Human Genet 67:471–485
11. Anderson MP, Gregory RJ, Thompson S et al (1991) Demonstration that CFTR is a chloride channel by alteration of its anion selectivity. Science 253:202–205
12. Anderson MP, Berger HA, Rich DP et al (1991) Nucleoside triphosphates are required to open the CFTR chloride channel. Cell 67:775–784

13. Rich DP, Anderson MP, Gregory RJ et al (1990) Expression of cystic fibrosis transmembrane conductance regulator corrects defective chloride channel regulation in cystic fibrosis airway epithelial cells. Nature 347:358–363
14. Welsh MJ, Smith AE (1993) Molecular mechanisms of CFTR chloride channel dysfunction in cystic fibrosis. Cell 73:1251–1254
15. Vergani P, Lockless SW, Nairn AC et al (2005) CFTR channel opening by ATP-driven tight dimerization of its nucleotide-binding domains. Nature 433:876–880
16. Blaug S, Quinn R, Quong J et al (2003) Retinal pigment epithelial function: a role for CFTR? Doc Ophthalmol 106:43–50
17. Miller SS, Rabin J, Strong T et al. Cystic fibrosis (CF) gene product is expressed in retina and retinal pigment epithelium. Invest Ophthalmol Vis Sci 1992; 33:#1597 ARVO Abstract
18. Reigada D, Mitchell CH (2005) Release of ATP from retinal pigment epithelial cells involves both CFTR and vesicular transport. Amer J Physiol 288:C132–C140
19. Weng TX, Godley BF, Jin GF et al (2002) Oxidant and antioxidant modulation of chloride channels expressed in human retinal pigment epithelium. Amer J Physiol 283:C839–C849
20. Loewen ME, Smith NK, Hamilton DL et al (2003) CLCA protein and chloride transport in canine retinal pigment epithelium. Amer J Physiol 285:C1314–C1321
21. Lara WC, Jordan BL, Hope GM et al (2003) Fast oscillations of the electro-oculogram in cystic fibrosis. Invest Ophthalmol Vis Sci 44:#4957 ARVO Abstract
22. Wu J, Marmorstein AD, Peachey NS (2006) Functional abnormalities in the retinal pigment epithelium of CFTR mutant mice. Exp Eye Res 83:424–428
23. Knave B, Persson HE, Nilsson SEG (1974) A comparative study on the effects of barbituate and ethyl alcohol on the retinal functions with specific reference to the c-wave of the electroretinogram and the standing potential of the sheep eye. Acta Ophthalmol (Copenh) 52:254–259
24. Pautler EL (1994) Photosensitivity of the isolated pigment epithelium and arachidonic acid metabolism: preliminary results. Curr Eye Res 13:687–695
25. Bialek S, Quong JN, Yu K et al (1996) Nonsteroidal anti-inflammatory drugs alter chloride and fluid transport in bovine retinal pigment epithelium. Amer J Physiol 270:C1175–C1189
26. Ikeda H (1963) Effects of ethyl alcohol on the evoked potential of the human eye. Vis Res 3:155–169
27. Arden GB, Wolf JE (2000) The human electro-oculogram: interaction of light and alcohol. Invest Ophthalmol Vis Sci 41:2722–2729
28. Skoog O-K, Textorius O, Nilsson SEG (1975) Effects of ethyl alcohol on the directly recorded standing potential of the human eye. Acta Ophthalmol (Copenh) 53:710–720
29. Arden GB, Wolf JE (2000) The electro-oculographic responses to alcohol and light in a series of patients with retinitis pigmentosa. Invest Ophthalmol Vis Sci 41:2730–2734
30. Arden GB, Wolf JE (2003) Differential effects of light and alcohol on the electro-oculographic responses of patients with age-related macular disease. Invest Ophthalmol Vis Sci 44:3226–3232
31. Gallemore RP, Steinberg RH (1991) Cobalt increases photoreceptor-dependent responses of the chick retinal pigment epithelium. Invest Ophthalmol Vis Sci 32:3041–3052
32. Griff ER, Steinberg RH (1982) Origin of the light peak: *in vitro* study of *Gekko gekko*. J Physiol 331:637–652
33. Gallemore RP, Griff ER, Steinberg RH (1988) Evidence in support of a photoreceptoral origin for the "light-peak substance". Invest Ophthalmol Vis Sci 29:566–571
34. Gallemore RP, Steinberg RH (1989) Effects of DIDS on the chick retinal pigment epithelium. II. mechanism of the light peak and other responses originating at the basal membrane. J Neurosci 9:1977–1984
35. Weleber RG (1989) Fast and slow oscillations of the electro-oculogram in best's macular dystrophy and retinitis pigmentosa. Arch Ophtalmol 107:530–537
36. Thorburn W, Nordstrom S (1978) EOG in a large family with hereditary macular degeneration. (Best's vitelliform macular dystrophy) identification of gene carriers. Doc Ophthalmol 56:455–464
37. Pinckers A, Cuypers MH, Aandekerk AL (1996) The EOG in Best's disease and dominant cystoid macular dystrophy (DCMD). Ophthalmic Genet 17:103–108
38. Rosenthal R, Bakall B, Kinnick T et al (2006) Expression of bestrophin-1, the product of the VMD2 gene, modulates voltage-dependent Ca^{2+} channels in retinal pigment epithelial cells. FASEB J 20:178–180
39. Marmorstein LY, Wu J, McLaughlin P et al (2006) The light peak of the electroretinogram is dependent on voltage-gated calcium channels and antagonized by bestrophin (Best-1). J Gen Physiol 127:577–589
40. Arden GB, Constable PA (2006) The electro-oculogram. Prog Ret Eye Res 25:207–248
41. Marmor MF (1991) Clinical electrophysiology of the retinal pigment epithelium. Doc Ophthalmol 76:301–313
42. Wu K, Marmor M (2005) Alcohol- and light-induced electro-oculographic responses in age-related macular degeneration and central serous chorioretinopathy. Doc Ophthalmol 110:237–246
43. Marmor M, Wu K (2005) Alcohol- and light-induced electro-oculographic responses: variability and clinical utility. Doc Ophthalmol 110:227–236
44. López-Jiménez J, Sánchez A, Fernández CS et al (1997) Cyclosporine-induced retinal toxic blindness. Bone Marrow Transplant 20:243–245
45. Garweg J, Wegmann-Burns M, Goldblum D. (2006) Effects of daunorubicin, mitomycin-C, azathioprine and cyclosporin A on human retinal pigmented epithelial, corneal endothelial and conjunctival cell lines. Graefe's Arch Clin Exp Ophthalmol 244:382–389
46. Schneck ME, Fortune B, Adams AJ (2000) The fast oscillation of the electrooculogram reveals sensitivity

of the human outer retina/retinal pigment epithelium to glucose level. Vision Res 40:3447–3453
47. Wolf JE, Arden GB (2004) Two components of the human alcohol electro-oculogram. Doc Ophthalmol 109:123–130
48. Marmor MF, Zrenner E (1993) Standard for clinical electro-oculography. International society for clinical electrophysiology of vision. Doc Ophthalmol 85: 115–124
49. Vaegan, Beaumont P (2005) The fast oscillation of the electroculogram Is a rapidly recorded independent parameter, sensitive to and specific for retinitis pigmentosa. Invest Ophthalmol Vis Sci 46:#515 ARVO Abstract
50. Marmorstein AD, Kinnick TR (2006)Focus on molecules: bestrophin (best-1). Exp Eye Res (in press)
51. Kunzelmann K (2001) CFTR: interacting with everything? News Physiol Sci 16:167–170
52. Schwiebert EM, Benos DJ, Egan, ME et al (1999) CFTR Is a conductance regulator as well as a chloride channel. Physiol Rev 79:145–166
53. Jovov B, Ismailov II, Berdiev BK et al (1995). Interaction between cystic fibrosis transmembrane conductance regulator and outwardly rectified chloride channels. J Biol Chem 270:29194–29200
54. Horisberger J-D (2003). ENaC-CFTR interactions: the role of electrical coupling of ion fluxes explored in an epithelial cell model. Pflügers Archiv Eur J Physiol 445:522–528
55. Simpson JE, Gawenis LR, Walker NM et al (2005). Chloride conductance of CFTR facilitates basal Cl^-/HCO_3^- exchange in the villous epithelium of intact murine duodenum. Amer J Physiol 288:1241–1251
56. Joris L, Dab I, Quinton PM (1993). Elemental composition of human airway surface fluid in healthy and diseased airways. Amer Rev Respir Dis 148:1633–1637
57. Linsenmeier RA, Steinberg RH (1984) Delayed basal hyperpolarization of cat retinal pigment epithelium and its relation to the fast oscillation of the dc electroretinogram. J Gen Physiol 83:213–232
58. Gallemore RP, Steinberg RH (1993) Light-evoked modulation of basolateral membrane Cl conductance in chick retinal pigment epithelium: the light peak and fast oscillation. J Neurophysiol 70:1669–1680
59. Oakley II B, Green DG (1976) Correlation of the light-induced changes in retinal extracellular potassium concentration with c-wave of the electroretinogram. J Neurophysiol 39:1117–1133
60. Dork T, Wulbrand U, Richter, T et al (1991) Cystic fibrosis with three mutations in the cystic fibrosis transmembrane conductance regulator gene. Hum Genet 87:441–446